Deciphering cryptic calcium signals in the human colonic epithelium

Nicolas Pelaez Llaneza

Submitted for the degree of Doctor of Philosophy

University of East Anglia

School of Biological Sciences

September 2019

Abstract

The colonic epithelium is constantly exposed to a harsh luminal environment. A monolayer of epithelial cells is organised into millions of blind ending flask-like invaginations called crypts. The regulation of the epithelial barrier is key in maintaining tissue integrity; failure to do so can result in the development of intestinal conditions such as inflammatory bowel diseases and cancer.

Stem cells residing at each crypt-base constantly proliferate to maintain tissue renewal and integrity. Physical barrier function provided by the epithelial monolayer is supported by goblet cells which secrete mucus and other antimicrobial proteins to protect the epithelium from noxious substances and the luminal microbiota. The regulation of this dynamic epithelial barrier and the associated physiological functions requires the complex integration of different signalling pathways. Calcium is a versatile intracellular messenger capable of integrating different signals to modulate cell biology and physiological function.

The aim of this thesis was to determine the molecular mechanism of cholinergic-induced intracellular calcium signals in the colonic epithelium and study the implications for tissue renewal and barrier function.

This thesis demonstrates that in the colonic epithelium intracellular calcium signals couple muscarinic receptors to the modulation of short-term and long-term physiological responses. In the stem cell niche, muscarinic receptor activation results in the generation of an intracellular calcium signal mediated by the endolysosomal Two-pore channels. The cholinergic calcium signal initiates in stem cells and results in the translocation of transcription factors to the nucleus and, over the long-term, stimulation of stem/progenitor cell proliferation and tissue regeneration. After a short delay, the stem cell-calcium signal registers in neighbouring goblet cells, hereby defined as Guardian goblet cells because they protect adjacent intestinal stem cells. Activation of the calcium signalling pathway in goblet cells induces mucus secretion and expansion in the crypt lumen which is accompanied by stimulated fluid secretion from neighbouring stem/progenitor cells; these short-term physiological responses culminate in flushing of the crypt luminal contents.

Taken together, these findings demonstrate a central role for intracellular calcium signalling in maintaining the fitness of the human intestinal stem cell niche and in promoting gut barrier function.

Declaration

I declare that this thesis represents my own work, except where due acknowledgement is made, and that it has not been previously included in a thesis, dissertation or report submitted to this University of to any other institution for a degree, diploma or other qualifications

_____

Nicolas Pelaez Llaneza

PhD candidate

Acknowledgments

I would like to thank all the people that make the completion of this project possible.

First of all, I would to express my gratitude to The Humane Research Trust for awarding me the studentship to undertake these studies.

I would particularly like to express my gratitude to my supervisor Dr Mark Williams, for the constant support and excellent guidance. In addition, I would especially like to thank Dr Victoria Jones and Alvin Lee for their help throughout the course of my studies.

Finally, I would like to thank my parents and Marina, for their unconditional support during these years.

Table of Contents

List of figures

List of Tables

Glossary

5-HT:	5-hydroxytryptamine (serotonin)
A83:	3-(6-Methylpyridin-2-yl)-1-phenylthiocarbamoyl-4-quinolin-4-ylpyrazole
ACh:	Acetylcholine
AChE:	Acetylcholinesterase
AMP:	Antimicrobial Peptide
ASCL2:	Achaete-scute complex homolog 2
BMP:	Bone Morphogenetic Protein
CRC:	Colorectal Cancer
CICR:	Calcium-induced calcium release
Ca^{+2}:	Calcium
CA:	Carbonic Anhydrase
cADPR:	Cyclic ADP-Ribose
CaM:	Calmodulin
cAMP:	Cyclic AMP
CaN:	Calcineurin
CBC cell	Crypt Base Columnar Cell
CCh:	Carbachol
CD:	Crohn's Disease
CFTR:	Cystic Fibrosis Transmembrane Conductance Regulator
ChAT:	Choline Acetyl Transferase
CHGA:	Chromogranin A
CNS:	Central Nervous System
COX:	Cyclooxygenase
DAG:	Diacylglycerol
DCLK1:	Doublecortin-Like Kinase 1
DSC:	Deep Secretory Cells
DZM:	Diltiazem
EEC:	Enteroendocrine Cell
EGC:	Enteric Glia Cell
EGF:	Epidermal Growth Factor

EGFR: Epidermal Growth Factor Receptor

EN: Enteric Neurons

ENS: Enteric Nervous System

FAPBP: Fatty Acid Binding Protein

FGF: Fibroblast Growth Factor

GAP: Goblet-associated Antigen Passage

GCG: Glucagon Precursor

GI: Gastrointestinal

GSNO: S-Nitrosoglutathione

Hh: Hedgehog

IBD: Inflammatory Bowel Disease

IP_3: Inositol trisphosphate

IP3R Inositol trisphosphate Receptor

IPAN: Intrinsic Primary Afferent Neuron

ISC: Intestinal Stem Cell

LGR5: Leucine-rich repeat-containing G-protein-coupled receptor 5

LRC: Label-Retaining Cell

MAChR: Muscarinic Acetylcholine Receptor

MGluR: Metabotropic Glutamate Receptor

MUC2: Mucin 2

NCC: Neural Crest Cell

NFAT: Nuclear Factor of Activated T-cells

NICE: National Institute for Health and Care Excellence

NKKC1: Sodium-potassium-chloride cotransporter

NO: Nitric Oxide

OCT: Organic Cation Transporter

OLFM4: Olfactomedin 4

Oxo: Oxotremorine-M

PGD2: Prostaglandin D2

PGDP: Proglucagon-derived Peptide

PLC: Phospholipase C

PMCA: Plasma Membrane Calcium ATPase

POU2F3: POU Class 2 Homeobox 3

PPAR-δ: Peroxisome Proliferator-Activated Receptor Gamma

PRR: Pattern Recognition Receptors

PTGS: Prostaglandin-endoperoxide Synthase

PTK7: Protein Tyrosine Kinase 7

PYY: Peptide YY

ROI: Region of Interest

ROS: Reactive Oxygen Species

RyR: Ryanodine receptor

SCFA: Short-Chain Fatty Acid

SMP: Submucosal Plexus

Shh: Sonic Hedgehog

SOCE: Store-operated Calcium Entry

SPCA: Secretory Pathway Calcium ATPase

TA Cell: Transit Amplifying Cell

TFF: Trefoil Factor

TGF-β: Transforming Growth Factor Beta

TNF-α: Tumour Necrosis Factor Alpha

TLR: Toll-like Receptor

TORC: Transducer Of Regulator CREB Activity

TPC: Two-Pore Channel

VAChT: Vesicular Acetylcholine Transporter

VGCC: Voltage-gated Calcium Channels

VIP: Vasoactive Intestinal Peptide

WFDC2: WAP Four-Disulfide Core Domain 2

YAP: Yes-associated Protein

Preface

The inner lining of the gut comprises of a monolayer of polarised intestinal epithelial cells. These cells form a selective barrier between the luminal contents on the apical-side and the systemic circulation on the other. The small intestine is formed by epithelial protrusions or villi and mucosal invaginations, or crypts, to maximise the absorption of nutrients, water and electrolytes and the secretion of different molecules. The colon is composed only of crypts and it is where water, ions and bile salts are absorbed; mucus is secreted, bacteria are sensed, and faeces are formed and expulsed. Importantly, the human large intestine hosts millions of microbes that reside in the lumen and ferment some dietary components that are otherwise indigestible, helping in the absorption of important nutrients. The inner layer of the gut also plays a major role as a barrier against potential threats such as bacteria, some metabolites and other toxic substances. The intestine epithelium is probably the fastest organ to self-renew as it is replaced almost entirely in 5 to 7 days (Clevers, 2013). Tissue renewal starts at the base of the crypts which is populated by intestinal stem cells (ISCs) and the resulting progeny differentiate into all types of cell lineages including enterocytes, enteroendocrine cells, goblet cells and tuft cells, as they migrate towards the top of the crypt. Cell signalling in the crypt is orchestrated by epithelial and mesenchymal cells. This is a tightly regulated process which functions as a gradient where Wnt, Notch and EGF signals induce proliferation at the base of the crypt whereas BMP and TGFβ pathways induce cell differentiation higher up the crypt axis (Gehart & Clevers, 2019; Reynolds et al., 2013).

The gut is innervated by neurons from the enteric nervous system (ENS) which can signal neurotransmitters that interact with the epithelium to regulate gut biology. (Bjerknes and Cheng, 2001; Neunlist et al., 2013). Acetylcholine (ACh) is a molecule synthesized from an ester of choline and Acetyl-CoA by the choline acetyltransferase (ChAT) enzyme, which has been traditionally considered a neurotransmitter since it is produced and secreted by neurons of the parasympathetic nervous system, including the ENS (Hebb and Whittaker, 1958; Taylor and Brown, 1999). However, recent studies have shown that ACh can be produced also by immune cells like macrophages (Kristen et al., 2014) or specialised epithelial cells like the tuft cells (Schneider et al., 2019). ACh signals are recognised by G-coupled protein receptors (GPCRs) present at the membrane of the cells of the colonic crypt (Nathanson, 2008). Cholinergic receptors are a type of GPCR that upon binding of the ACh molecule activate an intracellular signalling cascade that results in the release of calcium to the cytoplasm (Lindqvist et al., 1998). Calcium is an important second messenger that can integrate different cellular signals to activate specific routes to induce cellular responses like proliferation (Deng et al., 2015) in stem cells or mucus secretion in goblet cells (Ambort et al., 2012).

The colonic epithelium keeps bacteria and other potential threats away from the base of the crypt thanks in part to a dense layer of mucus produced by goblet cells that creates a barrier to protect the epithelium. Dysregulation in mucus secretion is related to the development of inflammatory bowel diseases such Crohn's disease and ulcerative colitis, which affect more than 250.000 people in the UK only (NICE, 2012, 2013). In the colon, the mucus is organised into two different layers, an outer one loose and easy for commensal bacteria to colonise and feed on, and the inner one which is thick and blocks any bacterial contact with the epithelium (Johansson et al., 2011). Secretion of mucus has been reported to be dependent on muscarinic activation of calcium signalling. ACh is sensed by muscarinic-cholinergic receptors like muscarinic receptor type 3 (MAChR3), that generate a calcium signal capable of inducing mucus secretion (Specian and Neutra, 1980; Ambort et al., 2012).

Stem cells reside at the base of colonic crypts where they proliferate to give rise to all cell types. In the gut, these cells can be identified by the expression of the LGR5 membrane receptor (Barker et al., 2007). Maintenance of stem cell function is regulated by cells located in close proximity to the stem cells like Paneth cells in the small intestine (Toshiro. Sato et al., 2011), goblet cells in the colon (Sasaki et al., 2016) and mesenchymal cells underlying the epithelium (Aoki et al., 2016; Stzepourginski et al., 2017) that secrete growth factors like Wnt and R-spondin proteins. Intestinal stem cells have been also shown to possess MAChR3 and it is thought that neuronal ACh secreted by the cholinergic neurons and non-neuronal ACh secreted by epithelial tuft cells can regulate stem cell biology (Lundgren et al., 2011; Zhao et al., 2014; Hayakawa et al., 2016). Muscarinic-coupled calcium activation has been reported to be key in regulating fluid secretion in the colon but the intracellular calcium mechanism that modulate mucus secretion and stem cell biology remain elusive.

This introduction will give an overview of the biology and regulation of the intestinal epithelium and the mechanisms of intracellular calcium signalling in homeostasis.

1 Chapter 1. General Introduction

1.1 The gastrointestinal tract

The gastrointestinal tract is made of a series of organs that process ingested food, absorb nutrients and water, and eliminate waste. These organs include the oral cavity, pharynx and oesophagus, stomach, small intestine, large intestine, rectum and the anus (**Figure 1.1**). The large intestine, also referred to as the colon, is located in the abdomen and it is approximately one and a half metres long. The colon is divided into four different regions: cecum and ascending colon, which connect with the small intestine region of the ileum; followed by the transverse colon, descending colon and sigmoid colon. The primary roles of the colon are the absorption of water and electrolytes, production and absorption of vitamins and the formation and further elimination of faeces through the anus. Most of the nutrients and approximately 90% of the water is absorbed in the small intestine. The luminal content enters the cecum from the small intestine and it moves up the ascending colon pushed by the contraction and relaxation movements of the colonic wall, also known as peristalsis. It is here where most of the remaining liquid and nutrients from the indigestible material are absorbed. The stools are formed as the digested content is dehydrated and stored in the descending colon. The faeces are moved into the rectum due to the contraction of the sigmoid colon and are eliminated when they exit the anus (Azzouz et al., 2019; Ogobuiro et al., 2019).

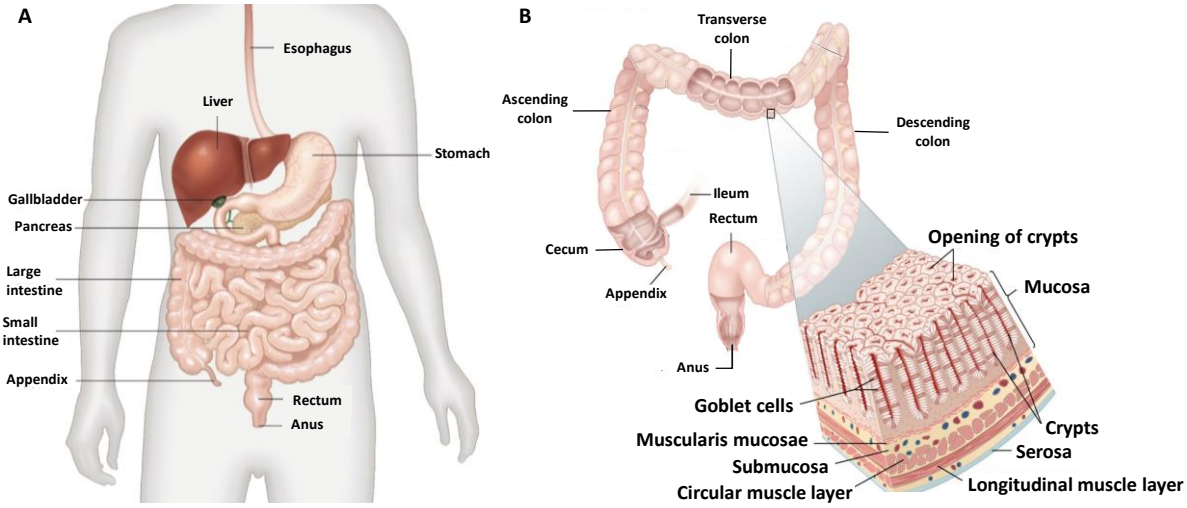

Figure 1.1. Anatomy of the human gastrointestinal tract. (A) The main components of the gastrointestinal tract include the oesophagus, stomach, small intestine, large intestine and anus. **(B)** Different layers of the GI comprising the mucosa, submucosa, muscularis propria and serosa. Adapted figures from Encyclopædia Britannica.

All the organs of the GI tract are formed by four different layers: mucosa (comprising epithelium, lamina propria and muscular mucosae), submucosa, muscularis propria (comprising inner circular muscle layer, intermuscular space, and outer longitudinal muscle layer) and serosa (**Figure 1.1**). All layers are joined to each other by connective tissue and by neural and vascular components. The mucosa is made of three layers, the innermost one being the epithelium. The epithelial cells are arranged as a monolayer of cells that are in contact with the luminal side. The next layer, the lamina propria is made of connective tissue and lymph nodes. The deepest layer, the muscularis mucosa; is formed by an uninterrupted sheet of smooth muscle cells. Underneath it, the submucosa is comprised of a range of inflammatory cells, lymphatic, autonomic nerve fibres and ganglion cells together with small arteries and venous channels. The muscularis propria is made of smooth muscle cells which are distributed into an inner circular layer and an outer longitudinal layer. The myenteric plexus contains autonomic neural fibres and ganglionic clusters which are situated in between both muscle layers (Azzouz et al., 2019; Ogobuiro et al., 2019).

The inner lining of the gut comprises a monolayer of polarised intestinal epithelial cells that varies in structure and composition between the small and the large bowel. The small intestine is formed by epithelial protrusions or villi and mucosal invaginations, or crypts, that maximise the absorption of nutrients, water and electrolytes and the secretion of different molecules (Collins et al., 2019; Pawel et al., 2016). The colon is composed only of crypts (**Figure 1.1**) which are specialised in absorbing water, ions and bile salts; secreting mucus, sensing bacteria and forming and expulsing faeces.

The intestinal lumen is home of millions of bacteria most of them living in symbiosis with the host. Many of these bacteria have a great impact on the local environment of the colon but also more general effects on the host metabolism. Microbes colonise the gut of infants during the first years of life and these colonies vary in composition and numbers during this time and later on in the life of the host. The microbiota undertakes important functions such as fermenting otherwise indigestible food components, metabolising oligosaccharides to generate short-chain fatty acids used as energy source, regulating hormone levels and producing inflammatory and anti-inflammatory signals (Flint et al., 2012; Skoczek et al., 2014; Tremaroli et al., 2012).

The microbiota population varies in number and composition along the GI tract due to the differences in nutrient composition and quantities, pH and oxygen levels, and the immune system components. The colon contains a higher bacterial density as compared to the small intestine. The reasons for this difference include the secretion from the small intestine of higher concentration of antimicrobial peptides which restrict microbial growth and the higher mucus density present in the colon. Moreover, while mucus is arranged in one tight layer in the small intestine, in the colon there

are two layers (Johansson, Larsson and Hansson, 2011). The outer one is a loose layer in contact with the lumen that bacteria find easy to colonise to create their own environment (Donaldson et al., 2017). In spite of the presence of such abundant number of bacteria, the colonic mucosa prevents any direct contact with the surface epithelium by generating the mucus film as a physical barrier, secreting antimicrobial proteins and regulating the epithelial intercellular flux with tight junctions.

1.2 The epithelial barrier

The human gut occupies an area of approximately 300 m^2, representing the largest boundary against the external environment. As part of the mucosa, intestinal crypts are constantly exposed to numerous antigens derived from nutrients or bacteria present in the lumen. The mucosal surface acts as a semipermeable structure that allows selective paracellular flux of water, ions and solutes, while preventing bacteria and toxins from penetrating the tissue. The capacity of the mucosa to selectively allow certain antigens to move across the tissue and to protect against luminal threats is called intestinal barrier function. Failure of the processes that regulate this barrier leads to pathological conditions.

To prevent the dysregulation of the intestinal mucosa, the action of the intestinal barrier starts in the lumen where commensal bacteria keep harmful bacteria at bay by producing antimicrobial substances and competing for nutrients (Coyte et al., 2019; Iacob et al., 2019). The next level of protection is obtained by the mucus secreted by the specialised epithelial goblet cells, which creates a physical barrier that coats the entire gut lining, separating it from the luminal content (**Figure 1.2**) (Johansson, Sjövall and Hansson, 2013). The mucus is a viscous substance made primarily of mucin glycoproteins, which in the colon is arranged in two different layers. The inner mucus layer is stratified and fixed to the intestinal epithelium and does not allow for any bacteria to access the mucosa easily. The outer mucus layer is loose in comparison and although the mechanism is not fully understood, it is thought to be generated after the degradation of the inner layer proteins by the host or the microbiota (Okumura et al., 2018). In the outer mucus layer, the long-term colonisation of commensal bacteria takes place. Fluid secretion into the lumen is a very important process that regulates colonic crypt homeostasis as it contributes to the flushing of potentially harmful substances and maintains a mucus coat that prevents from bacterial threats (Johansson et al., 2011; Johansson et al., 2008; Reynolds et al., 2007). Bacterial colonisation also influences mucus production and shapes the mucous barrier; in this way, gut bacteria modulate mucus production by augmenting goblet cell differentiation and inducing expression of genes that encode proteins involved in mucin glycosylation (Wrzosek et al., 2013).

Epithelial cells are polarised structures that are defined by their apical and basolateral membranes which present protein junctions comprised of tight junctions, adherens junctions and desmosomes (**Figure 1.2**). These protein junctions connect lateral membranes of neighbouring cells and seal the paracellular space while supporting the flux of ions, water and solutes (France et al., 2017). The hemidesmosomes are proteins located in the basolateral pole of the epithelial cells that connect them to the lamina propria. The tight junctions are the most apically located junctions and they work as transmembrane proteins regulating the intercellular passage of small molecules and water. These junctions interact with the cytoskeleton by being connected with the intracellular actin filaments. Tight junctions include members of the occludin and claudin families, the junction-adhesion-molecules (JAMs) and the Coxsackievirus and Adenovirus receptors (CAR) proteins (Guttman et al., 2009). At the apical pole of the cells, tight junctions form the apical junction complex together with adherens proteins and desmosomes to connect neighbouring cells. The role of the adherens proteins and desmosomes is to help assemble the tight junctions and to provide the strength that keeps the cells together. The most important adhesion protein is the E-cadherin which can interact with other cells and adherens proteins. Desmosomes in turn, interact with the cytoskeleton by creating connections with the intermediate filaments. In addition, Gap junctions are involved in regulating intracellular communication between neighbouring cells (France et al., 2017).

Together with mucus, there are also immune mediators that help maintain the mucosal barrier. IgA is present within the mucus coating, and its levels are higher in the small intestine. In the crypts of the small intestine, Paneth cells secrete antimicrobial proteins (AMPs) such as defensins, lysozyme and lectins such as REG3A (Johansson et al., 2016; Meyer-Hoffert et al., 2008) that associate with the mucus layer. Goblet cells of the colon can also secrete antimicrobial components such as WFDC2 which can inhibit bacterial serine and cysteine proteases (Parikh et al., 2019).

The mucosal immunity is the last line of defence. The lamina propria located underneath the mucosa presents both innate and acquired immune cells, enteric neurons, glial cells and the enteroendocrine system which form this microenvironment. Controlled antigen delivery to immune cells is key in maintaining a mature immune system. Microfold cells (M-cells) are specialised in sampling the lumen content where they take up bacterial antigens and deliver them to immune cells in the lymphoid tissue and the subsequent production and release into the lumen of IgA by the T-cells (Keita and Söderholm, 2010). Subepithelial mononuclear phagocytes also sample the luminal content through transepithelial dendrites (Chieppa et al., 2006). Intestinal epithelial cells are able to sense and integrate bacterial-derived signals into antimicrobial and immunoregulatory responses (Miron and Cristea, 2012; Knoop et al., 2014). The presence of pattern-recognition receptors enables them to recognise the microbial signals and communicate with the immune cells. These receptors

include the Toll-like receptors (TLRs), NOD-like receptors (NLRs) and RIG-I-like receptors (RLRs), each of which functions to activate a different and specialised signalling pathway (Peterson et al., 2014). Epithelial cell turnover plays another critical role in maintaining the mucosal barrier, whereby cells are constantly being created by proliferating stem cells at the base of the crypt but also being shed into the lumen at the top. The ratio of cell proliferation and shedding needs to be tightly regulated (Martini et al., 2017). When the control of the epithelial barrier is compromised, it can lead to increased antigen and bacterial passage, which can result in pathological conditions. A failure to resolve it can cause bacterial infections of the epithelium, chronic inflammation and loss of mucosal integrity, and the development of inflammatory bowel diseases (IBD) such as ulcerative colitis and Crohn's disease (Vancamelbeke and Vermeire, 2017). Recent studies have demonstrated that an altered microbiota composition, known as dysbiosis, is related to a number of immune, metabolic and neurological disorders like IBD (Okumura et al., 2018).

Lastly, the mechanism of autophagy has been suggested to play an important role in regulating the epithelial barrier. Autophagy is molecular process whereby impaired organelles, malformed proteins or invading microbes are carried to the lysosome to be degraded and recycled. Malfunctioning of autophagy is a critical factor that can result in the impairment of antimicrobial peptide secretion, the elimination of bacteria and the modulation of intestinal inflammation (Wu et al., 2019).

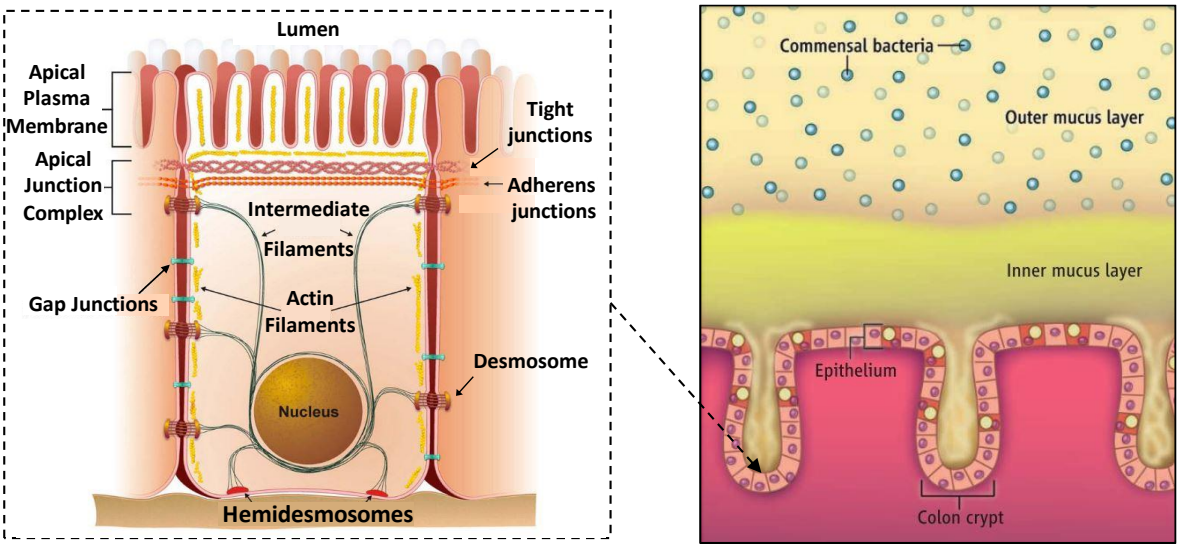

Figure 1.2. Main components of the epithelial barrier. (Left). Polarised epithelial cell showing the distribution of protein junctions that form the intercellular seals. These include gap junctions, tight junctions, adherens junctions, desmosomes and hemidesmosomes. **(Right)**. Goblet cells from the colonic epithelium secrete mucus to create a physical barrier to keep bacteria at bay. Figures were adapted from Guttman et al., 2008 and Johansson et al., 2011 respectively.

1.2.1 Epithelial regeneration

The gut epithelium is one of the fastest renewing tissues in the body as it can regenerate itself in 5 to 7 days (Clevers, 2013). Stem cells residing at the bottom of the crypts proliferate to give rise to progenitor cells that differentiate into all epithelial cellular types (enterocytes, enteroendocrine cells, tuft cells, goblet cells and Paneth cells in the small intestine) as they migrate up along the crypt axis, being shed in at the top (**Figure 1.3**). A tight balance regulates shedding of cells undergoing apoptosis and the subsequent replacement orchestrated by the intestinal stem cells during crypt homeostasis. It is thought that this fast epithelial renewal minimises the risks of disease and the accumulation of molecular damage (Medema et al., 2011). Excessive cell death can result in mucosal barrier defects and risk of infection, whereas insufficient cell death can drive the tumour formation (Edelblum et al., 2006).

Because of the importance of epithelial tissue regeneration, stem cells are located at the bottom of the crypts, protected from any potential luminal damage. In the small intestine, they are intermingled with Paneth cells that can secrete different antimicrobials to fight infection. In the colon, stem cells are located in between goblet cells which are thought to secrete mucus in response to a bacterial threat and flush away the pathogens. Together with underlying mesenchymal cells, these cells at the bottom of the crypt create the so called stem cell niche (Clevers, 2013). Under homeostatic conditions, proliferation occurs at a controlled rate and cells migrate upwards. However, upon acute injury stem cells are triggered and they proliferate at a faster rate to generate a large population of progenitor stem cells resulting in a transient enlargement of the crypt size and possible crypt fission to recover the tissue (Withers et al., 1970). Moreover, recent studies suggest that most epithelial cell types can migrate back to the base of the crypt and de-differentiate into stem cells to support the tissue recovery, making cellular plasticity key in tissue regeneration (de Sousa e Melo et al., 2019).

The Wnt signalling pathway (discussed later) is the major regulator of stem cell proliferation and it is prominent at the base of the crypt. As cells migrate up the crypt, presumably due to the pressure exerted by the newly generated cell, they are exposed to other signalling pathways including: Notch signals, bone morphogenetic protein (BMP) and the transforming growing factor β (TGF- β) signals (discussed later). These signals determine the cell fate (Reynolds et al., 2013). When cells are no longer required by the organism, they receive the appropriate signals to undergo cell death. This is a tightly regulated mechanism know as apoptosis or programmed cell death (Günther et al., 2013). Terminally differentiated cells reach the top of the crypt of villi after 3 to 4 days and they are shed into the lumen. Paneth cells, however, don't migrate up the crypt. Instead, via a poorly understood

mechanism, these cells remain next to the stem cells where they can live for more than 3 weeks (Clevers et al., 2013) to be later fragmented and phagocyted by infiltrating macrophages (Gassler, 2017). The cell shedding mechanism is another poorly understood process whereby cells stop receiving survival signals. These pro-apoptotic signals originate from their neighbouring cells and the underlying extracellular matrix, which activates programmed cell death or *anoikis*. The process of cell shedding, is believed to follow the 'zipper model' where the cell's tight junctions suffer remodelling and redistribution to allow the cell to be detached from the neighbouring cells and extruded into the lumen (Williams et al., 2015).

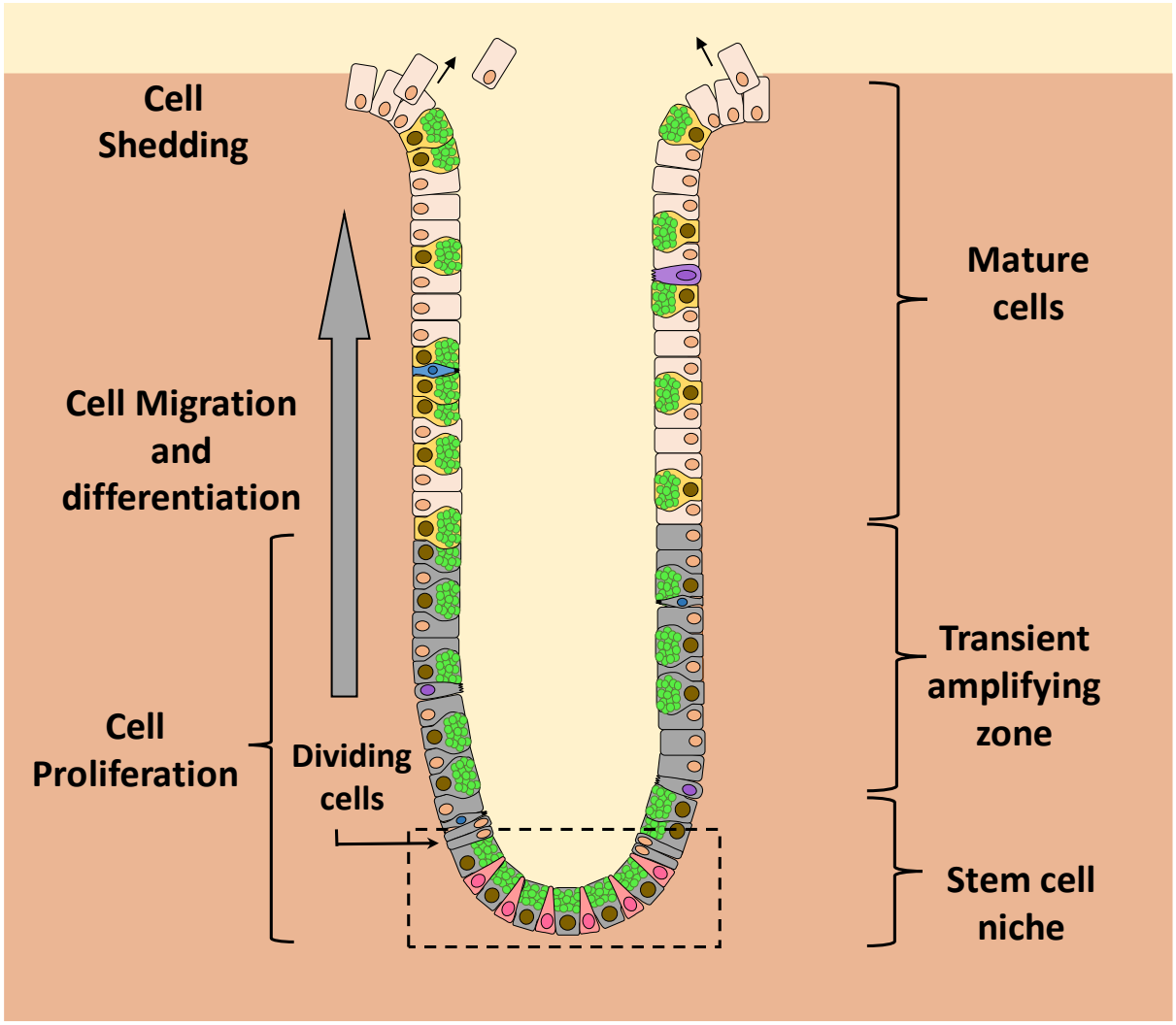

Figure 1.3.Regeneration of the intestinal epithelium. Stem cells located at the bottom of the colonic crypts self-renew and proliferate to give rise to transient amplifying cells. These cells differentiate into all cellular lineages as they migrate up the crypt axis and are eventually shed out into the lumen. The entire regeneration of the gut epithelium takes about 3 to 5 days.

1.2.2 Epithelial cell types in the gut

The epithelium of the gut is comprised of different cellular types (**Figure 1.4**) arranged as a monolayer that regulate nutrient and water absorption as well as maintaining the mucosal barrier. **Intestinal stem cells** (ISCs) reside at the base of the crypts, proliferate into transient amplifying cells (TA) and differentiate to give rise to the rest of the cell types (discussed later) (Beumer et al., 2016). The **enterocytes** are expert absorptive cells with a polarised structure whose main function is the uptake of nutrients derived from food digestion, water and electrolytes (Massey-Harroche, 2000). In the colon, they are present principally at the top of the crypts and are specialised in taking up electrolytes such as sodium, magnesium and chloride and vitamins. In the small intestine they represent the vast majority of the cells and are located in the protrusions of the gut lining also known as villi. Their apical surface is covered with microvilli, specialised in absorbing macromolecules from the lumen as well as maintaining the barrier function by degrading bacterial antigens. Ions and water can penetrate the epithelium through paracellular transport regulated by tight junctions whereas sugars and amino acids enter the enterocytes via endocytosis (Massey-Harroche, 2000). Enterocytes work as antigen presenting cells. They can recognise, internalise and process food and bacterial antigens and present them to intra-epithelium and lamina propria resident T-cells since they express MHC class II molecules. These absorptive cells are therefore involved in inducing the immunological tolerance to ingested protein and ensure no reaction to food antigens happen (Miron et al., 2012; Snoeck et al., 2005). Recently, researchers have identified a new type of colonic enterocyte which can sense luminal pH, and react by pumping protons into the cell cytoplasm when the extracellular pH decreases (Parikh et al., 2019).

The intestinal **enteroendocrine cells** (EECs) are cells specialised in the release of hormones that regulate metabolism by coordinating digestion, absorption, nutrient disposal and appetite. Taken together, they represent the largest human endocrine organ (Furness et al., 2013). In the traditional nomenclature there are 12 different types of cells classified depending on the hormones they secret, although they frequently co-express more than one, creating an overlap between lineages. Hormone production in a given EEC depends on the longitudinal location of the cell within the gastrointestinal tract (Gunawardene et al., 2011). These cells produce over 20 different types of hormones which have a wide range of targets and can act in close proximity, or be transported outside the GI tract to act in blood vessels, enteric neurons or the hypothalamus (Furness et al., 2013). Enterochromaffin cells are the most abundant type and they are widely distributed along the GI tract. These cells produce 5-HT (Serotonin) to increase gut motility and enhance intestinal transit (Diwakarla et al., 2017). D cells are also found across the entire gut but they only account for 3-5% of the EECs and

they are mainly located in the crypt region. These cells secrete somatostatin (SST), the major inhibitory hormone of the digestive system, which stops the release of all the GI hormones. SST is also responsible of inhibiting the immune system by reducing proliferation of T-cells and production of immunoglobulins and inhibiting secretion of cytokines. L cells are the second most common enteroendocrine cells type, primarily located in basal regions of the crypts. These EECs secret both the peptide YY (PYY) and proglucagon-derived peptides (PGDPs) such as GLP-1. PYY regulates intestinal transit by inhibiting it, whereas GLP-1 stimulates pancreatic insulin release in response to ingested glucose. This crucial processes must be tightly regulated by intracellular signalling mechanisms that underlie their release (Beumer et al., 2018; Gribble et al., 2019). Other EECs include cholestocystokinin-secreting cells, gastric inhibitory polypeptide-producing K cells, neurotensin-producing N cells and secretin-producing S cells (Gunawardene, Corfe and Staton, 2011).

Food digestion products such as fatty acids and amino acids or gut bacteria-produced short-chain fatty acids act as stimuli on enteroendocrine cells. Depending on the stimuli, enteroendocrine cells will release hormones to modulate food digestion and nutrient absorption, controlling blood nutrient levels by promoting hunger or satiety. The majority of the EEC can be regulated by the afferent neurons of the enteric nervous system and vice versa, which highlights the complexity of hormonal secretion (Gribble et al., 2019).

Goblet cells are a type of epithelial cells specialised in maintaining the epithelial barrier by secreting mucins and antimicrobial products. Their characteristics are discussed later.

Tuft cells are a group of chemosensory epithelial bottle-shaped cells presenting a characteristic apical brush formed by microvilli in contact with the intestinal lumen. In addition, some of them present cytospinules, which are lateral projections of the tuft cell that enter the neighbouring cells, making contact with the nucleus (Gerbe et al., 2012; Nevo et al., 2019). In the gut, they are located in the vicinity of the ISCs but also scattered in the mid and upper regions of the crypt-villi axis. While they account for over 20% of the epithelial cells of the major pancreatic duct, they are present in very low numbers (below 1%) in the gut (Middelhoff et al., 2017). Importantly, this cell type is present in non-mucosal and non-polarised tissues like the Thymus, a lymphoid organ implicated in the development and maturation of T cells (Nevo et al., 2019). These cells can be characterised by the presence of constituents of the taste receptor signalling cascade like TRPM5 (a calcium-activated ion channel), the expression of cytokine IL-25 and the presence of cyclooxygenase 1 and 2 (COX1 and COX2) involved in prostaglandin E_2 (PGE_2) synthesis. In addition, tuft cells also express choline acetyltransferase (ChAT), the enzyme responsible of ACh synthesis, and double cortin-like kinase 1

(DCLK1) which has a role in microtubule polymerisation (Schneider, O'Leary and Locksley, 2019). Recently, single-cell RNA sequencing has revealed that Tuft cells are present as a heterogeneous population across and within tissues. Previous research suggested the presence of two different Tuft cell subtypes in the small intestine, tuft-1 and tuft-2. Tuft 1 is rich in genes related to neuronal development while in Tuft 2 immune-related genes are predominant (Haber et al., 2017).

The number of signals and molecules that the tuft cells can sense is poorly understood, however it is known that they can sense luminal microbial and parasitical fermentation products like succinate. Succinate interacts with the G protein-coupled receptor (GPCR) SUCNR1 to trigger an intracellular calcium response that activates the cation channel TRPM5 causing membrane depolarisation. Ultimately, this activation leads to secretion of cytokine IL25 which activates ILC2 innate lymphoid cells in the lamina propria to release IL13. This results in the initiation of the type 2 inflammation and tissue remodelling causing activation of stem and progenitor cells and the expansion of goblet and tuft cells (Gerbe et al., 2016; Howitt et al., 2016; Lei et al., 2018; Nadjsombati et al., 2018; Schneider et al., 2018). The small intestine tuft cells present the taste receptor Tas2r, involved in sensing bitter tastants. Activation of this receptor by parasitic antigens causes TRPM5-dependent release of IL25 to induce an immune response (X.-C. Luo et al., 2019). The majority of tuft cells express ChAT, the enzyme that produces the neurotransmitter ACh. Activation of bitter receptors has been shown to induce ACh secretion from tuft cells which can cause muscle contraction, activation of enteric neurons or mucus secretion from goblet cells (Schneider, O'Leary and Locksley, 2019). Finally, long-lived $Dclk1^{+}$ tuft cells harbouring oncogenic mutations have been proposed as initiators of colorectal cancer. These cells can acquire mutations when in a quiescent state, but can become activated and progress to cancer when triggered by an inflammatory insult or by oversecretion of ACh (Hayakawa et al., 2016; Middelhoff et al., 2017). Recently, work by Goto and colleagues has demonstrated the presence of tuft cells expressing the IL17 receptor (IL17RB) as a potential marker in mouse intestine adenomas and human colorectal cancer, and identifying it as a possible therapeutic target (Goto et al., 2019).

The small intestine is home of the **Paneth cells,** a type of secretory cell which resides exclusively at the base of the intestinal crypts. These cells help control the epithelial barrier by secreting antimicrobial components like lysozyme, α defensins and REG3 A (Gassler, 2017). Paneth cells also develop an important role by maintaining the stem cell niche biology. These cells reside at the bottom of the crypts, intermingled with the intestinal stem cells, and they secrete factors that regulate stem cells such as the epidermal growth factor (EGF), the wingless protein Wnt3 and the Notch ligand D114 (H. C. Clevers et al., 2013; Sato et al., 2011). Paneth cells can also sense the nutritional status of the crypts and upon caloric restriction induce stem cell self-renewal (Yilmaz et

al., 2012). Malfunctioning of Paneth cells is linked to the development of IBD (Adolph et al., 2013). **Microfold (M) cells** are another subset of epithelial cells that play a key role in mucosal immune surveillance. M cells are usually found in the Peyer's patches (PPs) which are lymphoid follicles along the intestine containing immune cells such as B and T lymphocytes. These cells can sense microbial luminal content to induce release of AMPs from the epithelium and the production of IgA (Bennett et al., 2016).

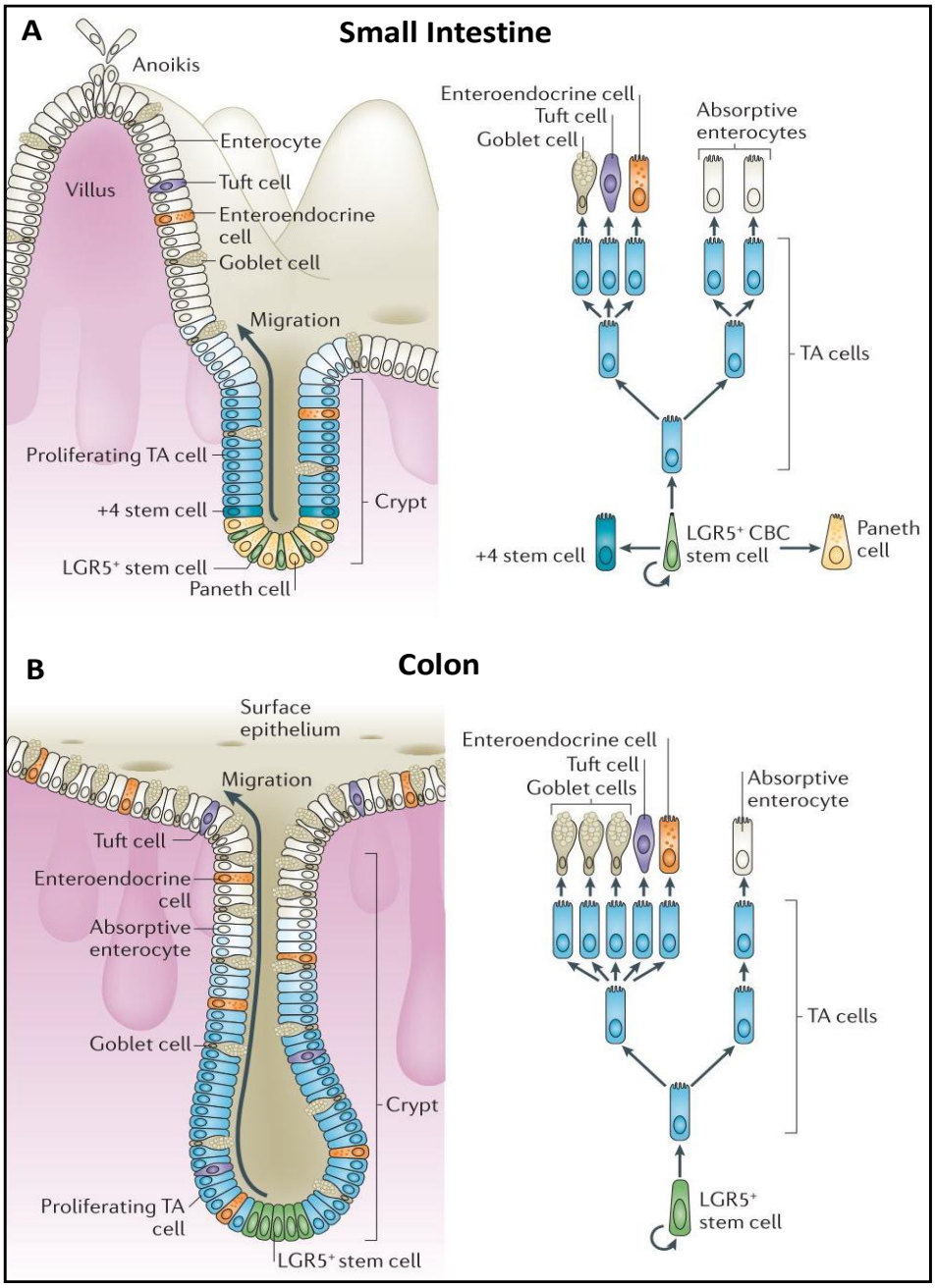

Figure 1.4. Cellular types of the small and large intestine. (A) The small intestine epithelium is composed of villi and crypts. Stem cells and antimicrobial secretors Paneth cells reside at the base of the crypts. The former proliferate and give rise to transient amplifying cells that migrate towards the villi and differentiate into absorptive enterocytes and secreting goblet cells, hormone secreting enteroendocrine cells and luminal sensors tuft cells. **(B)** The colon is formed by crypts only. Similar to the small intestine, stem cells at the base proliferate and give rise to all different cell types as they migrate up the crypt axis. Adapted from Barker et al., 2014.

1.3 Characterisation of goblet cells

Goblet cells are specialised epithelial cells responsible for maintaining the epithelial barrier integrity by secreting mucins that form the mucus layer and by releasing antimicrobial compounds to keep bacteria at bay. They are present in the GI tract, airway system and in the conjunctival epithelium of the eye. Goblet cells can be found in the entire gut and they are particularly numerous in the colon (McCauley et al., 2015). The number of goblet cells increases along the intestine, accompanied by the increase in number of microbes. In the duodenum they represent only 4% of the total number of epithelial cells, whereas this proportion elevates to 16% in the distal colon (Kim et al., 2010). These cells have a typical cup-like shape to allow storage of mucin granules in the cytoplasm (**Figure 1.6**). Goblet cells in the intestine can produce different types of mucins with MUC2 being the most common in the gut and MUC5B being present only in the colon at low levels (Johansson and Hansson, 2016). MUC2 is a secretory mucin and the major component of the mucus layers which helps to create a protective barrier, lubricate the lumen and flush out any pathogens (discussed later) (Knoop et al., 2018). The absence of these granules in mouse lacking the MUC2 mucin dramatically changes the morphology so that they lose their characteristic shape (Velcich et al., 2002).

Other products generated by goblet cells include intestinal trefoil factors, resistin-like molecule β (RELM-β) and Fc-γ binding protein (Fcgpb). Intestinal trefoil factors (ITFs) are small cysteine-rich peptides highly produced in the goblet cells of the GI tract and composed of three isotypes (TFF1, 2 and 3) (Dharmani et al., 2009). TFF3 is the second most abundant goblet cell product after MUC2. When secreted, they act on neighbouring epithelial cells to increase barrier function or to modulate intracellular signals. ITFs are important in protecting the epithelium and restoring the injured mucosa by stimulating epithelial restitution by inducing cell migration to the site of injury (Kjellev, 2009). Cells that need to migrate have to detach from their neighbours which makes them susceptible of receiving pro-apoptotic signals. ITFs secreted by goblet cells block these apoptotic signals via activation of Nuclear factor kappa enhancer of activated B cells (NFκB) (Kjellev, 2009). Moreover, ITFs play a role in mucus stabilisation by creating crosslinks with MUC2, in order to increase the viscosity of the gel layer (Kindon et al., 1995). The resistin-like molecule β (RELMβ) belongs to a family of cysteine-rich secretory proteins that can be secreted into the lumen by intestinal goblet cells in response to enteric bacteria colonisation, helminth parasitic infection and IBD to modulate intestinal innate immunity (Artis et al., 2004; Hogan et al., 2006; Nair et al., 2008). Studies in HT29 cells and mouse showed that RELMβ upregulated MUC2, 1 and 5AC expression and attenuated TNBS-induced colitis respectively (Krimi et al., 2008). In a different study in mouse,

Hogan and colleagues found that RELMβ acts downstream of IL-13 after DSS-induced colitis to modulate T_H2-associated inflammatory response (Hogan et al., 2006). *In vitro* work by Artis and co-workers demonstrated that upon nematode infection, RELMβ can bind to the parasite's chemosensory apparatus to inhibit its chemotaxic function (Artis et al., 2004). Nair and colleagues confirmed these results by showing that in mouse, RELMβ is needed to induce specific $CD4^+$ T cell-derived interferon gamma (IFN-γ) and tumour necrosis factor alpha (TNF-α) upon helminth infection (Nair et al., 2008).

Goblet cells can also secrete the Fcgbp protein, which binds to MUC2 to help create crosslinks to stabilise the complex in the inner mucus layer (Johansson et al., 2009). Moreover, Fcgbp has also been shown to bind to IgG in the lumen suggesting an important role in immunity and inflammation (Kobayashi et al., 2002). In addition to the aforementioned goblet cell-secreted proteins, Parikh and colleagues performed single cell analysis of human colon samples and showed the presence of a subpopulation of goblet cells residing in the bottom half of the crypt that express the WFDC2 protein. This protein is secreted by goblet cells to inhibit bacterial serine and cysteine proteases. By doing so it prevents the premature conversion of the inner mucus layer to the outer layer which would result in a weaker mucus barrier and would facilitate bacteria colonisation of the epithelium (Parikh et al., 2019).

As well as functioning as key epithelial barrier mediators, colonic goblet cells located at the base of the crypts are intermingled with ISCs where they regulate and support their functions, similar to the role of Paneth cells in the small intestine. These type of cells, named deep crypt secretory cells (DCS), were first identified by Altman and colleagues as different from the goblet cells located higher up the crypt (Altmann, 1983). Recently, Rothernberg et al. used fluorescence activated cell sorting (FACS) to isolate different regions of colonic crypts from mouse. Using single cell gene expression analysis of the sorted cells, they showed a subpopulation of goblet cells expressing cKit and CD117 proteins as well as Notch ligands Dll1 and Dll4, and epidermal growth factor (EGF). These researchers showed that DCS were located in between stem cells, regulated by Notch signalling and they could support the formation of in vitro cultures of colonic organoids when cultured together with $LGR5^+$ stem cells (Rothenberg et al., 2012). Further work by Sasaki and colleagues demonstrated the presence of the cKit protein in both epithelial and non-epithelial cells in the colon and suggested REG4 expressing cells as the *bona fide* DCS which could act as Paneth-like cells maintaining the ISCs (Sasaki et al., 2016).

1.3.1 Intestinal goblet cell development

Goblet cells originate from stem cells located at the base of the crypts. In the gut, these cells proliferate to give rise to trans-amplifying progenitor cells and move out of the stem cell zone. As they start to migrate upwards, the Notch-mediated lateral inhibition promotes progenitor cell differentiation. Cells with active Notch signalling trigger the activation of the Hes1 transcription factor which ultimately promotes cell differentiation into the absorptive lineage. Cells with inactive Notch signalling result in downstream activation of Atoh1 protein which activates the growth factor independent 1 (Gfi1) to subsequently induce activation of the transcription factor SPDEF (Sam pointed domain-containing ETS transcription factor), enabling differentiation into the secretory lineage (Katz et al., 2002; McCauley and Guasch, 2015). Unlike in the intestine, progenitor cells with active Notch signalling in the airway system and lung epithelium differentiate into goblet cells (Rock et al., 2013). Likewise, active Notch signalling is required in the eye conjunctive epithelium to promote cell differentiation into goblet cells (Zhang et al., 2013). The Krüppel-like transcription factors (KLF4 and 5) were also showed to be critical in promoting goblet cell differentiation in the gut, and studies in mice showed that overexpression of KLF4 induced goblet cell hyperplasia, whereas KLF4 null animals displayed a 90% reduction in mature colonic goblet cells. Therefore, Notch-active cells repress KLF4 and 5 which could work as a switch in cell lineage fate (Zheng et al., 2009). Moreover, Foxa1 and Foxa2 transcription factor activators have also been shown as potent activators of the expression of the goblet cell intestinal mucin MUC2 as well as controllers of goblet cell differentiation (van der Sluis et al., 2008; Ye et al., 2009) (**Figure 1.5**).

In addition to Notch signals, other signalling pathways are key in determining goblet cell differentiation. The Wnt/β-catenin signalling pathway is involved in goblet cell and Paneth cell fate (Nusse and Clevers, 2017a). Both cell types are genetically very similar, and a tight regulation is needed to determine their fate. A study by Heuberger and co-workers showed the tyrosine phosphatase Shp2 is involved in activating the MAPK signalling pathway and that Shp2-dependent MAPK activation attenuates Wnt signalling in progenitor cells by regulating the protein stability of the Wnt-related TCF4 transcription factor. This event drives cell differentiation to goblet cells while a reduction in MAPK and increase in Wnt signals induces Paneth cell differentiation (Heuberger et al., 2014). Together with Notch and Wnt, TGF-β signals have also been suggested to play an important role by negatively regulating goblet cell differentiation through SMAD proteins. Work by Takaku and colleagues revealed that loss of SMAD resulted in the development of adenocarcinomas characterised by the presence of large numbers of goblet cells (Takaku et al., 1999). Goblet cell differentiation is regulated by these signalling pathways during physiological conditions; however,

goblet cell fate can be also modulated by the interaction of the epithelium with the luminal content like bacterial or parasite-derived signals (McCauley and Guasch, 2015) (**Figure 1.5**).

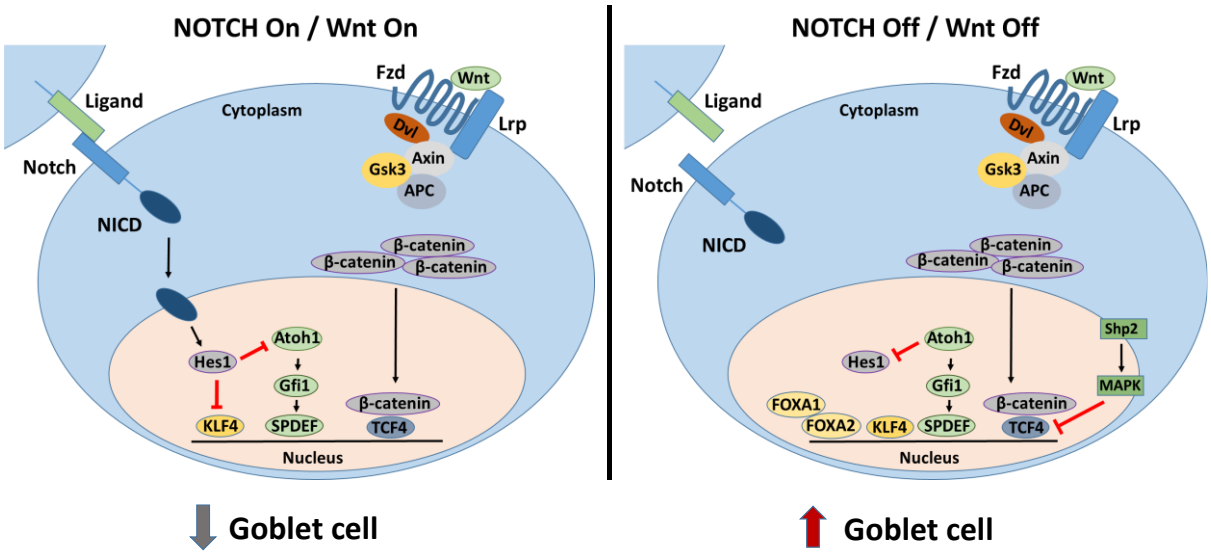

Figure 1.5. Goble cell differentiation. (Left) Activation of Notch and Wnt signalling pathways activates Hes1 and Tcf4 transcription factors respectively maintaining stemness of CBCs. **(Right)** Inactivation of Notch signalling pathway allows Atoh1-dependent SPDEF activation as well as KLF4, FOXA1 and FOXA2. In addition, Shp2-dependent activation of MAPK attenuates canonical Wnt signalling by blocking TCF4 transcription factor. These events result in cell lineage differentiation into goblet cell.

1.3.2 Goblet cells and the immune system

The mucus secreted by goblet cells helps keep bacteria far from the epithelial cells. In the small intestine, these cells can sense luminal stimuli and possible threats, and respond by inducing mucus secretion as well as signalling dendritic cells in close proximity to trigger an immune response (Knoop et al., 2014). The small intestine is made of a porous mucus layer that enables goblet cells to sense luminal content. Thanks to goblet cells, the epithelium accomplishes immune surveillance while maintaining the epithelial barrier with mucus secretion. Goblet cells can form goblet cell-associated antigen passages (GAPs) and are able to deliver small soluble antigens to dendritic cells (DCs)-expressing CD103 protein in the lamina propria. Using fluorescent dextran experiments, McDole and colleagues reported the creation of GAPs in the goblet cell membrane where the antigens were being internalised (McDole et al., 2012). Subsequently, Shan and colleagues demonstrated that the communication with DCs helps induce tolerance to food antigens. Therefore, the following interaction of DCs with regulatory T cells helps suppress inflammatory responses

during homeostasis by inhibiting NF-κB via β-catenin (Shan et al., 2013). Interestingly, the formation of GAPs are induced by ACh via activation of muscarinic receptor type 4 (MAChR4) in the membrane of goblet cells (Knoop et al., 2014). This study found that ACh, a molecule known to induce goblet cell mucus secretion via compound exocytosis (discussed later), induced GAP formation while mucus secretion induced by cholera toxin did not. Thus, the formation of these structures may depend on these stimuli. In the colon, GAPs are not present during homeostasis which suggests that the immune surveillance is operated by M cells. However, dysbiosis or disruption of goblet cell microbial sensing activates MAChR4, allowing GAP formation and subsequent antigen delivery to DCs. These results illustrate the differences in antigen delivery between the small intestine and the colon. These differences could owe to the different organ functions and the presence of larger amounts of bacteria in the colon, which would suppress GAPs to prevent inappropriate responses by the immune system (Knoop et al., 2014). Recent studies on *Salmonella* infection in the small intestine showed that bacteria can use GAPs to cross the epithelium. In this situation, the immune system is triggered and responds by inhibiting the expression of GAPs. The suppression of luminal sampling through GAPs prevents responses to dietary antigens, limits pathogen entry and minimises disease upon bacterial infection (Kulkarni et al., 2018).

1.3.3 Goblet cells and intestinal microbiota

The human gut is home of more than 400 bacterial species which include resident commensal bacteria and other species that reside temporally in the lumen. The mucus secreted by goblet cells is a source of nutrients for the microbiota that are able to colonise it, and it also serves as a "safe haven" preventing expulsion via the intestinal peristaltic movements (Dharmani et al., 2009). Bacterial population in the small intestine is less varied than in the colon, and they are usually found in the upper part of the villi where the mucus is more accessible. In the colon, bacteria are found in the outer layer of the mucus where they are able to metabolise the glycans present at the terminal ends of the mucins, providing them with a stable energy source (Johansson and Hansson, 2016). Preferentially, most bacterial species feed on the non-digested dietary polysaccharides which means that the diet has an influence on the gut microbiota composition. A diet low in fibre or plant material leads to a low microbiota diversity and shifts the population composition benefiting those species that can adapt better to glycan digestion; a factor that can impact mucus homeostasis (Marcobal et al., 2013).

The intestinal epithelium is able to distinguish commensal from pathogenic bacteria because it can recognise specific bacterial antigens through pattern recognition receptors (PPRs) which include Toll-like receptors (TLRs) expressed in the cell membrane, and nucleotide-binding oligomerisation

domain (NOD) proteins, expressed in the cytoplasm. During homeostasis, because the gut epithelium has tolerance for commensal bacteria, the expression and responsiveness of TLRs is low. Upon infection, PPRs can activate the production of NF-κB to induce the production of pro-inflammatory cytokines (Kim and Ho, 2010). The end product of bacterial metabolism and fermentation results in the production of highly valuable metabolites that are used by the epithelial cells as an energy source. The main products of fermentation are the short-chain fatty acids (SCFA) acetate, propionate and butyrate, and they all play a major role in maintaining metabolic homeostasis (Hamer et al., 2008). Butyrate in particular, has been shown to be important for gut physiology and its uptake is diminished in colorectal cancer due to the downregulation of butyrate membrane transporters (Lambert et al., 2002). In addition, many *in vitro* studies have demonstrated that butyrate increases MUC2 gene expression and MUC2 production and can also induce the production of TFFs and antimicrobial peptides (Finnie et al., 1995; Thim, 1997; Schauber et al., 2003; Willemsen et al., 2003; Gaudier et al., 2004), evidencing the key role it plays in reinforcing the epithelial barrier.

1.3.4 Inflammation and disease

The majority of intestinal infections trigger goblet cells to induce mucus synthesis and secretion during the acute phase. However, if the infection becomes chronic goblet cells may not be able to produce sufficient mucin leading to alterations in the composition and size of the mucus layers (Kim and Ho, 2010). Most pathogens have developed mechanisms to invade the epithelium by penetrating through the mucus layers. The protozoan parasite *Entamoeba histolyca* secretes cysteine proteases that cleave the C-terminal domain of the MUC2 mucin to disrupt the mucus gel and gain access to the epithelium (Lidell et al., 2006). Parasitic infections induce intestinal goblet cell hyperplasia and increase mucus production and secretion in a process mediated by T_H2 cells immune response (Moncada, Kammanadiminti and Chadee, 2003).

Pathogenic bacteria contain associated molecular patterns like lipopolysaccharide (LPS), peptidoglycans, flagellin or lipoteichoic acid (LTA) that are recognised by the Toll-like receptors in the membrane of epithelial cells and can stimulate mucin production (Sicard et al., 2017). This stimulation can be directly on goblet cells or mediated by cytokine production. LPS has been demonstrated to induce production of IL-8 which in turns triggers mucus secretion (Smirnova et al., 2003). The recognition of bacterial antigens leads to an immune response that provokes inflammation; the extent of the inflammation can vary depending on the type of bacteria and the type of the immune response. Immune deficiencies and defective mucus layers in the host can lead to spontaneously development of colitis (Johansson and Hansson, 2016). In the colon, the first cells

to be activated upon bacterial infection are the so called sentinel goblet cells (Birchenough et al., 2016). As shown by Birchenough and colleagues, the goblet cell population in the colon is heterogeneous. Goblet cells positioned in the upper region respond to TLR ligands (LPS, flagellin, etc.) by secreting mucus, whereas goblet cells in the base of the crypt secrete mucus when triggered by ACh (discussed later). These researchers concluded that an increased concentration of bacterial ligands near the crypt activates TLRs in special goblet cells in the upper region, named sentinel goblet cells. This event induces an intracellular calcium signal that results in mucus secretion and the transmission of the calcium signal to adjacent cells through gap junctions, causing a subsequent mucus secretion that flushes the bacteria away. The process finishes with the sentinel cells that have sensed the bacterial antigens being expelled to the lumen (Birchenough et al., 2016).

The status of mucus production and secretion is key in maintaining the epithelial barrier. The clinical expression of cystic fibrosis (CF) is characterised by accumulation of mucus in the airway system and the intestine. This is the result of a malfunctioning cystic fibrosis transmembrane regulator protein (CFTR), which is expressed in the membranes of the epithelium and mediates secretion of chloride, bicarbonate and fluid (De Lisle and Borowitz, 2013). Bicarbonate is crucial in mucus gel formation and secretion, and recent studies on mouse suggest that defective bicarbonate transport in animals with malfunctioning CFTR results in the formation of mucus aggregates, typically seen in CF (Garcia, Yang and Quinton, 2009). In ulcerative colitis, the synthesis and secretion of MUC2 is reduced and the mucus generated has an abnormal composition. This situation leads to inappropriate immune activation by commensal bacteria, pathogenesis and chronic inflammation (Dharmani et al., 2009). In a recent study by Van der Post and colleagues it was reported that in UC patients, the inner mucus layer was more penetrable to bacteria and this was due to a decrease in concentration of the MUC2 and Fcgbp mucus structural components (Van Der Post et al., 2019). Finally, overexpression of MUC2 and MUC5A in the intestine is characteristic of a subtype of colorectal cancer named mucinous adenocarcinoma (C. Luo et al., 2019). In this pathology, the malignant tissue contains pools of abundant amounts of extracellular mucin and its development is related with epigenetic alterations such as MUC2 promoter hypomethylation and increased binding of Hath1 to the MUC2 promoter (Kim and Ho, 2010).

1.3.5 Mucus structure and biosynthesis

In the human gut, goblet cells secrete mucins to create a physical barrier against potential pathogens. Mucins are large and highly glycosylated glycoproteins with a central region mainly composed of threonine and serine amino acid repeats, which are covalently bound to a great variety of *O*-linked oligosaccharides (Perez-Vilar, 2007). There are 20 different mucin genes identified and

their products can be classified into transmembrane mucins and gel-forming mucins. Transmembrane mucins are anchored to the cell membrane by a transmembrane domain and present a short cytoplasmic C-terminus and a long N-terminal domain on the outside. These transmembrane mucins are found in the apical pole of the cells and types MUC3, MUC12 and MUC17 are distributed on microvilli of the enterocytes where they form the glycocalix (Kim and Ho, 2010). The functions are not clearly understood but researchers believe they work by blocking undesired transport of large molecules and by sensing surface antigens (Hattrup and Gendler, 2008).

Gel-forming mucin structures are made of an N-terminal part involved in oligomerisation and a C-terminal region that forms dimeric structures. In the intestine, these molecules are produced and secreted by intestinal goblet cells where the main mucin is MUC2, although MUC5A can be found at low amounts in the colon. The MUC2 structure is formed by highly glycosylated tandem repeats of MUC2 monomers which are bordered on both sides by domains rich in cysteine. These domains include the C-terminal cysteine knot domain (involved in dimerisation) and four D domains of von Willebrand factor (vWF) involved in oligomerisation (Kim and Ho, 2010; Johansson and Hansson, 2016). These macromolecules first form mucin dimers by creating disulphide bonds between the cysteine knot domains and then trimers by creating more disulphide bonds between the N-terminal vWD3 assemblies (**Figure 1.6**) (Godl et al., 2002; Johansson and Hansson, 2016). As a result of this conformation, mucins are negatively charged highly hydrophobic and viscous multimer structures (Perez-Vilar, 2007). MUC2 monomers are synthesised in the endoplasmic reticulum where it is *N*-glycosylated in the mucin serine/threonine regions with *N*-acetylgalactosamine (GalNAc) residues and forms disulphide dimers. The dimers are then transported to the *cis*-Golgi compartments where the tandem repeats are *O*-glycosylated. When the dimers reach the *trans*-Golgi region they are assembled into disulphide-bonded trimers that bind to other trimers through their free cysteine residues forming multimers (Perez-vilar and Hill, 1999).

Once MUC2 has multimerised, it is packed and stored as concatenated six-sided ring structures in cytoplasmic granules located in the apical pole of the cell. The entire production and packaging processes depend on low pH and high calcium concentrations. In the ER, the pH starts at 7.2, then drops to 6.0 in the trans-Golgi compartments and subsequently to 5.2 in the secretory granulae, while in parallel, the intracellular calcium concentration increases (Ambort et al., 2012). It is thought that these conditions diminish the repulsive forces among the negatively charged mucin oligomers favouring the packaging (Perez-Vilar, 2007).

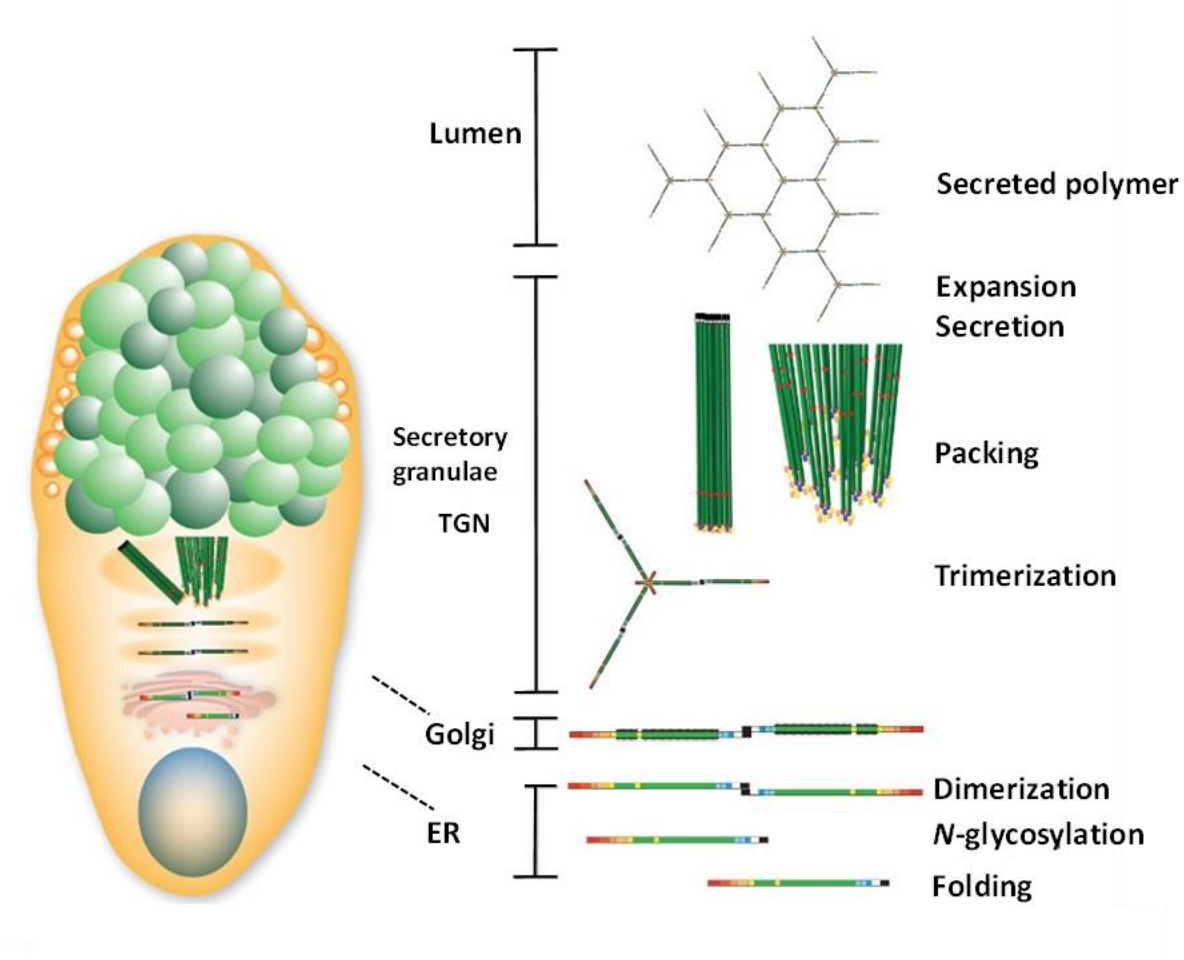

Figure 1.6. Synthesis and assembly of the MUC2 mucin in goblet cells. MUC2 monomers are produced in the ER and then *N*-glycosylated to later form dimers. These dimers are then transported to the *cis*-Golgi where they become *O*-glycosylated. In the *trans*-Golgi, mucins are assembled into trimers which can then multimerise by creating disulphide bonds between the free cysteine groups. These multimers are tightly packed into 6-side rings interconnected structures and transported into secretory granules. Figure adapted from Birchenough et al., 2015.

1.3.6 Mucus secretion

Mucin granule exocytosis is a calcium regulated process. During homeostasis, goblet cells constantly secrete mucus in small quantities via exocytosis in what is known as baseline or constitutive secretion. When goblet cells are stimulated, they can rapidly release their entire mucus content in a process called compound exocytosis. Baseline secretion is needed in order to maintain the thickness of the mucus gel, which is degraded over time and flushed away by peristaltic movements (Dharmani et al., 2009). It is thought that this type of secretion involves constant transit of MUC2 granules from the Golgi to the cell membrane, in a process mediated by microtubules (McCool, Forstner and Forstner, 1995). Research in mucus secretion in the airway system has shown that

constitutive secretion is induced by low levels of paracrine-secreted extracellular ATP and adenosine, whereas high levels of the same ligands induce compound exocytosis. ATP and adenosine bind and activate P2Y2 purinergic and A3 adenosine G protein-coupled receptors (GPCRs) in the membrane which activated phospholipase C (PLC) resulting in the generation of diacylglycerol (DAG) and IP_3. The latter induces calcium secretion from the ER which activates the low affinity calcium sensor Synaptotagmin-2 (Syt2) to allow mucus secretion during compound exocytosis. During mucus secretion, the mucus granules fuse with the membrane by SNARE-mediated fusion. The SNARE proteins mediate the tight docking of vesicles to the cell membrane and induce their fusion. Calcium-dependent Syt2 activation leads to full coiling of the SNARE proteins on each membrane to facilitate fusion (Adler, Tuvim and Dickey, 2013). Studies in pancreatic acinar cell secretion suggested that this process initiates when a primary granule fuses with a cell membrane to then become the target for a secondary fusion. This mechanism is termed sequential compound exocytosis and depends on the presence of the SNARE protein VAMP8 (Thorn and Gaisano, 2012). Cantero-Recasens and colleagues studied mucus secretion in colonic cell lines and reported that during baseline mucus secretion, the protein KChIP3 works as high-affinity calcium sensor as opposed to Syt2. In this study, the researchers propose that KChIP3 is constitutively attached to mucus granules acting like a brake, and that spontaneous calcium oscillations trigger KChIP3 changing its conformation to make it detach from the mucin granules and allow secretion in an agonist-independent manner. Lack of KChIP3 in knockout mice induces mucin hypersecretion (Cantero-Recasens et al., 2018) (**Figure 1.7**).

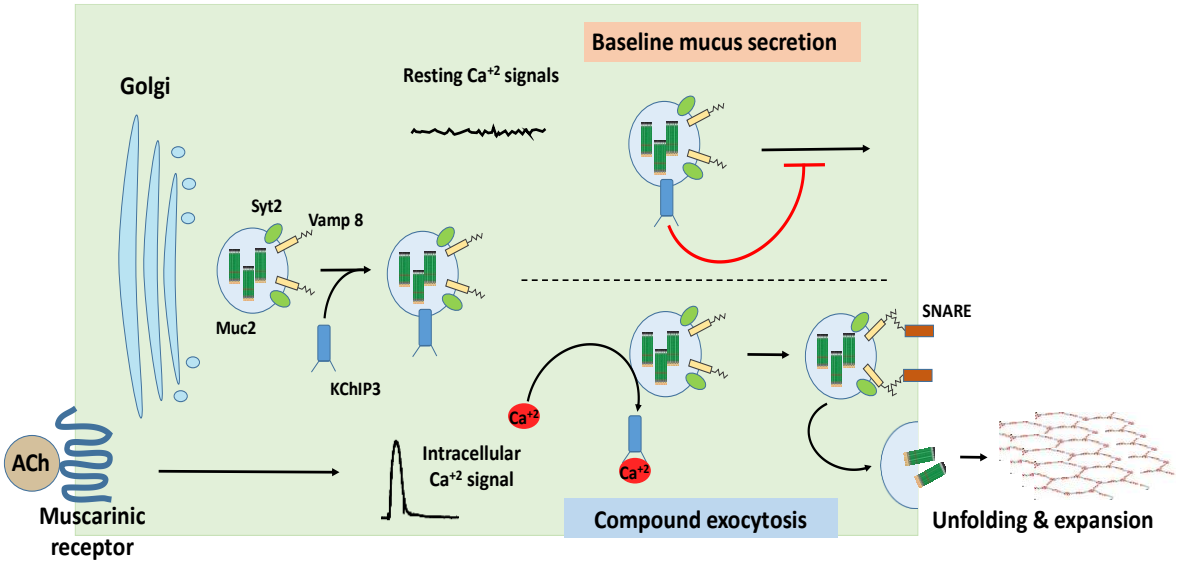

Figure 1.7. Models of mucus secretion. Under homeostatic conditions and resting intracellular calcium signals, mucus granules express high affinity calcium sensor KChIP3 on their membranes

which limits the capacity for granule exocytosis and reduces the process to baseline mucus secretion. External stimuli like ACh induce potent intracellular calcium signals by binding to muscarinic receptors which results in binding of calcium to KChIP3 and release from the membrane. High affinity sensor Syt2 gets activated and promotes binding of granules to the membrane mediated by SNARE proteins. The process is termed compound exocytosis and results in rapid release of great quantities of mucus. Figure based on Cantero-Recasens et al., 2018.

Reactive oxygen species (ROS) have been recently suggested to be needed for proper mucin granulae secretion in colonic goblet cells (Patel et al., 2013). ROS generation is modulated by autophagy, which is also an essential cellular process that directs cytoplasmic contents like impaired organelles, malformed proteins or microbes to the lysosomes for being degraded and recycled (Wu et al., 2019). The process starts with the generation of an autophagosome. The protein LC3 is key in mediating the generation and closing the curving membrane that form the autophagosome vacuoles that later fuses to an endosome (originated from the plasma membrane), creating an amphisome. This vacuole later fuses with a lysosome, generating a so called *endo-lysosome* where the degradation occurs (Levine, Muzishima and Virgin, 2011). In addition, ROS generated by the NADPH oxidase (Nox) enzyme is required to maintain the autophagy pathways and help degrade the cellular contents (Huang et al., 2009). Patel and colleagues showed that Nox co-expresses with LC3 and with the endosomal marker EEA1. Consequently, a reduction in ROS molecules by adding the ROS scavenger N-acetylcysteine (NAC) resulted in enhanced mucin accumulation. Nox-produced ROS is known to increase cytoplasmic calcium levels via activation of IP3Rs (Granados et al., 2006; Bedard and Krause, 2007; Espinosa et al., 2009). Patel and colleagues demonstrated that mucus secretion is dependent on the increase intracellular calcium which is regulated by ROS produced in the endo-lysosomes (Patel et al., 2013). In addition, a recent study by Wlodarska and colleagues highlighted the importance of autophagy in mucus secretion and its modulation by the immune system. Their work suggests the implication of the NLRP6 inflammasome in inducing autophagy-dependent mucus secretion. The inflammasome is a cytoplasmic multiprotein complex which works as sensor of endogenous or exogenous stress. NLRP6 is a protein part of this complex with roles in defence against infection and autoinflammation. In this study, the researchers suggest a role of the NLRP6 inflammasome in sensing bacterial infection and promoting autophagy in order to induce mucus secretion (Wlodarska et al., 2014).

When the densely packed mucus is secreted into the lumen, it requires an environment with increased pH and decreased calcium levels to be able to expand rapidly to levels of 100 to 1000 fold in volume. This requirement is fulfilled thanks to the secretion of bicarbonate (HCO_3^-) via the CFTR channel in the apical membrane of the epithelial cells of the small intestine. The mechanism in the

colon is still not fully understood. The decrease in pH and calcium weakens the N-terminal bonds which allows water to penetrate in the mucus structure and bind to the glycans making the mucin expand into large flat sheets (Ambort et al., 2012). As discussed previously, malfunctioning of the CFTR channel in cystic fibrosis results in low luminal HCO_3^- which prompts the formation of highly viscous aggregates of mucus (Gustafsson et al., 2012). In the small intestine, the mucus remains attached to the epithelium and needs the metalloprotease meprin-β to cleave the N-terminal region of the anchored MUC2 to release it into the lumen. MUC2 needs to expose the cleavage sites in order to be accessible to meprin-β, which requires cells to have functional CFTR channels to secrete HCO_3^- to allow for a proper mucus unfolding (Schutte et al., 2014) (**Figure 1.8**).

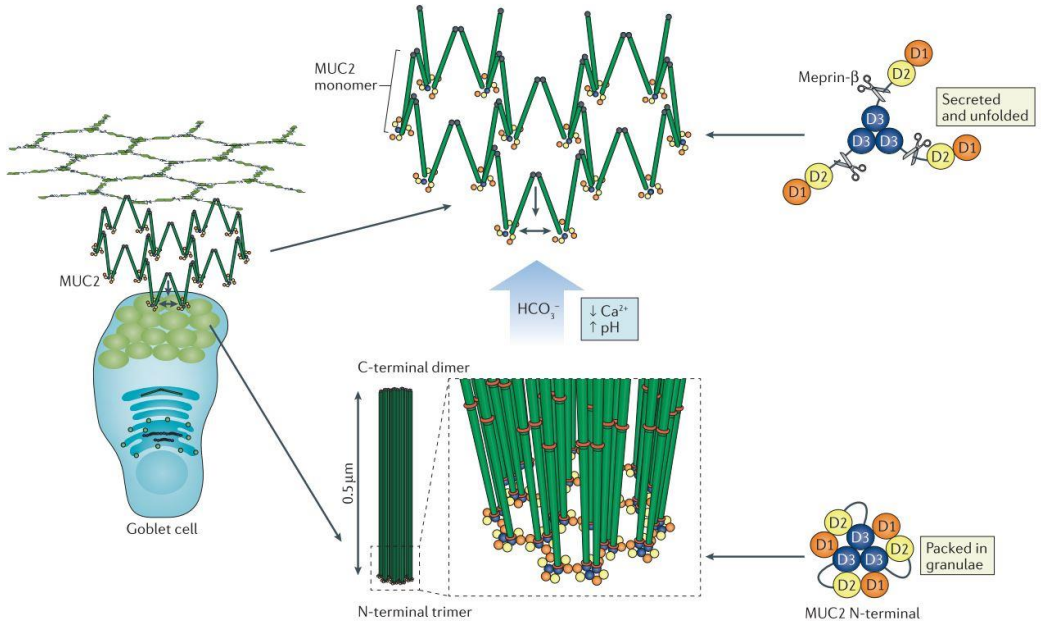

Figure 1.8. Mechanism of mucus release. Upon secretion into the lumen, mucus conformation changes from a tightly packed 6-ring-side multimers to an expanded structure of stratified and stacked sheets of polymerised MUC2. This process is strictly dependent on HCO_3^- secreted by CFTR channels. Detachment of mucus from the epithelium is mediated by meprin-β. Adapted from Johansson et al., 2016.

As described before, in the colon the mucus is organised in two layers; a loose outer layer and a firm inner layer attached to the epithelium. In the small intestine, the mucus does not form a continuous firm layer. It is secreted mainly by the goblet cells at the top of the crypts as a more soluble mucus and then it migrates up until reaching the villi. Although both small and large intestine secrete MUC2, it is not clear why mucus properties differ in each organ. The thickness of the inner mucus layer is still not known but it is expected to be thicker than 100 µm, which is the reference thickness measure in the rat colon (Atuma et al., 2001). The outer layer is thought to be twice as thick as the

inner one, but this depends on the bacteria that colonise it and degrade it. In the rat colon, it can reach approximately 700 µm. The composition of the mucus in the inner layer was characterised by Johansson and colleagues as a well organised stratified laminae. Based on this, the mucus is thought to be formed by sheets of polymerised MUC2 that do not allow passage of big size particles and therefore lack of bacteria (Johansson et al., 2008). In addition, these researchers demonstrated that the pattern of enzymatic proteolytic cleavage of MUC2, particularly from the C-terminus, determines the properties of the loose outer layer. These proteolytic processes still maintain an intact polymer but allow for volume expansion in the lumen. In the colon, the calcium-activated chloride channel regulator 1 (CLCA1) has been proposed as the main enzyme regulating the proteolysis of MUC2. This enzyme uses its proteolytic activity to mediate mucus expansion, transforming the attached dense inner mucus into the loose outer mucus (Nyström et al., 2018). The characteristics of the outer layer create an ideal environment for the microbiota, with MUC2 *O*-glycans providing attachment sites and acting as a nutrient source. In *in vivo* studies in mouse, fluorescently labelling of the GalNAc *O*-glycans bound to the MUC2 protein revealed the pattern of mucus turnover in the colon and small intestine. In the colon, the mucus turnover is a continuous event where the inner layer gets renewed every hour. Interestingly, the goblet cells at the top of the crypts can synthesise mucus faster than the ones at the base of the crypt highlighting the differences between goblet cell populations (Johansson, 2012). In the small intestine there are again distinct goblet cell populations characterised by a faster turnover in the villi compared to the crypt's goblet cells, which could be explained by the fast motility of luminal material (Johansson, 2012).

1.3.7 Mediators of mucus secretion

During steady-state mucus is constantly being released by means of baseline secretion. However, when goblet cells are exposed to potent secretagogues, MUC2 is released much faster by compound exocytosis in a process where goblet cells empty all their mucus content. A wide variety of stimuli can induce goblet cell compound exocytosis which includes neurotransmitters, gut hormones and immunity related molecules. Histamine which is mainly produced by immune cells like basophils and mast cells, was shown to strongly stimulate release of mucus from goblet cells in the crypts of rabbit colon (Neutra, O'Malley and Specian, 1982). In addition, vasoactive intestinal peptide (VIP), serotonin, peptide YY as well as interleukin-1β were also shown to induce mucus discharge in rat colonic crypts (Plaisancié et al., 1998). Prostaglandin E2 (PGE_2) is a known modulator of physiological, inflammatory and immunologic functions which signals through membrane receptors EP1-4. Recently, PGE_2 has been shown to be produced by intestinal epithelial tuft cells (Gerbe et al., 2011). Studies in rat and human colon have demonstrated that PGE_2 induces MUC2 secretion

helping to restore the epithelial barrier (Belley and Chadee, 1999; Halm and Halm, 2000). Goblet cell mucus secretion can be also modulated by the enteric nervous system which innervates the intestinal epithelium. Cholinergic neurons can secrete the neurotransmitter ACh to induce a massive mucin secretion which has been demonstrated in rabbit and human crypts (Specian and Neutra, 1980; Halm and Halm, 2000). This secretion is believed to affect only the goblet cells located in the crypts whereas the ones in the villi or the opening of the crypts seem unresponsive. Tuft cells are not fully yet characterised but researchers have shown that they are capable of producing ACh and therefore potentially stimulate mucus secretion of goblet cells (Dando and Roper, 2012; Gerbe, Legraverend and Jay, 2012).

The colonic epithelium secretes mucus into the lumen, but it can also secrete fluid in response to a number of stimuli. The secretion of fluid from crypt enterocytes changes the composition of the lumen making it more aqueous (Halm and Halm, 2000). Similar to mucus secretion, fluid secretion is thought to be constant and at low volumes in the steady-state. However, its secretion can increase quickly upon infection to help flush pathogens. The secretion of mucus and fluids do not necessarily occur simultaneously and it will depend on the secretagogue (Halm and Halm, 2000). In the colon however, it has been shown that the neurotransmitter ACh can induce calcium-dependent mucus secretion (Phillips, Phillips and Neutra, 1984; Patel et al., 2013) but also calcium-dependent fluid secretion (Reynolds et al., 2007).

1.4 Characterisation of intestinal stem cells

The intestinal stem cells, also known as crypt base columnar (CBC) cells, are slender cells located at the base of the crypts surrounded by Paneth cells in the small intestine and by goblet cells in the colon. CBC s are the only pluripotent crypt cell type that have the ability to self-renew (Beumer et al., 2016). As discussed previously, they proliferate to generate daughter progenitor cells which then migrate and give rise to the different epithelial lineages (enterocytes, enteroendocrine cells, goblet cells, Paneth cells and tuft cells). It has been proposed the existence of another population of stem cells located in the so called +4 position, that is, four cell diameters above the stem cell niche. These type of stem cells are characterised by their quiescence during homeostasis and their ability to revert phenotype to self-renewing stem cell upon crypt injury (Barker, 2014).

1.4.1 Discovery and identification of intestinal stem cells

Intestinal stem cells were first discovered by Cheng and Leblond in 1974 as continuously cycling cells at the bottom of the crypts (Cheng and Leblond, 1974). Winton and colleagues (Winton et al., 1988) working on mice were the first researchers to discover a method to label clonal cells produced

during stem cell proliferation in the intestine. Bjerknes et al. later showed that these CBCs could give rise to all epithelial cell types (Bjerknes et al., 1999). With the discovery of the genetic lineage tracing tools, Barker and co-workers identified for the first time a highly specific marker for intestinal stem cells, LGR5 (Barker et al., 2007). They first discovered that Wnt target genes are highly expressed in colorectal cancer and because Wnt signalling is central in regulating the biology of the crypt (van de Wetering et al., 2002), they hypothesised that a Wnt target gene driving proliferation should be present in the stem cells. They first generated a knock-in allele integrating an enhanced green fluorescent protein (EGFP) cassette at the first ATG codon of the LGR5 locus. In addition, they also included an internal ribosome entry site (IRES) and a CreERT2 recombinase enzyme, which can be activated in the presence of tamoxifen. The IRES sequence was used to prevent the fusion protein from being directed to the exocytotic pathway. Mice presenting the $LGR5^{EGFP–IRES–CreERT2}$ knock-in allele, showed LGR5 protein expression restricted to a few cells at the crypt base. They then crossed those mice with *Rosa26-lacZ*-inducible reporter mice (**Figure 1.9**); and administered tamoxifen to activate the CreERT2 fusion enzyme in LGR5-expressing cells. When the recombinase enzyme is active, it excises a sequence which otherwise blocks the transcription of the LacZ reporter by cutting its LoxP flanks, thereby activating LacZ and constitutively expressing LGR5-GFP proteins in $LGR5^{+}$ cells. Due to genetic recombination events, the progeny of these cells will no longer express GFP, but having an activated *LacZ* reporter serves as genetic marker that can be labelled and imaged, thereby enabling lineage tracing. Barker and colleagues then administrated tamoxifen to the mouse at different time points for one month and later prepared gut tissue sections where they visualised the number of $LacZ^{+}$ cells. The labelled cells appeared first at the bottom of the crypt regions at early time points, to then run up the crypt and villi axis at later time points (**Figure 1.9**). Importantly, they showed co-expression of induced clones and other epithelial markers for enteroendocrine, goblet and Paneth cells. These results illustrated that all those cells belonged to the $LGR5^{+}$ progeny cells and that these fulfilled the stem-cell requirements in being pluripotent and maintaining epithelial self-renewal over long periods of time (Barker et al., 2007).

In addition to the CBCs, a population of +4 cells located just above the uppermost Paneth cell of the crypt base was proposed to be another stem cell candidate in the intestinal crypts. These cells were first reported by Potten and colleagues as uncommon slow-cycling DNA-label-retaining cells. This cell type revealed mitotic quiescence, capable of remaining functional after a high dose of radiation (Potten et al., 1978). Further research identified potential specific markers of these cells like *Bmi1* and *Hopx* (Sangiorgi et al., 2008; Takeda et al., 2011), and subsequent single cell expression analysis revealed these cell populations are overlapped with each other but are different from the CBCs marked with $LGR5^{EGFP–IRES–CreERT2}$ (Yan, Chia and Li, 2012). It was speculated that this +4 cell population

or label-retaining cells (LCRs) with high resistance to radiation (as opposed to LGR5^{+} cells) and infrequent cell division, could work as reserve stem cells that could give rise to the pool of CBCs if required, after acute damage to the crypt (Ning et al., 2016). At present, researchers believe that the fate of the epithelial cells is not hardwired and instead there is a plasticity mechanism whereby cells can differentiate and de-differentiate into and from stem cells depending on the needs of the epithelium (de Sousa e Melo and de Sauvage, 2019).

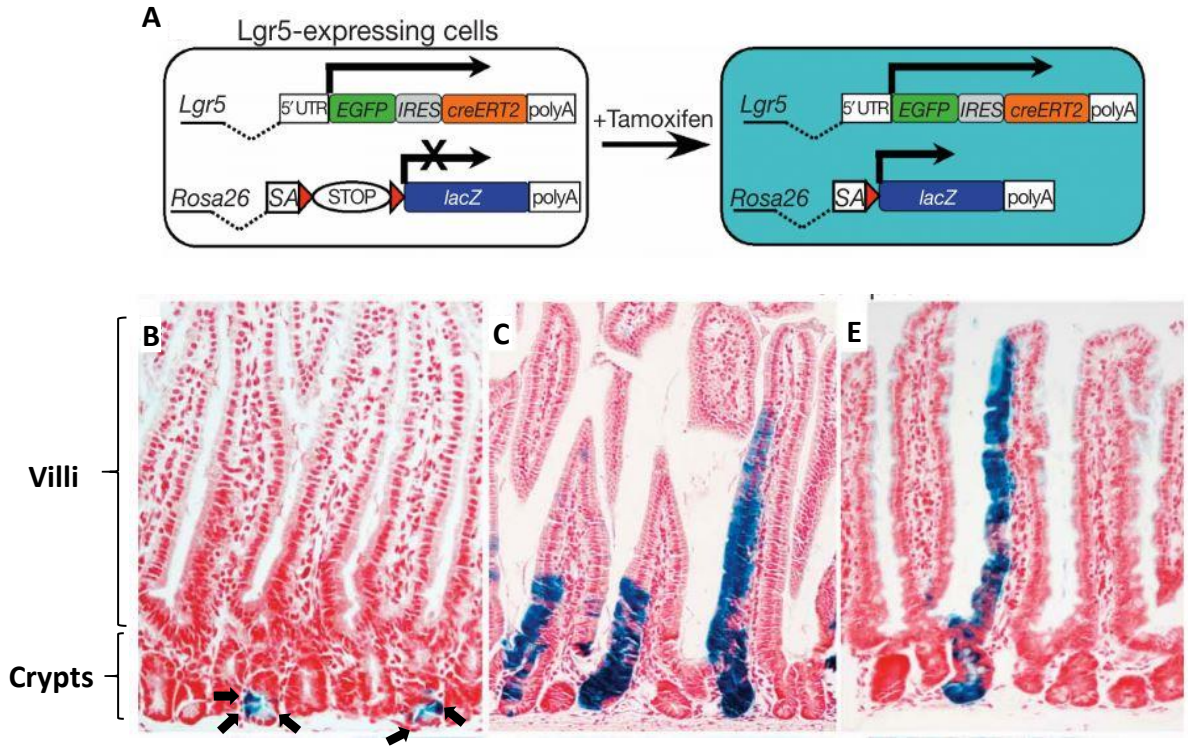

Figure 1.9. Generation of LGR5$^{EGFP–IRES–CreERT2}$ mice knock-in and lineage tracing of LGR5^{+} cells. (A) Mice were engineered to carry a knock in cassette in the LGR5 gene. The cassette contains the GFP sequence to allow visualisation under fluorescent microscopy, an IRES sequence to prevent exocytosis of the LGR5 protein and a creERT2 sequence that codes for a recombinase enzyme. When crossed with *Rosa26-lacZ* mice and upon tamoxifen administration, the active creERT2 enzyme cleaves the STOP sequence upstream the lacZ sequence, thus constituently activating its expression. **(B, C, & E)** Vibratome sections of small intestine showing nuclei in red labelled with ToPro3, and LacZ labelled in blue with β-galactosidase. **B** to **E** images show early to later tamoxifen incubation time points illustrating the lineage tracing of LGR5^{+} cells. Black arrows in B show presence of LGR5^{+} at the bottom of the crypt after 1h incubation with tamoxifen. Figure and images adapted from Barker et al., 2007.

1.4.2 Other stem cell markers

Prior to the discovery of LGR5 as a marker of intestinal stem cells, Potten and co-workers described the expression of the *Musashi-1* (*Msi-1*) gene as a putative stem cell marker by means of immunocytochemistry and *in situ*-hybridisation (Potten et al., 2003). Msi1 is a protein that interacts with the cell proliferation-related protein Notch and with the transcription factor Tcf-4. The latter was shown by Korinek and co-workers to be important in maintaining crypt stem cells and being part of the proliferation-related Wnt signalling pathway (discussed later) (Korinek et al., 1998). Tcf-4 was later shown to bind the Achaete-scute-Like 2 (ASCL2) transcription factor which was also a direct target of the Wnt pathway (van der Flier, van Gijn, et al., 2009; Schuijers et al., 2015). These studies used fluorescence activated cell sorting (FACS) of GFP-positive epithelial cells from LGR5$^{-EGFP\text{-}ires\text{-}CreERT2}$ mice and showed two different populations, GFP^{high} and GFP^{low}. These two populations were interpreted as being LGR5^{+} stem cells and their transient amplifying daughters respectively. This group then used quantitative real-time PCR (qRT-PCR) to measure the relative gene expression of LGR5 and ASCL2, which were found to be only enriched in the GFP^{high} group. Further studies demonstrated that ASCL2 can bind to the β-catenin/Tcf-4 complex to induce transcription of genes that regulate stem cell biology (Schuijers et al., 2015; Yan and Kuo, 2015). In parallel, van der Flier and colleagues identified the Olfactomedin-4 (OLFM4) gene as another strong LGR5^{+} stem cell marker in human small intestine and colon (van der Flier, Haegebarth, et al., 2009). OLFM4 is a secreted protein that acts as a BMP inhibitor (discussed later) promoting proliferation (Inomata et al., 2008). Van der Flier and his team first performed *in situ* hybridisations showing OLFM4 presence at the base of the crypts. In a follow-up study, Schuijers and colleagues developed an OLFM4$^{-IRES\text{-}eGFPCreERT2}$ knock in allele in mice that was subsequently crossed with *Rosa26-LacZ* mice. Similar to the experiments with LGR5, lineage tracing of OLFM4 showed how after tamoxifen induction for 7 days the entire crypt-villus axis contained OLFM4 daughter cells, making it a good LGR5^{+} stem cell marker (Schuijers et al., 2014). Finally, Jung et al. characterised the protein tyrosine pseudokinase 7 (PTK7) as another potential stem cell marker. Using *in vitro* culture of human colonic crypts in the form of organoids (discussed later) they searched for surface markers to enable discrimination of distinct cell populations. They treated the colonic organoids with proliferation-inducing media and differentiation-inducing media. They then analysed the membrane-enriched protein fractions using quantitative mass spectrometry and found that PTK7, a regulator of the Wnt signalling during embryo development, was upregulated in the proliferation-inducing media. Using flow cytometry, Jong and colleagues discovered a heterogeneous distribution of PTK7 in the membrane. However, they found that cells with high PTK7 surface content had a higher re-seeding capacity, presented more organoid forming cells and had higher expression levels of the stem cell marker LGR5 as well as

the enteroendocrine marker chromogranin A (CHGA). These researchers concluded that PTK7$^+$ human colonic epithelial population expresses gene programs of both ISCs and of LRCs, suggesting the existence of LRC-like cells in the human colonic epithelium which implies the presence of a phenotypic heterogeneity in human colonic stem cells (Jung, et al., 2015).The discovery of alternative LGR5$^+$ markers such as OLFM4 has been key in helping studying crypt stem cells since the protein LGR5 is expressed in low quantities in the membrane and antibodies lack of high-affinity needed to isolate stem cells.

1.4.3 Stem cell plasticity

The gut can recover after suffering substantial damage. Potter and co-workers demonstrated that the intestinal epithelium is able to regenerate after high doses of radiation that nearly eliminates CBCs in its entirety (Potten, 1977). Upon radiation damage, cells undergo apoptosis which leads to crypt shrinkage (Merritt et al., 1994), but the epithelium can compensate it by triggering proliferation in the remaining cells. This situation prompts temporary enlargement of crypts followed by crypt fission to recover the epithelium (Withers, Brennand and Elkind, 1970). When the stem cell compartment is compromised and LGR5$^+$ stem cells are eliminated, the intestinal epithelium can recover and LGR5$^+$ stem cells reappear in a matter of days (Tian et al., 2011).

Recent discoveries have highlighted the complexity of intestinal tissue regeneration and have shown that various cell types can revert their phenotype to become stem cell-like upon tissue damage. Research done by Buczacki and his team investigated the functional role of quiescent LCRs and demonstrated that their fate is to become Paneth and enteroendocrine cells but retain the ability to re-acquire stem-cell function. When tissue regeneration is critically needed, quiescent cells proliferate extensively and can give rise to clones presenting all the main epithelial cell lineages (Buczacki et al., 2013). Van Es and colleagues showed that a subset of transient amplifying progenitor cells expressing *Dl11* can de-differentiate into stem cells *in vitro* when provided with exogenous Wnt signals, as well as *in vivo* following tissue damage (van Es et al., 2013). Work done by Asfaha and colleagues also showed that a group of transient amplifying radio-resistant progenitors expressing the *Krt19* marker can give rise to LGR5$^+$ CBCs in the colon (Asfaha et al., 2015). A lineage of enteroendocrine cells containing the *Bmi1* and *Prox1* was demonstrated to contain a reservoir of homeostatic cells that could also be transformed into ISCs upon injury (Yan et al., 2017).

Furthermore, Jadhav and his team showed that when native ISCs are eliminated, a subset of *Bmi1* expressing enteroendocrine precursor cells and CD69$^+$CD274$^+$ goblet precursor cells can revert to ISC state and that this is dependent on their chromatin accessibility (Jadhav et al., 2017). Tetteh and colleagues showed that even a subset of Alpi$^+$ enterocyte progenitors can revert to stem cells and

Paneth cells during regeneration by inducing *Alpi-CreERT2* knock-in in mice and trace their lineage (Tetteh et al., 2016). Moreover, the intestinal epithelium can respond to inflammation and loss of $LGR5^+$ stem cells by de-differentiation of Paneth cells induced by activation of the SCF/c-Kit signalling, a major regulator of cell proliferation (Schmitt et al., 2018). Finally, recent studies done by Nusse and colleagues demonstrated that the intestinal epithelium is also remodelled upon parasitic infection-triggered inflammation. The infection triggers the formation of immune cell structures called granulomas and crypts that are associated with them are able to regenerate in the absence of $LGR5^+$ stem cells. Nusse and his team discovered that stimulation of the inflammatory-related interferon gamma (IFN-γ) in crypts could activate a different transcriptional programme with genes generally expressed in foetal epithelium (Nusse et al., 2018). Along with the gut, de-differentiation of cell lineages has also been reported in other organs like the liver (Tarlow et al., 2014) and the stomach (Stange et al.,2013).

Recently, the intestinal cell fate has been related to the chromosomal configuration of the epithelial cells. The stem cell niche is constantly receiving signals from its neighbouring epithelial and subepithelial cells and it is thought that this microenvironment can re-programme progenitor and mature cells. A number of studies have demonstrated that the DNA methylation and histone modification signatures in differentiating cells show an open and accessible chromatin state (Jadhav et al., 2017; Kim et al., 2014; Yu et al., 2015). Because changes in epigenetic signatures are allowed during cell fate specification, stimuli emanating from the stem cell niche microenvironment are thought to modulate the signalling episodes needed to induce cell lineage variations.

The discovery of the majority of these new cell types has been possible thanks to the development of new techniques such as single cell RNA sequencing (Parikh et al., 2019). The specific gene expression profile each cell contains permits comparing differences and similarities and obtain highly detailed characterisation of the intestinal epithelial cell population. All these discoveries have made the scientific community change their views on the unidirectional model of cell differentiation. Researchers have shown that differentiated secretory and absorptive progenitors can revert to stem cells upon tissue injury which illustrates a more dynamic and plastic characteristic of the intestinal epithelium (**Figure 1.10**).

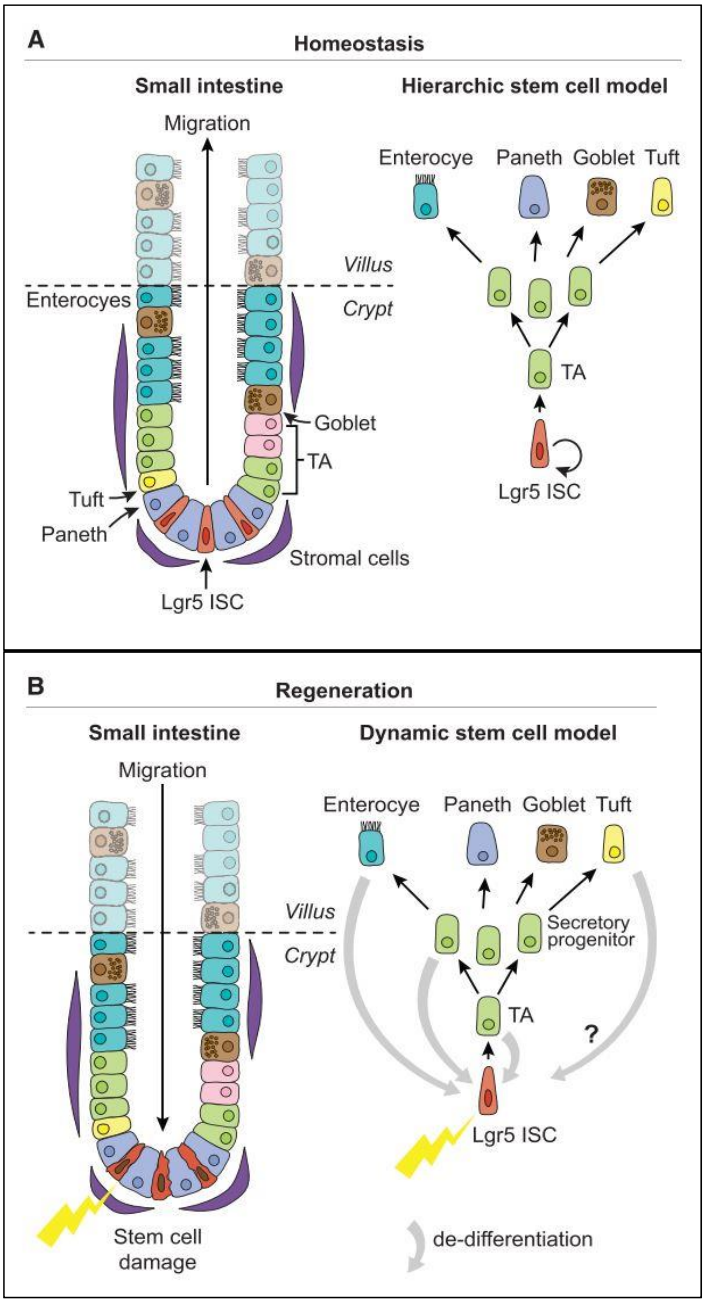

Figure 1.10. Models of Intestinal Stem Cell Hierarchy during homeostasis and regeneration. (A) Hierarchical stem cell model. Under homeostatic conditions, stem cells residing at the base of the crypt proliferate to give raise to all different crypt cell types. **(B)** Dynamic stem cell model. Upon tissue damage and loss of LGR5^{+} stem cells, progenitor cells as well as differentiated cells can revert their phenotype to become stem cells, proliferate and restore the epithelium. Figure adapted from de Sousa e Melo et al., 2019).

1.4.4 Intestinal Stem cell replacement

Stem cells at the base of the crypts are continually replicating to compensate the constant loss of differentiated cells and sustain the tissue architecture. The way these stem cell populations are

maintained depends in part on the type of cell division pattern that they undergo. These cells can divide asymmetrically or symmetrically. A symmetrical cell division will render two identical stem cells with the same chance of remaining in the stem cell niche, whereas an asymmetrical cell division and segregation involves a stem cell giving rise to two cells with different fate, one remains a stem cell and the other one a transient amplifying cell. This fate asymmetry can either be achieved as the invariant result of every stem cell division (invariant asymmetry) or orchestrated from the whole population (population asymmetry) whereby cell fate is unpredictable or stochastic and is decided only up to some limited probability. These two models are controlled by cell autonomous and environmental signals (Krieger et al., 2015). The asymmetrical cell division phenomenon has been demonstrated in *C.elegans* and *Drosophila* models and only upon tissue damage, stem cells will divide symmetrically to help regenerate the epithelium (Neumüller and Knoblich, 2009). A study by Potten and colleagues first supported the idea of intrinsic asymmetry by showing that DNA segregates asymmetrically during cell division (Potten et al., 2002). Lineage tracing studies by Lopez-Garcia and his team showed that ISCs follow a pattern of neutral drift whereby stem cell loss through differentiation is compensated by the replication of an ISC neighbour (Lopez-Garcia et al., 2010). They hypothesised that this process could be achieved through stochastic stem cell loss triggering self-renewal, or through overpopulating the stem cell pool leading to loss. Interestingly, Snippert and colleagues, following pulse-chase lineage tracing of LGR5 expression studies and mathematical analysis of clonal evolution, showed that their results favoured a stochastic model where every $LGR5^{+}$ stem cell has the same potential stemness. This similarity in stemness results in a neutral competition for niche space, leading to neutral drift dynamics. In this scenario, stem cells are under a highly competitive environment, where there is limited niche space and stem cells will try to get closer to Paneth cells to receive growth factors (Snippert et al., 2010). Little differences in cell fitness have major effects in the chances of a stem cell in remaining in the stem cell niche. A stem cell with mutations that diminishes its proliferative capacity will stand a lower chance and will be displaced from the crypt bottom. Intestinal tumour development relies on cancer cells having to gain the capacity to replicate outside the stem cell niche before being pushed out of the bottom of the crypt. In this case, because cancer cells compete with healthy stem cells, only the cancer cells that contain mutations to promote stem cell niche independency will prevail (Gehart and Clevers, 2019).

1.4.5 The intestinal stem cell niche

As discussed before, stem cells reside at the bottom of crypts, where they are far away from any potential luminal threat. In the small intestine, they are surrounded by Paneth cells, which unlike other cell types can migrate down the crypt axis to be located next to the stem cells (Gassler, 2017).

Paneth cells alternate with stem cells so that these are in contact with them and can receive pro-stemness paracrine signals such as Wnt, epidermal growth factor (EGF), Notch ligands (discussed later) (Toshiro. Sato et al., 2011), and other proteins like Phospholipase A2 that promote stem cell homeostasis (Schewe et al., 2016). The number of Paneth cells determines how many stem cells are present in a stem cell niche. Because stem cells depend so much on being in direct contact with Paneth cells, ISCs residing in the centre of the crypt and bordered by Paneth cells have higher possibility of becoming a dominant clone than those at that only contact one Paneth cell (Ritsma et al., 2014). Paneth cells also secrete antimicrobial proteins such as defensins and lysozyme to maintain the crypt base sterile (Gassler, 2017). In addition, Paneth cells contribute to stem cell regulation by secreting lactate, the end product of glycosylation, which is then converted in pyruvate by the ISCs to generate ATP via the mitochondrial oxidative phosphorylation. This event results in increased mitochondrial activity and subsequent reactive oxygen species (ROS) generation that contributes to crypt formation (Rodríguez-Colman et al., 2017). In the colon, because of the lack of Paneth cells, a population of goblet cells expressing the regenerating family member 4 (REG4) marker and residing intermingled with stem cells, is believed to regulate and maintain the stem cells in mice (Sasaki et al., 2016).

In addition to Paneth or $REG4^+$ goblet cells, other non-epithelial cell types contribute to the regulation of the stem cell niche. These cells include myofibroblasts, fibroblasts, perycites, telocytes, smooth muscle cells, endothelial cells and neural cells. This cell population is located in the mesenchyme that lies underneath the epithelial monolayer and serves as an alternative source of paracrine signals (Santos et al., 2018). Paneth cells were shown not to be the only source of Wnt signals, as ablation of Paneth cells had no effect in $LGR5^+$ stem cell function (Kim et al., 2012) and epithelial-specific deletion of Wnt showed no effect on ISCs in mice (Farin et al., 2012). These results suggested the existence of another different source of signals that can regulate ISCs. Work developed by Greicius and colleagues demonstrated an alternative source of Wnt and R-spondin (Wnt signalling amplifier) proteins. These researchers showed in *ex vivo* cell cultures that pericryptal intestinal myofibroblasts that express the PDGF receptor alpha (PDGFRα) can secrete R-spondin 3 (RSPO3) and Wnt protein. In addition, *in vivo* work in mice showed and that excision of *Porcn* (a protein needed for Wnt formation) in $PdgfR\alpha^+$ cells resulted in decreased Wnt/β-catenin signalling and Paneth cell differentiation, blocking crypt formation (Greicius et al., 2018). Research done by Aoki and colleagues revealed the presence of a subset of mesenchymal fibroblasts that express the Forkhead box I1 (FoxI1) transcription factor capable of producing Wnt and R-spondin proteins. By specific ablation of $Fox1^+$ mesenchymal cells in mice, these researchers demonstrated a subsequent disruption of the epithelium, highlighting the relevance of this cell type in stem cell maintenance

(Aoki et al., 2016). Similarly, work by Stzepourginski et al. indicated the existence of a subset of mesenchymal cell residing in close proximity to the ISCs, specifically characterised by the expression of CD34 and Gp38 proteins, capable of producing Wnt, R-spondin and the growth factor Gremlin (Stzepourginski et al., 2017). Intestinal subepithelial myofibroblasts (ISEMFs) that locate right below ISCs have been shown to regulate the stem cell niche. Horoguchi and colleagues (Horiguchi et al., 2017) showed that ISEMFs secrete the agiopoietin-like protein 2 (ANGPTL2). The secretion of this protein balances the levels of signalling between pro-differentiation BMP and pro-proliferation β-catenin, regulating intestinal homeostasis after tissue damage in mice with induced colitis (Horiguchi et al., 2017). Recently, a population of mesenchymal cells named telocytes, characterised by their long cytoplasmic extension and expression of Foxl1 and PdgfRα were similarly shown to secrete Wnt proteins (Shoshkes-Carmel et al., 2018). Finally, as shown by Mao et al.; the gut epithelium can also regulate the underlying mesenchyme through the Hedgehog (Hh) signalling pathway, where Hh proteins act as paracrine mitogens to stimulate the development of the neighbouring mesenchymal progenitor cells (Mao et al., 2010) (**Figure 1.11**).

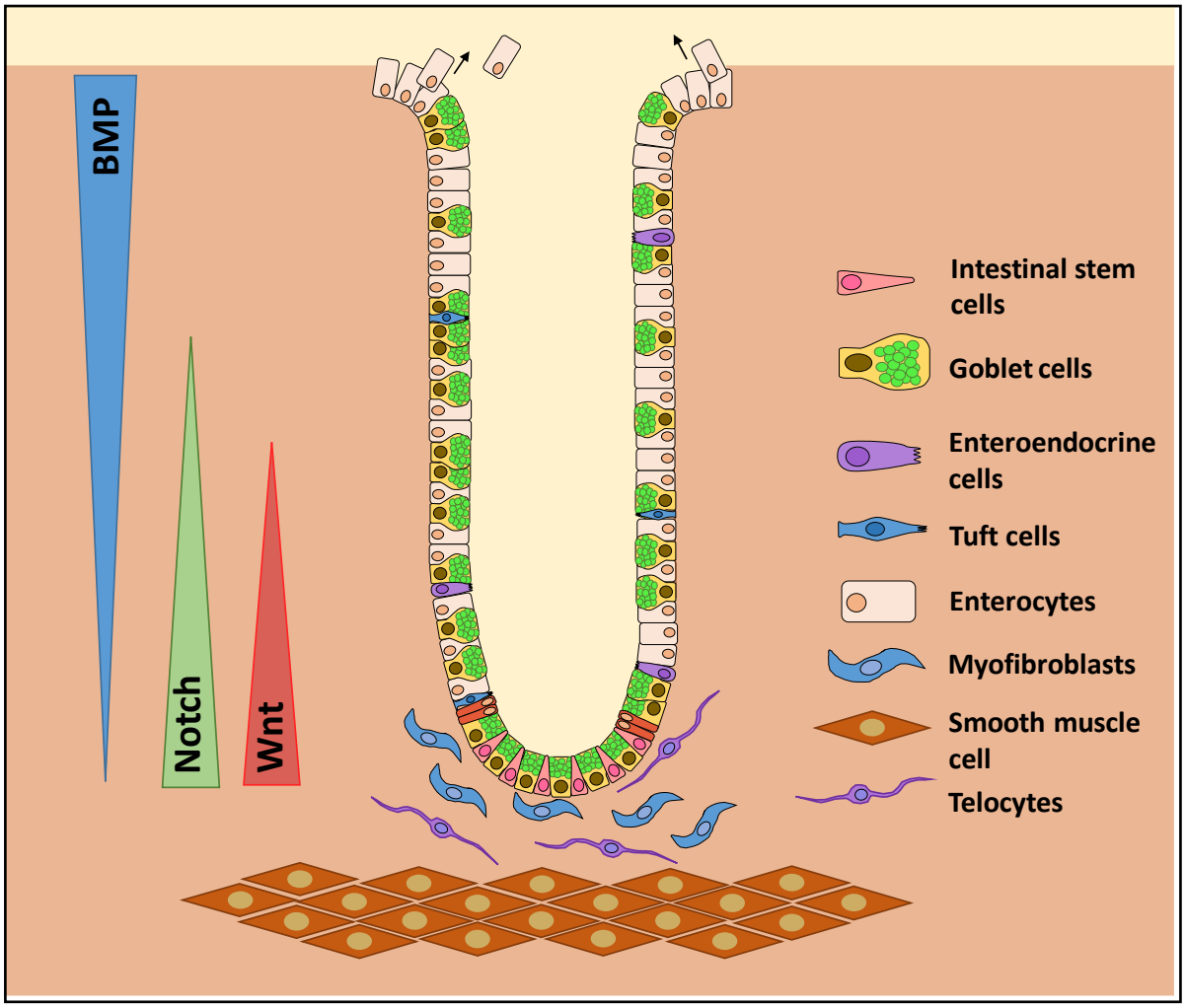

Figure 1.11. Signalling pathways and the regulation of the stem cell niche in colonic crypts. Goblet cells and other non-epithelial cells such as myofibroblasts, smooth muscle cells and telocytes in close proximity to the crypts base regulate ISCs biology. These cells secrete molecules like Wnt, R-spondin, Notch and Noggin to maintain stemness by activating the Wnt and Notch signalling pathways and inhibiting the BMP/TGFβ signalling pathways. These signals diminish in intensity along the crypt axis whereas BMP/TGFβ are enhanced promoting cell differentiation and inhibiting proliferation.

1.5 Crypt signalling pathways

As previously described, the biology of the intestinal epithelium is tightly regulated by specific signals emanating from the actual epithelium and the underlying mesenchyme. The major regulators of the epithelium include the Wnt, Notch, EGF, BMP, TGF-β, YAP/TAZ and Hh signalling pathways. Specific spatio-temporal activation of these signals determines the fate of the epithelial cells

1.5.1 Wnt signalling

The Wnt signalling pathway is the most important driver of proliferation and cell fate of ISCs. In the Wnt canonical pathway, Wnt proteins bind to the Frizzled (FZD) receptor in the membrane of the ISCs which lead to the activation of the co-receptors LRP5 and LRP6, causing the dimerization of the two receptors (Nusse et al., 2017). The formation of this receptor complex induces conformational changes that result first in the binding of the cytoplasmic part of FZD to Dishevelled (DVL) which in turn facilitates the recruitment of the scaffold protein Axin that binds to the LRP tail. Axin interacts with β-catenin, which is otherwise being degraded by the tumour suppressor protein adenomatous polyposis coli (APC) together with other proteins. This event results in β-catenin accumulation in the cytoplasm which then translocates to the nucleus where it binds to the transcription factor T cell factor (TCF). The binding β-catenin to TCF regulates the expression of genes that control stem cell biology and tissue growth (**Figure 1.12**) (Nusse et al., 2017). The Wnt signal can be enhanced by the R-spondin proteins. These proteins bind with high affinity to transmembrane Lgr receptors. As described before, LGR5 was found to mark stem cells in intestinal crypts (Barker et al., 2007) and binding of R-spondin induces the interaction of this protein with the Rnf43/Znrf3 protein ubiquitin-ligase complex. This complex functions by clearing the Wnt receptors from the membrane and R-spondin binding to LGR5 induces clearance of the Rnf43/Znrf3 complex, persistence of activated Wnt/FZD/LRP receptor complex and subsequent amplification of the Wnt signal (**Figure 1.12**) (Nusse et al., 2017). Absence of R-spondin implies a quick turnover of the Wnt receptors by the ubiquitin-ligase complex, shortening the Wnt signal gradient (Farin et al., 2016). As discussed before, Wnt proteins can be secreted by epithelial and mesenchymal cells, with Paneth cells specifically producing Wnt3 (Toshiro. Sato et al., 2011). The origin of the R-spondin proteins is still not clear. As reported earlier mesenchymal cells can secrete Rspo1 (Aoki et al., 2016; Stzepourginski et al., 2017) although it is thought the major regulators of crypt biology are Rspo2 and Rspo3 (Storm et al., 2015).

As discussed previously, Wnt signalling is key in maintaining stem cell biology in ISCs. Loss of Wnt signalling by genetic knock out of the β-catenin or inhibition of Wnt receptors causes a complete loss of intestinal crypt structures (Fevr et al., 2007; Pinto, et al., 2003). The expression of Wnt targets like β-catenin is higher at the cells residing at the base of the crypt and gradually decreases towards the crypt opening, highlighting the presence of a Wnt signalling gradient (Kosinski et al., 2007) (**Figure 1.11**).

Abnormal Wnt signalling has been linked with cancer in the gut and other tissues. The gene that codes for APC is mutated in the majority of sporadic colorectal cancers and familial adenomatous polyposis patients (Kinzler et al., 1996). In addition, mutations in the Axin gene or genes that are

involved in promoting β-catenin destruction can originate colorectal cancers, even in the absence of aberrant APC mutations (Morin et al., 1997; Liu et al., 2000). Any mutations that result in uncontrolled Wnt activation are likely to induce tumour formation but the progression of tumour formation in later stages is dependent on inactivation of tumour suppressor genes like p53, SMAD4 and PTEN (Janssen et al., 2006; Marsh et al., 2008; Luo et al., 2009) or activation of proto-oncogenes like RAS (Fearon et al., 1990).

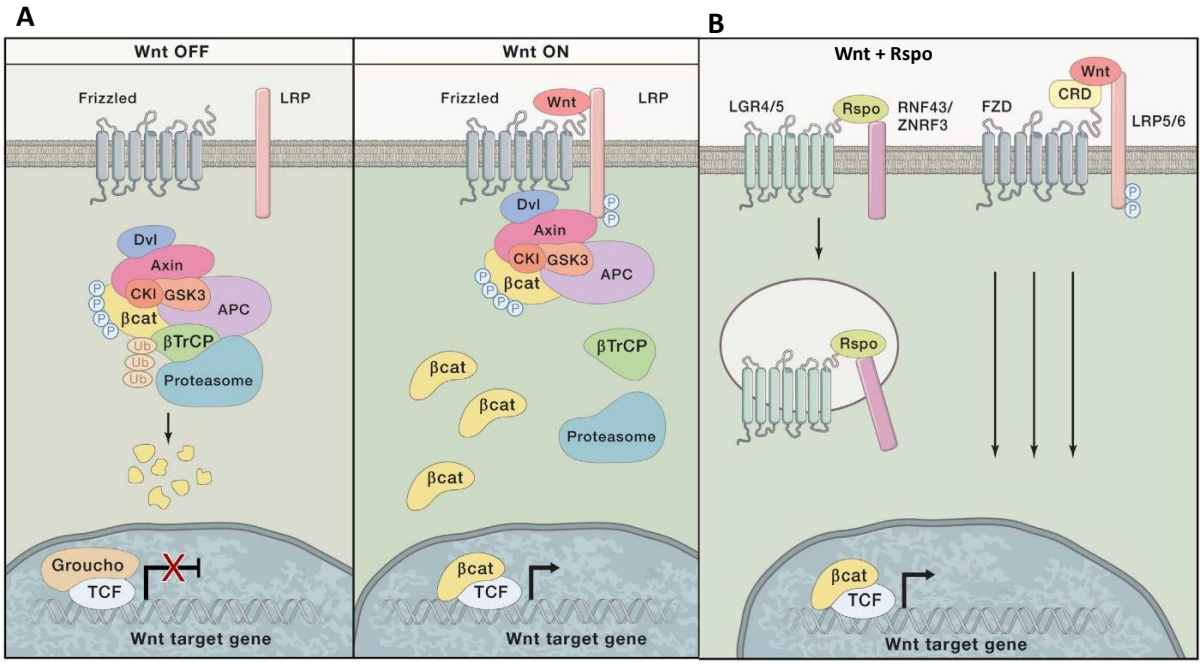

Figure 1.12. Canonical Wnt signalling. (A-left) When the Wnt signalling is not active, FZR receptors are internalised and degraded and β-catenin forms a complex with Axin and APC and other components which are constantly degraded by the proteasome. **(A-right)** Binding of the Wnt protein prompts association of Axin with the LRP receptor resulting in inactivation of the proteasome complex allowing β-catenin to translocate to the nucleus and activate TCF transcription factor to induce expression of Wnt target genes. **(B)** Binding of Rspo to receptor LGR5 triggers internalisation of the RNF43/ZNRF43 ubiquitin-ligase complex that otherwise would recycle the FZD receptors, amplifying Wnt signalling. Adapted from Nusse et al., 2017.

1.5.2 Notch signalling

Notch signalling pathway plays another major role in maintaining intestinal crypt biology as it is key in regulating cell fate. Lateral inhibition is a cell mechanism that requires direct cell-to-cell contact by which Notch can signal neighbour cells to generate different cell types (Sancho et al., 2015). Notch receptors are expressed in the membrane of epithelial cells and undergo conformational changes

upon binding of a transmembrane ligand, such as delta-like ligands (DLL1, DLL3 and DLL4 or Jagged1 and Jagged 2). The Notch intracellular domain (NICD) is removed by a two-step proteolytic cleavage by an ADAM-metalloprotease and a γ-secretase and it is then translocated into the nucleus where it binds transcription factor CSL and Mastermind-like protein (MAML). This binding induces transcription of Notch target genes like the helix transcription factor HES1 (**Figure 1.13**) (Vanuytsel et al., 2013). Upon activation, HES1 represses the transcription factor ATOH1 (which otherwise will activate transcription of delta-like ligands) resulting in the incapability of the cell to express Notch ligands like DLL in what is called lateral inhibition. In this scenario, the cell that produces more Notch ligands activates Notch signalling in the neighbour cell making it reduce the expression of Notch ligands. In turn, this enables the cell with low Notch signalling to produce more Notch ligands because its neighbour cell cannot produce inhibitory signals in a feedback loop. This means that any slight difference in the Notch activity whether unpredictable or due to epigenetics is amplified to drive the neighbour cell into the opposite signalling status and therefore into different development and fate (Vanuytsel et al., 2013). In the crypts of the small intestine, Notch signalling is key in maintaining stem cell biology whereby Paneth cells (Sato et al., 2011) or other mesenchymal cells (Demitrack et al., 2016) continuously secret Notch ligands to keep the Notch signal active in the ISCs, preventing them from differentiating (Fre et al., 2005). In the TA region, progenitor cells with active Notch signalling will differentiate into absorptive enterocytes pushing the Delta ligands-expressing neighbours into a secretory lineage (van Es et al., 2013), promoting balance between cell types (Sancho, Cremona and Behrens, 2015). When Notch-mediated lateral inhibition is disrupted, or ATOH1 overexpressed, proliferative cells differentiate into postmitotic secretory cells (Milano et al., 2004; Vandussen et al., 2010). Notch signalling outcome depends on the status of the Wnt signalling pathway. When Wnt signalling is active at the base of the crypt, β-catenin can bind to Hes1 promoter together with NICD which results in stabilisation of the Notch pathway. This event promotes initial absorptive or secretory cell differentiation based on lateral inhibition. Further up the crypt, where Wnt signals are weak, the absence of β-catenin results in oscillatory Notch activation which means that the fate of the cell to become goblet cell or enteroendocrine cells will be determined stochastically (Kay et al., 2017) (**Figure 1.13**).

1.5.3 EGF signalling

EGF signalling is another signalling pathway that plays an important role in promoting stem cell proliferation. It is known to be secreted by Paneth cells (Toshiro. Sato et al., 2011) but similar to other growth factors it is likely to be secreted by the underlying mesenchyme. EGF binds to EGF receptor ERB1, which is a tyrosine kinase protein expressed in ISCs (Gehart et al., 2019). Activation

of ERB1 starts a complex signalling cascade. It activates AKT, whose downstream targets like mTORC1 are involved in cell proliferation (Efeyan et al., 2010). At the same time, it also activates the mitogen-activated protein kinase (MAPK) signalling pathway that results in ERK activation which can then promote cell proliferation and inhibit cell differentiation (Aliaga et al., 2017; Lemieux et al., 2011). Studies by Basak et al. showed that blocking ERB1 or MAPK signalling pathway resulted in diminished cell proliferation and induction of quiescence state on $LGR5^{+}$ ISCs (Basak et al., 2017). In addition, stimulation of ERB1 activates tyrosine kinases JAK and SRC who subsequently activate transcription of STAT proteins to induce transcription of proliferation target genes. The JAK/STAT pathway has been reported to be key during intestinal regeneration following injury (Richmond et al., 2018) (**Figure 1.13**).

1.5.4 BMP/ TGF-β signalling

Bone morphogenetic proteins (BMPs) belong to the transforming growth factor (TGF-β) protein family. Their main role in the intestine is to promote cell differentiation and supress cell proliferation as well as acting as tumour suppressor proteins (Gehart et al., 2019). Mutations on the BMP/ TGF-β pathway or overexpression of BMP inhibitors can initiate intestinal tumorigenesis (Howe et al., 1998; Davis et al., 2015). BMP ligands are sensed by type I receptors (BMPRI) in the cellular membrane which subsequently activate R-Smads proteins (Smad1, 5 and 8). These Smads form a protein complex with Smad4 that can translocate to the nucleus to regulate gene expression (Massagué, 2014) (**Figure 1.13**). The main ligands in the intestine are BMP2 and BMP4, which are secreted by intravillus and intracrypt mesenchymal cells (Hardwick et al., 2004). The BMP/ TGF-β signalling is inhibited by Noggin or Gremlin1 proteins by direct binding to the ligand. These inhibitors are secreted at the base of the crypt and therefore maintain stemness of ISC (Gehart et al., 2019). The presence of BMP inhibitors is weaker towards the crypt opening which generates a signalling gradient where BMP/ TGF-β signals are low in the bottom of crypts and more powerful higher up the crypt axis. Conversely, Wnt signals decrease toward the crypt tops and are intense at the base of the crypt. This signalling gradient acts as a balance promoting stem cell maintenance as well as cell differentiation towards the crypt top (Reynolds et al., 2013) (**Figure 1.11**).

1.5.5 Hippo-YAP/TAZ signalling

The Hippo signalling pathway has been shown recently to be key in regulating the stem cell niche. It was first discovered to control tissue size during organ development, but it has also been linked to regeneration of adult tissues like the gut (Totaro et al., 2018). The Hippo pathway integrates a great variety of signals: mechanotransduction, GPCR signalling, metabolite sensing and receptor tyrosine

kinase signalling. These signals activate a kinase cascade comprising Ste20-like kinase I (MST1) and 2 (MST2), the large tumour suppressor kinase 1 (LATS1) and 2 (LATS2), the adaptor proteins Salvador 1 (SAV1), MOB1A and MOB1B and the homologous transcriptional co-activators YAP and TAZ. During epithelial regeneration following tissue injury the Hippo signalling pathway is switched off. In this situation YAP/TAZ can bind to the TEAD transcription factors to suppress the expression of genes that regulate cell cycle and cell migration. Activation of the Hippo pathway induces MST1/MST2 activation which ultimately results in the phosphorylation of YAP/TAZ and its proteosomal degradation (Moya et al., 2019) (**Figure 1.13**). YAP/TAZ acts by limiting Wnt signalling overexpression in tissue regeneration after injury, and it does so by suppressing Wnt signals and excessive Paneth cell differentiation. The effect of YAP and TAZ repress classic Wnt target genes like LGR5 and AXIN2 (Gregorieff et al., 2015). In this way, YAP/TAZ temporarily suppresses the normal homeostatic programme of ISCs during injury and induces a more embryonic stem cell programme (Moya and Halder, 2019). It has been suggested that YAP and TAZ can bind directly to the β-catenin destruction complex, which induces a higher rate of β-catenin destruction. When the cell starts receiving Wnt signals, both factors detach to allow activation of the proliferation pathway (Azzolin et al., 2014).

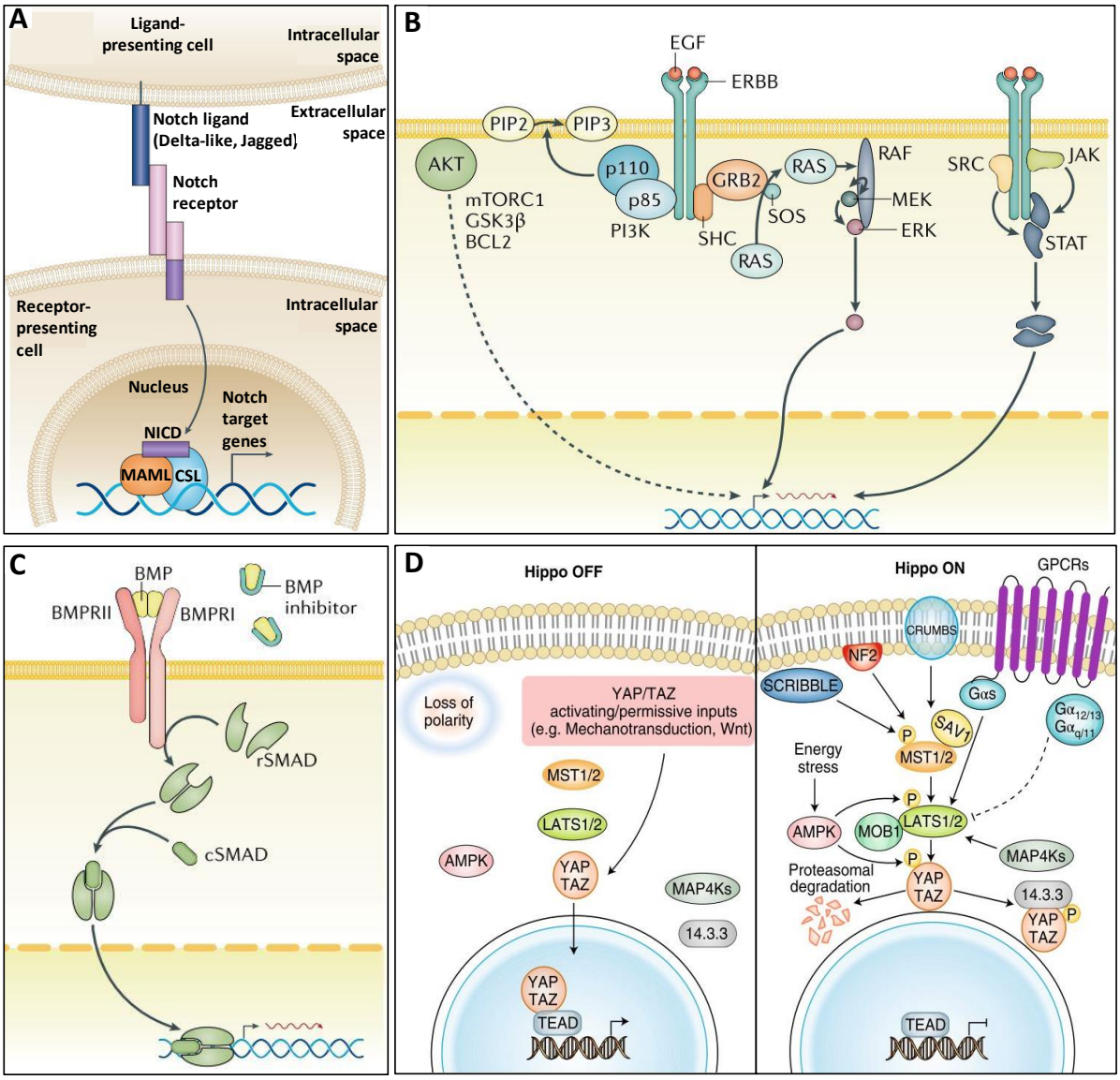

Figure 1.13. Crypt signalling pathways. (A) Notch signalling pathway. Activation of Notch receptor induces translocation of NICD and transcription of Notch related genes. **(B)** EGF signalling pathway. Binding of EGF to the receptor ERBB activates a complex pathway that involves AKT, MAPK and JAK/STAT signalling pathway resulting in transcription of EGF related genes. **(C)** BMP signalling pathway. Activation of the BMP receptor by BMP induces the formation of a SMAD protein complex that translocates to the nucleus to regulate BMP related genes. **(D)** Hippo-YAP/TAZ signalling pathway. When the Hippo pathway is turned off (left) by signals such as Wnt; YAP and TAZ can translocate to the nucleus and bind the transcription factor TEAD to modulate stem cell response to injury. Activation of the Hippo pathway (right) induces a downstream signalling that results in the phosphorylation and further degradation of YAP and TAZ. Figures adapted from Gehart et al., 2018; Anderson et al., 2014 and Totaro et al., 2018.

1.5.6 Other crypt regulators

In addition to the signalling pathways described before, the **Hedgehog (Hh) signalling** route is also relevant in maintaining the physiology of the intestinal epithelium as it plays a critical role during gut development. The Hedgehog ligands Sonic Hedgehog (Shh) and Indian Hedgehog (Ihh) are secreted by the intestinal epithelium and activate Hh target genes Pathed (Ptch1) and Gli1 in the mesenchyme (Büller et al., 2012). Recent studies suggest Hh acts on myofibroblasts to limit the size of the crypt and the ISC pool (Kosinski et al., 2010) whereas mutations that cause downregulation of Hh are implicated in colon cancer development (Gerling et al., 2016).

Interleukins are soluble cytokine proteins critical for intracellular communication and with an important role in inflammation. These proteins can be derived from innate and adaptive immune cells as well as from intestinal epithelial cells (Andrews, et al. 2018). Upon infection or stress signalling, these cytokines have been shown to modulate ISCs in the midgut of *Drosophila* by inducing the Jak/Stat signalling. This signal activation promotes rapid division and progenitor differentiation to regenerate the epithelium (Jiang et al., 2009). Interleukin 22 (IL22) can be secreted upon inflammation and it has been shown to activate STAT3 in epithelial cells to recover mucus-producing goblet cells, resulting in improvement of the epithelium during ulcerative colitis (Sugimoto et al., 2008). IL22 presence in organoid *in vitro* cultures has been suggested to target $LGR5^{+}$ cells to mediate tissue recovery and regeneration (Lindemans et al., 2015). Other important interleukins include IL10 which has been shown to maintain epithelial permeability (Zheng et al., 2017) and IL25, which has been shown to be secreted by tuft cells upon parasitic infection to activate IL4 and IL3-producing ILC2 cells. This cell activation ultimately promotes goblet cell differentiation and mucus secretion (Gerbe et al., 2016).

Nutrient availability has been recently shown to modulate ISCs biology. Following acute nutrient deprivation, quiescent ISCs are activated and induced to proliferate via PTEN-dependent phosphorylation and the inhibition of the nutritional sensor mTORC1 (Richmond et al., 2015; Yousefi et al., 2018). In addition, calorie restriction promotes regeneration of the small intestine by inducing more ISC self-renewal. Reduction in calorie intake attenuates mTORC1 activity in Paneth cells which in turn stimulates ISC proliferation (Yilmaz et al., 2012). Interestingly, a high fat diet also induces an increase in the number of ISCs by almost 50% but a decrease in the number of Paneth cells. Beyaz and colleagues found that under these conditions, ISCs become Paneth cell independent and more sensitive to Wnt signalling, which results in a higher number of ISCs up the crypt axis, increasing the chances of tumour formation (Beyaz et al., 2016). Finally, another source of signals that regulate the

intestinal epithelium derive from the neurons of the **enteric nervous system** that innervate the tissue (discussed later).

All these signals are responsible for ensuring a good maintenance of the gut epithelium. Their spatio-temporal functioning is key in securing a controlled cell proliferation of stem cells at the base of the crypt and differentiation towards all types of cell lineages as they migrate up the crypt axis. In recent times, the development of new techniques has allowed to investigate the physiology of the gut epithelium. Researchers can now isolate colonic crypts and intestinal stem cells derived directly from rodents or human patients and culture them in a 3D environment maintaining a polarised crypt-villus structure. This culture system is a powerful tool that permits the study of regulatory and pathological mechanisms of the intestinal epithelium at the molecular and macromolecular level.

1.6 3D *in vitro* culture of colonic crypts

The need for new model systems that could recapitulate body functions and molecular and cellular processes has been driving current biomedical research. Animal models like mouse or rat can closely epitomise most of the *in vivo* human physiology but they still exhibit certain biological differences. The use of 2D cultures relies on the culture of a monolayer of cells; this can be advantageous for certain studies but they still lack of complex cell-cell and cell-matrix interactions that orchestrate a variety of cellular signals and signalling pathways (Yin et al., 2016). Stem cells have the capability to grow and organise complex structures when placed in 3D matrices or gels and fed a number of growth factors. These stem cells can generate 3D organised tissues named organoids, which can recapitulate a number of biological processes like cell to cell and cell-matrix interactions. Moreover, organoids can be propagated *ad infinitum* and are easy to manipulate (Date et al., 2015).

The first successful culture of primary adult intestinal crypts was developed by Evans and co-workers. In this culture system, rat crypt epithelial cells were embedded in a matrix of collagen type I and could be propagated for 1 to 2 weeks (Evans et al., 1992). Sato and colleagues managed to develop a 3D organoid culture system by embedding mouse isolated small intestinal crypts devoid of mesenchymal cells in Matrigel; a more complex matrix containing laminin which is a protein enriched in the crypt base (**Figure 1.14**). By supplementing the culture with EGF, Noggin (blocker of BMP signalling) and R-spondin, organoids could be propagated for more than a year while maintaining genomic stability. These spherical organoids recapitulate the *in vivo* crypt-villus structures, where stem cells are found at the base of crypt to give rise to the rest of cell types (Sato, et al., 2011). Human colonic organoids were developed subsequently with the addition of Wnt3A,

prostaglandin E2 (PGE_2) and nicotinamide (ROCK kinase inhibitor) to the mouse organoid media (Jung et al., 2011).

In addition to the organoid model, human intact colonic crypts can also be isolated and placed in culture. Early research done by Withehead and colleagues and Gibson and co-workers (Gibson et al., 1989; Whitehead et al., 1987) first managed to isolate and culture crypts. However, the lack of cell-matrix interactions drives crypt cell to apoptosis. Culture of colonic crypts in collagen type I matrix improved the culture conditions (Reynolds et al., 2007), though the use of Matrigel in combination with a range of specific growth factors previously described by Sato et al. and Jung et al. significantly improved the crypt viability. This type of *ex vivo* culture rendered a system that can recapitulate the hierarchy of crypt cell renewal along the crypt axis and functional epithelial polarity (Parris & Williams, 2015). The development of this near-native model allows the study of the status of signalling pathways by modulating stem cell proliferation and cell migration and differentiation (Reynolds et al., 2013). In addition, the physiology of the crypt can be studied over time with live imaging microscopy to monitor events such as cell division, cell migration, mucus and fluid secretion. Furthermore, this model is also amenable to the study of intracellular calcium signals with the use of calcium indicators like Fura-2 and Fluo-4, and it can provide valuable information on specific protein localisation with the use of immunocytochemistry methods (Parris & Williams, 2015).

Organoids are an extremely useful tool because they recapitulate a great variety of *in vivo* functions and are easily propagated. They are cell cultures amenable for genetic engineering and many groups have been able to manipulate their genome via transfection, lentivirus or electroporation. Moreover, organoids can be grown from single stem cells containing the desired genetic modification (Koo et al., 2011; Yilmaz et al., 2012). Recently, the development of the CRISPR/Cas technology for gene editing has been proven really useful because of its efficacy and specificity (Knott and Doudna, 2018). Organoids can be used for regenerative medicine therapies, whereby these structures can be grown *in vitro* to be later transplanted and engrafted into the patient to help regenerate the epithelium, as it has been reported in mouse (Yui et al., 2012). This culture system can be also used to model diseases. A recent study has made use of the CRISPR/Cas technology to correct the CFTR protein, which is not functional in patients suffering from cystic fibrosis (CF) (Schwank et al., 2013). Importantly, organoids can be used to develop personalised medicine and drug discovery where patient-derived organoids are screened for the best drug to cure a disease so it can then be administered to the patient. Inflammatory disorders, chemotherapy, radiotherapy and drug-mediated toxicity are some of the classic intestinal epithelial conditions that can be investigated using organoids (Takahashi, 2018). Recently, Berkers et al. successfully confirmed

intestinal organoids as a tool for personalised medicine. These researchers tested a variety of anti-CF drugs in patient derived organoids and gave the patient the best performing drug showing a high correlation between the *in vitro* and the *in vivo* model (Berkers et al., 2019).

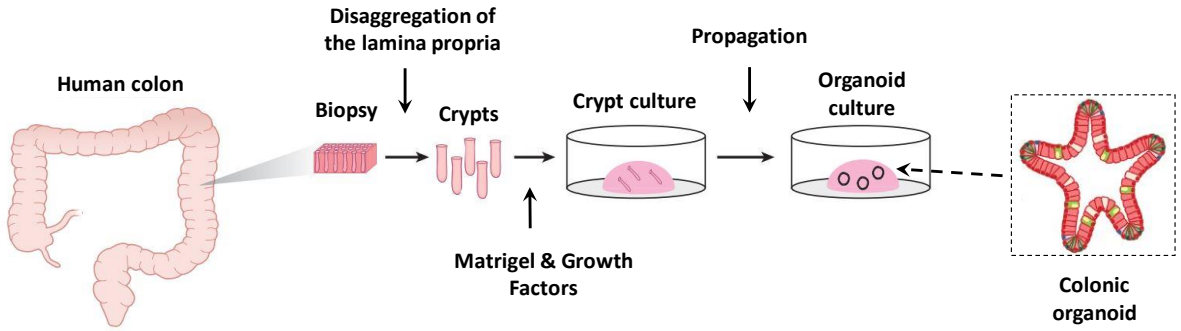

Figure 1.14. Human colonic organoids culture. Human colonic crypts can be isolated from biopsies cultured in matrix where they create a 3D culture that recapitulates *in vivo* tissue morphology and cell polarity. Cultured crypts can be propagated in the form of organoids and cultured *ad-infinitum*. Figure adapted from Sato et al., 2018 and Takahashi et al., 2018).

1.7 Acetylcholine

Acetylcholine (ACh) is a molecule often regarded as a neurotransmitter, but in the gut, it is implicated in several other physiological processes. ACh can regulate muscle contraction to induce peristalsis, fluid and ion transport to maintain epithelial barrier, immune regulation, mucus secretion and stem cell proliferation (Furness et al., 2013; Campoy et al., 2016; Ramirez et al., 2019). The sources of ACh can be neuronal when produced and secreted by cholinergic enteric neurons innervating the intestine, or non-neuronal when released by immune cells and tuft cells from the epithelium. Neuronal ACh is synthesized within the nerve terminals from acetyl-CoA and choline by the choline acetyltransferase (ChAT) enzyme and stored in vesicles. In neurons, the vesicular ACh transporter (VAChT) transports the molecule to the synaptic vesicles to be rapidly released when triggered by the generation of a membrane action potential, facilitating a quick transmission of the signal (Hebb and Whittaker, 1958) (**Figure 1.15)**. The acetyl-CoA needed for the synthesis of ACh is generated in the mitochondria after the metabolism of pyruvate from glucose. Choline is brought inside the cell together with Na^+ through the high affinity choline transporter (CHT1). This event constitutes a limiting factor for ACh synthesis. Most of the choline used in ACh synthesis is believed to come from the recycling of secreted ACh, which is metabolised extracellularly by the acetylcholinesterase (Taylor and Brown, 1999). ChAT is a single strand globular protein and it was first discovered to generate ACh by Nachmanshon and colleagues (Nachmansohn and Machado,

1943).The major isoform of human ChAT is a soluble protein of 69 kDa but alternative splicing generates other two subtypes of 74 and 82 kDa, the latter being located in the nucleus and whose activity is still poorly understood (Resendes et al., 1999). In neurons VAChT guides the synaptic vesicle to the membrane to be released, whereas in non-neuronal tissues this transporter has not been found yet. Recent studies suggest that in the gut this role is carried out by the organic cation transporters (OCT), as isoforms OCT1, 2 and 3 have been found expressed in colonic epithelium (Bader, Klein and Diener, 2014).

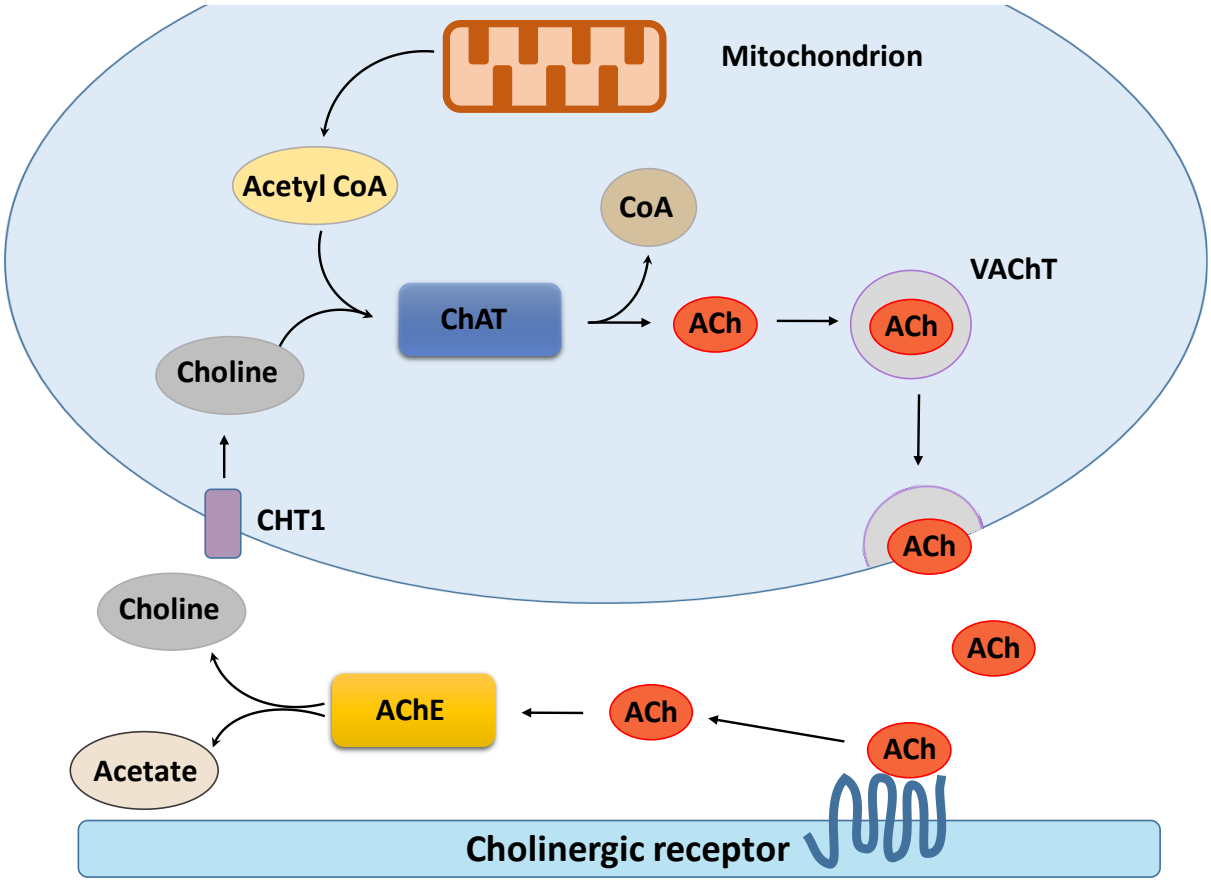

Figure 1.15. Synthesis of ACh. In neurons, the enzyme choline acetyltransferase (ChAT) synthetises ACh from acetyl CoA resulting from the mitochondrial metabolisation of pyruvate and choline coming from previous ACh degradation. ACh is brought into vesicles and transported to the membrane by the vesicular acetylcholine transferase (VAChT). ACh is released into the synaptic space to stimulate cholinergic receptors and rapidly degraded by the enzyme acetylcholinesterase (AChE).

1.7.1 Enteric nervous system

In the gut, neuronal ACh is secreted by the cholinergic neurons of the enteric nervous system (ENS). The enteric nervous system is a division of the peripheral and autonomic nervous system that innervates the digestive system of vertebrates. The ENS is formed of an intricate network of neurons and glia cells that are gathered into ganglia situated in two important plexuses: the myenteric and the submucosal plexus, which cover the whole gastrointestinal (GI) tract (Furness, 2012) (**Fig.1.16)**. The ENS, although not fully autonomous, directs all the critical functions of the digestive system such as the motility control of the digestive tract, vascular blood flow, fluid exchange through the gut mucosa and secretion of gut hormones (Sasselli, Pachnis and Burns, 2012). The total government of the GI tract is carried out by the coordinated action of the enteric neuronal signalling, signals that pass through sympathetic ganglia and other neuronal signals that pass from the gut back through the central nervous system (CNS) (Furness, 2012). The myenteric plexus mainly controls muscle contraction and intestinal motility whereas the submucosal plexus' major role is to regulate epithelial transport. The nerve extensions of the enteric neurons and glia cell are in close proximity with the epithelial layer or cells which facilitates mutual communication through the release of different substances. More recently the ENS has also been implicated in maintaining gut epithelial homeostasis and barrier function by regulating cellular permeability, mucus secretion, tissue repair and intestinal epithelial proliferation (Neunlist et al., 2013; Walsh and Zemper, 2019). The ENS interacts with the intestinal epithelium and communicates by exchanging paracrine signals (**Figure 1.16**). Enteric neurons can regulate the epithelial barrier by secreting ACh to increase paracellular and transcellular permeability (Cameron and Perdue, 2007; Reynolds et al., 2007). ACh has also been shown to activate immune cells like eosinophils and mast cells to mediate barrier dysfunction during ulcerative colitis (Wallon et al., 2011). Conversely, the vasoactive intestinal polypeptide (VIP) has been shown to reduce paracellular permeability (Neunlist et al., 2003).

The ENS is also composed by glia cells which were long thought to be mere mechanical support for the enteric neurons. Recent discoveries have demonstrated that glial cells can help regulate intestinal epithelial permeability through their secreted mediator, S-Nitrosoglutathione (GSNO) by improving expression of tight junction proteins (Cheadle et al., 2013). Glia cells have also been reported to play an important role in tissue repair (Van Landeghem et al., 2011). As discussed before, ACh is known to be a potent secretagogue for mucus in goblet cells which helps maintain the epithelial barrier and expel any potential threat (Specian and Neutra, 1980).

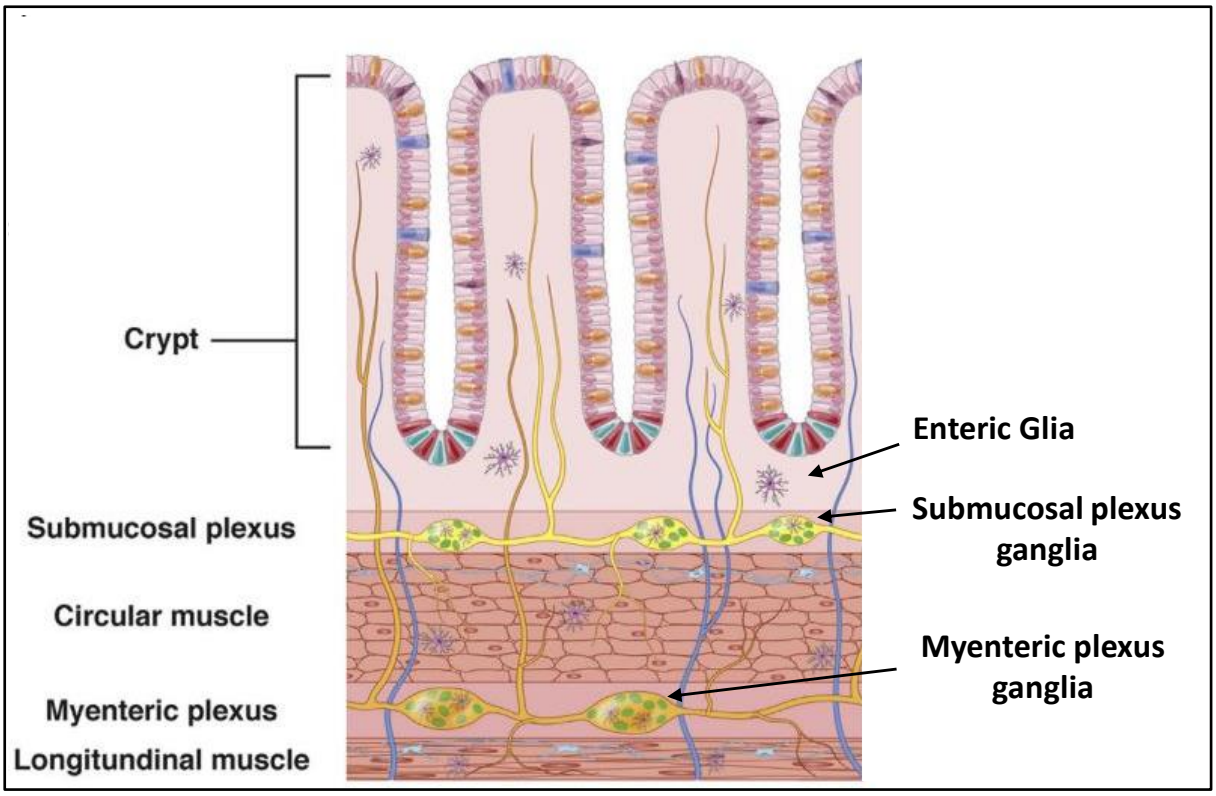

Figure 1.16 Anatomy of the enteric nervous system. The enteric nervous system is arranged into a complex network of neurons and enteric glia gathered into ganglia. The myenteric plexus is located in between the longitudinal and circular muscle layers. The submucosal plexus is situated in between the circular muscle layer and the mucosa. Enteric glia and neurons innervate the entire gut and are in close proximity to the epithelial cells. Figure adapted from Walsh et al., 2019.

The ENS has been suggested to modulate cell proliferation in the gut. Serotonin secreted by enteric neurons has been shown to induce crypt proliferation, crypt depth and villus height (Gross et al., 2012). ACh secreted by cholinergic neurons has also been implicated in controlling proliferation: researchers have demonstrated that it can induce epithelial growth in gastric organoids (Hayakawa et al., 2016) and cell proliferation in human cell lines (Cheng et al., 2008). A recent study in nematodes by Labed et al. proposed that upon infection, cholinergic neurons signal ACh to induce Wnt production in gut epithelial cells. Wnt production in turn induces the expression of lectins and lysozyme which are potent antimicrobials (Labed et al., 2018). Conversely, noradrenaline has been suggested to reduce cell proliferation as observed in small intestinal organoids (Davis, Zhou and Dailey, 2018). Enteric neurons can signal enteroendocrine cells (EECs) in the gut epithelium and recent data suggest this interaction could be via synapsis. Kaelberer and colleagues showed that this population of enteroendocrine cells, called neuropods, can signal to vagal neurons using glutamate as a neurotransmitter and this signal can be transmitted to the brain (Kaelberer et al., 2018). EECs

can also secrete serotonin to stimulate enteric neurons to induce muscle contractions (Nozawa et al., 2009) and have recently been proposed as chemosensors to integrate different luminal signals ,and convey this information to the serotonergic neurons (Bellono et al., 2017). Tuft cells have been reported to also play and important role in mediating ENS proliferative signals to the epithelium as enteric neuron signals are required for maintaining tuft cells in culture (Westphalen et al., 2014). In addition, tuft cells produce and secrete ACh which could signal to enteric neurons to enable bidirectional communication (Schneider, O'Leary and Locksley, 2019).

Finally, enteric neurons have been heavily linked with the onset of cancer. Presence of dense innervation within tumours is correlated with a short-term survival. Recent studies demonstrated that denervation of cholinergic neurons in the stomach and pancreas was linked with a reduction in $LGR5^+$ stem cells and weakening of tumorigenesis (Magnon et al., 2013; Zhao et al., 2014). Hayakawa and colleagues recently demonstrated that release of ACh from cholinergic neurons and tuft cells in tumour cells of the stomach epithelium induces the secretion of nerve growth factor (NGF), which in turn promotes neuron and tuft cell expansion leading to spontaneous gastric tumours. As proposed by Zhao and co-workers, nerve-induced tumorigenesis depends on overstimulation of the Wnt signalling pathway, which is dependent on ACh activation of the cholinergic muscarinic receptor 3 (MAChR3) (Hayakawa et al., 2016). Research on colorectal cancer suggests that tumours can adhere to enteric neuronal networks and use them to migrate and expand through the tissue (Duchalais et al., 2018).

1.7.2 Non-neuronal acetylcholine

ACh has been shown to be produced by non-neuronal cells in organisms like plants, protists, algae and bacteria (Wessler and Kirkpatrick, 2012), as well as in many different human tissues including skin cell keratinocytes (Grando et al., 1993), skin fibroblasts (Kurzen et al., 2004), lung fibroblasts (Matthiesen et al., 2006), immune T and B cells (Kawashima and Fujii, 2003; de Jonge et al., 2005) and differentiated embryonic stem cells (Serobyan et al., 2007). In the intestine, tuft cells express ChAT and are able to secrete ACh through a process whose regulation is still not well understood. Tuft cells have been proposed as luminal sensors. Researchers have recently suggested that epithelial cells of the rat colon secrete ACh in response to luminal addition of the bacterial metabolite propionate, through organic cation transporters located in their basolateral membranes (Yajima et al., 2011; Bader, Klein and Diener, 2014). Takahashi and colleagues reported the existence of non-neuronal ACh producing cells in organoid cultures devoid of neurons and suggested the molecule could regulate proliferation and differentiation of $LGR5^+$ stem cell via activation of cholinergic muscarinic receptors (Takahashi et al., 2014). As discussed before, Hayakawa and co-

workers demonstrated that tuft cells are the major producer of ACh in the stomach together with the cholinergic neurons, and that overexpression of ACh induces nerve overgrowth and promotes carcinogenesis (Hayakawa et al., 2016). In addition to epithelial cells, intestinal immune cells also secrete ACh and have been shown to play and important role in fighting infection. Work in mouse demonstrated that upon pathogen infection, a population of $CD4^+$ $ChAT^+$ T-cells can be recruited to the colon and secrete ACh to induce expression of IFN-γ and nitric oxide to aid host defences (Ramirez et al., 2019).

1.7.3 Muscarinic-acetylcholine receptor signalling

Cholinergic receptors constitute a family of membrane signal integrators formed by the muscarinic and nicotinic receptors which are expressed in both neuronal and non-neuronal cells throughout the body and regulate distinct physiological functions according to their location and receptor subtype (Tiwari et al., 2013). Although they can both be activated by binding of ACh, their structure and mechanism of action vary. Nicotinic receptors are ionotropic receptors and upon activation they form an ion channel in the membrane. This change in conformation allows influx of cations into the cell causing depolarisation of the membrane and an action potential depending on the strength of the signal. Muscarinic receptors are G-coupled protein receptors which generate second messengers when activated by ligand binding (Albuquerque et al., 2009).

1.7.3.1 Muscarinic receptors

Muscarinic acetylcholine receptors (MAChR) are part of the G-protein-coupled receptors family, and they are organised in five subgroups; M_1 to M_5. Muscarinic receptors are encoded by intronless genes and exhibit a high sequence homology across species (Eglen, 2006). GPCRs receptors are the largest family of signalling proteins in animals and structurally they are formed by seven trans-membrane domains. The current view sees them as dynamic proteins that are able to change conformational states; this plasticity allows them to interact with a wide variety of ligands and induce different spatio-temporal signals (Wootten et al., 2018). Activation of GPCRs promotes its association with a heterotrimeric G protein composed of three subunits, the Gα monomer and the Gβγ dimer. When inactive, Gα binds to GDP but activation of GPCR induces the release of GDP and subsequent binding of GTP. This event leads to conformational changes that result in separation of the Gα and Gβγ subunits which will then go on to activate different effector proteins (**Figure 1.17**). Gα can activate proteins such as adenylyl cyclase (catalyser of cyclisation of ATP into cAMP), phospholipase C or RhoGEFs (GTPase regulators), which in turn activate other intracellular signalling pathways. Gβγ can recruit proteins to the membrane such as G protein-coupled receptor kinases

(GRKs) as well as regulate the activity of ion channels, protein kinases or phospholipases to modulate other signalling pathways (Mahoney and Sunahara, 2016). Importantly, GPCRs undergo cycles of dynamic trafficking regulated by their own ligands in a key process that ensures desensitisation of signalling transducer, change in mode of signalling and downregulation of the receptor response and subsequent degradation. GPCRs can be internalised into endosomes by forming a complex with the arrestin protein and carried to the Golgi apparatus and other intracellular sites to exert non-canonical signalling (Wootten et al., 2018).

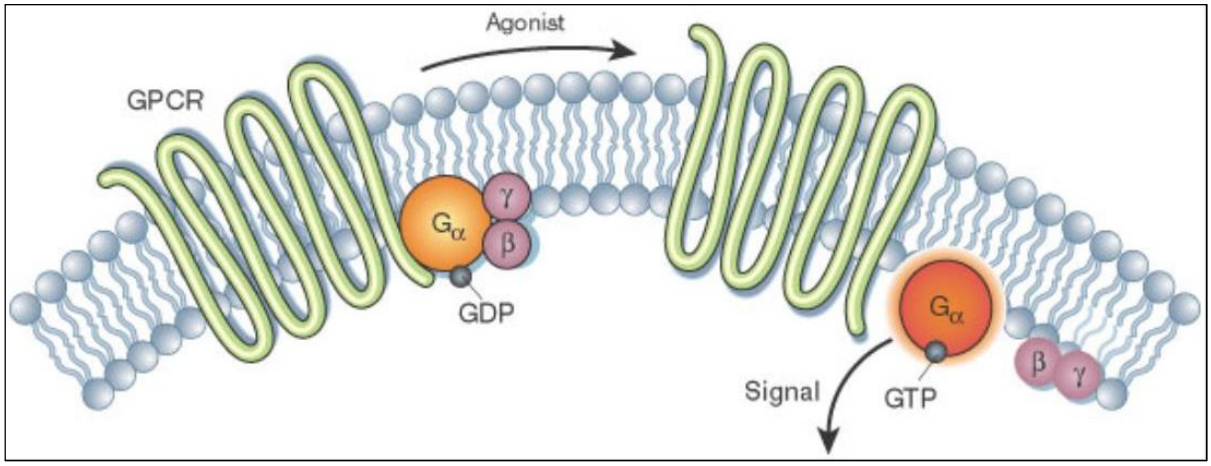

Figure 1.17. GPCR activation. Upon binding of an agonist, GPCRs associate with a complex of G proteins formed by Gα, Gβ, Gγ. Activation of the complex leads to the exchange of Gα-bound GDP for GTP causing the separation of the protein complex into a Gα monomer and a Gβγ dimer. Each complex subunit becomes active to modulate of specific effector proteins. Figure adapted from Li et al., 2002.

The different muscarinic subtypes have different modes of action. Upon triggering, M1, M3 and M5 act through $G\alpha_q$ proteins to activate phospholipase C (PLC) that produces inositol trisphosphate (IP3) and diacylglycerol (DAG) and eventually an intracellular increase of calcium, whereas M2 and M4 act through $G\alpha_i/G\alpha_0$ proteins to inhibit adenylate cyclase decreasing the production of the second messenger cyclic AMP (cAMP) (Nathanson, 2008). As a result of separate receptor physiology and different signalling transduction, muscarinic receptors can modulate a great variety of signals. Characterisation of the muscarinic distribution along the intestinal epithelium, and in particular in the colon, showed that M3 is the dominant receptor and that it is expressed in the basolateral membranes along the tissue (Dickinson, Frizzell and Sekar, 1992; O'Malley et al., 1995; Reynolds et al., 2007). In addition, M1 receptors have been also reported to be present in mouse colon and to contribute in ion secretion induced by cholinergic stimulation (Haberberger, Schultheiss and Diener, 2006).

As described previously, ACh-induced muscarinic activation in the gut is involved in several physiological responses which include regulation of cellular permeability (Reynolds et al., 2007), mucus secretion (Specian and Neutra, 1980), tissue repair and intestinal epithelial proliferation (Walsh and Zemper, 2019). In addition, muscarinic receptors have been shown to be involved in development of ulcerative colitis (Hirota and McKay, 2006) and the development and progression of gastrointestinal cancer (Raufman et al., 2008; Zhao et al., 2014; Hayakawa et al., 2016).

1.8 Intracellular calcium signalling

Tissue development and regulation is organised by a compendium of intricate cellular processes. Calcium is a highly resourceful signalling ion that can integrate a sophisticated network of signalling pathways to regulate cell physiology and cellular responses to the tissue environment. In cells, calcium signals operate as transient increases of cytosolic free calcium that originate from the release of calcium to the cytoplasm from outside the cell or from intracellular calcium stores (Dodd, Kudla and Sanders, 2010). When calcium signals are triggered, the nature of the stimulus determines the frequency and amplitude of the calcium flux to the cytoplasm, which occurs in the form of repetitive oscillations. The spatio-temporal characteristics of this calcium oscillations determine the type of cellular response which ranges from extremely quick events like neurotransmission or muscle contraction to much slower responses such as cell proliferation, division, differentiation and apoptosis (Dupont et al., 2011).

The concentration of intracellular free calcium varies depending on its location. During homeostasis, the baseline calcium concentration in the cytoplasm is approximately 100 nM, which is 10^4 lower than the extracellular one, set to be around 1 mM. Other organelles that function as calcium stores like the endoplasmic reticulum (ER) or the sarcoplasmic reticulum (SR) in the smooth muscle, and endolysosomes contain higher concentrations than the cytoplasm (1 mM-3 mM and ~500 μM respectively) (Bagur and Hajnoczky, 2017). The intracellular calcium is regulated by a series of calcium transporters. Under resting conditions, the plasma membrane Calcium ATPase (PMCA) and the Na^+/Ca^{+2} exchanger (NCX) maintain the concentration of calcium in the cytoplasm. When calcium is released into the cytoplasm and the concentration increases, other transporters like the SE Calcium-ATPase (SERCA) pump can refill the ER/SR with Calcium in order to regain the homeostatic conditions (Bagur and Hajnoczky, 2017) (**Figure 1.18**).

Each cell type is composed of different types of channels, pumps and other molecules from the calcium signalling toolkit with different characteristics which are adapted to the physiological properties of the cell (Berridge, Lipp and Bootman, 2000). Generally, the mechanism of calcium

signalling integration in mammalian cells starts with a signal that can be membrane depolarisation in excitable cells (Catteral, 2011), stretch forces (He et al., 2018) or just a specific ligand sensed by a membrane receptor (GPCRs such as muscarinic receptors and receptor tyrosine-kinase such as EGF receptors), as well as signals derived from an internal store. The downstream effect of the signal is the release of calcium from the intracellular stores which results in a steep increase in the calcium concentration, followed by a decay which originates cytoplasmic calcium oscillations, aided by the different positive or negative feedback. These oscillations are promoted by the activation or deactivation of intracellular calcium channels and the calcium channels that maintain a calcium gradient across the different cellular compartments (SERCA pump in the ER/SR, PMCA pump and NCX in the membrane) (Brodskiy and Zartman, 2018) (**Figure 1.18**). The regulation of cytosolic calcium concentration is key because of all the important physiological processes that calcium modulates, therefore aberrant signalling can induce cell dysregulation and death (Berridge, 2016; Pchitskaya, Popugaeva and Bezprozvanny, 2018).

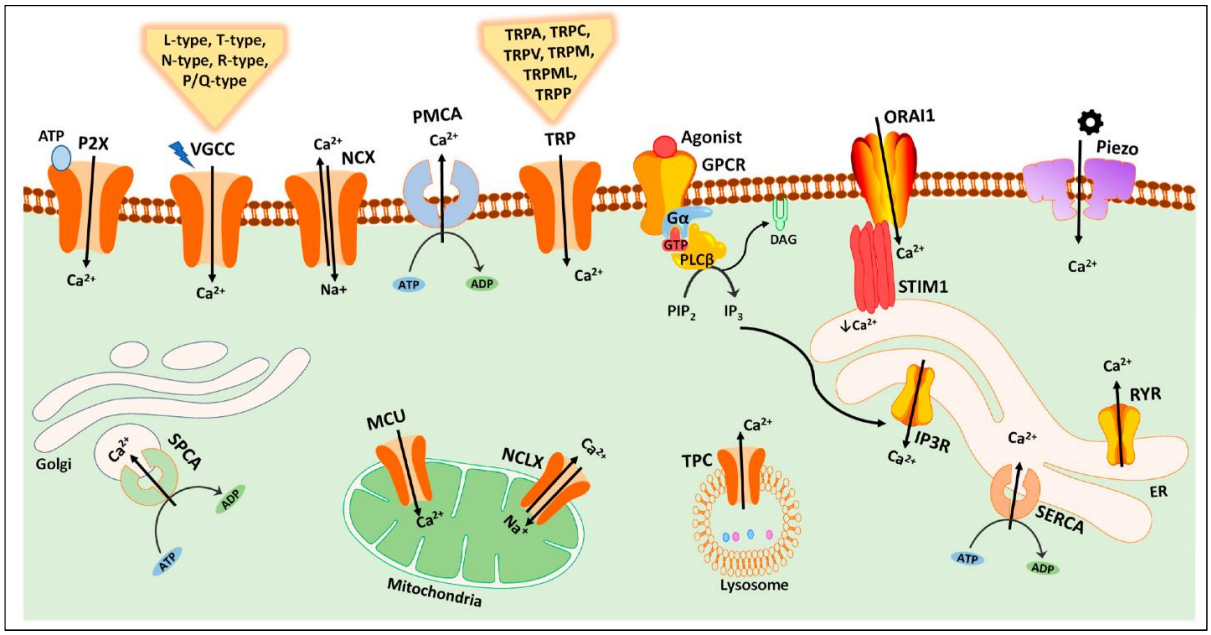

Figure 1.18. Overview of the main cellular calcium channels, pumps, exchangers and sensors. Calcium influx into the cells is regulated by a series of channels such as store-operated calcium channels like ORAI1 and STIM1 channels, voltage-gated calcium channels (VGCCs), ligand-gated ionotropic P2X receptors and mechanosensitive Piezo channels. Intracellular calcium stores can secrete calcium into the cytoplasm through inositol 1,4,5-trisphosphate receptors (IP3Rs) and Ryanodine receptors (RyRs) in the endoplasmic reticulum, mitochondrial Na^{+}/Ca^{+2} exchanger or the endolysosomal two-pore channels (TPCs). Calcium can be pumped back into the intracellular stores by the SE Calcium-ATPase (SERCA) and the mitochondrial calcium uniporter (MCU) and released out

of the cell by the plasma membrane Calcium-ATPase (PMCA) and Na^{+}/Ca^{+2} exchanger (NCX). Figure adapted from Maklad et al., 2019.

The information that the cytoplasmic calcium signals carry can be decoded when calcium binds to a series of different effectors, which contain calcium binding motifs. In this way, calcium can bind to other calcium channels such as IP3Rs or RyRs, cytoplasmic enzymes (Calcineurin) and proteins that associate with other effector proteins (Calmodulin); all of which will function in different ways depending on the nature of the signal and their localisation. The majority of proteins can bind calcium through their EF-hand motifs which induces a conformational change and function (Ikura, 1996). The EF-hand domains can bind calcium with different affinity, and proteins with high affinity (Calbindin) can buffer cytoplasmic calcium modulating the duration of the signal (Gifford, Walsh and Vogel, 2007). Calmodulin (CaM) is a well characterised calcium sensing protein which can identify variations in calcium concentration and generate a downstream response by targeting effector proteins (Cheung, 1979). CaM has four calcium binding sites which upon activation by calcium change structure and reveal an opening in the protein that can be used to bind its targets (Bagur and Hajnóczky, 2017). CaM can rapidly bind and activate its target enzymes such as calmodulin kinase (CaMK) or calcineurin (CaN) when the levels of cytoplasmic calcium are high. When the levels are low or homeostatic, CaM can still form a low affinity complex with its targets but still needs an increase in calcium to activate them. Such functioning confers this mechanism with a sensitive switch for controlling the enzyme activity with low differences in calcium concentration (Kincaid and Vaughan, 2006). In addition, the CaM calcium-free form (Apo-CaM) can also bind a different number of target proteins to modulate different cellular responses (Jurado, Chockalingam and Jarrett, 2019).

The enzyme CaMK is one of the main targets of CaN which acts as a phosphatase of target proteins when activated by CaM (Saucerman and Bers, 2008). The CaMK can autophosphorylate to increase its affinity for CaM at low concentrations of calcium. As the frequency of oscillations increases, CaMK can recruit more CaM molecules dissociated from other CaM targets and become increasingly active (Meyer et al., 1992). CaN is another member of the decoding components of the calcium toolkit that can be activated directly by calcium through interaction with its EF-domain, as well as by CaM. When active, CaN acts as a phosphatase catalysing the dephosphorylation of downstream targets implicated in important functions such as lymphocyte activation, neuronal and muscle development and morphogenesis of vertebrate heart valves (Crabtree, 2001). Downstream targets of activated CaMK include transcription factors like the serum response factor (SRF) which once phosphorylated can translocate to the nucleus. Once inside, SRF can bind to the serum response element (SRE) which is associated with a variety of genes that control cell growth and differentiation, neuronal

transmission and muscle development (Miranti et al., 1995; Chai and Tarnaswski, 2002). Activated CaMK can also activate the cAMP-response element binding protein (CREB) by phosphorylating it, which in turn regulates gene expression of regulators of nervous system development, cell proliferation and survival (Shaywitz and Greenberg, 1999). The transcription factor NFAT (nuclear factor of activated T-cells) is another downstream target of intracellular calcium signals. Increase in intracellular calcium activates CaN via CaM activation to dephosphorylate NFAT and allow nuclear translocation (Jain et al., 1993; Garcia-Cozar et al., 1998).

NFAT was first identified as an inducible nuclear factor which binds to the interleukin-2 (IL-2) promoter, upregulating its transcription following stimulation of T-cell antigen receptor (Shaw et al., 1988). NFAT belongs to a family of proteins that include NFATc1 (NFAT2), NFATc2 (NFAT1), NFATc3 (NFAT4), NFATc4 (NFAT3) and NFAT5, and are present in many cell types. NFAT binds to its gene targets with relatively low affinity and it is thought to regulate gene expression partnering with other transcription factors like Fos and Jun (Chen et al., 1998), making NFAT a potential integrator of different signals (Buchholz and Ellenrieder, 2007). Inactivation of nuclear NFAT occurs when it is re-phosphorylated by specific kinases such as the glycogen synthase kinase 3 (GSK3), that induce its translocation back to the cytoplasm (Neal and Clipstone, 2001). NFAT proteins have been linked with regulating numerous physiological processes like the development and differentiation of the cardiovascular system (Mammucari et al., 2005). NFATc1 has been linked with regulation of cell proliferation and apoptosis of epithelial cells, fibroblasts and adipocytes (Hogan et al., 2003; Neal and Clipstone, 2003). Other members of the NFAT family have been demonstrated to modulate angiogenesis (Graef et al., 2001) and apoptosis of immune cells (Chuvpilo et al., 2002). In the colon NFATc1 and NFATc3 have been identified as having potential roles in tumour development (Tripathi et al., 2014; Peuker et al., 2016). Work done by Peuker and colleagues demonstrated that NFATc3 was expressed in primary human colorectal cell lines and that it can be CaN-dependent activated upon binding of microbiota antigens to TLRs in the membrane of epithelial cells. These events demonstrate that a weak epithelial barrier can result in bacterial activation of stem cell tumorigenesis (Peuker et al., 2016). According to their hypothesis, activated TLRs induce PLC-γ-mediated release of calcium from the ER via IP3Rs which in turn activates store-operated calcium entry through calcium release-activated channels. Increased cytosolic concentration of calcium subsequently activates CaM-CaN; this activates NFAT promoting translocation to the nucleus. By inducing overexpression of NFATc3 in mouse, Peuker et al. showed an increase in tumour formation that was dependent on the presence of functional calcineurin, while blocking of NFATc3 expression ameliorated its progression. In addition, these researchers found that wild-type mice expressed predominantly cytoplasmic NFATc3 in $LGR5^{+}$ ISCs suggesting unaffected proliferation in those cells,

while knockdown of CaN was associated with decreased LGR5 expression in human cancer cell lines and in mice. Previous work has showed that Wnt signalling is key for maintain $LGR5^+$ ISC biology (Clevers, Loh and Nusse, 2014) and that Wnt signalling promotes activation of NFAT (Takeo et al., 2002; Köenig et al., 2010). Moreover, chromatin immunoprecipitation (ChIP)-qPCR analysis determined that NFATc3 exhibited calcineurin-dependent binding to the promoters of Cd44, LGR5, OLFM4 and Dclk1 in intestinal tumors *in vivo*. Taken together, these resutls suggest that calcium-activated CaN can activate nuclear translocation of NFAT to induce expression of Wnt signalling related genes and promote expression of cell proliferation in $LGR5^+$ stem cells and that a weak epithelial barrier can lead to bacterial induced aberrant signalling resulting in tumorigenesis (Peuker et al., 2016).

1.8.1 Spatial and temporal properties of calcium signalling

The majority of the calcium signalling components are organised in subcellular compartments within the cell that are able to buffer the calcium released into the cytoplasm following a calcium response. The existence of different intracellular calcium stores adds another layer of complexity to the generation of the calcium signals. Each store contains different calcium channels sparsely distributed such as IP3Rs and RyR and some being able to act independently from the main signalling events in the cellular membrane. Calcium can be released from only one channel in what is known as a *blip* and can also be released by multiple channels operating at the same time in what is known as a *puff*. Calcium signals of great magnitude can be propagated to neighbouring cells through GAP junctions (Toyofuku et al., 1998) or via paracrine signalling, which result in intracellular calcium long-range signals or waves (Zumerle et al., 2019) and highlights the ability of calcium to modulate tissues physiology.

The calcium signal responses vary in time depending on their nature. Responses to synaptic activity or cardiac contraction last just nanoseconds to microseconds; mechanical or wound healing responses last seconds while other processes that depend on changes in basal concentration take longer (Justet et al., 2016; Narciso et al., 2017). As mentioned before, oscillations are originated as a result of an increase in cytoplasmic calcium which is followed by a decay when buffered or when calcium channels become inactive in order to restore homeostasis. These oscillations are dynamic and allow for the activation of different downstream effectors in different ways. When a signal induces a fast response to calcium, which is referred to as a spike, it creates a sustained response with high amplitude which decays fast and that does not oscillate. This type of signal can activate targets with low activation threshold like the myosin light-chain kinase (MLCK). This same type of targets are not sensitive to an oscillatory signal of high frequency, low amplitude and slow decay

kinetics. This type of response will activate targets with high activation threshold like NFAT, which needs to integrate calcium signals over time to be fully active (Brodskiy and Zartman, 2018). Other molecules that are responsible for decoding frequency modulated calcium signals include CaMKII (Koninck and Schulman, 1998) and PKC (Oancea and Meyer, 1998). The calcium signal that makes calcium oscillations spread through the cytoplasm as a wave depends of successive rounds of calcium release primarily from clusters of IP3Rs or RyRs and recovery from the SERCA pump in the ER. In addition, most tissues have a population of pacemaker cells that are able to set the pace of oscillations of the neighbouring cells, highlighting the importance of spatio-temporal signals in controlling cellular and tissue processes (Fridlyand, Tamarina and Philipson, 2010). The specificity of the calcium signal effectors can be remodelled to ensure that every key player continues to work properly. In this way, if the spatio-temporal characteristics of an output signal are altered, there is a system that monitors it and there are mechanisms to compensate it (Berridge, Bootman and Roderick, 2003). Calcium-induced calcium signalling has been proposed to be able to regulate its own pathway to fix the activity components that no longer function. Calcium can undertake this role by modulating calcium dependent transcription factors, protein kinases (CaMKs) protein phosphatases (CaN), and gene expression to activate MAPK or cAMP signalling pathways and modify the expression levels of pumps and channels (Berridge, Bootman and Roderick, 2003). Examples of this compensatory mechanisms have been described in mice carrying a mutation in the SERCA2 gene that codes for the SR/ER pump in the heart. These mutations affect the concentration of calcium in the ER which drops by 40-60%. The system is able to balance this situation by increasing the expression of the calcium channels phospholamban and NCX to generate moderate calcium spikes (Ji et al., 2000).

Calcium is well suited to act as a second messenger with a role as a central integrator of different inputs. Its ability to interact and regulate so many functions quickly and efficiently, and to create single messages of multiple stimuli makes it a key ion for maintaining cellular homeostasis. Calcium signalling can regulate a great variety of cellular functions which include morphogenesis, regeneration and wound healing by modulating cell division, death, migration, secretion and differentiation (Brodskiy and Zartman, 2018). Calcium has been shown to be a crucial integrator of stimuli derived from the diet to regulate stem cell biology. In a study by Deng and colleagues in *Drosophila*, the dietary component L-glutamate was shown to activate GCPRs in the membrane and to induce a calcium signalling response mediated by IP3-activation of IP3Rs, as well as from calcium entry via store-operated calcium entry (SOCE). Using the genetically encoded calcium reporter GCaMP and two-photon microscopy live imaging of stem cells, researchers revealed that L-glutamate-induced calcium signals activated a particular pattern of oscillations of low frequency and

high amplitude. These oscillations activated CaN which in turn dephosphorylated the CREB-regulated transcriptional co-activator (Crtc), allowing nuclear translocation and transcription of stem cell genes (Deng, Gerencser and Jasper, 2015). In addition, exposure of ISCs to other factors such as stress or mitogens also induced oscillatory calcium signals with patterns of low frequency and high amplitude that regulated stem cell proliferation. These results proposed that calcium can integrate various signals from the environment to respond appropriately. Moreover, the signals that result in the increase in average calcium concentration in the cytosol are suggested to mediate stem cell regulation and not just the intensity of individual calcium spikes.

1.8.2 Intracellular calcium stores

In order to maintain cytoplasmic calcium levels at low concentration, the cell must store the free calcium. The main intracellular calcium stores are the ER (SR in the smooth, cardiac and skeletal muscle), the mitochondria, the Golgi apparatus, the nucleoplasm reticulum of the nucleus and the endolysosomes. These stores are all tightly controlled and can respond to a variety of stimuli to release calcium into the cytoplasm with different spatio-temporal characteristics. Each organelle contains specific proteins and channels that regulate the whole calcium cycle.

1.8.2.1 Endoplasmic Reticulum

The endoplasmic reticulum represents the major intracellular calcium store in non-excitable cells, and it is implicated in great number of cellular processes. In order to maintain the homeostatic calcium gradient, the ER makes use of a series of enzymes and channels located in its membranes. The ER contains molecular chaperones to buffer calcium, mechanisms to import calcium into ER to increase the calcium concentration, and channels and pores that release or leak calcium into the cytoplasm when stimulated. The crosstalk between these effectors is key in maintaining a balance in the calcium concentration (Carreras-Sureda, Pihán and Hetz, 2018). This balance is also crucial to create a luminal environment needed for the ER to carry out its enzymatic activities such as protein folding or lipid synthesis (Wuytack-2002).

The concentration of free calcium in the lumen of the ER varies between 50 to 500 μM, however the total concentration is approximately 1 to 3 mM. The vast majority of the ER calcium is kept trapped to the buffer chaperone proteins in the membrane. These proteins contain several binding sites or possess a low calcium association/dissociation ratio and are therefore able to catch numerous calcium molecules (Coe and Michalak, 2009). Calnexin (CNX) and calreticulin (CRT) are the main ER chaperones which in addition to binding calcium, can also interact with other channels and pumps in the membrane and modulate their functions. CNX is a transmembrane protein that can act as a

molecular switch and bind to SERCA2b to stop calcium oscillations (Roderick, Lechleiter and Camacho, 2000).

The calcium-ATPase proteins, SERCA pumps, are responsible for importing the cytosolic calcium back into the ER against the gradient, in a process that involves ATP consumption (**Figure 1.18**). They represent a family of various proteins whose expression and characteristics varies depending on the cell type. The ER of vertebrates contains the variant SERCA2 protein, which in humans has two major isoforms; the specialised isoform SERCA2a, found in skeletal and cardiac muscles, and the housekeeping SERCA2b which differs in their affinity to bind calcium. Due to its key role in maintaining cellular calcium gradients, SERCA pumps are tightly regulated and can form multicomplex structures with other proteins like chaperones that vary across cell types and tissues. The SERCA pump can be inhibited by high selective pharmacological drugs such as Thapsigargin and cyclopiazonic acid (CPA) which prevent calcium reuptake and result in depletion of the ER calcium pool. Given the importance of having a balanced calcium concentration, the influx of calcium into the cell from the SOCE plasma membrane calcium channels modulate ER functioning. The SOCE complex is composed of calcium release-activated calcium channels (CRAC), of which ORAI proteins are the most relevant. The ORAI proteins are formed by the mammalian homologues ORAI1, 2 and 3 are located in the plasma membrane. ORAI proteins are activated by direct interaction with the STIM proteins in the ER. Upon activation, ORAI proteins organise into multimer structures, this allows them to create CRAC channels or pores that permit flux of calcium into the cytoplasm. The potent pharmacological agent 2-APB blocks the receptors stopping the calcium influx (Smyth et al., 2010). The stromal interaction molecules (STIM) protein STIM1 and STIM2 are very important in coordinating calcium release and entry signals and regulating calcium homeostasis. Under resting conditions, they are distributed throughout the ER and can be triggered when the ER calcium levels are low. These circumstances promote its rapid translocation into close proximity to the plasma membrane where they create special junctions by interacting with ORAI proteins. This activation results in the entry into the cell of calcium ions which provides a special local signal. The inactive form of STIM under resting conditions binds calcium through the EF-hand domain but decreased ER calcium levels makes calcium dissociate which results in activation and oligomerisation of STIM. Conversely, when calcium levels are restored, STIM detaches from ORAI protein complex and binds to calcium to become deactivated (Soboloff et al., 2012).

The release of calcium from the ER is mediated by the IP3Rs and the RyRs (**Figure 1.18**). IP3Rs are commonly activated by its physiological ligand IP3 which is produced in the cytoplasm downstream of the activation of GPCR membrane receptors in response to diverse stimuli (Mak and Foskett,

2015). IP3Rs were physiologically characterised by the development of patch clamp electrophysiology techniques. Because of the intracellular location of the ER, these techniques were only successful when applied in isolated nuclei where the nuclear membrane continues with the ER. By exchanging culture bath solutions with different ionic environments, the patch clamps can detect dynamic responses of the IP3R channels (Mak et al., 2013). In mammals, the IP3R is expressed in all types of cells and so far, three different isotypes have been described (IP3R1, IP3R2 and IP3R3). Activation of IP3Rs by IP3 starts with the sensing of an external stimuli by the membrane GPCRs or the tyrosine kinase-linked receptors. The triggering of these receptors results in the activation of phospholipase C (PLC) which hydrolyses the membrane lipid phosphatidylinositol 4,5-bisphosphate (PIP_2) to generate IP3 and diacylglycerol (DAG). IP3 diffuses in the cytoplasm and binds to IP3Rs to activate them and induce calcium release (Foskett et al., 2007).

The number and distribution of the calcium binding proteins and the calcium release channels allow the signals from IP3Rs to have different spatio-temporal characteristics, making it a highly versatile and complex signalling mechanism. IP3-induced calcium signals are usually organised to provide different signals in specific regions of the cell. These signals are structured in different levels with different signalling functions. The basic signals are a result of the weak activation of individuals IP3Rs by low concentration of IP3, which induces localised calcium release or blip at discrete sites (**Figure 1.19**) (Parker, Choi and Yao, 1996). When the IP3 signal is stronger, it can activate the opening of multiple IP3Rs organised in a cluster in process called puff (Swillens et al., 1999). The synchronised activation of multiple channels is triggered by the secreted calcium from one of the IP3Rs acting as a ligand to stimulate opening of neighbour channels in a process known as calcium-induced calcium release (CICR). This signalling is modulated by co-localised effector proteins to create different spatial responses in order to induce different cellular actions. When an increased extracellular stimuli induces the concentration of IP3 to become very high, the calcium signal from one cluster can trigger different clusters in a CICR manner capable of generation of calcium waves that propagate in cycles of calcium release, dissemination and CIRC (Dawson, Keizer and Pearson, 1999). The distribution of IP3Rs clusters within the ER and its regulation by IP3 and CICR permit local and long-range calcium signals to be carried out by the actions of single IP3Rs (Foskett et al., 2007).

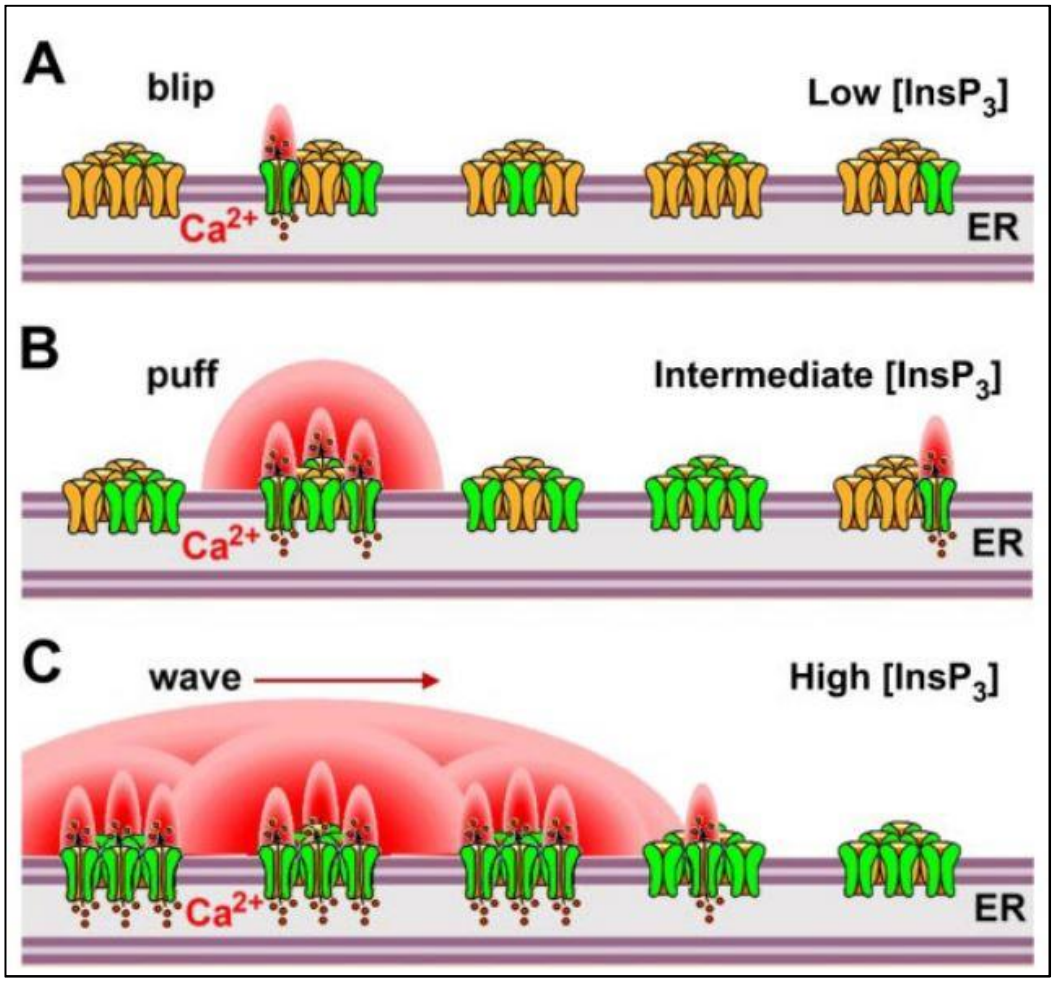

Figure 1.19. Responses of IP3R to different concentrations of IP3. (A) The IP3R are organised in groups. During low concentrations of IP3 only a few IP3Rs are activated, allowing highly localised small calcium responses called "blips". **(B)** When the levels of IP3 are higher, the coordinated opening of IP3Rs is mediated by CICR, whereby calcium release from one channel acts as a ligand to stimulate gating of neighbouring channels. **(C)** Potent stimuli that induce great levels of IP3 result in the global propagation of calcium signals as waves. CICR induced in one IP3R cluster triggers calcium release from other nearby clusters by CICR which induces a calcium wave that propagates by successive cycles of calcium release, diffusion and CICR. Figure adapted from Foskett et al., 2007.

The RyRs are a family of tetramer molecules believed to be the largest ion channels. In mammals, RyRs consist of three different isoforms RyR1, RyR2 and RyR3. These calcium channels reside on the ER or SR membrane forming a macromolecular complex with a wide variety of proteins and calcium channels including L-type calcium channels, protein kinase A (PKA), CaM, CaMKII, and others. This macrostructure interacts with RyR cytoplasmic region regulating the receptor function to open or close the ion channel (Lanner et al., 2010). Activation of RyRs results in amplification of the calcium signalling by means of calcium-activated calcium release and its functions are particularly relevant in

the skeletal muscle and the heart. In skeletal and cardiac muscles, the L-type voltage dependent calcium channels ($Ca_v1.1$ and $Ca_v1.2$ respectively) are voltage sensing and poring forming channels. They are located next to each other so that the molecular mechanism of excitation-coupling (E-C) can occur between them. In skeletal muscle $Ca_v1.1$-RyR calcium release is voltage dependent, whereas in the cardiac muscle, $Ca_v1.2$-RyR calcium release is triggered by extracellular calcium (Lamb, 2000). Mg^{+2} and ATP regulate RyRs in the cytoplasm while calcium can modulate them both in the cytoplasm (directly or via CaM and CaMKII regulation) and in the ER lumen. The changes in cytoplasmic concentration of calcium modulate the RyR1 and while low concentrations of calcium enable activation of the receptor, high concentrations can inhibit it (Meissner et al., 1997). Mg^{+2} has been suggested to be an inhibitor of the RyRs via direct competition with high-affinity calcium activation sites (Meissner, Darling and Eveleth, 1986). RyRs can be activated by adenine nucleotides and ATP is known to be the most efficient activator (Meissner, 1984). In addition, cyclic ADP-ribose (cADPR) has also been shown to modulate CICR function in RyRs (Galione, Lee and Busa, 1991). CaM can also regulate RyRs function. When bound to calcium, CaM inhibits RyRs whereas when not bound to calcium, it acts as a partial agonist (Lanner et al., 2010). Phosphorylation is a crucial event that modulates the calcium release from the ER/SR and the current view is that proteins like PKA and CaMKII induce RyR activation by phosphorylating the receptor, promoting calcium release to the cytoplasm. Ryanodine, a plant alkaline, is a pharmacological selective blocker at high concentrations (Meissner, Darling and Eveleth, 1986).

1.8.2.2 Mitochondria

The mitochondria are organelles with many important functions that regulate cellular physiology such as energy production and cell death. These organelles also play an important role as a regulator and decoder of calcium signals. Mitochondria can localise at specific sites in the cell shaping the spatial and temporal characteristics of the calcium signal. The mitochondria can absorb large quantities of cytosolic calcium and increase its concentration from 100-200 nM to 1-2 µM (Giorgi, Marchi and Pinton, 2018). By being able to collect large amounts of calcium in specific cellular locations, these organelles can moderate the propagation of calcium waves and therefore regulate the processes of those calcium signals (Contreras et al., 2010). In order to enter the mitochondria, calcium needs to pass first the outer mitochondrial membrane (OMM) and then the inner mitochondrial membrane (IMM). The OMM is highly permeable to calcium channels thanks to the voltage-dependent anion-selective channel proteins (VDACs) which form a pore in the membrane to allow flux of calcium and other molecules like ADP and ATP. In order to enter the IMM, calcium generally passes through the mitochondrial calcium uniporter (MCU) complex, which is the

dominant calcium entry mechanism (Ryu et al., 2010) (**Figure 1.18**). The MCU complex is formed of a channel forming protein, the MCU protein, accompanied by other regulators such as the mitochondrial calcium uptake protein 1 (MICU1) and 2 (MICU2) which form a dimer and first bind to incoming calcium. MICU1 and MICU2 function as gatekeepers and activate MCU only at high calcium concentrations (Mallilankaraman et al., 2012).

Mitochondria localisation next to the ER is crucial in regulating calcium signalling. The mitochondria and the ER form inter-organelle associations, named mitochondria-associated membranes (MAMs) (Giorgi et al., 2015). This contact sites ensure that calcium can be taken up by the MCU complex when calcium release is induced in the ER IP3Rs. Depending on the intensity and pattern of the calcium signalling, the mitochondria can exhibit different functions (van Vliet, Verfaillie and Agostinis, 2014). When the mitochondria receives high frequency oscillatory calcium signals, it triggers respiration and production of ATP via activation of calcium dependent enzymes (Tarasov, Griffiths and Rutter, 2012). Basal calcium transfer to the mitochondria is necessary to avoid mitochondrial energetic failure (Cárdenas et al., 2010) but prolonged calcium uptake can activate mitochondrial-induced cell death (Pinton, Romagnoli and Giorgi, 2008). The mitochondria can also connect with the plasma membrane creating the plasma membrane-associated mitochondria (PAM) (Suski et al., 2014) and uptake calcium upon the activation of CRACs in the membrane. Mitochondria can secrete the accumulated calcium into the intermembrane space through the mitochondrial Na^{+}/Ca^{+2} exchanger (mNCX), present predominantly in excitable tissues, and H^{+}/Ca^{+2} exchanger (mHCX) expressed in non-excitable cells. From the mitochondrial lumen, calcium is then released into the cytoplasm via VDACs (Brodskiy and Zartman, 2018).

1.8.2.3 Nucleus

The nucleus together with the ER and mitochondria also works as an autonomous calcium signalling system that is able to produce and process its own calcium transients (Bootman et al., 2009). This important organelle is protected by the nuclear envelope (NE) which controls the transport of molecules and ions, regulates gene expression and acts as a platform for cellular signalling (Malhas, Goulbourne and Vaux, 2011). The NE can create a series of complex branched network invaginations across the nucleus, referred to as the nucleoplasmic reticulum (NR) because of its morphological similarities with the ER. This structure if formed by an inner nuclear layer (INM) and an outer nuclear membrane (ONM) which creates an intermediate space (IMS). The presence of this structure increases the surface-to-volume ratio in the nucleus, enabling the exchange of calcium. The NR invaginations can store calcium in the lumen and present similar calcium release and uptake mechanism to the ER such as IP3Rs, RyRs and SERCA pumps (Malhas, Goulbourne and Vaux, 2011).

IP3Rs are expressed both in the ONM and in the INM; the latter can trigger the release of calcium from the NE lumen into the nucleoplasm. In addition, IP3Rs have been suggested to be present in small vesicles within the chromatin (Seung et al., 2007). The calcium sensing protein CaM has also been reported to be present inside the nucleus, as it can be translocated upon cellular stimulation (Wu and Bers, 2007).

A controversial issue within the nuclear calcium signalling is whether the calcium signals can be generated by the NE or they depend on signals originated from the cytoplasm. Perinuclear calcium signals, that is, calcium signals occurring immediately outside the nucleus, have been reported to cause calcium elevations within the nucleoplasm (Chamero et al., 2002). Changes in the calcium concentration in the nucleosome have been shown to be happening only in that organelle and not anywhere else in the cell, although researchers could not conclude whether they had been originated inside the nucleus (Luo et al., 2008). Recent studies demonstrate that nuclear calcium signalling modulates gene transcription and cell progression. As described before, calcium signals activate CaN to allow translocation of NFAT and CaN to the nucleus. When calcium concentrations are high in the nucleus, CaN remains actively bound to NFAT promoting gene transcription and preventing it from being deactivated by phosphorylation (Bootman et al., 2009).

1.8.2.4 Endolysosomes

The endolysosomes are acidic organelles that originate from the endocytosis of the plasma membrane, mature into late endosomes and later form endolysosomes by merging with lysosomes. First discovered by Metchnikoff at the beginning of the 20th century, lysosomes are responsible for some crucial cellular physiological process which include the enzymatic degradation of endocytosed, phagocytosed and autophagocytosed macromolecules, nutrient sensing, and calcium signalling (Luzio, Pryor and Bright, 2007).

The lysosomal membrane contains heavy glycosylated membrane proteins named lysosomal-associated membrane proteins (LAMPs) which coat the luminal side of the membrane and prevent the degradation by the acid hydrolases (Settembre et al., 2013). In addition, the lysosomal membrane also contains proteins that regulate the traffic of molecules to be degraded and proteins that maintain intracellular pH and regulate ion transport. The pH inside the lysosome is around 5 to favour enzymatic hydrolysis of target macromolecules, and in order to maintain it, the organelle contains pumps that translocate H^+ into the lumen (Morgan et al., 2011). The vacuolar-type H^+-ATPase (V-ATPase) utilises ATP to pump H^+ inside the lysosome. This enzyme is tightly regulated in order to maintain the pH acidic and the potent inhibitors like Bafilomycin block it resulting in the

alkalinisation of the organelle and release of intracellular calcium. In addition, lysosomes contain H^+ exchangers that release H^+ and replace it with other cations or anions to regulate the pH. Cation exchangers inhibit organelle acidification by pumping in Na^+ and extruding H^+, whereas anion exchangers release H^+ and pump in $2Cl^-$ to neutralise the charge. In addition, lysosomes present the electrogenic pump Na^+/K^+-ATPase which pumps in $3Na^+$ and releases $2K^+$ and used to control lysosomal acidification. The intraorganelle pH is determined by the pump and leak ratio of H^+. Calcium storage in the endolysosomes is achieved by the Ca^{+2}/H^+ exchanger and regulated by the V-H^+-ATPase (Morgan et al., 2011).

Endolysosomal calcium can be released through the Two-pore channels (TPCs) (**Figure 1.20**) upon binding of nicotinic acid adenine dinucleotide phosphate (NAADP). NAADP was discovered to induce calcium release in homogenates of sea urchin by a different mechanism and from different calcium stores than the ones regulated by IP3 and cADPR (Galione et al., 2010). NAADP is synthesised by the ADP-ribosyl cyclase CD38 from the substrate $NADP^+$. Alternatively, CD38 can also synthesise cADPR from NAD^+. The enzyme CD38 has been found to be associated with the endolysosomes which suggests an important function in regulating NAADP-induced calcium release from the endolysosomes (Galione et al., 2010). The TPC belong to a family of voltage-gated ion channels located in the endolysosomes and arranged to create two pores (**Figure 1.20**). In human, two subtypes have been identified: TPC1 and TPC2 (Calcraft et al., 2009). NAADP was first discovered to induce calcium secretion in a sea urchin egg model by Churchill and colleagues (Churchill et al., 2002) and although it has been shown to activate RyRs, its main target was confirmed to be the TPC (Brailoiu et al., 2009; Calcraft et al., 2009; Zong et al., 2009; Ogunbayo et al., 2011). The regulation of TPC by NAADP is still not fully understood although the general view is that these channels are primarily modulated by NAADP and can be also co-regulated by $PI(3,5)P_2$, Mg^{+2} and MAPKs (Jha et al., 2014), as well as being permeable to Na^+ and Ca^{+2}. TPCs can be inhibited by the pharmacological drugs Ned-19, an NAADP antagonist, and by L-type channel blockers like diltiazem (DZM) (Genazzani et al., 1997; Naylor et al., 2009).

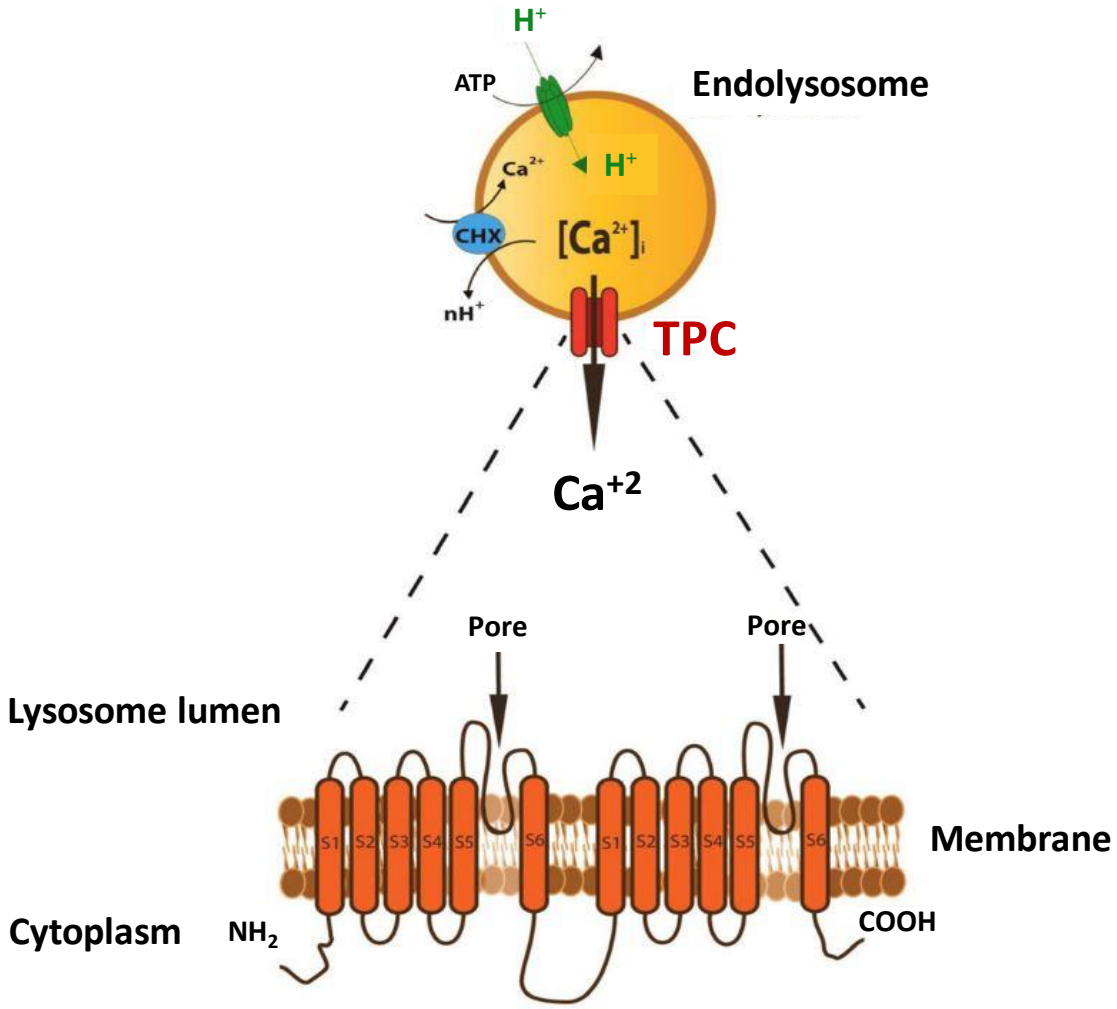

Figure 1.20. Channels of the endolysosome. Endolysosomes uptake calcium from the Ca^{+2}/H^{+} exchanger (CHX) located in the membrane. Calcium can be secreted into the cytoplasm through two-pore channels (TPCs) which are transmembrane proteins forming two pores in the membrane. The endolysosomal pH is regulated by the vacuolar-type H^{+}-ATPase which is dependent of ATP. Figure adapted from Parrington et al., 2015.

Endolysosomes are highly dynamic and change in shape, volume and position within the cell. These organelles can contact the ER to create microdomains by membrane contact sites and provide local calcium signals. It is thought that NAADP-induced calcium release can trigger calcium release from the ER to amplify the signal and convert them into global cytosolic calcium responses. In the heart, calcium release via TPC increases the RyR-mediated calcium spikes (Macgregor et al., 2007). Moreover, endolysosomes can buffer cytosolic calcium around the ER to inhibit IP3R-induced calcium release (López-Sanjurjo et al., 2013). The dialogue between both calcium stores is believed to be bidirectional. Retrograde signals from the ER to the endolysosomes also occur and although

not fully understood, it has been suggest that ER calcium release could trans-activate the NAADP pathway and possibly induce an endolysosomal CICR (Morgan, 2016).

Besides the ER amplification of the endolysosomal calcium signal, growing evidence indicates that these organelles can produce their own local calcium signals to regulate other cellular process like autophagy. As part of their role in nutrient sensing, lysosomes have been shown to bind to the mammalian target of rapamycin complex 1 (mTORC1), which is a master regulator of cell growth (Laplante and Sabatini, 2012). mTORC1 is activated by a variety of stimuli including growth factors, hormones, amino acids, glucose, oxygen and ROS to regulate the balance between biosynthetic and catabolic states. When nutrients are present, mTORC1 is able to induce autophagosome biosynthesis, whereas during starvation, mTORC1 is inhibited and released from the lysosomal membrane which promotes the nuclear translocation of TFEB to induce transcriptional activation of autophagy (Settembre et al., 2013). Recent findings propose that autophagy is regulated by calcium released through the mucolipin 1 (MCOLN1 or TRMPL1) channel present in the lysosomes. This calcium signal activates CaN which can bind and dephosphorylate TFEB to promote its nuclear translocation (Medina et al., 2015; Wang et al., 2015). Conversely, other findings suggest a role of NAADP-mediated calcium signalling in the induction of autophagy. Rah and colleagues showed that in hepatocytes, the CD38/NAADP/Ca^{+2}/TFEB pathway induced autophagy to protect against bacterial LPS-induced liver injury (Rah, Lee and Kim, 2017). Ogunbayo and co-workers demonstrated the mTORC1 can control lysosomal calcium release through TPC2. These researchers showed that both NAADP and rapamycin, an inhibitor of mTORC1, induced global calcium signals in pulmonary arterial myocytes and HEK293 overexpressing TPC2. Importantly, these signals were absent in myocytes derived from TPC2 knockout mice (Ogunbayo et al., 2018). These studies highlight the importance of lysosomes in regulating nutrition levels and the functionality of a lysosome-to-nucleus calcium signalling. Furthermore, NAADP induced calcium signalling has also been linked with the stimulation of exocytosis in T cell to deliver the immune response (Davis et al., 2012) and in adipocytes, it is suggested to regulate insulin-stimulated glucose uptake (Song et al., 2012).

1.8.3 Muscarinic-induced calcium signalling in the human colonic epithelium

As discussed before, calcium acts as a crucial second messenger to regulate a multitude of cellular functions. The majority of the research in muscarinic receptors and calcium signalling in the gut has been developed in cell lines derived from animal models such as mouse, rat and rabbit or human cell lines like HT-29 or Caco2. 2D cultures fail to represent tissue and cell polarity and lack of cell-to-cell connections which might affect the properties of the calcium signal generation.

Previous research done by the Williams lab has led to the development of a 3D culture system of the native human colonic epithelium capable of recapitulating the topological hierarchy of stem cell-driven tissue renewal, which enables the study of physiological processes on polarised cells such as calcium signalling and fluid secretion (Parris and Williams, 2015). Early studies from the Williams lab first characterised the ACh-induced calcium signalling along the colonic crypts of rat. These studies revealed the spatiotemporal characteristics of muscarinic receptor type 3 (MAChR3)-coupled calcium signalling where the response initiates at the base of the crypt and propagates up the crypt axis (Lindqvist et al., 1998). These results were further confirmed using human colonic crypts (Lindqvist et al., 2002). Follow-up studies showed that cholinergic calcium signals regulate fluid secretion by modulating the expression of the Na^+-K^+-$2Cl^-$ co-transporter (NKCC1) in the membrane of human colonic epithelial cells. Reynolds and colleagues showed that ACh is sensed by muscarinic receptors at the base of the crypt which activates an intracellular calcium signal that results in a cycle of recruitment of the NKCC1 transporter to basolateral membranes and subsequent activation. This process is followed by internalisation and degradation of the transporter, finishing in NKCC1 re-expression. These results revealed a novel mechanism of regulation of NKCC1 to limit intestinal fluid loss and validated the use of 3D human colonic crypts as a powerful tool for investigating the physiology of the colonic epithelium (Reynolds et al., 2007).

Research in the William's lab has demonstrated the effects of muscarinic-induced calcium signals in fluid secretion of cultured human crypts. Calcium signals start at the base of the crypt and propagate up towards the crypt opening. As discussed previously, intestinal stem cells reside at the bottom of the crypts and in the colon they are located intermingled with goblet cells (Reynolds et al., 2013; Sasaki et al., 2016) suggesting a role in the initiation of the calcium signals. The mechanism of the muscarinic-activated calcium signals has been recently characterised by the former laboratory member Dr Christy Kam. In her studies, Dr Kam demonstrated that binding of ACh to muscarinic receptors induces NAADP-dependent release of calcium from the TPC of the endolysosomes which activates IP3Rs and RyRs in the ER to amplify the response. This signalling ultimately results in mucus secretion in colonic goblet cells (Dr Christy Kam, PhD Thesis). In addition to cultured human colonic crypts, colonic organoids have been shown by other groups to represent a great platform for the study of gut physiology and calcium signals (Zietek et al., 2015; Fujii, Clevers and Sato, 2019).

1.9 Hypothesis

In the recent years, a lot of effort has been placed by the research community in understanding the biology of human colonic crypts in health and disease. However, some of the different signalling mechanisms that govern crypt functioning remains poorly understood.

The Williams lab has previously shown the importance of muscarinic-activated calcium signalling in the maintenance of the crypt cell hierarchy and the regulation of fluid (Reynolds et al., 2007, 2013) and mucus secretion (Dr Christy Kam, PhD thesis) using a culture model of primary human colonic crypts. Mucus and fluid secretion are crucial in maintaining the epithelial barrier (Johansson et al., 2011) and it is known to be induced by calcium signalling upon activation of muscarinic receptors by ACh (Halm and Halm, 2000; Reynolds et al., 2007; Johansson et al., 2008; Birchenough et al., 2016). However, the mechanisms of the intracellular calcium signals that leads to mucin and fluid secretion have not been fully characterised. In this thesis, the author tries to elucidate which calcium stores are implicated in inducing ACh-induced mucus release and how these signals shape the mucus secretion spatio-temporal characteristics (**Figure 1.25**).

Another question that this thesis tries to answer is the role of muscarinic-activated calcium signals in modulating stem cell biology. A great body of evidence suggests that calcium signalling regulates cell proliferation, and it has recently been proposed that calcium is a second messenger capable of integrating a great variety of external stimuli to regulate stem cell proliferation using *Drosophila* as a model (Deng, Gerencser and Jasper, 2015). The transcription factor NFATc3, which is activated by calcium signalling has been suggested to induce expression of intestinal stem cell markers in human colonic epithelium (Peuker et al., 2016). Moreover, ACh has been linked with stem cell proliferation and tumorigenesis (Magnon, Freedland and Frenette, 2013; Zhao et al., 2014; Hayakawa et al., 2016). The use of organoid cultures to study gut physiology has been proven to be a useful tool because they can recapitulate most of the physiological characteristics of the gut, they can be originated from single cell cultures and propagated indefinitely, and are amenable to genetic modifications (Sato et al., 2009; Schwank et al., 2013). How ACh-induced calcium signals regulate stem cell proliferation in human colonic crypts it still unknown and will be investigated in this thesis.

In summary, this thesis' hypothesis is that muscarinic-activated calcium signals are crucial in regulating the stem cell niche of human colonic crypts and organoids, promoting stem cell renewal and inducing mucus and fluid secretion.

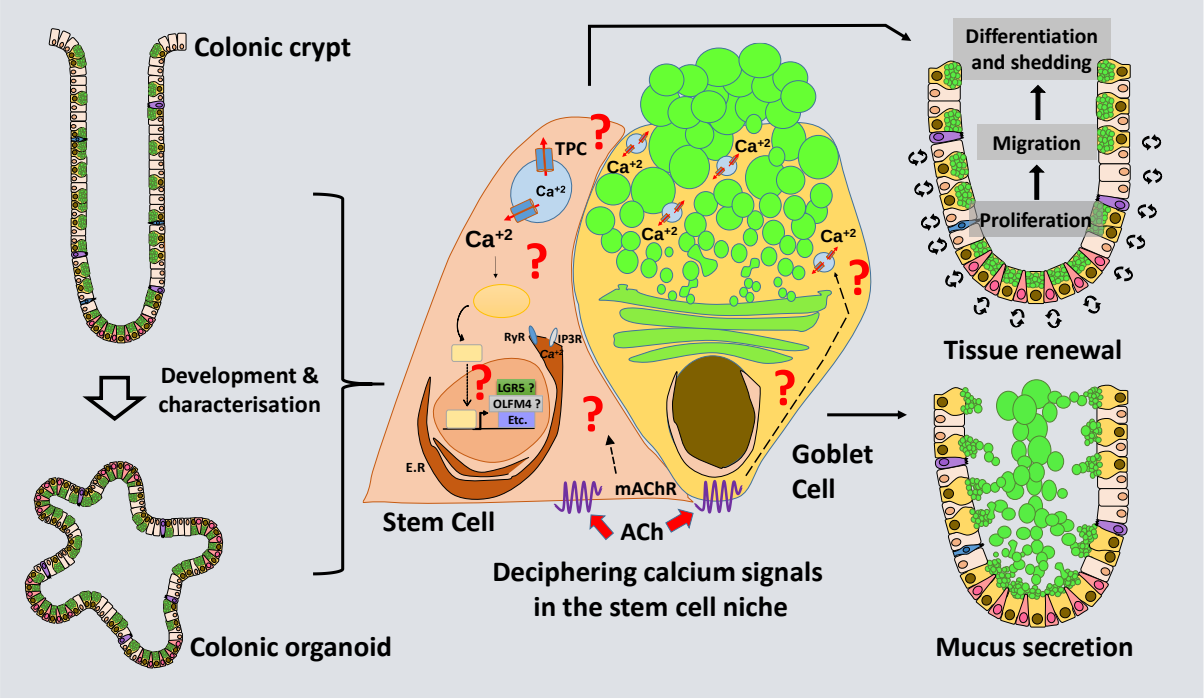

Figure 1.21. Deciphering calcium signals in the stem cell niche. Primary human colonic crypts and colonic organoids are used to test the hypothesis that muscarinic activation of stem cells and goblet cells in the base of the crypt induces calcium release from the endolysosomes which results in stem cell proliferation and induced mucus and fluid secretion.

1.10 Aims

1. To develop and characterise human colonic organoids as a model of human colon physiology along with primary cultured human colonic crypts.

2. To examine the role of acetylcholine-derived calcium excitation-mucus and fluid secretion in the stem cell niche of colonic crypts and organoids.

3. To investigate the role of acetylcholine-derived calcium signals in cell proliferation in the stem cell niche of colonic crypts and organoids.

2 Chapter 2. Materials and Methods

2.1 Overview

During the course of this research project a number of techniques and methods were utilised in order to study the regulation of calcium signals and its implication in the colonic epithelium fitness. The foundation for all the experiments was the acquisition of human colonic tissue of patients undergoing colon cancer surgery. This colonic native tissue was immediately fixed, and DNA and RNA were isolated to provide insights into the status of gene and protein expression and localisation.

Two different culture models, isolated human colonic crypts and human colonic organoids were used to study the physiology of the gut epithelium. Human colonic crypts were isolated from the patients' tissue samples and cultured in a 3D culture system that mimics the *in vivo* functioning of the gut. Previous work done by the Williams lab (Reynolds et al., 2007, 2013; Parris and Williams, 2015) demonstrated that this model can be used to study the hierarchy of the crypt cell renewal and the functional epithelial cell polarity. The use of this model permits the study of protein localisation and expression with immunofluorescence techniques and the visualisation using brightfield time-lapse, fluorescence and confocal microscopy. At the same time, DNA and RNA can be extracted and genomics and transcriptomic analysis such as PCR, qRT-PCR, RNA sequencing and whole exome sequencing can give valuable clues of the status of the colon epithelium.

Long term cultured colonic crypts can be propagated as organoids and cultured *ad infinitum*. This culture system was validated to be used for the study of intracellular calcium signals, protein localisation and tissue regeneration. Analysis on single cells originated from organoids can be used to develop clonal expansion assays, which can be used as a read out for stem cell activity. Organoids are also amenable to genetic manipulation at the genomic (CRISPR/Cas technology) and are a good platform for the studies of changes in gene expression (qRT-PCR, PCR).

With the use of the culture systems, calcium sensitive dyes such as Fura-2 and Fluo-4 in combination with the appropriate microscopy were used to investigate the status of intracellular calcium signalling in real time. The presence and distribution of colonic epithelial cell markers such as OLFM4, MAChR3 and MUC2, were observed and validated in native tissue, cultured colonic crypts and colonic organoids using immunofluorescence techniques and genomic studies. The use of these culture systems and techniques allowed for the study of gut physiology and the understanding of the role of calcium signals in mucus and fluid secretion and stem cell proliferation in the colon epithelium.

2.2 Reagents and buffers

2.2.1 Chemicals and reagents

Table 2.1. List of Chemicals and Reagents

Chemical or Reagent	**Supplier**
Acetic Acid	Sigma
Advanced/DMEM	Invitrogen
Agarose	Sigma
Ammonium Chloride (NH_4Cl)	Fisher Scientific
Bovine Serum Albumin (BSA)	Sigma
Bovine Serum Albumin Fraction V 7%	Gibco
Calcium Chloride ($CaCl_2$)	VWR International
Click-IT EdU reaction kit	Fisher Scientific
D-Glucose	Fisher Scientific
Dimethyl Sulfoxide (DMSO)	Sigma
Disodium hydrogen phosphate (Na_2HPO_4)	Fisons Scientific Apparatus
Donkey Serum	Sigma
DTT	Fisher Scientific
EDTA	Sigma
Ethanol	Sigma
Fetal Bovine Serum (FBS)	Sigma
Fluo-4	Invitrogen
FM 1-43FX	Fisher Scientific
Fura-2	Invitrogen
Goat Serum	Abcam
Growth factor reduced Matrigel	VWR International
HEPES	Fisher Scientific
Hoescht	Life Technologies
L-Glutamine	Gibco
Magnesium Chloride ($MgCl_2$)	Fluka (Sigma)
MEM Non-essential aminoacids solution (MEM NEAA)	Fisher Scientific
Methanol	Sigma
Paraformaldehyde (PFA)	Sigma

Penicillin Streptomycin (P/S)	Gibco
Phosphate buffered saline	OXOID
Potassium Chloride (KCl)	Fisher Scientific
Sodium Bicarbonate ($NaHCO_3$)	Fisher Scientific
Sodium Chloride (NaCl)	Fisher Scientific
Sodium Dodecyl Sulfate (SDS)	Melford
Sodium Hydroxide	Fisher Scientific
SYTOX Blue	Invitrogen
Triton-X-100	Roche
Vectashield	Vector laboratories

2.2.2 Buffers

Table 2.2. List of buffers used

Buffer	Formula
HEPES Buffered Saline (HBS), pH 7.4	NaCl (140nM), KCl (5mM), HEPES (10mM), D-Glucose (17.5mM), Na_2HPO_4 (1mM), $NaHCO_3$ (10mM), $MgCl_2$ (0.5mM), $CaCl_2$ (1mM), MEM NEAA (1x), P/S (50U/ml, 50µg/ml), L-Glutamine (3mM)

2.2.3 Primary and Secondary Antibodies

Table 2.3. List of primary and secondary antibodies used in the study

Antibody	Species Origin	Clonality	Working concentration	Supplier
anti-β-catenin	Rabbit	Monoclonal	1:100	Abcam
anti-CD38	Rabbit	Monoclonal	1:100	Abcam
anti-ChAT	Goat	Polyclonal	1:100	Milipore
anti-Chromogranin-A (CHGA)	Mouse	Monoclonal	1:100	Abcam
anti-E-cadherin	Goat	Polyclonal	1:100	R&D Systems
anti-E-cadherin	Mouse	Monoclonal	1:100	Abcam

anti-Ki67	Rabbit	Polyclonal	1:100	Abcam
anti-LGR5 (212)	Mouse	Monoclonal	1:100	Origene
anti-LGR5 (2A2)	Mouse	Monoclonal	1:50/1:100	Origene
anti-MUC2	Mouse	Monoclonal	1:100	Santa Cruz
anti-Muscarinic receptor 1 (MAChR1)	Rabbit	Polyclonal	1:100	R&D Systems
anti-Muscarinic receptor 2 (MAChR2)	Rabbit	Monoclonal	1:100	Abcam
anti-Muscarinic receptor 3 (MAChR3)	Rabbit	Polyclonal	1:100	R&D Systems
anti-Muscarinic receptor 4 (MAChR4)	Rabbit	Polyclonal	1:100	Abcam
anti-Muscarinic receptor 5 (MAChR5)	Rabbit	Polyclonal	1:100	R&D Systems
anti-NFATc3	Rabbit	Polyclonal	1:100	Sigma
anti-NKCC1	Goat	Polyclonal	1:100	Santa Cruz
anti-OLFM4	Rabbit	Polyclonal	1:100	Abcam
anti-PTK7	Mouse	Monoclonal	1:100	Miltenyi Biotec
anti-REG4	Goat	Polyclonal	1:100	R&D Systems
anti-TORC1	Rabbit	Monoclonal	1:100	Abcam
anti-TPC1	Rabbit	Polyclonal	1:100	Abcam
anti-TPC2	Rabbit	Polyclonal	1:100	Abcam
anti-VAChT	Rabbit	Polyclonal	1:100	Abcam
anti-YAP1	Mouse	Monoclonal	1:100	Santa Cruz
Antibody	**Species Origin**		**Working concentration**	**Supplier**
anti-mouse Alexa Fluor 488	Donkey		1:200	Invitrogen
anti-mouse Alexa Fluor 568	Donkey		1:200	Invitrogen
anti-mouse Alexa Fluor 647	Donkey		1:200	Invitrogen
anti-rabbit Alexa Fluor 488	Donkey		1:200	Invitrogen

anti-rabbit Alexa Fluor 568	Donkey		1:200	Invitrogen
anti-rabbit Alexa Fluor 647	Donkey		1:200	Invitrogen
anti-goat Alexa Fluor 488	Donkey		1:200	Invitrogen
anti-goat Alexa Fluor 568	Donkey		1:200	Invitrogen
anti-goat Alexa Fluor 647	Donkey		1:200	Invitrogen
anti-mouse Alexa Fluor 488	Goat		1:200	Invitrogen
anti-rabbit Alexa Fluor 568	Goat		1:200	Invitrogen
anti-goat Alexa Fluor 647	Goat		1:200	Invitrogen

2.3 Methods

2.3.1 Human colorectal tissue samples

This study was performed in accordance with the Norfolk and Norwich University Hospital and approved by the East of England National Research Ethics Committee [2013/2014–62 HT (ongoing approval)]. Samples from colorectal tissue were obtained with the consent of patients undergoing sigmoid endoscopy, right-hemicolectomy or anterior resection. The histologically-normal mucosa samples were obtained from at least 10 cm away from the tumour locations, and only used if there was no apparent intestinal pathology.

2.3.2 Human fixed tissue sections

A small fraction of the colorectal tissue sample was immediately fixed in 4% paraformaldehyde (PFA) for 2 hours on ice cold temperature after the surgical resection and washed overnight in PBS. The samples were embedded in OCT compound and frozen on liquid nitrogen in isopentane. Sections of 8 µM of thickness were cut using the cryostat and processed for immunohistochemistry as described in section 2.3.6.

2.3.3 Colonic crypt isolation and culture

Human colonic crypts were isolated by members of the Williams lab as previously described (Reynolds et al., 2007, 2013; Parris and Williams, 2015). In short, fresh tissue samples were collected in ice cold PBS and transferred to the laboratory to be placed in HBS containing DTT (1 mM) and EDTA (1 mM) for 1h at room temperature. Crypts were liberated by vigorous shaking and left to sediment. Once settled, crypts were collected and embedded in growth factor reduced Matrigel and seeded in no.0 glass coverslips arranged in 12 well plates. The Matrigel containing colonic crypts was

left to polymerise at 37°C for 10 minutes and then the crypts were flooded with human colonic crypt culture medium (hCCCM): advanced F12/DMEM containing B27, N2, n-acetylcysteine (1 mM), Hepes (10 mM), Pen/Strep (100U/mL), L-Glutamine (2 mM), Wnt-3A (100ng/mL), IGF-1 (50ng/mL), Noggin (100ng/mL), RSPO-1 (500ng/mL) and A83-01 (0.5 µM). Colonic crypts were cultured at 37°C and 5% CO_2 for 0 to 4 days in hCCCM, which was further modified depending on the experimental conditions.

2.3.4 Colonic organoid culture

Human colonic organoids were obtained by members of the Williams lab after the passage of colonic crypts grown for 7 days. The samples were detached from the bottom of the plate by scratching the surface and mechanically dissociated into smaller fragments using a pipette. The suspension containing the crypt fragments was transferred into centrifuge tubes and pelleted at 4^0C. The supernatant containing cell debris and Matrigel leftovers was aspirated and then fresh media was added, and the crypt fragments resuspended. The final pellet was embedded in Matrigel, left to polymerise, and the organoids were flooded with hCCCM. Organoids were cultured at 37^0C and 5% CO_2, fed every 3 days and passaged every 5 to 7 days.

2.3.5 Colonic single cell culture

Human colonic single cells were obtained by members of the Williams lab after the passage of colonic organoids grown for 7 days. Similar to the protocol for organoid culture, samples were detached from the bottom of the plate by scratching the surface and mechanically dissociated into very small fragments using a pipette. These fragments were then filtered using a 10 µm cell strainer to ensure a uniform size population. The suspension containing the single cells was transferred into centrifuge tubes and pelleted at 4^0C. The supernatant containing cell debris and Matrigel leftovers was aspirated and then fresh media was added, and the single cells resuspended. The final pellet was embedded in Matrigel, left to polymerise and the single cells were flooded with hCCCM. Single cells were cultured at 37^0C and 5% CO_2, fed every 3 days and passaged every 5 to 7 days.

2.3.6 Immunohistochemistry

Colonic crypts or organoids were fixed with 4% (PFA) on ice for 1h and then washed two times with PBS. The samples were then treated with NH_4Cl for 13 minutes to remove the excess of aldehyde bonds, after which 1% SDS and 1% Triton 100-X were added to permeabilise the membrane. The samples were later treated with donkey or goat serum and 1% BSA for 2h to prevent non-specific binding of the antibodies. Samples were incubated over night with the primary antibodies at 4^0C

(**Table 2.3**). Specific Alexa Fluor-conjugated secondary antibodies were added to the crypts for 2h (**Table 2.3**) and then embedded in Vectashield mounting solution containing cell nuclear stain Sytox Blue or Hoescht. Crypts or organoids when then mounted into slides and the immunolabelling was imaged using laser confocal microscopy (Zeiss LSM) or epifluorescence microscopy (Nikon). Primary antibody negative controls were used to determine antibody specificity. Alternatively, colonic crypts were fixed with a 3:1 solution of methanol and acetic acid, methanol-Carnoy (Methacarn) for 5 minutes at -20^{0}C and then washed 5 times with PBS. Samples were treated with NH_4Cl and subsequently permeabilised with 0.1% SDS for 2 minutes. From this point on, crypts were processed following the same protocol as described above for PFA-fixed specimens. In addition, for the characterisation of certain cell markers, colonic crypts were labelled with the primary antibody prior to fixation with %4 PFA and subsequently incubated with specific Alexa Fluor-conjugated secondary antibodies.

2.3.7 Organoid formation efficiency assays

Human colonic organoids were passaged and plated in hCCCM with or without the cholinergic agonists carbachol (CCh) and Oxotremorine (Oxo) at different concentrations. The organoids were imaged every other day from the day they were plated using the epi-fluorescence microscope (Nikon-Ti) in a chamber at with 5% CO_2 supply at 37^{o}C. Growth was assessed by measuring the cross-sectional area over the course of 8 days.

2.3.8 Organoids swelling assays

Human colonic organoids were passaged and plated in hCCCM. On day 1 of culture, muscarinic agonist CCh was added at 10 µM for 2 hours while the inhibitor of intracellular calcium signalling Ned19 (500 µM) was pre-incubated for 1 hour. The organoids were live imaged during the course of the treatment using the epi-fluorescence microscope (Nikon-Ti) in a chamber at with 5% CO_2 supply at 37^{o}C.

2.3.9 Intracellular vesicle labelling

Human colonic crypts, organoids and organoid-derived single cells were plated in Matrigel containing hCCCM. Upon plating, cultured cells were loaded with the lipophilic dye FM-143 FX (4 µM) overnight at 37^{0}C. On day 1 of culture, cells were fixed with PFA and mounted using Vectashield containing Sytox blue nuclear stain, and then imaged under confocal microscope (Zeiss LSM). For the live imaging assays, the samples were placed in a coverslip cell chamber with HBS and imaged at room temperature under the confocal microscope (Zeiss LSM). Images were acquired at one frame

per second. Addition of mucus secretagogue CCh was performed by aspirating the existing solution and replacing it with the desired drug, previously diluted in HBS.

2.3.10 EdU labelling of isolated crypts

After crypts were fixed in PFA, the Click-IT reaction was prepared following the manufacturer's instructions and colonic crypts were incubated for 40 minutes in the dark at room temperature. The reaction was stopped with 3% BSA and the samples were then treated for 2h with 10% donkey serum and 1% BSA to avoid unspecific binding of the antibodies. Colonic crypts were incubated with primary antibodies overnight at 4^0C and then treated with the appropriate Alexa fluor-conjugated secondary antibodies (**Table 2.3**) for 2h at 4^0C. Samples were mounted with Vectashield with the nuclear stain Hoescht and imaged using an epifluorescence microscope (Nikon Ti) or laser confocal microscopy (Zeiss LSM).

2.3.11 Gene expression analysis

2.3.11.1 RNA isolation and cDNA generation

RNA from freshly isolated colonic primary mucosa, freshly isolated crypts and human colonic organoids was isolated using the ReliaPrep ™ RNA Miniprep System (Promega) according to the manufacturer's instructions. Total RNA concentration and purity was measured using a NanoDrop ND-1000 spectrophotometer (Thermo Fisher Scientific). Using reverse-transcription PCR, cDNA was generated from 500 nM of RNA using oligo-dT primers (Promega) and M-MLV Reverse Transcriptase kit (Thermo Fisher Scientific) (**Table 2.4**).

2.3.11.2 Reverse Transcription PCR (RT-PCR)

RT-PCR was performed using 25ng/µl of cDNA in a final volume of 25µl. The reaction comprised 200 nM of forward and reverse primers, 200 µM of dNTPs, 0.04 U/µl of GOTaq® G2 DNA Polymerase (Promega), PCR buffer (Promega) and 2.5 mM of $MgCl_2$ (**Table 2.4**) and was carried out using a G-Storm thermocycler. cDNA was amplified following 1 initial denaturation cycle at 94^0C for 1 minute, 35 cycles comprising denaturation at 94^0C for 30 seconds, annealing at a temperature ranging from 55 to 65^0C (optimised for each set of primers) for 30 seconds, and extension at 72^0C for 1 minute; finishing with 1 cycle of final extension at 72^0C for 5 minutes. Primers were designed to span intron-exon boundaries when possible; sequences are listed in **Table 2.5**. The following primers were kindly provided by Dr Christy Kam: ChAT, Nested ChAT, FABP2, LGR5, MAChR1, MAChR2, MAChR3, MAChR4, MAChR5, MUC2, OLFM4, TPC1, VAChT, Nested VAChT and GAPDH. The PCR products were run in 3% agarose gel containing 0.5 µg/ml of ethidium bromide and visualised under UV light.

2.3.11.3 Generation of DNA and RNA biobank

A biobank was generated containing the DNA and RNA from primary isolated colonic mucosa, crypts and colonic organoids of matching patients. Colonic crypt and isolated mucosa samples were obtained after a colonic crypt isolation. Colonic crypts were cultured and propagated into organoids and the DNA and RNA were isolated approximately after the 4th passage. The isolation of DNA and RNA was performed using the ReliaPrep ™ DNA Miniprep System (Promega) and ReliaPrep ™ RNA Miniprep System (Promega) according to the manufacturers' instructions and the samples were stored at -20^{0}C and -80^{0}C respectively.

Table 2.4. Conventional PCR chemicals and reagents utilised in the study

Name	Supplier
Gene Ruler™ 100bp Plus DNA Ladder	Fermentas
GoTaq® G2 Flexi DNA Polymerase	Promega
Low Molecular Weight DNA Ladder	New England Biolabs
M-MLV Reverse Transcriptase	Invitrogen
Oligo(dT15) Primer	Promega
PCR Nucleotide Mix	Promega
ReliaPrep™ RNA Tissue Miniprep System	Promega
RNasin® Plus RNase Inhibitor	Promega

Table 2.5. List of primary and secondary antibodies used in the study

Gene	Accession Number	Primer Sequence F	Primer Sequence R	Product size (bp)
CD38	NM_001775.3	GCTCAATGGATCCCGCAGTA	GGATCCTGGATAAGTCTCTGG	149
CHAT	NM_020985.3	GGACAACATCAGATCGGCCAC	GAACATCTCCGTGGTTGTGGG	300
Nested CHAT	NM_020985.3	TTTGTGAGAGCCGTGACTGA	ATCCATGAACATCTCGGGCA	195

FABP2	NM_000134.3	CAATCTAGCAGACGGAACTGAA	CCGTTTGAATTTTCCAATAAGTTT	76
LGR5	NM_001277226.1	ACCAGACTATGCCTTTGGAAAC	TTCCCAGGGAGTGGATTCTAT	77
MAChR1	NM_000738.2	CAAGTGGCCTTCATTGGGATCAC	GCATTGCTGGCCACATAGTCC	260
MAChR2	NM_000739.2	GAGCTCCAATGACTCCACCTCAG	GGAAGGAGGAGGCTTCTTTTTTG	298
MAChR3	NM_000740.2	CAACCTCGCCTTTGTTTCCAAAC	CCAGGATGTTGCCGATGATGG	242
MAChR4	NM_000741.3	GGCAGTTTGTGGTGGGTAAG	CGCTCTGCTTCATTAGTGGGC	248
MAChR5	NM_012125.3	GTCTGGCTTGTGACCTTTGGC	GGTGGGCTCAGAGAGAAACTG	278
MUC2	NM_002457.4	GCTGCTATGTCGAGGACACC	GGGAGGAGTTGGTACACACG	90
NEGF1	NM_001321386	ACTGGAAGTCTGAAGCGAGC	GCTTGGTCAGTTTGCCACAG	94
NFATc3	NM_173165.3	GGACAAGATGGACGACCTCA	TCAAGGACAATGTGAGCCCC	80
OLFM4	NM_006418.4	ATCAAAACACCCCTGTCGTC	GCTGATGTTCACCACACCAC	74
PTK7	NM_002821.5	CAGTTCCTGAGGATTTCCAAGAG	TGCATAGGGCCACCTTC	82
PPP3CA (CALCINEURIN)	NM_000944.5	GATATTGATGCGCCAGTCAC	CCCTAAGAAGAGGTAGCGAGTG	114
TPCN1	NM_001143819.2	GCATCACCCTTGAGAAGGAAATC	GGCATGCTCCTCATACCACTC	233
TPCN2	NM_139075.4	TTCCAGAACCTGCCTGAGTC	TTGGAATACGCAGGAATCATC	89
SLC18A3 (VAChT)	NM_003055.2	CTACCCTACGGAGAGCGAAG	GGCTCCTCCGGGTACTTATC	282

Nested VAChT	NM_003055.2	GAAGATCGGGGTGCTGTTTG	GAACAGCGTGGCGTA	172
GAPDH	NM_002046.5	GTCAGTGGTGGACCTGACCTG	TGCTGTAGCCAAATTCGTTG	245

2.3.11.4 Quantitative Real Time PCR (qRT-PCR)

This technique was performed using TaqMan® probes containing a FAM™ reporter dye at the 5' end and a non-fluorescent quencher at the 3'end. In short, following a normal PCR amplification set up, the primers and probe bind to the single stranded DNA after denaturation of the template. The *Taq* DNA polymerase will then synthesise new strands, ultimately cleaving the probe with its nuclease activity. This results in the separation of the dye from the quencher. After every cycle, fluorescence is recorded, and its intensity will be proportional to the amount of amplicon synthesised. For these experiments, 5ng (20ng when relative gene expression of candidate genes was low) of cDNA were used on a final volume of 25µl together with the TaqMan® PCR cocktail (**Table 7**) containing 900 nM of both forward and reverse primers and 250 nM of TaqMan® probe (**Table 8**). The plate containing the samples was analysed using a 7500 Fast Real-Time PCR System (Thermo Fisher Scientific) and the readouts further examined using the7500 software v2.3. With the use of this tool, the relative gene expression of the genes of interest was assessed by means of their Ct value (cycle threshold); this being the number of cycles required for the fluorescent signal to cross the threshold. For these experiments, reference gene expression measurements were included to normalise the genes of interest values. Subsequently, the double delta Ct method was utilised to calculate the relative fold change in gene expression of the samples by comparing the normalised expression measures of the genes of interest between different conditions.

Table 2.6. Quantitative RT-PCR chemicals and reagents utilised in the study

Reagent	Supplier
2x qPCRBIO Probe Mix Lo-ROX	PCR Biosytems
Homo sapiens reference gene assay with Double-dye	Primer Design
DEPC treated water	Invitrogen

Table 2.7. Quantitative RT-PCR primers utilised in this study

Gene	Assay ID	Supplier
ANPEP	Hs00969422_m1	Fisher Scientific
ASCL2	Hs00266139_m1	Fisher Scientific
CA1	Hs00270888_s1	Fisher Scientific
CEACAM7	Hs04260396_g1	Fisher Scientific
LGR5	Hs03988977_m1	Fisher Scientific
MKi67	Hs00758143_m1	Fisher Scientific
YWHAZ	Hs01122445_g1	Fisher Scientific

2.3.12 RNA sequencing (RNAseq)

Following RNA isolation and purification, an RNAseq library was prepared from isolated colonic primary mucosa, freshly isolated crypts and human colonic organoids of matching patients. Illumina RNAseq (175 bp PE HiSeq 4000; 100 million reads/sample) was performed at Earlham Institute Genome Centre. Data is expressed in reads per kilobase million (RPKM) which is a normalised value to correct differences in sample sequencing and gene length.

2.3.13 Intracellular calcium imaging in human colonic crypts and organoids

Isolated colonic crypts and organoids in culture for 1 to 3 days were loaded with HBS containing 5 µM of fluorescent calcium indicators Fura-2 or Fluo-4 for 2h at room temperature and protected from the light. The samples where then washed two times with HBS for 1h to allow for the de-esterification of the dye inside the cells. The Fura-2 loaded samples were then mounted in a coverslip cell chamber and imaged on an inverted fluorescent microscope (Nikon TE200) using a 40x 1.1 NA oil lens. The calcium indicator Fura-2 was excited using fluorescence wavelengths of 340 nm and 380 nm and the emission was detected at 510 nm using a cooled CCD camera (Quantum, Roper Scientific). Using the Easy Ratio pro software (Horiba), regions of interest were drawn along the crypt axis and for each of them the average of the background-corrected 340/380 ratio was recorded live over time with an acquisition time of one frame per second. The experimental solutions (**Table 2.8**) were diluted in HBS and added by aspirating the existing solution and replacing it. The ratiometric changes in fluorescence were presented as pseudo-colour images (**Figure 2.1**) and traces plotted over time (**Figure 2.3**). Colonic crypts and organoids loaded with Fluo-4 were

visualised using laser scanning confocal microscopy (Zeiss 510 META). The calcium dye was excited at 488 nm and the emission recorded at 520 using a 40x 1.3 NA WD 0.21mm oil immersion objective, using a pinhole diameter of 5 airy units (AU) to increase overall intensity. The samples were zoomed in to the cellular level and then treated with calcium signalling activators and/or inhibitors diluted in HBS (**Table 2.8**) by replacing the buffer content. The calcium imaging was recorded at one frame per second and changes in fluorescence were normalised by expressing the intensity of fluorescence relative to the intensity at the start of the experiment (F/F_0) using ImageJ's Times series analyser plug in, and presented as pseudo-colour images (**Figure 2.2**). Fluorescence changes were also presented as traces plotted over time (**Figure 2.3**).

Table 2.8. Calcium signalling reagents utilised in the study

Name	Working Concentration	Supplier
2-APB	10 µM	Sigma
4-DAMP	100 µM	Sigma
BAPTA-AM	66 µM	Sigma
Calcineurin Inhibitor VIII (CN585)	60 µM	EMD Milipore
Carbachol (CCh)	10 µM	Sigma
Cyclopiazonic Acid (CPA)	20 µM	Sigma
Diltiazem (DZM)	250 µM	TOCRIS
Dantrolene	10 µM	TOCRIS
Oxotremorine	1 µM	Sigma
Trans-NED19	250 µM	TOCRIS

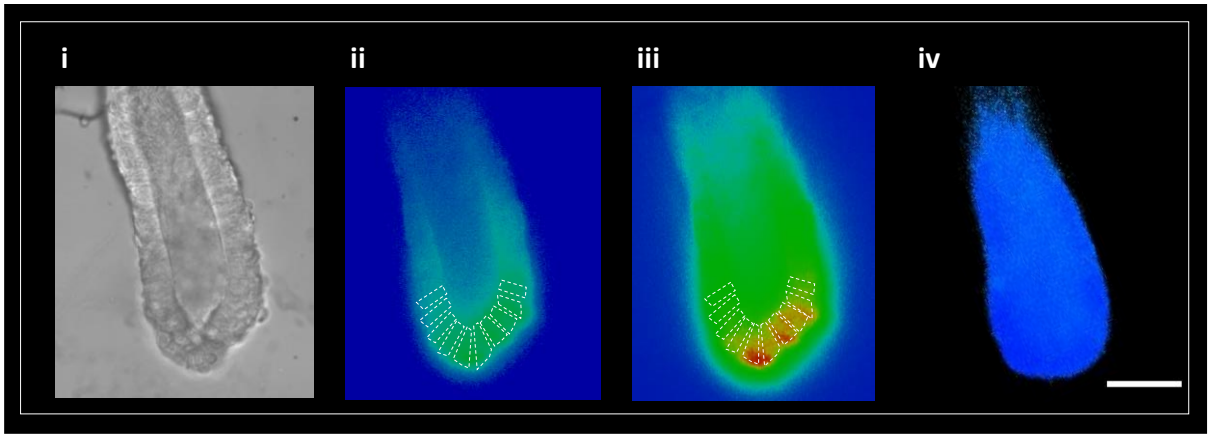

Figure 2.1. Fluorescence images of Fura-2 loaded cells. Representative epifluorescence images of human isolated colonic crypts loaded with Fura-2 (5 µM). (**i**) Brightfield image. (**ii**) Fura-2 fluorescence recorded at 340 nm excitation wavelength. (**iii**) Fura-2 fluorescence recorded at 380 nm

excitation wavelength. (**iv**) Fura-2 fluorescence recording of the background subtracted 340/380 nm ratio. Dashed lines represent ROIs. Scale bar 50 µm.

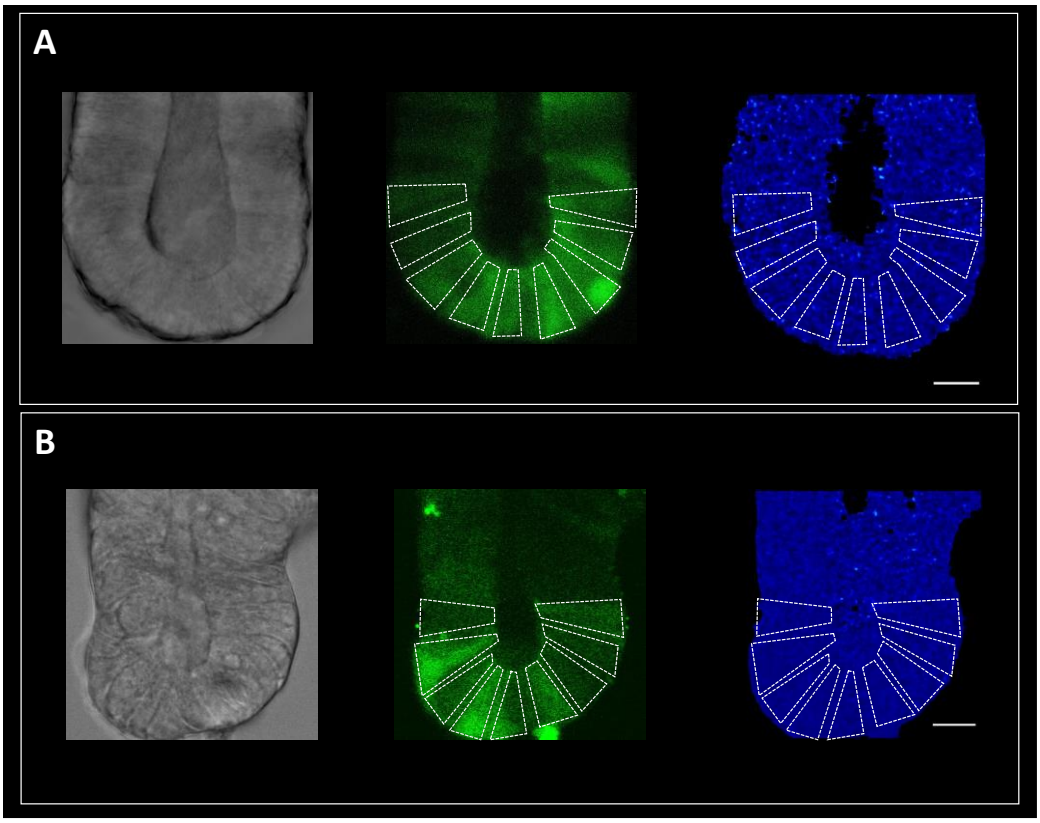

Figure 2.2. Fluorescence images of Fluo-4 loaded cells. Representative confocal images of the base of human isolated colonic crypts (A) and colonic organoids (B) loaded with Fluo-4 (5 µM). Left images represent brightfield. Middle images represent Fluo-4 loaded crypts recorded at 488 nm excitation wavelength. Right images represent F/F0 background corrected Fluo-4 loaded crypts recorded at 488 nm excitation wavelength. Dashed lines represent ROIs. Scale bar 10 µM**.**

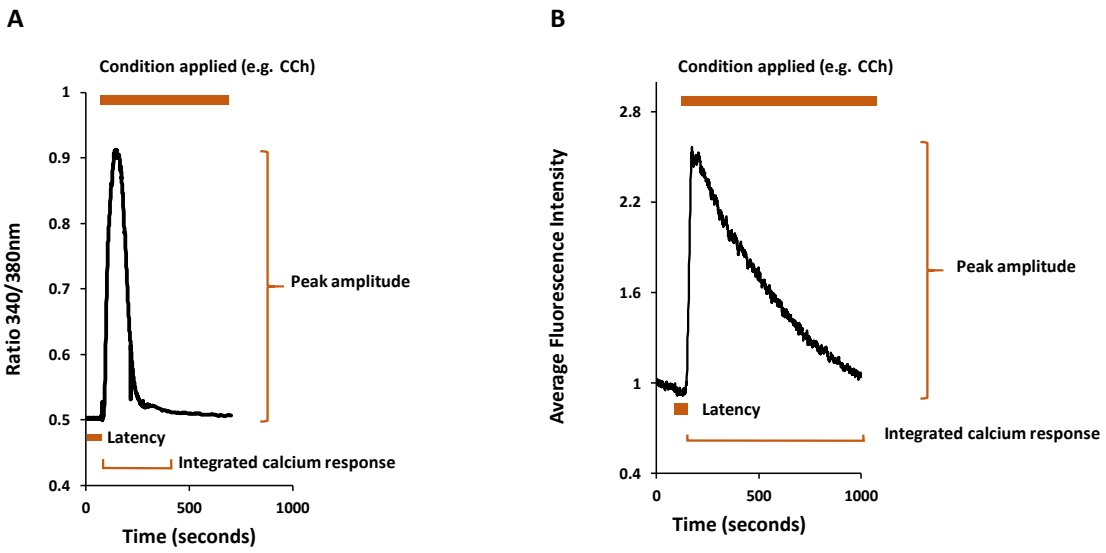

Figure 2.3. Parameters for measuring cellular calcium signals. Representative traces of a calcium signal induced by the muscarinic agonist CCh (10 µM) and the factors used to study the response in cells loaded with Fura-2 (A) and Fluo-4 (B).

2.3.14 CRISPR/Cas technology

Genomic DNA from human colonic organoids was used to introduce the fluorescent reporter mKate2 (Evrogen) in the MUC2 gene by using the CRISPR/Cas technology. Firstly, a region was selected in the genome where to precisely create a Cas9 protein-driven DNA cleavage using the manufacturer's website design tool (Dharmacon). In order to obtain a DNA template, genomic DNA (gDNA) from human colonic organoids was isolated using the ReliaPrep ™ DNA Miniprep System (Promega) according to the manufacturer's instructions. With the aim of knocking in mKate2, a plasmid donor was generated containing the insert (mKate2) flanked by two homology arms (HA) required for the homology-directed repair (HDR), using the Dharmacon™ Edit-R™ HDR plasmid donor kit for fluorescent reporter knock-in. HDR is a process of homologous recombination whereby a genomic DNA template offers the homology needed for an exact repair of a double-strand break. 5' and 3' HAs (**Table 2.9**) were amplified using 25ng/µl of gDNA in a final volume of 25µl. The reaction comprised 500 nM of forward and reverse primers (Table 2.10), 200 µM of dNTPs, 0.04 U/µl of Phusion™ Hot Start II High-Fidelity DNA polymerase (Thermo), 5x Phusion HF buffer (Thermo) 2.5 mM of $MgCl_2$ and DMSO 100% and was carried out using a G-Storm thermocycler. gDNA was amplified following 1 initial denaturation cycle at 98^0C for 30 seconds, 35 cycles comprising denaturation at 98^0C for 10 seconds, annealing at a temperature ranging from 55 to 65^0C (optimised for each set of primers) for 20 seconds and extension at 72^0C for 40 seconds; finishing with 1 cycle of final extension at 72^0C for 10 minutes. Purification of the amplified 5' and 3' HAs was performed by

loading the PCR product on a 1% agarose gel containing 0.5 µg/ml of ethidium bromide and visualised under UV light. Fragments with the appropriate size band where cut and DNA were extracted using Thermo Scientific™ GeneJET Gel Extraction Kit according to manufacturer's instructions. Extracted DNA was quantified by using a NanoDrop™ ND-1000 spectrophotometer (Thermo). In order to generate the plasmid donor, ligation of the 5' and 3' HA together with mKate2 insert and a vector backbone (Dharmacon) was performed using NEB Gibson Assembly® Cloning Kit according to manufacturer's instructions. The ligation product was then transformed into *E.coli* competent cells following the manufacturer's instructions and these were plated in LB Agar plates containing Carbenicillin (100µg/mL) and incubated at 37^0C overnight. In order to screen for plasmids containing the right construct, a colony PCR was carried out. For each bacterial colony, two PCR were set up using two different sets of primers in order to amplify either part of insert and the 5'HA, or part of the insert and 3'HA. The setup of the PCRs consisted on 200 nM of forward and reverser primers (**Table 2.9**), 200 µM of dNTPs, 0.04 U/µl of GOTaq® G2 DNA Polymerase (Promega), PCR buffer (Promega) and 2.5 mM of $MgCl_2$ (**Table 2.10**) and was carried out using a G-Storm thermocycler. Genomic DNA was amplified following 1 initial denaturation cycle at 98^0C for 10 minutes, 30 cycles comprising denaturation at 98^0C for 10 seconds, annealing at a 55^0C for 20 seconds and extension at 72^0C for 1 minute and 30 seconds; finishing with 1 cycle of final extension at 72^0C for 5 minutes. Size check of the fragments of interest was carried out using agarose gels as previously described. Candidate colonies containing the desired plasmid construct were propagated in LB Agar plates containing Carbenicillin (100µg/mL) and plasmid DNA was isolated using the Pure Yield Plasmid Miniprep (Promega) according to manufacturers' instructions and stored at -20^0C. DNA samples at a concentration of 75 ng/µl were sequenced using the Sanger method by Eurofins Genomics and the resulting sequences blasted to original template by using the BioEdit Sequence Alignment Editor.

Table 2.9. CRISPR/Cas reagents utilised in the study

Primers	Primer Sequence (5'-3')	Adapter sequence (5'-3')
5' Homology Arm Forward	TCCGTCACACTTCCTTACTGGA	ACAGAGTGATATTATTGACACGCCC
5' Homology Arm Reverse	GGTGATACACTTATCCATGGGCC	ATCAGCTCGCTCACGCTGCCACCAGC
3' Homology Arm Forward	ACTCCCAGCCCTCCAACTAC	CAAACTGGGGCACAGAGGAGGTAGC
3' Homology Arm Reverse	GTTGTTAGAGGGCTGGAAGTGG	ATAACGGAGACCGGCACACTGGCCAT
Colony PCR mKate2 Forward	GGCCGACAAAGAGACCTACG	
Colony PCR mKate2 Reverse	GTTGTTCACGGTGCCCTCCA	
Colony PCR Backbone Forward	TCGCCCGGTTTATTGAAATG	
Colony PCR Backbone Reverse	TTCGCCACCTCTGACTTGAGC	

Table 2.10. CRISPR/Cas primers utilised in the study

Reagents	Supplier
Phusion Hot Start II DNA Polymerase	Thermo Scientific
5x Phusion HF Buffer	Thermo Scientific
MgCl2	Thermo Scientific
DMSO	Thermo Scientific

2.3.15 Microscopy

Samples processed for immunocytochemistry were visualised using fluorescence microscopy, where the proteins labelled with fluorescent dyes were irradiated with a selected band of wavelengths in order to detect the emission light. During the course of these studies, visualisation of the

immunocytochemistry experiments was achieved by using either the epi-fluorescence microscope (Nikon Ti) or the confocal laser scanning microscope (Zeiss 510 META).

The epi-fluorescence microscope was used to capture the fluorescently labelled EdU in colonic crypts using a 40x 1.1 NA oil lens. In addition, this system was also used to record the time course imaging of organoids' growth. The samples were place in a chamber at 37^0C with 5% supply of CO_2 and imaged with a 4x 0.20 NA dry objective.

Immunofluorescence labelled samples that required of high-resolution imaging were obtained utilising the Zeiss 510 META confocal laser scanner microscope. This microscope scans the object plane in a point-by-point raster using an XY light deflection system and assembles the pixel information to one image. In addition, the emission light projected on the detection pinhole, which is a tiny aperture that removes all emission not originated from the focal plane, is registered by the detector which generates an image free from the blur caused by unwanted light. Immunoflorescent labelling of fixed colonic crypts or organoids was recorded using a 63x 1.4 NA 0.75 mm WD oil immersion objective and a 40x 1.3 NA 0.21 mm WD oil immersion objective. Different focal planes on the z axis were imaged at 2-3 µm intervals to cover the regions of interest of the samples.

2.3.16 Image analysis

Calcium imaging analysis of Fura-2 loaded crypts and organoids was done on ROIs drawn at the base of crypts. Fluorimetric measurements were performed by plotting the fluorescence intensity of 340/380 nm ratio with respect to time and subsequently calculating the amplitude of the response to a given condition by subtracting the resting ratio from the peak ratio recorded (**Table 2.3A**). Intensity measurements were background corrected.

The measurement of organoid formation and growth was carried out by quantifying the cross sectional area of 46 organoids treated with different concentrations of the ACh analogue CCh and Oxo, and imaged on day 0, day 2, day 4, and day 6 of culture using the software Fiji ImageJ (**Figure 2.4**).

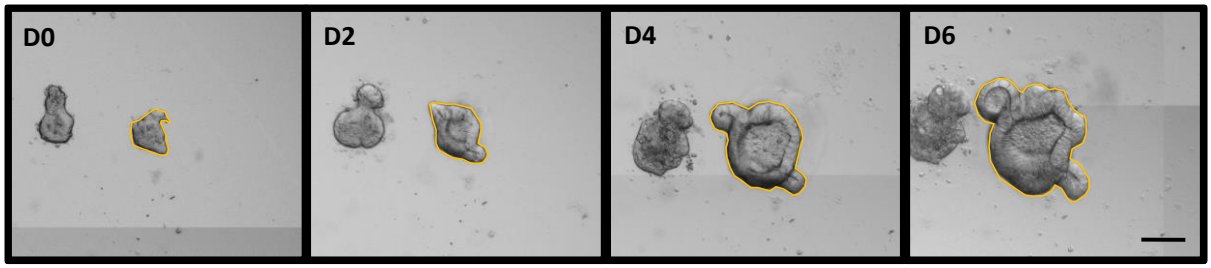

Figure 2.4. Organoid growth measurement. Colonic organoids were imaged from the day of passaging (D0) until day 6. Orange lines indicate cross sectional area measurements. Scale bar 150 µm.

The swelling of the organoids was assessed by measuring the increase of luminal area from resting conditions and after the addition of the pharmacological drugs. A minimum of 15 organoids were measured per conditions for a total of 3 samples on day 1 of culture. (**Figure 2.5**).

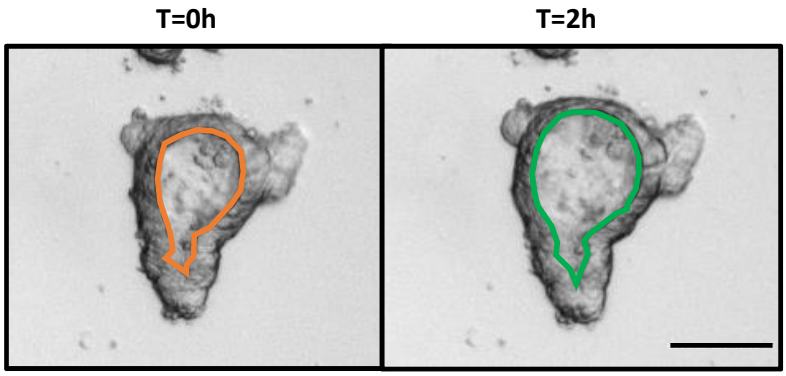

Figure 2.5. Organoid swelling measurement. Colonic organoids were imaged on day 1 of culture for 2 hours and the swelling was assessed by measuring the luminal membrane area. Orange and green lines indicate luminal membrane areas at T=0h and T=2h respectively. Scale bar 100 µm.

Proliferation experiments were analysed by counting the percentage of EdU positive crypts in crypts relative to total number of Hoescht-labelled cell nuclei. This analysis was performed using the software Fiji ImageJ. A minimum of 20 crypts and organoids were examined per condition. Experiments were repeated two times at least. Colonic crypts were divided into four regions (base, supra-base, mid and top) containing the same number of nuclei and each region was analysed separately (**Figure 2.6**).

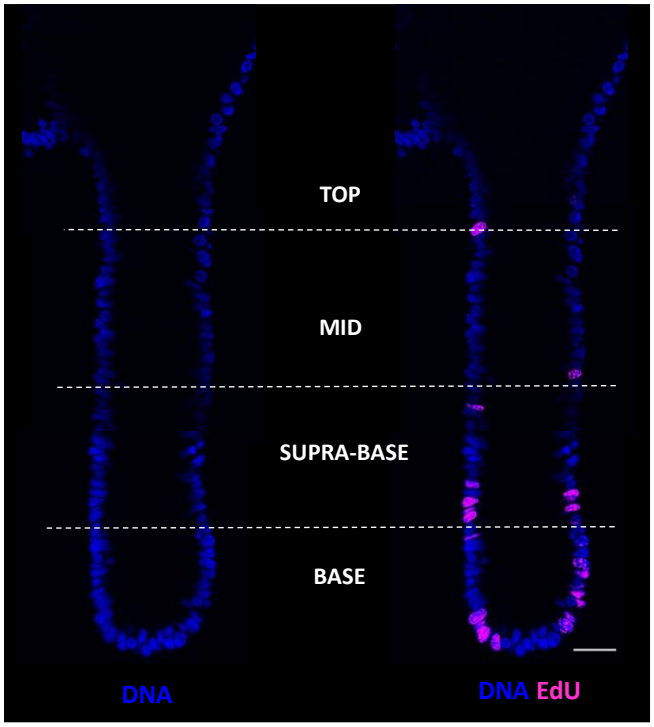

Figure 2.6 Analysis of cell proliferation in human colonic crypts. Colonic crypts were divided into four different regions of similar cell number along the crypt axis (base, supra-base, mid and top regions). For each region, the number of cell nuclei and EdU was counted separately. Scale bar 25 µm.

Transcription factor translocation to the nucleus was analysed by measuring the fluorescence intensity of immunolabelled proteins of interest. Using the Fiji ImageJ software, two independent regions of interest were drawn in each cell of the first 28 that form the base of the crypts; one around the nucleus and the other one around the cytoplasm (**Figure 2.7**). The intensity of fluorescence of the transcription factor activator was then measured and compared between conditions. The results were corrected to the background and normalised to control conditions.

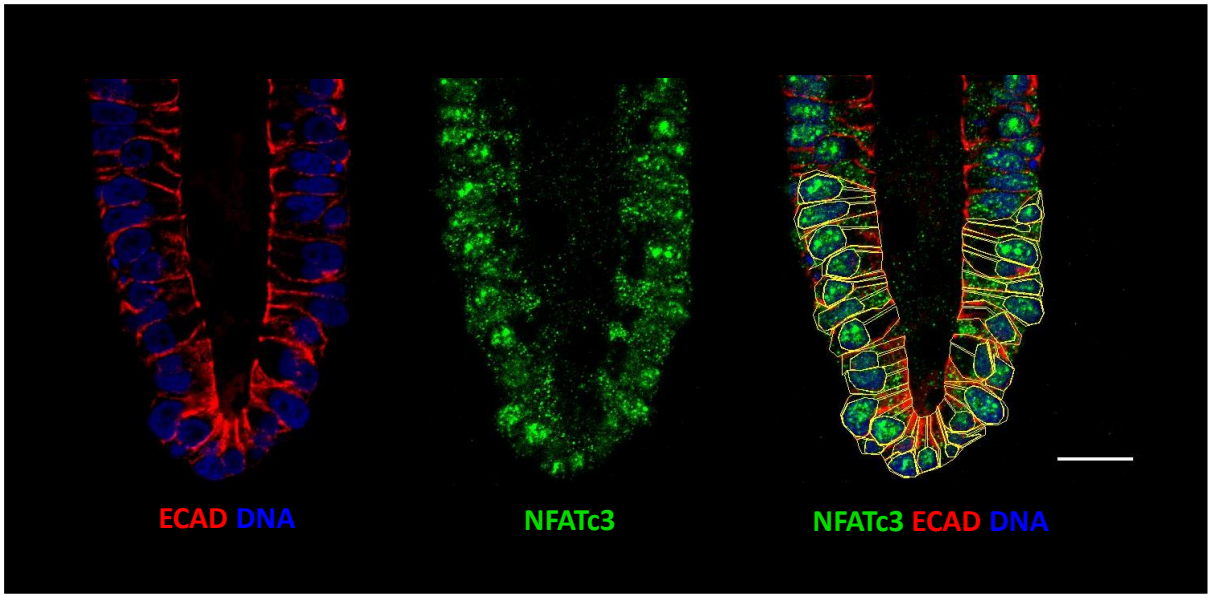

Figure 2.7. Fluorescence measurement of nuclear translocation of transcription factor activators. Quantification of translocation of transcription factor activators to the nucleus was determined by measuring the fluorescence intensity of the NFATc3 antibody. Regions of interest were drawn around the nucleus and cytoplasm of colonic crypts bases using the antibody E-cadherin and the nuclear dye Sytox Blue as reference (left), and the fluorescence intensity of the marker of interest was recorded (middle). Right image shows merged markers with ROIs drawn. Scale bar 10 µm.

Similarly, mucus secretion experiments were quantified by measuring the intensity of fluorescence of the MUC2 antibody used to label mucus. Regions of interest were drawn around the apical pole of the all the mucus positive cells at the base of colonic crypts and organoids (**Figure 2.8**) and the fluorescence intensity was measured, background corrected, normalised to control results and compared between conditions.

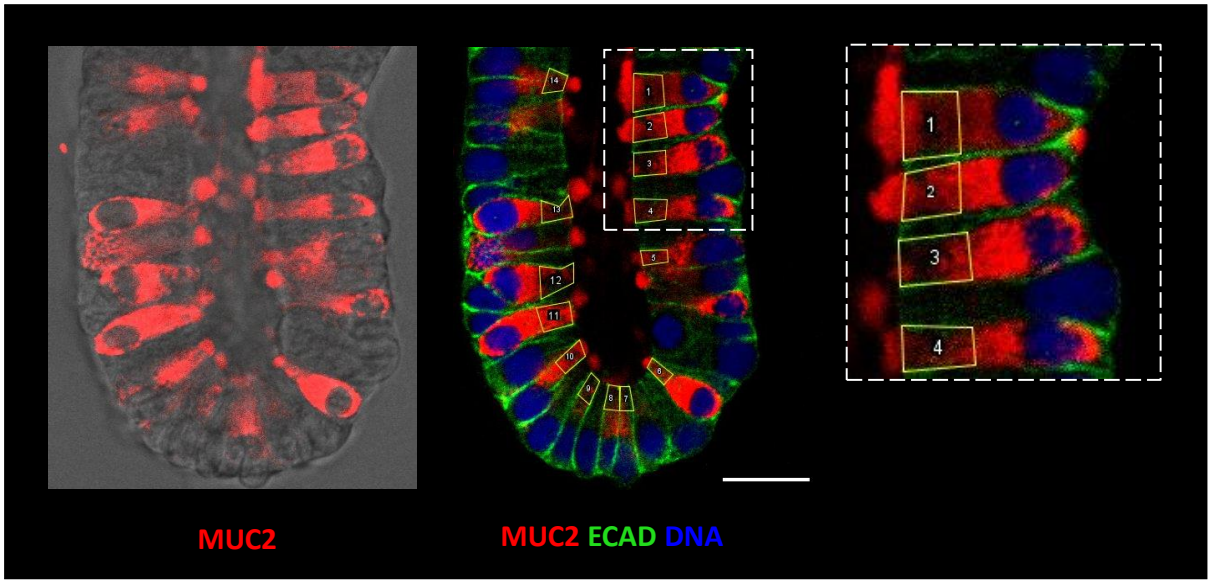

Figure 2.8. Fluorescence measurement of mucus secretion. Analysis of mucus secretion was performed by measuring the fluorescence intensity of the MUC2 antibody (left). E-cadherin antibody and the nuclear dye were used as reference. Regions of interest were drawn at the apical pole of all MUC2 containing goblet cells at the base of the colonic crypt (right). Scale bar 10 µm**.**

2.3.17 Statistical analysis

Data are expressed as mean +/- SEM. Comparison between two groups was evaluated by using paired student's t-test analysis, and comparison between two and more groups was assessed using a one-way ANOVA with Tukey's post-hoc analysis. P value of less than 0.05 was considered significant. 'N' refers to the number of subjects (i.e. patients) and 'n' to the number of crypts or organoids analysed from those subjects.

3 Chapter 3. A human colonic organoid system to study gut epithelial physiology

3.1 Introduction

The study of colonic epithelial physiological functions has been facilitated with the early development of human cell lines like Caco-2 (Sambuy et al., 2005) and T84 (Devriese et al., 2017) which grow as 2D monolayers. This type of *in vitro* cell culture offers some advantages such as low cost and easy maintenance and provides highly reproducible results. However, these cell culture systems have major limitations; 2D culture of human cell lines fail to recreate the physiological cell-to-cell and cell-to-extracellular matrix interactions and fail to recreate the cell polarity present in tissues. Also, Caco-2 and T84 cell lines are derived from intestinal tumours and harbour mutations in oncogenes and tumour suppressor genes that will influence their physiological function. Alternatively, animal models also serve as *in vivo* and (short-term) *ex vivo* systems for the study of gut physiology and are useful to confirm phenomena observed *in vitro*. These platforms allow for the study of gut epithelial cell biology (e.g. polarity), cell physiology (e.g. membrane transport, cell proliferation and migration) pharmacology (e.g. drug testing) and tissue development. Utilising animal models allows work with more complex systems, although they present a genetic difference gap with humans which contributes to the low rate of concordant results with human clinical trials (Mak, Evaniew and Ghert, 2014). The recent development of the organoid 3D culture system has circumvented those limitations by recreating *in vivo*-like tissue architecture, cell polarisation and maintaining genetic profile of the tissue they are derived from without any significant variations. Gut organoids were first developed in mouse by Sato and colleagues (Sato et al., 2009) by embedding dissociated small intestinal crypts in a complex mixture of extracellular matrix proteins (Matrigel) and supplementing it with extracellular matrix growth factors. These conditions allowed for the development of a 3D structure that resemble the crypt morphology and recapitulates the intestinal epithelial characteristics. Stem cells and Paneth cells reside at the bottom the crypt-like structures named buds and proliferate to give rise to all types of differentiated cells. Mouse and human colonic organoids were developed afterwards with the latter needing a different cocktail of growth factors (Jung et al., 2011; Toshiro Sato et al., 2011).

Alongside these discoveries, the Williams lab pioneered the development of a culture model of human colonic crypts. In this model, colonic crypts are isolated and plated in Matrigel and fed with a similar cocktail of growth factors, and are able to retain *in vivo*-like morphology for a few days (Parris and Williams, 2015). Different studies in the lab have validated this culture system as it epitomises

two major characteristics of intestinal crypts biology which are the hierarchy of crypt cell renewal along the axis and functional epithelial cell polarity. The use of isolated human colonic crypts has enabled the study of the regulation of muscarinic-induced intracellular calcium signals (Lindqvist et al., 2002). Furthermore, this culture system was utilised to describe the spatio-temporal characteristics of the major cell signals that regulate crypt renewal (Reynolds et al., 2013), as well as demonstrating the regulation of the expression pattern of NKCC1, a key protein in controlling fluid secretion in gut polarised epithelial cells (Reynolds et al., 2007). Although this culture system is amenable to some molecular techniques such as in situ hybridisation, the development of genetic engineering protocols like siRNA-mediated gene silencing or CRISPR/Cas-mediated gene knock-in and knock-out requires a system with longer-term *ex vivo* viability. Isolated colonic crypts can be mechanically disrupted and passaged to generate colonic organoids. These structures can be propagated indefinitely with no significant physiological or genetic variations, making then a very useful tool. In addition, organoids have been demonstrated to recapitulate nutrient absorption and transport, fluid secretion and epithelial ion transport (Foulke-Abel et al., 2016; Middendorp et al., 2014; Zietek et al., 2015) and shown to be a useful model for host-microbe interaction (Leslie et al., 2015; Saxena et al., 2016). Furthermore, organoids have been demonstrated to be amenable to genetic engineering with the CRISPR/Cas system to enable the modelling of colorectal cancer progression (Melo et al., 2017) and the repair of transmembrane ion transport (Schwank et al., 2013; Berkers et al., 2019). All of these discoveries highlight the importance of the gut organoid model as a powerful tool to study intestinal physiology and pathophysiology which encouraged our lab to develop and adopt this culture system for our research purposes.

Colonic crypts are finger-like invaginations of the epithelium composed of a population of different specialised cells. The base of the crypt is populated by stem cells that proliferate to give rise to all the different cell types as they migrate and differentiate towards the crypt opening. Stem cells can be characterised by the expression of protein markers such as LGR5 (Barker et al., 2007), OLFM4 (van der Flier et al., 2009) and PTK7 (Jung et al., 2015). Stem cells give rise to cells of secretory function that include goblet cells, enteroendocrine cells and tuft cells as well as cells with absorptive roles which include enterocytes. Goblet cells are of the most abundant cell types and their main role is to secrete mucus and antimicrobial proteins to protect the epithelial barrier. They are distributed along the entire crypt-axis including the base of the crypt where they are thought to regulate and maintain the stem cell population (Sasaki et al., 2016). In the colon, goblet cells secrete the mucin glycoprotein MUC2 which is used as a specific cell marker (Johansson et al., 2008). Enteroendocrine cells are specialised in secreting a great range of hormones such us serotonin or somatostatin to modulate digestion, absorption and appetite. They are present along the crypt-axis in lower

numbers than goblet cells and are routinely identified by the expression of the protein chromogranin A (CHGA), a major component of the endocrine secretory granules (Gut et al., 2016). Tuft cells are a group of chemosensory cells that can sense a wide variety of signals through mechanisms still not very well understood to regulate the immune response via cytokine secretion as well as the secretion of other important molecules such as prostaglandin E_2 (PGE2) and ACh (Gerbe et al., 2012). This cell type represents less than 1% of the cells of the crypt and in the colon it can be identified by the expression of the choline acetyltransferase (ChAT) enzyme that catalyses the generation of ACh (Hayakawa et al., 2016). Finally, the enterocytes are a cell lineage whose role is to absorb nutrients, water and electrolytes resulting from the food digestion. These are the most abundant cell type in the colon and can be identified by the expression of protein markers such as carbonic anhydrase (CA) enzyme that catalyses the hydration of CO_2 (Bekku et al., 1998) and fatty acid-binding protein (FABP), thought to be involved in nutrient absorption (Agellon, Toth and Thomson, 2002). These cell types define the crypt epithelium and govern its functioning. Therefore, in order to validate our organoid culture system as a model capable of recapitulating these characteristics, it is critical that they retain the expression of all undifferentiated and differentiated cell types and recapitulate cellular signals that govern the physiological function of the gut epithelium.

ACh is molecule implicated in the regulation of key physiological processes in the gut epithelium which include fluid and mucus secretion to maintain the epithelial barrier integrity, immune regulation and stem cell proliferation (Birchenough et al., 2016; Campoy et al., 2016; Halm & Halm, 2000; Ramirez et al., 2019). ACh can be produced by cholinergic neurons (Neunlist et al., 2013) and has recently been shown to be produced by tuft cells (Nevo, Kadouri and Abramson, 2019). Upon secretion, ACh can bind to cholinergic receptors located in the cellular membrane of the gut epithelial cells. The family of cholinergic receptors include the muscarinic receptors which constitute a subfamily of GPCR that can generate intracellular second messengers upon binding of a ligand (Albuquerque et al., 2009). Muscarinic receptor type 3 (MAChR3) has been shown to be the dominant receptor subtype expressed in the basolateral membranes of the colon (Dickinson, Frizzell, & Sekar, 1992; Lindqvist et al., 2002; O'Malley et al., 1995; Reynolds et al., 2007) which together with MAChR1 and MAChR5 are coupled to the release of calcium from intracellular stores. Binding of ACh to muscarinic receptors in the gut activates the G_α proteins to mediate the production of IP3 and DAG via activation of the enzyme phospholipase C (PLC). Production of IP3 induces the increase in intracellular calcium by activating IP3R in the membrane of the endoplasmic reticulum (ER) to allow the ion flux into the cytoplasm (Eglen, 2006).

Calcium is a second messenger that functions as a powerful intracellular signalling ion capable of integrating a sophisticated network of signalling pathways to regulate cell physiology and cellular responses of the tissue environment. External stimulation of cells by hormones, neurotransmitters or grow factors can elevate intracellular calcium concentrations to provoke a cellular response (Bootman and Bultynck, 2019). The type of response will depend on the complex spatio-temporal characteristics of the signal and can result in the activation of many cellular processes some of them being rapid events such as muscle contraction or neurosecretion and others being slower like cell proliferation, differentiation or apoptosis (Dupont et al., 2011). The source of calcium needed to generate a cellular signal can be the intracellular calcium stores such as the endoplasmic reticulum (ER), mitochondria or the endolysosomes as well as the influx from the extracellular space. In both cases, the influx from the outside of the cell or the release and reabsorption from intracellular stores is mediated by a series of ion channels (Berridge, Lipp and Bootman, 2000). The ER is the biggest intracellular calcium store and regulates the flux of calcium into the cytoplasm via the IP3R and the RyRs. Activation of IP3Rs are primarily regulated by calcium and the messenger IP3 whereas RyRs are predominantly regulated by calcium and cADPR. A sustained activation of the calcium signals by a potent stimulus can induce the release of calcium from various channels of the ER. This released calcium can subsequently activate the secretion of calcium from more ER calcium channels by a process named CICR which results in the generation of a calcium wave signal that can modulate different cellular processes (Berridge, Bootman, & Roderick, 2003). The endolysosomes are acidic organelles which play a major role in nutrient sensing, autophagy and calcium signalling (Gómez-Suaga et al., 2012; Ogunbayo et al., 2018). These organelles are also able to store calcium and release it upon stimuli to induce local or global (via ER-dependent CICR) calcium signals. Calcium was shown to be mobilised from these stores via nicotinic acid adenine dinucleotide phosphate (NAADP)-mediated activation of the endolysosomal two-pore channels (TPCs) (Calcraft et al., 2009). NAADP is synthesised by the enzyme CD38 from the substrate $NAPD^+$ and nicotinic acid, and is regarded as the most potent calcium mobilising messenger discovered so far, which is efficacious at low nanomolar concentrations (Galione et al., 2010).

Research in the Williams lab has demonstrated that ACh and its analogue Carbachol (CCh) activate MAChR3 in a culture system of human isolated colonic crypts. The binding of this ligand induces a calcium signal that originates at the apical pole of the cells located at the base of the crypt, then propagates to the basal membrane and is then amplified up the crypt-axis (Lindqvist et al., 2002; Reynolds et al., 2007). These calcium signals were monitored by live imaging of crypts loaded with the calcium-sensitive fluorescence indicator Fura-2. This molecule binds to intracellular calcium and can record alterations in the ion concentration by changes in fluorescence. In polarised epithelial

cells, it is thought that under normal conditions the ER is located predominantly in the vicinity of the nucleus at the basal pole of the cell, whereas endolysosomes are mostly located in the apical pole. The observation that the muscarinic-induced calcium signal originates at the apical pole of the cell, prompted the question to whether endolysosomes were responsible for the initiation of the signal. Subsequent work carried out in the Williams lab studied the mechanisms of intracellular calcium mobilisation upon muscarinic activation in human isolated colonic crypts. Preliminary results suggested a role of the endolysosomal TPCs in mediating the muscarinic-induced calcium response. In order to validate colonic organoids as an effective culture system it is needed to demonstrate their capability in recreating the same physiological and cellular responses and present the major components of the muscarinic-calcium signalling toolkit.

The use of organoid culture system has been shown to be a major advance in the biomedical field as it provides a platform for the study of organ and tissue physiological and cellular mechanisms in an environment that recapitulates most of the *in vivo* characteristics. The study of intracellular calcium signals has historically been carried out in other organisms or cell culture systems and is yet to be studied in human organoids. Preliminary work from Dr Christy Kam suggest that muscarinic signals induce an intracellular calcium response via release of calcium to the cytoplasm via TPC. The aim of this chapter is to develop and characterise a human colonic organoids system and validate it as a model for the study of intestinal tissue physiology as well as a tool for the study of intracellular calcium signals.

3.2 Results

In order to develop, characterise and validate human colonic organoids as an effective 3D tissue culture model system for the study of gut physiology, a series of techniques were carried out through the course of this study. Firstly, the cell culture and growth conditions were determined empirically based on current literature and the previous expertise on culturing human isolated crypts. Next, the organoids were genetically characterised in order to be compared to native human tissue and freshly isolated crypts with the use of RNA sequencing, PCR and quantitative real-time PCR to measure gene expression. Immunofluorescence and confocal imaging was used to determine the presence and localisation of key cellular markers and components of the muscarinic-calcium signalling toolkit. Finally, live imaging of calcium signalling using the calcium fluorescence indicator Fura-2 was used to investigate the mechanism of muscarinic receptor-induced intracellular calcium signals in cultured colonic crypts and organoids.

3.2.1 Development of a human colonic organoid culture

Gut organoids from mouse were the first to be generated and further validated as a powerful research tool by the pioneering work of Sato, Clevers and colleagues (Sato et al., 2009). Subsequent research has led to the development of a human colonic organoid culture system (Jung et al., 2011; Toshiro Sato et al., 2011; Jung, Sommer, Francisco M. Barriga, et al., 2015), which can now be used as an alternative and resourceful platform for the study of the colon epithelium. In order to develop human colonic organoids, human colonic crypts were first isolated from the mucosa obtained from colorectal surgery, following the well stablished protocol from the Williams lab (Parris and Williams, 2015). First, the residual muscularis mucosa was removed manually and discarded and crypts were incubated in a crypt isolation solution to help dissociate epithelial structures. Liberated crypts were then placed in media, embedded in the extracellular matrix-like Matrigel and seeded in 24 well culture plates. Crypts were then fed with human colonic crypt culture media (hCCCM) supplemented with a cocktail of growth factors (see materials and methods chapter) and incubated at 37^0C and 5% CO_2. Isolated crypts retained the same finger-like morphology *in vitro*, displaying a distinctive crypt-base and opening at opposing ends of a crypt lumen (**Figure 3.1A**). Colonic crypts were grown for 7 days after which they were ready for passage. Cultured crypts were detached from the plate and mechanically disrupted into smaller fragments. These fragments were embedded in Matrigel, fed with hCCCM and incubated at 37^0C and 5%CO_2 and eventually gave rise to organoids that displayed a spherical shape with no clear opening. The organoids started to develop different numbers of crypt-like structures or buds after the first 2-3 days in culture as well as showing a well-defined lumen, suggesting apicobasal polarity (**Figure 3.1B and 3.2A**). Under these culture conditions, organoids increased in size over time and retained the formation and growth of the crypt-like structures, suggesting the presence of fully differentiated cells. Organoids were passaged every 5 to 7 days at which time, RNA and DNA were isolated to create a genetic biobank. In addition, a population of organoids were frozen and stored in liquid nitrogen to generate an organoid tissue biobank. The starting size of the organoids was adapted to the type of functional experiment. Experiments that required fully matured organoids (i.e. presenting buds) such as those for the study of intracellular calcium signals or mucus secretion were seeded as big fragments, whereas experiments where the aim was to investigate organoid growth were seeded as small fragments. Furthermore, a single cell culture system was developed, derived from the organoid cultures. In a similar fashion, organoids were mechanically disrupted and filtered to obtain only single cells of a homogenous size which were plated and fed as described above (**Figure 3.1C and 3.2**). Single cell cultures were developed with the aim of studying the biology of cells in the absence of neighbouring cell signals as well as to help determine the capacity of forming organoids under different growth conditions.

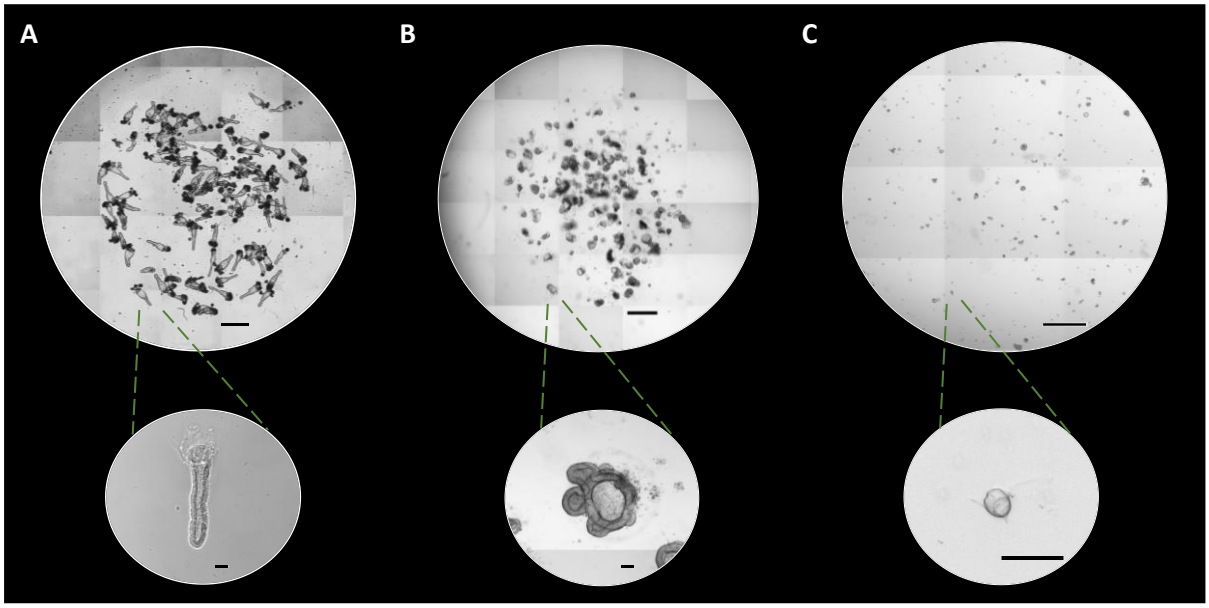

Figure 3.1. Different culture systems for the study of the colon epithelium. Representative brightfield images of the culture of (**A**) human isolated colonic crypts, (**B**) budding human colonic organoids and (**C**) spherical colonic organoids formed from single cells. The bottom row shows high magnification images of individual structures depicting their representative morphology. Scale bar is 500 µm in the upper row of images and 50 µm in the lower row of images.

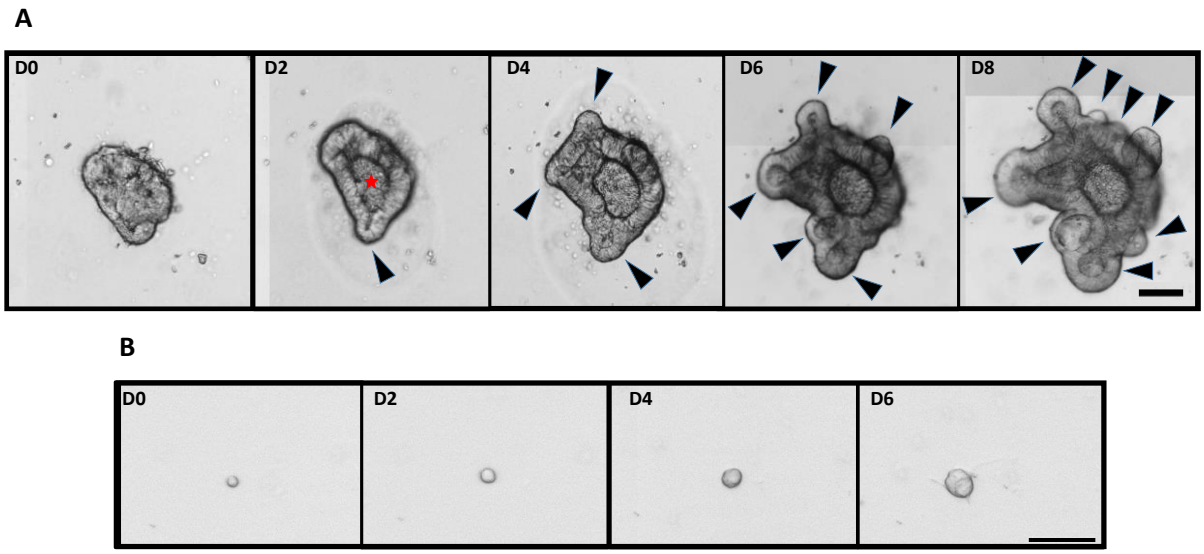

Figure 3.2. Growth of cultured colonic organoids and single cells. (**A**) Colonic organoids grow and develop buds over time. Red star indicates presence of lumen. Arrowheads mark buds. Scale bar 150 µm. (**B**) Single cell grow over time. Scale bar 50 µm.

3.2.2 Characterisation of the cellular types in the colon epithelium

The morphological analysis of organoid growth revealed the presence of crypt-like domains with a lumen, suggesting a strong structural similarity with cultured crypts and native tissue. To further evaluate the organoid culture system, we decided to analyse gene expression and proteins of key cell-type markers in order to study the cellular diversity across the different tissue samples.

3.2.2.1 The gene signatures of colonic organoids closely match those of isolated colonic crypts and native tissue.

In order to study comparative bulk gene expression, RNA and DNA samples from the mucosal native tissue containing a mixture of cells including epithelial cells, mesenchymal cells or immune cells, were isolated immediately after the patient's colorectal surgery, as wells as from crypts liberated from the muscularis mucosa prior to their seeding. In addition, RNA and DNA were also purified from organoid cultures established from the same patient's colonic crypts.

Our first approach was to investigate the presence of the different epithelial cell types including stem cells, secretory and absorptive cells, by carrying out reverse transcription PCR for cell-type enriched transcripts on RNA samples obtained across all systems. Isolated and purified RNA was first reverse transcribed to cDNA and PCR amplified using specific primers (see materials and methods). The PCR product was then run in 3% agarose gels containing ethidium bromide and visualised under a gel imager. The results confirmed the expression at the mRNA level of the stem cell markers LGR5, OLFM4 and PTK7 in the mucosa, crypts and organoids (**Figure 3.3**). Interestingly, the stem cell marker PTK7 expression in mucosa was fainter than the one observed in crypts and organoids. The goblet cell marker MUC2, the main constituent of colonic mucus, and the enterocyte marker fatty acid-binding protein 2 (FABP2), involved in fatty acid transport, were also consistently expressed in all samples. The presence of Tuft cells was evaluated by analysing the expression of ChAT, the enzyme that catalyses the formation of ACh, and VAChT, the marker for the vesicular transporter of ACh to the membrane. The conventional PCR amplification of both markers showed faint bands across all conditions (data not shown), so a nested PCR was carried out using another set of primers to amplify a broader genomic region where these genes are located. The resulting PCR product was subsequently amplified using the original primers which showed the expression of VAChT in all samples. However, although expressed in native mucosa and isolated crypts, our results showed no expression of ChAT in colonic organoids (**Figure 3.3**). In addition, we analysed the expression of the nerve growth factor (NGF), which has been implicated in promoting a NGF/CHAT/ACh/MAChR/NGF positive feedback loop to regulate gastric epithelial cell growth (Hayakawa et al., 2016) and confirmed its expression in native mucosa and isolated crypts. The enzyme glyceraldehyde-3-

phosphate dehydrogenase (GAPDH) was used a positive control since its expression is constant in the colon epithelium (Barber et al., 2005) and was shown to be present in all three samples derived from one patients' tissue (**Figure 3.2**).

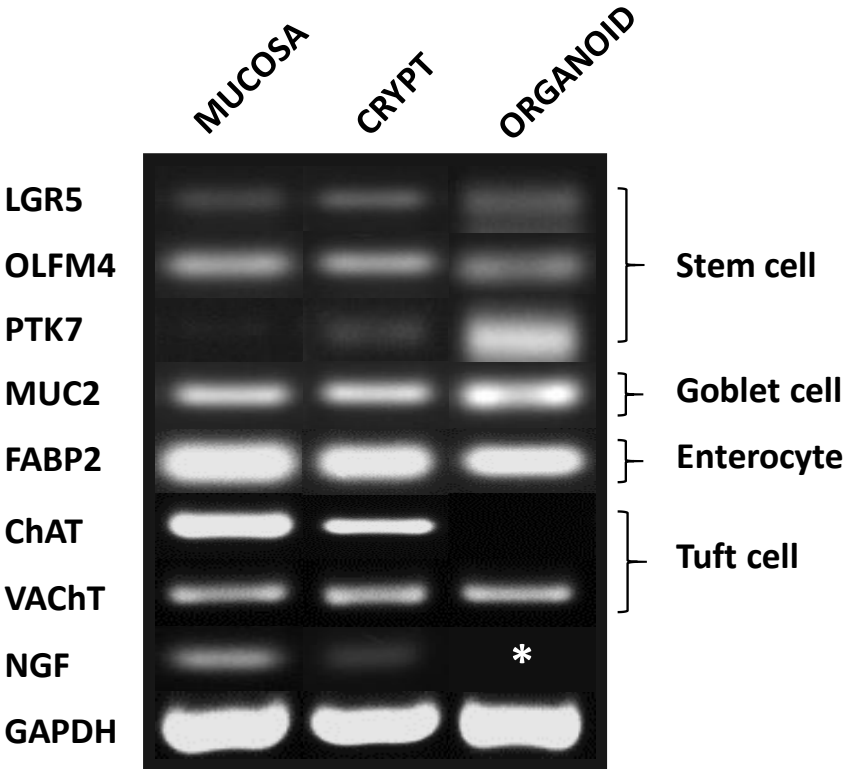

Figure 3.3. Genetic expression of key cellular markers. Agarose gel showing the RNA expression of the different colonic epithelial cell types in native mucosa, isolated crypts and organoids. Colonic organoids present all cellular makers except from ChAT. Asterisk indicates missing sample. The image is a construct of different experiments.

In order to obtain a more comprehensive analysis to determine the genetic similarities between the native tissue, isolated crypts and organoids, we analysed the gene expression characteristics of markers of the different colonic epithelial cellular types using bulk RNA sequencing of isolated genetic material from the mucosa, isolated crypts and organoids derived from the healthy mucosa of 6 CRC patients. The number of reads derived from next generation sequencing was normalised to correct the differences in sample sequencing and gene length and presented as reads per kilobase million (RPKM) (**Appendix A, Figure A1**). The expression of stem cell markers LGR5, OLFM4, ASCL2 and PTK7 (Barker et al., 2007; van der Flier, Haegebarth, et al., 2009; Jung, Sommer, Francisco M. Barriga, et al., 2015; Yan and Kuo, 2015) was confirmed in all patients and across all different tissue sample for each patient. The proportions varied across samples with LGR5, ASCL2 and PTK7 showing

higher gene expression in colonic crypts whereas the expression of OLFM4 was found to be higher in organoids (**Figure 3.4**).

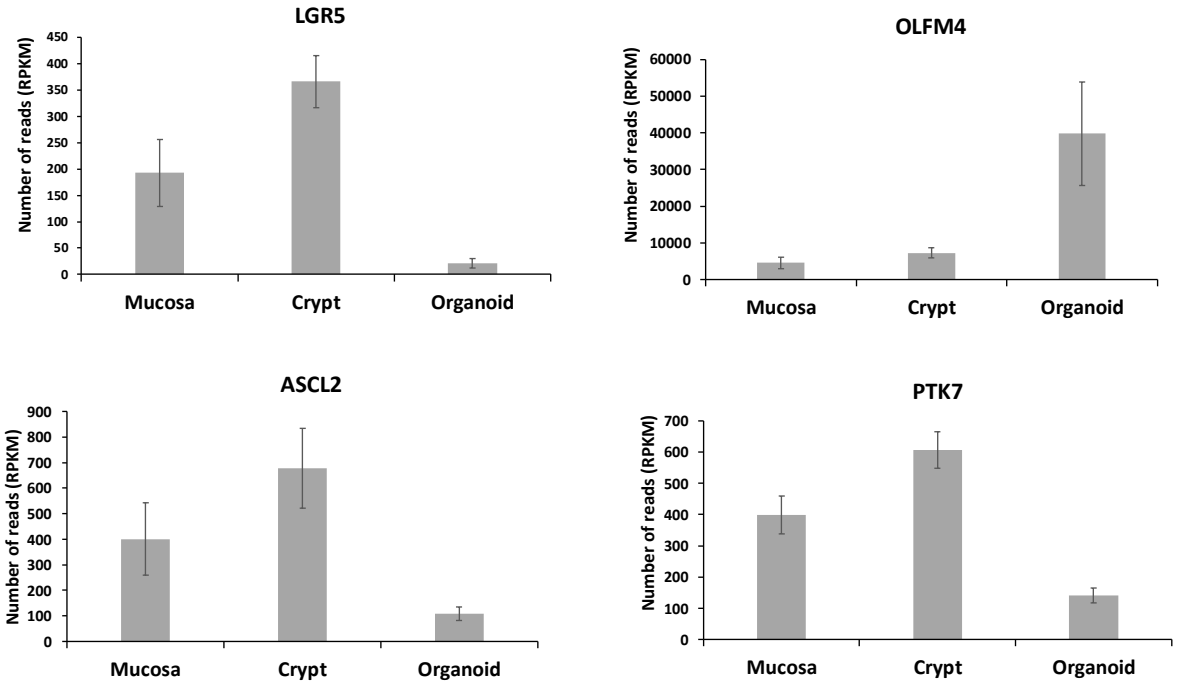

Figure 3.4. Gene expression of colonic epithelial stem cell markers. The bar charts represent the presence and the mean RNA expression levels of the stem cell markers LGR5, OLFM4, ASCL2 and PTK7 across human colonic mucosa, isolated crypts and organoid samples from 6 patients. Data is expressed as number of reads (RPKM).

The presence of goblet cells was evaluated by analysing the gene expression of the canonical colonic goblet cell marker MUC2, as well as WFDC2, which has been shown to be prominently expressed in goblet cells located at the base of the crypt (Parikh et al., 2019). In addition, we analysed the expression of the goblet cell secreted trefoil factors, which help protect the epithelial barrier. The family is formed of three isotypes (TFF1, 2 and 3) of which TFF3 is thought to be expressed in the goblet cells located in upper regions of the crypt (Taupin and Podolsky, 2003). RNAseq analysis of genetic expression confirmed the presence of all goblet cell markers in the different tissue samples. The high number of MUC2 gene reads possibly indicates the presence of a big population of goblet cells. Interestingly, organoids showed highest expression of these goblet cell markers, including MUC2 and WFDC2 (**Figure 3.5**).

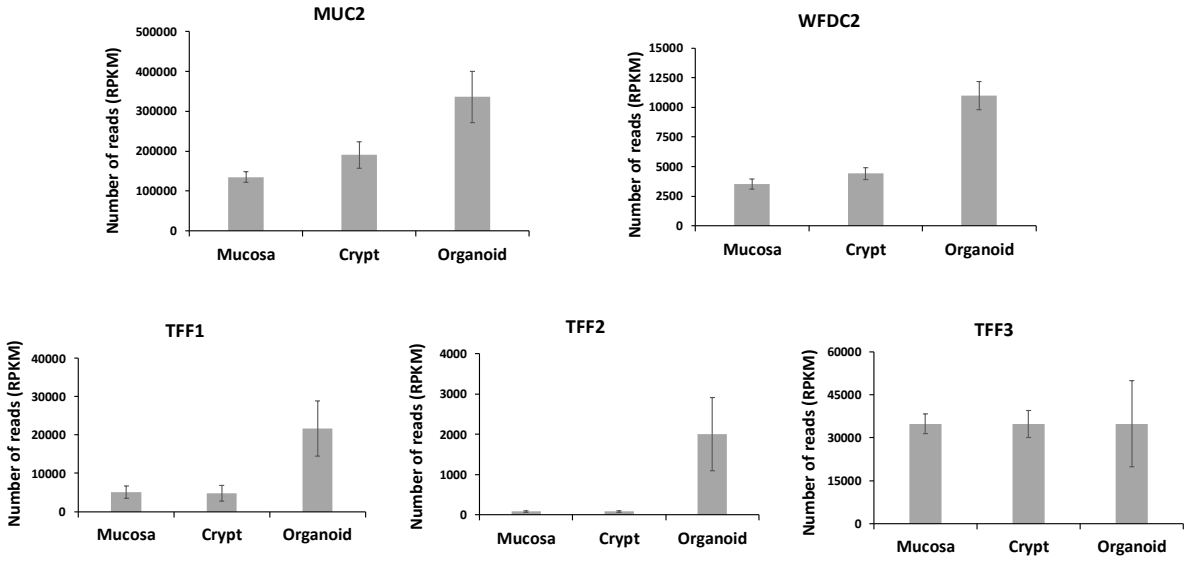

Figure 3.5. Gene expression of colonic epithelial goblet cell markers. The presence of goblet cells in colonic tissue samples was assessed by analysing the RNA expression of the goblet cell markers MUC2, WFDC2, TFF1, 2 and 3 across human colonic mucosa, isolated crypts and organoid samples from 6 patients, represented in the bar charts. Data is expressed as number of reads (RPKM).

We then analysed the presence of enteroendocrine cells, the other main secretory cell type present in the colon epithelia. To do so, we looked at the expression of the pan-enteroendocrine marker chromogranin A (CHGA) which is implicated in the generation of hormone secretory vesicles (Gut et al., 2016), together with the expression of the glucagon-like peptide 1 gene (GCG) which is characteristic of enteroendocrine subtype L cells (Brubaker and Drucker, 2004). Transcriptomic analysis of the tissue samples revealed simultaneous presence of both CHGA and GCG (**Figure 3.6**).

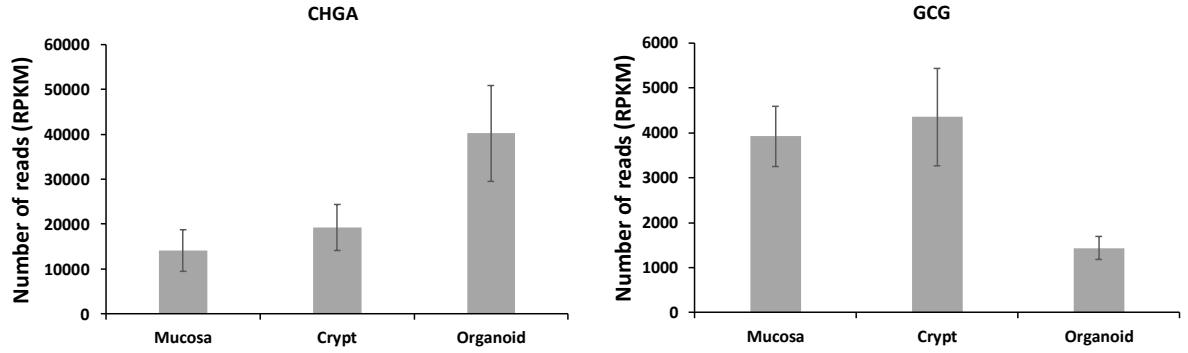

Figure 3.6. Gene expression of enteroendocrine cell markers. Measurement of gene expression in human colonic mucosa, isolated crypts and organoids of the enteroendocrine cell markers CHGA and GCG is represented in the bar charts. Data is expressed as number of reads (RPKM).

In order to investigate the presence of enterocytes, we analysed the gene expression of carbonic anhydrase (CA) isoforms 1 and 2, regulators of the levels of water and electrolytes (Bekku et al., 1998) as well as the expression of the fatty acid-binding protein (FABP) subtypes 1 and 2, involved in nutrient absorption (Agellon, Toth and Thomson, 2002). The examination of the gene expression levels determined the presence of the enterocyte markers in all the tissue samples and revealed a different expression pattern where CA levels were higher in crypts whereas FABP gene expression was greater in organoids (**Figure 3.7**).

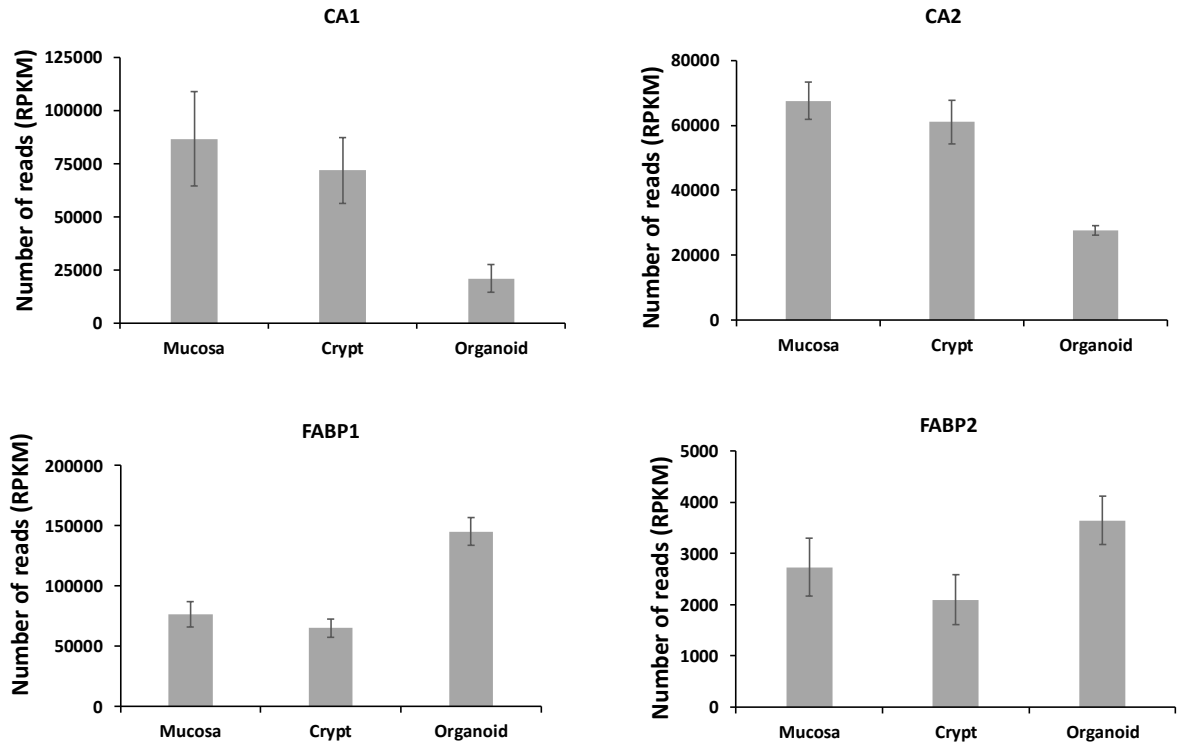

Figure 3.7. Gene expression of enterocyte markers. Bar chart shows presence and expression levels of CA1 and 2 as well as FABP1 and 2 in human mucosa, isolated crypts and organoids (N=6). Data is expressed as number of reads (RPKM).

Finally, we evaluated the presence of tuft cells, which are known to secrete ACh and prostaglandins (Banerjee et al., 2018). The presence of this cell type was assessed by studying the gene expression of the markers choline acetyltransferase (ChAT) which catalyses the production of ACh as well as the genes PTGS1 and 2 that code for Cox1 and Cox2 respectively, and are responsible for prostaglandin synthesis (Eberhart and Dubois, 1995). In addition, tuft cells can be identified by the expression of the doublecortin-like kinase 1 (DCKL1) and the Pou domain class 2 (POU2F3) involved in the generation of taste receptors (Matsumoto et al., 2011). RNA sequencing analysis of these markers showed that whereas the expression of POU2F3 was constant across tissue samples, we reported low expression of CHAT, DCLK1 and PTGS1 and 2 in crypts and organoids compared to mucosal

samples. In organoids, the expression was minimal which could suggest an absence of mature tuft cells (**Figure 3.8**).

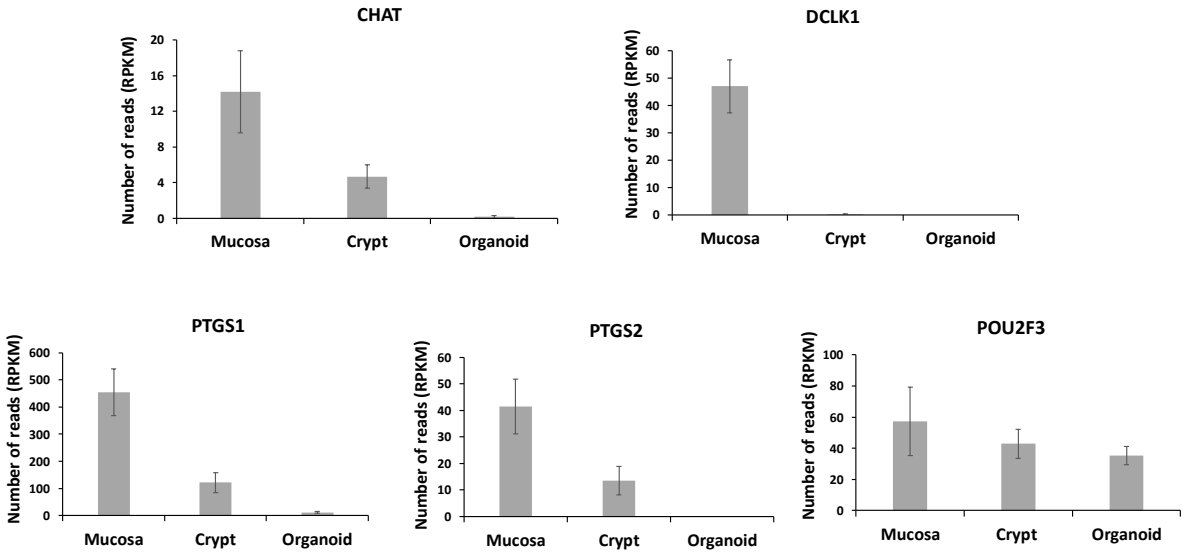

Figure 3.8. Gene expression of tuft cell markers. RNA expression of tuft cell markers was studied by analysing the presence of ChAT, DCLK1, PTGS1, PTGS2 and POU2F3 across the different tissue samples. N=6. Data is expressed as number of reads (RPKM).

Next, we decided to investigate how our culture conditions influence gene expression in organoids. Cultured crypts and organoids are fed with hCCCM media supplemented with stem cell niche ligands such as Wnt and R-spondin, that stimulate cell proliferation and migration (Reynolds et al., 2013). We therefore chose to test the levels of expression of a set of cell proliferation markers (LGR5, ASCL2 and Ki67) and compare it to a set of differentiation markers (CA1, AMPEP, CEACAM7) by using quantitative real time PCR (qRT-PCR), following a similar approach to previous research done by Jung and colleagues (Jung et al., 2015). As described earlier in this chapter, LGR5 and ASCL2 are both important stem cell markers, whereas Ki67 is a protein expressed in active proliferating cells (Gerdes et al., 1984). CA1, AMPEP and CEACAM7 are all markers of differentiated enterocytes (Bekku et al., 1998; Schölzel et al., 2000; Kramer et al., 2005). To understand how the components of the culture media affect the biology of organoids we compared the expression of the markers of interest in organoids cultured in standard hCCCM (for this experiment referred as STEM media) to those cultured in a media devoid of the growth factors Wnt and R-spondin, to promote cell differentiation (hereafter referred as DIFF media). Colonic organoids were passaged and cultured for 8 days. On the last 5 days two groups were prepared, one of which was kept in STEM media, whereas the other group was changed to DIFF media.

For this experiment we first analysed the relative gene expression of different housekeeping genes with a constant expression between the native tissue, isolated crypts and organoids, in order to normalise our results to a reference. To do so, we compared the relative gene expression of the genes 18s rRNA, GAPDH, beta-2-microbulin (B2M), actin-beta (ACTB) and phospholipase A2 (YWHAZ) (Vandesompele et al., 2002) across 8 samples including 2 of isolated crypts and 3 pairs of different organoid lines, previously cultured in STIM of DIFF media. The results showed that YWHAZ expression was the most stable as it presented the lowest standard deviation between samples (**Figure 3.9**). We then measured the expression of the genes of interest and demonstrated that the proliferation markers LGR5, ASCL2 and particularly Ki67 were all upregulated in the STEM media whereas their expression was substantially reduced in the DIFF media. Conversely, the differentiation markers ANPEP and CA1 in particular, were found to be upregulated in organoids treated with DIFF media and downregulated when kept in STEM media, suggesting that Wnt and R-spondin maintain stem cells and tissue renewal of organoids. Interestingly, the relative gene expression of the cell differentiation marker CEACAM7 showed a slight upregulation in organoids grown in STEM media (**Figure 3.10**).

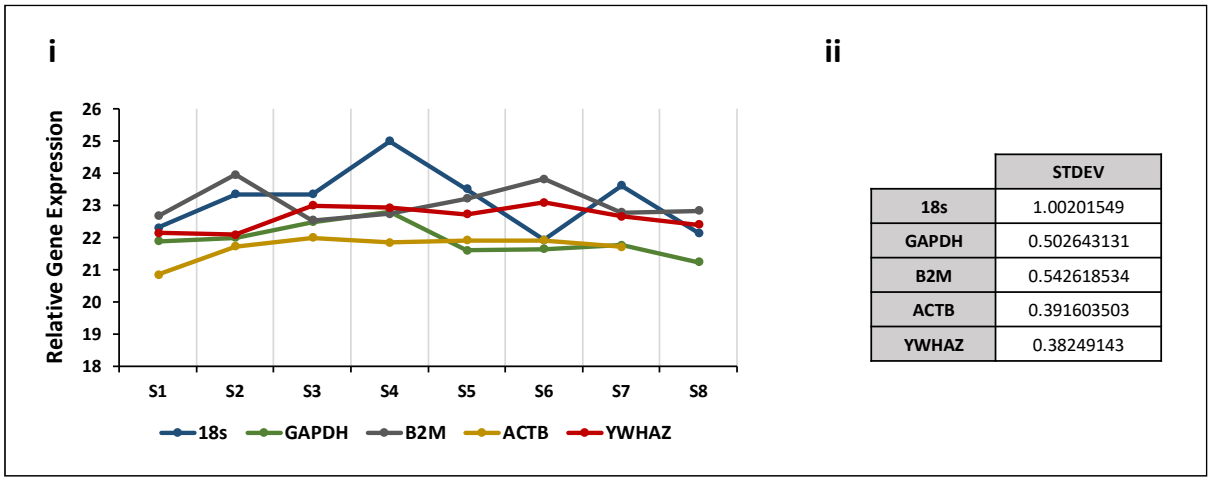

	STDEV
18s	1.00201549
GAPDH	0.502643131
B2M	0.542618534
ACTB	0.391603503
YWHAZ	0.38249143

Figure 3.9. YWHAZ is an ideal reference gene in all culture systems. (**i**) The chart represents the relative gene expression of candidate housekeeping genes across the different samples, shown as variations in the average of Ct values (N=8, n=2). (**ii**) The measurement of the standard deviation across samples indicates that YWHAZ expression is the most stable.

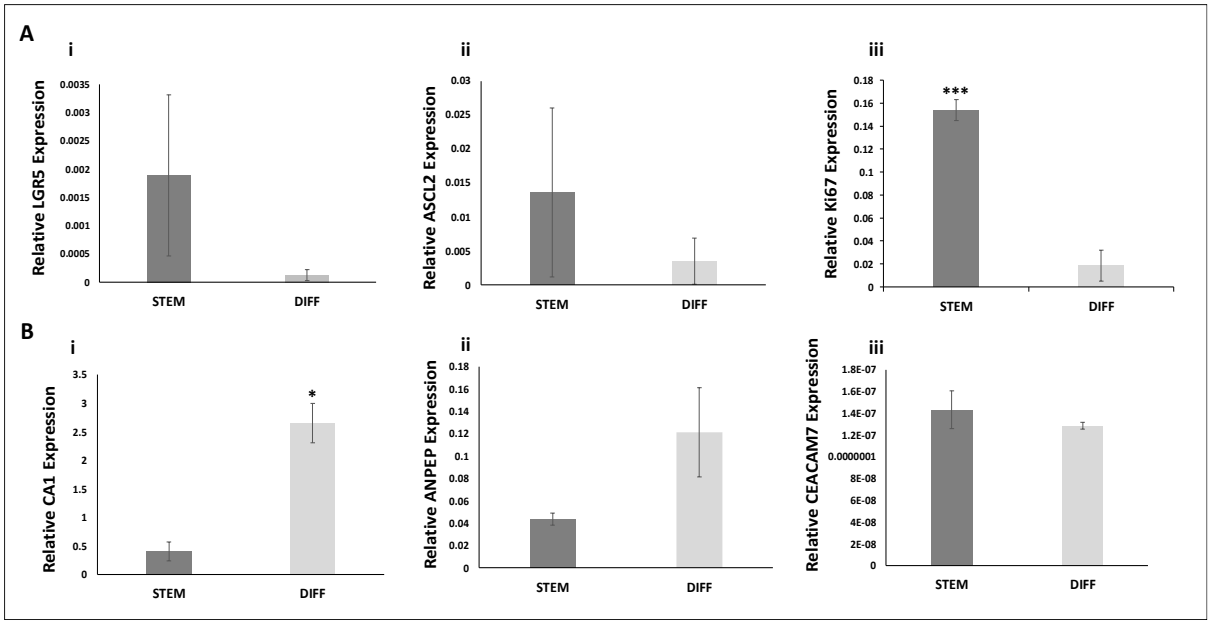

Figure 3.10. Differential gene expression of candidate genes in STEM versus DIFF media. (**A**) The bar charts show the relative gene expression of the cell proliferation markers in organoids cultured with STEM or DIFF media. (**i**) LGR5, (**ii**) ASCL2, (**iii**) Ki67. (**B**) The bar charts show the relative gene expression of the cell differentiation markers in organoids cultured with STEM or DIFF media. (**i**) CA1, (**ii**) ANPEP, (**iii**) CEACAM7. The relative gene expression is shown as the expression fold change of the averaged Ct value normalised to YWHAZ (N=2 biological replicates, n=2 technical replicates, *P<0.05, **P<0.01).

3.2.2.2 Cell types and distribution in human colonic epithelium

The gene expression measurements demonstrated the presence of the major cellular markers in organoids. We next sought to confirm these results by analysing the presence of these cell makers at the protein level. First, we evaluated the expression of the stem cell marker OLFM4 in native tissue (obtained from sectioning mucosa samples), cultured crypts and organoids. To do so, the native tissue was immediately fixed after the surgical resection of the colon sample and sectioned using a cryostat microtome. Colonic crypts and organoids were fixed on day 1 after passage and all samples were stained with OLFM4, E-cadherin (ECAD) and the nuclear stain Sytox blue. Confocal imaging revealed the expression of the stem cell marker to be localised in the bottom of the crypt. In native tissue, the expression was predominant at the base and could also be seen at the suprabase but became almost inexistent in the upper regions of the crypt (**Figure 3.11A**). Similarly, the expression of OLFM4 was located to the base of the buds in organoids and was absent in regions above (**Figure 3.11B**). In addition, colonic crypts were also shown to express the stem cell marker in the base of the crypt (**Figure 3.11C**).

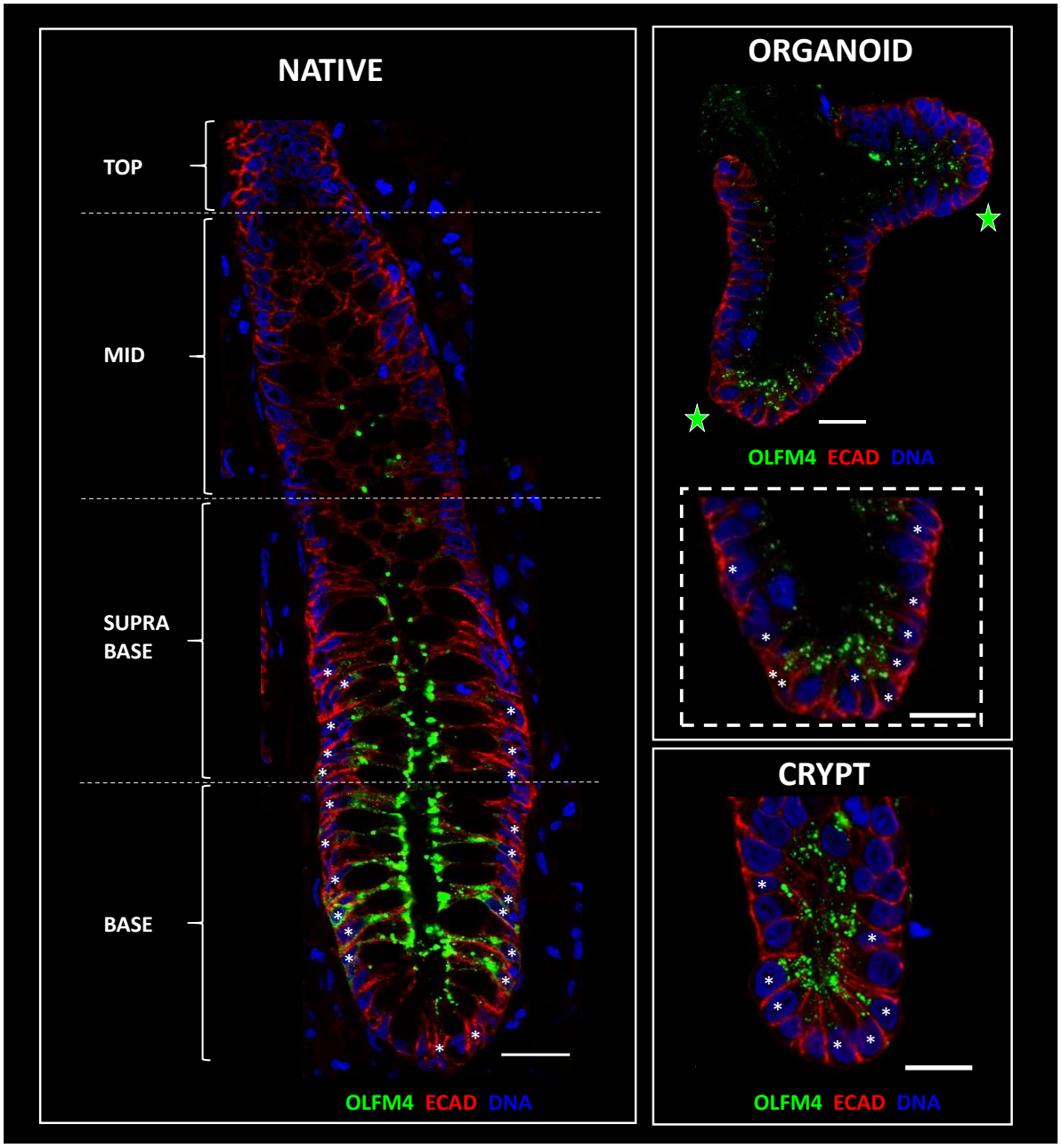

Figure 3.11. Stem cells reside at the base of the crypts. Confocal images illustrate the presence of OLFM4 (green) (**A**) OLFM4 positive cells are expressed in the base and supra-base regions in native tissue and absent in the upper regions. (**B**) OLFM4 positive cells are present in the base of buds in organoids. Green-filled stars indicate presence of buds. Dashed region indicates high magnification image of an organoid bud. (**C**) Presence of OLFM4 labelled cells in the base of colonic crypts. Asterisks indicate presence of stem cells. Data also contributed to by Alvin Lee. Scale bar 25 µm.

Next, we analysed the presence of the goblet cell secretory marker MUC2, known for generating the mucin layer that helps maintaining the epithelial barrier (Johansson et al., 2011). Samples were fixed and immunolabelled with MUC2 antibody. Confocal imaging of the base of the crypts and buds

demonstrated the presence of a large number of goblet cells (**Figure 3.12**), which were also present along the entire tissue sample (**See chapter 4, figure 4.2**).

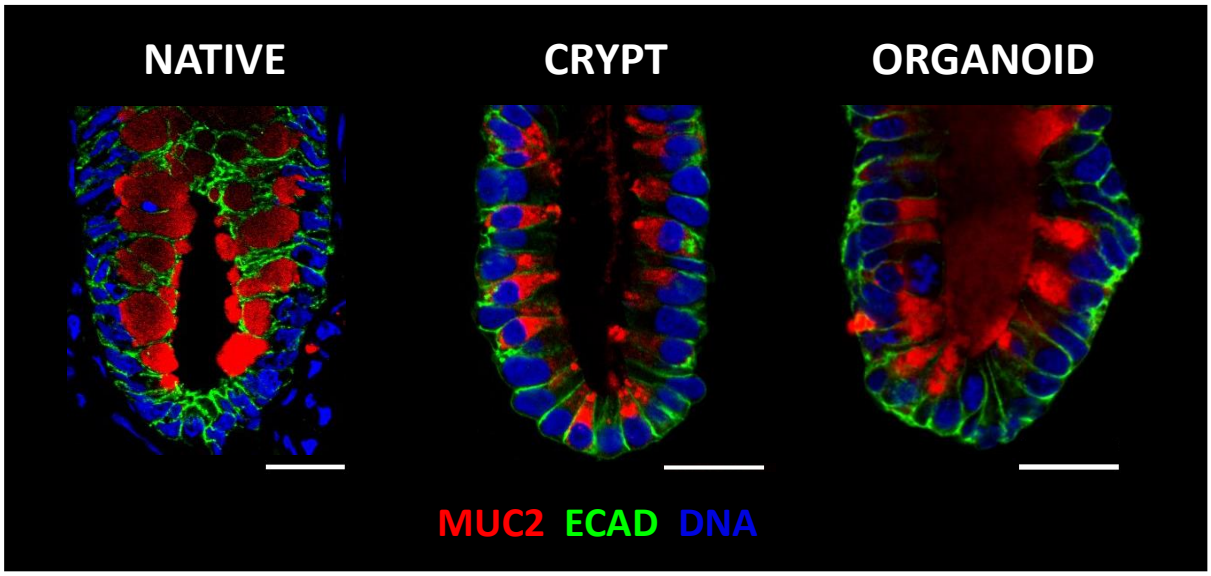

Figure 3.12. Goblet cells are expressed at the base of the crypt. Representative confocal images showing presence of goblet cells labelled with MUC2 (red) in the base of the crypt. ECAD (green), nuclei stained with Sytox blue (DNA). (**i**) Native tissue, (**ii**) colonic crypt, (**iii**) organoid bud. Data also contributed to by Alvin Lee. Scale bar 25 µm.

Furthermore, we studied the presence of enteroendocrine cells which can be identified by the expression of the protein chromogranin A (CHGA). Confocal imaging of fixed and immunolabelled cultured colonic crypts and organoids showed the expression of a few enteroendocrine cells which were present in the base of colonic crypts and buds but also distributed across the crypt-axis (**Figure 3.13A-B**). Finally, in order to identify the presence of tuft cells we studied the expression of the cell marker ChAT across all samples. Fixed and immunolabelled native tissue images showed the presence of low number of ChAT positive cells, usually around 3 or 4, which were mostly found in base and mid regions of the crypt (**Figure 3.14A**). Immunolabelled colonic crypts showed the presence of ChAT positive cells, and these were distributed in similar positions as the ones found in the native tissue. ChAT immunolabelling was distributed across the entire cell, connecting the apical and basal membranes (**Figure 3.14B & C**). However, we noticed that the number of positive cells was always lower, with crypts presenting 1 or 2 ChAT-labelled cells. In addition, ChAT positive cells were not found in colonic organoids (data not shown).

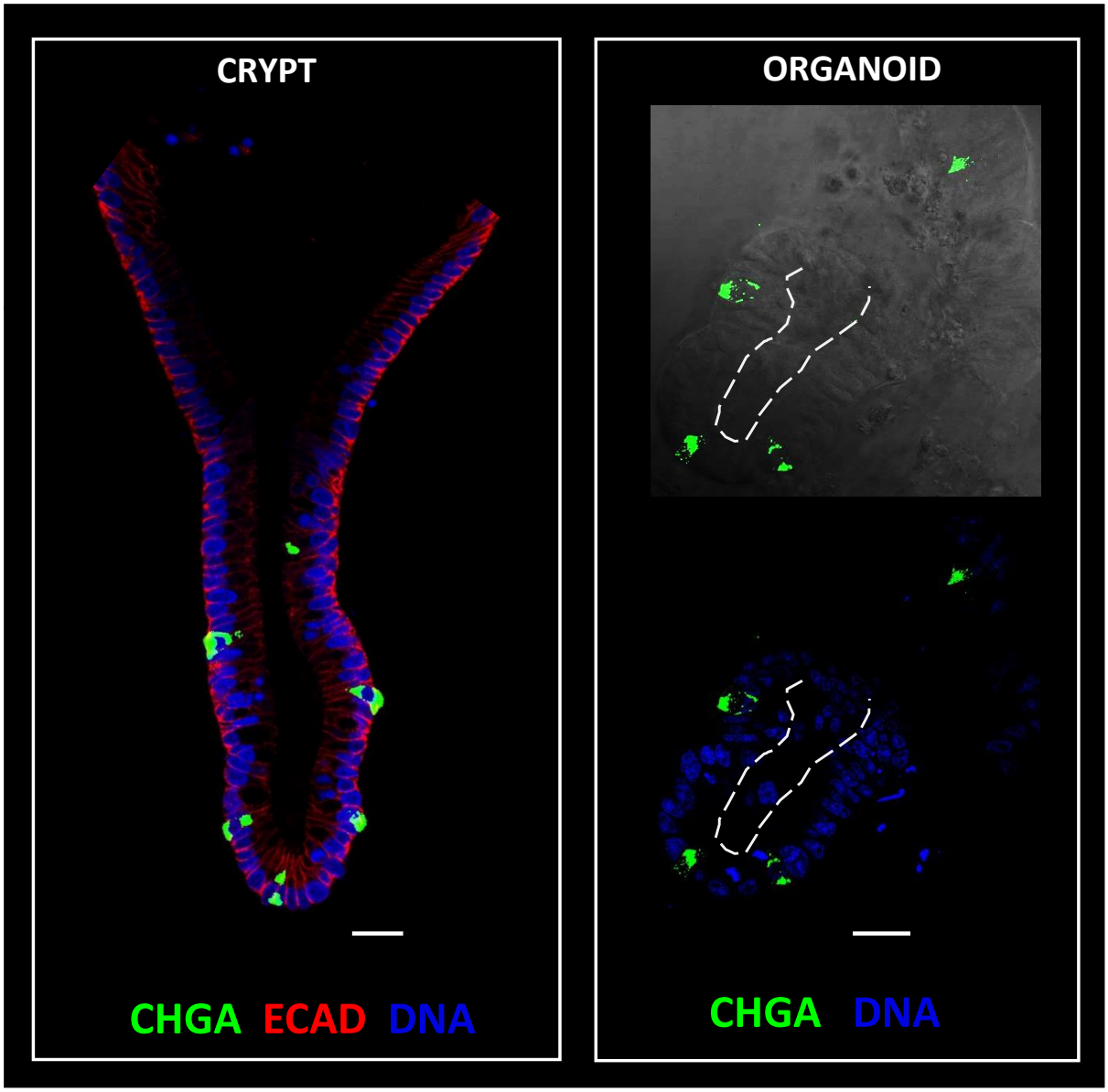

Figure 3.13. Presence and distribution of enteroendocrine cells in crypts and organoids. (**A**) Cultured colonic crypt showing CHGA positive cells (green), ECAD (red). (**B**) Representative confocal images of an organoid showing CHGA positive cells (green) and brightfield at the top and CHGA positive cells and nuclear stain Sytox blue (DNA) at the bottom. Dashed lines indicate position of the cell apical membrane. Scale bar 25 µm.

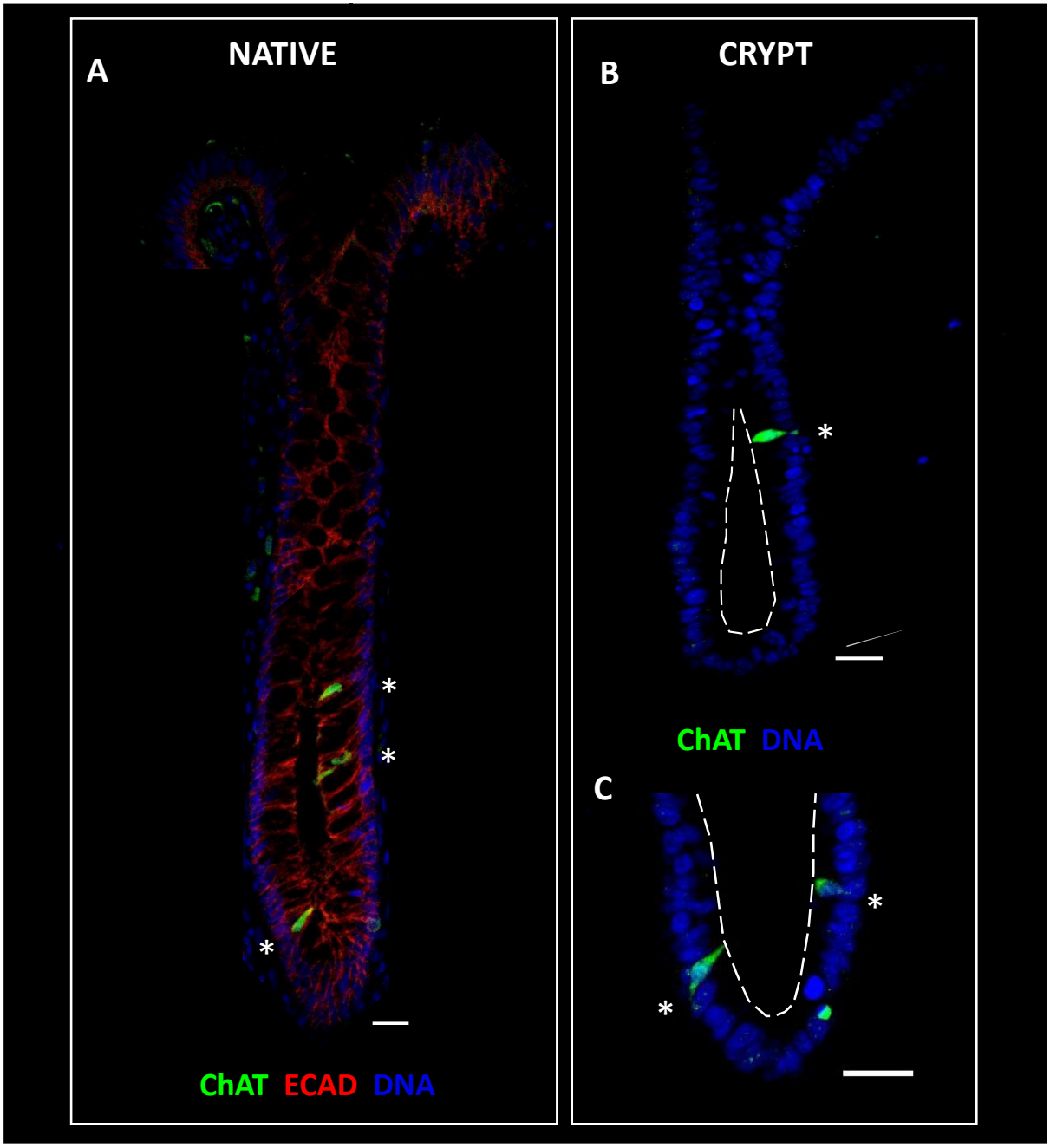

Figure 3.14. Presence and distribution of tuft cells in native tissue and colonic crypts. (**A**) Illustrative image of a native tissue colonic crypt depicting ChAT positive cells (green) (**B**). Entire colonic crypt showing a ChAT positive cell (green) and nuclear stain Sytox blue. **C**) Representative confocal image of the base of a colonic crypt displays two ChAT positive cells (green). Dashed lines indicate position of the lumen and asterisks represent location of ChAT positive cells. Data also contributed to by Alvin Lee. Scale bar 25 µm.

3.2.3 Characterisation of the calcium toolkit components in the colon epithelium

Previous work in the Williams lab has investigated the mechanism of muscarinic activation of the intracellular calcium signals in isolated colonic crypts (Lindqvist et al., 2002; Reynolds et al., 2007, Dr Christy Kam, PhD Thesis). This work suggested that ACh activation of muscarinic receptors induces a calcium signal response mediated by release of calcium from the endolysosomes via TPCs. In this chapter we wanted to investigate the presence of the main components of the calcium toolkit that orchestrate the muscarinic-induced calcium signal in organoids, by comparing its genetic and protein expression to that in the native mucosa and isolated crypts.

3.2.3.1 Genetic characterisation of the calcium toolkit components

First, we analysed RNA expression of the main markers of the calcium toolkit by reverse transcriptase PCR. These results showed all muscarinic receptors (MAChR1-5) to be expressed in the native mucosa, isolated crypts and organoid tissue (**Figure 3.15**). Next, we showed the expression of CD38, which catalyses the formation of NAADP in native mucosa and isolated crypts. NAADP has been suggested to activate TPC to induce calcium release (Calcraft et al., 2009). Here we show that both TPC1 and TPC2 are expressed across all tissue samples. However, the gel band for TPC1 in organoids was found to be very faint, suggesting a lower expression (**Figure 3.15**). In addition, we analysed the expression of calcium sensor calcineurin (CaN) and the transcription factor NFATc3, both downstream effectors of the calcium signal linked to cell proliferation (Urso et al., 2019). The PCR results showed the expression of both markers in all three samples. We found the expression of CaN in organoids and mucosa to be faint compared to the crypts (**Figure 3.15**). GAPDH was used as a reference gene and its expression is shown in **Figure 3.3**.

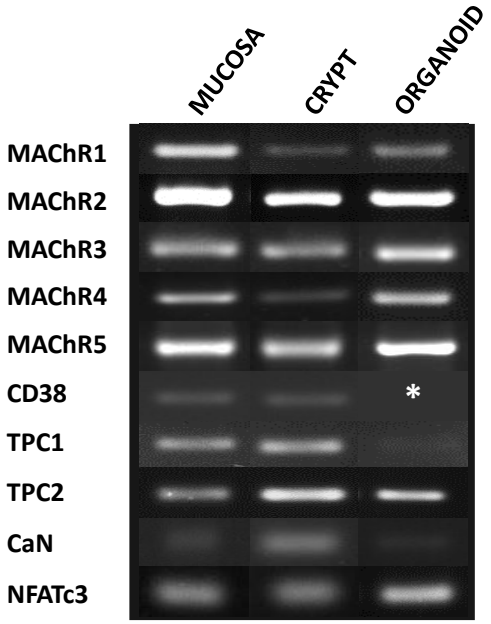

Figure 3.15. **Genetic expression of main components of the calcium signalling toolkit.** Agarose gel showing the RNA expression of key muscarinic-induced calcium signalling markers of the colonic epithelium in native mucosa, isolated crypts and organoids. Asterisk indicates missing sample. The image is a construct of different experiments.

In order to further investigate the genetic similarities of the calcium toolkit of organoids compared to the native mucosa and colonic crypts we sequenced the RNA of all three types of sample using the same experimental design to the one undertaken for the analysis of gene expression of markers of cellular types. We focused our attention on the expression of the main calcium channels present in the ER (IP3Rs, RYRs, and SERCA pump), Golgi (SPCA pump), endolysosomes (TPCs) and plasma membrane (PMCAs) (**Appendix A, Figure A2**). The analysis of IP3R gene expression confirmed the presence of all three subtypes across all tissue samples. This data also revealed a greater number of reads for IP3R3, which could suggest a higher presence in the colonic epithelium compared to the other subtypes. In addition, we showed a proportional expression of all three receptor types between crypts and organoids (**Figure 3.16**).

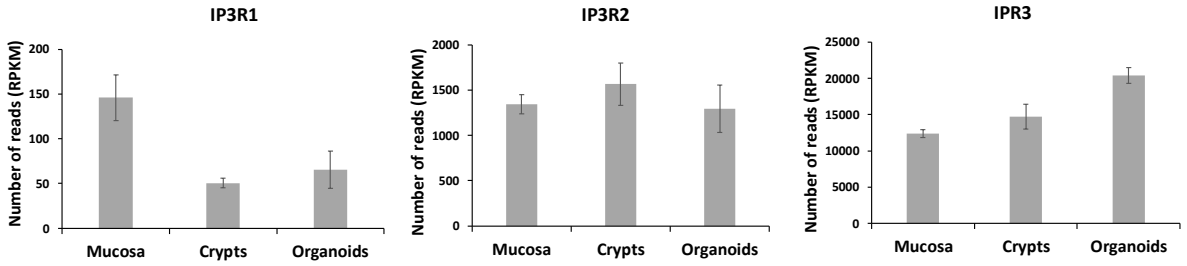

Figure 3.16. Gene expression of IP3Rs. Bar charts represent the differential gene expression of the three IP3R subtypes in the different tissue samples (N=6). Data is expressed as number of reads (RPKM).

Interestingly, the gene expression of all three RyRs was found to be low across all tissue samples as judged by the number of reads, suggesting the presence of low levels of mRNA (**Figure 3.17**).

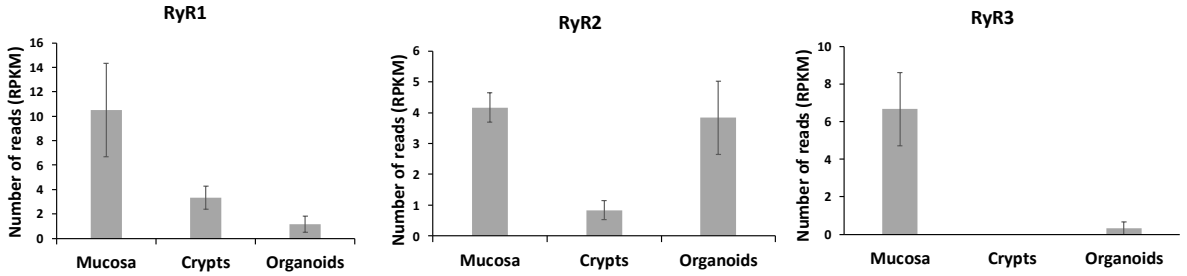

Figure 3.17. Gene expression of RyRs. The gene expression of the different RyR was analysed and compared between mucosa, crypts and organoids (N=6). Data is expressed as number of reads (RPKM).

The analysis of TPC gene expression revealed the presence of both subtypes in all the tissue samples. TPC1 was found to be more abundant that TPC2 but their expression levels were similar between colonic crypts and organoids (**Figure 3.18**).

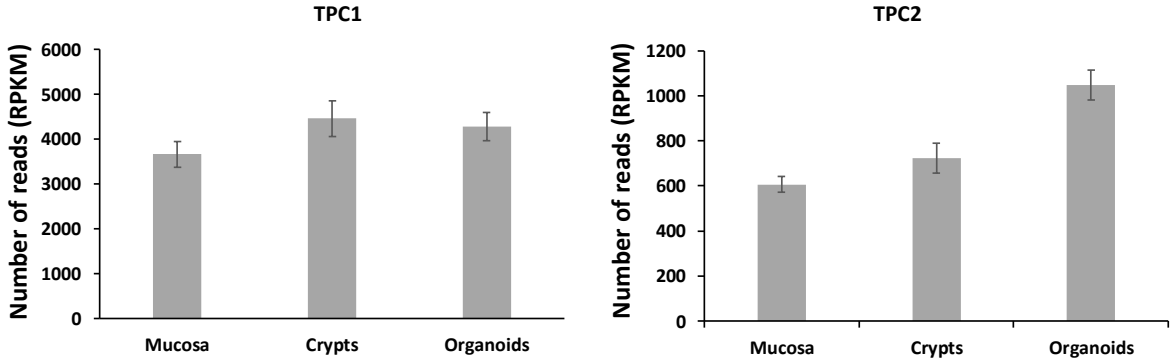

Figure 3.18. Gene expression of TPCs. Bar charts indicate the presence and expression of the TPC1 and 2 in all tissue samples derived from 6 patients. Data is expressed as number of reads (RPKM).

In addition, the study of the gene expression of the main calcium ATPases confirmed the presence of all three across our tissue samples (**Appendix A, Figure A3**). The SERCA pump family of receptors (ATP2A1, 2 and 3) were found to be expressed at low levels as judged by the number of reads, however the proportions were similar between mucosa, isolated crypts and organoids (**Appendix A, Figure A3A**). The expression of the different plasma membrane calcium-transporting ATPases (PMCP) isotypes (ATP2B1, 2, 3 and 4) was proportional across samples with ATP2B1 and 3 showing a higher number of reads, suggesting more abundance than the other two isotypes (**Appendix A, Figure A3B**). The expression of the Golgi SPCA isotypes was found to be high as judged by the number of reads and was also shown to be similar between samples (**Appendix A, Figure A3C**).

3.2.3.2 Presence and distribution of the calcium signalling toolkit

The genetic expression analysis suggested the presence of the calcium signalling toolkit in colonic organoids at the RNA level as well as revealing a similar expression profile to cultured crypts. To test whether these components were also present at the protein level, we performed immunofluorescence analysis of fixed colonic crypts and organoids. We first characterised the presence of the different muscarinic receptors (MAChR1-5). To do so, colonic crypts and organoids were fixed and immunolabelled with the muscarinic receptor antibodies. Confocal imaging of the samples revealed the presence MAChR1, 3 and 5 in both colonic crypts and organoids (**Figure 3.19**). In colonic crypts, MAChR1, 3 and 5 were found to be expressed in the basolateral membrane of cells at the base of colonic crypts. The expression of MAChR3 and 5 was found along the crypt-axis although it was prevalent at the base of the crypt. The expression of MAChR1 followed a decrease gradient of expression towards the upper region of the crypt, were it was almost unnoticeable (**Figure 3.19A & B**). Interestingly, the expression of MAChR5 was found to be present around the Sytox blue positive nuclei, suggesting the presence of this receptor in the nuclear membrane (**Figure 3.19B**). Colonic organoids showed the expression of all receptors in their basolateral membranes. Of note, unlike in crypts, MAChR1 was found to be expressed with similar intensity in all cells of organoids. In addition, similar to cultured crypts, the expression of the MAChR5 was found to be present around the nuclei as well (**Figure 3.19C**). These results were followed by the imaging of the muscarinic receptors that are not coupled to intracellular calcium stores, MAChR2 and 4. Both receptors were found present in cultured crypts and organoids (**Figure 3.20**). In crypts, MAChR2 is present in the basolateral membranes of the epithelial cells along the entire axis. The expression of MAChR4 was found to be present in the basolateral membranes of some cells but it was more abundant in the cytoplasm and apical pole of all the epithelial cells. Although MAChR4 was found at the base (**Figure 3.20B**), the expression increased in intensity towards the upper regions (**Figure**

3.20A). In organoids, MAChR2 was found to be ubiquitously expressed in the basolateral membranes of all epithelial cells, whereas the expression of MAChR4 was found to be higher in the upper region of the buds compared to the base. In that zone, most cells showed immunolabelling of the receptor in the basolateral membranes as well as in the apical ones (**Figure 3.20C**).

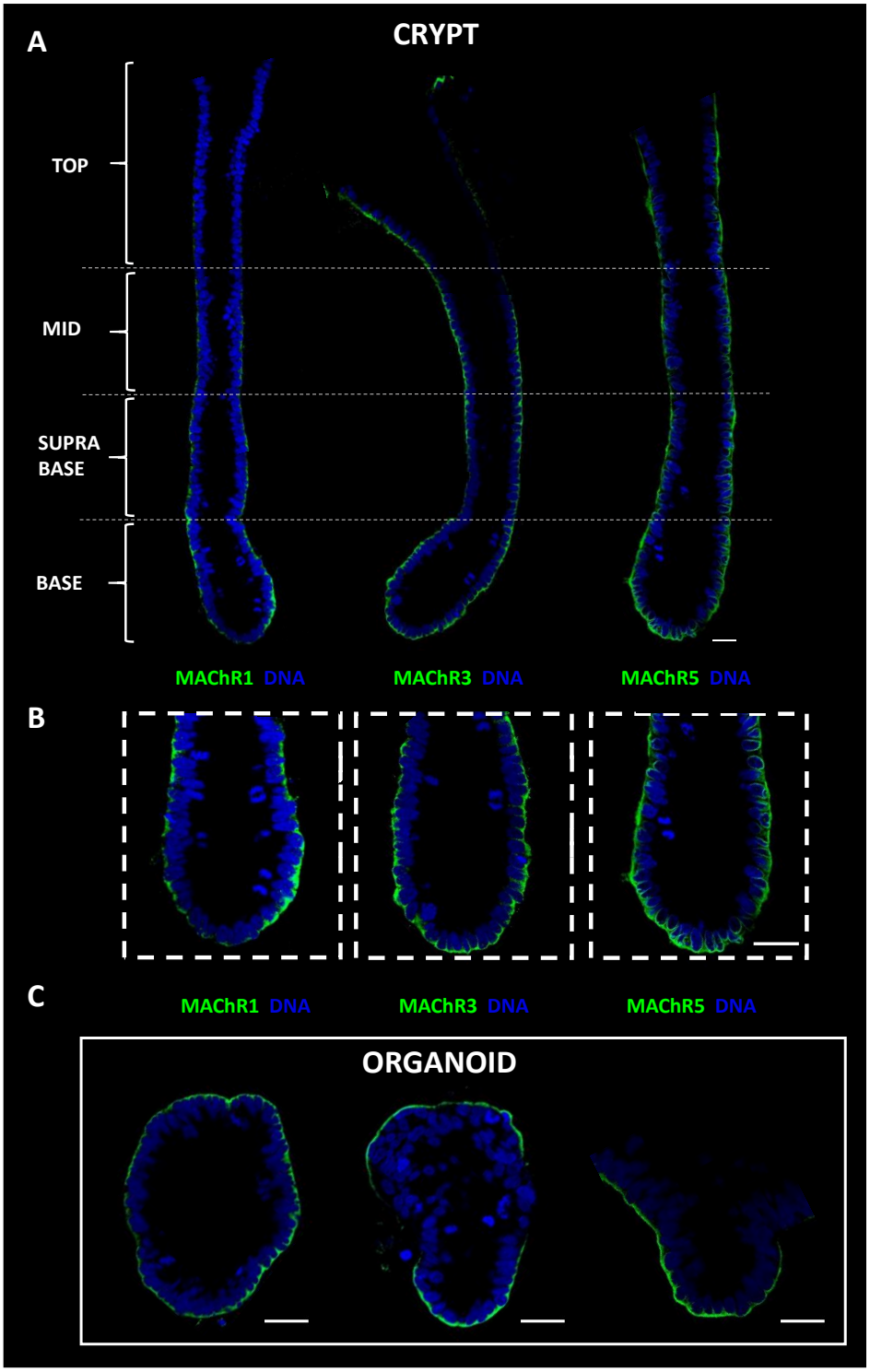

Figure 3.19. Colonic crypts and organoids express MAChR1, 3 and 5. (**A**) Representative confocal images of entire isolated colonic crypts immunolabelled from left to right with MAChR1, 3 and 5

(green) and nuclei stained with Sytox blue (DNA). (**B**) High magnification confocal images representing the base of isolated human colonic crypts (**C**) Confocal images illustrate expression of (from left to right) MAChR1, 3 and 5 in human colonic organoids. Scale bar 25 µm.

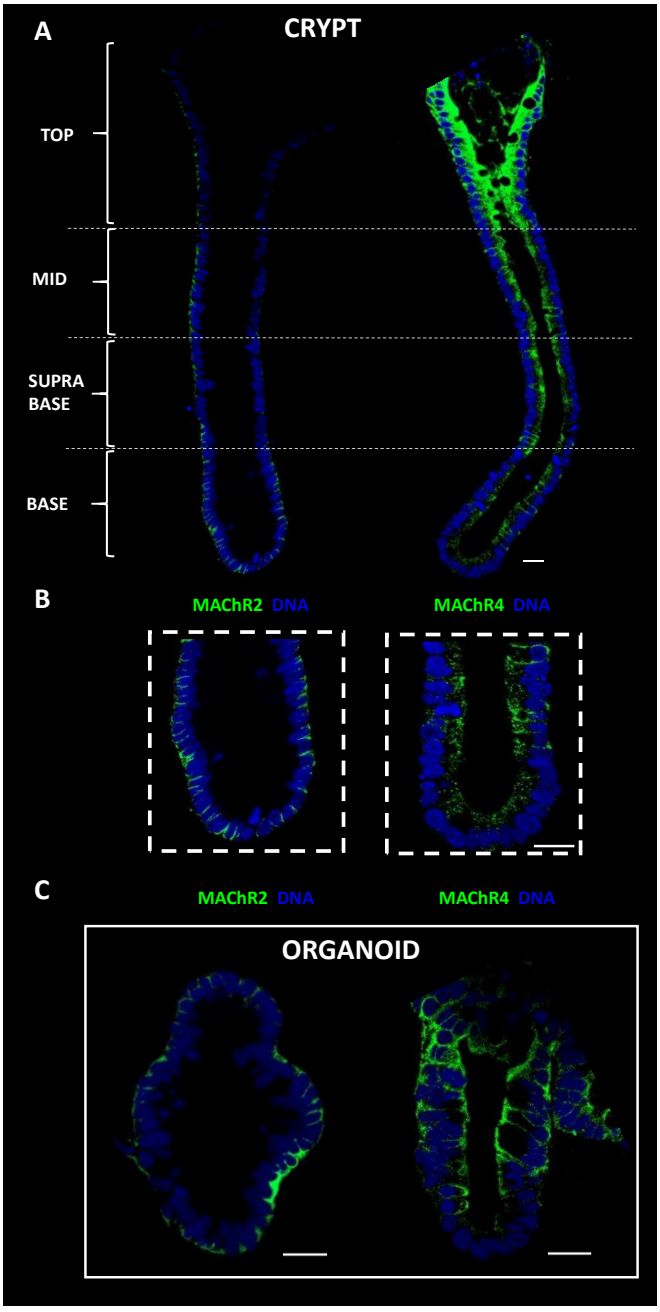

Figure 3.20. Colonic crypts and organoids express MAChR2 and 4. (**A**) Representative confocal images of entire colonic crypts immunolabelled in green with MAChR2 (left) and 4 (right) (**B**) High

magnification images of the base of isolated human colonic crypts (**C**) Representative confocal images of colonic organoids labelled in green with MAChR2 (left) and 4 (right). Scale bar 25 µm.

We subsequently studied the presence and distribution of the main calcium intracellular stores in organoids. The samples were incubated for two hours with Lysotracker (1 µM) and Mitotracker (100 nM) in order to label the acidic secretory granules and acid endolysosomes, and mitochondria respectively. Live imaging of Lysotracker loaded organoids revealed the presence of acidic secretory granules and endolysosomes in the apical pole of the cells and was not found in the perinuclear region (**Figure 3.21i**). Next, live imaging of Mitotracker loaded organoids showed the expression of the organelle to be present all around the cell but it was found to be more intense around the perinuclear region (**Figure 3.21ii**). In addition, the presence of the ER was confirmed by immunolabelling of organoids with KDEL marker (Capitani and Sallese, 2009) which was found to be located in the basal membranes as well as in the perinuclear area (**Figure 3.21v**). Interestingly, some cells displayed a more intense antibody labelling, which was also present in the lateral membranes and cytoplasm. Co-labelling with the goblet cell marker MUC2 showed overlapping of both antibodies possibly indicating a higher ER content in mucus secreting cells (**Figure 3.21v & vi**).

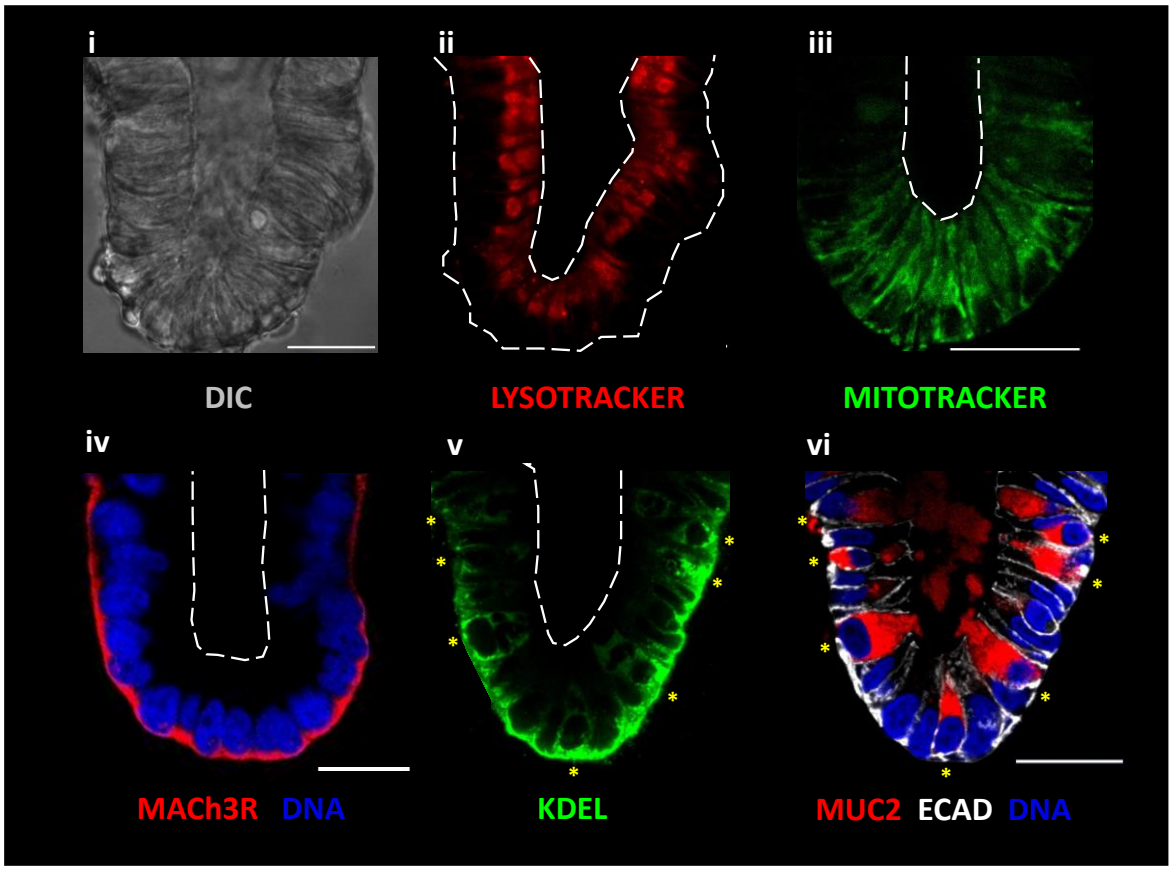

Figure 3.21. Presence and distribution of the main cellular organelles. Representative confocal images of the base of organoids buds. (**i**) Brightfield image. (**ii**) Acidic secretory granules and

endolysosomes labelling with Lysotracker (red). (**iii**) Mitochondrial labelling with Mitotracker (green). (**iv**) Expression of MAChR3 in the base of the crypt. (**v**) ER marker KDEL (green) (**vi**) Goblet cells (red), ECAD (white) and nuclei (blue). Yellow stars indicate co-localisation of KDEL and MUC2 labelled cells. Dashed lines indicate luminal area and asterisks represent position of MUC2 positive cells. Data also contributed to by Dr Victoria Jones. Scale bar 25 µm.

Following the characterisation of the different organelles, we decided to investigate the presence of the protein CD38. Imaging of the immunolabelled crypts and organoids demonstrated the presence of the marker to be nuclear in both models as well as showing a defined expression in the apical membrane of the cells at the base of crypts and buds (**Figure 3.22**). Next, we decided to examine the presence and distribution in organoids of the calcium channels located in the ER and endolysosomes and suggested to be responsible for the increase of intracellular calcium after muscarinic activation. Firstly, we looked at the immunolabelled expression of the IP3R subtypes in colonic organoids. Confocal imaging of the samples showed all the receptors to be present in organoids. IP3R1 was found in the nucleus but it was primarily expressed in the cytoplasm of all cells (**Figure 3.23i**). The expression of IP3R2 was observed in all epithelial cells and although present in both the cytoplasm and the apical pole of the cell, the intensity of the antibody was higher in the basal membrane. (**Figure 3.23ii**). Conversely, the expression of IP3R3 was found to be located in the apical pole of all cells in the bud, where the antibody labelling was particularly intense, possibly indicating abundance of the receptor (**Figure 3.23iii**).

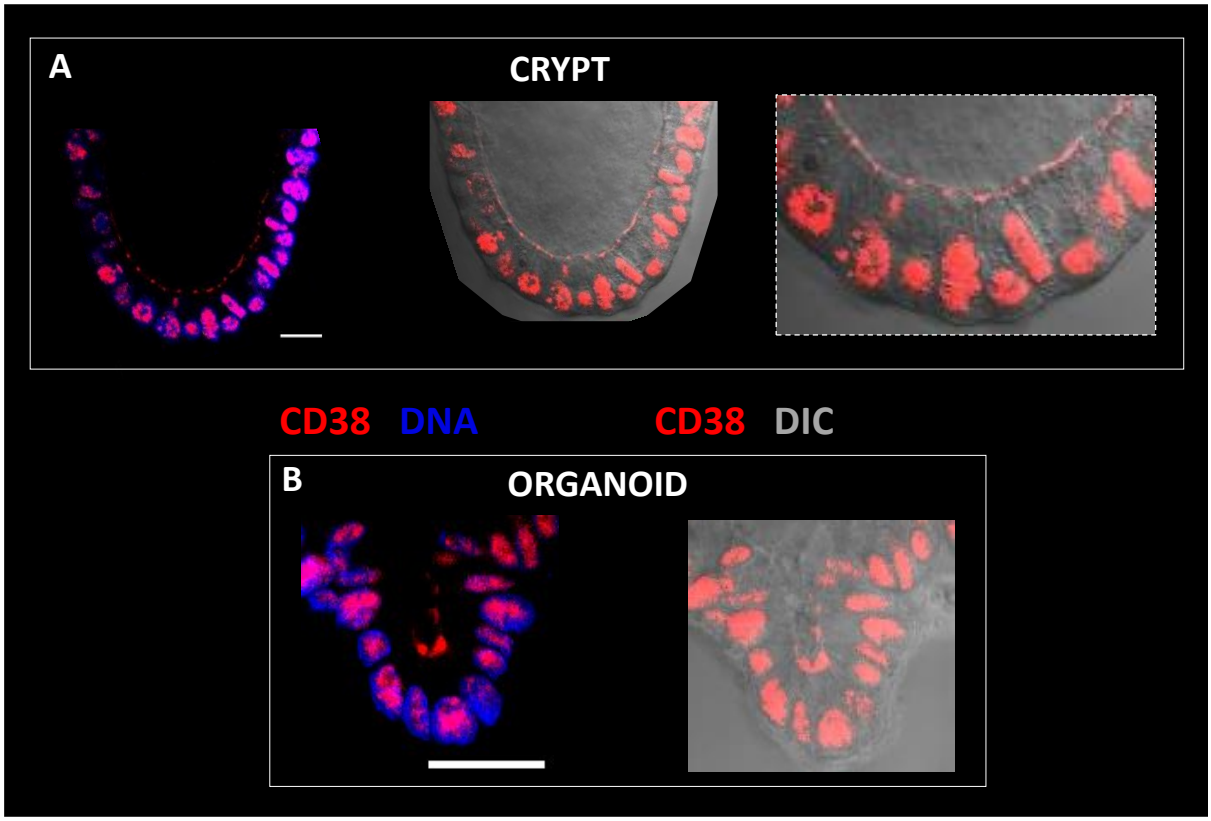

Figure 3.22. Expression and distribution of CD38 in colonic crypts and organoids. (**A**) Representative confocal images of cultured colonic crypts labelled on the left with CD38 (red) and nuclear stain (blue) and in the middle a merged image of brightfield and CD38. Right image indicates high magnification to highlight CD38 expression. (**B**) Representative confocal images of organoids labelled on the left with CD38 (red) and nuclear stain (DNA) and on the right a merged image of brightfield and CD38. Scale bar 25 µm.

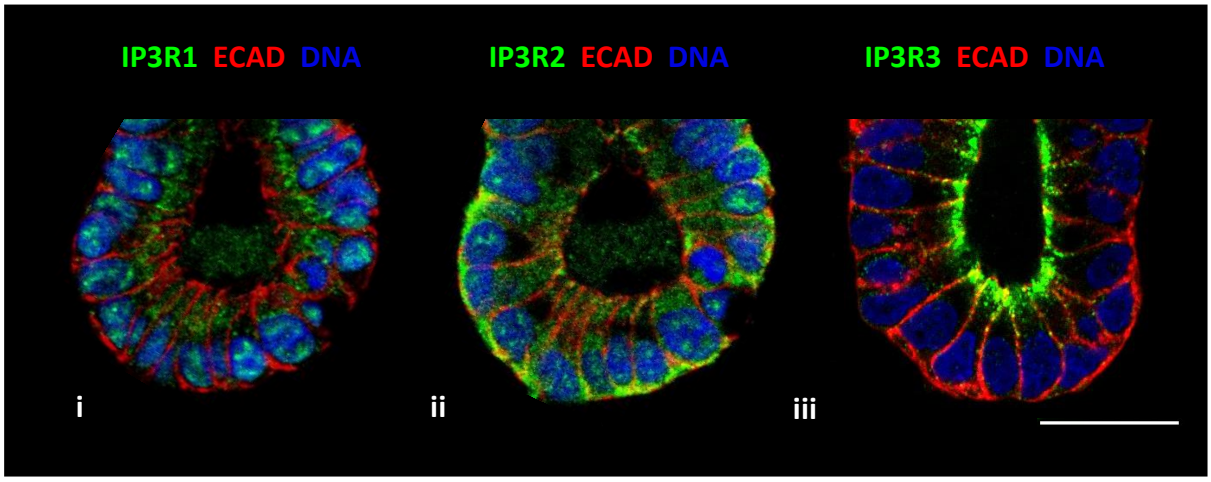

Figure 3.23. Expression and distribution of the IP3R1, 2 and 3 ion channels. Representative confocal images of colonic organoids expressing ECAD (green) and Sytox blue (blue) and (**i**) IP3R1, (green), (**ii**) IP3R2 (green) and (**iii**) IP3R3 (green). Data also contributed to by Victoria Jones. Scale bar 25 µm.

Secondly, we investigated the location of the endolysosomal TPC1 and TPC2 in the base of crypts and organoids. Following a similar immunolabelling and imaging protocol, the expression of TPC1 was found to be predominant in the apical membrane of all cells (**Figure 3.24A**). However, the protein was also observed in the nucleus and was particularly intense in organoids (**Figure 3.24B**). The expression of TPC2 was also found to be present in both models, located primarily in the cytoplasm and apical membrane of all cells. The expression of the calcium channel was present in the nuclei of the cells but with a lower intensity than the one seen for TPC1 as judged by the antibody immunolabelling (**Figure 3.24C & D**).

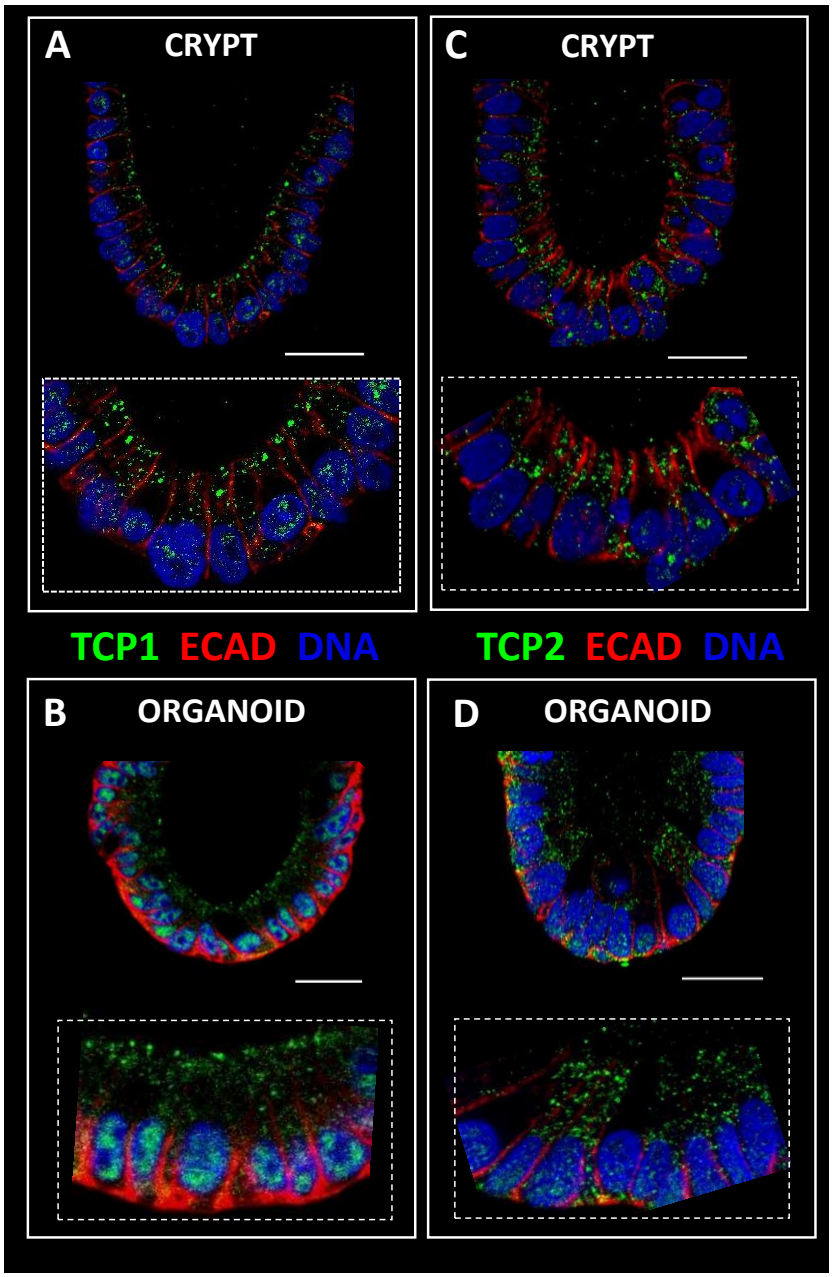

Figure 3.24. Expression and distribution of the TPC1 and 2 ion channels in colonic crypts and organoids. (**A**&**B**) Representative confocal images showing the expression of distribution of TPC1 (green) in crypts (**A**) and organoids (**B**). (**C**&**D**) Illustrative confocal images displaying the expression and distribution of TPC2 in crypts (**C**) and organoids (**D**). Scale bar 25 µm.

3.2.3.3 The calcium signalling toolkit is present in stem cells and goblet cells

Muscarinic-induced calcium signalling has been shown in the literature to regulate mucus secretion in goblet cells (Neutra, O'Malley and Specian, 1982; Halm and Halm, 2000) and cell proliferation in stem cells (Campoy et al., 2016). As described in this chapter, we demonstrated the presence of both goblet and stem cell markers as well the calcium toolkit elements in crypts and organoids. To

investigate in more detail whether the latter are present in goblet and stem cells we analysed the co-localisation of representative immunolabelled markers. First, we studied the presence of the toolkit components mACh3R, CD38, TPC1 and TPC2 in goblet cells identified by the expression of MUC2 or morphologically by the presence of large cytoplasm. To do so, colonic crypts and organoids were fixed and labelled with the different antibodies. Confocal imaging of the samples confirmed the presence of the MAChR3 in all MUC2 immunolabelled goblet cells of colonic crypts (**Figure 3.25A**). CD38 expression in colonic crypts was revealed to be present in the nucleus and apical membrane of goblet cells which were identified by their morphology (**Figure 3.25B**). The expression of TPC1 in crypts was shown to co-localise with $MUC2^{+}$ goblet cells and was found present primarily and in the apical pole of the cell (**Figure 3.25C**). Finally, confocal images of colonic crypts labelled with TPC2 showed the calcium channel to be present in goblet cells identified by their morphology, with a faint expression in the nuclei and more prominent one in the cytoplasm (**Figure 3.25D**).

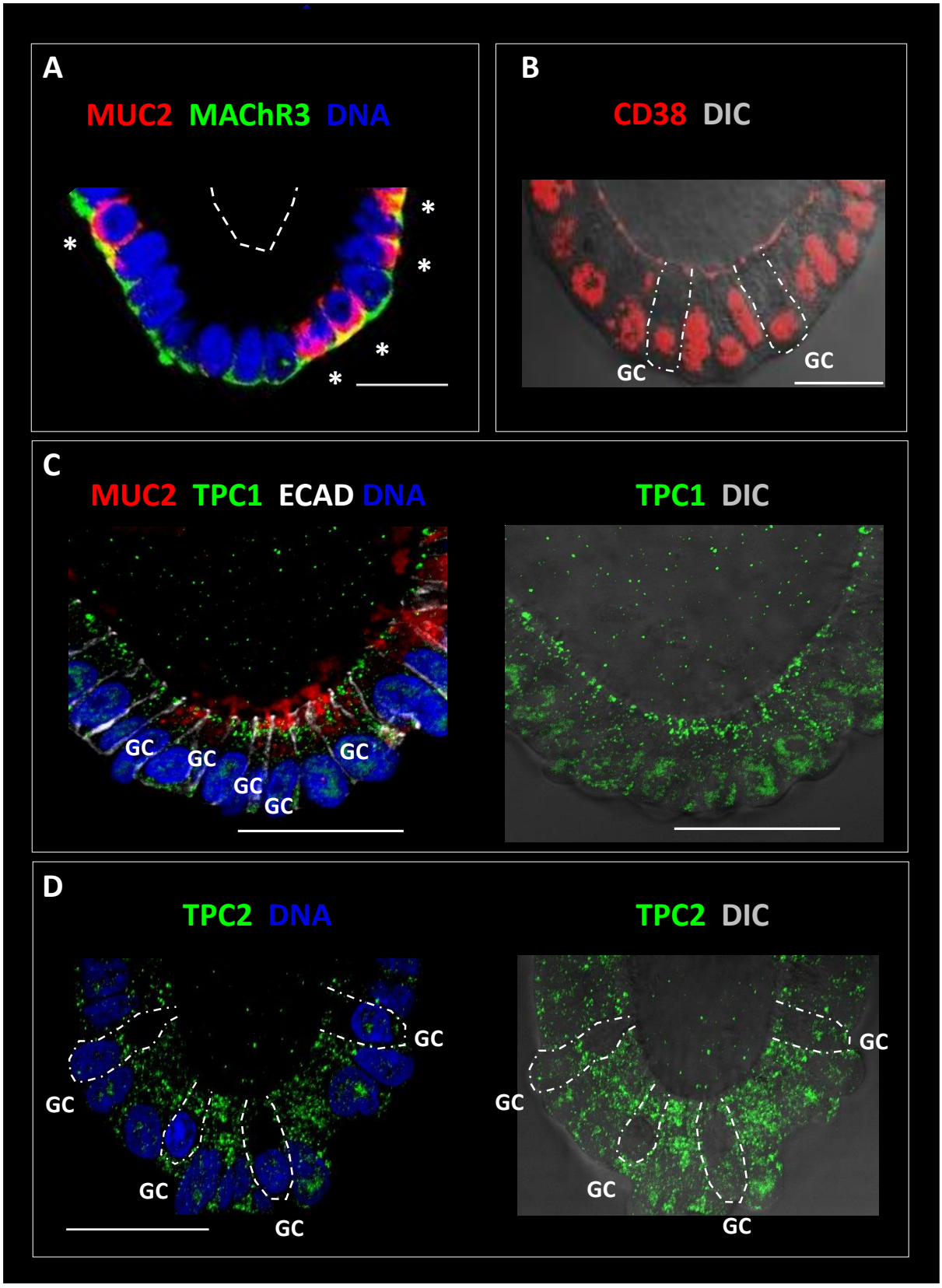

Figure 3.25. Goblet cells express the calcium signalling toolkit. (**A**) MUC2 (red) and MAChR3 (green) co-localise in colonic crypts (**B**) Colonic crypts show presence CD38 (red) in goblet cells circled with dashed lines. (**C left**) Crypt immunolabelled with MUC2 (red), TPC1 (green) and ECAD (white). (**C-**

right) TPC1 (green) and brightfield. (**D-left**) Colonic crypts displaying TPC2 (green) in goblet cells together with blue stained nuclei and brightfield (**D-right**). Dashed lines outline of goblet cell shape in (B and D). Asterisks indicate co-localisation of makers. Scale bar 25 µm.

Similarly, for the characterisation of the calcium toolkit in stem cells, colonic crypts were fixed and immunolabelled with the markers MAChR3, CD38 and TPC2 and the stem cell markers LGR5 and PTK7. Expression of MAChR3 co-localised with all LGR5^{+} stem cells (**Figure 3.26A**). Moreover, CD38 was shown to be expressed in the nuclei and apical membrane of LGR5^{+} cells (**Figure 3.26B**) and the presence of TPC2 was confirmed in PTK7^{+} cells, where it labelled the cytoplasm (**Figure 3.26C**).

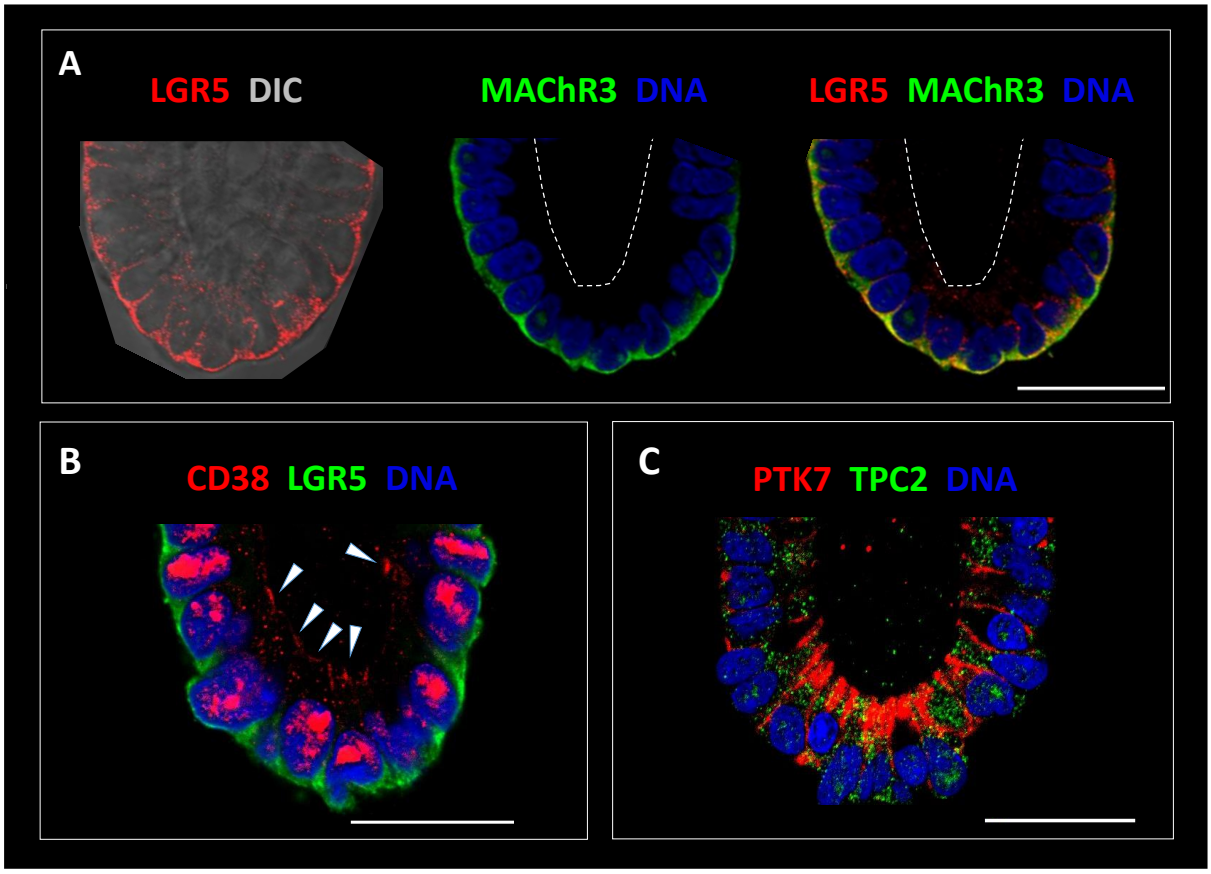

Figure 3.26. Stem cells express the calcium signalling toolkit. (**A**) Illustrative images of LGR5^{+} cells (left), MAChR3^{+} cells (middle) and merged imaged showing antibody co-localisation (right). Representative confocal images of the base of colonic crypts displaying co-localisation. (**B**) Co-localisation of CD38 (red) and LGR5 (green). Arrowheads indicate apical expression of CD38 (**C**) Co-localisation of PTK7 (red) and TPC2 (green). Scale bar 25 µm.

3.2.4 Characterisation of the muscarinic-induced calcium signal in colonic crypts and organoids.

Previous research in the Williams lab has demonstrated that ACh activation of muscarinic receptors induces an intracellular calcium signal in cultured colonic crypts (Lindqvist et al., 2002; Reynolds et al., 2007). In addition, preliminary work from Dr Christy Kam have suggested that the muscarinic-induced calcium signal is mediated by the release of calcium through the TPCs present in the endolysosomes (Dr Christy Kam, PhD Thesis).

3.2.4.1 Topology and polarity of the calcium signal in human colon epithelium

In order to test whether the calcium signal initiates in the base of the crypt, we decided to study the topology and polarity of the intracellular calcium signals in human colonic crypts. To do so, cultured crypts grown for 24 or 48 hours were loaded with cell permeable calcium sensitive fluorescence dye Fura-2 for 2 hours in Hepes buffer saline solution (HBS). The dye is incorporated into the cells thanks to its lipophilic acetoxylmethyl ester group which is later cleaved by cellular esterases preventing efflux of de-esterified Fura-2. Crypts were placed on a chamber slide and imaged under an epifluorescence microscope. Colonic crypts were then stimulated with the ACh analogue, Carbachol (CCh) to induce an intracellular calcium signal. The ratiometric fluorescence imaging of the Fura-2 340/380 nm excitation wavelengths revealed an increase in fluorescence that first originated in the ROI located in the most basal position and gradually propagated to the neighbouring cells located (**Figure 3.27**).

In order to study the topology of the calcium signal, we drew regions of interest (ROI) around cells located at different heights across the crypt (**Figure 3.28A**). The fluorimetric measurements confirmed and increase of the ROIs fluorescence over time and showed that the calcium signal is first generated in the apical pole of the cells at base of the crypt which then travels to the basal pole. The calcium signal is later propagated as a wave that moves to the neighbouring crypts and continues up the crypt-axis (**Figure 3.28A**). We next sought to determine the polarity of the calcium signal. A close look at the ratiometric images revealed that muscarinic activation with CCh induced an increase in fluorescence in the apical pole of the cells first to then travel to the basal pole. In order to validate these observations, ROIs were drawn in the apical and basal pole of the cells and the fluorimetric analysis confirmed the starting of the calcium signal was always first in the apical ROIs and second in the basal ones (**Figure 3.28B**).

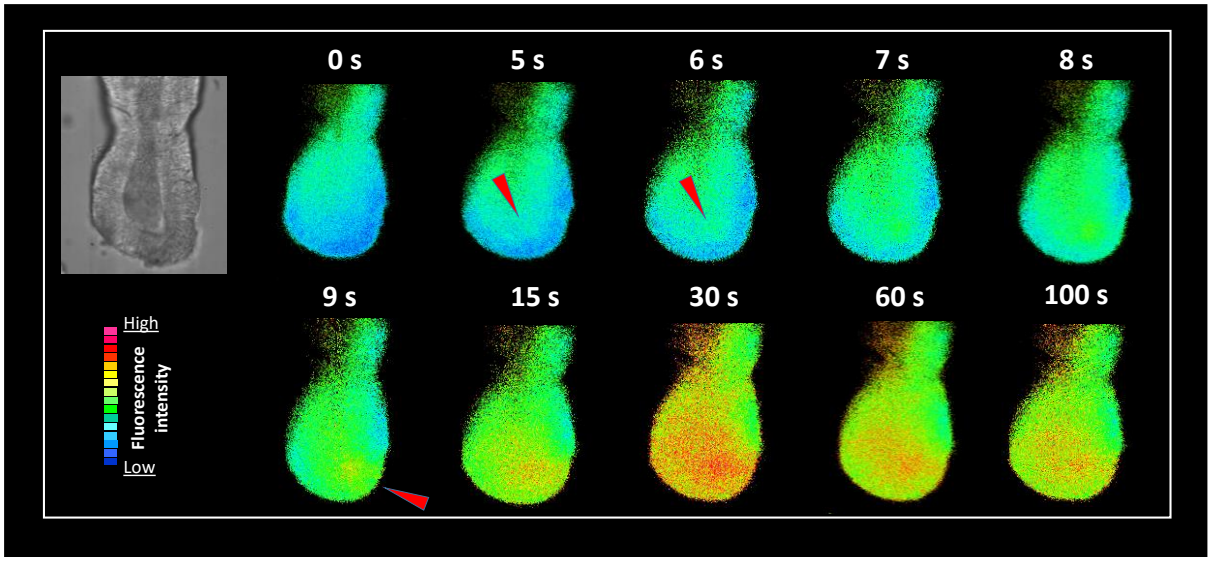

Figure 3.27 Calcium signalling originates at the base of the crypt. Representative confocal series of live images of a crypt loaded with Fura-2 (5 µM) after stimulation with CCh (10 µM). Calcium signals start in the apical pole of the cells at the base of the crypt and spread to the basal side to then propagate up the crypt-axis (red arrowheads). The calcium signal develops rapidly, reaching its highest intensity 30 seconds after stimulation to decay slowly afterwards.

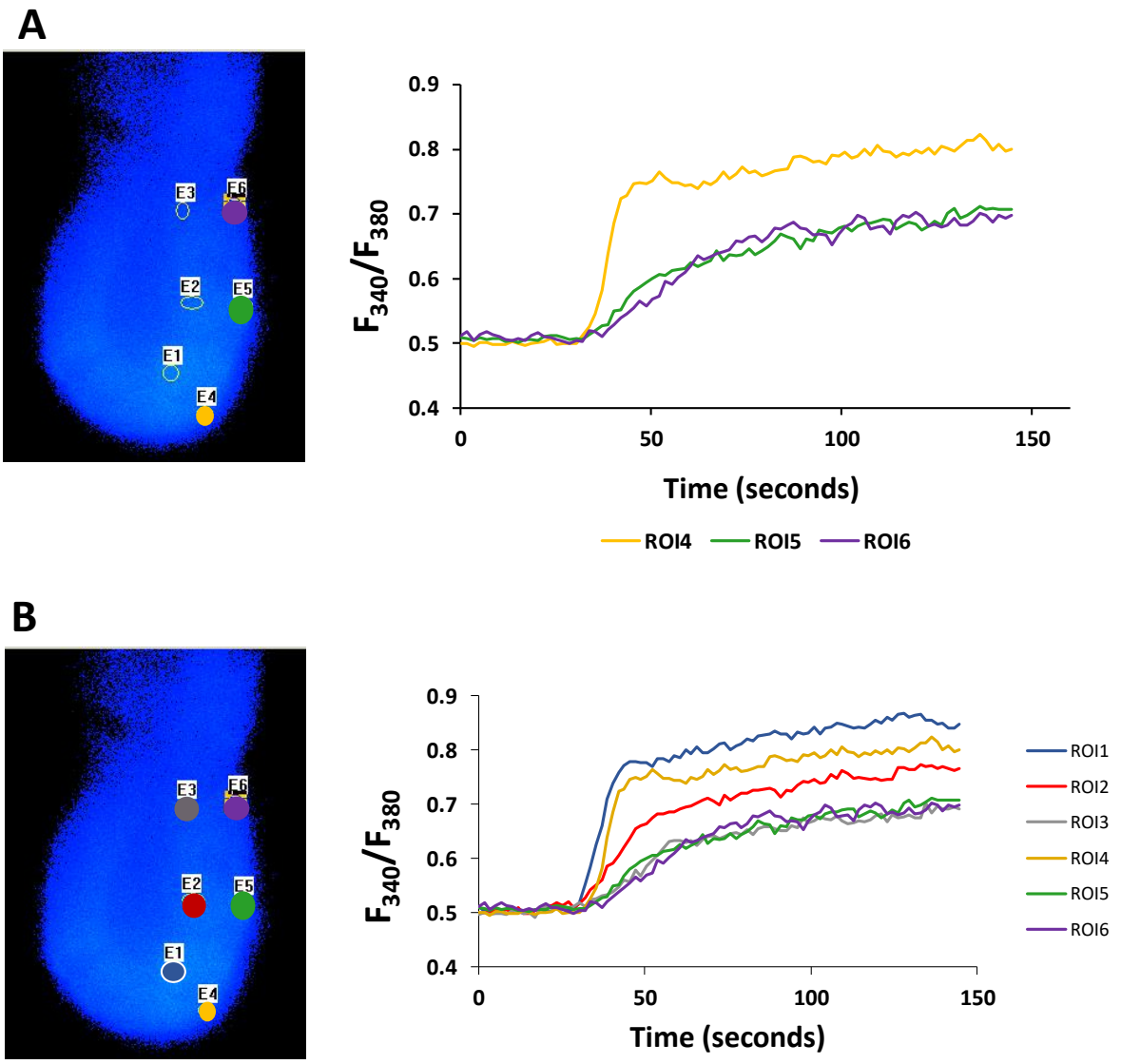

Figure 3.28. Topology and polarity of the calcium signal. (**A-Polarity**) Left image represents a Fura-2 loaded crypt with ROIs distributed along the crypt-axis. Right, the ratiometric analysis indicates the initiation of the signal in ROI4, located at the base. (**B-Topology**) Left image represents a Fura-2 loaded crypt with ROIs distributed in the apical and basal membranes of the crypts. Right, the ratiometric analysis shows the origin of the signal to be in the apical pole and then propagate to basal pole.

3.2.4.2 Carbachol induces intracellular calcium signals via activation of muscarinic receptors.

The ACh analogue CCh is a potent activator of both the muscarinic and nicotinic cholinergic receptors which are often used in research instead of the neurotransmitter due to its chemical structure. This structural characteristic makes it difficult for enzyme cholinesterase present in the media to degrade it, prolonging its time of action (Streichert and Sargent, 1992). In order to study

the role of CCh in calcium signal initiation, we first sought to determine the optimal concentration of use in colonic crypts. Colonic crypts cultured for 24 or 48 hours were loaded with Fura-2 and imaged under the epifluorescence microscope. In order to determine the ideal concentration of use of CCh, we stimulated colonic crypts with different concentrations of the ACh analogue (100 nM, 300 nM, 1 µM, 3 µM, 10 µM, 30 µM and 100 µM) and recorded the fluorescence response until it reached plateau. The analysis of ROIs drawn at the base of the crypt revealed a dose response effect of CCh, which was minimal at 100 nM and gradually increase to be maximal at 100 µM (**Figure 3.29A**). The average peak amplitude of the different concentrations of CCh was plotted together and the EC_{50} calculated showing that a concentration of 6.1 µM induces the half-maximal effective response (**Figure 3.29B**). Previous work done in the Williams lab has demonstrated the use of CCh at a concentration of 10 µM to be optimal (Lindqvist et al., 2002; Reynolds et al., 2007) so we decided to use that tested concentration for the following experiments .

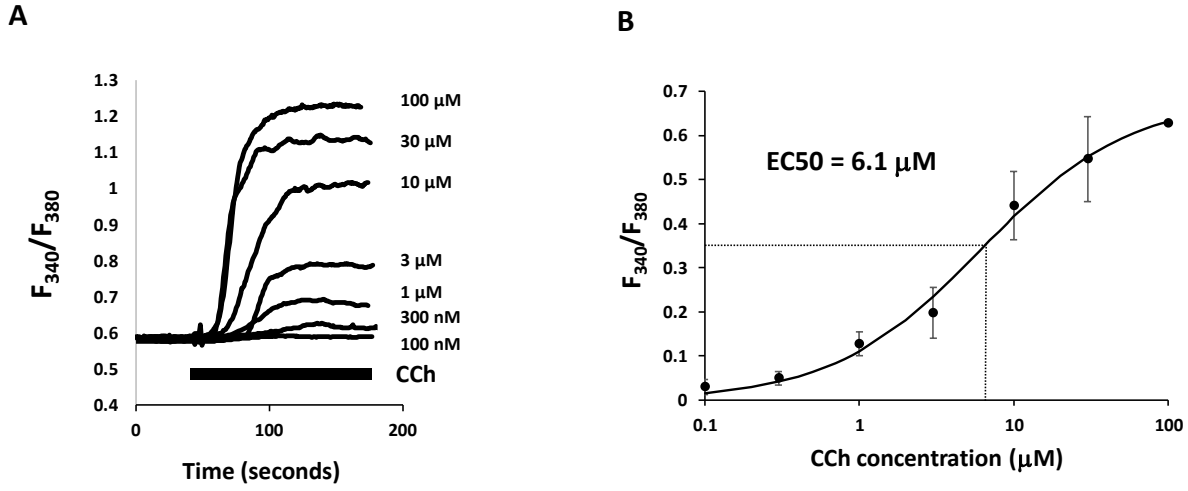

Figure 3.29. Characterisation of the CCh dose response. (**A**) Fluorimetric analysis of colonic crypts showing calcium response to different CCh concentrations over time. (**B**) Scatter chart representing the peak amplitude of the response of colonic crypts to different concentrations of CCh. Dashed lines indicate the EC_{50} (6.1 µM) (N=4, n=3).

Next, we decided to investigate which type of cholinergic receptor is involved in initiating the CCh-induced intracellular calcium signal. To do so, we first stimulated colonic crypts with the analogue of ACh, Oxotremorine (Oxo) which is a selective activator of muscarinic receptors (Boschero et al., 1995). Colonic crypts were loaded with Fura-2 and imaged under the epifluorescence microscope. Stimulation with Oxo (1 µM) resulted in a potent increase of intracellular calcium and the fluorescence measurement of ROIs located in the base of the crypt showed a response with a peak amplitude of 0.5 (**Figure 3.30**). Secondly, we chose to block muscarinic receptors and test whether

we could induce a calcium signal by stimulating colonic crypts with CCh. Firstly, we designed a paired control experiment to evaluate the capacity of the cells to induce a calcium signal in response to two successive stimulations with CCh (10 µM) spaced apart by a recovery time of 25 minutes, and test whether the second response was similar to the first one. Stimulation with CCh (10 µM) resulted in an increase in fluorescence ratio and was reversed by washing after the signal reached plateau of the peak response (**Figure 3.31A**). The crypt was left to recover for 25 minutes which was accompanied by the decay of the fluorescence ratio to levels close to resting conditions. A second stimulation with CCh (10 µM) elicited a calcium response of similar peak amplitude to the first one (**Figure 3.31A**). Fluorescence intensity analysis of the ROIs showed minimal differences in the averaged peak amplitudes of the firs CCh stimulation and the second (**Figure 3.31A**). In order to inhibit the activity of the muscarinic receptors we carried out a similar paired experiment where colonic crypts were incubated with 4-DAMP (100 µM) (Kilbinger et al., 1984) for 25 minutes after the first CCh stimulation. While the first CCh stimulation resulted in an increase in the fluorescence intensity of similar peak amplitude to control, the subsequent stimulation of CCh in the presence of 4-DAMP had minimal effects. (**Figure 3.31B**). The analysis of the changes in fluorescence recorded in the ROIs revealed a complete ablation of the calcium signal in crypts stimulated with CCh in the presence with 4-DAMP as judged by the peak amplitude levels (**Figure 3.31B**).

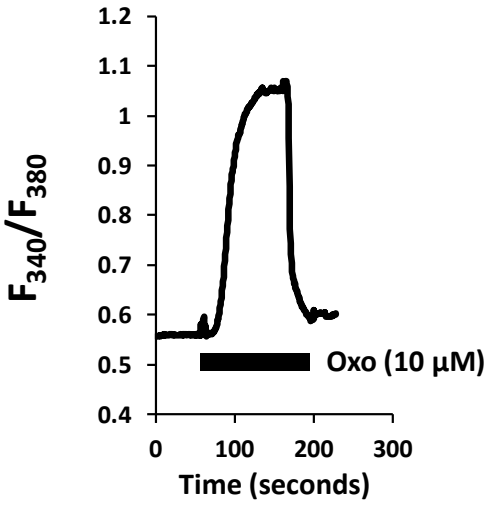

Figure 3.30. The muscarinic selective agonist Oxo induces a calcium signalling response.
Representative calcium traces of a human colonic crypt stimulated with Oxo (1 µM).

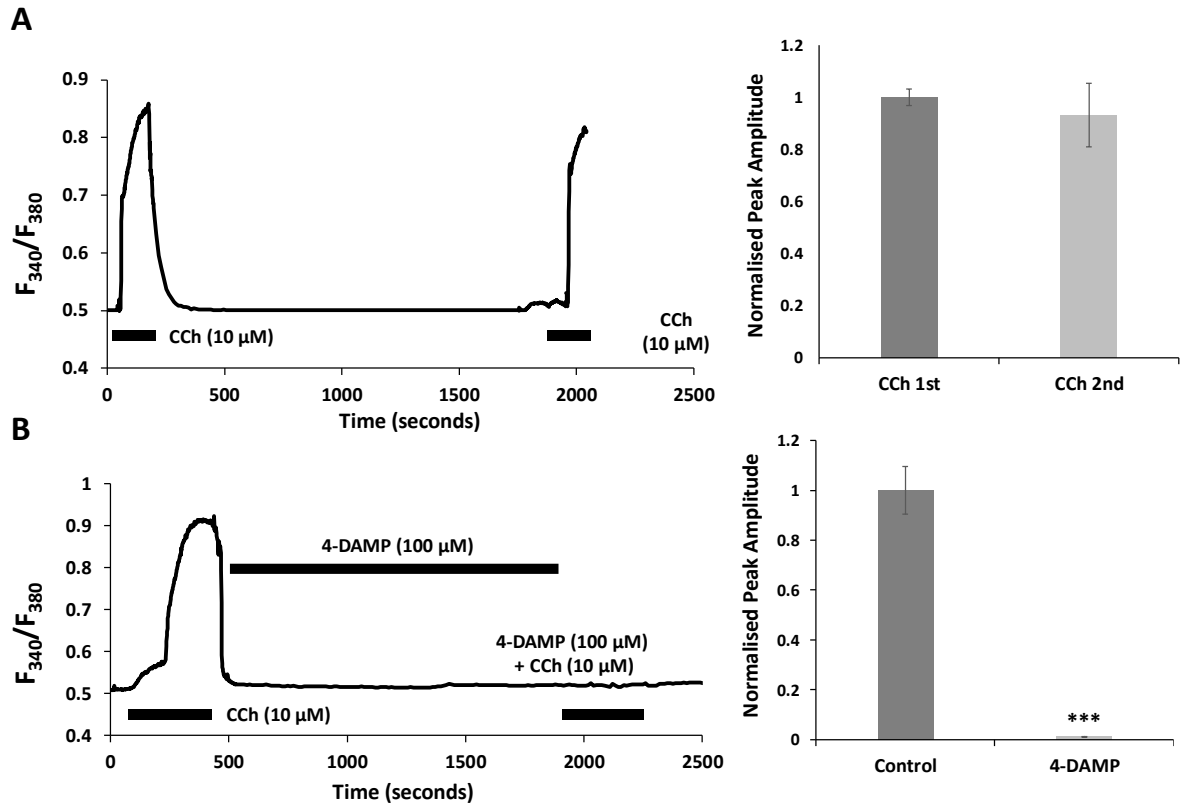

Figure 3.31.-DAMP blocks the CCh-induced calcium signal. (**A-left**) Representative calcium traces of a human colonic crypt stimulated first with CCh (10 µM), then rested for 25 minutes and subsequently stimulated with CCh (10 µM). (**A-right**) Bar chart indicates the comparison of the average peak amplitude of the calcium response between conditions. Fluorescence values normalised to first CCh response (N=1, n=3). (**B-left**) Representative calcium traces of a human colonic crypt stimulated first with CCh (10 µM), then incubated with 4-DAMP (100 µM) for 25 minutes and subsequently stimulated with CCh (10 µM) and 4-DAMP (100 µM). (**B-right**) Bar chart illustrates the comparison of the average peak amplitude of the calcium response between conditions. Fluorescence values normalised to first CCh response (***P<0.001, N=2, n=8). Data also contributed to by Alvin Lee.

3.2.4.3 Muscarinic calcium signals are not initiated in the ER

We next looked at the role of ER in mediating the ACh-induced calcium signal by first emptying the stores with the SERCA pump blocker CPA (20 µM) (Seidler et al., 1989) and subsequently inducing muscarinic stimulation. The experiments were conducted in organoids pre-incubated with calcium free media with EGTA (1mM) for 2 hours in order to observe a response independent of extracellular calcium influx. CPA stimulation of organoids elicited a calcium response and a subsequent CCh stimulation still induced an attenuated response (**Figure 3.32).**

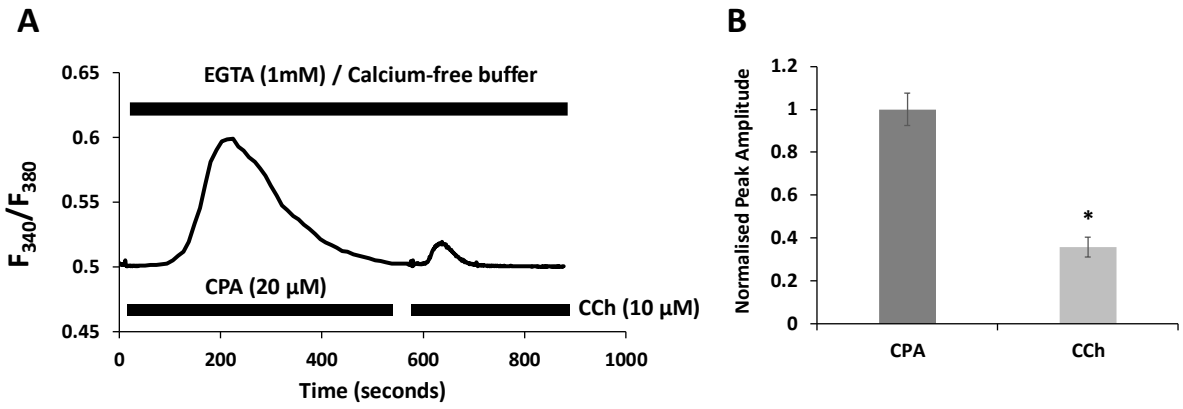

Figure 3.32. Calcium depletion of the ER attenuates muscarinic activated calcium signals. (**A**) Calcium traces represent Fura-2 ratio recorded over time after stimulation with CPA (20 µM) first and subsequent stimulation with CCh (20 µM) in the presence of EGTA (1mM) in organoids. (**B**) Bar chart represents the normalised peak amplitude of the calcium response (N=1, n=2). Data also contributed to by Alvin Lee.

3.2.4.4 Endolysosomal TPCs mediate the muscarinic-induced calcium signals

The TPC-mediated endolysosomal calcium release has been shown to regulate critical cellular processes such as autophagy and nutritional sensing (Gómez-Suaga et al., 2012; Ogunbayo et al., 2018). In our culture systems, we have demonstrated that endolysosomes and TPCs are expressed in the apical pole of the cells at the base of the crypt (**Figures 3.20 and 3.23**). Furthermore, the study of the topology and polarity of the calcium signal induced by muscarinic activation was shown to initiate in the apical pole of colonic crypts. The evidence that TPC are located in the cellular zone where the calcium signal initiates suggest a role of these calcium channels in initiating the muscarinic induce calcium response. In order to test this hypothesis, we blocked TPCs by pre-incubation with the antagonist Ned19 (500 µM) (Naylor et al., 2009) for 2 hours and studied the calcium response to CCh stimulation in Fura-2 loaded colonic crypts and organoids. Experiments where Ned19 was pre-incubated for less than 2h showed no inhibition of the CCh signal (data not shown). In colonic crypts, the stimulatory effect of CCh was abrogated in the presence of Ned19 (**Figure 3.33A**). The same effect was reported in colonic organoids (**Figure 3.33B**), suggesting that the initiation of the muscarinic-induced calcium signal depends on the activity of TPC in both culture systems. These results were supported by pharmacological inhibition of TPCs with Tetrandrine (20 µM), Diltiazem (250 µM) and Verapamil (50 µM) in colonic crypts and organoids pre-incubated for 2 hours (data not shown).

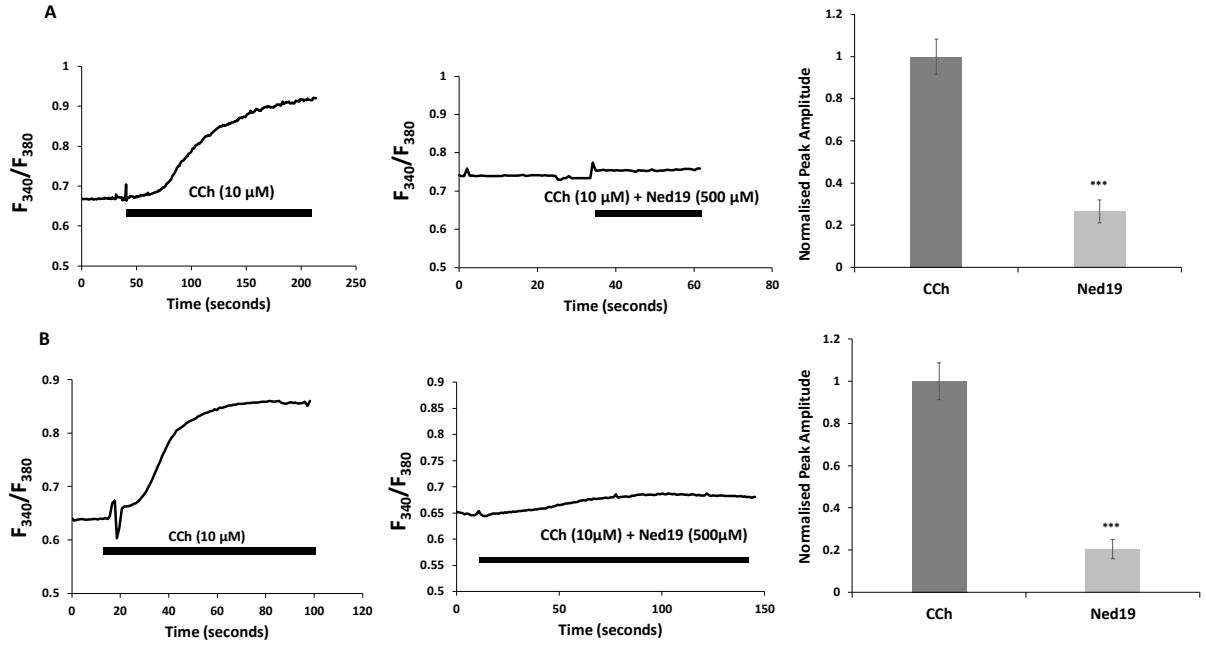

Figure 3.33. Ned19 abrogates the CCh response. (**A**) Calcium traces indicate that pre-incubation with Ned19 abrogates the response to CCh (10 µM) in colonic crypts which is confirmed by the comparison of the peak amplitude. (**B**) Cholinergic calcium response is inhibited in the presence of Ned19 in colonic organoids. Data also contributed to by Alvin Lee.

In order to understand the role of the main ER calcium release channels in the response to muscarinic activation we blocked IP3Rs and RyRs respectively in colonic crypts. The tissue samples were pre-incubated with the IP3R antagonist 2-APB (100 µM) (Maruyama et al., 1997) and with the RyR blocker Dantrolene (10 µM) (Zhao et al., 2001) for 2 hours and their calcium signal assessed by measuring the Fura-2 ratio. To evaluate the role of 2-APB we undertook an unpaired experimental approach and compared the effects of the CCh stimuli in crypts pre-incubated with 2-APB for 2 hours to a control CCh stimulation and showed that response to CCh in crypts was attenuated by approximately 30% in the presence of 2-APB. To test the effect of Dantrolene we compared the effect to the CCh signal in an unpaired experiment. The results showed that the presence of RyR inhibitor blocks the muscarinic activated signal. Taken together these results suggest that release of calcium via TPCs induces a calcium signal that is amplified by calcium-induced calcium release from the ER (**Figure 3.34**).

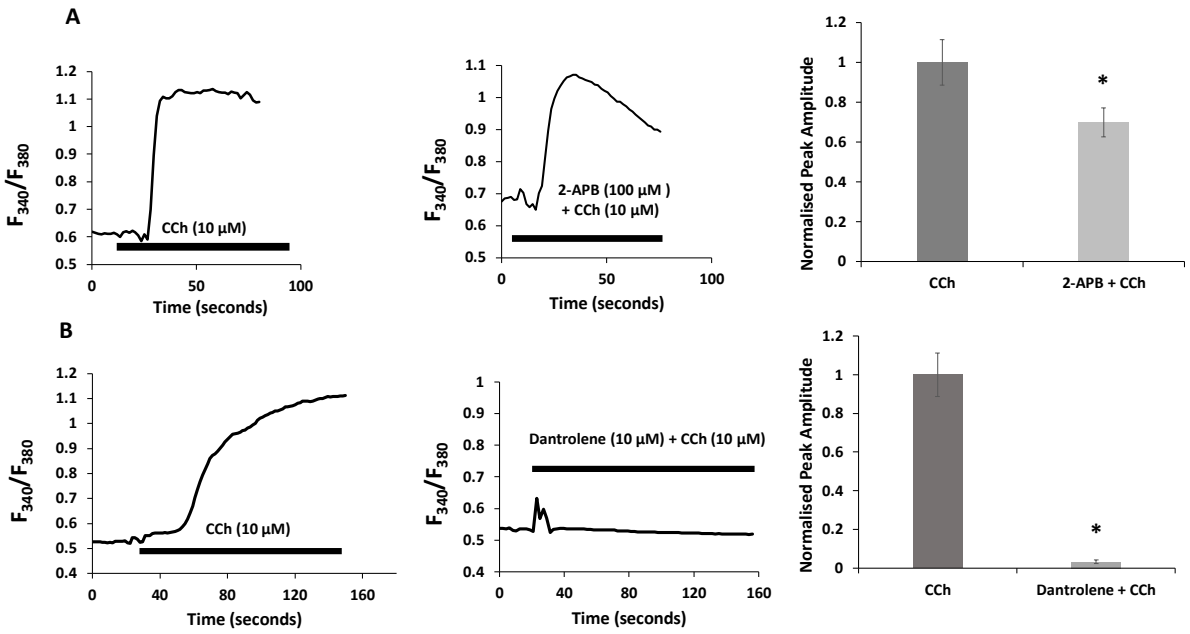

Figure 3.34. Role of the ER in the muscarinic-calcium response. (**A**) Calcium traces represent crypt response to CCh (10 µM) (left) and CCh (10 µM) in crypts pre-incubated with 2-APB (100 µM) for 2h (right). Bar chart represents the normalised peak amplitude of the calcium response (N=1, n=4, *P<0.05) (**B**) Calcium traces represent the crypt response to CCh (10 µM) (left) and CCh (10 µM) in crypts pre-incubated combination with Dantrolene (10 µM) for 2h (right). Bar chart represents the normalised peak amplitude of the calcium response (N=1, n=2, *P<0.05). Data also contributed to by Alvin Lee.

3.3 Discussion

The results of this chapter validate the use colonic organoids as a powerful tool to study gut physiology as it recapitulates the similar genetic features and largely conserves the cellular diversity present in the native tissue and colonic crypts. Measurement of organoid RNA expression with the use of RNAseq, RT-PCR and qRT-PCR demonstrated the presence of similar gene signatures existing *in vivo* and in isolated colonic crypts. Immunofluorescence labelling confirmed these findings by revealing at the protein level the expression and location of all colonic epithelium cellular types and thus confirming the differentiated cell diversity of our culture systems. Furthermore, gene expression and immunofluorescence analysis verified the presence of the muscarinic-calcium signalling toolkit in colonic crypts and organoids. The study of intracellular calcium signals with the use of fluorescence calcium indicators in organoids corroborated the physiological similarities with cultured crypts and help advanced the research field by aiding in the study of the regulation of colonic calcium signalling.

3.3.1 Development of an organoid culture system

The development of 3D culture systems of gut epithelial cells, known as gut organoids, has helped bridged the gap between the 2D cell culture and live tissues by creating a platform that recreates the *in vivo* like tissue architecture. Gut organoids are grown in a gel where they can present adhesions distributed in all 3 dimensions and are able to generate epithelial cell polarity in a relatively low stiffness environment similar the one present in tissues. These characteristics allow the organoids to recapitulate tissue topology where the hierarchy of stem cell-driven tissue renewal is maintained (Almeqdadi et al., 2019; Date & Sato, 2015).

In this chapter we presented the development of a successful long-term human colonic organoid culture system that is able to recreate the physiological characteristics of the live tissue. Passage of isolated cultured crypts into smaller fragments that are embedded in Matrigel, generates organoids that grow to resemble the mini-gut morphology comprising a circular array of crypts with a central lumen. Over the first days in culture we showed that colonic organoids develop crypt-like structures with a luminal space that recapitulates the architecture of the native tissue. The colonic epithelium is dependent on the submucosa that lies underneath as it provides structural support and the secretion of key molecules and growth factors to create a cellular microenvironment that regulates crypt biology (Meran et al., 2017). Following the pioneering work by the Williams lab in generating and culturing near-native colonic crypt cultures and from Sato and colleagues in the development of gut organoids (Reynolds et al., 2007, 2013; Sato et al., 2009), organoids were embedded in extracellular-like matrix called Matrigel which allows for epithelial cells to grow in three dimensions. This gel presents a high concentration of laminin, which is enriched in the crypt cell base to support epithelial cell growth (Sasaki et al., 2002). Because crypt biology is dependent on a tightly regulated secretion of growth factors in the stem cell niche, organoids were incubated with culture media containing a balanced concentration of these molecules. High concentrations of growth factors such as Wnt and R-spondin can overstimulate the Wnt signalling pathway and suppress differentiation, which has been reported to induce organoids with a cystic-like structure that is mainly formed by undifferentiated cells (Yip et al., 2018). Here we show that our culture conditions contain optimal levels of growth factors which support stem cell proliferation in the base of crypts but also allow cells to differentiate towards the upper region, resulting in the formation of crypt-like structures or buds (**Figure 3.1B and 3.2A**). The generation of these buds is reminiscent of the *in vivo* crypt fission events that occur naturally during organogenesis or can be triggered upon epithelial damage and are generated from the stem cell compartments. Our organoids vary in the number of buds they produce, which can be related to the number of stem cells present in the fragment they were

originated from after passage. Importantly, we showed that these organoids can be propagated indefinitely, and we have successfully grown organoid lines for more than a year that are able to maintain the same morphology and physiological characteristics. In addition to the development of colonic organoids, we successfully generated single cell cultures derived from colonic crypts. This culture system aims to answer physiological questions such as the capacity for forming organoids under different growth conditions or the study of cellular responses in cells lacking signals from neighbours. In principle, the population of single cells can be immunolabelled and sorted using fluorescence activated cell sorting (FACS) to achieve cultures with the desired cell types as well as to allow for further single cell RNA sequencing to study the genetic differences between cell lineages of the colon epithelium.

3.3.2 Colonic organoids recapitulate the differentiated cell diversity of native tissue and cultured crypts

Colonic crypt and organoid cultures conserve all the cell lineages that constitute the colon epithelium. Making use of gene expression level measurements with RT-PCR, qRT-PCR and RNAseq in conjunction with immunofluorescence experiments to study protein location and distribution, we validated the presence of all colonic epithelial cell types in our culture systems except mature tuft cells. We first demonstrated the presence of stem cells across our tissue samples by analysing the gene expression and protein localisation of the validated markers LGR5, OLFM4, ASCL2 and PTK7 (Barker et al., 2007; Jung et al., 2015; van der Flier et al., 2009; van der Flier et al., 2009). Measurement of mRNA expression with RT-PCR showed the presence of LGR5, OLFM4 and PTK7 in both cultured crypts and organoids (**Figure 3.3**) and was further confirmed by RNAseq (**Figure 3.4**). The expression of OLFM4 was found to be more abundant than the other stem cell markers. This marker is a secreted protein of an unknown function, but its high levels could be explained by the need of the cell for replenishing the content of the secreted protein, indicating a higher demand for protein formation and thus of mRNA. Imaging of immunolabelled colonic crypts and organoids revealed the presence of OLFM4, LGR5 and PTK7 to be restricted to the stem cell niche which matched what was observed in native tissue (**Figure 3.11 & Chapter 5, Figure 5.2**). These results confirm the existing literature that locates stem cells and proliferative cells at the base of the crypts (Clevers, 2013; Reynolds et al., 2013; Barker, 2014; Gehart and Clevers, 2019).

The expression of the secretory cell types, goblet and enteroendocrine cells was assessed in a similar fashion. Goblet cell location was evaluated primarily with the marker MUC2, which is the main mucin expressed in the human colon and is responsible for the formation of the mucus layers (Johansson et al., 2013; Johansson et al., 2009). In this study we show MUC2 to be expressed both at

the gene and the protein level in colonic crypts and organoids (**Figures 3.3, 3.5 and 3.11**) and the results showed the marker to be present in high levels as judged by the number of RNA reads and number of $MUC2^+$ immunolabelled goblet cells (goblet cell distribution is further discussed Chapter 4). The existence of these high numbers is representative of the importance of this cell type, which is more prominent in the colon, where the gut microbiota is more abundant. This fact explains the need for the colonic epithelium to present a high number goblet cells capable of secreting mucus to maintain the epithelial barrier (Atuma et al., 2001; Johansson et al., 2011; Kim & Ho, 2010). Another finding that we report is the existence of different goblet cell subtypes in our tissue samples. WFDC2 has recently emerged as a marker of a population of goblet cells located at the basal regions of the crypt (Parikh et al., 2019). Our RNAseq analysis confirmed the presence of this gene (**Figure 3.5**) and the immunofluorescence analysis corroborated its presence in the base of crypts and organoids (discussed in Chapter 4). In addition, goblet cells are known to secrete trefoil factors to help maintain the epithelial barrier (Taupin and Podolsky, 2003). The RNAseq results show the presence of all three family members (TFF1, 2 and 3) in our culture models, of which TFF3 is known to be expressed in a subpopulation of goblet cells located at the upper regions of the crypt (Taupin and Podolsky, 2003). Sentinel goblet cells have been suggested as a subpopulation of goblet cells that also reside at the upper crypt region where they can trigger mucus secretion in response to bacterial metabolites (Birchenough et al., 2016). To date, these goblet cells lack a selection marker and further research is needed to characterise them. The presence of a heterogeneous population of goblet cells in our organoid culture system opens the possibility to study the complex regulation of mucus secretion and the role of these cells in protecting the epithelial barrier.

Enteroendocrine cells are specialised hormone secreting cells that regulate digestion, nutrient absorption and appetite in the gut epithelium (Gribble and Reimann, 2019). To study their expression we have evaluated the presence of the pan-enteroendocrine marker chromogranin A (CHGA), a protein expressed in the hormone containing granules (Gut et al., 2016). Using RNAseq (**Figure 3.6**) and immunofluorescence analysis (**Figure 3.12**) we confirm the presence of this cell type across our culture systems. Imaging of $CHGA^+$ cells reveals a scattered distribution of these cells along the crypt and organoid axis. Importantly, we report their presence in the stem cell niche in both culture systems which could indicate a potential role in modulating stem cell biology; a mechanism that has been described in mammary glands (Simoes et al., 2015). Although the number of reads observed in the gene expression analysis was high, the presence of $CHGA^+$ cells in crypts and organoids was low. This fact can be explained by the abundance of hormone containing granules in enteroendocrine cells, which are known to be able to secrete more than one type (Furness et al., 2013) and would imply a greater presence of the marker in those cells. Furthermore, we

demonstrate the existence of a subpopulation of L-type enteroendocrine cells that can be characterised with the expression of the family of glucagon-like peptides (GCG) 1. RNAseq analysis showed lower gene expression of this cell type marker in organoids, perhaps indicating an inferior proportion of L-type enteroendocrine cells compared to colonic crypts. Further analysis should determine whether our colonic crypts and organoids are capable of producing other hormones like serotonin or cholecystokinin.

In addition to determining the existence of secretory goblet and enteroendocrine cells, we have also confirmed the expression of the nutrient and liquid absorptive enterocytes at the gene expression level. In this analysis we show the presence of Carbonic anhydrase (CA) proteins 1 and 2 together with the fatty acid-binding proteins (FABP) 1 and 2, which are enzymes that regulate nutrient absorption (Bekku et al., 1998; Agellon, Toth and Thomson, 2002) in the gut epithelium. The high levels observed as judged by the number of reads, are consistent with the number of enterocytes reported in the literature, where it has been demonstrated they account for 80% of the total cell population of the small intestine (Snoeck et al., 2005). The crucial role of the colon in absorbing nutrients, liquids and electrolytes from the diet also suggests the abundance of this cell type in the epithelium.

This study also validates the presence of tuft cells in colonic crypts and their POU2F3^{+} precursors in organoids. Although little is known about their function, emerging literature suggests they play a role in sensing the luminal content of the gut and are able to induce cellular responses upon detection of nutrients and bacterial metabolites (Gerbe et al., 2012; Schneider et al., 2019). In this chapter we successfully identify tuft cells in colonic crypts by the expression of choline acetyltransferase (ChAT) at the gene and protein level (**Figure 3.8 and 3.14 respectively**). The literature suggests that tuft cells are able to produce and secrete non-neuronal ACh mediated by ChAT (Dando and Roper, 2012). In our immunofluorescence analysis we report the presence of ChAT^{+} cells in the native tissue as well as in cultured crypts (**Figure 3.14**). Similar to CHGA^{+} cells, we found low number of tuft cells distributed along the crypt's axis including the stem cell niche. Because tuft cells can synthesize ACh as well as prostaglandins (Eberhart and Dubois, 1995), the precise location in the proximity of stem cells could imply a potential role in regulating stem cell biology (**Discussed in Chapter 5**). While we were able to confirm the presence of ChAT^{+} tuft cells in colonic crypts, our results showed the absence of the marker in organoids in both the RT-PCR and RNAseq gene expression analysis (**Figure 3.3 and 3.8 respectively**), as well as in our immunofluorescence imaging (data not shown). Because tuft cells can secrete prostaglandins (PGE), their expression can be characterised by the presence of the PTGS gene family 1 and 2 that encodes the enzymes COX1 and COX2 (which generate PGE) but immunofluorescence analysis of COX1 and

COX2 could not confirm expression in colonic crypts or organoids (data not shown). Nevertheless, analysis of gene expression of POU2F3, a transcription factor present in tuft cells (Matsumoto et al., 2011), was found to be consistent across the native tissue, crypts and organoids which suggests the existence of this lineage in all our culture models. In addition, the presence of vesicular ACh transporter (VAChT) was found in crypts and organoids by RT-PCR analysis of mRNA expression. This transporter has been well documented in cholinergic neurons where it works by delivering the ACh into synaptic vesicles (Matsuo et al., 2011). However it is still unclear how ACh is transported in tuft cells (Middelhoff et al., 2017). Moreover, the study of mRNA expression by RT-PCR also revealed the presence of the nervous growth factor (NGF) in colonic crypts (sample not tested in organoids) which has been shown to be induced by the release of ACh from tuft cells (Hayakawa et al., 2016). The fact that tuft cells constitute less than 0.5% of the total gut epithelial population (Banerjee, Coffey and Lau, 2018) could explain a low presence of their cell markers. This observation could suggest that the techniques used in this study are not sensitive enough to detect their expression. Other research groups have reported the presence of $POU2F3^+$ tuft cells in their human organoid cultures by use of single cell RNAseq (scRNAseq) analysis (Fujii et al., 2018), although the expression of CHAT was not discussed. In addition, a possible scenario that could explain these results would involve the presence in our organoids of immature $POU2F3^+/ChAT^-$ cells which in our current culture conditions cannot fully differentiate into mature Tuft cells. Currently, the Williams lab is working on detecting tuft cell secretion of non-neuronal ACh by mass spectrometry analysis of conditioned media obtained from organoids. Mass spectrometry is a more sensitive analytical technique that has been shown to successfully identify the presence of ACh in plants (Murata et al., 2015). The finding of ACh secreted in the organoid media could help verify the presence of $ChAT^+$ tuft cells.

By confirming the expression of all colonic epithelial cell types and while the ratio of cells compared to crypts was not evaluated, we demonstrate that organoids maintain the colonic epithelial cellular diversity and are able to recapitulate all the gut physiological processes including tissue growth and self-renewal, hormone secretion to modulate nutrient incorporation and tissue motility, mucus production to protect the epithelial barrier, nutrient and bacterial antigen sensing, and nutrient, liquid and electrolyte absorption.

This chapter also validated the presence of stem and differentiated cells in our organoid system as well as the plasticity of our culture system by qRT-PCR gene expression analysis. We showed that changes in the growth factor composition of the media modulate the gene expression of stem cells and differentiated cells. Because organoids cultured in media lacking of Wnt and R-spondin revealed lower numbers of stem (LGR5 and ASCL2) and proliferation markers (Ki67), and conversely expressed higher numbers of differentiated cells (CA1 and ANPEP) (**Figure 3.5**) we confirmed that our standard

culture conditions favour an environment that promotes stem and tissue renewal. The lack of difference in expression found for the cellular marker CEACAM7 could be explained by the low numbers registered, which could suggest that its expression is reduced in our culture system. The outcome of this experiment shows that the organoid culture can adapt to changes in the growth factor composition by promoting or reducing the expression of proliferation or differentiation related genes. This finding can be useful with regards to study of the signals that regulate crypt physiology by analysing the gene expression of markers of interest in response to addition or removal of nutrients and growth factors in the media. In the literature, Fujii and colleagues demonstrated in their model of human colonic organoids that changes in the growth factor composition can modify the cellular composition as well as the culture efficiency (Fujii et al., 2018). While we have shown that bulk RNAseq is a powerful methodology for sequencing multiple genes across multiple samples, in this chapter we also validate the use of quantitative PCR as a tool for the study of gene expression in organoids, which is proven useful when analysing a low number of known targets.

3.3.3 Colonic organoids express the components of the muscarinic-calcium signalling toolkit

In this chapter we demonstrate for the first time that colonic organoids are endowed with an array of calcium channels and cellular receptors that mediate the muscarinic activation of intracellular calcium signals. Early work by the Williams lab has demonstrated that human cultured colonic crypts respond to the stimulation with ACh by activating a complex intracellular calcium signalling pathway which originates at the base of colonic crypts (Lindqvist et al., 2002; Reynolds et al., 2007, Dr. Christy Kam, PhD Thesis), but no previous studies have characterised the expression and presence in colonic organoids of its regulatory elements. In this study, we show by RT-PCR analysis of mRNA expression that all muscarinic receptors (MAChR1-5) are present in colonic crypts and organoids (**Figure 3.15**). Immunolabelling of the receptors further demonstrates the tissue distribution of these markers (**Figures 3.19 and 3.20**) in both culture systems. The receptors MAChR 1, 3, and 5 are all coupled to release of calcium from intracellular stores (Lechleiter et al., 1990). Our immunofluorescence results indicate the presence of these markers in the base of colonic crypts and organoid buds, in line with the exsisting literature (Reynolds et al., 2007), and confirms that ACh can signal in the stem cell niche. Lysotracker live labelling reveals the presence of acidic stores in the cytoplasm and the apical pole of epithelial cells. The presence of a high number of goblet cells containing acidic secretory granules explains the large cytoplasm labelled areas. In addition, Lysotracker also labels endolysosomes and highlights the presence of a polarised distribution of the calcium signalling

organelles, where mitochondria and ER are primarily located in the perinuclear region, as seen by the Mitotracker and KDEL labelling (**Figure 3.21**). Labelling of the ER with the KDEL marker shows prominent expression of the protein in goblet cells which could suggest an important role for this organelle in regulating goblet cell biology (**Figure 3.21v and vi**). Goblet cells demand a constant production of mucins to fill the cytoplasmic globules destined for release into the lumen (Johansson et al., 2013) which could explain the presence of a more abundant ER network to generate enough protein to meet the demand.

Preliminary work in the Williams lab suggested TPCs as the mediators of the muscarinic-induced calcium signalling (Dr. Christy Kam, PhD Thesis). In order to elaborate on this hypothesis, we analysed the expression of the elements of the signalling pathway that contribute to calcium release from the endolysosomal TPCs. We demonstrated the mRNA expression of CD38, which catalyses the formation of NAADP, as shown by RT-PCR analysis, to be present in colonic crypts (data not analysed in organoids) (**Figure 3.15**) and confirmed the protein expression by immunofluorescence examination of the antibody labelling (**Figure 3.22**) in both colonic crypts and organoids. The expression was observed in the nucleus and also in the apical membrane of epithelial cells as previously reported in the literature (Ramaschi et al., 1996; Adebanjo et al., 1999). RNAseq analysis revealed the presence in organoids of all the major cellular calcium channels and calcium ATPases including the ones present in the ER (IP3R, RyR and SERCA pump) endolysosomes (TPCs), Golgi (SPCA pump) and plasma membrane (PMCA) with expression levels similar to the ones found in crypts. Surprisingly, the gene levels of RyR were very low. However, this does not necessarily correlate with protein expression as analysis of calcium signalling with the selective blocker Dantrolene showed blockage of the CCh-induced calcium response (**Figure 3.34**), indicating the presence of RyRs in our culture systems. Further immunofluorescence analysis is needed to determine the cell localisation of these calcium channels. The protein distribution revealed the presence of IP3Rs and TPCs in the base of organoid buds. Our immunofluorescence analysis indicates a cytoplasmic and nuclear presence of IP3R1 and 2, with the latter being highly expressed in the basal membrane. Interestingly, the expression of IP3R3 was restricted to the apical pole of epithelial cells (**Figure 3.23**). This difference in the protein distribution suggest specialised spatial function of each of the receptors which has been previously reported in the rat colonic epithelium (Siefjediers et al., 2007). The mRNA transcript of TPC was also confirmed by RT-PCR to be present in crypts and organoids. Immunofluorescence visualisation of TPC1 and 2 showed the calcium channels to be preferentially expressed in the apical pole of the cells (**Figure 3.24**) which correlates with the location of the endolysosomes previously reported and with the role of the organelle in membrane trafficking (Luzio, Pryor and Bright, 2007). Expression of TPC1 was found to be higher both at the gene expression and protein level which

could indicate a more abundant presence of this subtype in the colon epithelium. However, it remains unclear whether the two subtypes develop the exact same role and if they respond to the same activator. Further research into the development of selective antagonist could elucidate their function independently. In addition, the presence of TPC1 was also observed in the nuclei which suggests that this calcium channel could be present in more than one organelle. Our observations indicate the presence of IP3R3 and TPCs to be prominently expressed in the apical pole, while the localisation of RyR remains to be studied. Previous research has suggested the existence of a crosstalk between the ER and the acidic organelles, where depending on the nature of the calcium signal, calcium can activate calcium release from one store and vice versa (Boittin, Galione and Evans, 2002; Kinnear et al., 2004). Another possible scenario would involve the presence of IP3R3 in the membrane of endolysosomes, which remains to be studied. In addition, preliminary work by Alvin Lee suggest that IP3Rs do not play a key role in ACh-induced calcium signals but are essential in generating calcium signals coupled to purinergic P2Y2 receptors located in the apical pole of epithelial cells, suggesting the presence of two different calcium signalling pathways (Alvin Lee, unpublished). Importantly, we show that goblet cells and stem cells of the base of the crypt are endowed with components of the muscarinic-calcium signalling toolkit (**Figures 3.25 and 3.26**), indicating the possibility for this signals to be expressed those cell types.

3.3.4 Muscarinic-induced calcium signals are dependent on TPC

The study of the topology and polarity of the calcium response to muscarinic activation confirmed that the signal originates in the stem cell niche of crypts and then propagates as a wave to the upper regions (**Figure 3.27**). Importantly, the signal is elicited in the apical pole of the cells and then spreads to the basal pole where the muscarinic receptors are expressed. Although uncommon, this long distance communications between muscarinic receptors and calcium release channels have been reported in pancreatic acinar cells (Ashby et al., 2003). The fact that muscarinic activation elicits a calcium response in the apical pole of the cell correlates with the cellular location of the endolysosomal TPCs.

The characterisation of the muscarinic-activated calcium signal showed that the use of the selective muscarinic agonist Oxo induces a calcium response while the inhibition of muscarinic receptors with 4-DAMP abrogates it. This result confirm that CCh-induced calcium response is mediated by muscarinic and not by nicotinic receptors (**Figures 3.30 and 3.31**). In the absence of extracellular calcium, depletion of the ER with CPA elicited an intracellular calcium response. Importantly, a subsequent muscarinic stimulation with CCh still induced a calcium response of lower amplitude (**Figure 3.32**). This indicates that muscarinic activation elicits an intracellular calcium response

independent on extracellular influx of calcium. In addition, the presence of a CCh-induced signal after ER depletion indicates that there is another store that functions independent of the ER. Further analysis is needed to confirm the possible endolysosomal source of calcium implicated in the second calcium response stimulated by CCh. To this end, the CCh-induced calcium response needs to be assessed in the presence of TPC blockers such as Ned19, Tetrandrine or Diltiazem. In addition, in a different experimental set up, inhibition of the TPCs with Ned19 abrogated the calcium signal in response to CCh in both colonic crypts and organoids. These results were also confirmed in the presence of the TPC inhibitors Tetrandrine, Diltiazem and Verapamil (data not shown), which suggests that intracellular calcium signals are dependent on calcium release from the TPC upon muscarinic activation (**Figure 3.33**). Blocking of IP3Rs with 2-APB attenuates the calcium response to CCh while inhibition of RyR1 and/or RyR3 with Dantrolene blocks it in both culture systems (**Figure 3.34**), which suggests that muscarinic stimulation induces release from TPC which is then amplified via calcium-induced calcium release from IP3Rs and RyRs. These findings confirm a key role of endolysosomal TPCs in releasing calcium in response to CCh stimulation (possibly mediated by NAADP activation of the receptors, which is generated by CD38), which is observed in the endolysosomes located in the apical pole of the cells at the crypt base. Based on this evidence, we suggest that this calcium signal is then amplified by activation of calcium release from the ER via IP3Rs and RyRs, which is observed as the intracellular calcium wave that spreads to the basal pole of the cell. We have shown that this signal originates in the stem cell niche and that the main elements involved are present in goblet cells and stem cells. These findings beg the question of which kind of downstream effect these calcium signals have and which aspects of their cell biology they regulate.

In addition to the work presented in this chapter, parallel studies in the Williams lab have confirmed the expression of RyR1, 2 and 3 in colonic epithelial cells at the base of crypts at RNA messenger level by conducting RT-PCR analysis, and at the protein level by conducting immunofluorescence assays (data not shown). Moreover, we have carried out other pharmacological experiments (data not shown) where colonic crypts pre-incubated with Ryanodine (50 μM), a known inhibitor of RyR1 and/or RyR2, attenuated the CCh-induced calcium response by 30%. Furthermore, pre-incubation with Procaine (1 mM) reduced the cholinergic-induced calcium response by approximately 80%, suggesting that RyR1, RyR2 and possibly RyR3 are involved in the response of colonic epithelial cells to cholinergic activation. In this thesis, we have shown the presence at the RNA and protein level of CD38, which catalyses the formation of NAADP or cADPR, the latter known to activate RyR1 (Ogunbayo et al., 2011). Previous research conducted by Dr Christy Kam (PhD thesis) has shown that pre-incubation of colonic crypts with 8-Bromo-cADPR (30 μM), an antagonist of cADPR (Walseth and Lee, 1993), has minimal effect on the CCh-induced calcium signal. These results suggest that

activation of RyR1 by cADPR is not involved, and that production of NAADP is favoured upon activation of the signalling cascade. Whether RyR1 engages in CICR in our system or if it just depends on the action of RyR2 and RyR3 remains to be studied. Selective inhibition of all three RyR subtypes and CD38 using siRNA will be conducted to clarify the role of each of these receptors in the cholinergic-induced calcium signalling.

3.4 Conclusion

This chapter has described the development of a colonic organoid culture system and validated it by confirming its capacity to self-renew and maintain a differentiated cell diversity. Colonic organoids present the components of muscarinic-induced calcium signalling toolkit. This signal initiates in the stem cell niche and is triggered by release of calcium from TPCs. The colonic stem cell niche is populated by stem cells and goblet cells. In view of these findings, we decided to study the physiological consequences of cholinergic calcium signal activation in these cell types, which will be the subject of the following results chapters.

4 Chapter 4. Guardian goblet cells protect the human intestinal stem cell niche

4.1 Introduction

The maintenance of the intestinal epithelial barrier is crucial to safeguard the intestine from any potential luminal threats. Mucus and fluid secretion from goblet cells and the epithelium form one of the major lines of defence as they are able to flush and expel noxious substances trying to contact the colonic crypts. Goblet cells are present along the entire gut-axis but are prominent in the colon, where most of the microbiota resides. Intestinal stem cells reside at the base of colonic crypts where literature suggest they are found intermingled with goblet cells (Reynolds et al., 2013; Sasaki et al., 2016). Together with other mesenchymal cell types like myofibroblasts and telocytes, stem cells and goblet cells generate the stem cell niche (Meran, Baulies and Li, 2017). All these different cell types help maintain stem cell biology and regulate their function during homeostasis and tissue regeneration. Protection of the stem cell niche is crucial for the maintenance of the crypt, and goblet cells located at the base are thought to play a protective role. However, to date little is known about the way these cells are regulated.

The population of colonic goblet cells has been suggested to vary in function along the crypt-axis. A recent publication by Birchenough and colleagues highlighted the important role of the so-called sentinel goblet cells which reside at the top of the crypts. These cells play a critical role in sensing bacterial metabolites that have breached the mucus barrier and rapidly activate neighbouring goblet cells to induce mucus secretion and expel the bacterial threat (Birchenough et al., 2016). At the bottom of the crypt, goblet cells reside interspersed with stem cells. These type of goblet cells, named deep secretory cells, are thought to develop a key role similar to Paneth cells in regulating the biology of stem cells (Toshiro. Sato et al., 2011) and recent findings suggest they can be identified by the expression of the REG4 marker (Sasaki et al., 2016). Unlike Paneth cells, little is known about the secretion of antimicrobial peptides by goblet cells, which includes molecules like human defensins (Cobo and Chadee, 2013). However, recent discoveries show that a population of goblet cells residing at the base can secrete the protein WFDC2. This protein works as a defence factor to prevent pathogen invasion by inhibiting the proteolytic activity of bacterial enzymes needed for breaching the inner mucus layer (Parikh et al., 2019).

Intestinal fluid secretion is crucial for maintaining an appropriate level of fluidity required for digestion (Frizzell and Hanrahan, 2012) but it also serves as another mechanism by which the colonic epithelium can fight bacterial invasion. Activated secretion of fluid induces the swelling of crypts and

the subsequent flushing of the luminal content to maintain a sterile epithelium. Fluid secretion into the lumen depends on the movement of chloride ions (Cl^-) as water follows through osmosis. On polarised epithelial cells Cl^- uptake is mediated by the Na^+-K^+-$2Cl^-$ co-transporter NKCC1 located in the basolateral membranes. The presence of this co-transporter has been shown to be also crucial for mucus formation (Gustafsson et al., 2014) and the expression has been localised to the basolateral membranes of the epithelial cells of colonic crypts (Reynolds et al., 2007). Cl^- movement into the lumen is primarily regulated by the cystic fibrosis transmembrane conductance regulator (CFTR) located in the apical membrane of epithelial cells (Barrett and Keely, 2000), which also mediates release of HCO_3^- needed for proper formation and secretion of mucus (Garcia, Yang and Quinton, 2009; Yang, Garcia and Quinton, 2013).

A great body of work has demonstrated the effect of different secretagogues in the regulation of mucus and fluid secretion in the colonic epithelium. Intestinal epithelial cells have been shown to secret fluid under the stimulation of vasoactive intestinal peptide (VIP) (Schwartz et al., 1974), serotonin (Cooke et al., 1991), histamine (Homaidan et al., 1997), ACh (Tapper, Powell and Morris, 1978; Halm and Halm, 2000) and prostaglandin E_2 (PGE2) which is suggested to be the most potent activator (Halm and Halm, 2000; Fujii et al., 2016). Regarding mucus secretion, histamine has also been shown to act as a secretagogue in the airway system as well as in the colon (Neutra, O'Malley and Specian, 1982; Kang et al., 2017). Importantly, cholinergic activation by ACh has been demonstrated to be the most potent secretagogue in colonic crypts (Specian and Neutra, 1980, 1982; Halm and Halm, 2000; McGuckin and Hasnain, 2017).

As discussed in the previous chapter (**Figure 3.27**), we have demonstrated that muscarinic activation of colonic epithelial cells induces a calcium signal response which starts at the apical pole membrane of cells located at the base of the crypts and then exhibits intracellular propagation to the basal pole and intercellular propagation up the crypt-axis (S. Lindqvist et al., 2002; S. M. Lindqvist et al., 1998; Reynolds et al., 2007). The role of the second messenger calcium has been shown to be involved in modulating fluid secretion and mucus formation, packaging and release. As shown by Reynolds and colleagues, activation of the muscarinic receptor type 3 (MAChR3) by ACh induces an intracellular calcium response that modulates NKCC1 trafficking to the membrane, therefore regulating Cl^- uptake and the subsequent fluid secretion (Reynolds et al., 2007). A high calcium concentration is needed during the formation and packaging of mucus because its interactions with the protein diminish the repulsive forces among the negatively charged mucin oligomers, which favours a dense packaging of the mucin (Perez-Vilar, 2007; Ambort et al., 2012).

Although the mechanism by which elevated intracellular calcium promotes mucus release is still not clearly understood. Cantero-Recasens and colleagues have proposed the existence of a calcium-sensitive mechanism that regulates docking of the mucus granule to the plasma membrane and subsequent exocytosis. KChIP3 is a high affinity calcium sensor that under resting calcium conditions prevents fusion of the mucus granules to the membrane. An increase in intracellular calcium will enable the second messenger to bind to KChIP3 to inactivate it, inducing its removal from the granule membrane, thereby allowing granules to bind to the plasma membrane and release their contents (Cantero-Recasens et al., 2018). However, as is often the case for studies on the physiology of mucus secretion, this investigation was over reliant on a cell line that did not express the main mucin protein secreted by the native intestinal epithelium, MUC2.

Previous work in studying mucus secretion has involved the use of different animal models like mouse (Schneider et al., 2018), guinea pig (Cooke, Sidhu and Wang, 1997), rabbit (Neutra, O'Malley and Specian, 1982), monkey and human mucosal explants (Halm and Halm, 2000), and human colonic cell lines (Warhurst et al., 1991; Bou-Hanna et al., 1994). Recent work by Dr Christy Kam made use of isolated colonic crypts (Parris and Williams, 2015) to study mucus secretion (Dr Christy Kam, PhD Thesis), however studies using human colonic organoids for investigating fluid secretion are limited, while mucus secretion using our model has not been studied yet to our knowledge. In addition to the advantages discussed in the previous chapter, colonic organoids are amenable to genetic engineering. Live imaging of labelled mucus secretion in human tissue could be extremely advantageous to monitor its spatio-temporal characteristics. However, a model that would enable this study is yet to be developed.

Our observations from the study of muscarinic-induced calcium signals in colonic organoids together with the work of Dr Christy Kam (PhD Thesis) suggest that endolysosomes play a key role in the initiation of the muscarinic-induced calcium response by TPC-dependent calcium release. This increase in intracellular calcium could be involved in mucus secretion (**Figure 4.1**). The aim of this chapter is to determine the characteristics of the calcium signals induced by muscarinic activation in fluid and mucus secretion of human colonic crypts and organoids. In order to study the status of mucus secretion, immunofluorescence labelling and confocal imaging was used. Time lapse microscopy was also used to monitor organoid swelling. In addition, PCR was used to generate a fluorescent reporter cassette to be knocked in the MUC2 gene (**Appendix B**). The data presented suggest calcium release from the endolysosomal two-pore channels is crucial in regulating fluid and mucus secretion in goblet cells of the stem cell niche.

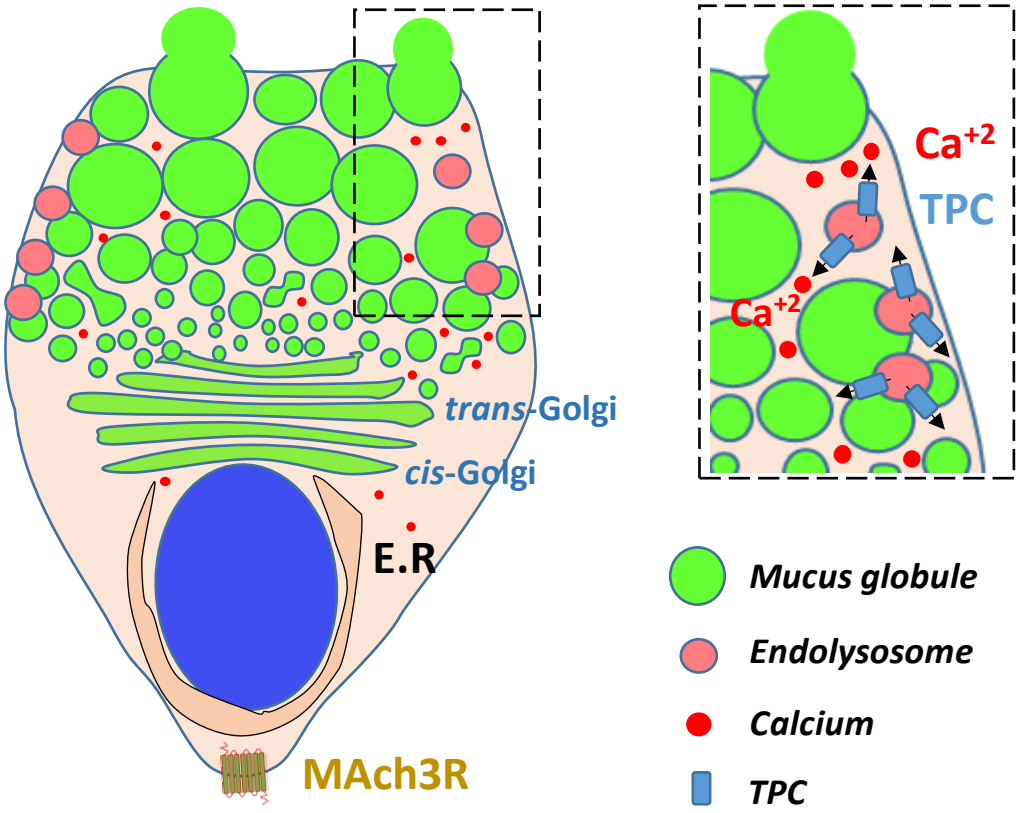

Figure 4.1. Proposed mechanism of calcium induced mucus secretion. Activation of muscarinic receptors on goblet cells by ACh results in release of calcium from the endolysosomes located in the apical pole of the cells into the cytoplasm via TPCs. Released calcium possibly activates IP3Rs and RyRs to induce global calcium signals that ultimately trigger mucus secretion from the goblet cells into the lumen of colonic crypts.

4.2 Results

The study of goblet cell mucus secretion and fluid transport was carried out using primary cultures of human colonic crypts and organoids. The role of muscarinic-induced calcium signals in regulating mucus secretion was investigated by using selective pharmacological agents that modulate the calcium signalling pathway components, prior to imaging the mucin content in goblet cells using antibodies against MUC2. Goblet cell calcium signals in response to muscarinic stimulation were monitored with live imaging of the calcium-sensitive fluorescence indicator Fluo-4. In addition, stimulation of fluid secretion in organoids by muscarinic receptor-coupled calcium signals was assessed by time lapse microscopy and measurement of their cross-sectional area. Finally, mucus granule trafficking and exocytosis by goblet cells was monitored by confocal live imaging of a fluorescence lipid dye in goblet cells.

4.2.1 Goblet cell presence and distribution in human colonic crypts

Goblet cells are expressed along the entire gut-axis but are more abundant in the colon (Kim and Ho, 2010). The presence and distribution of goblet cells was characterised in native tissue as well as cultured human colonic crypts derived from human tissue samples. We also validated our organoid and single cell culture models by demonstrating expression of $MUC2^+$ goblet cells. Human native tissue was fixed immediately after the surgical resection of the colon sample to preserve the *in vivo* tissue integrity and thin sections were obtained with a cryostat microtome (8 μm). Crypt sections were immunolabelled for MUC2 and E-cadherin (ECAD) protein to visualise goblet cells and cellular membranes, respectively. Cell nuclei were stained with nuclear dye Sytox blue. Confocal fluorescence images revealed the distribution of goblet cells along the entire length of the crypt-axis (**Figure 4.2 Left**). High magnification images of the crypt base demonstrated the presence of goblet cells in the stem cell niche (**Figure 4.2 Left and bottom**). Similarly, cultured human colonic crypts were fixed on day 1 of culture and processed for immunofluorescence labelling. Confocal microscopy revealed a similar distribution of goblet cells in cultured crypts as compared to native tissue (**Figure 4.2 Centre**). Moreover, the number of $MUC2^+$ goblet cells was found to be comparable along the crypt axis (**Figure 4.3A**). Goblet cells were shown to be present in the stem cell niche (**Figure 4.2 Centre and bottom**). Having established that cultured colonic crypts exhibited a similar number and distribution of goblet cells as visualised in native tissue, we next investigated the number and distribution of goblet cells in colonic organoids in the exact way as for isolated colonic crypts. Goblet cell distribution was comparable to those of native tissue and isolated crypts (**Figure 4.2 Right and top**). In addition, the total number of $MUC2^+$ goblet cells were found to be similar across all culture systems. (**Figure 4.3B**). Moreover, high magnification images also revealed the presence of goblet cells in the stem cell niche of the organoids' crypt-like domain (**Figure 4.2 Right and middle**). Finally, single cells were obtained from the enzymatic and mechanical degradation of organoids and plated as a heterogeneous cell population. Single cells were processed and imaged on day 1 in the same way as colonic crypts and organoids. Single goblet cells retained their goblet-like shape and demonstrated the potential for carrying out experiments in goblet cells lacking neighbouring epithelial cells (**Figure 4.2 Right and bottom**).

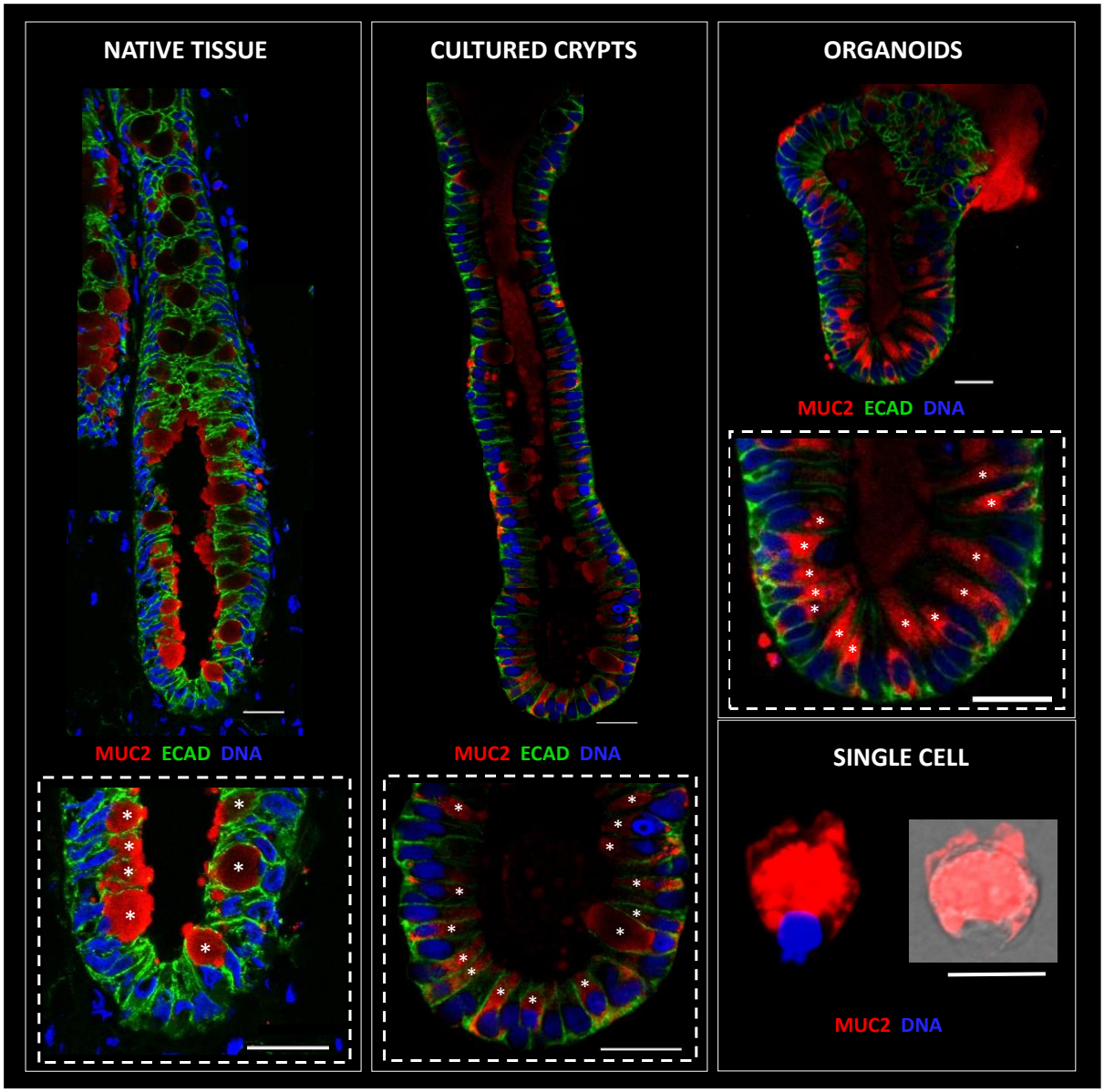

Figure 4.2. Presence and distribution of goblet cells across different models. Representative confocal images of human mucosal (native) sections, isolated human colonic crypts, human colonic organoids and single goblet cells, respectively. Images display goblet cell marker MUC2 (red), cell membrane marker ECAD (green) and nuclear dye Sytox blue (DNA). Bottom images show high magnification images of the base of crypt and highlight presence of goblet cells in the stem cell niche. Asterisks mark presence of goblet cells. Scale bar 25µm. Bottom right section depicts a high magnification confocal image of a single goblet cell. Left image shows composite image of MUC2 (red) and nuclear dye Sytox blue (DNA) and right shows composite image of MUC2 (red) and brightfield. Scale bar 10µm. Imaging also contributed to by Alvin Lee.

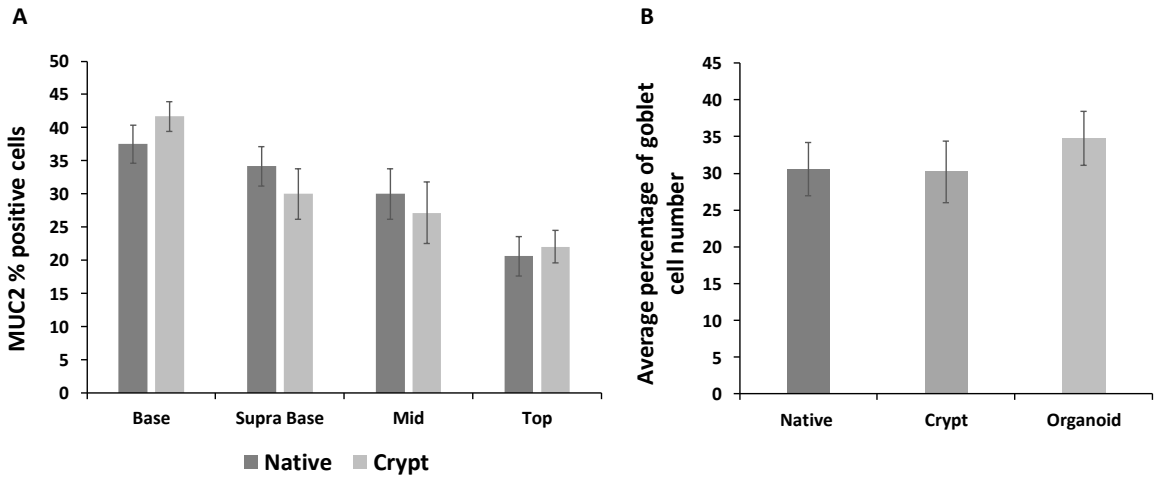

Figure 4.3. Goblet cell number is similar across the different culture systems. (**A**) Bar chart represents the percentage of MUC2$^+$ goblet cells distributed along the different regions of the crypt axis of native and cultured human colonic crypts (N=3). (**B**) Bar chart represents the average percentage of MUC2$^+$ goblet cells present in native crypts, cultured crypts and organoids (N=3).

Recent literature has suggested the existence of different populations of goblet cells along the crypt-axis (Birchenough et al., 2016; Parikh et al., 2019; Sasaki et al., 2016). Researchers revealed the presence of a population of special goblet cells, termed deep secretory cells, which can be identified by the expression of the REG4 protein. These cells reside at the base of the colonic crypts and undertake a similar role of Paneth cells of the small intestine in regulating the biology of stem cells (Sasaki et al., 2016). In order to characterise the presence of this goblet cell population we fixed and processed isolated colonic crypts and labelled with antibodies against MUC2 and REG4. Confocal imaging of these samples revealed the presence of REG4$^+$ cells at the base of the crypt (**Figure 4.4B**). However, REG4$^+$ cells were also found along the entire crypt-axis congruent with MUC2$^+$ goblet cells (**Figure 4.4A**). A different type of goblet cell suggested to be present in human colonic crypts is the WFDC2-producing goblet cell (Parikh et al., 2019), which secretes the protein WFDC2 to inhibit bacterial proteases. In order to check for the presence of this marker we labelled human mucosal sections as well as isolated colonic crypts with the antibodies against MUC2 and WFDC2. Confocal imaging of tissue sections revealed the presence of WFDC2$^+$ cells expressed with particular abundance in the base and supra-base regions of the crypt, and to a minor extent in the middle region, and with minimal expression in the upper region (**Figure 4.5A and 4.5C**). The anti-WFDC2 antibody labelled both the perinuclear region as well as the cytoplasm (**Figure 4.5B**) and was shown to co-express in its entirety with MUC2$^+$ goblet cells (**Figure 4.5D**). In addition, isolated colonic crypts were fixed and labelled with the same antibody combination. Imaging of the base of the crypts revealed expression of WFDC2 in some cells, and similar to the native tissue, WFDC2 and MUC2

were co-expressed. (**Figure 4.6A and D**). High magnification images revealed WFDC2 labelling was particularly intense in the basal cell membrane as well as being present in the cytoplasm of most labelled cells (**Figure 4.6B and C**).

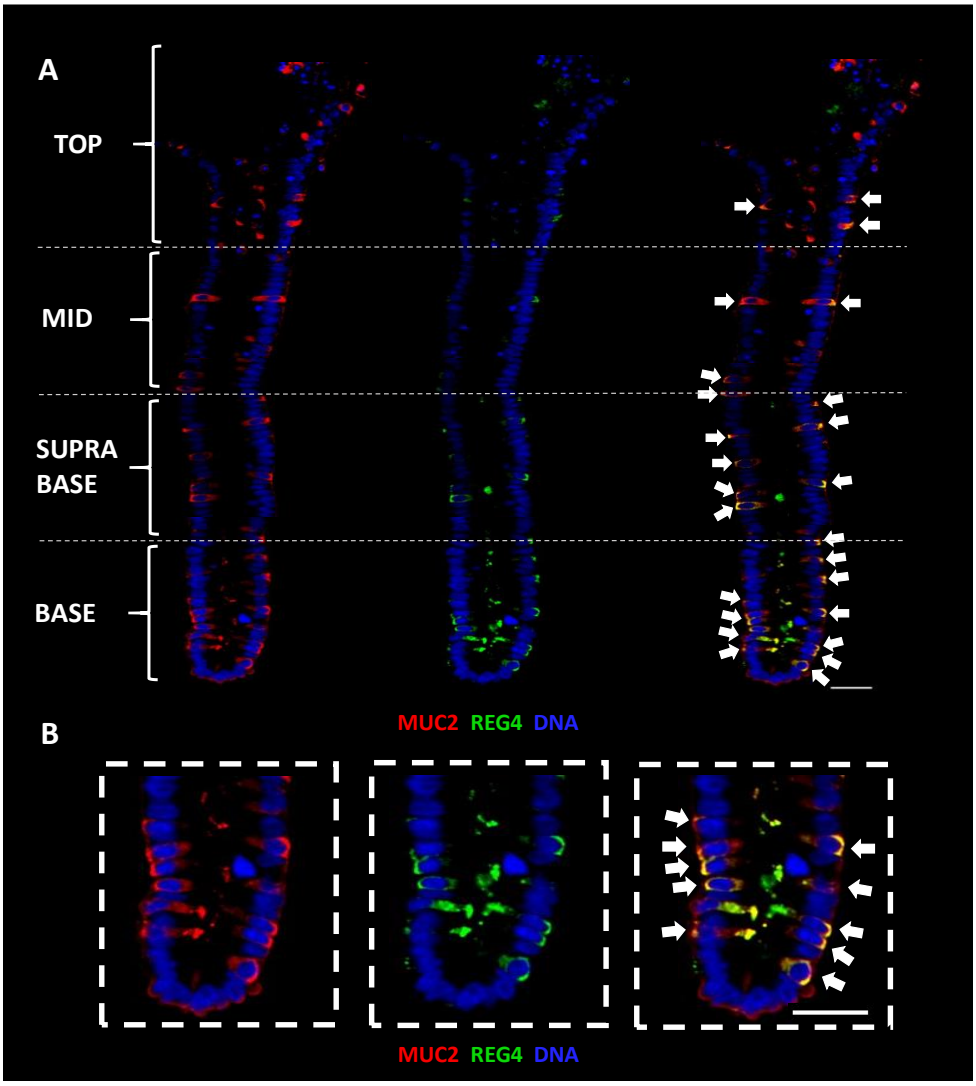

Figure 4.4 REG4 and MUC2 co-express in colonic crypts. Representative images of an isolated colonic crypt showing MUC2 (red) REG4 (green) and the nuclear stain Sytox blue (DNA). **(A)** Distribution of the MUC2^{+} and REG4^{+} cells across the crypt-axis. Right image displays MUC2 and REG4 merge labelling. Arrow heads indicated overlapping expression of both markers. Scale bar 25 µm. **(B)** High magnification images of the crypt displayed in (A). Image on the right demonstrates presence of MUC2^{+} and REG4^{+} cells in the stem cell niche. Arrow heads indicate overlapping expression of both markers. Scale bar 25 µm.

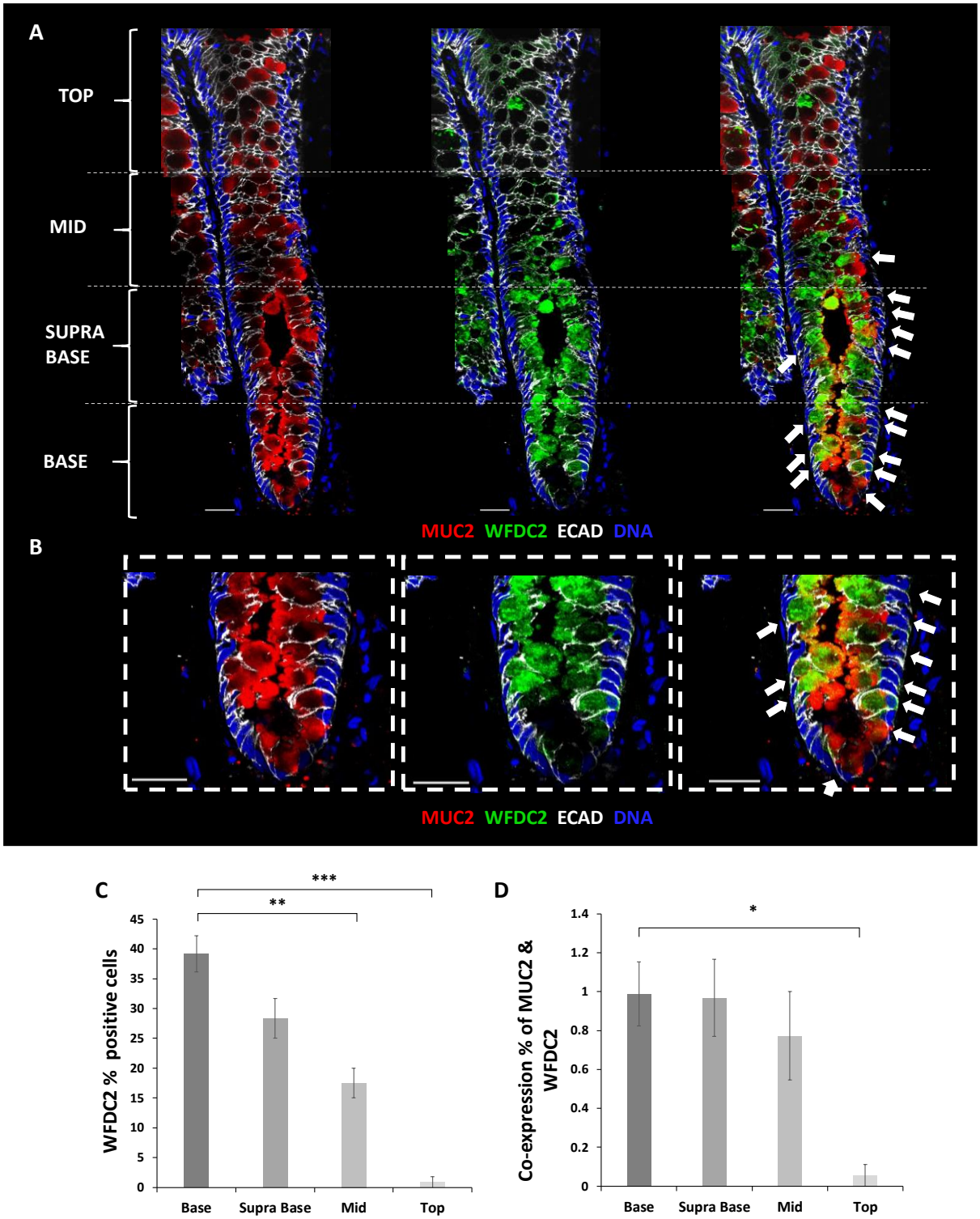

Figure 4.5. WFDC2 expression in human mucosal samples. (**A**&**B**) Illustrative confocal images showing WFDC2 (green), MUC2 (red), ECAD (white) and nuclear dye Sytox blue (DNA) expression in cryostat sections of the human colonic crypt. (**A**) Left image shows MUC2 labelled goblet cells. Middle images show expression of WFDC2 is predominant in the base and supra-base regions, moderate in the mid regions and weak in the top of the crypt. Right image displays WFDC2 and MUC2 overlapping expression in all WFDC2 positive cells. Scale bar 25 µm (**B**) High magnification

images reveal WFDC2 labels baso-lateral membranes as well as the cytoplasm. Scale bar 25 µm. Data contributed to by Alvin Lee. (**C**) Bar chart shows the percentage of WFDC2$^+$ cells along the crypt axis (N=3, ***P<0.001) (**D**) Bar chart represents the co-expression percentage of MUC2$^+$ and WFDC2$^+$ cells along the crypt axis (N=2, *P<0.05).

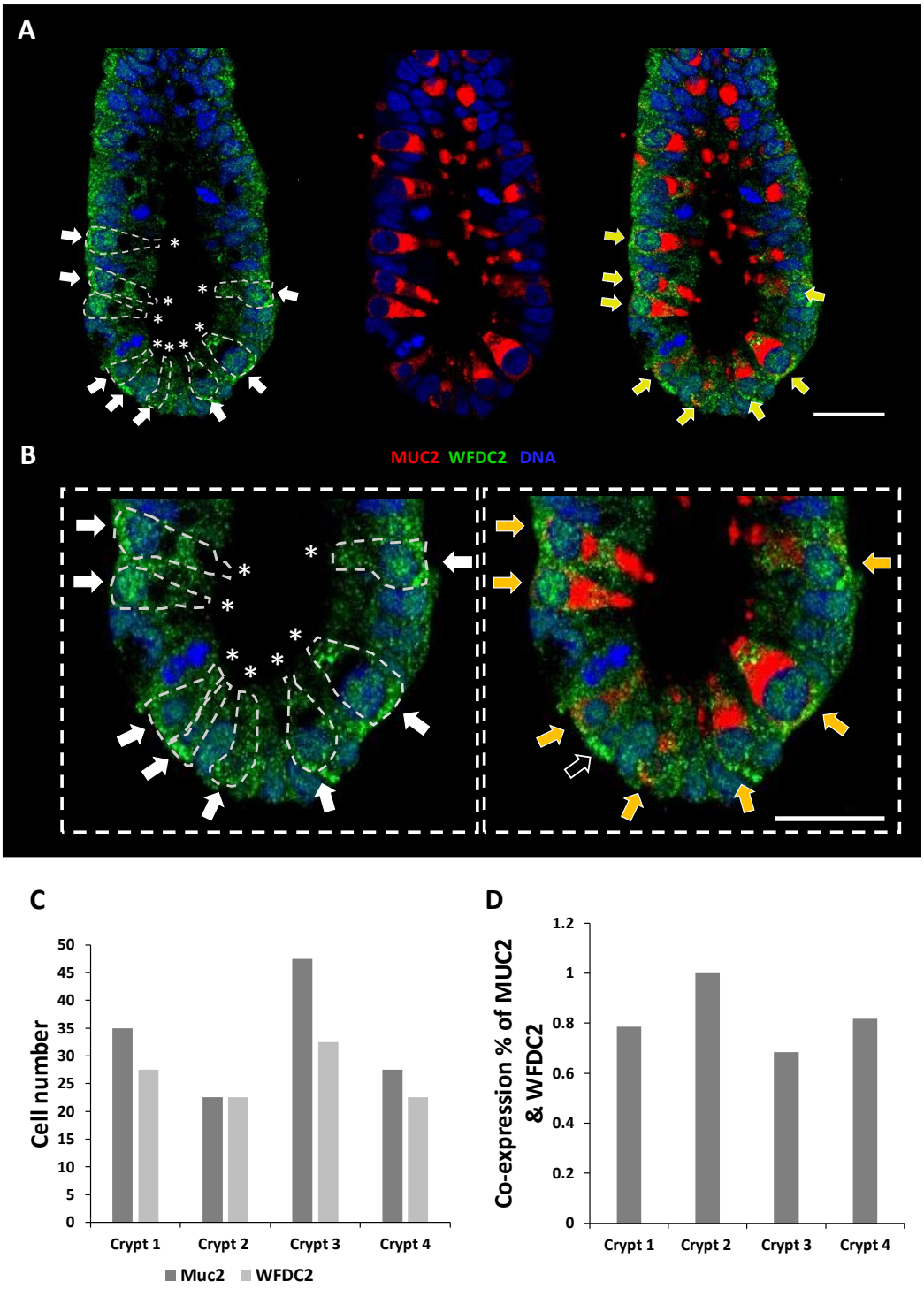

Figure 4.6. WFDC2 expression in isolated colonic crypts. (**A**&**B**) Representative confocal images showing WFDC2 (green), MUC2 (red) and nuclear dye (DNA) labelling in isolated human colonic

crypts. (**A**) The left-hand image shows expression of WFDC2 in cells at the base of the crypt marked with white arrows. The cell shape is outlined with white dashes. Middle image shows distribution of MUC2 labelled goblet cells. The right-hand image shows merged MUC2 and WFDC2 labelling. Yellow arrows indicate co-labelling of both markers. Scale bar 25 μm. (**B**) High magnification left image shows that WFDC2 labelling is evident in both the basal pole (as marked by white arrows) and apical pole (in cells marked with the asterisk). Right image shows overlapping labelling of MUC2 and WFDC2. Yellow arrows indicate $MUC2^+$ goblet cells co-labelling with WFDC2. Empty arrows show $WFCD^+/MUC2^-$ cells. Scale bar 25 μm. (**C**) Bar chart shows number of $MUC2^+$ and $WFDC2^+$ cells present in the base of colonic crypts (N=4). (**D**) Bar chart shows the percentage of co-expression of $MUC2^+$ and $WFDC2^+$ cells at the base of colonic crypts (N=4).

4.2.2 Characterisation of fluid secretion markers in colonic crypts

Fluid secretion is a physiological mechanism of the colonic epithelium used together with mucus secretion to flush the lumen of noxious substances. Regulation of fluid secretion in the colon is orchestrated by the uptake of Cl^- across the basal membrane by the NKCC1 co-transporter and secretion of Cl^- (or HCO_3^-) by the CFTR channel (Frizzell and Hanrahan, 2012). Immunolabelling and fluorescence microscopy demonstrated that NKCC1 was expressed predominantly in the base and supra-base regions of crypts and progressively diminished along the crypt axis (**Figure 4.7A Middle**). $MUC2^+$ goblet cells were shown to be positive for $NKCC1^+$ cells (**Figure 4.7A Right**), as were neighbouring enterocytes. High magnification images revealed the labelling of NKCC1 to be present in the baso-lateral membranes of the epithelial cells (**Figure 4.7B Middle**). Conversely, CFTR

expression was found predominantly in the apical membrane of cells located in the lower half of the crypt **(Figure 4.8 Middle**) and co-expressed with some MUC2^{+} goblet cells (**Figure 4.8 Right**).

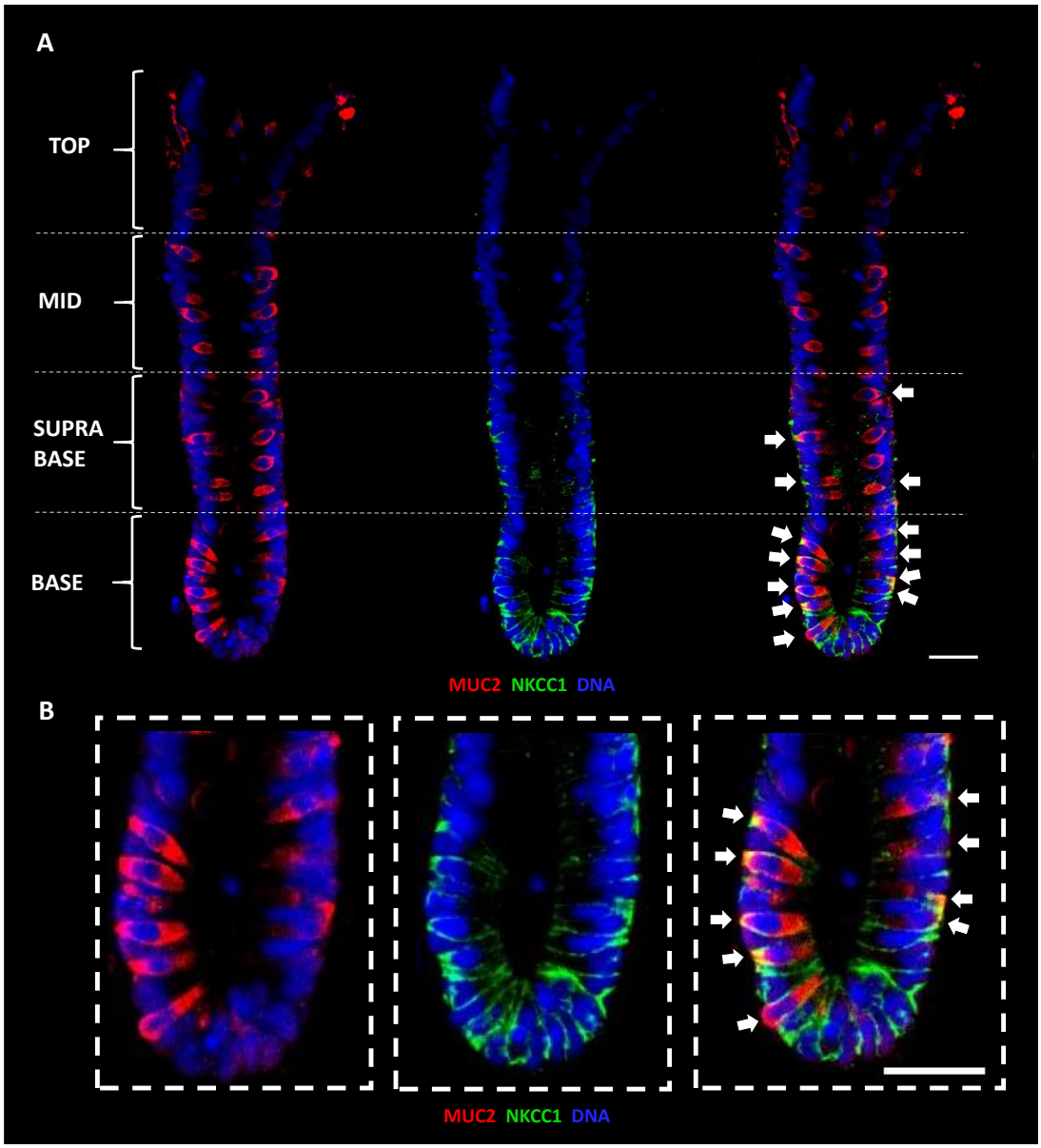

Figure 4.7. NKCC1 expression in isolated colonic crypts. Representative confocal images showing NKCC1 (green), MUC2 (red) and nuclear dye Sytox blue (DNA) labelling in isolated human colonic crypts. (**A**) Left-hand image shows goblet cells labelled with MUC2 present across the entire crypt-axis. Middle image shows expression of NKCC1 is prominent in the base and supra base regions but weak and absent in the mid and top regions. Right-hand image depicts merging of NKCC1 and MUC2 markers. Arrowheads shows expression of NKCC1 overlaps with the majority of MUC2^{+} goblet cells and neighbouring cells. (**B**) Middle image represents baso-lateral labelling pattern of NKCC1 on high magnification crypt base images. Arrow heads in the right image represent co-expression of NKCC1 and MUC2 located in the majority of goblet cells. Scale bar 25 µm.

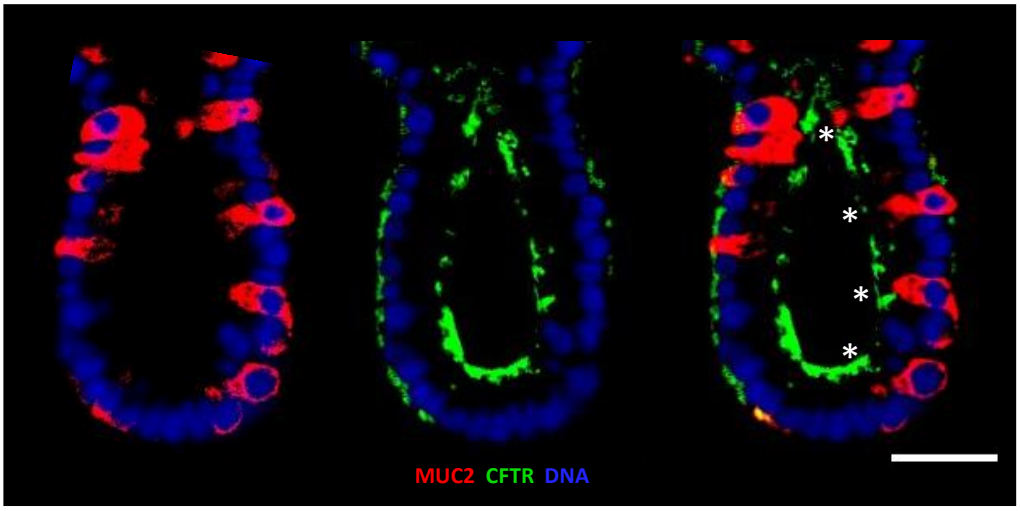

Figure 4.8. CFTR expression in isolated colonic crypts. Left-hand image shows presence of MUC2^{+} cells (red) in the base of the crypt. Middle image shows distribution of CFTR labelling (green) to be predominant in the apical membrane of cells at the base of the crypt. Right-hand figure shows merged image of MUC2 and CFTR. Asterisk marks co-expressions of both markers to be present in some goblet cells. Scale bar 25 µm.

4.2.3 CCh-induces rapid mucus secretion

Goblet cells are known to secrete mucus upon activation of muscarinic receptors with ACh (Specian and Neutra, 1980; Halm and Halm, 2000), however the temporal characteristics of the response in the base of colonic crypts have yet to be described. In order to determine the kinetics of mucus secretion in goblet cells, a mucus depletion assay developed by Stappenbeck and colleagues was adopted (Patel et al., 2013). Isolated colonic crypts were stimulated with CCh for 5, 15 and 30 minutes and then fixed and labelled with antibodies for MUC2 (red) and ECAD (green), and nuclei stained with Sytox blue (blue). Mucus secretion was assessed by measuring the cytoplasmic fluorescence intensity of MUC2 immunolabelling at the different time points including T=0 minutes. While the level of intracellular mucus content at the base of the crypt was relatively constant with respect to time, goblet cells were found to be more depleted of their mucus content after stimulation with CCh. In addition, acutely stimulated crypts exhibited concomitantly more content of secreted MUC2 in the lumen (**Figure 4.9**). Normalised MUC2 fluorescence intensity inside the cytoplasm of goblet cells revealed that mucus depletion was higher after 5 and 15 minutes stimulation with CCh, where the amount of mucus was approximately 30% lower than in control (**Figure 4.10**). CCh stimulation for 30 minutes was shown to reduce mucus content by less than 15% as compared to control (**Figure 4.10**).

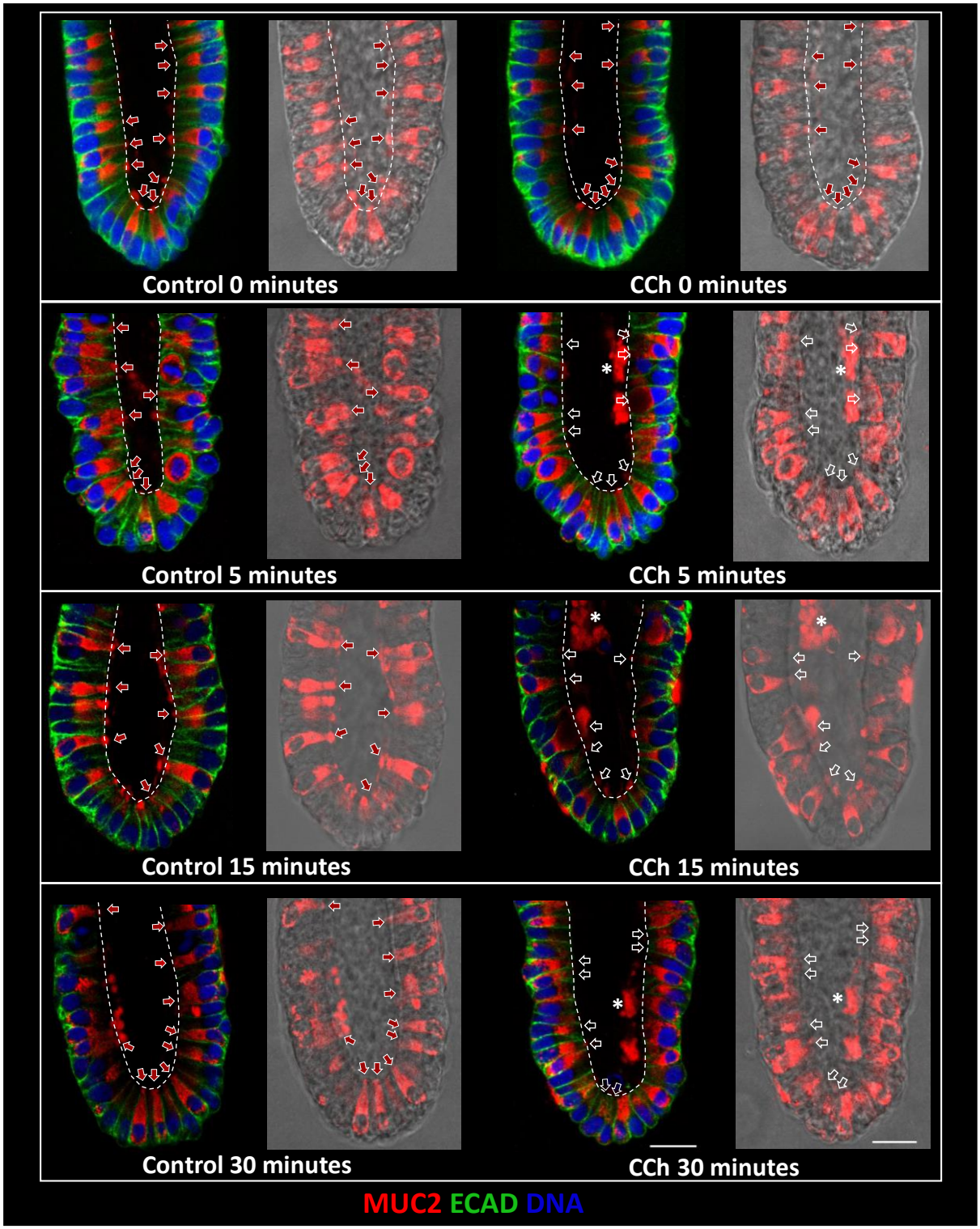

Figure 4.9. Time course analysis of CCh-induced mucus secretion. Representative confocal images of control and CCh (10µM) stimulated colonic crypts at 0, 5, 15 and 30 minutes were labelled with MUC2 (red) and ECAD (green) antibodies and the nucleus stained with Sytox blue. In additon, brigthfield images merged with MUC2 reveal the cytoplasmic mucus content of goblet cells. Red filled arrow heads mark full goblet cells whereas empty arrow heads mark goblet cells with lower

mucus content. Asterisks indicate presence of secreted luminal mucus. Dash lines mark crypt lumen. Scale bar 20 µm.

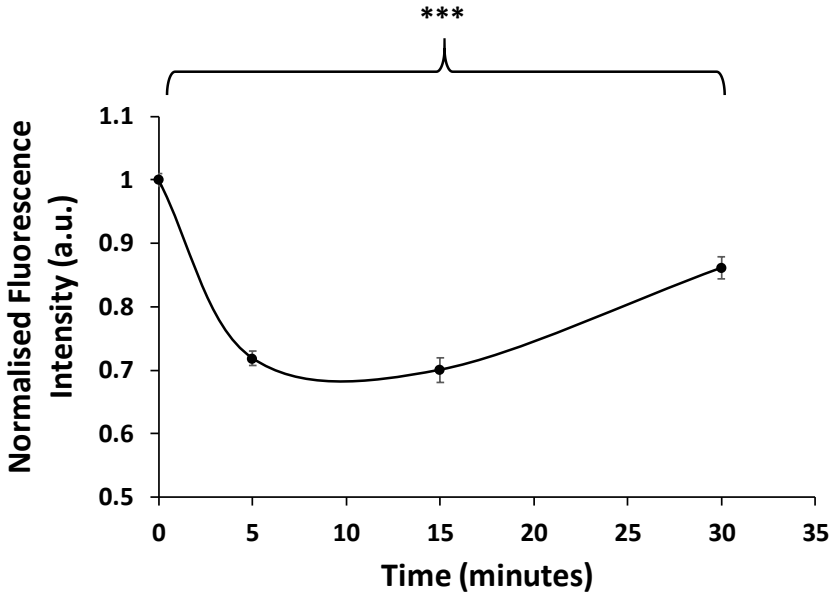

Figure 4.10. Time course fluorescence intensity analysis. The scatter plot represents the time course fluorescence intensity normalised to control. Results show maximum decrease in MUC2 fluorescence intenisty in crypts stimulated with CCh (10 µM) after 5 and 15 minutes as compared to control, followed by a increase in fluoresecence at 30 minutes (2≤N≤4 subjects, n>30 rypts, n_gc>400 goblet cells, ***P<0.001 w.r.t T=0).

4.2.4 Muscarinic-induced calcium signalling originates in goblet and stem cells of the base of human colonic crypts

Previous work done in the Williams lab has demonstrated that calcium signals induced by muscarinic activation originate at the base of colonic crypts and then propagate up the crypt-axis (Reynolds et al., 2007), however it is not clear in which cells this signal is first activated. In order to investigate the cells-of-origin of colonic crypt calcium signals, day 1 cultured human colonic organoids were first loaded with Fluo-4 (5 µM) for 2 hours in HBS and live imaged with a confocal microscope. Stimulation with CCh (10 µM) initiated a rapid calcium signal five seconds after addition, that started at the apical pole of 2 distinct cells located at the very base of the crypt-like domain (**Figure 4.11**). The signal propagated to the basal pole of these cells approximately 6 seconds after stimulation and was followed by the sequential activation of calcium signals with the same apicobasal direction in cells neighbouring the cells-of-origin. The signal reached its maximum fluorescence intensity after 30 seconds and followed a slow decay afterwards (**Figure 4.11**).

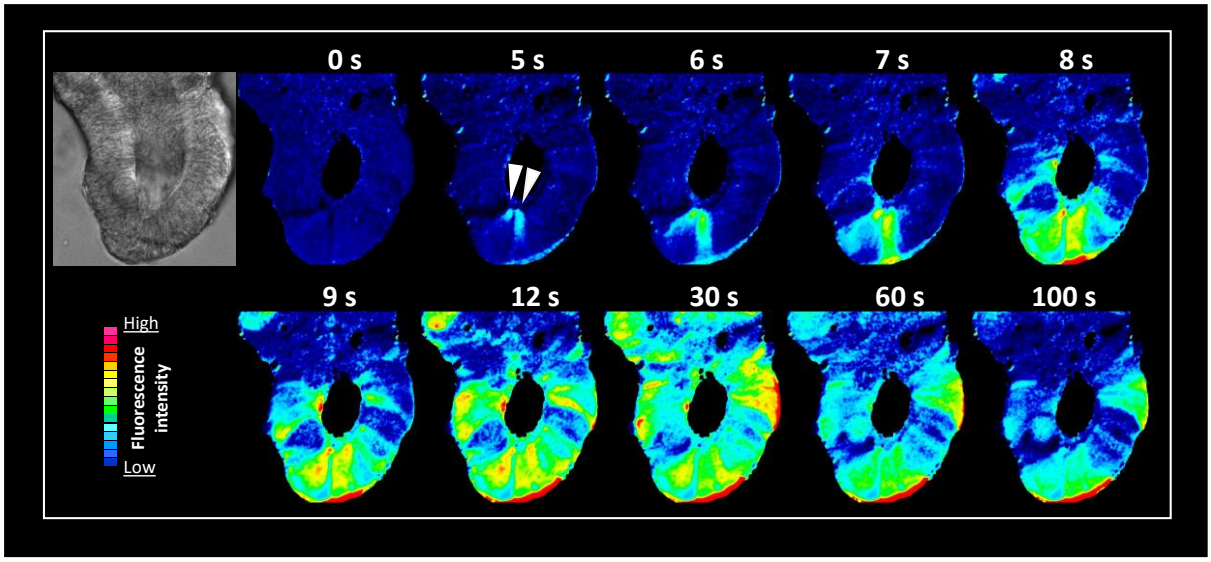

Figure 4.11. Calcium signalling originates at the base of the crypt. Representative confocal series of live images of an organoid loaded with Fluo-4 (5 µM) after stimulation with CCh (10 µM). Calcium signals start in the apical pole of two distinct cells at the base of the crypt (marked with arrow heads) and spread to the basal side to then propagate up the crypt-axis. Calcium signals developed rapidly, reached highest intensity 30 seconds after stimulation and decayed slowly afterwards.

In order to characterise the cell types where the calcium signal had originated, the same crypts were subsequently fixed and labelled with the goblet cell marker MUC2 (red), the stem cell marker OLFM4 (green), the membrane marker ECAD (white) and the nuclear stain Sytox blue and further imaged on the confocal microscope. 'Landmarks' such as two dividing mitotic nuclei were used to register the corresponding image planes for the 'live' and 'post-fixed' image series. Based on the location of goblet and stem cells observed in the immunofluorescence image, the cell types were drawn in the Fluo-4 live imaged organoids and named and numbered by their position with respect to the middle of the base of the crypt (L-left, R-right) (**Figure 4.12A**). The analysis of the immunolabelled cells revealed a position match between two OLFM4 labelled stem cells with the cells where the fluorescence calcium signals had first originated (**Figure 4.12A**). The study of the Fluo-4 live imaged calcium response overlapped with the cell type dashed lines further confirmed the start of the calcium signal in the apical pole of two stem cells, labelled ISC L1 and L3 (**Figure 4.12B**). This event is followed one second after, by the start of the calcium signal in the goblet cell L2 located in between stem cells L1 and L3.

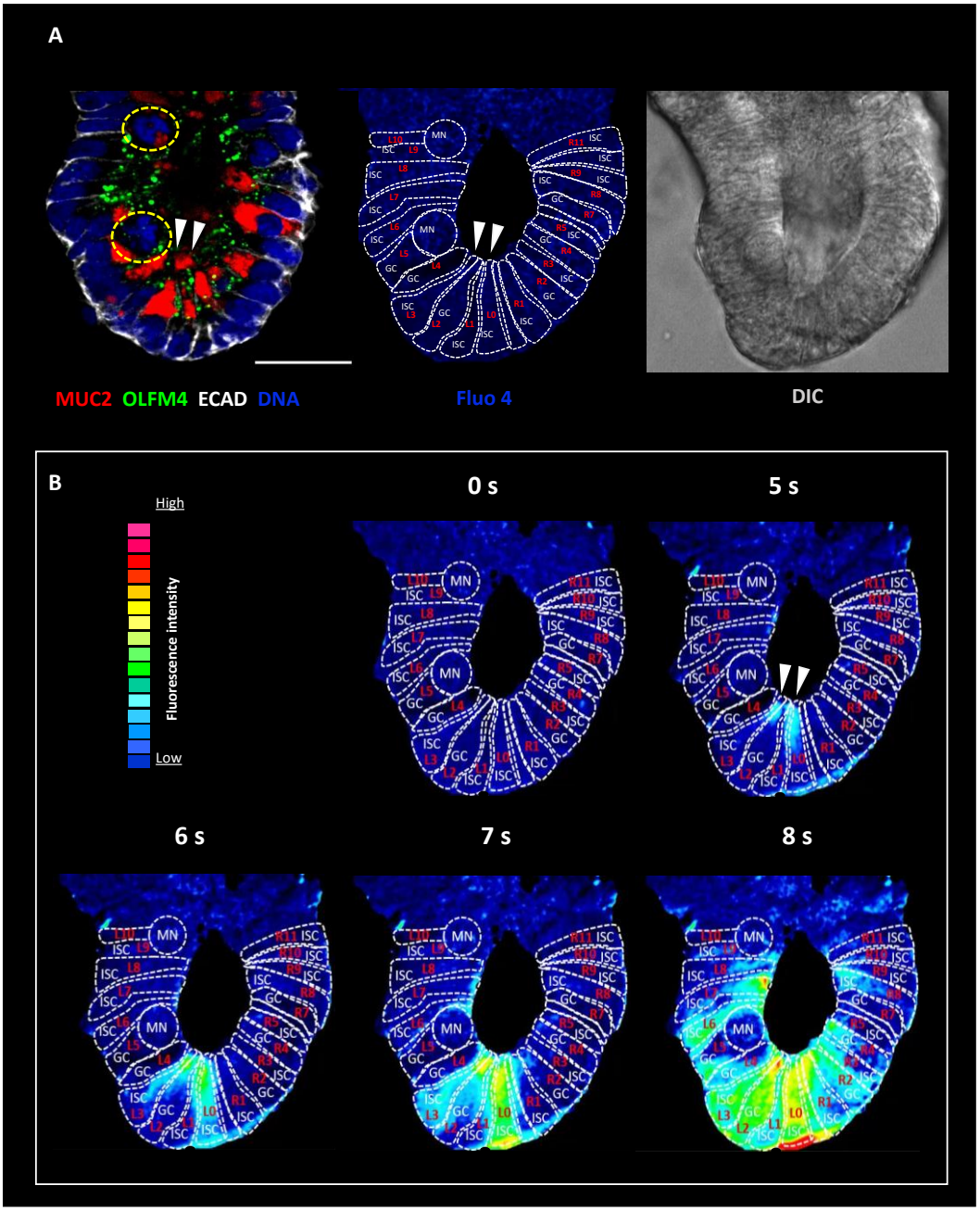

Figure 4.12. Calcium signals originate in stem cells. (**A**) On the left, an organoid labelled with stem cell marker OLFM4 (green) and MUC2 (red) reveals the cell type distribution. Arrowheads indicate two OLFM4^{+} stem cells where the calcium signal starts. Yellow dashed circles indicate reference mitotic nuclei. In the middle, the image of a Fluo-4 loaded organoid containing the different cell types drawn with white dashed lines. White arrowheads indicate stem cells. On the right, brightfield image of the organoid. (**B**) Representative confocal series of live images of an organoid loaded with Fluo-4 (5 µM) after stimulation with CCh (10 µM). Calcium signals start in the apical pole of stem cells L1 and L3 marked with white arrowheads and is followed by the initiation of the calcium signal in the goblet cell 'L2' one second after. Scale bar 25 µm.

In order to support these findings, we studied the topology and polarity of the calcium signals in the stem cell niche. For the study of the topology of the signals, ROIs were drawn in the apical pole of cells distributed on the left side of the organoid (L1-L10) and the changes in fluorescence were monitored over time after stimulation with CCh (**Figure 4.13**). The fluorimetric analysis confirmed L1 and L3 stem cells to be the first cells to show an increase in fluorescence intensity, immediately followed by the L2 goblet cell. The response was gradually recorded in the different ROIs located up these cells (**Figure 4.13A**). Finally, in order to study the polarity of the calcium signal, ROIs were drawn in the apical and basal poles of two cells, one located at the bottom of the crypt (L0) and the other up in the stem cell niche (L7). Using a similar approach, the fluorimetric analysis revealed the spatio-temporal characteristics of the calcium signal initiation in the stem cell niche, where the increase in fluorescence was first observed in the apical pole of the L0 cell and two seconds after in the basal pole. The increase in fluorescence in the L7 followed a similar apicobasal order but was delayed for approximately 2-3 seconds compared to L0 (**Figure 4.13B**).

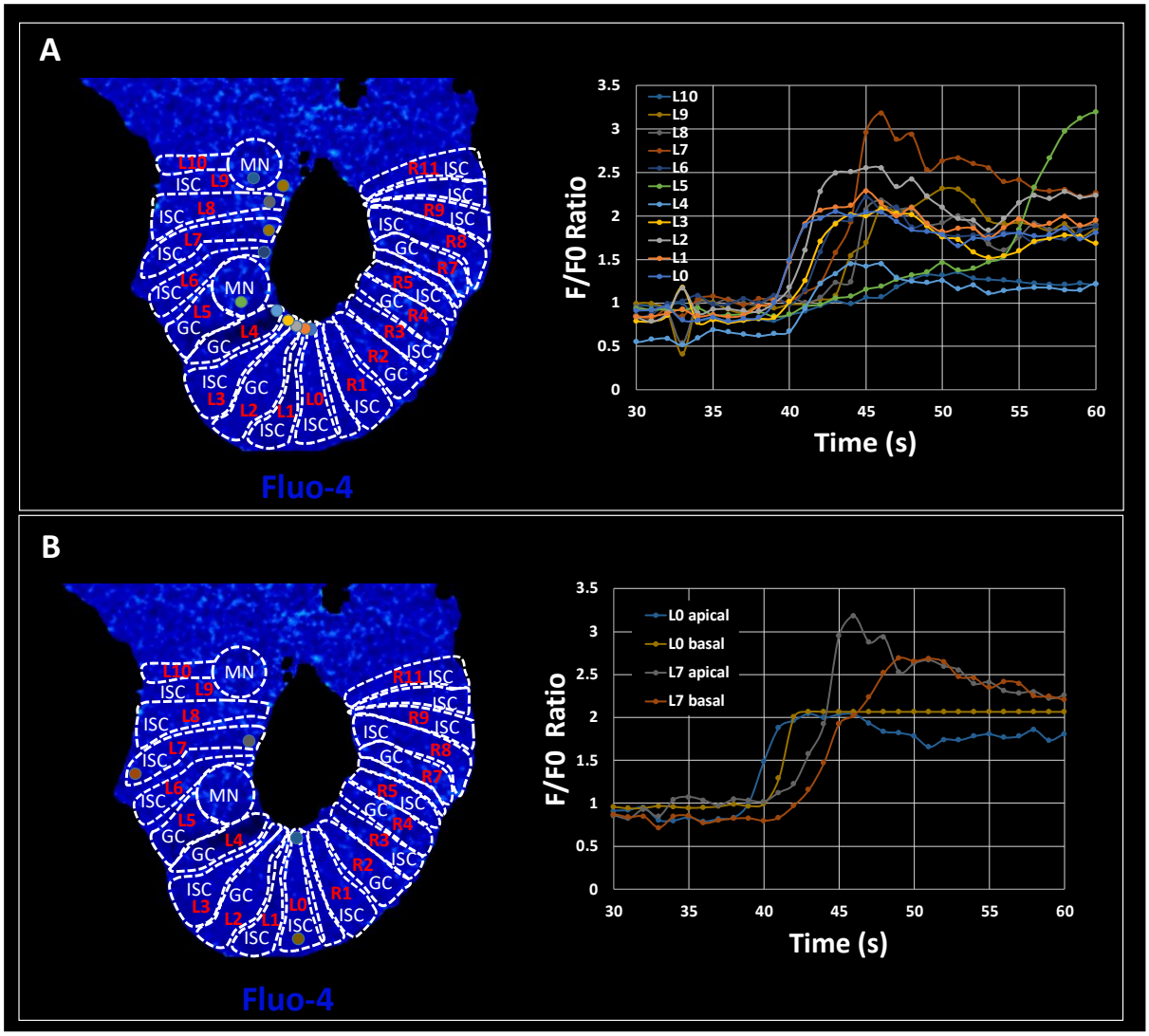

Figure 4.13. Topology and polarity of the calcium crypt signals in the stem cell niche. (**A**) On the left, representative confocal image of a Fluo-4 loaded organoid. Dashed lines indicate cell type. Coloured dots indicate ROIs distributed along the left side of the stem cell niche. On the right, fluorimetric analysis of the topology of the calcium signal. (**B**) On the left, the confocal image of a Fluo-4 loaded organoid with coloured dots indicating ROIs distributed in the apical and basal regions in the cells L0 and L7. On the right, fluorimetric analysis of the polarity of the calcium signal. Data also contributed to by Dr Mark Williams.

4.2.5 Calcium dependent mucus secretion

Mucus secretion has been shown to be dependent on intracellular calcium mobilisation in mouse models (Patel et al., 2013; Birchenough et al., 2016) and in the airway epithelium (Abdullah et al., 1997; Adler, Tuvim, & Dickey, 2013). In order to test this hypothesis in our culture model, isolated human colonic crypts were incubated with the intracellular calcium chelator BAPTA (66 µM) for 1h

prior to stimulation with CCh (10 µM) for 5 minutes. The samples were then fixed and labelled with antibodies for MUC2 and ECAD in order to assess intracellular MUC2 content. Confocal images revealed a decrease in MUC2 immunofluorescence intensity in the cytoplasm of CCh treated crypts whereas samples pre-treated with BAPTA exhibited an increase in MUC2 immunofluorescence (**Figure 4.14A**). Image analysis revealed a decrease in mucus content of approximately 20% after incubation with CCh (10 µM) for 5 minutes as compared to control. However, MUC2 immunofluorescence intensity after pre-incubation with BAPTA (66 µM) was found to be 20% higher than control (**Figure 4.14B**). Stimulation with CCh (10 µM) for 5 minutes in the presence of BAPTA (66 µM) showed no decrease in MUC2 fluorescence intensity as compared to control, and instead revealed an increase in approximately 15%. (**Figure 4.14B**).

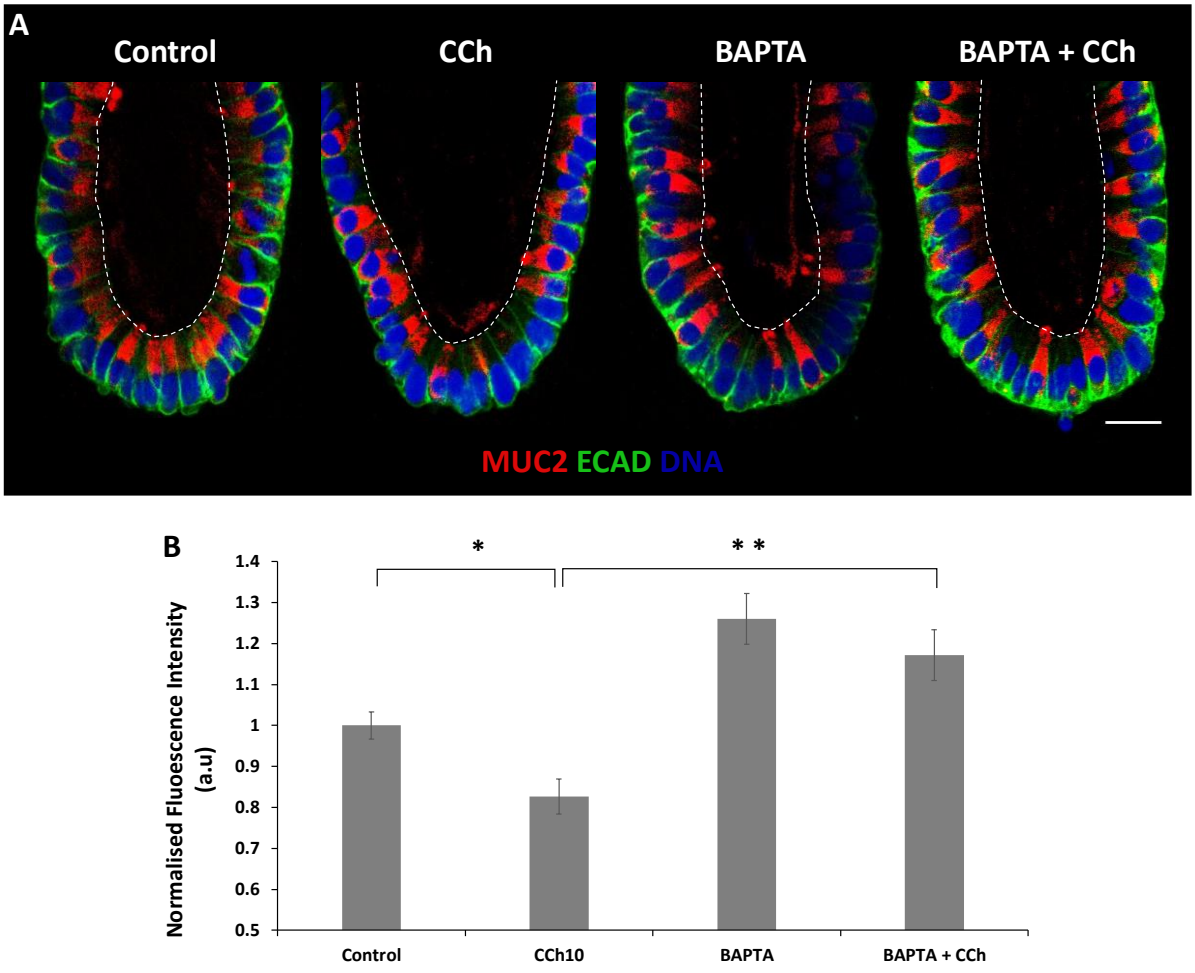

Figure 4.14. The intracellular calcium chelator BAPTA decreases mucus secretion. (**A**) Representative confocal images of the base of colonic crypts labelled with MUC2 (red), ECAD (green) and stained with nuclear dye Sytox blue and stimulated with CCh (10 µM), BAPTA (66 µM) or both CCh and BAPTA. Scale bar 20 µm. (**B**) Bar chart showing a decrease in fluorescence intensity of crypts in samples stimulated with CCh (10 µM) for 5 minutes as compared to control. Pre-incubation with

BAPTA blocks the CCh-induced mucus secretion. Fluorescence intensity was normalised to control (N=1, n≥90, **P<0.01). Data also contributed to by Alvin Lee.

In order to investigate whether an increase in cytoplasmic calcium was sufficient to stimulate cytoplasmic mucus depletion, the levels of intracellular calcium in colonic crypts were elevated by using the ER Calcium-ATPase transporter blocker cyclopiazonic acid (CPA) (20 µM) for 5 minutes. Similar to the previous experiment, colonic crypts were fixed and labelled with MUC2 and ECAD antibodies. Confocal images of the base of the crypts revealed lower quantities of mucus in goblet cells after addition of CCh (10 µM) for 5 minutes as judged by the intensity of the MUC2 antibody in the cytoplasm of goblet cells. Stimulation of colonic crypts with CPA (20 µM) for 5 minutes revealed similar levels of fluorescence intensity to control (**Figure 4.15A**). Quantification of the MUC2 cytoplasmic immunofluorescence intensity in crypts stimulated with CCh showed an approximate reduction of 20% fluorescence intensity while stimulation with CPA for 5 minutes showed similar fluorescence levels to control (**Figure 4.15B**).

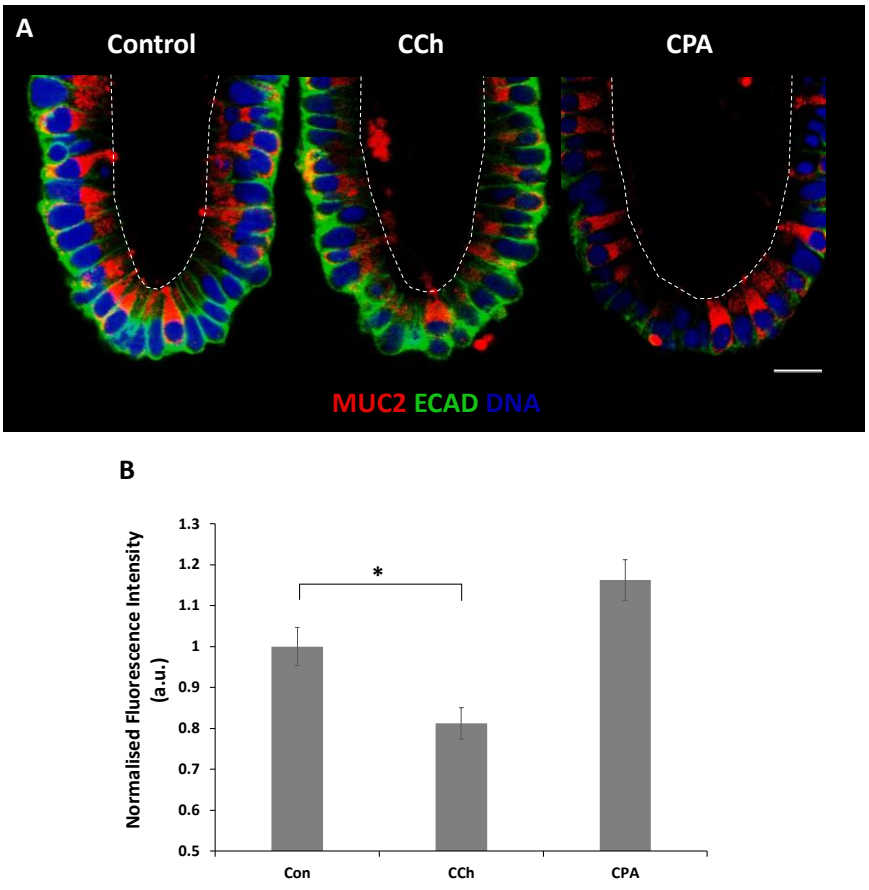

Figure 4.15. CPA-induced elevated intracellular calcium is not sufficient to stimulate mucus secretion. (**A**) Representative confocal images of the base of colonic crypts labelled with MUC2 (red), ECAD (green) and stained with nuclear dye Sytox blue (DNA) and stimulated with CCh (10 µM) and

CPA (20 μM). Scale bar 20 μm. (**B**) Bar chart showing a decrease in fluorescence intensity of crypts stimulated with CCh (10 μM) as compared to control. Fluorescence intensity was normalised to control (N=1, n≥56, *P<0.05). Data also contributed to by Alvin Lee.

4.2.6 Muscarinic-induced mucus secretion is dependent on endolysosomal two-pore channels

Calcium signalling orchestrated by the release of calcium from the endolysosomes has been suggested to regulate key cellular processes like autophagy (Pereira et al., 2011; Gómez-Suaga et al., 2012), receptor trafficking (Song et al., 2012; Grimm et al., 2014; Ruas et al., 2014), exocytosis (Arredouani et al., 2015; Cane et al., 2016; Davis et al., 2012; Hamilton et al., 2018) and has recently been linked to mucus secretion (PhD Christy Kam, PhD Thesis). Using a similar approach as in chapter 3 (**Figure 3.27**) we used the inhibitor of the TPC, Ned19 in order to determine the effects of endolysosomal TPC-mediated calcium release on mucus secretion. Day 1 colonic crypts were stimulated with CCh (10 μM) for 5 minutes, pre-incubated with Ned19 (250 μM) for 2 hours and also stimulated with CCh (10 μM) for 5 minutes in the presence of Ned 19 (250 μM) that had been pre-incubated for 2 hours. Colonic crypts were fixed and labelled with MUC2 and ECAD and the base of the crypt imaged under the confocal microscope. Stimulation with of CCh resulted in depletion of the goblet cell mucus whereas crypts pre-incubated with Ned 19 displayed levels similar to those of control, as revealed by the cytoplasmic intensity of the antibody labelling (**Figure 4.16A**). The measurement of the cytoplasmic MUC2 fluorescence intensity showed a decrease of 20% mucus content after stimulation of CCh when compared to control. Ned19 pre-incubation as well as CCh stimulation of crypts pre-incubated with Ned19 showed no significant differences in mucus content when compared to control (**Figure 4.16B**).

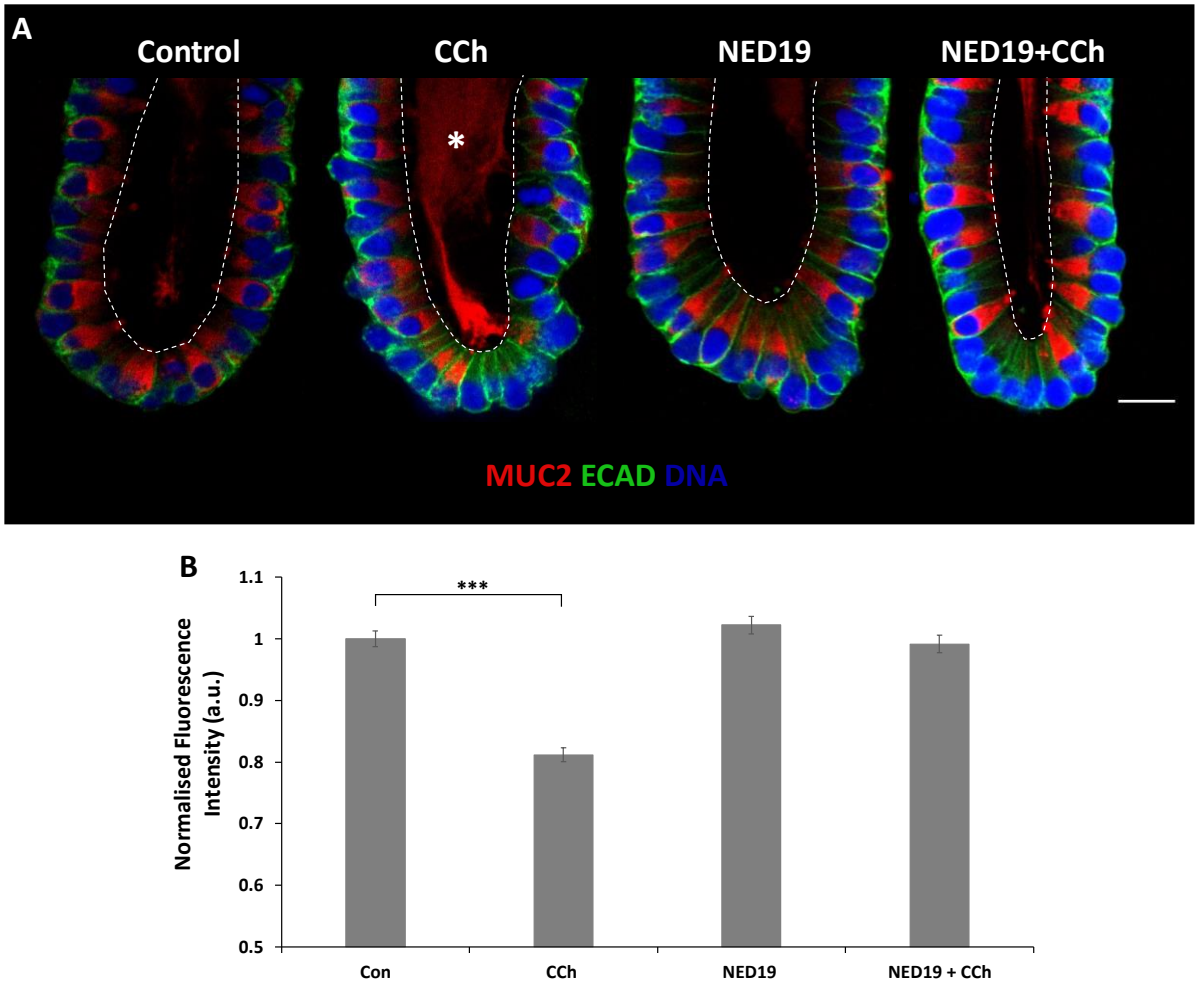

Figure 4.16. Ned19 inhibits mucus secretion in human colonic crypts. (**A**) Representative confocal images of the base of colonic crypts labelled with MUC2 (red) and ECAD (green), stimulated with CCh (10 µM) and treated with Ned19 (250 µM) or both CCh and Ned19. Asterisk signals presence of luminal mucus. Scale bar 20 µm. (**B**) Bar chart demonstrates decrease in fluorescence intensity of crypts stimulated with CCh. Fluorescence intensity of crypts pre-incubated with Ned19 and stimulated with CCh shows similar levels to control. Fluorescence intensity was normalised to control (N=3, n≥972, ***P<0.001). Data also contributed to by Dr. Victoria Jones.

In order to validate our organoid culture system as a complementary tool for assessing mucus depletion of goblet cells, we carried out the same experimental plan on day 1 organoids and analysed the MUC2 fluorescence of crypt-like buds. Similar to the results observed on crypts, confocal imaging of MUC2 labelled organoids treated with CCh (10 µM) for 5 minutes resulted in lower cytoplasmic fluorescence intensity. Organoids pre-incubated with Ned19 (250 µM) for 2 hours and then stimulated with CCh (10 µM) for 5 minutes showed more mucus-filled goblet cells with increased fluorescence intensity (**Figure 4.17A**). In line with the results obtained in crypts, the measurement of cytoplasmic MUC2 immunofluorescence intensity showed a 20% decrease in mucus

content in organoids stimulated with CCh as compared to control. Pre-incubation with Ned19 blocked the secretion of mucus induced by CCh (**Figure 4.17B**).

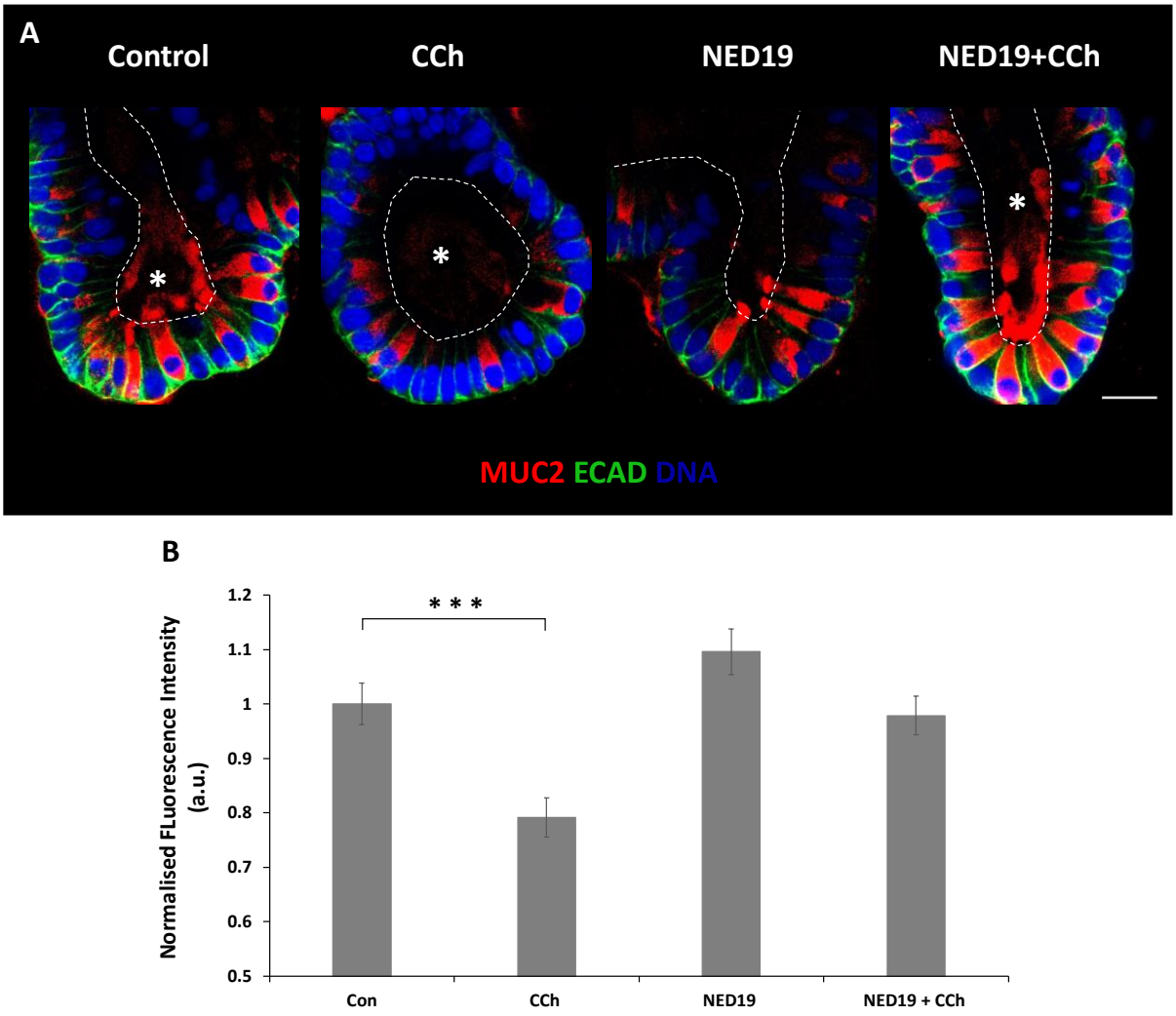

Figure 4.17. Ned19 inhibits mucus secretion in human colonic organoids. (**A**) Representative confocal images of the crypt-like organoid buds labelled with MUC2 (red) and ECAD (green) and treated under different conditions. Asterisks indicate presence of luminal mucus. Scale bar 20 µm. (**B**) Bar chart showing the decrease in immunofluorescence intensity of MUC2 in goblet cells stimulated with CCh. Pre-incubation with Ned19 inhibits the muscarinic-activated mucus secretion. Immunofluorescence intensity was normalised to control (N=2, n≥279, ***P<0.001).

Endolysosomal calcium signalling has been shown to induce global calcium responses via amplification of the signal through calcium-induced calcium release activation of the ER calcium channels IP3R and particularly RyR (Galione, 2011; Ronco et al., 2015). We sought to understand the implications of these channels in muscarinic receptor-induced mucus release from goblet cells. Firstly, we analysed the role of IP3R by using the receptor antagonist 2-APB. Colonic crypts were pre-

incubated with 2-APB (100 µM) for 2 hours and then stimulated with CCh (10 µM) for 5 minutes. The samples were fixed and labelled with MUC2 and ECAD and the base region of the crypts was imaged under the confocal microscope. CCh-stimulated crypt images showed induced release of mucus into the lumen and together with depleted cytoplasm (**Figure 4.18A**). Interestingly, confocal images of CCh stimulated crypts that had been previously incubated with 2-APB revealed similar levels of cytoplasmic immunofluorescence labelling as the CCh-only group (**Figure 4.18A**). Quantification of the immunofluorescence intensity in the cytoplasm of goblet cells stimulated with CCh showed a decrease in 20% mucus content as compared to control (**Figure 4.18B**). Incubation with 2-APB had no significant effect as compared to control, whereas addition of CCh to 2-APB pre-incubated crypts showed a reduction in MUC2 immunofluorescence intensity comparable to the effect of CCh alone (**Figure 4.18B**).

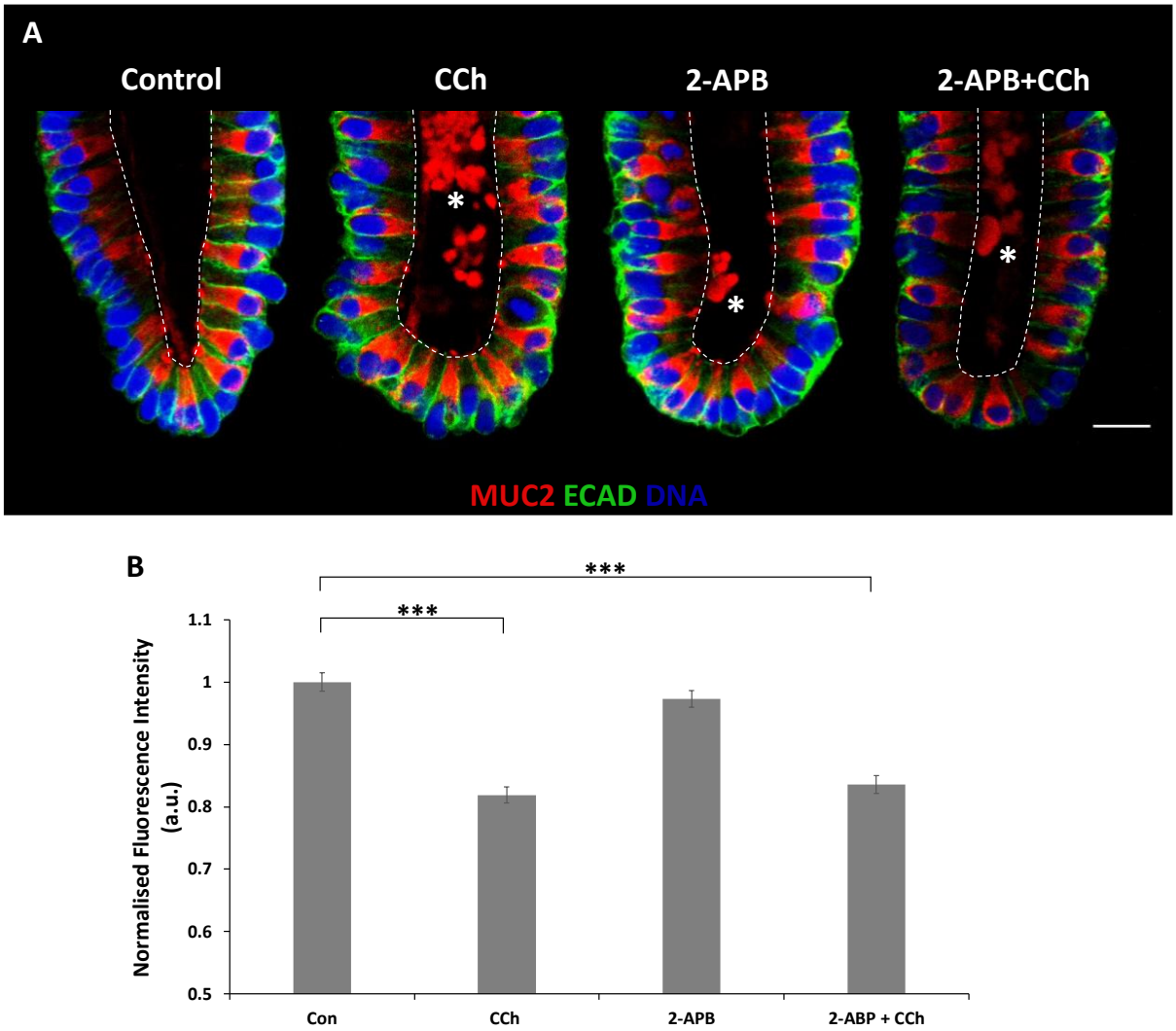

Figure 4.18. Effects of 2-APB in mucus secretion. (**A**) Representative confocal images of colonic crypt bases labelled with MUC2 (red), ECAD (green) treated under different conditions. Asterisks indicate

presence of luminal mucus. Scale bar 20 µm. (**B**) Bar chart showing a mild decrease in MUC2 immunofluorescence intensity of crypts treated with 2-APB (100 µM) and a bigger decrease in immunofluorescence intensity of crypts pre-incubated with 2-APB and stimulated with CCh (10 µM) similar to stimulation with CCh alone. Immunofluorescence intensity was normalised to control (N=3, n≥992, ***P<0.001). Data also contributed to by Dr. Victoria Jones.

We next tried to determine the role of RyRs in muscarinic-mediated mucus release. To do so, we utilised the inhibitor of RyRs, Dantrolene (Zhao, Li et al., 2001) by pre-incubating crypts at a concentration of 10 µM for 2 hours and analysed goblet cell MUC2 depletion in the presence of CCh (10 µM). Similar to previous experiments, colonic crypts were processed for immunofluorescence and imaged under the confocal microscope. CCh stimulated crypts showed lower content of mucus in the majority of goblet cells, whereas crypts stimulated with CCh in the presence of Dantrolene showed similar levels of cytoplasmic mucus content as compared to control (**Figure 4.19A**). The analysis of the goblet cell immunofluorescence intensity revealed a strong depletion of approximately 50% of mucus content in CCh treated crypts as compared to control, however Dantrolene pre-incubated crypts showed similar levels of immunofluorescence intensity to control when stimulated with CCh (**Figure 4.19B**). Similar results were obtained in the presence of another blocker of RyRs, Procaine (1mM) under similar experimental conditions (data not shown).

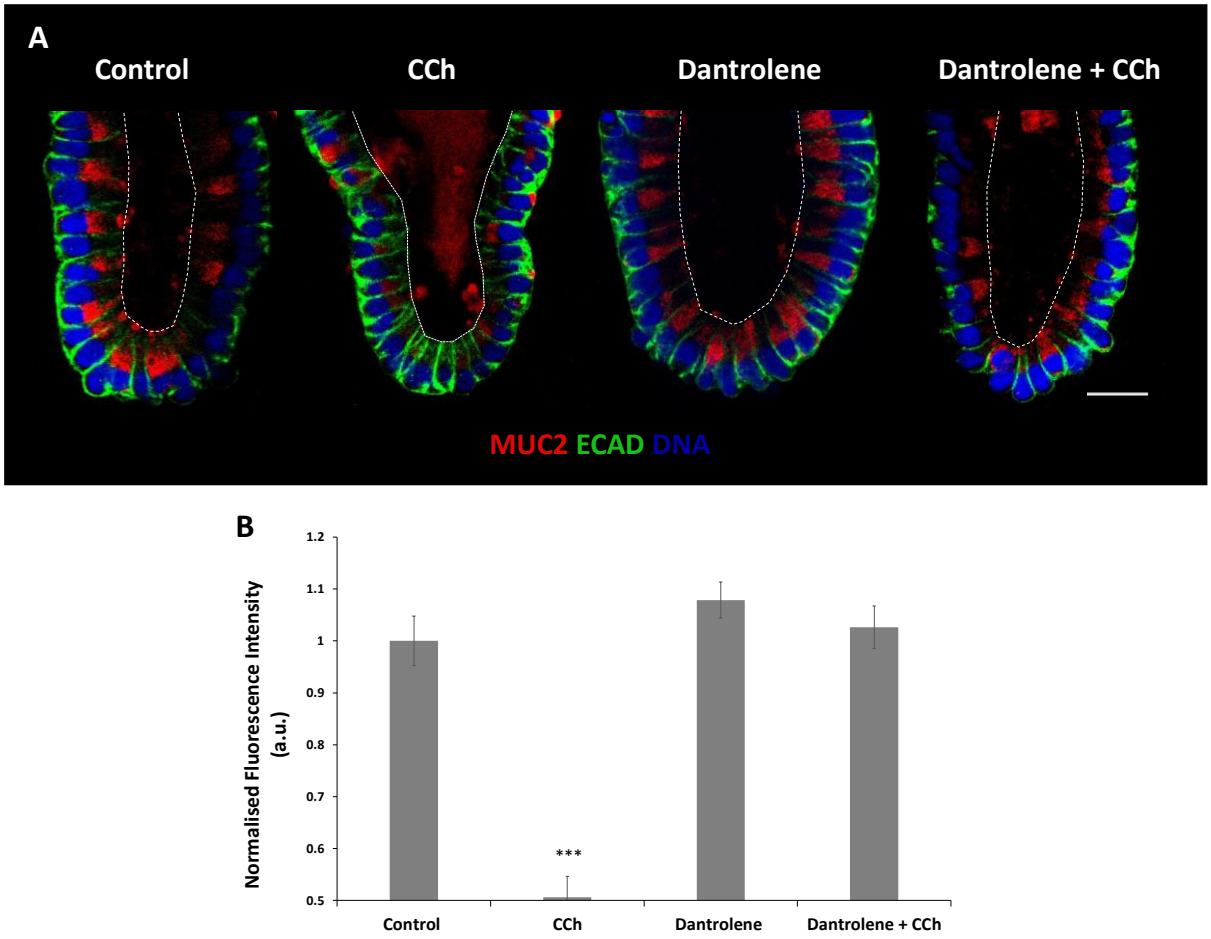

Figure 4.19. Dantrolene blocks mucus depletion. (**A**) Illustrative confocal images of colonic crypt bases labelled with MUC2 (red), ECAD (green) and stained with nuclear dye stimulated with CCh (10 µM), Dantrolene (10 µM) or both CCh and Dantrolene. Asterisks indicate presence of luminal mucus. Dashed lines mark lumen. Scale bar 20 µm. (**B**) Bar chart showing CCh induced goblet cell depletion which is blocked by the presence of Dantrolene (N=1, n≥122, ***P<0.001). Data also contributed to by Alvin Lee.

4.2.7 Muscarinic-induced fluid secretion is dependent on endolysosomal two-pore channels

Epithelial cell fluid secretion is driven by epithelial chloride transport. In the gut, this process is regulated by NKCC1 and the K^+ channel in the basal membrane to allow influx of Cl^-, Na^+, and K^+ and efflux of K^+ respectively. In the apical membrane, the coordinated action of the CFTR channel and the TMEM16A Cl^- channel allow for the efflux of Cl^- and HCO_3^- and Cl^- respectively into the lumen which is followed by water through osmosis (Frizzell and Hanrahan, 2012). Importantly, NKCC1 activation in colonic epithelial cells has been shown to be dependent on intracellular calcium signals (Reynolds et al., 2007). In addition, the release of HCO_3^- and a functional epithelial chloride transport has been

shown to be crucial for generating the ideal conditions for mucus to hydrate and unfold in the lumen. In the gut, fluid secretion into the lumen causes swelling of colonic crypts. In order to understand the role of calcium signalling in fluid secretion, colonic organoids were analysed for changes in the luminal cross-sectional area following stimulation or inhibition of intracellular calcium signalling during the course of 2 hours. Imaging of organoids using time lapse microscopy revealed that addition of CCh (10 µM) for 2 hours notably increased the luminal volume as compared to the homeostatic state (**Figure 4.20A**). Inhibition of the TPCs with Ned19 in the absence and presence of CCh did not show major morphological changes (**Figure 4.20A**). Measurement of the luminal area of the organoids at T=0 and T=2 hours, showed that stimulation with CCh (10 µM) induced more than a 20% increase in luminal volume as compared to control, whereas organoids pre-incubated with Ned19 showed no blocking of the CCh-induced organoids swelling(**Figure 4.20B**). These results were confirmed in organoids pre-incubated with another TPC inhibitor, Tetrandrine (20 µM) for 2 hours (data not shown).

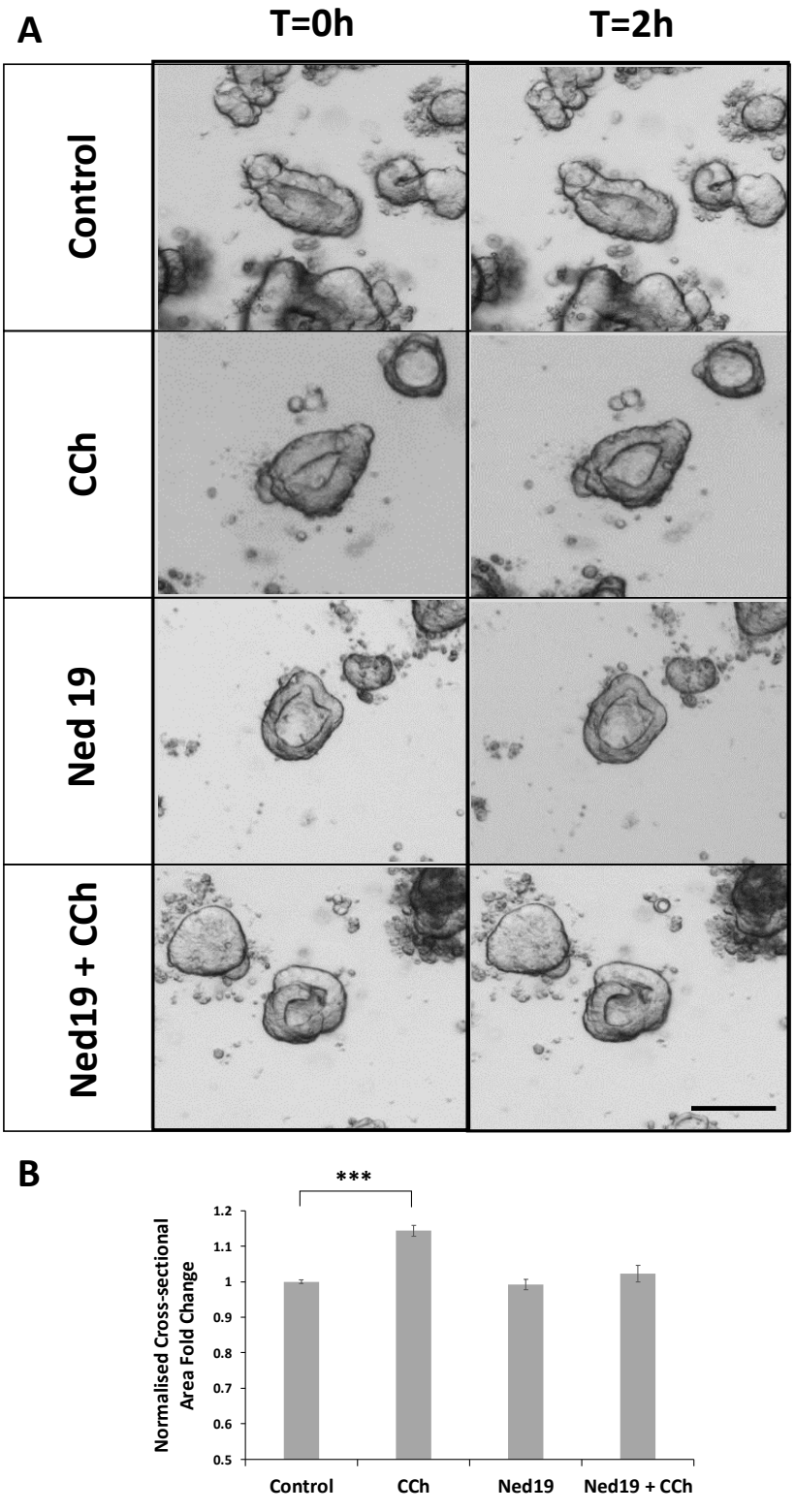

Figure 4.20. CCh-induced organoid swelling is calcium dependent. (**A**) Representative high magnification time lapse images of organoids at T=0 and T=2h under control conditions, stimulation with CCh (10 µM), incubation with Ned19 (500 µM) and stimulation with CCh (10 µM) after incubation with Ned19 (500 µM). Scale bar 100 µm (**B**) Bar chart representing the increase luminal area of organoids stimulated with CCh (10 µm) compared to control, Ned19 (500 µm) and Ned19

and CCh. Luminal area was normalised to control and displayed as mean ±SEM (N=2, n≥40, ***P<0.001). Data also contributed to by Sean Tattan.

4.2.8 Labelling of intracellular mucus globules and its secretion

Intracellular vesicle trafficking and exocytosis can be monitored by using special lipophilic dyes to label cell membranes. Because mucus is stored in globules bounded by a double lipid layer originating from the plasma membrane, we tried to localise these subcellular organelles in goblet cells of colonic crypts and track their movements by using the lipid dye FM-143 FX. In order to use this dye in our culture system, colonic crypts were stained overnight with the dye and fixed on day 1 of culture. Crypts were imaged under confocal microscopy and the FM dye immunofluorescence was recorded using the 488 nm excitation laser and visualised in green pseudo-colour. The lipid labelling showed immunofluorescence to be particularly intense in numerous cells along the base of the crypt (**Figure 4.21A**). High magnification images of these cells revealed the presence of fluorescent hot spots located around the perinuclear region but predominantly intense and numerous in the cytoplasm (**Figure 4.21B**).

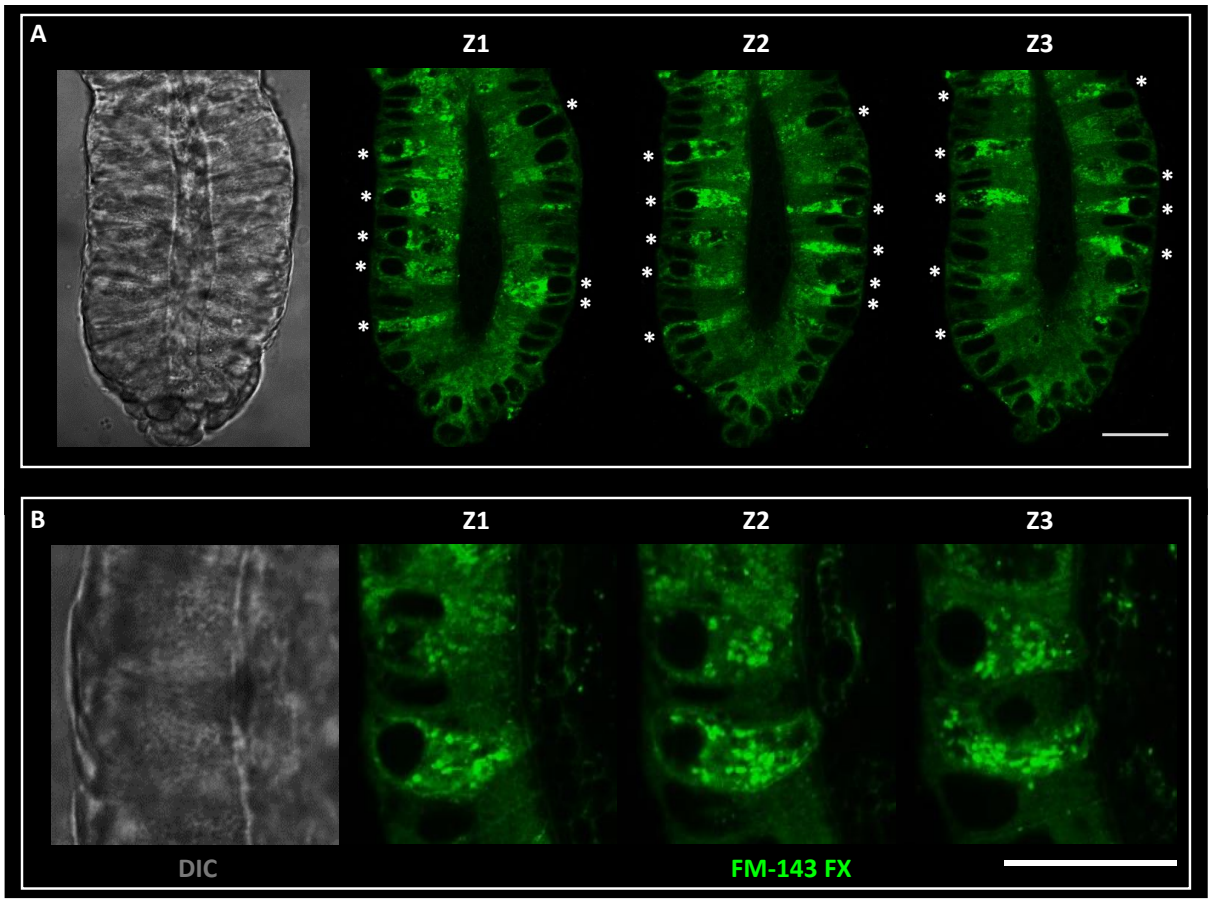

Figure 4.21. Labelling of intracellular globules in goblet cells. (**A**) Representative confocal z stacks of images of the base of colonic crypts labelled with FM-143 FX (green) reveal labelling of intracellular vesicles is more prominent in a particular subset of cells. Scale bar 25 µm. (**B**) High magnification images of FM-143 FX-labelled cells at the base of colonic crypts reveal perinuclear location of vesicles but prominent presence in the cytoplasm. DIC images show presence of intracellular globules similar of those in goblet cells. Scale bar 25 µm.

With the aim to understand how this vesicle trafficking and exocytosis is orchestrated in goblet cells, day one colonic crypts were incubated overnight with FM-143 FX (green) and stimulated with CCh (10 µM) in order to induce mucus secretion. Live confocal recording of the base of the crypt monitored the effect of the secretagogue in the goblet cells during a 5 minutes stimulation period. Because goblet cells contain multiple intracellular MUC2 granules that can be labelled with the lipophilic dye, they could be identified by the strongest immunofluorescence intensity as compared to their neighbouring epithelial cells. CCh stimulation revealed the induction of exocytosis and could be appreciated by the increase in size of the apical membrane of the cell which could be easily visualised in the last minute of stimulation (**Figure 4.22**). The increase in size of the apical membrane eventually forms a sphere that retains the FM-143 FX label and it is secreted into the lumen.

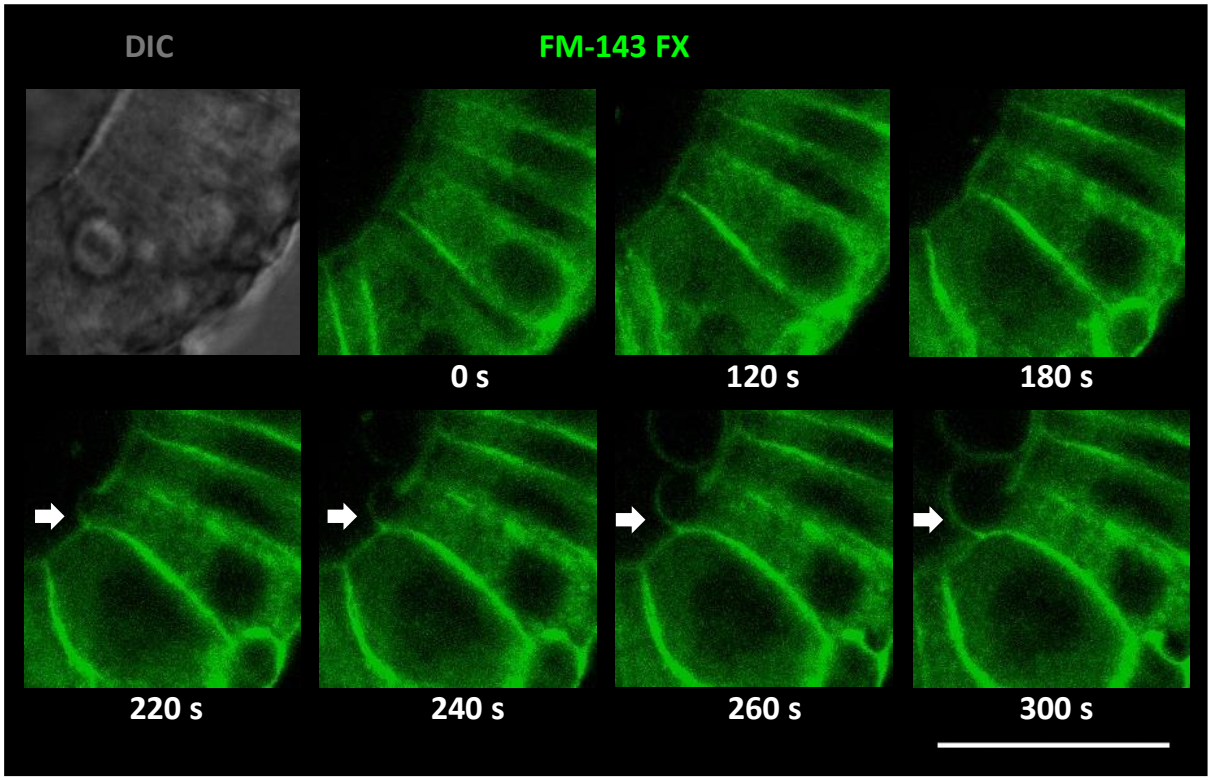

Figure 4.22. CCh induces mucus exocytosis. Representative confocal time series images of live microscopy of the base of colonic crypts labelled overnight with FM-143 FX (green) and stimulated with CCh (10 µM) for 300 seconds (5 minutes). High resolution images of goblet cells reveal the formation of a sphere on the apical membrane over time which starts to form 220 seconds (3.6 minutes) after addition of CCh. Reduction in cytoplasmic volume becomes apparent towards the end of the recording. Scale bar 25 µm.

Having established the methodology for live monitoring goblet cell granule formation we decided to study the effect of CCh stimulation of colonic crypts using FM-143FX labelled crypts to analyse the response of the cells located in the crypt base. As previously described, colonic crypts were incubated with the lipophilic dye overnight and live imaged under the confocal microscope. Stimulation with CCh (10 µM) resulted in the formation of globules in the apical membrane of goblet cells, identified by the presence of multiple intracellular vesicles, that became apparent 6 minutes after treatment (**Figure 4.23**). The globules increased in size and were released into the lumen 12 minutes after stimulation. Moreover, live labelling of cell membranes allowed us to monitor the changes in luminal size, which expanded following muscarinic stimulation-induced fluid secretion. In addition, we could examine the effects crypt base flushing by means of fluid and mucus secretion on the luminal content, using a labelled luminal particle as a reference. Stimulation with CCh seems to induce an influx of fluid into the lumen directed towards the base in the first 5-6 minutes of the

response, as judged by the sinking of the particle over time. However, coinciding with the starting granule formation and fluid secretion, the particle starts to migrate upwards (**Figure 4.23**).

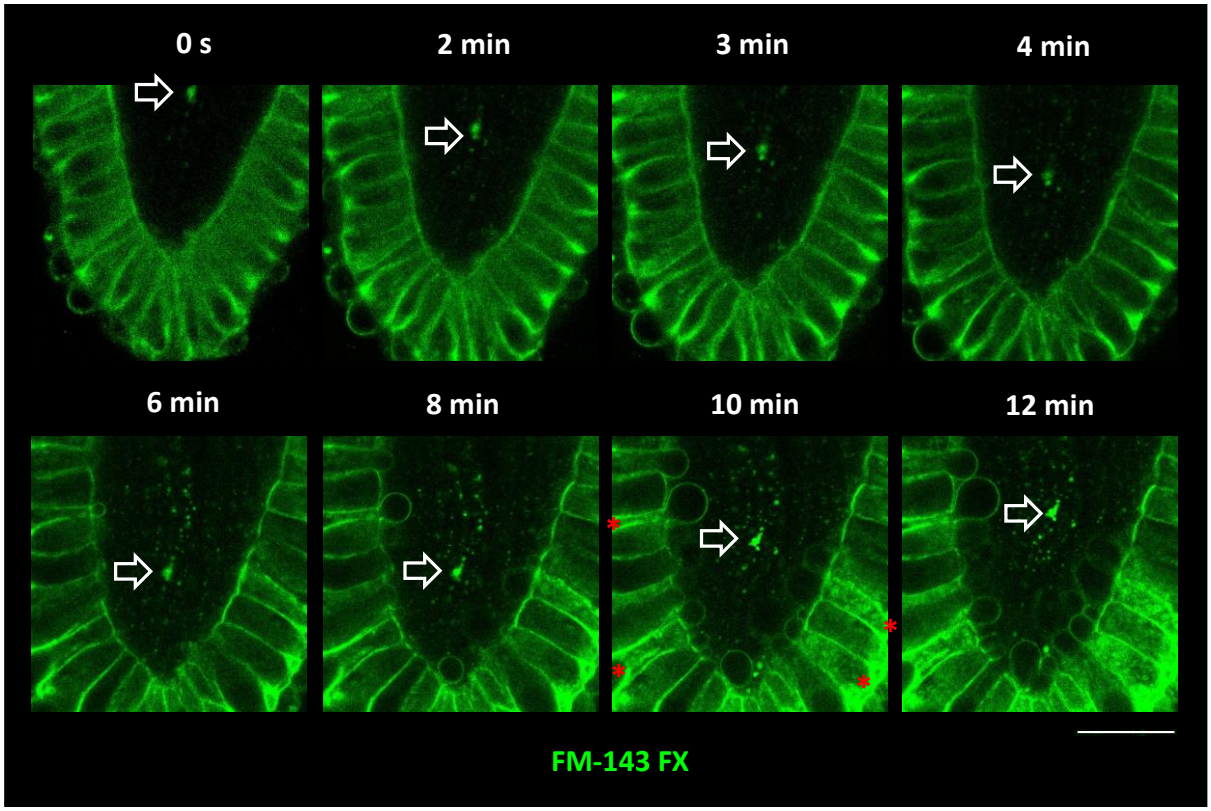

Figure 4.23. CCh stimulation induces granule formation and exocytosis as well as and fluid secretion. Representative time-lapse confocal images of FM-143FX live labelled colonic crypts stimulated with CCh (10 µM). White arrow indicates position of the luminal labelled particle over time. Red asterisks indicate presence of goblet cells. Scale bar 25 µm.

In order to confirm that mucus is present in the globules secreted into the lumen, we decided to live image FM-143FX-labelled granule secretion and post-fix it with MUC2 antibody to study their co-expression. As described before, FM-143FX labelled crypts were stimulated with CCh (10 µM) and the response was live imaged under the confocal microscope. Colonic crypts were shown to form and release globules into the lumen, visible in the brightfield too (**Figure 4.24**). Next, crypts were immediately fixed and immunolabelled with MUC2 antibody. Subsequent confocal imaging revealed the presence of $MUC2^+$ cells that co-localised with the FM-143FX-labelled goblet cells observed during live labelling. In addition, $MUC2^+$ mucus was found in the lumen, in the same location as the secreted FM-143FX-labelled globules observed during the live imaging (**Figure 4.24**).

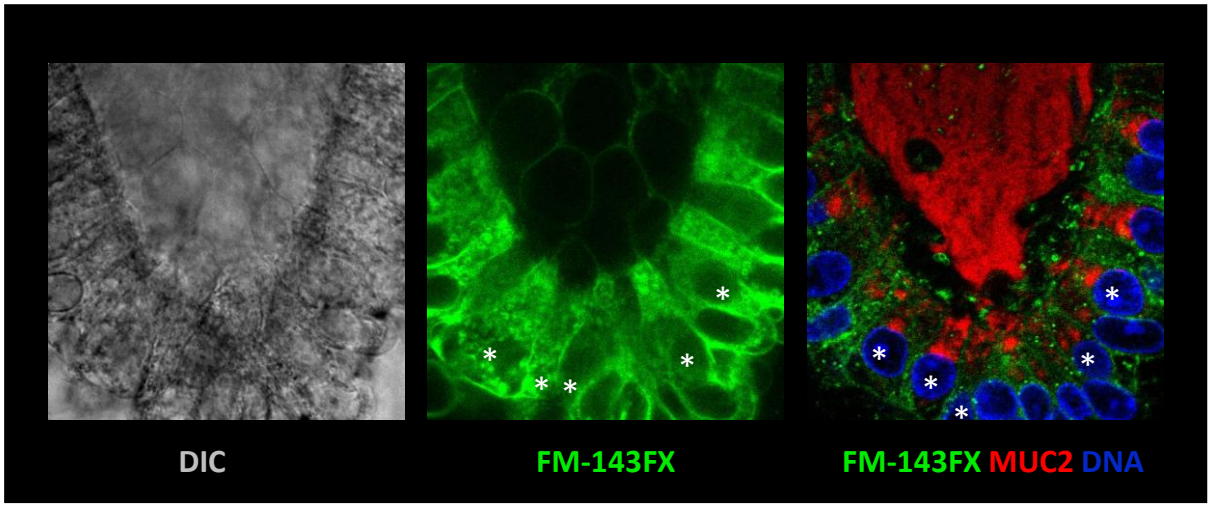

Figure 4.24. Mucus is contained within FM-143FX-labelled globules. Representative confocal images of a CCh stimulated colonic crypt. Left image represents brightfield displaying luminal globules. Middle image represents luminal presence of FM-143FX-labelled globules. Right image represents post-fix crypt displaying FM-143FX (green), MUC2 (red) and nuclear stain. White asterisks represent co-localisation of goblet cells.

4.2.9 Morphological characterisation of mucus compound exocytosis

The possibility of labelling mucus secretion in goblet cells of fixed colonic crypts allows for the characterisation of the mechanism of compound exocytosis. With the aim of capturing the different stages of mucus secretion, day 1 cultured crypts were fixed and labelled with MUC2 (red), ECAD (green) and nuclei stained with Sytox blue (DNA) and subsequently imaged using confocal microscopy. The study of different crypts revealed the changes in morphology of the goblet cells that lead to compound exocytosis. Cells that have not received a secretory stimulus were shown to retain all the mucus content (**Figure 4.25i**), whereas cells that have been activated to secrete their content, mobilise the mucus globules to the apical pole of the cell pushing the plasma membrane (**Figure 4.25ii**). Compound exocytosis continues with the fusion of the mucus granules to the membrane and the release of mucus into the lumen (**Figures 4.25iii and iv**) and finalises with the emptying of the cytoplasmic mucus content (**Figure 4.25v**).

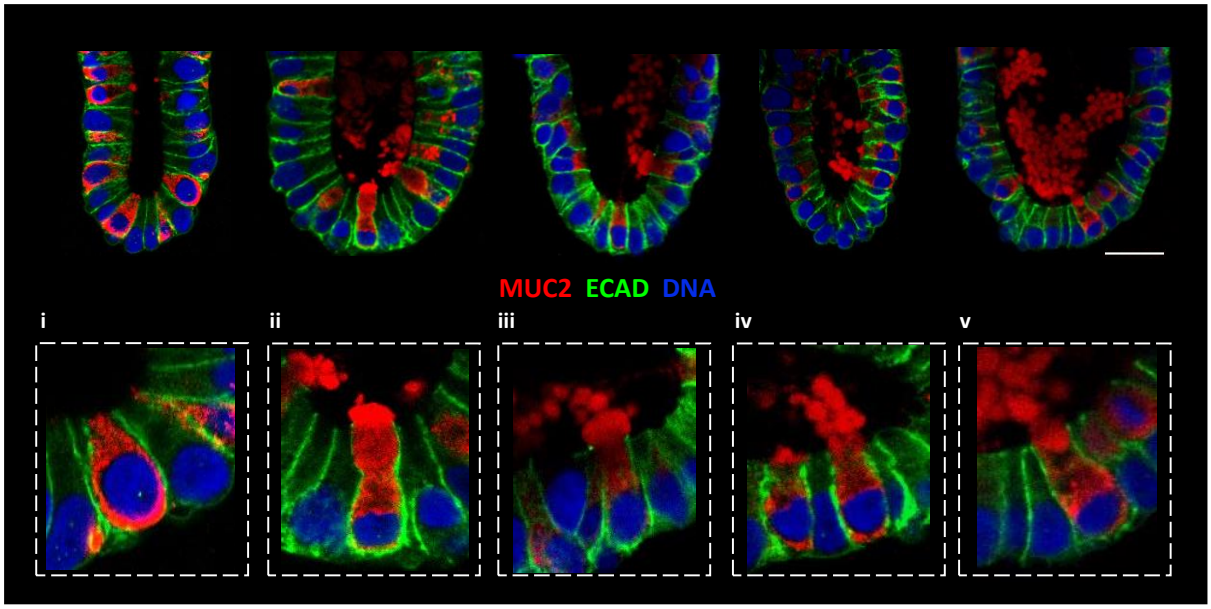

Figure 4.25. Labelling of mucus compound exocytosis in goblet cells. Representative images of the base of colonic crypts labelled with MUC2 (red) and ECAD (green) and nuclear stain Sytox blue (DNA). Withe dashed lines (i-v) represent high magnification images of the different stages of mucus compound exocytosis in goblet cells. Scale bar 25 µm.

4.3 Discussion

The results in this chapter demonstrate a role for muscarinic receptor activation in stimulating intestinal mucus and fluid secretion. Two-pore channels are proposed to be responsible for triggering muscarinic receptor-induced calcium release from endolysosomes in intestinal stem cells located at the base of human colonic crypts. A role for calcium in coupling muscarinic receptor activation to stimulation of mucus secretion and fluid secretion is also demonstrated in human colonic organoids. Cholinergic calcium signals initiate in stem cells located at the crypt base and propagate to neighbouring goblet cells and to other cell types throughout the stem cell niche and the entire crypt-axis. Buffering of intracellular calcium with BAPTA inhibits the CCh-mediated mucus secretion, while inhibition of TPCs and RyRs also block muscarinergic-coupled mucus depletion and fluid secretion suggesting a requirement for cross-coupling of intracellular calcium stores. These observations imply that goblet cells in the stem cell niche play a vital role in guarding adjacent intestinal stem cells against noxious luminal agents and organisms. Cholinergic-coupled mucus secretion by guardian goblet cells is accompanied by calcium stimulated secretion of fluid, which flushes the crypt lumen with hydrated mucus to help preserve the sterility of the stem cell niche and contribute to the maintenance of the epithelial barrier.

4.3.1 Characterisation of goblet cell markers in human colon

In this chapter we studied the presence and location of different markers to identify goblet cell subpopulations as well as to characterise markers important for fluid and mucus secretion. We compared the number and distribution of goblet cells across a series of models including native human colonic mucosal tissue sections, cultured human colonic crypts and colonic organoids, and single intestinal epithelial cells. Fluorescence imaging of immunolabelled native tissue sections, isolated crypts and organoids showed MUC2 labelled goblet cells to be distributed in high numbers along the entire crypts-axis (**Figure 4.2A,B,C**) which was consistent with what has been previously reported in the literature (Greco et al., 1967; Matsuo et al., 1997; Reynolds et al., 2013). MUC2 immunolabelling in crypts and organoids revealed some goblet cells to be empty of mucus as well as showing the presence of the mucin in the adjacent lumen. This result demonstrated that both models were suitable for the study of mucus secretion by measuring the MUC2 content of goblet cells by means of antibody fluorescence intensity measurement. In addition, we showed that single cells can also be labelled with MUC2 (**Figure 4.2D**). This result opens the possibility of studying the status of mucus secretion in goblet cells in the absence of neighbouring signals as well as a potentially enabling fluorescence activated cell sorting (FACS) of goblet cells.

The human colonic epithelium has been suggested to present a heterogeneous population of goblet cells that vary in functions depending on the location along the crypt's axis. Deep secretory cells are goblet cells that populate the base of the crypt and are thought to regulate the biology of the stem cells they are interspersed with. These goblet cells have been suggested to express the REG4 protein marker in mouse colon (Sasaki et al., 2016). We show that in isolated human colonic crypts REG4 positive cells co-labelled with MUC2 positive cells not only at the crypt-base, but also along the entire crypts-axis (**Figure 4.3**). This result suggest that the expression of this protein is not restricted to the base of the crypts in humans and hence implies that in our near-native model, REG4 cannot be considered an ideal marker of a subpopulation of goblet cells at the base of the crypt. Single cell transcriptomics of human colonic crypts has recently revealed the existence of a subpopulation of goblet cells residing at the base crypts that express the antimicrobial protein WFDC2 (Parikh et al., 2019). However, the presence of this marker in isolated cultured crypts had not been assessed to our knowledge. In this study we demonstrate that WFDC2 is present at the protein level in goblet cells since all WFDC2 positive cells were found to express MUC2 as well. By analysing its distribution along the crypt-axis we confirm that the expression is high in the base and suprabase regions and decreases towards the top of the crypt (**Figure 4.4**). These findings correlate with the results previously described by Parikh et al. In addition, we also confirm the presence of WFDC2 in the base region of isolated colonic crypts where it is co-expressed with most of the $MUC2^+$ goblet cells. However, the labelling pattern of the marker was different compared to native colon sections, being expressed mostly in the basal pole and to a lesser extend in the cytoplasm (**Figure 4.5**). This expression pattern suggests the antimicrobial protein can be secreted basally and apically, which is consistent with the results reported by Parikh et al. These researchers also demonstrated that WFDC2 expression was lower during inflammation in ulcerative colitis. This finding makes WFDC2 a potential marker for ulcerative colitis and with the use of our culture models it opens the possibility to study its effects in health and disease.

Previous studies reported the importance of the ion transporters NKCC1 and CFTR in mediating fluid and mucus secretion in the colon epithelium (Reynolds et al., 2007; Gustafsson et al., 2012, 2014). In near-native colonic crypts we first show by immunofluorescence that NKCC1 is located in basolateral membranes of crypt epithelial cells, including goblet cells, and that its expression is prominent in the base and suprabase regions of colonic crypts and diminishes further up the crypt-axis (**Figure 4.6**). These results are consistent with the expression patterns previously demonstrated by Reynolds and colleagues (Reynolds et al., 2007). We further confirm the expression of CFTR on the apical membrane of epithelial cells in the base of the crypt (**Figure 4.7**), which is in line with the literature that describes CFTR to regulate secretion of Cl^- and HCO_3^- from the apical membrane into the colon

lumen (Geibel, 2004). Co-expression with MUC2 labelled cells was found in a subset of goblet cells which could indicate the presence of a subpopulation of CFTR expressing goblet cells. In order to confirm whether CFTR is expressed in a subpopulation of goblet cells, single cell RNA sequence of colonic crypt cells could help profile and map the cellular diversity, as it has been shown for other goblet cell markers like WFDC2 (Parikh et al., 2019). The finding of NKCC1 and CFTR membrane presence supports the existence of transepithelial ion transport activity on epithelial colonic cells and reinforces the importance of fluid and mucus secretion on the stem cell niche.

4.3.2 Muscarinic mediated mucus secretion in the colon

In the absence of cholinergic stimulation, crypt goblet cells secrete mucin at a slow baseline rate (Phillips, 1992). Upon cholinergic stimulation, goblet cells are activated to rapidly accelerate their release of mucin by compound exocytosis. Previous *in vivo* results in rat suggest that mucus secretion in colonic goblet cells induced by muscarinic activation is higher at 5 minutes (Phillips, 1992) and CCh stimulation of human and monkey colonic explants revealed that the mucus granule release is maximum at a half time of 3.3 minutes (Halm and Halm, 2000). However, the temporal characteristics of the mucus production and secretion in goblet cells located at the base of the crypt have not been studied in a human primary cell culture model. Our time course results show that CCh (10 µM) stimulation of muscarinic receptors induces mucus secretion that is maximum at 5 and 15 minutes as seen by the presence of cavitation in the cytoplasm of MUC2 labelled goblet cells (**Figure 4.9**). Goblet cells stimulated for a longer period (30 minutes) show a decrease trend in mucus secretion which can be interpreted as a reduction in signal strength to allow restoration of the mucin content by the promotion of the protein production. Mock treated controls showed minimal goblet cell mucus secretion across all time points as seen by the presence of large amounts of mucus in the cytoplasm (**Figure 4.9**). This event is consistent with a baseline mucus secretion process under resting conditions. Stimulation of crypts for 5 and 15 minutes with CCh (10 µM) reduces the cytoplasmic mucus content of goblet cells by approximately 30% as compared to control (**Figure 4.10**) which is comparable to morphological measurements in human colonic explants (Halm and Halm, 2000). Goblet cells stimulated for 30 minutes showed less than 15% decreased in mucus content compared to control (**Figure 4.10**). Taken together, these results suggest that CCh (10 µM) stimulation of muscarinic receptors induces a rapid response that leads to mucus release by compound exocytosis, which is higher after 5 minutes and remains high also 15 after stimulation. We postulate that subsequent to the maximum mucus release, goblet cells undergo a period of recovery time whereby they start to form and accumulate mucus in the cytoplasm which gets full again approximately 30 minutes after (**Figure 4.10**). Importantly, we believe that a rapid secretion of

mucus from the goblet cells in the base of the crypt is critical for ensuring that any potential pathogen gets expelled before threatening the stem cells and it therefore suggests the idea that goblet cells at the base of the crypt are key in guarding of the stem cell niche. Moreover, we validate the culture of isolated human colonic crypts as useful model for the study of mucus turnover.

Recent work by Johansson and colleagues investigated the mechanism of mucus turnover in the mouse colon under homeostatic conditions and showed different dynamics in the goblet cells of the surface epithelium compared to the ones in the base (Johansson, 2012). In order to do so, these researchers labelled the mucin glycoproteins with GalNAz, an analogue of N-Acetylgalactosamine (GalNAc) which is present in mucus and fixed the samples at different time points. Using this novel methodology, Johansson et al. were able to study the mucus dynamics in goblet cells from the production in the Golgi, until the secretion into the lumen. In this thesis we followed the same approach in cultured colonic crypts, although the outcome of the experiment was not successful, perhaps due to lack specificity of GalNAz in our system.

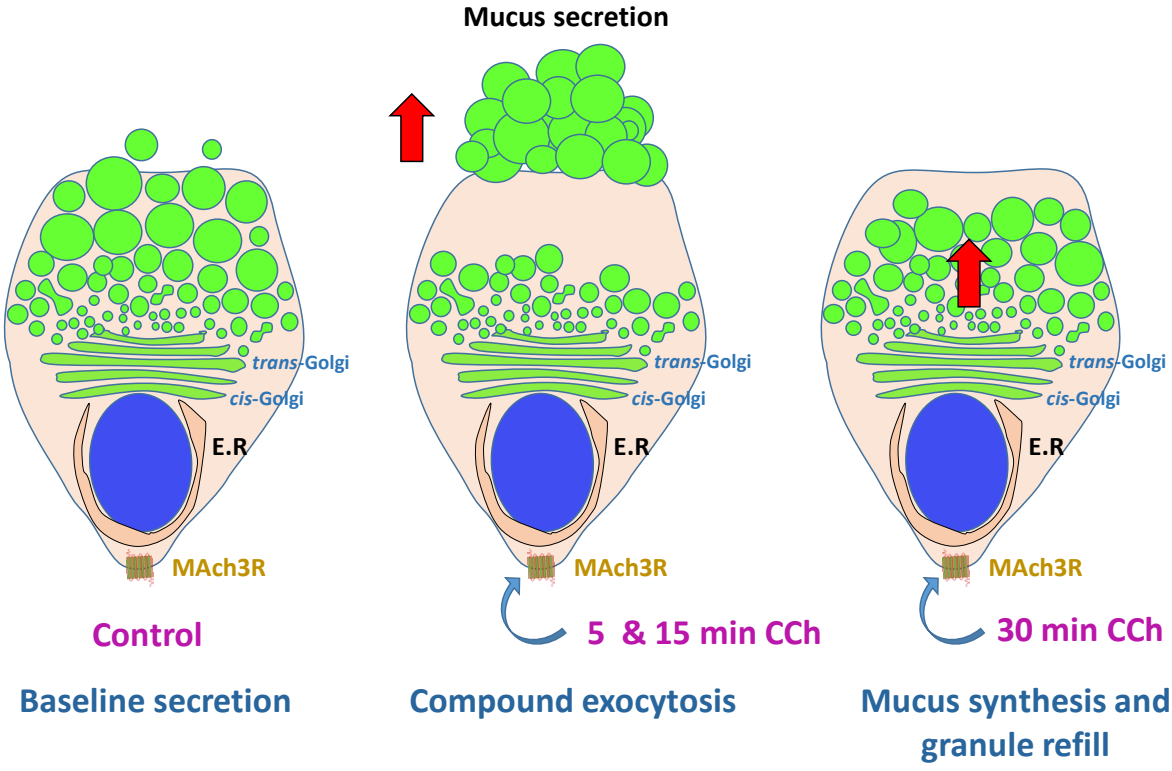

Figure 4.26. Goblet cell mucus turnover. Goblet cells of the human colon secrete minimal mucus under resting conditions. Stimulation of muscarinic receptors with CCh (10 µM) for 5 and 15 minutes induces maximum levels of mucus secretion. The cytoplasm of goblet cells subsequently starts to refill until being full again approximately after 30 minutes post-stimulation.

4.3.3 Calcium-dependent mucus secretion

The second messenger calcium has been shown to induce mucus secretion in mouse colonic explants and organoids (Patel et al., 2013; Birchenough et al., 2016) and it has been also demonstrated to promote mucin release upon stimulation of membrane GPCR receptors in human goblet cells of the airway system (Rossi et al., 2007; Rossi, Sears, & Davis, 2004). In human colorectal cell lines, this process has been shown to be driven by muscarinic activation (Marcon et al., 1990; McCool, Forstner, & Forstner, 1994; Yedgar et al., 1992). However, the role of calcium in the stem cell niche of human colonic crypts and organoids is yet to bed studied. In this chapter, we show that buffering of intracellular calcium with BAPTA (Collatz, Riidel and Brinkmeier, 1997) in isolated colonic crypts abrogates mucus secretion and leads to accumulation of mucin in colonic goblet cells (**Figure 4.14A**). Stimulation with CCh confirmed the role of muscarinic activation in mucus release by emptying 20% of the content of goblet cells compared to control. However, it had a minimal impact on mucus secretion on crypts in which intracellular calcium increases were buffered with BAPTA (**Figure 4.14B**). This result suggests that mucus secretion requires the presence of intracellular calcium, which has been previously shown to be induced by muscarinic activation (Lindqvist et al., 2002). The increase in intracellular calcium can be due to influx from the extracellular fluid via activation of plasma membrane ion channels or by release from intracellular calcium stores. In order to understand which mechanism drives the increase of intracellular calcium coupled to muscarinic activation we decided to deplete the calcium content of ER, the biggest intracellular calcium store, using the SERCA pump inhibitor CPA (Seidler et al., 1989). While stimulation with CCh reduced the content of goblet cell mucus in approximately 20% compared to control, crypts where the ER was emptied with CPA showed mucus levels similar to control (**Figure 4.15**). This observation suggests that the muscarinic activated mucus secretion in the base of the crypt is dependent on the release of calcium from intracellular stores rather than extracellular influx. These results correlate with previous findings from Lindqvist et al. where they demonstrated that ACh induced calcium signals at the base of the crypts depend on the release of calcium from intracellular stores (Lindqvist et al., 2002). Interestingly, incubation of crypts with CPA induced an approximate 10% increase in the mucus content of goblet cells compared to control. A possible explanation could be that an increase in cytoplasmic calcium per se is insufficient to stimulate mucus granule exocytosis. In this scenario, following GPCR activation with CCh, there are other signals in addition to an increase in cytoplasmic calcium that are probably required to stimulate mucus secretion. Moreover, these findings also suggest that calcium release from the ER is not enough to induce mucus release and suggest the existence of other intracellular stores implicated in this process.

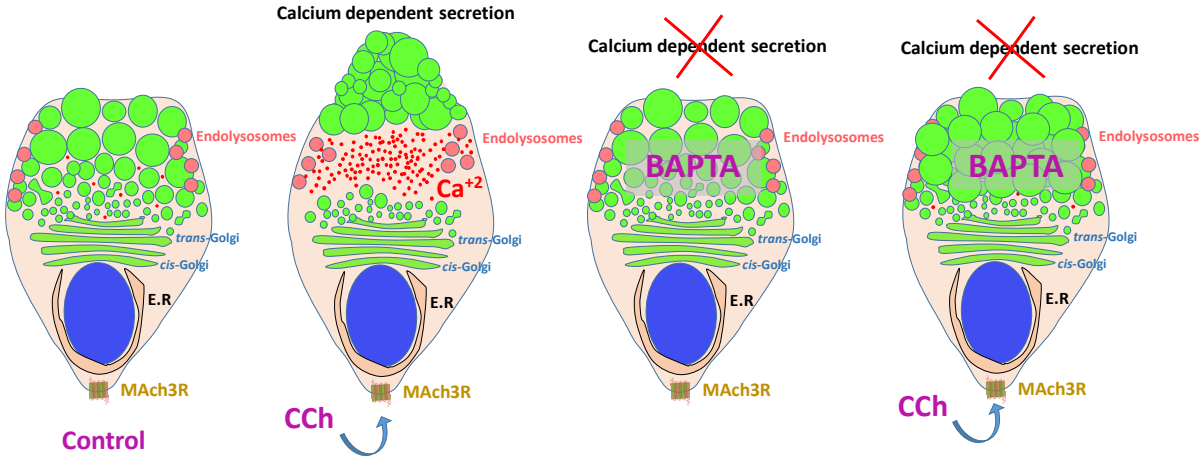

Figure 4.27. Mucus secretion is dependent on intracellular calcium release. Chelation of intracellular calcium with BAPTA inhibits mucus secretion even after muscarinic activation.

Calcium signals have been shown to originate in the base of human colonic crypts (Lindqvist et al., 2002). The exact cells responsible for initiating the calcium signal response have not been yet identified which begs the question as to who is responsible for orchestrating the reaction and amplification of the muscarinic signal, to therefore regulate mucus secretion in the base of the crypt. As shown in **Chapter 3**, the stem cell niche at the base of the crypts is populated mainly by goblet and stem cells. In this chapter we show that using single cell resolution confocal microscopy we were able to capture the calcium signal of crypts loaded with the calcium sensitive dye Fluo-4 in specific cells of the crypt base of colonic organoids. Activation of muscarinic receptors with CCh induced a rapid calcium response which first originated in the apical pole of two single cells at the very base of the crypt and then travelled to the basal pole to be later propagated to the cells above and amplified higher up the crypt (**Figure 4.12**). The topology and polarity characterisation of these calcium signals confirmed these observations (**Figure 4.13**). This result was consistent with the previous evidence obtained with the calcium sensitive dye Fura-2, described in **Chapter 3, Figure 3.27**. In order to discover the nature of the cell types where calcium signal initiates, we fixed and labelled organoids from which the calcium signalling response to CCh had already been recorded. Using confocal imaging of goblet and stem cell markers (MUC2 and OLFM4 respectively) we revealed that the CCh-induced calcium signal was initiated in stem cells and quickly transmitted to neighbouring goblet cells (**Figure 4.12B**). This finding suggests that stem cells respond first to muscarinic activation by inducing a calcium signal in a key location such as the stem cell niche. We speculate that the starting of the signal in a goblet cell of the stem cell niche is key in inducing a rapid response to secrete mucus and flush any potential pathogen to ensure the viability of the stem cells. With this theory we also suggest that the first goblet cell in receiving the signal could amplify it to its neighbour epithelial

cells through GAP junctions and reach other goblet cells of the stem cell niche to induce a potent mucus secretion. These results create a scenario comparable to that demonstrated by Birchenough and colleagues, where only a subset of goblet cells in the top of the crypt can sense bacteria and induce a mucus response in the neighbouring goblet cells via transmission of calcium signals (Birchenough et al., 2016). However, some questions remain to be elucidated. Firstly, it would be interesting to understand what makes stem cells respond first to muscarinic activation. It could be hypothesised that these cells are endowed with a more abundant presence of the calcium toolkit, which could facilitate a rapid response to the stimuli. Finally, more research is needed in understanding how these calcium signals propagate. Similar to Birchenough and colleagues, we have also hypothesised that the transmission of the calcium signal could be enabled by GAP junctions on the basolateral membranes of epithelial cells. Testing the effect of selective GAP blockers like carbenoxolone (CBX) or quinine (QUIN) (Manjarrez-Marmolejo and Franco-Pérez, 2016) could be use in preventing the transmission of the muscarinic-induced calcium signals in the base of the crypt. Further analysis of the mucus secretion under those circumstances would give an insight on whether GAPs are needed.

4.3.4 TPC-mediated calcium release induces fluid and mucus secretion

As discussed in the previous chapter, we have suggested that muscarinic activation induces the release of calcium from the endolysosomes via two-pore channels. The positioning of these organelles in close proximity to the mucus granules could indicate a direct action between the calcium release from these stores and a subsequent and rapid mucus secretion upon activation of the muscarinic signal. This work shows that blocking the calcium release with the TPC inhibitor Ned19 abrogates the release of mucus from human colonic goblet cells. As shown before, CCh induces fast mucus secretion by emptying the mucus content by more than 20% in goblet cells at the base of the crypt when compared to control. We show that pre-incubation with Ned19 prevents the release of mucus from goblet cells and induces MUC2 accumulation in the cytoplasm (**Figure 4.16**). Similar to the action of BAPTA and CPA, we suggest that the inhibition of mucus secretion does not impede the synthesis of new mucus and that this could explain the reason the mucus content is higher in goblet cells when exocytosis is prevented. Importantly, we show that the stimulation with CCh of crypts where the TPCs had been previously blocked with Ned19 results in minimal mucus secretion. We therefore hypothesise that the calcium release from the endolysosomes via TPC is crucial for inducing muscarinic activated mucus secretion in the base of colonic crypts. The same results were observed in organoids derived from human colonic crypts which indicates that signalling mechanism is conserved in the organoid model (**Figure 4.17**). In our studies we also

reported that incubation of crypts and organoids with a higher concentration of Ned19 (500 µM) resulted in a greater increase in mucus accumulation (data not shown). Importantly, the use of a high concentration might exert cytotoxicity and thus the inhibition of mucus secretion could be a result of toxicity. In order to confirm this possibility, cell viability assays with different Ned19 concentrations will need to be carried out. Having obtained the same results validates the use of organoids as another model for the study of mucus secretion. Since organoids are amenable to genetic editing and can be propagated indefinitely, the use of this model opens the possibility to study the status of mucus secretion in organoids with targeted genetic modifications. In addition, the particular role of TPC1 and TPC2 separately remains to be elucidated. Having not found any literature describing the use of specific TPC antagonist, follow up studies could make use of techniques like siRNA to prevent protein transcription of the receptor and further assess the role of each one them distinctly.

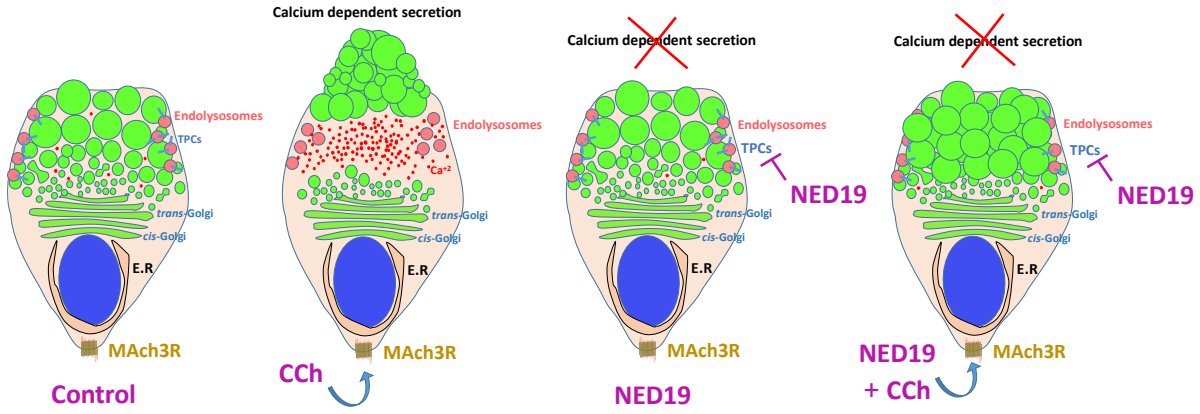

Figure 4.28. TPC regulate calcium-couple mucus secretion. Inhibition of TPC with Ned19 abrogates mucus secretion. Stimulation with CCh does not induce mucus secretion in the presence of Ned19.

Mucus and fluid secretion have been shown to be dependent of calcium signals originating from the ER. Recent studies in mice suggest that IP3Rs-dependent release of calcium upon muscarinic activation is needed for fluid secretion in the eye (Inaba et al., 2014) and mucus release in the olfactory gland (Fukuda et al., 2008). In order to test the influence of IP3Rs in mediating the calcium-coupled mucus secretion in goblet cells of the base of the crypt we blocked the receptor using 2-APB (Takayuki et al., 1997). Inhibition of the IP3Rs in the presence of 2-APB showed no difference in the mucus content in the goblet cells of the base of the crypt compared to control (**Figure 4.18**), whereas pre-incubation with 2-APB showed no effect on CCh stimulation of mucus release. Importantly, these results show that inhibition of IP3Rs does not lead to an increase in mucus secretion upon muscarinic stimulation, which suggests that the IP3R-mediated calcium release is not the main driving force of mucus secretion.

RyRs located in the ER play an important role in amplifying intracellular calcium signals by the mechanism of calcium induced calcium release (Dawson, Keizer and Pearson, 1999). Recent studies suggested that release of calcium from RyRs is key in inducing mucus secretion in goblet cells of the airway system (Chen et al., 2011) and in the colon (Cantero-Recasens et al., 2018). To test the role RyR in mucus secretion of human colonic crypt goblet cells we used Dantrolene (10 μM) to block the calcium channel (Zhao et al., 2001) and thus any calcium dependent release. While CCh induced depletion of the cytoplasmic mucus, the presence of Dantrolene completely blocked the CCh induced mucus secretion (**Figure 4.19**). A possible explanation to this finding is that following activation of the muscarinic receptors, an intracellular signalling pathway activates CD38 at the apical membrane of the cells to produce NAADP. Under these circumstances, NAADP activates TPCs to induce a local calcium signal. This local response activates the RyRs in the ER to amplify the signal by CICR. While Dantrolene effectively blocks the CCh-induced mucus secretion by inhibiting RyR1 and/or RyR3, the RyR subtypes involved in CICR remain to be studied. Ongoing work in the Williams lab has shown that Procaine (known to inhibit RyR1 & 2 and possibly 3) reduced the CCh-induced calcium response by 80%. Follow up experiments using siRNA to selectively inhibit the expression of each of the three RyRs will aim to elucidate their role in CICR and their involvement in mucus secretion

The effector proteins that are activated by the cholinergic-induced calcium signal that facilitate the release of mucus have not been studied in this thesis. However, recent work by Recasens et al. in the human cell line HT29-18N2 has suggested the presence of the calcium sensor KChiP3 that is expressed in the mucus globules under resting conditions. Under this circumstances, KChiP3 prevents the docking of the globules to the membrane but an increase in cytosolic calcium promotes the recycling of this protein from the granules to allow membrane fusion with the plasma membrane to induce the release of mucus (Cantero-Recasens et al., 2018). In this regard, it would be of interest in the future to characterise the presence of this protein in our culture model.

In the literature, other researchers have made use of different protocols to measure mucus secretion which include the measuring of mucus content with enzyme-linked immunosorbent technique (Garcher, 1998) or more recently by measuring the mucus thickness in mouse colonic explants (Birchenough et al., 2016). We here present a method to quantify mucus secretion based on the measurement of the antibody fluorescence intensity which is capable of recording with accuracy the modulations in the goblet cell physiology that lead to mucus secretion.

Inside the mature mucus granules, the mucins are arranged as tightly packed multimers. For the mucus molecules to be organised in such way, the concentration of calcium and pH varies as the

mucins are processed inside the organelles. Mucus is synthesised in the ER and arranged into dimers. In the trans-Golgi the pH decreases to 6.2 while the concentration of calcium rises to allow for the molecules to trimerise. The final arrangement into multimers in the mature mucus granules is achieved at pH of 5.2 and a greater concentration of calcium (Birchenough et al., 2015). The mechanism is similar to the one observed in the packaging of the zymogen granules in pancreatic acinar cells. In this cell types, exocytosis is mediated by calcium release from the vesicles into the cytoplasm following stimulation (Williams, 2010). In a similar scenario, we could hypothesise that mucus globules also present the same components (e.g. TPCs) and follow a similar intracellular regulation. Once the granules are secreted into the lumen the increase in pH and the presence of HCO_3^- allow the water to penetrate inside the structure which results in the unfolding and expansion of MUC2 (Gustafsson et al., 2012). Secretion of HCO_3^- is mediated by the apical membrane receptor CFTR but the whole mechanism is dependent on epithelial chloride transport. In the colon, increases in intracellular calcium activate NKCC1 and the K^+ in the basal membrane to allow influx of Cl^-, Na, and K^+ and efflux of K^+ respectively (Reynolds et al., 2007). At the same time calcium also activates the Cl^- channel TMEM16A in the apical membrane to release Cl^- ions into the lumen which is followed by water (Frizzell and Hanrahan, 2012). Fluid secretion is another physiological response of the colonic epithelium that together with mucus secretion helps to clear the base of colonic crypts. Seminal work by Halm and colleagues demonstrated that muscarinic activation induces fluid secretion in the human colonic epithelium (Halm and Halm, 2000). However, the origin of the calcium signals that induce fluid secretion have not been fully characterised. Recent work using gut organoids has demonstrated the validity of this culture system to investigate fluid secretion (Fujii et al., 2016; Schwank et al., 2013). The stimulation of fluid secretion induces the swelling of the organoids which can be compared between different conditions. Utilising a similar approach, we show in this chapter that human colonic organoids swell after stimulation with CCh and that the endolysosomes are responsible for the release of calcium via TPC that mediates CCh-induced fluid secretion. Stimulation of organoids with CCh induced fluid secretion which increased the luminal cross-sectional area by 20% compared to control (**Figure 4.20)**. In order to assess the role of TPC we used the inhibitor Ned19 to block calcium release (Sakurai et al., 2015). Incubation of colonic organoids with Ned19 showed no apparent effect on swelling as compared to control, however it abrogated the CCh induced swelling response. This result suggest that TPC-release of calcium is crucial in regulating muscarinic induced fluid secretion (**Figure 4.20**) as well as to allow for mucus expansion in the lumen. Similar results were obtained in the presence of Tetrandrine (data not shown) which further support the key role of TPCs in mediating this physiological process. These results correlate with the previous findings on mucus secretion and suggest that calcium signalling is

key in regulating fluid secretion. Studies in the salivary gland indicate that fluid secretion is dependent on muscarinic-activated calcium release from the ER via IP3R (Ambudkar, 2000). The role in the ER in fluid secretion has not been tested in our model but follow up work could determine whether release of calcium from IP3R and RyR is needed to orchestrate fluid secretion together with the endolysosomal TPC. It could be possible to speculate that due the role of calcium in activating different channels in different regions of the polarised epithelial cell, the spatial characteristics of the calcium signal could involve the action of different calcium stores and channels.

4.3.5 Intracellular trafficking and exocytosis of mucus granules

To follow up our findings on the molecular regulation of mucus secretion we wanted to study and visualise the actual movement of the mucus granules to the membrane that leads to mucin secretion. The use of the fluorescent lipid dye FM-143FX has been reported in the literature as a tool to record granule exocytosis (Balseiro-Gomez et al., 2015). We first showed that this dye can be used to visualise putative goblet cells in fix samples of human colonic crypts (**Figure 4.21**). High magnification images revealed the presence of presumed mucus granules which were particularly intense and rich in the cytoplasm. Goblet cells are the most abundant secretory cell type in the colon and thus their cytoplasm is filled with lots of granules wrapped in a lipid membrane that originates from the plasma membrane. We hypothesise that mucus secreting cells incorporate more dye-labelled plasma membrane than their neighbours to be used for the generation of the mucus granules, which makes FM-143FX labelled cells good candidates for being goblet cells. In addition, high magnification of DIC images reveal the presence of mucus granules in intense FM-143FX labelled cells (**Figure 4.21**). We also reported that the use of this dye can be a useful tool to study mucus granule exocytosis. Using live confocal imaging of FM-143FX labelled crypts stimulated with CCh we showed the enlargement of the apical membrane of an intense labelled and presumed goblet cell, which progresses over the course of 5 minutes forming a sphere (**Figure 4.22**). This sphere is eventually shed into the lumen at the same time that the cellular membrane is sealed again (data not shown). In addition, using this methodology and following stimulation of colonic crypts with CCh, we were able to record in real time the effect of fluid and mucus secretion and visualise the flushing of the luminal content (**Figure 4.23**), which correlates with the previous results that indicate the regulation of this mechanism by the muscarinic-coupled calcium signalling. These findings suggest the possibility of labelling intracellular mucus granules and their exocytosis. Follow up studies will aim to elucidate the nature of mucus compound exocytosis and determine whether this is a multivesicular process where mature mucus granules are fused to each other before fusing to the plasma membrane, or whether they follow a sequential mechanism in which individual

mature vesicles fuse to the plasma membrane which is followed by the secondary fuse of deeper-lying granules (Pickett and Edwardson, 2006). This method represents a good model for the study of live mucus secretion which can be altered upon the addition of secretagogues or inhibitors. In addition, we show that FM-143FX labelled and live imaged crypts stimulated with CCh can be subsequently fixed and labelled for the presence of $MUC2^+$ goblet cells and mucus to confirm that FM-143FX labelled cells are also $MUC2^+$ goblet cells and that FM-143FX-labelled luminal globules contain mucus (**Figure 4.24**). Moreover, we show that screening fixed samples of goblet cells has allowed us to capture the exocytosis of mucus at different stages in different cells, which follows a similar pattern as the one reported in live imaging experiments (**Figure 4.25**).

4.3.6 Generation of MUC2 knock-in fluorescent reporter

The development of a human colonic organoid culture system enabled us with a platform suitable for genetic engineering. In order to study the release of mucus in human colonic goblet cells we aimed to generate an organoid line containing a MUC2 fluorescence reporter. The development of the CRISPR/Cas system for genetic engineering has been shown to be a great tool to edit the genome in organoid cultures (Schwank et al., 2013). The knock-in of a MUC2 fluorescence reporter has been previously demonstrated by Birchenough and colleagues who engineered mice to constitutively express the fluorescent marker in goblet cells (Birchenough et al., 2016). Based on the work of Birchenough and others we chose to incorporate our fluorescent reporter, mKate2 in a region of the MUC2 gene containing many repetitive sequences that would not disrupt the protein function. In order to generate the cassette containing the fluorescent reporter we first had to amplify each of the components to later ligate them together and propagate it in *E. coli* competent cells. We showed that we can successfully generate a cassette containing the homology arms needed for the recombination with the template DNA, as well as containing the reporter mKate2 (**Appendix B**). However, genomic sequencing of the final construct showed a low level of genomic similarity of one of the homology arms with the template, which could result in poor recombination probability with the host genome upon transformation. Our efforts are now focused on generating a fully functional cassette. The main challenge to overcome is the amplification of one of the homology arms which is located in region with high number of repetitive sequences, limiting the efficacy of primer binding. However, the generation of an organoid line constitutively expressing a MUC2 fluorescent reporter would enable the in-depth study of the precise spatio-temporal characteristics of the mucus secretion in the base of the crypts. Moreover, live imaging of organoids loaded with the calcium fluorescent indicator Fluo-4 could help to better characterise the initiation and transmission of the calcium signals between $mKate2^+$ goblet cells.

4.4 Conclusion

This chapter has characterised the presence of a subpopulation of goblet cells residing in the stem cell niche which are activated by muscarinic-coupled calcium signals to induce mucus and fluid secretion at the base of the crypt to clear out the luminal content. The specific location of these goblet cells in the vicinity with stem cells suggest a role for their protection, therefore we identify them as guardian goblet cells. Importantly, we have identified stem cells as the cells responsible for the initiation of the muscarinic-induced calcium signal, which is immediately transferred to the neighbour goblet cells potentially by intercellular communication. Importantly, TPC-mediated calcium release from the endolysosome has been determined to be the mechanism that regulates fluid and mucus secretion upon muscarinic activation in human colonic crypts and organoids. These results validate the use of our culture models for investigating goblet cell mucus and fluid secretion.

5 Chapter 5. Cholinergic calcium signals regulate intestinal stem cell biology

5.1 Introduction

Stem cells are the cellular maestros that orchestrate tissue renewal. In the colon epithelium, these cells reside at the base of colonic crypts protected from any potential luminal threat. Colonic stem cells are constantly proliferating to counteract the loss by shedding of epithelial cells at the opening of the crypts and thus maintain a constant cell population (Clevers, 2013). In homeostasis, stem cells proliferate to give rise to progenitor cells which then differentiate into absorptive or secretory cell lineages as they migrate up the crypt axis (Clevers, 2013). The biology of stem cells is tightly regulated by the components of the stem cell niche which include cells from the underlying mucosa and in the case of the colon, potentially also by goblet cells that reside intermingled with them (Santos et al., 2018). These cells secrete an array of different molecules and growth factors to ensure stemness and prevent differentiation. Growth factors like Wnt and R-Spondin activate the Wnt signalling pathway and promote Notch signalling to induce stem cell proliferation whereas molecules like gremlin (the physiological analogue of noggin in the human colon) inhibit the BMP/TGFβ signalling pathway that promotes cell differentiation (Toshiro. Sato et al., 2011). These growth factors are abundant in the stem cell niche but decrease toward the upper regions of the crypt to facilitate cell differentiation, aided by an increase in BMP and TGFβ proteins. The gut can recover from an injury by regenerating the epithelium. Recent literature suggests that upon damage of the stem cell compartment, differentiated cells can revert their phenotype to that of a stem cell and proliferate to help the tissue recover, illustrating the existence of a complex mechanism of stem cell plasticity (de Sousa e Melo and de Sauvage, 2019).

Operational colonic stem cells were proposed by early work from Cheng and Leblond in 1974 as continuously cycling cells at the bottom of the crypts (Cheng and Leblond, 1974). Characterisation of intestinal stem cells remained elusive until the discovery of the bona fide cell marker leucine-rich repeat GPCR (LGR5) (Barker et al., 2007). This marker encodes a GPCR that can bind R-spondin to enhance Wnt signalling in stem cells. In addition, colonic stem cells present other enriched markers that allow for its characterisation. The secreted protein Olfactomedin-4 (OLFM4) and the transcription factor achaete scute-like 2 (ASCL2) are both highly expressed in the base of the crypt and have been identified in LGR5 stem cell enriched genes which are found absent in immediate daughters. Moreover, the protein tyrosine pseudokinase 7 (PTK7) was recently shown to mark colonic stem cells and is thus considered a surrogate of the LGR5 marker (Jung et al., 2015).

In addition to the growth factors mentioned above, stem cells can also be modulated by interleukins and the nutritional status of the crypt. Lymphoid cells located in the vicinity of stem cells can be activated upon intestinal injury to secrete the cytokine IL22 which induces cell proliferation needed for the regeneration of the damaged epithelium (Lindemans et al., 2015). Stem cells can integrate dietary and energy signals by nutrient-sensing pathways to respond to stress conditions or to preserve epithelial growth. Caloric restriction has been shown to be beneficial for the stem cell niche as it improves the intestinal stem cell functions (Mihaylova et al., 2018). Nutrient overabundance, on the other hand, increases the stem cell number and promotes its proliferation instead of differentiation towards the other cell lineages, enhancing tumorigenesis in the stem cell compartment (Beyaz et al., 2016). Another important signalling molecule in this tissue is the prototypical neurotransmitter ACh, that is secreted by cholinergic neurons that innervate the gut to regulate the biology of the colon epithelium and gut motility (Furness, 2012). In recent years it has been demonstrated that ACh can be produced in a non-neuronal manner by the tuft cells of the colonic epithelium. This cell type functions as a chemosensor of the luminal content and can identify bacterial cues through taste receptors to induce an immune response (Nadjsombati et al., 2018; von Moltke et al., 2015). In the trachea, upon sensing of bacterial signals, tuft cells can release ACh to activate cholinergic neurons to reduce breathing rate to help eliminate the bacteria (Krasteva et al., 2011). In the urethra, identification of bacterial antigens induces ACh release from these cells to stimulate sensory nerves and enhance the activity of the bladder detrusor muscle to fight infection (Deckmann et al., 2014). Recent literature has suggested an important role of ACh in mediating cell proliferation and tumorigenesis in the GI tract epithelium. In the stomach and pancreas, cholinergic innervation signal muscarinic receptor types 3 and 1 respectively to enhance the Wnt signalling pathway in stem cells. Aberrant signalling from these nerves induces tumour growth and progression (Magnon et al., 2013; Zhao et al., 2014). In the stomach, dysregulation of ACh production by cholinergic neurons and tuft cells induces nerve growth factor (NGF) expression to promote neuron expansion and tumorigenesis. Importantly, ACh signals MAChR3 of gastric stem cells to trigger the YAP signalling pathway that results in the activation of Wnt target genes (Hayakawa et al., 2016).

In the colon epithelium, seminal work by the Williams lab has shown that activation of MAChR3 induces an intracellular calcium response that originates in the stem cell niche (Lindqvist et al., 1998; Reynolds et al., 2007). As discussed before in **Chapter 3** (**Figure 3.27**) **and Chapter 4** (**Figure 4.12**), the muscarinic-induced calcium signalling response initiates first in the stem cells to then propagate to the neighbouring cells. The second messenger calcium is an important regulator of cell biology and changes in its intracellular concentration can modulate diverse array of cellular functions such as cell proliferation, migration, differentiation or apoptosis (Dupont et al., 2011). Recent discoveries

have highlighted the role of calcium as a remarkable messenger to integrate a wide variety of signals to mediate stem cell activity. Jasper and colleagues presented an elegant study in *Drosophila* where they demonstrated that calcium can integrate and transduce nutritional and stress signals from the environment and respond by promoting stem cell proliferation via activation of calcineurin and the transcription factor CRTC (also known as CREB regulated transcription coactivator or TORC) (Deng, Gerencser and Jasper, 2015). The type and intensity of the cellular stimulus determines the duration and amplitude of the intracellular calcium signals, and the downstream effects are defined by the affinity and the intracellular location of the cellular calcium sensors that decode the calcium signal (Berridge, Bootman and Roderick, 2003). Calcium sensors such as calmodulin (CaM) and calcineurin (CaN) have been demonstrated to be required for cell cycle progression (Rasmussen & Means, 1989; Tomono et al., 1998). CaN also regulates the transcription factors that control the G1 to S transition like the nuclear factor of activated T cells (NFAT). NFAT is located primarily in the cytoplasm but increases in cytosolic calcium can activate CaN to de-phosphorylate NFAT to allow translocation to the nucleus (Hogan et al., 2003). Recent findings indicate that increases in cytosolic calcium can activate CaN to promote nuclear translocation of NFATc3 to stimulate the expression of proliferative genes such as LGR5 and OLFM4 (Peuker et al., 2016). In addition, upon ACh stimulation, the transcription factor YAP has been showed to translocate to the nucleus to activate the expression of Wnt in $LGR5^{+}$ stem cells of the stomach (Hayakawa et al., 2016). Our findings in the study of the intracellular calcium signals in the colonic epithelium (**Chapter 3. Figure 3.32**) support the idea that muscarinic stimulation triggers a local calcium response that depends on the release of calcium from the endolysosomes via TPCs, which is potentially amplified via calcium-induced calcium release from the IP3Rs and RyRs in the ER. Calcium signalling involving NAADP and calcium release from TPCs has been implicated in differentiation (Notomi, Ezura and Noda, 2012), migration (Nguyen et al., 2017) and autophagy (Pereira et al., 2011). Importantly, calcium release from TPCs has also been shown to induce proliferation and angiogenesis (Favia et al., 2014) and in the colon, our recent findings indicate that these channels mediate goblet cell mucus and fluid secretion (**Chapter 4**).

ACh has been suggested to induce proliferation of stem cells in the colon epithelium, however the underlying mechanism is not fully understood. Our recent findings suggest muscarinic activation induces a calcium signal response that first originates in the stem cells and is mediated by TPC release of calcium. The aim of this chapter is to determine whether the muscarinic calcium signal activates tissue growth and cell proliferation of stem cells, and whether these signals are regulated by TPC-mediated calcium release and subsequent activation of nuclear translocation of transcription factors (**Figure 5.1**).

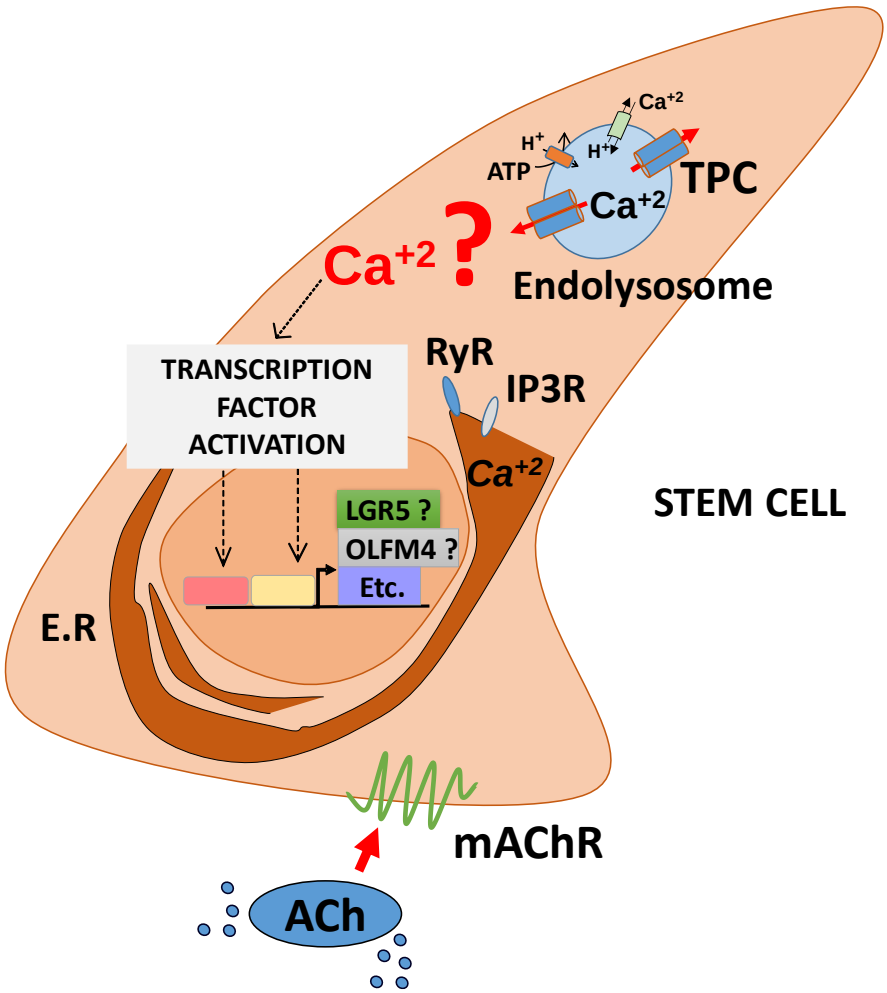

Figure 5.1. Proposed mechanism for the regulation of stem cell biology by muscarinic-induced intracellular calcium signals. ACh stimulates a calcium response that originates in the apical pole of the cell, which is highly populated with endolysosomes. TPCs present in endolysosomes are able to decode the ACh signal and induce an intracellular calcium response that results in the activation of gene transcription to promote cell proliferation.

5.2 Results

In this chapter, we aimed to study the role of ACh in initiating the intracellular calcium signals to induce proliferation in the stem cell niche of human colonic crypts and organoids. To do so, we first made use of immunofluorescence imaging to characterise the presence of proliferation and stem cell markers in our culture systems. We developed an organoid growth assay using time-lapse microscopy, to monitor the increase in size under muscarinic stimulation. Next, we blocked muscarinic-induced endolysosomal calcium release from TPCs with Ned19 and evaluated its role in cell proliferation by measuring DNA synthesis with Click-iT EdU technology. Finally, we used immunofluorescence imaging to study nuclear translocation of transcription factors involved in cell proliferation under the influence of muscarinic stimulation.

5.2.1 Characterisation of stem cells in colonic crypts and organoids

Stem cells reside at the base of colonic crypts where they proliferate to maintain epithelial regeneration and homeostasis of the tissue (Barker, 2014). Cell proliferation can be identified by the expression of the protein Ki67, which is highly expressed in cycling cells and strongly downregulated in resting G0 cells (Gerdes et al., 1984). To localise the proliferative region of the crypt, we imaged colonic crypts immunolabelled with the antibody Ki67. Confocal images revealed the majority of Ki67 positive cells to be present in the base and supra-base region of the crypt with the presence gradually decreasing towards the upper region (**Figure 5.2**). In order to characterise the presence of stem cells in our culture system we looked for the expression of the bona fide markers. As previously described, we reported the expression of the OLFM4 stem cell marker in native and cultured crypts as well as in organoids (**Chapter 3**, **Figure 3.11).** However, the protein LGR5 is regarded as the canonical stem cell marker for intestinal stem cells in the gut, where it mediates Wnt signalling (Barker et al., 2007). In order to study its presence in our culture systems, we immunolabelled colonic crypts and organoids with the LGR5 antibody and analysed its expression under the confocal microscope. Because of the low expression of the protein in the membrane we decided to immunolabel the samples prior to fixation in order to prevent any loss of the protein antigen during the process. Confocal imaging revealed the expression of the stem cell marker to be present in the basolateral membranes of discrete cells of the base of the crypt (**Figure 5.3A**) and organoids (**Figure 5.3B**). Antibody labelling was also found in some cells in supra base and mid regions of the crypt which could indicate the presence of progenitor proliferative cells. In addition, we also investigated the expression in colonic crypts of PTK7. Using a similar approach, the immunolabelling of the samples showed the presence of this marker to be prominently expressed in the base of the crypt where it labelled the basolateral membranes of the cells. Our images reported the expression of this marker to immunolabel the entire membrane of a few number of cells along the crypt axis, which could indicate the presence of a subpopulation of progenitor cells destined to undergo cell differentiation to the enteroendocrine cell lineage as indicated by Jung and colleagues (Jung et al., 2015).

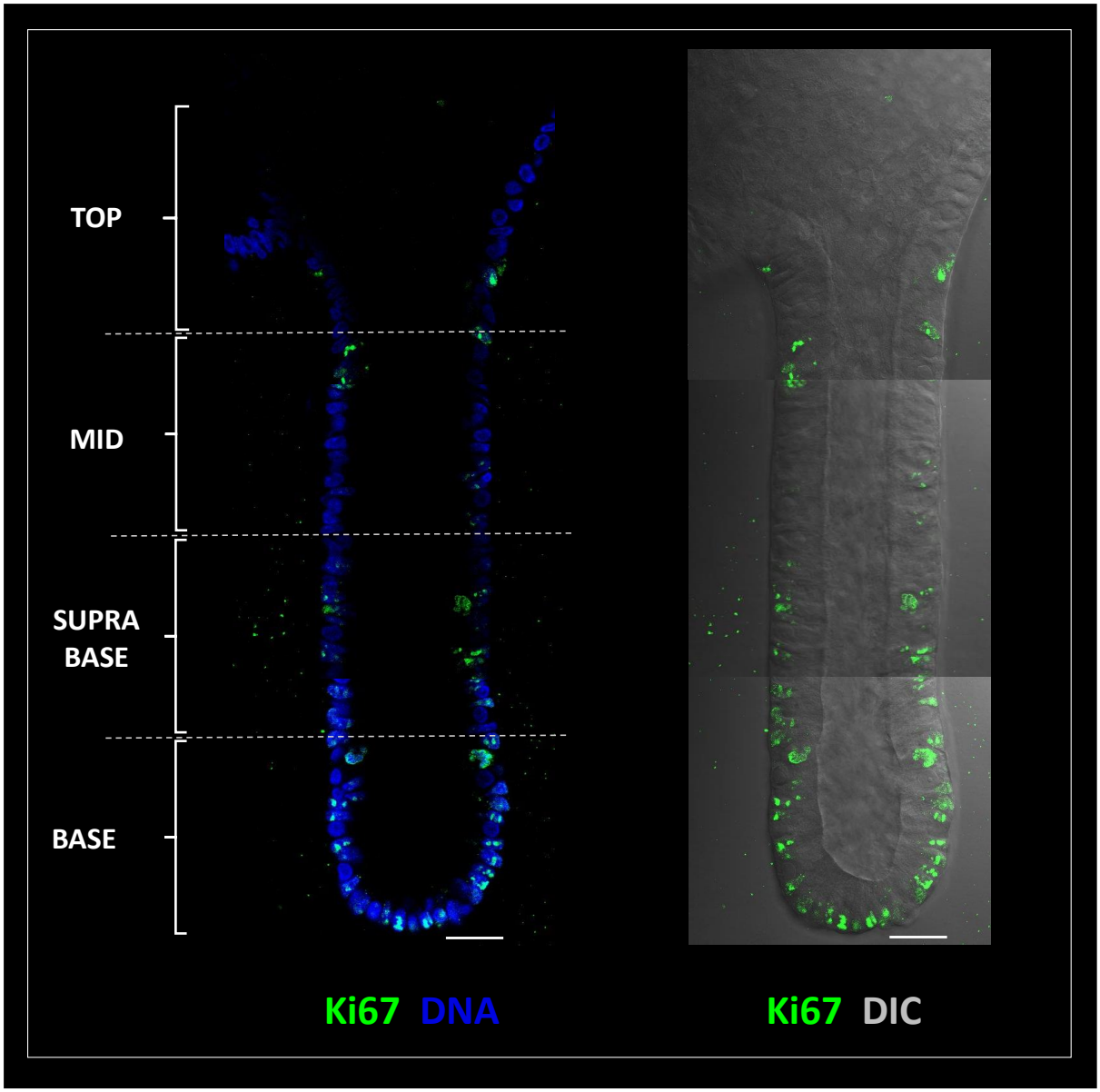

Figure 5.2. Presence and distribution of Ki67. Confocal immunofluorescence images illustrate the presence and distribution along the crypt axis of Ki67 (green) positive cells merged with nuclear dye, Hoescht 3342 (DNA), on the left and with brightfield on the right. Scale bar 25 µm.

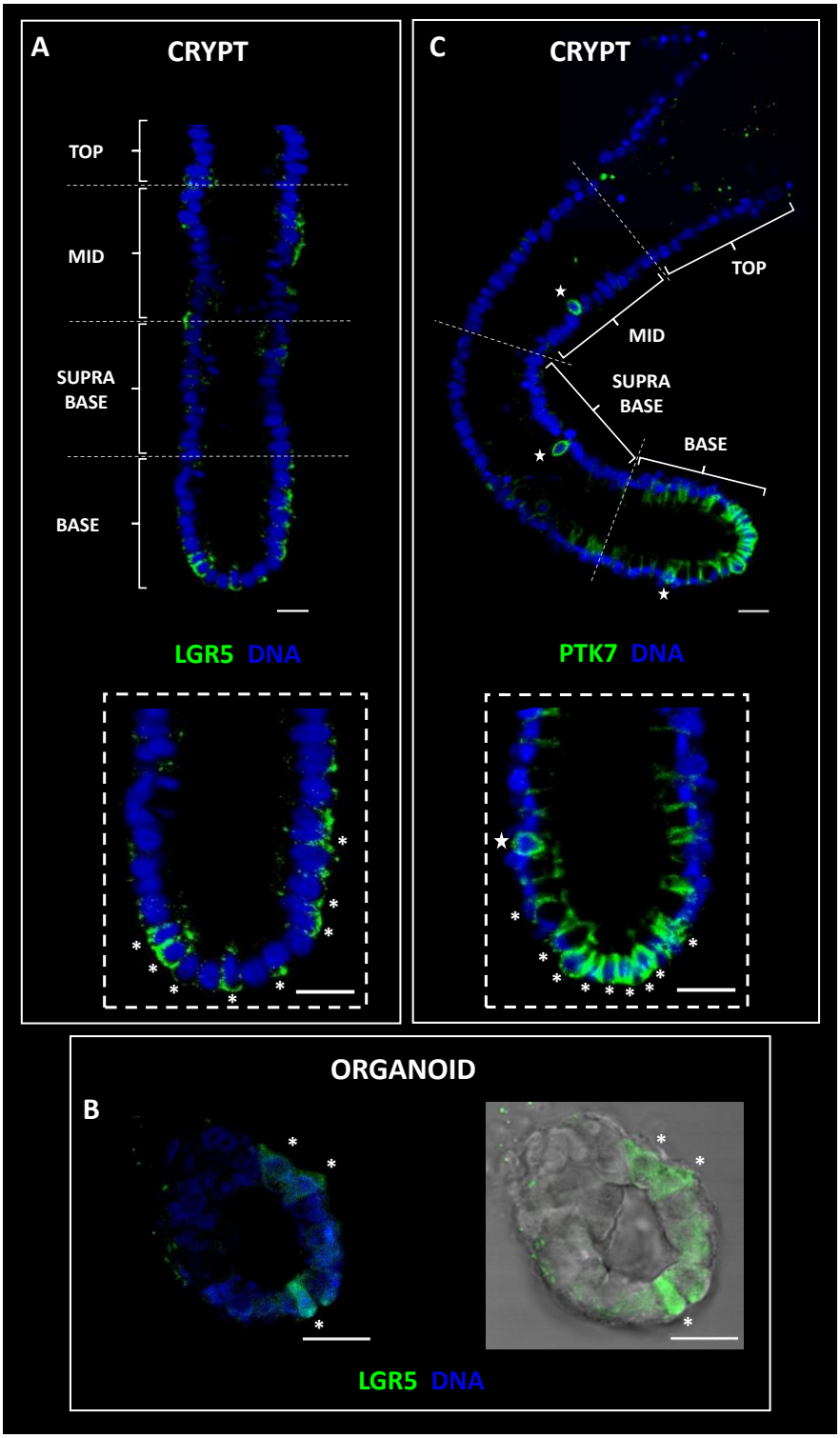

Figure 5.3. Presence and distribution of colonic stem cell markers. (**A** & **B**) Confocal images show immunolabelling of LGR5 marker (green) in colonic crypts (**A**) and organoids (**B**). At the top, the image shows distribution of the protein along the crypt axis. Below, a high magnification image displays basolateral labelling of the marker. In **B**, the bottom image shows LGR5 expression in an organoid, co-labelled with nuclear DNA (left) and brightfield (right). Asterisks indicate LGR5^{+} cells. (**C**) Expression of the marker PTK7 along the crypt axis. White stars indicate possible enteroendocrine

cells. Below, high magnification image of the crypt base. Asterisks indicate basolateral labelling of PTK7^{+}cells. Scale bar 25 μm.

5.2.2 Muscarinic activation induces organoid growth

Recent literature has suggested that ACh can induce stem cell proliferation in the mouse stomach via muscarinic receptor activation (Hayakawa et al., 2016) and intracellular calcium signals have been demonstrated to regulate cell proliferation in *Drosophila* gut epithelial cells (Deng, Gerencser and Jasper, 2015). In addition, our previous results indicate that the muscarinic-induced calcium signal originates in the stem cells which express the calcium signalling toolkit (**Chapter 3, Figure 3.27 and Chapter 4, Figure 4.12**). In order to test whether muscarinic stimulation induces stem cell activation of tissue growth we stimulated colonic organoids with different concentrations of CCh (1, 10 and 100 μM) and analysed the growth every other day over the course of 6 days (**Figure 5.4A**). The analysis of the organoid cross-sectional area measurements over the course of the experiment revealed that CCh stimulation induced an increase in organoid size as compared to control, which was greater at a concentration of 100 μM (**Figure 5.4B**). In addition, stimulation with CCh resulted in the development of more crypt-like structures as compared control (**Figure 5.5**).

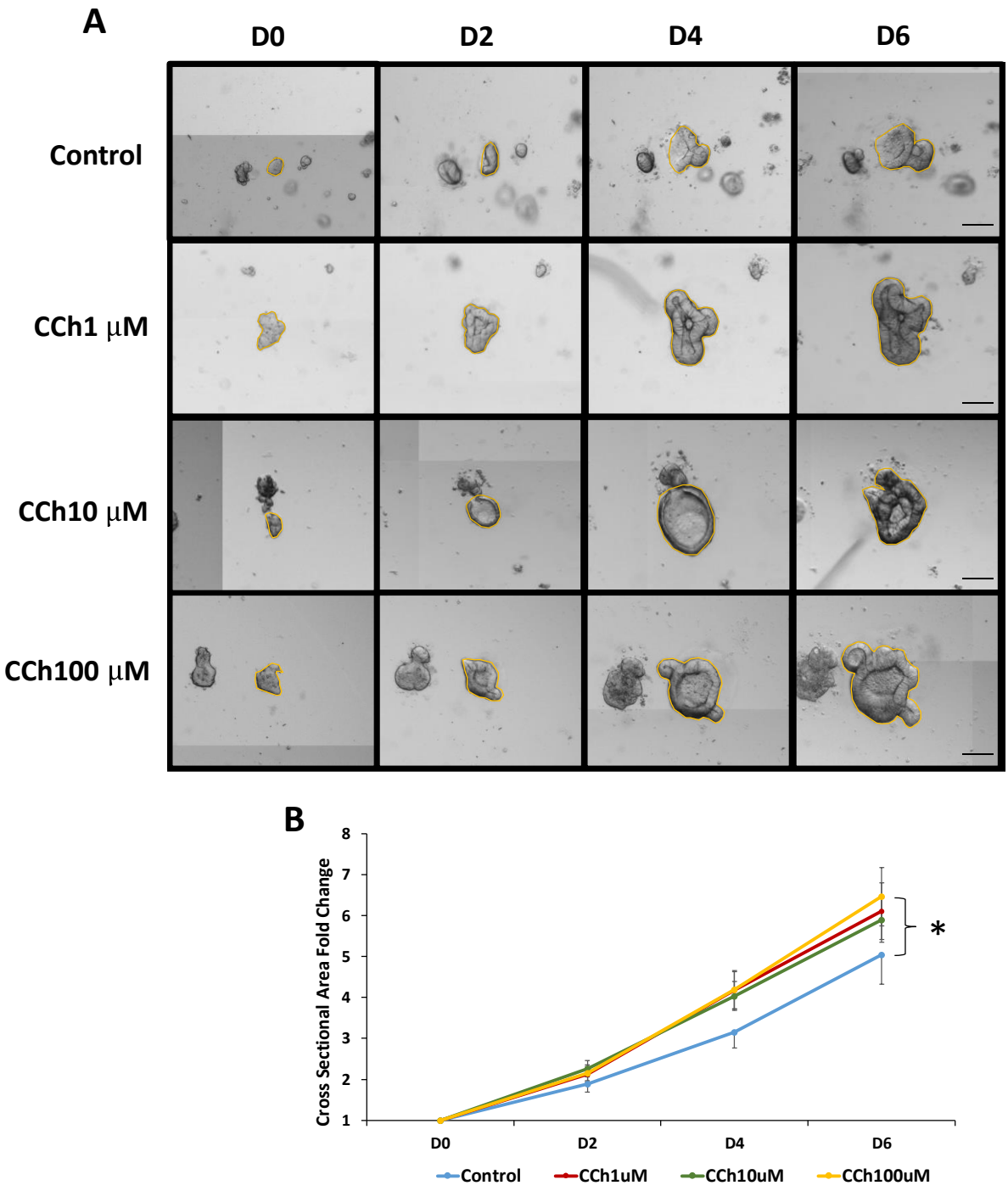

Figure 5.4. CCh induces organoid growth. (A**).** Brightfield representative images of organoids grown in different concentrations of CCh over the course of 6 days. Yellow line indicates image analysis of cross-sectional area. Scale bar 150 μm (**B**) Scatter plot represents the increase in growth over time as judged by the normalised cross-sectional measurements. (N=1, n=46, *P<0.05).

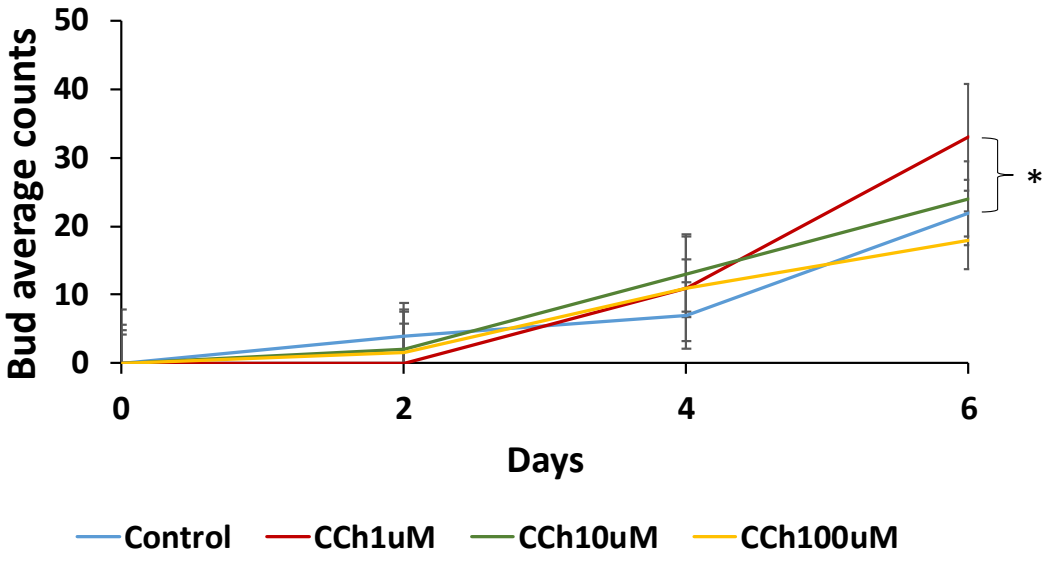

Figure 5.5. CCh induces bud formation. Scatter plot represents the increase in number of buds of organoids stimulated with different concentration of CCh over the course of 6 days (N=1, n=46, *P<0.05).

Similarly, we investigated whether CCh-induced organoid growth is mediated by muscarinic receptors by stimulating the samples with different concentrations of the selective agonist Oxo (**Figure 5.6A**). Cross-sectional area measurements showed an increase in size of organoids stimulated with Oxo as compared to control through the course of 6 days, which confirmed that activation of tissue growth is dependent on muscarinic stimulation (**Figure 5.6B**). The average of the total number of buds developed over the course of 6 days revealed no significant differences compared to control. Stimulation with Oxo 10 µM resulted in a lower number of buds compared to lower doses of the ACh agonist and control (**Figure 5.7**).

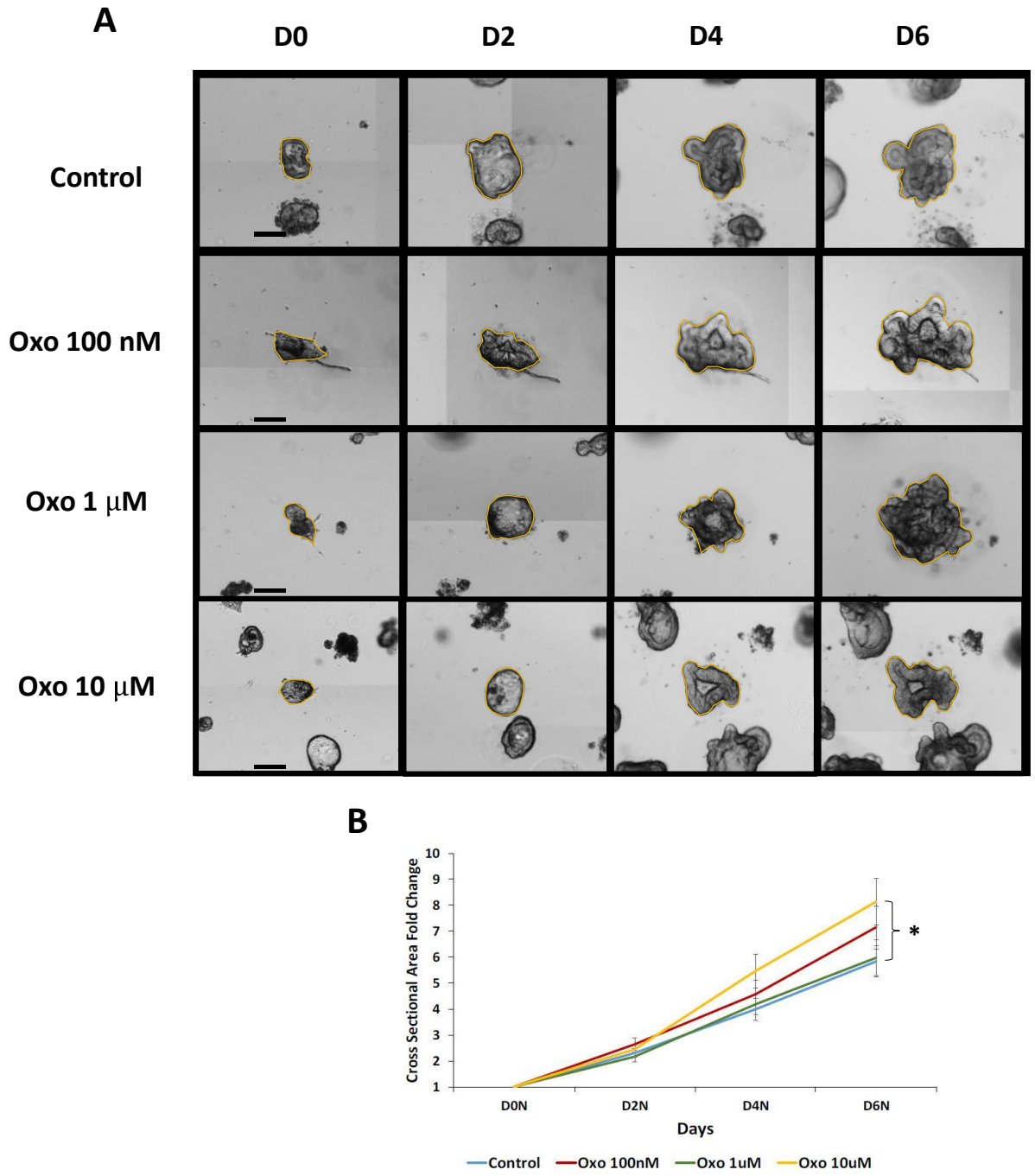

Figure 5.6. Muscarinic stimulation induces organoid growth. (**A**) Illustrative brightfield images of the growth of organoids over time under different concentrations of Oxo. Yellow lines indicate cross-sectional area. Scale bar 150 μm. (**B**) Scatter plot represents an increase in cross-sectional area of organoids stimulated with Oxo over the course of 6 days. Cross-sectional area was normalised to control (N=1, n=46 P*<0.05).

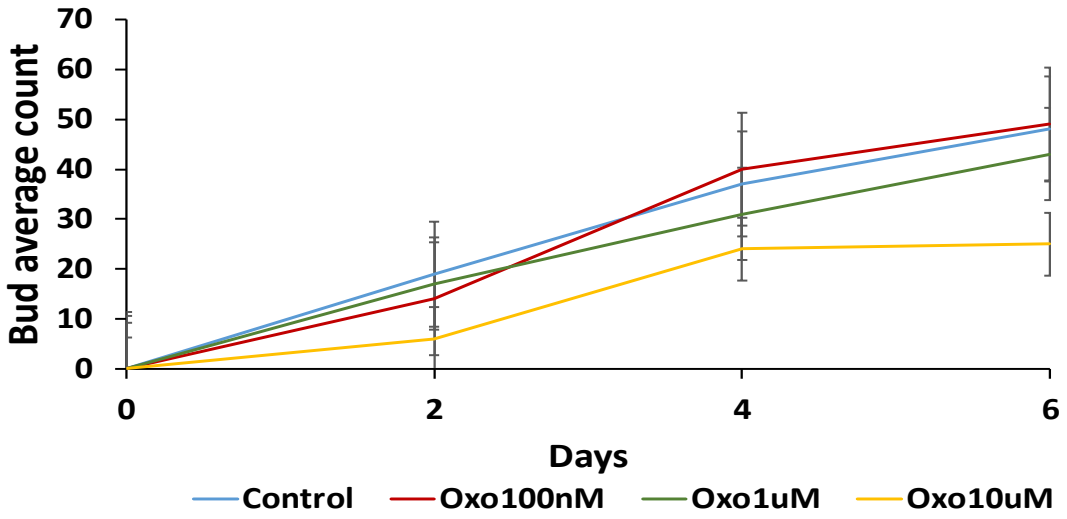

Figure 5.7. Oxo has no effect on bud formation. Scatter plot represents the average number of buds in untreated organoids versus organoids stimulated with different concentrations of Oxo over the course of 6 days. (N=1, n=46).

5.2.3 TPC mediates cell proliferation

Our previous findings suggest that the CCh stimulation of muscarinic receptors triggers an intracellular calcium response that is controlled by release of calcium from endolysosomes through TPCs (**Chapter 3, Figure 3.32**). With the aim to study whether TPC-mediated release of calcium is needed for inducing cell proliferation in the colon epithelium, we analysed the number of proliferative cells in colonic crypts where TPCs were blocked by pre-incubation with Ned 19 (125 µM). In addition, we used CCh (10 µM) to test whether muscarinic activation induces cell proliferation and whether is dependent on TPCs. In order to quantify cell proliferation, we used the EdU assay, which inserts a fluorescent analogue of thymidine every time a cell replicates its DNA. Colonic crypts were stimulated for 2 days to maintain a constant activation of the muscarinic signal and were later fixed and stained with the nuclear dye Hoescht. To prevent cytotoxicity derived from long exposure to high concentrations of Ned19, the concentration of the TPC inhibitor was lowered to 125 µM. The study of cell proliferation revealed an increase in the number of EdU^+ cells in crypts stimulated with CCh as compared to control which were present up to the mid region of the crypt axis while control EdU^+ cells were restricted to the base and supra-base (**Figure 5.8A**). Analysis of the percentage of EdU^+ cells showed a reduction in 50% of the number of proliferative crypts pre-incubated with Ned (125 µM) as compared to control which was not restored in the presence of CCh.

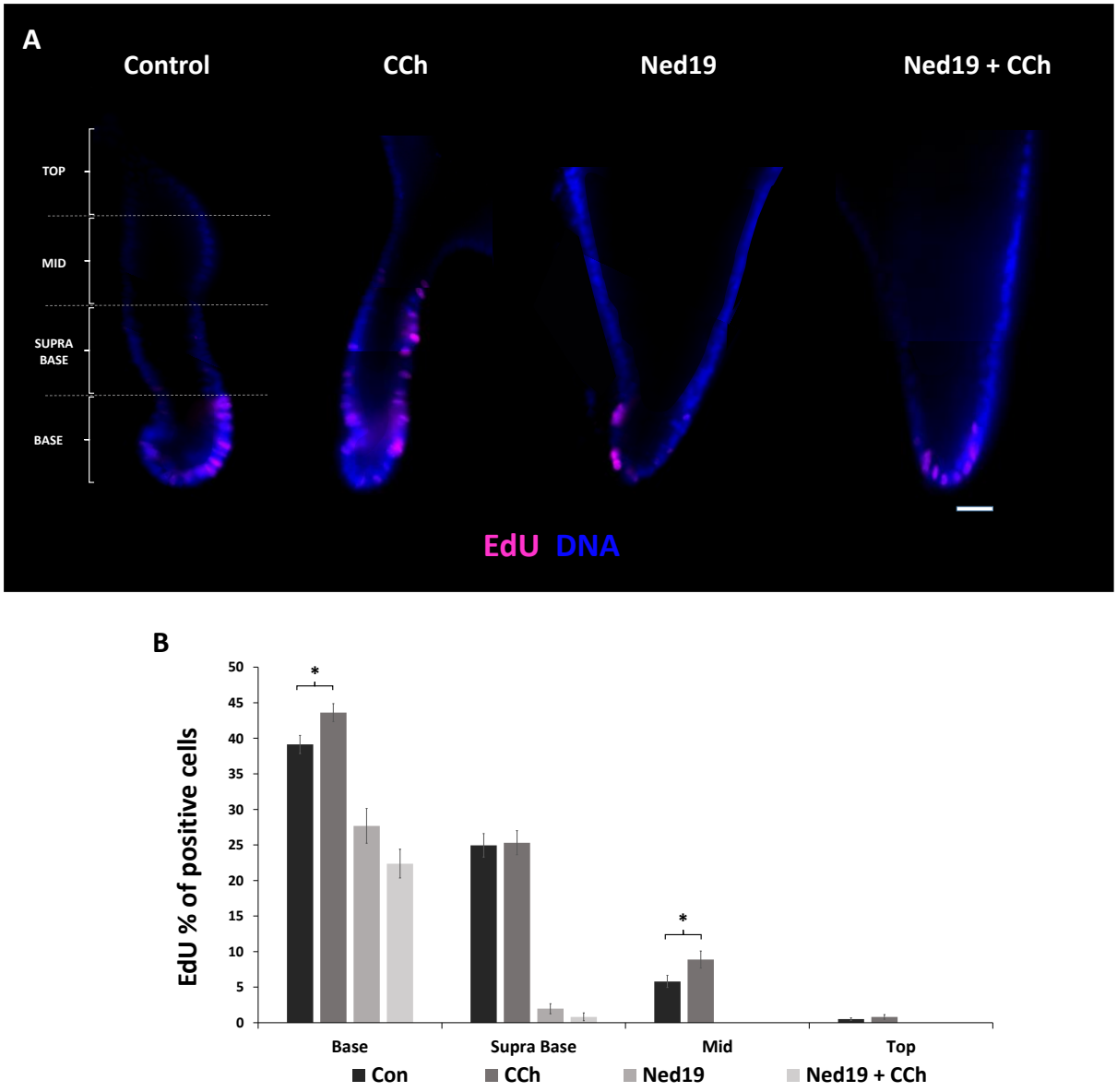

Figure 5.8. CCh-induced cell proliferation is dependent on TPC. (**A**) Representative epifluorescence images of colonic crypts labelled with EdU (pink). Scale bar 25 µm. (**B**) Bar chart indicates percentage of positive EdU cells across the different crypt regions as compared to the total number of nuclei stained with Hoescht (N=2, n≥15, *P<0.05).

5.2.4 Characterisation of the presence of proliferation-related transcription factors in colonic crypts

Calcium signals can activate intracellular calcium sensors such as calcineurin to induce nuclear translocation of transcription factors, some of which can signal cell proliferation. In order to test whether our culture system is endowed with such molecules, we analysed the expression of NFAT, TORC and YAP in the base of colonic crypts where stem cells reside. The isoforms NFATc3 (NFAT4), YAP1 and TORC1 (not to be confused with target of rapamycin complex 1) were used in this study

based on its consistent expression in human colon (Peuker et al., 2016; Schumacher et al., 2016; Wei et al., 2017). Immunofluorescence analysis of fixed samples showed the presence of all three in the cytoplasm and nucleus of the epithelial cells (**Figure 5.9**). Expression of TORC1 was found to be lower compared to NFATc3 and YAP1 and its location was abundant in the cellular apical membrane (**Figure 5.9ii**).

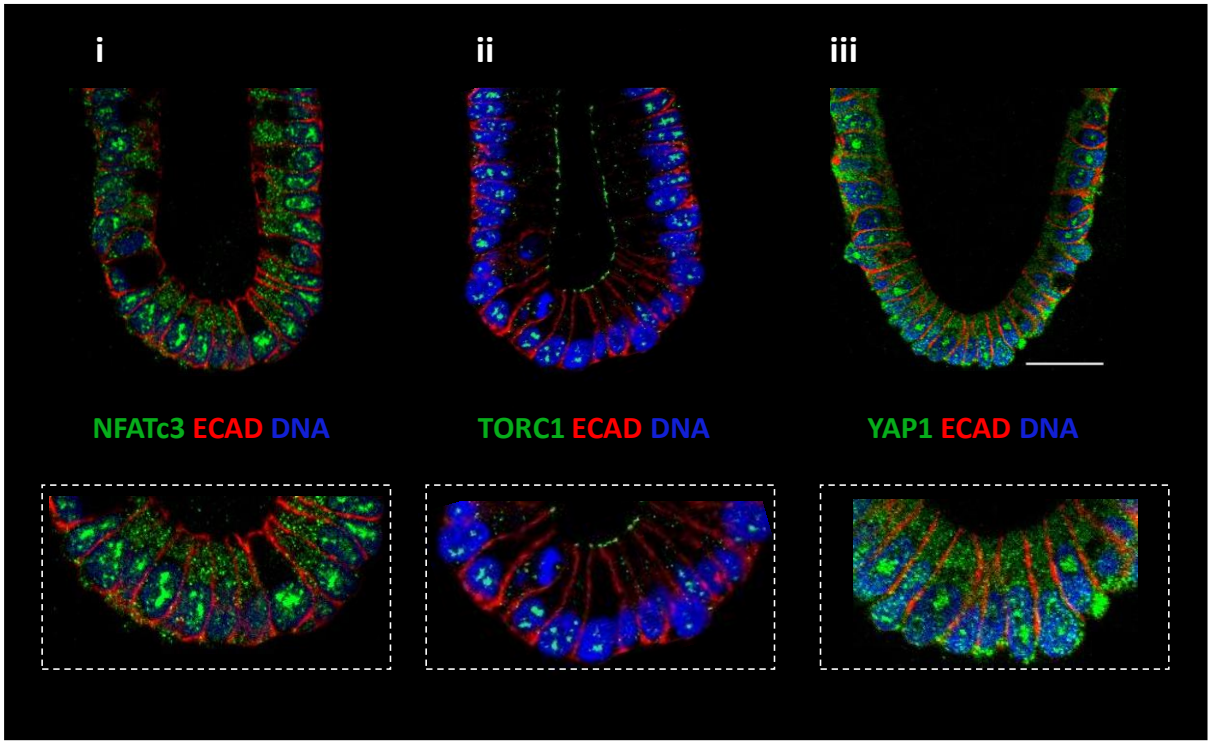

Figure 5.9. Colonic crypt expression of different transcription factors. Representative confocal images of the base of colonic crypts immunolabelled with NFATc3 (i), TORC1 (ii), and YAP1 (ii). Bottom, high magnification image highlighting cellular localisation. Scale bar 25 µm.

5.2.5 Muscarinic activation induces NFAT and YAP nuclear translocation

Nuclear translocation of NFAT can be induced by stimulation of muscarinic receptors 2 and 4 in lymphoid cells (Boss, Talpade and Murphy, 1996), however this mechanism has not been studied in the colon epithelium to our knowledge. We know from our previous results (**Chapter 3, Figure 3.28 and Chapter 4, Figure 4.12**) and literature (Lindqvist et al., 2002; Reynolds et al., 2007) that activation of muscarinic receptors induces an intracellular calcium signal and so we decided to investigate whether the nature of that signal can also induce nuclear translocation of NFAT in the stem cell niche. Because the kinetics of nuclear accumulation of transcription factors can vary depending on the nature of the stimuli (Bilgin et al., 2016), we performed a time course analysis where crypts were stimulated with CCh (10 µM) for 5, 15 and 30 minutes and then fixed and

immunolabelled. Confocal images revealed a more abundant nuclear concentration of NFATc3 in crypts stimulated for 15 minutes (**Figure 5.10A**), which was further confirmed by immunofluorescence measurement of the nuclear antibody intensity (**Figure 5.10B**).

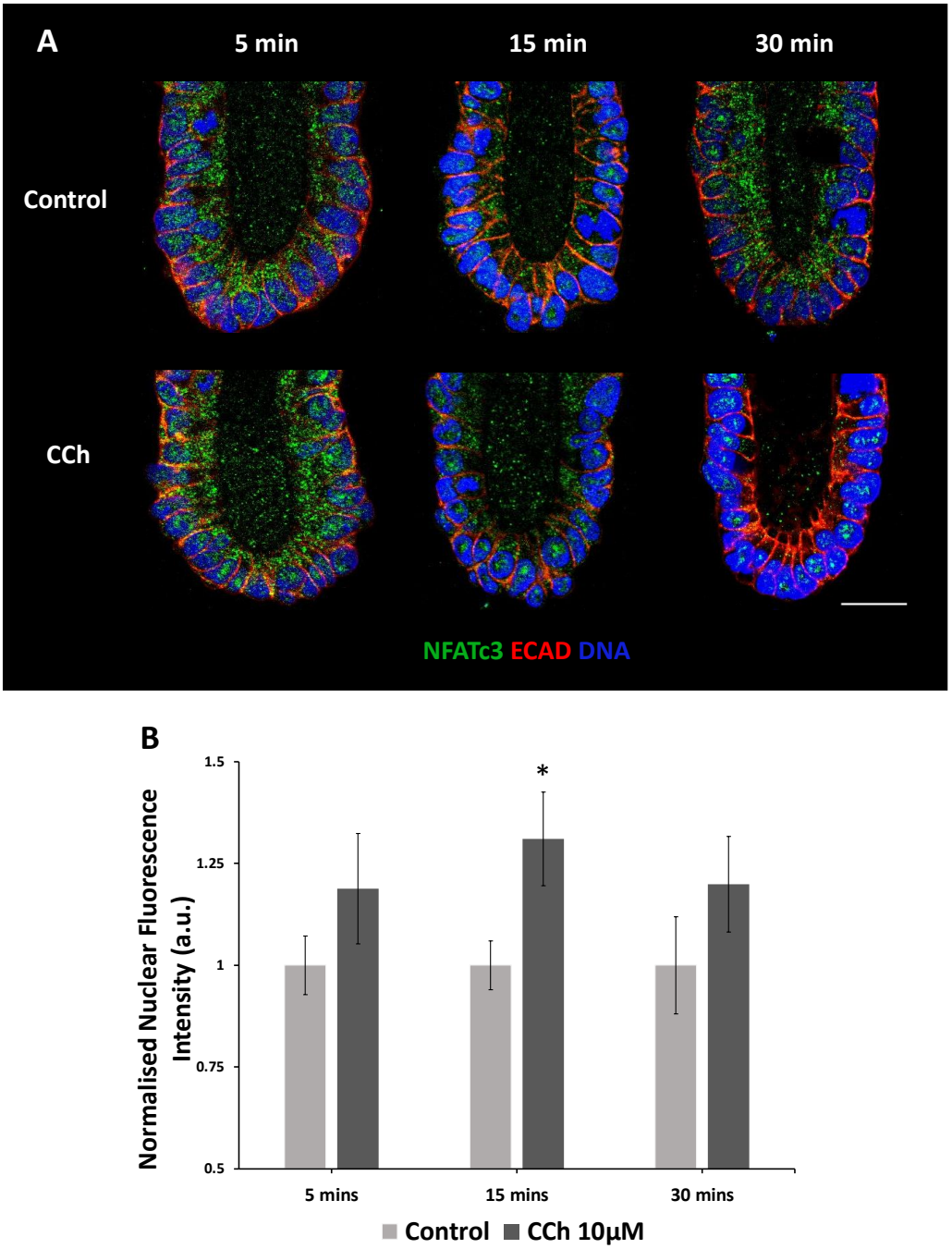

Figure 5.10. CCh stimulates NFATc3 nuclear translocation. (**A**) Confocal images illustrate NFATc3 cellular labelling (green) in control and CCh-stimulated colonic crypts at 5, 15 and 30 minutes. Scale bar 25 µm. (**B**) Nuclear fluorescence measurements reveal higher NFATc3 nuclear translocation 15

minutes post CCh stimulation. Fluorescence intensity was normalised to control (N=1, n=168, *P<0.05).

Similarly, muscarinic stimulation has been shown to induce YAP activation and translocation to the nucleus to regulate cell proliferation in the stomach epithelium (Hayakawa et al., 2016). In order to verify this mechanism in the colon, we stimulated cultured crypts with CCh (10 µM) for different time periods (5, 15 and 30 minutes) and observed the transcription factor nuclear mobilisation by immunofluorescence of fixed samples. Unlike the results detected in the NFATc3 analysis, the antibody labelling was found to be more intense after 5 minutes (which although not statistically significant, suggests a trend in nuclear translocation) and specially after 30 minutes of CCh stimulation (**Figure 5.11A**), which was confirmed by measurement of the nuclear fluorescence intensity (**Figure 5.11B**).

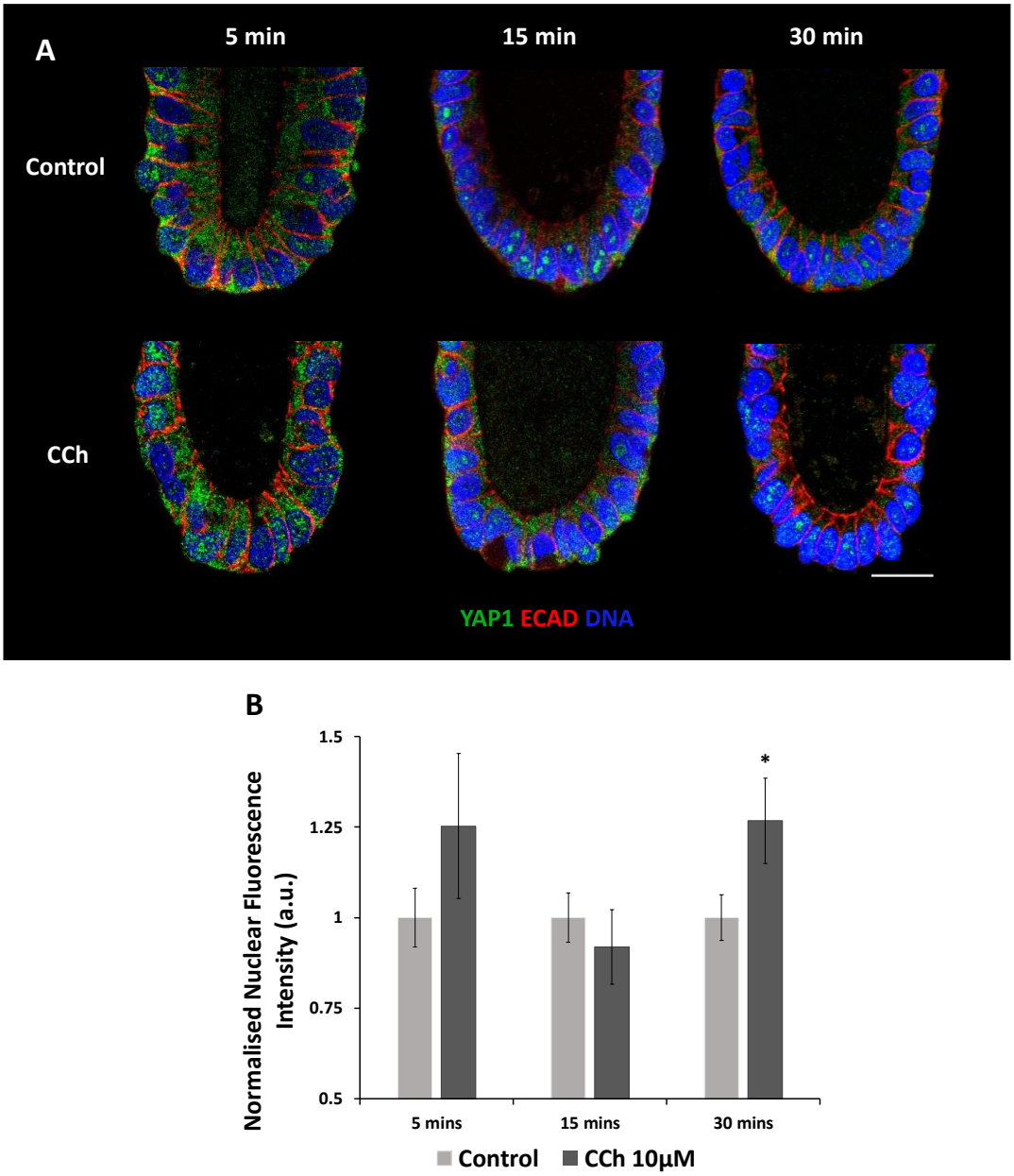

Figure 5.11. CCh induces YAP1 nuclear translocation. (**A**) Representative confocal images of the nuclear translocation of YAP1 (green) in stimulated and non-stimulated colonic crypt cells at different time points. Scale bar 25 µm. (**B**) Nuclear translocation is greater following 30 minutes of CCh stimulation. Fluorescence intensity was normalised to control (N=1, n=168, *P<0.05).

5.2.6 NFATc3 nuclear translocation is dependent on calcium release via TPC

Our recent findings suggest that muscarinic activation stimulates nuclear translocation of NFATc3 (**Figure 5.10**). Activation of NFATc3 has been shown to be dependent on intracellular calcium (Hogan et al., 2003) and as described previously (**Chapter 3. Figure 3.33**) we show that the muscarinic-induced calcium signal is dependent on release of calcium from the endolysosome via TPCs. To test

whether nuclear translocation of NFATc3 is mediated by calcium released from TPCs we pre-incubated colonic crypts with the calcium channel blocker Ned19 (250 µM) for 2 hours and analysed the potential nuclear translocation of NFATc3 after stimulation with CCh (10uM) for 15 minutes. Confocal analysis of immunolabelled crypts revealed the nuclear presence of the antibody in crypts pre-incubated with Ned19 and stimulated with CCh to be similar to that of control (**Figure 5.12A**). Further fluorescence intensity analysis showed that inhibition of TPCs reduces the CCh stimulatory response and prevents the nuclear translocation of NFATc3 (**Figure 5.12B**).

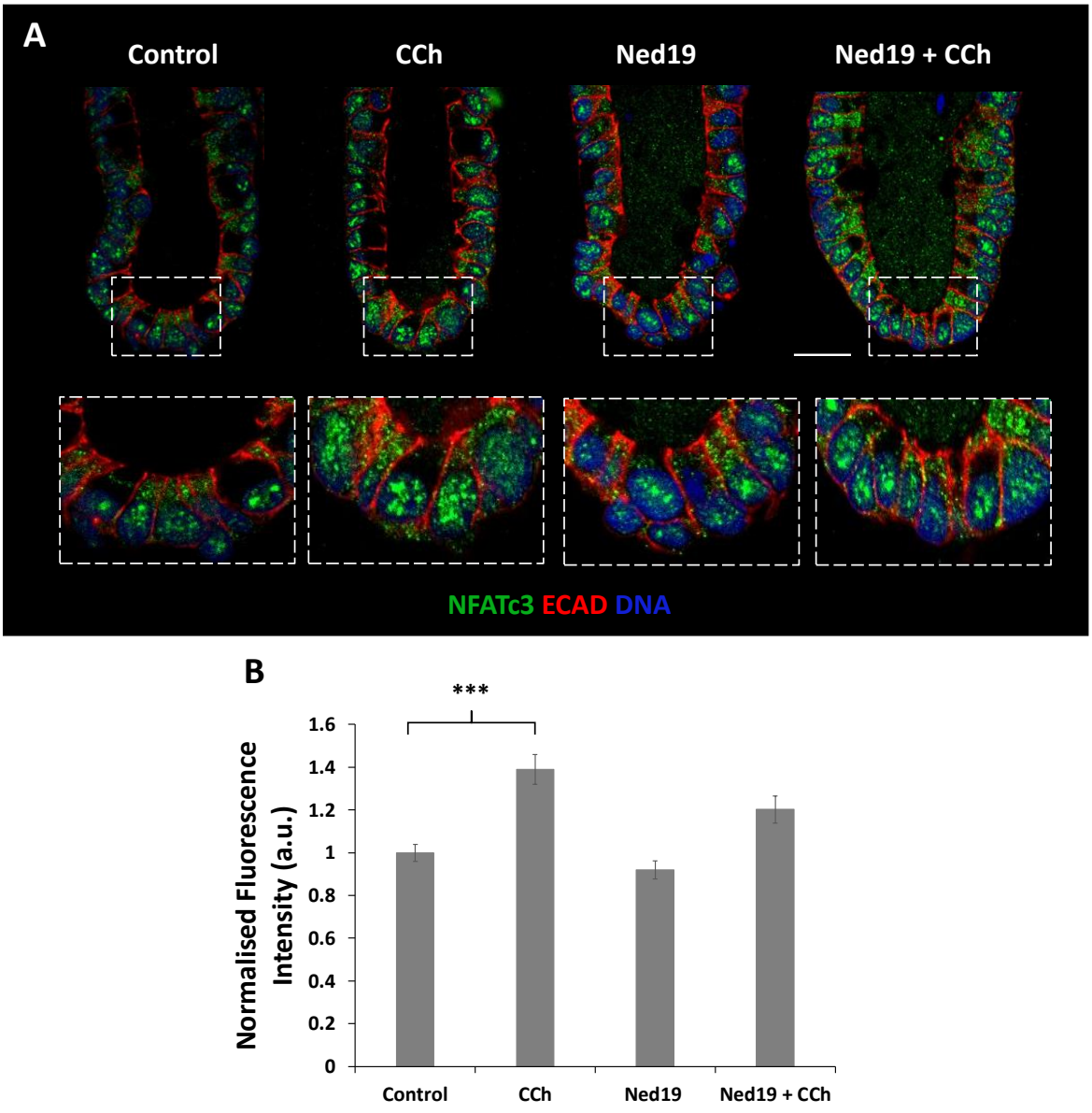

Figure 5.12. Ned19 blocks CCh-induced nuclear translocation of NFATc3. (**A**) Illustrative confocal images of the cellular presence of NFATc3 (green) in colonic crypts under different conditions. Bottom, high magnification images show nuclear presence of the antibody. Scale bar 25 µm. (**B**) Bar

chart shows reduction of the CCh-induced nuclear translocation of NFATc3 under the presence of Ned19. Fluorescence intensities were normalised to control. (N=2, n=168, *P<0.001).

5.2.7 NFATc3 nuclear translocation is dependent on calcineurin

Recent literature suggest that transcription of cell proliferation genes in stem cells is dependent on calcium-mediated CaN activation (Deng et al., 2015; Peuker et al., 2016). In colonic crypts, we have shown that muscarinic stimulation induces calcium release from the endolysosomes via TPCs. Recent literature shows that lysosomal calcium signalling can regulate CaN to promote activation of the transcription factor TFEB, to induce lysosomal biogenesis and autophagy (Medina et al., 2015). In order to analyse whether endolysosomal calcium signals mediate CaN-dependent transcription factor translocation to the nucleus in the stem cell niche, we blocked CaN and analysed the capacity of NFATc3 to translocate to the nucleus after stimulation with CCh. To this end, colonic crypts were pre-incubated with the selective inhibitor of CaN, CN585 (60 μM) (Erdmann et al., 2010) for 2 hours and subsequently stimulated with CCh (10 μM) for 15 minutes. Confocal imaging of NFATc3 immunolabelling revealed similar antibody labelling intensity between control and CNC585 pre-incubated crypts simulated with CCh (**Figure 5.13A**) and measurements of fluorescence intensity showed CCh simulation of NFATc3 nuclear translocation is prevented when CaN is inhibited by CN585 (**Figure 5.13B**).

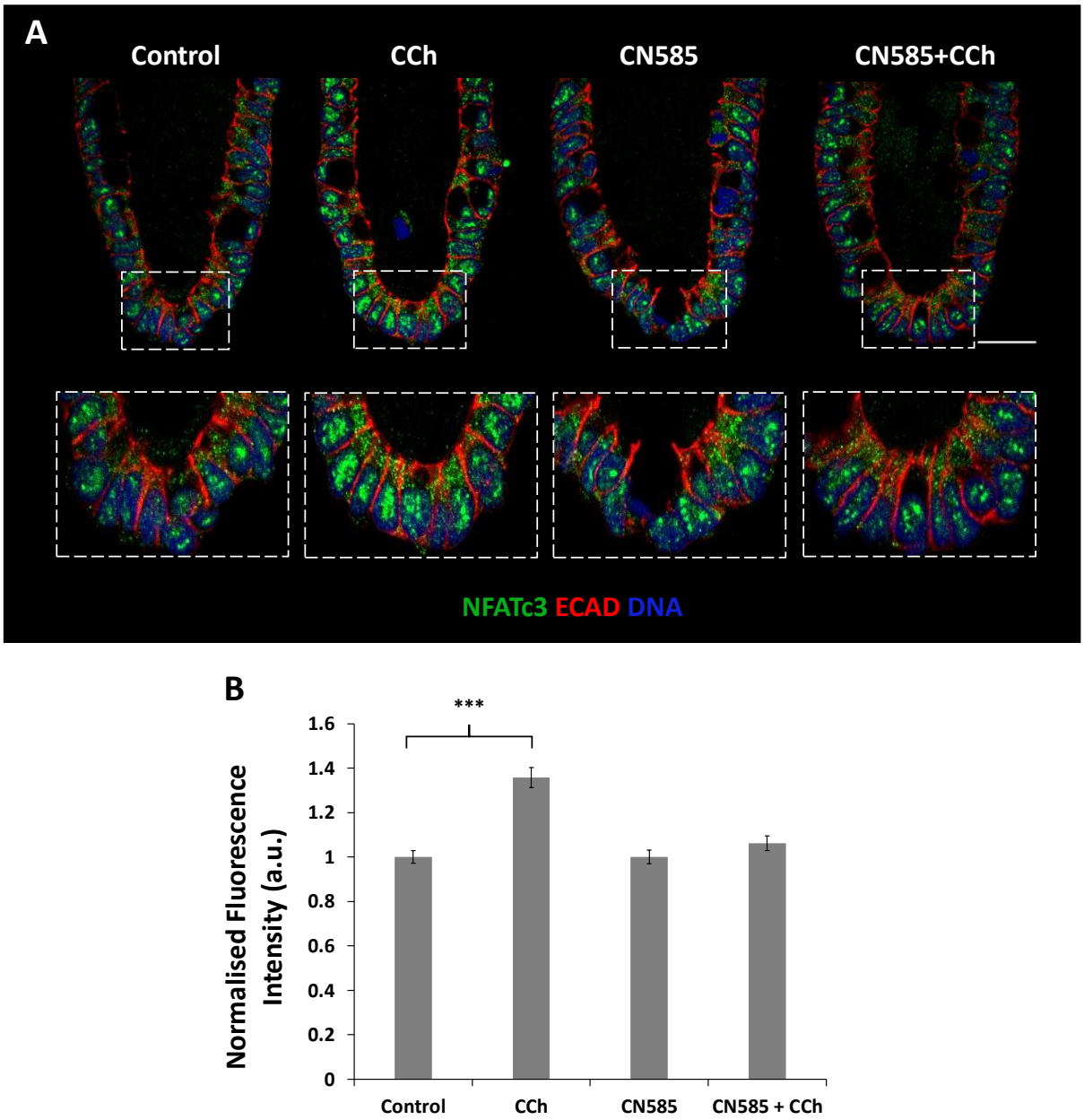

Figure 5.13. CCh-stimulated nuclear translocation of NFATc3 is dependent on CaN. (**A**) Illustrative confocal images of the cellular presence of NFTAc3 in colonic crypts under different conditions. Bottom, high magnification images indicate NFATc3 nuclear abundance. Scale bar 25 µm. (**B**) CaN is needed to activate NFATc3 nuclear internalisation following CCh stimulation. Fluorescence intensity was normalised to control (N=2, n=168, *P<0.001).

5.3 Discussion

In this chapter we have evaluated the role of intracellular calcium in regulating stem and progenitor cell proliferation and tissue growth. Our results suggest that neuronal and/or non-neuronal ACh released in the stem cell niche can be sensed by stem and progenitor cells to induce an intracellular calcium response that is dependent on calcium release from the endolysosomes via TPCs. Endolysosomal calcium signals act on the calcium sensor CaN which in turn activates the nuclear translocation of transcription factors to potentially promote expression of cell proliferation-related genes. These findings suggest a new role for ACh in regulating the colon epithelium by promoting stem-cell driven tissue regeneration. In addition, we highlight the importance of intracellular calcium in integrating proliferation-related signals to regulate gene expression in the stem cell niche of colonic crypts.

5.3.1 Human cultured colonic crypts and organoids retain stem cell expression.

In this chapter we confirm the presence of stem cells in colonic crypts and organoids. Ki67 immunolabelling results indicate that proliferative cells are located in the lower regions of the crypt (**Figure 5.2**). Stem cell markers LGR5 and PTK7 as well as OLFM4 (**see Chapter 3, Figure 3.11**) were found to label the basolateral membranes of epithelial cells at the base of colonic crypts which is consistent with the existing literature (Barker et al., 2007; Jung et al., 2015). The presence of these markers in the stem cell niche confirms our previous gene expression results (**Chapter 3, Figure 3.4**). In addition, we have validated a new method for live immunolabelling of stem cells, which to our knowledge has not been reported before. We show that live immunolabelling can be a useful technique for the detection of markers with low membrane expression due to receptor internalisation (**Figure 5.3**). In particular, LGR5 has been shown to be rapidly and constitutively internalised to the Golgi network (Snyder et al., 2013), which suggests a mechanism for the stem cells to regulate Wnt signalling and prevent overstimulation of cell proliferation and tumorigenesis (Morgan, Mortensson and Williams, 2018). In this scenario, antibody labelling prior to fixation of freshly isolated crypts ensures binding to the antigen that could otherwise be lost by protein internalisation or damaged after fixation. Our results also show PTK7 presence in cultured colonic crypts by imaging of the immunolabelled marker (**Figure 5.3C**). To our knowledge, the existing literature only reports its expression in immunolabelled tissue sections, which highlights the novelty of our finding. In addition, we show that PTK7 can also label individual cells along the crypt axis. According to the literature, PTK7 can be also expressed by a small subset of $CHGA^+$ progenitor cells undergoing differentiation towards the enteroendocrine lineage (Jung et al., 2015). Overall, the

presence of stem cells demonstrates that our culture models are capable of driving the renewal of the colon epithelium.

5.3.2 Acetylcholine promotes cell proliferation and tissue growth in the colon epithelium

Muscarinic stimulation of colonic organoids with the ACh analogues CCh and Oxo promotes tissue growth. ACh has been shown to be secreted by cholinergic neurons as well by tuft cells of the colonic epithelium (Furness, 2012; Nevo, Kadouri and Abramson, 2019). In the stomach, researchers have identified that ACh-mediated stimulation of muscarinic receptor type 3 (MAChR3) stimulates Wnt and Yap signalling to promote cell proliferation in $LGR5^+$ cells under homeostasis, which can lead to tumorigenesis under aberrant signalling (Zhao et al., 2014; Hayakawa et al., 2016). We have previously shown that both cultured colonic crypts and organoids express all muscarinic receptors including MAChR3 and that this one is prominently expressed in the stem cell niche (**Chapter 3, Figure 3.19**). To date, no one has studied the effect of ACh in cell tissue growth of human colonic organoids. Previous research in mouse small intestine has suggested that ACh can signal through nicotinic ACh receptors to induce Wnt signalling and regulate intestinal cell proliferation (Takahashi et al., 2018). Our results show that stimulation of muscarinic receptors with CCh induces organoid growth (**Figure 5.4**). In addition, tissue growth is also induced in the presence of Oxo, which suggests this process is mediated by muscarinic receptors only (**Figure 5.6**). Crypt formation in the normal colonic epithelium requires a tight balance between cell proliferation and cell differentiation that is achieved through signalling gradients. Wnt and Notch signalling promote cell proliferation of $LGR5^+$ stem and progenitor cells at the base of the crypt, whereas BMP and TGFβ signals induce differentiation in upper regions (Gehart and Clevers, 2019). In our organoid system, the standard culture conditions conserve a differentiated cell diversity where the majority of organoids develop fully functional crypt-like structures or buds (**Figure 3.2**). Organoid crypt formation is a mechanism that has not been fully investigated. Studies in mouse colonic organoids suggested that organoid bud formation is dependent on the presence of epidermal growth factor (EGF) and independent of Wnt signals (Yip et al., 2018), however, mouse and human organoids have different culture requirements (Sato et al., 2011). In this chapter we show that in addition to tissue growth, stimulation with CCh also induces bud formation in colonic organoids (**Figure 5.5**), which suggests that ACh could act as growth factor in the colon epithelium promoting tissue regeneration. Following stimulation with Oxo, we did not observe any major changes in the number of buds compared to control. Increased cell proliferation and decreased budding is a hallmark of increased Wnt signalling that may result from chronic activation of muscarinic receptors by Oxo. Future studies will investigate this prospect.

The human colon presents two known sources of ACh, cholinergic neurons and tuft cells and as suggested in the literature, MAChR3 activation by ACh can activate epithelial proliferation and stem cell division during mucosal regeneration (Hayakawa et al., 2016). In this scenario, tuft cells, which have been linked to luminal sensing of bacterial metabolites (Schneider et al., 2018; Nadjsombati et al., 2018) could trigger the secretion of ACh in response to infection and tissue damage, and signal to other cholinergic neurons or directly to stem cells in a paracrine fashion to induce stem cell proliferation and tissue regeneration.

5.3.3 Calcium signals dependent on TPCs mediate cell proliferation

We have previously shown that CCh stimulation of muscarinic receptors induces an intracellular calcium signal which we suggest originates in the apical pole of stem cells (**Chapter 4, Figure 4.12**). This calcium signal is mediated by calcium release from the TPCs present in the endolysosomes (**Chapter 3, Figure 3.33**). Characterisation of the muscarinic-calcium toolkit revealed the presence of endolysosomal TPCs in the apical pole of stem cells (**Chapter 3. Figure 3.27**). We hypothesised that this calcium signal regulated by TPCs could modulate stem cell biology. In this chapter we demonstrate that CCh activates cell proliferation by stimulating the cell cycle as judged by the number of EdU positive cells (**Figure 5.8**). This result correlates with the increase in organoid size previously reported and strongly suggests a role for muscarinic activation in promoting tissue growth. Calcium signals originating from endolysosomes of endothelial cells have been implicated in promoting cell proliferation following growth factor stimulation of membrane receptors (Favia et al., 2014). Favia et al. demonstrated that Ned19 blocks endolysosomal calcium release resulting in the reduction of different markers of cell proliferation. In our studies we find that inhibition of TPCs with Ned19 blocks CCh-induced cell proliferation (i.e. EdU nuclear incorporation) suggesting that these calcium channels are implicated in the muscarinic response that regulates stem cell biology (**Figure 5.8**). Together with Ned19, we have demonstrated that TPC blockers Tetrandrine and Verapamil also inhibit the cholinergic-induced calcium response (data not shown). While its effects on organoid growth, cell proliferation and nuclear translocation of transcription factors have not been addressed in this thesis, we hypothesise that the results will be similar to those of Ned19, highlighting the key role of TPCs in regulating stem cell biology and tissue regeneration.

Cell proliferation is dependent on transcription factor activation of proliferative genes which in stem cells include those who regulate the Wnt signalling pathway like LGR5, β-catenin, PTK7 or ASCL2 (Barker et al., 2007; Jung et al., 2011; Jung et al., 2015; Schuijers et al., 2015). Several transcription factors have been reported to be implicated in cell proliferation (Deng et al., 2015; Hayakawa et al., 2016; Peuker et al., 2016; Tripathi et al., 2014; van der Flier et al., 2009; Vu et al., Ghosh, 2013; Wu

et al., 2018). In this chapter we demonstrate the presence of NFATc3, YAP1 and TORC1 in the cells of the stem cell niche of colonic crypts (**Figure 5.9**). The activity of NFATc3 and TORC1 has been shown to be regulated by calcium (Deng et al., 2015; Peuker et al., 2016), while ACh has been shown to modulate YAP1 activity (Hayakawa et al., 2016). Therefore, the characterisation of their presence in our culture system makes them good candidates for the study of the muscarinic signals and its effect on calcium-dependent cell proliferation. Following stimulation with CCh, we show an increase in nuclear translocation to the nucleus of NFATc3 and YAP1 which suggests that these transcription factors are controlled by muscarinic activation (**Figure 5.10 and Figure 5.11**). Interestingly, our results indicate variations in their location levels, which peak at different time points in the presence of the same stimuli. Literature suggests that the time required for a transcription factor to enter the nucleus is different between molecules and is also dependent on the nature of the stimuli. Based on our results that show the muscarinic-induce calcium response propagates rather quickly through the cell (**Chapter 4. Figure 4.12**), we assumed that the kinetics of transcription factor translocation under muscarinic stimulation to be a rapid event and decided to analyse the transcription factor presence during the course of 30 minutes. Our findings show that following CCh stimulation, NFATc3 presence in the nucleus is enhanced throughout the different time points but becomes maximal at 15 minutes. These results suggest that CCh is a potent activator of NFATc3, which becomes apparent soon after muscarinic stimulation and is maintained throughout the course of 30 minutes (**Figure 5.10**). Conversely, the kinetics of YAP1 activation differ to those of NFATc3 since we report a quick increase in nuclear translocation 5 minutes post CCh stimulation, which although it does not reach statistical significance, suggests the presence of an increasing trend. Importantly, this increase in YAP1 nuclear translocation returns to basal levels at 15 minutes to be followed by a maximal increase in nuclear translocation 30 minutes after CCh stimulation, suggesting a complex regulatory mechanism (**Figure 5.11**). Preliminary chronic stimulation with CCh has given rise to colonic crypt calcium oscillations with a frequency of 14 minutes (unpublished). Transcription factor activation of gene expression is a very tightly regulated mechanism and cells can mediate its nuclear export by inactivation or degradation to prevent gene over-expression (Mognol et al., 2016). Our confocal live imaging results showed the propagation of the intracellular calcium signals from the apical pole across the cell and into the basal nucleus (**Chapter 4. Figure 4.12**). However, the role for nuclear calcium levels in regulation of transcription factor translocation and activation has not been assessed.

In this study we also demonstrate that activation of TPCs is needed for NFATc3 to translocate to the nucleus following stimulation with CCh. The existing literature indicates that nuclear import of NFAT following GPCR activation is dependent on calcium influx into the cytoplasm via SOCE, which in turn

is activated by calcium release from the ER (Mognol et al., 2016). Our findings suggest that inhibition of TPCs with Ned19 blocks the nuclear translocation of NFATc3, indicating that the calcium signals evoked by these channels are required to enable the mobilisation of the transcription factor to the nucleus (**Figure 5.12**). In addition, we show that following muscarinic activation, nuclear translocation of NFATc3 is dependent on CaN. Blocking CaN with the selective inhibitor CN585 prevents the transcription factor from entering the nucleus. CaN can be activated by an increase in cytosolic calcium, either by direct binding of the molecule or by interaction with calcium-activated calmodulin (Rusnak and Mertz, 2000). Our results show that muscarinic stimulation is needed to induce an intracellular calcium signal that can elevate the calcium cytoplasmic levels required for calcineurin activation (**Figure 5.13**). A schematic of these results is shown in **Figure 5.14.** While other techniques have been used in the past to study the kinetics of transcription factors (Mueller et al., 2013), in this thesis we have also demonstrated that measurement of fluorescence intensity of immunolabelled transcription factors is a useful tool for the analysis of the kinetics of nuclear translocation in colonic cultured crypts. In addition to the previous findings on NFATc3, follow up studies are needed to confirm whether the proposed calcium signalling mechanism regulates the translocation to the nucleus of YAP1 and TORC1 in stem cells in the presence of ACh.

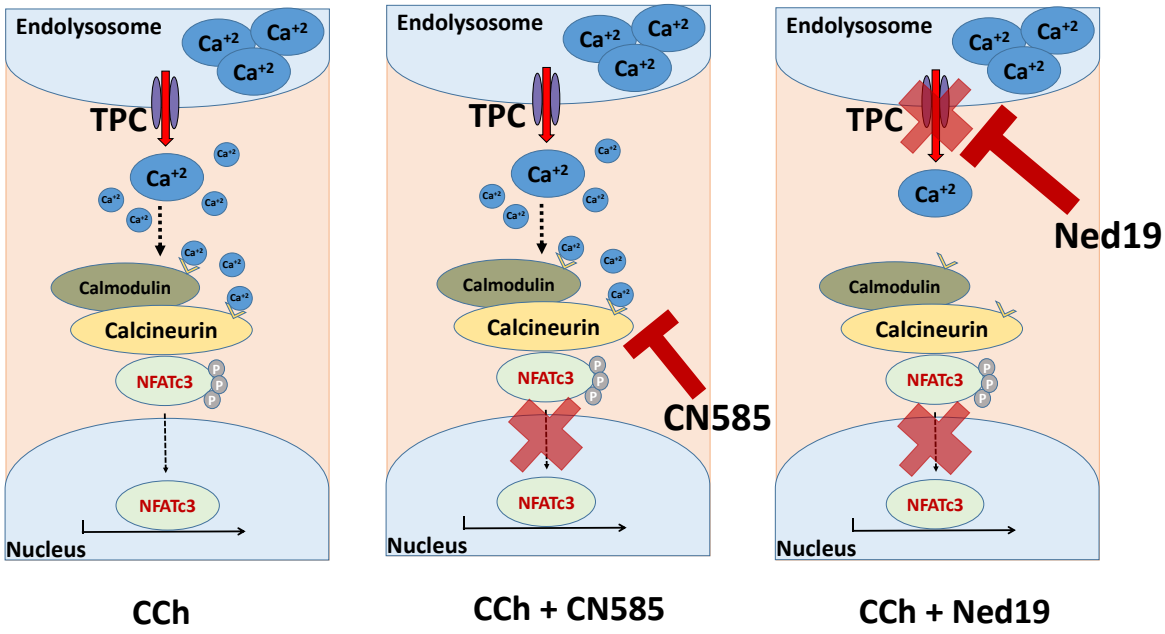

Figure 5.14. Nuclear translocation of NFATc3 is mediated by calcium signals originated by activation of TPCs. Left, CCh induces NFATc3 translocation via activation of calcium release via TPC. Middle, CN585 blocks CCh-induced nuclear translocation. Right, Ned19 blocks CCh-induced nuclear translocation.

5.3.4 Limitations of the study

NAADP has been postulated as the major activator of calcium release from the endolysosomes (Calcraft et al., 2009). The direct role of NAADP in activating TPCs has not been able to be assessed in this thesis due to the limitations in the use of this molecule. Since NAADP is not cell-permeant, its entry through the plasma membrane is impeded. Alternative techniques such as direct cellular delivery by injection constitute another possibility, although the penetration of the cell by a glass needle can in it itself induce an increase in cytosolic calcium. Recent reports suggest the use of the chemically synthesised acetoxylmethyl ester of NAADP (NAADP-AM) to overcome the cell permeability issue (Parkesh et al., 2008). However, previous studies in our lab have tried to modulate calcium release from the endolysosomes with the use of NAADP-AM but have been unsuccessful (data not shown). In addition, the mTORC inhibitor rapamycin has been postulated as an alternative TPC activator. Ogunbayo and colleagues showed that different concentrations of this molecule can elicit calcium responses of different frequency and intensity that localise to the endolysosomes of HEK293 cells (Ogunbayo et al., 2018). Recent work with rapamycin in our lab was not able to reproduce those results in colonic crypts and organoids (data not shown); therefore, a selective TPC activator is desirable to support the above studies. Subsequent experiments with the use of a molecule capable of directly stimulating TPCs would further confirm the implication of these channels in the signal pathway that induces stem cell to proliferate. On the other hand, we have previously showed that stem cells are endowed with a muscarinic-calcium signalling toolkit (**Chapter 3, Figure 3.26**). By confirming the expression of CD38, we postulate that stem cells have the capability to generate NAADP to activate TPCs. Measurement of elevated NAADP levels in this context is also desirable.

Calcium release initiated from the endolysosomes has been reported to trigger ER-mediated calcium release to amplify the signal (Morgan, 2016). Our studies on the regulation of the calcium signals that induce mucus and fluid secretion in colonic crypts suggest that IP3Rs and RyRs are directly implicated in amplifying the calcium signals evoked by release of calcium from the endolysosomes (**Chapter 4, Figure 4.15 and 4.16**). The receptor IP3R3 has been shown to be present in the apical membrane of cells in the stem cell niche (**Chapter 3, Figure 3.23**) which indicates that this cross-talk between endolysosomes and ER could potentially take place in stem cells as well. Further experiments targeting the ER are needed to elucidate whether this calcium store is involved in the intracellular cell signal that drives stem cell proliferation in the colon epithelium. In this way, we have planned to target these receptors pharmacologically using inhibitors of IP3Rs and RyRs in a similar approach to the one used for the study of mucus secretion. Moreover, we intend to inhibit

the expression of these calcium channels as well as the TPCs genetically using small interfering RNA (siRNA) in colonic organoids. By doing so, we expect to evaluate the direct implication of each channel in response to muscarinic activation to complement the existing findings. In addition, we would also like to study how the ACh induced signal pathway modulates gene expression. It remains to be elucidated which genes are upregulated following the ACh→TPC→CaN→NFATc3 signalling pathway. Using qRT-PCR on organoid samples, we expect to compare the differences in gene expression of canonical stem cell markers such LGR5, ASCL2, OLFM4 and PTK7, which we have previously shown to be present in our culture system. As described in Chapter 3 (**Figure 3.2**) we have developed a single cell culture system of epithelial colonic cells. Follow up studies are aimed to confirm whether ACh promotes stem cell proliferation by assessing the capacity of single cells to form organoids.

5.4 Conclusion

Human colonic crypts and organoids respond to ACh by inducing cell proliferation of progenitor and stem cells, and tissue regeneration. These cells integrate the ACh signal through the endolysosomal TPCs located in the apical pole of the cell. Calcium release from TPCs activates the calcium sensor calmodulin which promotes nuclear translocation of transcription factors to induce cell proliferation in stem cells. The outcome of this study underscores the importance of ACh as an important regulator of the colonic epithelium regeneration and emphasises the relevance of calcium as an integrator of growth and proliferation signals. Future work is needed to investigate the status of the cholinergic coupled calcium signalling pathway with respect to ageing, cancer and inflammatory bowel disease.

6 Chapter 6. General discussion and Future work

During the course of this thesis a number of important findings have helped elucidate some of the mechanisms that regulate the physiology of the colonic epithelium. This study proposes that cholinergic input protects the stem cell niche by inducing mucus and fluid secretion (**Chapter 4**) and promoting tissue renewal (**Chapter 5**). A subpopulation of guardian goblet cells has been demonstrated to reside at the base of colonic crypts and are stimulated by ACh to secrete fluid-rich mucus to clear bacteria, safeguard the stem cell niche and maintain homeostasis (**Chapter 4**). This study also provides new insights on the intracellular transduction of the ACh signal and identifies the endolysosomal TPCs as a key mediator of goblet and stem cell physiology. These findings confirm the importance of calcium as a signal integrator and its versatility to control different cellular processes. Furthermore, this study describes the development of a human organoid culture system derived from primary colonic tissue which largely recapitulates the *in vivo* cellular diversity and physiological functions of the human gut epithelium and validates organoids as an important tool for the study of colon physiology in health (**Chapter 3**). The novel findings present in this thesis provide new insights into the regulation of the gut epithelium and establish a new platform for the study of colonic diseases such as inflammatory bowel disease and cancer.

6.1 Development of an organoid culture as a model system for the study of the human colonic epithelium

The development of 3D culture systems of gut epithelial cells, known as gut organoids, has helped to bridge the gap between the 2D cell culture and live tissues by creating a platform that recreates the *in vivo* like tissue architecture. Gut organoids are grown in a gel where they can present adhesions distributed in all 3 dimensions and are able to generate epithelial cell polarity, maintain cell-to-cell and cell-to-matrix communication in a relatively low stiffness environment, similar to the one present in tissues. These characteristics allow the organoids to recapitulate tissue topology where the hierarchy of stem cell-driven tissue renewal is maintained (Reynolds et al., 2013; Date and Sato, 2015; Almeqdadi et al., 2019).

The colon epithelium is formed by a monolayer of cells organised in flask-like invaginations called crypts. This tissue is organised in such way to protect the stem cells that reside at the base and minimise their exposure to luminal hazards. The morphological analysis of our organoid cultures reveals the presence of crypt-like structure of buds which recreate the *in vivo* structure. Because of the harsh luminal environment that the epithelial cells are exposed to, they have a very short life and are sloughed-off from the luminal surface after 5-7 days (Gehart and Clevers, 2019). Colonic

stem cells are constantly proliferating to produce new cells that can restore the natural cell loss in a process of tissue renewal. In our organoid model, the buds grow bigger over time by expanding the crypt-like axis longitudinally which confirms the capability of the culture system to recapitulate crypt cell renewal/regeneration along the axis. In addition, the presence of a luminal bud in organoids is indicative of functional cell polarity where the various organelles and cellular machinery is organised differently along the cell axis. This observation was further confirmed by immunofluorescence analysis of membrane protein localisation of markers of basal cellular membrane (e.g. muscarinic receptors), cytoplasm (e.g. mucus), apical membrane (e.g. CD38) as well as nuclear positioning at the basal pole of the cell.

The colonic epithelium is comprised of different cell types that originate from the stem cells at the base of the crypt and are able to perform the different tissue functions. Organoids that lack cellular diversity develop into spheres or cysts. Our observations at the gene and protein level confirm the presence of all cell types, which suggests they can potentially recapitulate all the tissue physiological functions including hormone secretion, nutrient absorption and mucus release (**Chapter 3**). Of all cell types, we were not able to confirm the presence of the canonical tuft cell marker ChAT (mediator of the production of ACh), as the presence of this enzyme was not found in both the gene expression and immunolabelling assays, while it was reported in cultured colonic crypts. A possible explanation could be that mature tuft cells are not expressed in our culture system. However, our gene expression analysis did reveal the presence of another tuft cell marker, POU2F3, which has been reported to be expressed in human colonic organoids by other groups (Fujii et al., 2018) and VAChT which mediates the transport of ACh to the secretory vesicles in neurons. The function of the latter has only been characterised in cholinergic neurons and its role in tuft cells remains to be elucidated. Experiments are underway to restore lineage specification of Tuft cells in the organoid culture system.

The use of next generation RNA sequencing for gene expression profiling allowed us to compare which genes are active and how much they were transcribed between our culture systems (crypts and organoids) and also in comparison to patient-matched native colonic mucosa tissue samples. While the analysis of these results was presented as a comparison between samples of the number of reads registered for each candidate gene transcript (i.e. the number of times our transcript was amplified), using a more sophisticated bioinformatic analysis, this complete dataset can also be subjected to cluster analysis. The use of algorithms like the principal component analysis (PCA) allows comparative gene expression to be visualised in a simple 2D scatter plot according to the level of similarity in gene expression (Son et al., 2018). In view of our results we hypothesise that the analysis of the complete RNAseq data set for organoids, isolated crypts and the native colonic

mucosa would generate clusters for colonic crypts and organoids that would locate in close proximity.

Alongside the validation of our organoid system at the gene and protein level, we find that these cultures also recapitulate the physiological processes observed in cultured crypts. In this regard, we show that organoids are able secrete mucus and release fluid (**Chapter 4**). Analysis of goblet cell depletion after muscarinic activation with CCh rendered similar results to those observed in cultured crypts, which indicates the presence of the same regulatory pathway. Organoid swelling induced by CCh correlates with liquid secretion from the epithelium, which is a mechanism used by the tissue to expel noxious substances from the crypt lumen. Our findings are indicative of the presence of the same machinery that mediates liquid transport *in vivo*. In the Williams lab we have previously confirmed that the study of the intracellular calcium signals with calcium fluorescence indicators is a highly reproducible methodology (Lindqvist et al., 2002; Reynolds et al., 2007). Cultured colonic crypts from different patients elicit similar calcium responses when stimulated with the same agonists. Our findings on the study of the intracellular calcium signals induced by ACh in organoids show equivalent results to those performed in cultured crypts, which confirms the conservation of a native physiological regulatory pathway in organoids. In addition, it further reinforces the use of calcium signalling measurements as a robust readout for the study of gut biology in health and disease.

Another important feature of this culture system is the possibility to propagate organoids indefinitely while retaining the same phenotypic signatures. In our lab we have successfully cultured organoids for over a year and confirmed their phenotypic and physiological stability by analysing morphology, cell diversity and intracellular calcium signals. While the genetic variability of organoids during time has not been assessed, RNAseq results reveal high similarities in gene expression. In addition, previous research has addressed this matter and confirmed that organoids are genetically stable over time (Sato et al., 2011). While colonic organoids can routinely be passaged, we have also generated a cryopreserved library or biobank of each of the samples. In our observations, the freeze-thaw process does not damage the integrity of the organoid and following thawing they have a short recovery period. These characteristics provide us with immediate availability of tissue sample and the possibility to study the same tissue sample at different periods of time.

A key attribute of the organoid system is the ability to manipulate the genetic identity of the epithelial cells. Genetic engineering of organoids can be achieved by different ways including the use of CRISPR/Cas technology. This form of gene editing has quickly become very popular owing to its high efficiency and specificity in targeting the DNA. One of the main interests in the lab is the

possibility to study mucus generation and secretion in real-time, in order to comprehend the spatio-temporal characteristics of this phenomena, as well as to understand the functioning of the intracellular pathway that regulates it. To this end, we have started to develop a vector containing a fluorescence reporter to be inserted in the gene MUC2, which is the main glycoprotein constituent of mucus in the goblet cells of the colon (**APPENDIX B**). In addition, CRISPR/Cas9 technique permits high efficiency gene knock outs to be generated to study the role of candidate genes in gut health and disease. Future studies could be aimed at targeting the key elements suggested to be involved in mucus secretion like the muscarinic-calcium toolkit components to further elucidate its role. Moreover, recent literature has demonstrated the possibility of using CRISPR/Cas technology in organoids for modelling intestinal diseases (Schwank et al., 2013). This finding opens the possibility for the study of candidate genes for colorectal cancer. Using CRISPR/Cas gene editing in organoids, it is possible to induce mutations in genes that are generally found upregulated in cancer and analyse their capacity to form tumours in culture, independently of the standard growth factors (Matano et al., 2015).

The study and development of personalised medicine is one of most promising features of research using organoids as a model. Organoids can be grown from tissue samples of patients suffering from a disease (e.g. colorectal cancer) and be treated with different drugs to find a best candidate. Owing the fact that organoids do not require long culture times and the possibility to scale up the numbers, this culture model becomes an ideal platform to study patient-personalised drugs and treatments.

In this thesis we confirm the organoid culture as powerful tool for the study of cell and tissue biology and we highlight the relevance of this model for investigating gut physiology. A general summary of the current applications of this model and its futures uses is displayed in **Figure 6.1**.

Although this model has been proven extremely useful for the study of the regulation of the colon epithelium, this system still carries some disadvantages. The materials needed for generating this model, in particular Matrigel, make it an expensive culture system. In addition, Matrigel is formed of extracellular matrix proteins (laminin and collagen mainly) derived from mouse which contain a certain number of growth factors of unknown concentration. To overcome these limitations, the Williams lab is currently developing an alternative matrix that can support the 3D growth of colonic organoids maintaining the tissue physiology.

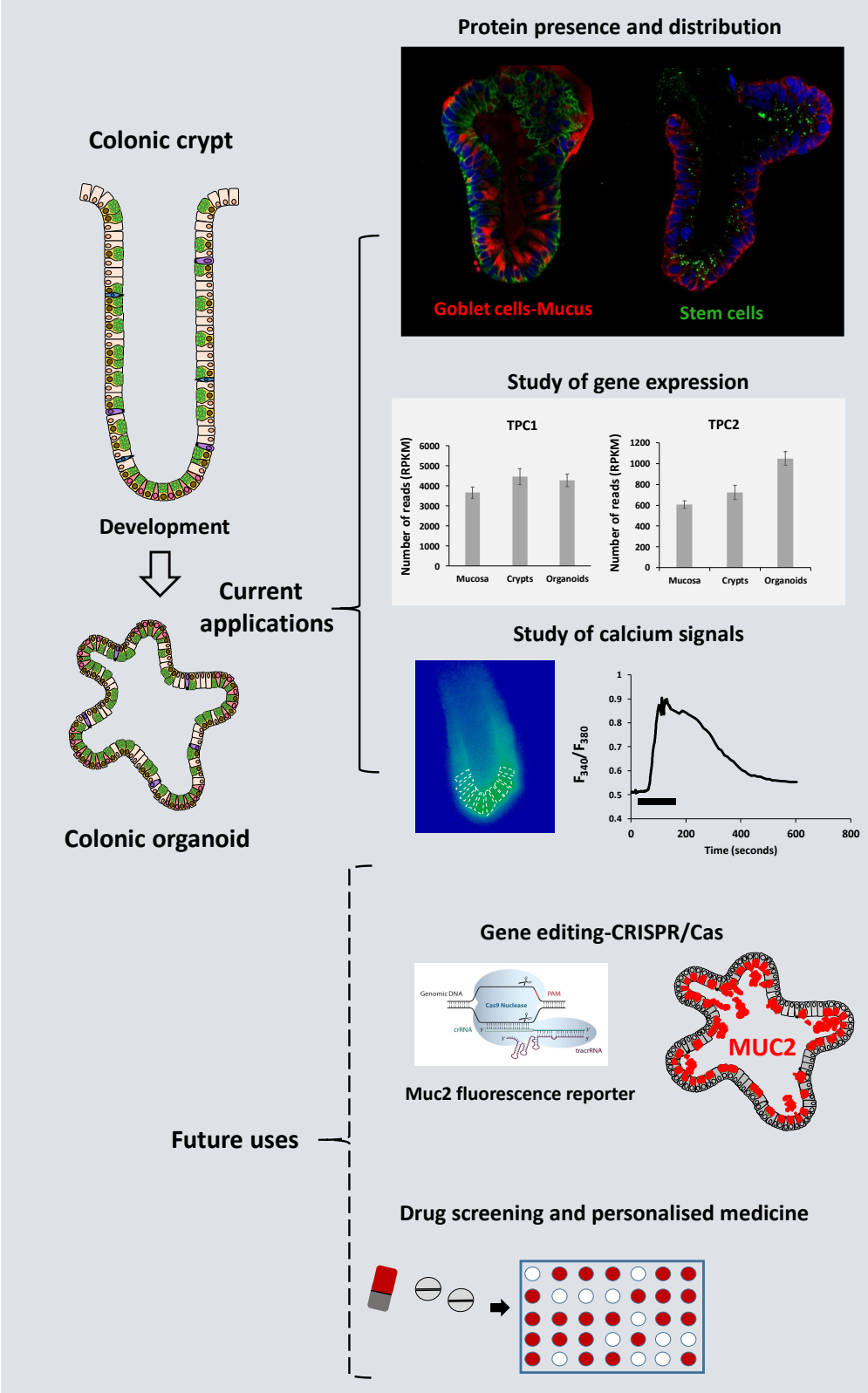

Figure 6.1. Current applications and future uses of the colonic organoid culture system. Our organoid model system has been successfully validated and can be used as a platform for the study of protein expression and distribution, gene expression analysis and the study of intracellular calcium signals. Future work will exploit this tool for the generation of genetic modifications (e.g.

gene knock-in and knock out) and the development of personalised therapies for intestinal related diseases.

6.2 Sources of ACh

This thesis highlights the importance of ACh in the regulation of colonic epithelial physiology. This molecule works as a mitogen to stimulate tissue renewal and at the same time it functions as a potent secretagogue stimulating epithelial fluid secretion and mucus release from goblet cells. ACh can be generated by cholinergic neurons that innervate the gut as well as by the specialised tuft cells located in the epithelium. Previous work in the Williams lab has characterised the distribution of these neurons and showed that they reside in close proximity to the colonic stem cells (Dr Christy Kam, PhD Thesis). In addition, our data confirms the expression of ACh producing tuft cells in the colon epithelium, which importantly, are also present in the stem cell niche. Tuft cells are specialised chemosensors of the lumen that can recognise the presence of bacteria and parasites and respond by activating the immune system (Schneider et al., 2018; von Moltke et al., 2015). However, the role of ACh secreted by tuft cells is still not clear. We propose that in the colon epithelium, Tuft cell-mediated release of ACh is an alarm signal triggered by penetration of the mucus barrier. The proximity of the microbiota or pathogens is sensed by stimulation of chemoreceptors that are expressed on the apical 'tuft' membranes of Tuft cells. The secreted ACh can activate cholinergic neurons that reside in close proximity and it can also act in a paracrine fashion to directly activate the cells of the stem cell niche. The signal is rapidly transmitted to goblet cells to induce a quick response resulting in mucus and fluid secretion for the removal of the pathogen. In parallel, an increase in ACh levels quickly evoke an intracellular calcium response in stem cells which in the long-term promotes tissue regeneration to restore epithelial integrity.

6.3 Calcium as a signal integrator in colonic epithelial cells

The colonic epithelium requires complex coordination between the different cell types to fulfil all tissue functions and maintain integrity. The gut is continuously processing a wide variety of signals that regulate its physiology and for this to happen, cells need to present a sophisticated communication network that allows them to process all the different inputs. Calcium is a versatile second messenger that is capable of coordinating different cellular signals and regulate the downstream transduction and its effects on cell biology (Berridge, Lipp and Bootman, 2000). All cells are endowed with an array of calcium signalling components that can regulate the concentration of this molecule in the cytoplasm and organelles. These elements are referred to as the calcium signalling toolkit, and its specific expression and regulation can vary depending on the cell type

resulting in different cell behaviours. Within a cell, calcium signals can have pleiotropic actions that determine the activation or inhibition of a variety of cellular processes. The different cellular location of the elements of the calcium toolkit is also important to determine the dynamics of the response and ultimately the effect on the cellular function (Bootman and Bultynck, 2019). Calcium signals have been extensively characterised in excitable cells of the muscle or neurons, however there is limited information on the mode of action in intestinal epithelial cells (Brini et al., 2014; Kuo & Ehrlich, 2015). Colonic epithelial cells are polarised structures with distinct apical and basolateral plasma membrane domains to separate the luminal content form the underlying mucosa. The establishment of cell polarity requires specific subcellular machinery to transport and recycle proteins to their appropriate location. These structural characteristics determine the location of the calcium toolkit elements (Petersen and Tepikin, 2008).

In this thesis we have focused on the role of the cells located at the base of the crypt, mainly goblet and stem cells because of their relevance in maintaining tissue renewal and epithelial barrier functions. The epithelial cells of the colon can respond to a great variety of stimuli to regulate the tissue's specific functions. Amongst the known stimulants, previous studies have demonstrated the role of ACh in the release of mucus from goblet cells and fluid secretion (Specian and Neutra, 1980; Halm and Halm, 2000) as well as cell proliferation in other organs of the GI tract (Zhao et al., 2014; Hayakawa et al., 2016; Renz et al., 2018). The signal is received by the cholinergic receptors in the membrane which in turn triggers a calcium signalling pathway that results in the activation of the specific cellular function. The characterisation of this signalling pathway has been a focus of this thesis. Firstly, we confirm that the calcium signal initiates in the apical pole of individual cells at the base of the crypt and then travels to the basal pole (**Chapter 3**). The combined analysis of the calcium signal and the immunolabelling of cell markers suggests that these individual cells are stem cells (**Chapter 4**). The calcium signal is then rapidly transmitted to the neighbour cells as a wave which is then propagated further up the crypt axis. The generation of the calcium signal in the apical pole of cells seems *a priori* counterintuitive as the receptor for ACh is expressed the basal pole (**Chapter 3**). This mechanism has been studied in pancreatic acinar cells and the general consensus is that polarised cells can present a higher concentration of critical calcium release channels, transporters and signalling proteins in the apical pole (Petersen and Tepikin, 2008). The geometry of the colonic crypt-base may contribute to this, where the apical pole of numerous cells within the stem cell niche converge at the lowest point of the blind-ending crypt lumen. Observations in this thesis confirm that epithelial cells express calcium channels required to generate a calcium response and these components are specifically distributed inside the cell (**Chapter 3**). Firstly, mapping of the distribution of the calcium-storage organelle revealed the apical location of endolysosomes, which is

in concordance with their role in membrane trafficking and autophagy (Luzio, Pryor and Bright, 2007). These acidic organelles are endowed with a series of calcium channels including TPC1-2 that can release calcium to modulate lysosomal function (Li, Gu and Xu, 2019). In the colon epithelium we show that endolysosomes express TPC1 and 2 (**Chapter 3**). TPCs are believed to be activated by NAADP, which is synthesised by the enzyme CD38. This protein has been shown to locate to the membrane and our studies confirmed its expression in the apical membrane of cells of the stem cell niche. The ER is the biggest intracellular calcium store and it functions as an important regulator of the calcium signal by mediating the release into the cytoplasm via IP3R and RyR receptors and the subsequent uptake to the organelle by the SERCA pump. In this thesis, our results indicate the expression of these calcium channels in colonic epithelial cells (**Chapter 3**). We show that all members of the IP3R family are differentially expressed in the cell. This observation correlates with the idea that the expression of the calcium toolkit varies along the cell and different positioning could imply a different cellular function. Interestingly, we report that IP3R3 is highly expressed in colonic epithelial cells, both at the transcriptomic level and at the protein level. In addition, we show their presence to be prominent in the apical pole (**Chapter 3**). Paradoxically, IP3R3 does not play a major role in muscarinergic coupled calcium signalling but does play a central role in generating calcium signals coupled to metabotropic purinergic P2Y2 receptors (Alvin Lee, unpublished). Overall these findings confirm the presence of a calcium toolkit capable of generating calcium signals in response to ACh stimulation. In order to understand how calcium integrates this cellular input we characterised the role of the calcium toolkit components present in the colonic epithelium. The general consensus of the research community is that following the binding of ACh to the muscarinic receptors 1, 3 and 5, a signalling pathway is triggered that results in the activation of the protein PLC by the $G\alpha_q$ to generate IP3 and DAG. IP3 is a second messenger which acts as a potent activator of IP3Rs in the ER inducing calcium release (Nathanson, 2008). However, ACh has also been shown to activate NAADP to induce calcium signals mediated by TPC release of calcium in the endothelium (Brailoiu et al., 2010), and preliminary studies by Dr. Christy Kam in the Williams lab have suggested the implication of this calcium channel in the response to ACh stimulation in the colon epithelium (Christy Kam, PhD Thesis). By undertaking a pharmacological approach, we revealed that blocking of TPC activation with the antagonist Ned19 completely inhibits the calcium response to muscarinic receptor activation. The inhibition of IP3Rs with 2-APB attenuates the calcium response while the inhibition of RyRs with Dantrolene blocks it, suggesting the ACh signal is first mediated by release of calcium via TPCs and that RyRs in particular are important in propagating the signal. The generation of this local calcium signal activates the ER via a cross-coupling mechanism to induce calcium-induced calcium release and the amplification of the signal (**Chapter 3**). Parallel work in the Williams

lab has confirmed that all RyRs subtypes are expressed and appear to be co-expressed in all cells located at the crypt base (data not shown). In addition, the action of the RyR inhibitor Procaine implicates RyR1 and RyR2, and possibly RyR3 in the globalisation of the calcium signal via CICR (data not shown), while the minimal effects of the 8-bromo-cADPR in the cholinergic-induced calcium response suggests that CD38-mediated generation of cADPR and subsequent activation of RyR1 is not involved (Dr. Christy Kam, PhD). Follow up studies will aim to elucidate the role of each of the different RyR subtypes in the CICR amplification of cholinergic-induced calcium signalling.

Importantly, a comprehensive pharmacological profile of the calcium mobilisation pathway coupled to muscarinic receptor activation supports a role for TPCs. Tetrandrine, diltiazem, verapamil and Ned19 all block muscarinergic-coupled calcium signals, but not those coupled to purinergic P2Y2 receptors; while dantrolene blocks calcium signals coupled to both GPCR receptor types (Alvin Lee, unpublished).

In light of these findings we propose the following novel mechanism of intracellular calcium signalling of the colonic epithelial cells from the stem cell niche upon stimulation with ACh: 1) ACh is sensed by muscarinic receptors located at the cellular basal membrane. 2) The activation of muscarinic receptors coupled to calcium (MAChR1, 3 and 5) induces a signalling pathway that ultimately results in the activation of the TPCs, potentially stimulated by NAADP generated via CD38. 3) Activated TPCs release calcium to the cytoplasm generating a local calcium response. 4) This response is immediately amplified via CICR activation of IP3Rs (potentially IP3R3) and RyR receptors present in close proximity, which propagates as a wave through the cell and is transmitted to the neighbour cells (possibly through membrane GAPs). A schematic diagram represents the proposed signalling pathway in **Figure 6.2**.

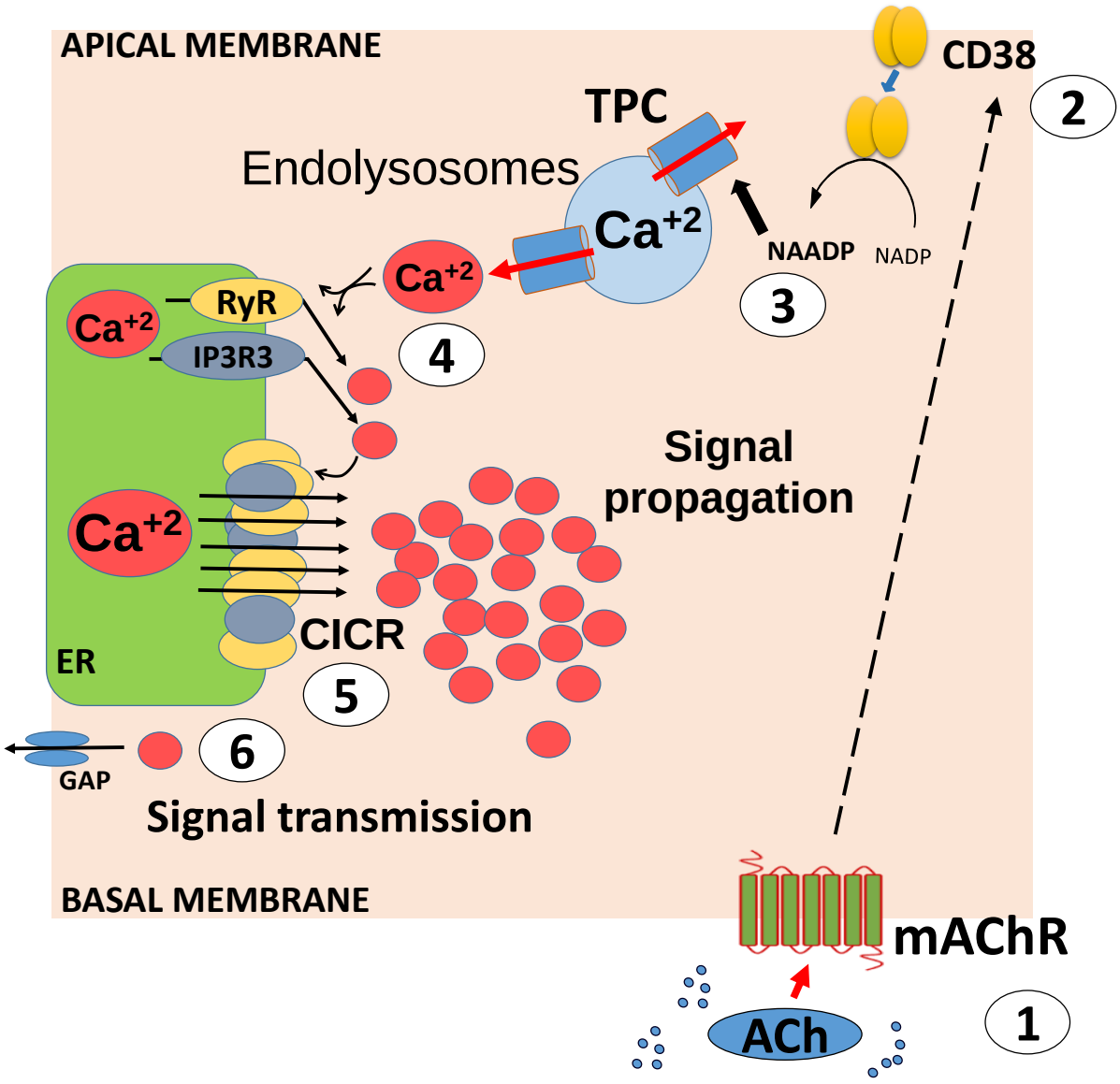

Figure 6.2. Proposed mechanism of muscarinic-coupled calcium signals in the stem cell. (1) Muscarinic receptor activation by ACh induces an intracellular signalling pathway that results in the activation and internalisation of CD38 (2). CD38 catalyses production of NAADP which activates TPC to release calcium (3). Local calcium signal activates RyR and IP3Rs (possibly IP3R3) to induce release of calcium from the ER (4). Calcium signal is amplified by CICR and propagates through the cell (5). Signal is transmitted to neighbour cells (possibly by gap junctions) (6).

6.4 Physiological functions of the muscarinic-coupled calcium signals

ACh has been shown to be a potent modulator of mucus and fluid secretion as well as an activator of cell proliferation (Specian and Neutra, 1980; Halm and Halm, 2000; Hayakawa et al., 2016). In this thesis we show that ACh activates a calcium signal response that initiates in the stem cells of colonic crypts and is mediated by calcium release from the TPCs. In addition, our findings highlight the different physiological responses that this signal evokes in the epithelium. These responses are ultimately integrated by calcium, which depending on the particular characteristics of the cell, can result in the activation of different cellular processes. The effects of the stimulation of the muscarinergic signal in stem cells activate a long-term process which involves calcium-dependent activation of gene expression, and transcription of proteins needed for cell proliferation. Conversely, the same stimulus in the neighbouring goblet cells induces the calcium-dependent short-term process of mucus and fluid secretion that is evident minutes after cell stimulation.

6.4.1 Cell proliferation and tissue growth

In the gastrointestinal tract, ACh regulates epithelial stem cell proliferation via activation of the muscarinic receptors and the modulation of the Wnt and Yap signalling (Zhao et al., 2014; Hayakawa et al., 2016). In the colon, ACh release into the stem cell niche is first sensed by the stem cells. The activation of muscarinic receptors induces an intracellular signalling pathway that results in the activation of the TPCs present in the membrane of endolysosomes. These apically located organelles release calcium via TPCs which induces a local response. This response is amplified by CICR release of calcium from the ER via activation IP3Rs and RyR.

Cells are endowed with a specific machinery to decode calcium signals and transduce them into cellular processes. The regulation of gene expression by calcium signalling can involve the activation of specific cytosolic calcium sensors which can then induce the translocation of transcription factors to the nucleus to promote the expression of different genes. Our studies in the stem cell niche of colonic crypts revealed the presence of TORC1, YAP1 and NFATc3; three transcription factors known to induce activation of cell proliferation in the GI tract (Deng, Gerencser & Jasper, 2015; Hayakawa et al., 2016; Peuker et al., 2016). While the study of TORC1 remains to be analysed, the study of the muscarinic-calcium coupled signals revealed that both YAP1 and NFATc3 are translocated to the nucleus following the elevation of the calcium cytoplasmic levels (**Chapter 5**). In addition, we show that both transcription factors have different mobilisation kinetics, perhaps owing to the presence of different regulatory mechanisms defined by the nature of the cellular process they modulate. The existing literature has limited references on calcium-dependent activation of YAP. Recent studies in

brain tissue suggest a negative regulation of YAP, which functions via SOCE activation of calcium signals (Liu et al., 2019). However, in colonic crypts we show that the increase in calcium following muscarinic activation induces YAP activation and nuclear translocation. The exact mechanism of YAP activation by calcium signals has not been addressed in this thesis, and it will be of interest to study which elements are responsible for it and how are they modulated by calcium. Our studies were focused on the mechanism of activation of NFATc3 and confirmed that the generation of a calcium signal is needed for the transcription factor to translocate to the nucleus. While the exact role of other calcium sensors such as calmodulin has not been studied, our findings indicate that translocation of NFATc3 to the nucleus is likely mediated by calcineurin, which is known to dephosphorylate the transcription factor to activate it. Moreover, we also confirm that this calcium-dependent process is mediated by release of calcium from the TPCs as its inhibition blocks the muscarinic receptor-induced nuclear translocation of the transcription factor.

Considering the above stated lines of evidence, we propose the following regulation of stem cell function by muscarinic-coupled calcium signals: 1) Activation of TPCs induces a local signal which is amplified by CICR 2) Elevated cytosolic levels of calcium activate the calcium sensor calcineurin (possibly via activation of calmodulin). 6) Activated calcineurin decodes de calcium signal by dephosphorylation of the transcription factor NFATc3. 7) Removal of phosphate ions allows NFATc3 to translocate to the nucleus to promote gene expression of proliferation genes (possibly LGR5, OLFM4 and other components of the Wnt signalling pathway) 8) Increase in gene expression of these markers induces cell proliferation and tissue growth in the stem cell niche. A schematic diagram represents the proposed signalling pathway in **Figure 6.3**.

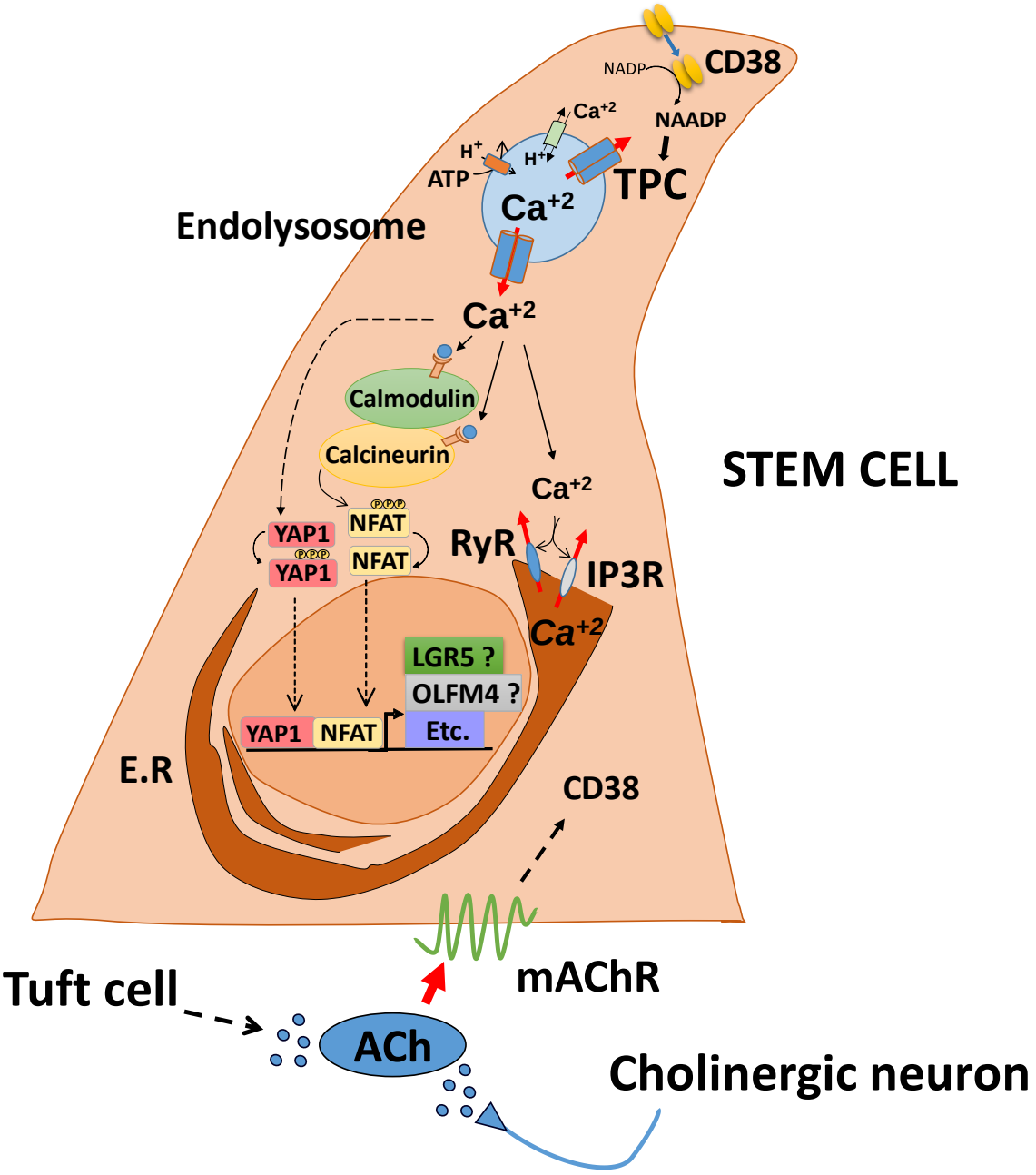

Figure 6.3. Proposed regulatory mechanism of stem cells by muscarinic-coupled calcium signals. ACh activates muscarinic receptors in the basal membrane which initiates and intracellular signalling pathway that results in the activation of CD38 and the generation NAADP. This molecule induces calcium release from TPC which results in the generation of a local signal that is amplified by IP3Rs and RyRs via CICR. Elevated levels of calcium activate nuclear translocation of transcription factors. NFATc3 mobilisation to the nucleus is mediated by calcium activate calmodulin. Once in the nucleus, the transcription factors activate gene expression of proliferation-related genes.

Cell proliferation requires of the activation of gene expression and the transcription of a number of proteins that regulate the cell cycle. This is a slow biological process and the effects of this

mechanism become apparent hours after the initiation of the signalling pathway. Our analysis revealed the effects of muscarinic-coupled signalling in the stem cell niche correlate with an increase cell proliferation and tissue renewal. Activation of proliferation-related genes induces the expression of growth-dependent proteins that promote the cell cycle progression and synthesis of new DNA (Schepers and Clevers, 2012). These effects were reported in colonic crypts by measuring DNA synthesis using fluorescence analysis of EdU nuclear incorporation. Cell proliferation of stem cell and progenitor cells results in the generation of more epithelial cells which promotes tissue renewal or regeneration. In our studies with organoids, this effect became visible by measuring the increase in size over time (**Chapter 5**). In addition, the activation of this signalling pathway also induces the generation of more buds. The new buds are formed in the stem cell niche and start to project out from the crypt axis and elongate to form a mature daughter crypt containing all the different cell types. In the human colon, the formation of new crypts occurs during organogenesis or upon intestinal damage (Yip et al., 2018). We propose that the ACh is secreted into the epithelium, stimulates stem cells to proliferate and induce tissue regeneration which results in the production of more epithelial cells that contribute to the growth of the colonic tissue. This mechanism is regulated by calcium which integrates this mitotic signal and orchestrates the generation of this cellular process.

In view of these findings, an interesting question that remains to be elucidated is why these signals specifically initiate in stem cells. One possible explanation would be that the elements required to integrate the muscarinic-coupled calcium signals, including muscarinic receptors and the rest of the components of the calcium toolkit are more abundant in this cell type, which potentiates the effect of this signal as compared to the neighbouring cells. To confirm this theory, future work is needed to quantify the presence of these elements in the different cell types of the colon epithelium. To this end, a possible approach could be the analysis of gene expression at the single cell level. The development of single cell RNA sequencing methodology has been shown in recent times to be a useful technique for analysing the cellular characteristics of the different cell types that constitute the colonic epithelium (Fujii et al., 2018; Parikh et al., 2019) and therefore it holds a great potential for gene expression comparative analysis of the calcium toolkit components.

Bud formation and organoid growth are indicative of the presence of stem cells that are capable of generating all different cell types. Stem cells express a series of markers such as LGR5, ASCL2, OLFM4 or PTK7 that enables them to integrate mitogen signals that induce cell proliferation (Gehart and Clevers, 2019). Based on our findings, we hypothesise that the downstream effects of the calcium signal activate the gene expressions of those makers and possibly others. To confirm this theory, it

would be of great interest to analyse the effect of the muscarinic-coupled signalling in the gene expression of these markers. As described before (**Chapter 3**), qRT-PCR has been shown to be a resourceful technique for the analysis of gene expression and thus, it could serve as good platform for subsequent studies.

The integrity of the epithelial barrier in colonic crypts is dependent on stem cell-driven tissue renewal and the generation of daughter cells that differentiate into all cell lineages as they migrate up the crypt axis to be shed off in the upper region. Our studies in organoid growth following activation of cell proliferation suggest that stem cells produce a progeny of cells that are expelled out of the stem cell niche and migrate upwards increasing the crypt size. However, it remains to be analysed whether cell migration is driven by cell proliferation and if this process is promoted by activation of the muscarinic-coupled calcium signalling. A functional way to test it would be to do a pulse-chase study that relies on the administration at different time points of fluorescence analogues of thymidine that bind DNA when this is being replicated in the nucleus. In this experimental procedure, we would first pulse live cells with one fluorescence thymidine analogue (e.g. BrdU) to mark the cells that are replicating at the beginning of the experiment and then wash it off to stop the reaction. Subsequently, we would pulse our cells with a different fluorescence thymidine analogue (e.g. EdU) at different time points. Imaging of both fluorescence markers would reveal the migration distance along the crypt axis of cells originated at the crypts base and would help elucidate the dynamics of this cellular process. Since some diseases result in aberrant cell turnover (e.g. colorectal cancer), this methodology could be applied to study the migration dynamics under different pharmacological treatments.

6.4.2 Mucus and fluid secretion

The epithelial barrier protects the colonic epithelium from the hazards of the luminal content by the generation a mucus layer and the secretion of fluid to flush bacteria away. Under homeostatic conditions, goblet cells maintain a baseline secretion of mucus to replenish the layer that is constantly being degraded by the microbiota and swept along the gut, transported by the movements of the luminal content. In the event of a barrier breach, goblet cells respond by inducing a massive release of mucus in a process known as compound exocytosis. In the colon epithelium, we have shown that ACh is a potent mucus secretagogue, which functions by activating an intracellular calcium signal that results in the depletion of the mucus stores.

Stem cells reside at the bottom of the crypt where they orchestrate the tissue renewal of the epithelium. The integrity of the tissue is dependent on the proper functioning of the stem cells,

which suggests the presence of mechanisms that can protect them. In this thesis we show that the stem cell niche is populated with numerous goblet cells that can release their mucus content in response to muscarinic receptor activation with ACh. We suggest that these cells have the mission of protecting the stem cell niche from any potential threat and therefore we refer to this population as guardian goblet cells (**Chapter 4**). Similar to stem cells, this cell type is also endowed with the elements of the calcium toolkit. Importantly, the calcium signal elicited upon muscarinergic stimulation is rapidly transmitted from the stem cells to their neighbouring cells including the guardian goblet cells (**Chapter 3**), possibly via GAPs. In order to study the implication of this calcium signal in the regulation of goblet cell function, we investigated its effects based on the capacity of this signal to induce mucus depletion from the cytoplasm. To this end, we used a novel approach based on the measurement of immunofluorescence intensity of the mucus marker MUC2 present in the cytoplasm of goblet cells, in conjunction with pharmacological modulation of intracellular calcium release.

Our findings described in **Chapter 4** confirmed that mucus secretion induced by muscarinic receptor activation is driven by calcium signalling. Similar to stem cells, the release of calcium from the acidic stores by TPCs is needed to initiate a calcium response. Cross-coupling with the ER enables the calcium signal to be amplified by CICR and an increase in the cytosolic concentration of calcium results in the depletion of goblet cells.

Future studies should aim to further characterise the guardian goblet cells. A potential marker could be WFDC2 which has been shown to be expressed predominantly in the goblet cells of the lower regions of the crypt (Parikh et al., 2019). Our findings have confirmed the presence of this protein in the base of colonic crypts which highlights the capacity of our culture system to recapitulate the cellular complexity observed *in vivo* (**Chapter 4**). With the use of this system and a similar approach to the one utilised for the study of mucus secretion, future work aims to elucidate whether the secretion of this antimicrobial protein is also regulated by the muscarinic-coupled calcium signalling. The presence of this cell type would suggest the existence of at least to different populations of goblet cells: the sentinel goblet cells that reside in upper regions and are stimulated by the sensing of bacterial antigens (Birchenough et al., 2016) and the guardian goblet cells, another specialised subpopulation of cells that reside in the stem cell niche and is activated by ACh to release mucus and protect the stem cells.

Secretion of mucus into the lumen is followed by the production of more mucus by the goblet cells in order to refill their cytoplasmic content in what is known as mucus turnover. Previous work by Johansson and colleagues investigated this mechanism in the mouse colon under homeostatic

conditions, and showed different dynamics of mucin turnover in the goblet cells of the surface epithelium compared to the ones in the base (Johansson, 2012). In this thesis we studied this mechanism in the goblet cells present in the stem cell niche. Our time course experiment on mucus secretion induced by CCh indicates that mucus turnover is rather quick (**Chapter 4**). Stimulation of goblet cells induces depletion of the cytoplasmic globules that is maximal between 5 and 15 minutes after the addition of CCh. These cells are then triggered to produce more mucus to refill the stores, reaching full capacity after 30 minutes. The characterisation of this mechanism in the goblet cells located at the upper regions of the crypt remains to be studied, and it would be of interest to compare the dynamics to the ones observed in the guardian goblet cells. However, given the important role in protecting the stem cell niche, we suggest that the mucin turnover observed is a rather quick mechanism which ensures that guardian goblet cells are always ready to secrete mucus.

The exact mechanism that follows the elevation of calcium levels to trigger mucus secretion was not addressed in this thesis. However, recent findings suggest the presence of calcium sensors that regulate the docking of the mucus globules to the membrane to allow the release of mucus (Cantero-Recasens et al., 2018). Recasens and colleagues suggest the presence of a high-affinity calcium sensor, KChiP3, expressed in the membrane of the mucus globules which under resting conditions prevents their interaction with the plasma membrane. These observations allow us to propose a scenario where the activation of muscarinic receptors induces an intracellular response that culminates with the activation of TPCs which in turn release calcium into the cytosol to generate a local response. The ER amplified signal elevates the concentration of calcium in the cytoplasm. The increase in calcium levels is sensed by KChiP3, which in turn is removed from the membrane of the mucus globules. The removal of KChiP3 allows the interaction of the docking protein Vamp8, present in the globule membrane, with the SNARE proteins expressed in the plasma membrane, facilitating the membrane contact (Cantero-Recasens et al., 2018). This event results in membrane fusion and the release of their content into the lumen (**Figure 6.4**). The proposed mechanism of KChiP3 as a calcium sensor and modulator of mucus secretion has shed some light on how the calcium signals are transduced in goblet cells. While this finding was reported in cultured cell lines by Cantero-Recasens and colleagues, it will be interesting to characterise the presence of this mechanism in our culture system and confirm its mode of action.

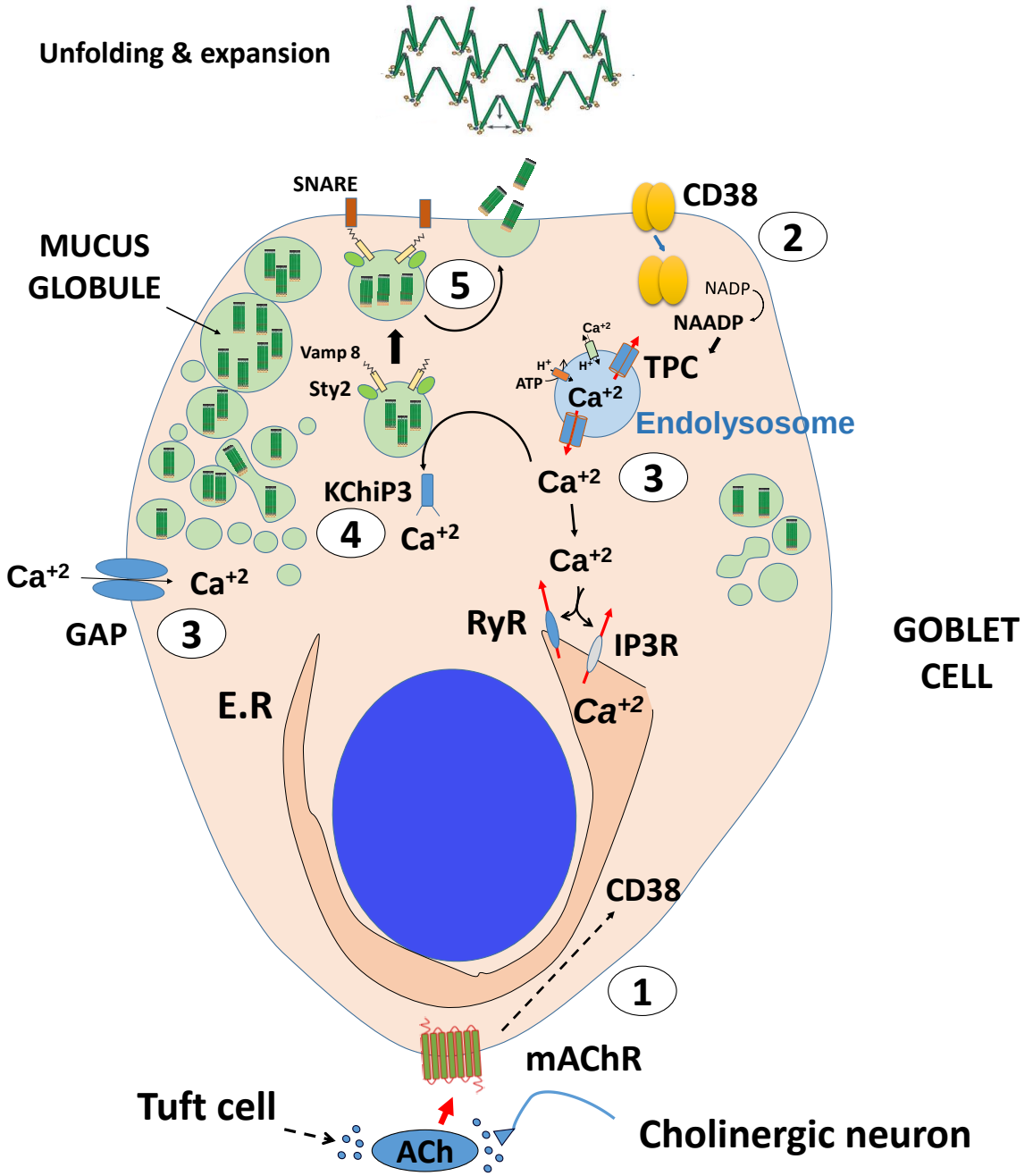

Figure 6.4. Proposed mechanism of the regulation of mucus secretion by calcium. (1) ACh is sensed by muscarinic receptors which activates a signalling pathway that results in the production NAADP mediated by CD38 (2). NAADP activates TPC and induces the release of calcium into the cytoplasm (3). This local calcium signal is amplified by CICR from the IP3R and RyR present in the ER (4). Elevated levels of intracellular calcium are sensed by KChiP3 which induces its recycling form the membrane of mucus globules. (5) Removal of KChiP3 allows interaction of the mucus globule membrane protein Vamp8 and the plasma membrane protein SNARE resulting in the fusion of the membranes and the release of mucus into the lumen.

Another important event that occurs in the goblet cell during mucus secretion is the unfolding of the densely packed mucins in the lumen. MUC2, the main mucin present in colonic goblet cells is synthesised in the ER where is arranged into dimer structures and N-glycosylated. The proteins are then transported into the Golgi apparatus where there are first O-glycosylated in the cis-Golgi and arranged into trimers in the trans-Golgi (Birchenough et al., 2015). When transported into the mucus globules, these proteins are arranged into tightly packed multimers. The steps required for the organisation and packaging of the mucin are dependent on the presence of low pH levels and high calcium concentration inside the organelles. A similar mechanism has been demonstrated in the packaging of the zymogen granules in pancreatic acinar cells. In this cell types, exocytosis is mediated by calcium release from the vesicles into the cytoplasm following cell stimulation (Williams, 2010). In view of these observations, we could hypothesise that mucus globules also present the same components (e.g. TPCs) and undergo a similar intracellular regulation. Once secreted into the lumen the presence of lower calcium concentrations and the increased levels of the pH and HCO_3^- secreted from the cell, allow for water to penetrate the mucin structure which is then able to expand to levels of 100 to 1000 fold in volume (Birchenough et al., 2015). Importantly, the release of HCO_3^- is dependent on the correct epithelial transport of chloride anions (Gustafsson et al., 2014). This transport is mediated primarily by the protein NKCC1 located in the basal membrane which facilitates the influx of Na^{+2}, K^+ and Cl^- into the cell, and the CFTR protein located in the apical membrane which releases Cl^- and HCO_3^- into the lumen. The system is balanced with the presence of K^+ channels in the basal membrane that pump out K^+ and Cl^- channels in the apical membrane that secrete Cl^- into the lumen. Of note, the K^+, Cl^- and NKCC1 channels have been shown to be regulated by intracellular calcium (Reynolds et al., 2007; Frizzell and Hanrahan, 2012). In our studies we have confirmed the presence in colonic crypts of NKCC1 and CFTR in the basal and apical membranes respectively (**Chapter 4**) which suggests the presence of this chloride epithelial transport mechanism. In addition, in this thesis we show evidence that the muscarinic-coupled calcium signal is involved in the secretion of fluid into the lumen. Using colonic organoids as a model, we demonstrated that the swelling of these structures induced by muscarinic receptor activation was blocked when the TPCs where inhibited, which indicates that this specific calcium signal can regulate several different physiological functions. Moreover, the secretion of fluid and mucus induces the flushing of the luminal content out of the crypt, as seen in our live recording of mucus secretion (**Chapter 4**).

In view of this observations we propose that following the activation of the muscarinic-coupled calcium signal, the increase in calcium levels activates NKCC1 and the K^+ channel in the basal membrane of the goblet cell which induces chloride influx. At the same time calcium activates the Cl^-

channel in the apical membrane to release the anion which is accompanied by cAMP activation of CFTR (mediated possibly by calcium) to release Cl^- and HCO_3^- into the lumen and water that would follow via osmosis. The increase in pH and HCO_3^- generates the environment necessary for the mucus to unfold and expand. In addition, this same mechanism is also activated in the rest of the epithelial cells of the crypt which results in a massive secretion of fluid which can clear out the contents of the crypt lumen (**Figure 6.5**).

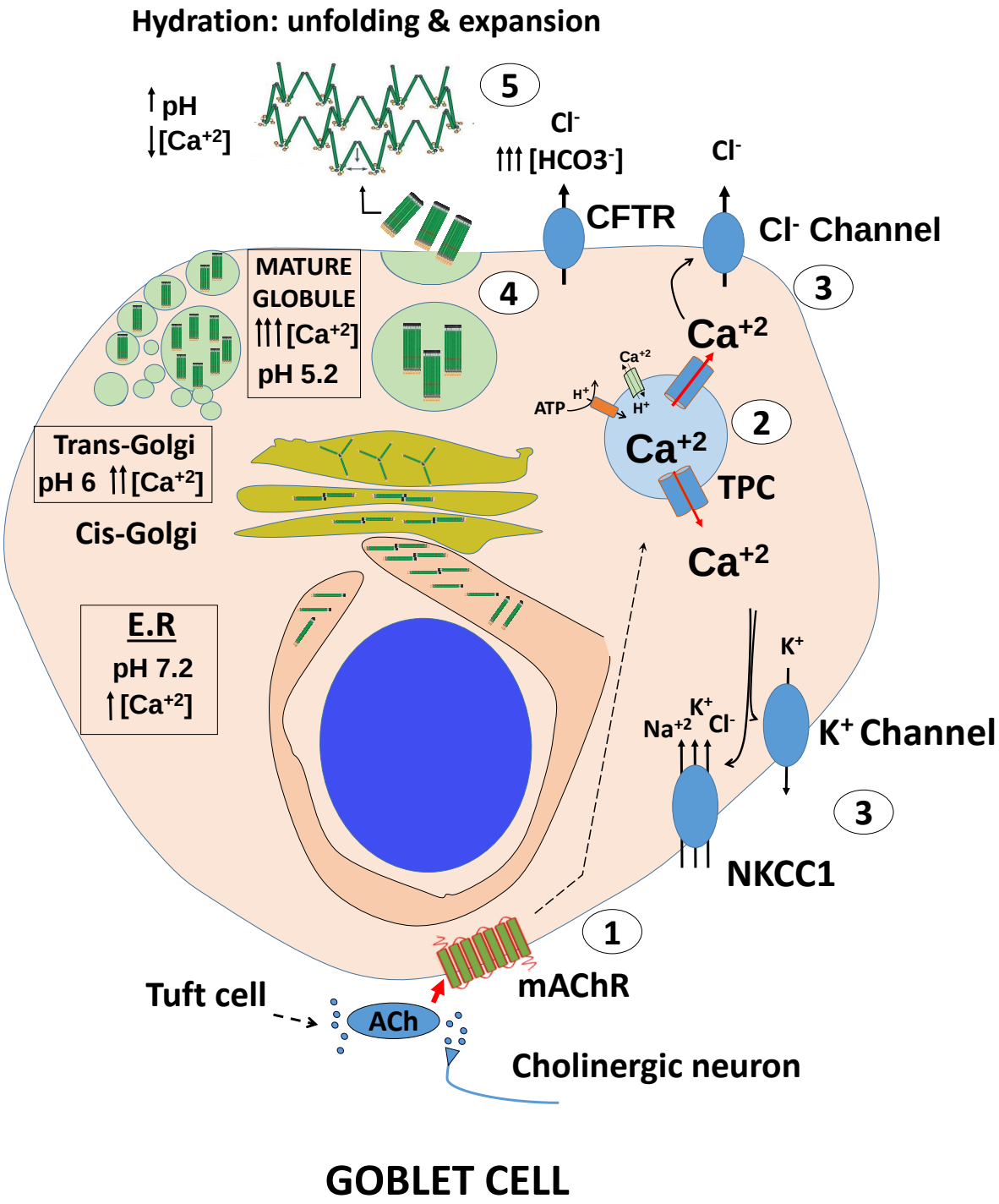

Figure 6.5. Proposed mechanism of muscarinic-coupled calcium induced epithelial chloride transport. Activation of muscarinic receptors (1) triggers an intracellular calcium signal that induces calcium release from TPCs which is further amplified by CICR from the ER (2). The increase in calcium levels activates NKCC1 and the Cl^- transporters in the basal membrane inducing Cl^- influx. At the same time calcium activates the Cl^- channels in the apical membrane and cAMP stimulates CFTR to secrete Cl^- and HCO_3^- efflux to the lumen, which is followed by liquid via osmosis (3). Changes in the

pH and increase in the HCO_3^- allow mucus expansion. Liquid secretion induces flushing of the luminal content (4).

6.4.3 Other potential physiological functions

The studies in this thesis have characterised the muscarinic-coupled calcium signals in the stem cell niche of colonic crypts and focused on the physiological functions in stem and goblet cells. However, it is possible that these same signals also regulate the cellular functions of enteroendocrine cells. In the colon, these cells can sense the luminal content and secrete a variety of hormones to control blood nutrient levels, modulating digestion and absorption (Gribble and Reimann, 2019). Similar to goblet cells, the hormones synthesised by enteroendocrine cells are accumulated in secretory vesicles. Upon stimulation, these vesicles are secreted into the interstitial space where they can act in a paracrine fashion or be transported in the bloodstream to reach distant targets. Enteroendocrine function has been shown to be modulated by activation of GPCRs and calcium signalling to induce hormone release (Sternini, Anselmi and Rozengurt, 2008). These observations suggest that these cells could be potentially regulated by the same calcium signal that induces cell proliferation in stem cells and mucus and fluid secretion in goblet cells. Therefore, future work should aim to elucidate the role of muscarinic-coupled calcium signalling in enteroendocrine cells. If hormone release by these cells is confirmed to be mediated by this signalling pathway, this finding will highlight the versatility of calcium in regulating different cellular processes to exert different cellular functions. In addition, it will confirm the importance of muscarinic-coupled calcium signals in regulating tissue physiology and organ systems such as the gut-brain axis, and gut-pancreas axis via release of neurotransmitters, hormones such as incretins (e.g. GLP-1).

6.4.4 Summary of physiological functions

The work in this thesis has characterised the complex regulation of the colonic epithelium physiology and evidenced the critical role of the second messenger calcium in integrating the ACh-induced signals to modulate different cellular functions. In summary, we propose that ACh is first sensed in the stem cells located at the base of the crypt which triggers a signalling pathway that ultimately activates the TPCs present in the endolysosomes. Upon activation, TPCs release calcium into the cytosol which initiates a calcium signal. The close proximity of ER facilitates cross-coupling of the signal and in this way, calcium activates IP3Rs and RyRs to release calcium. The increase in calcium activates more IP3Rs and RyRs and therefore, the signal is amplified and propagated through the cell. At this point the high levels of intracellular calcium can activate calcium sensors like calmodulin to induce the translocation to the nucleus of transcription factors. This event ultimately promotes

gene expression of proliferation genes which drives stem cell to proliferate and contribute to tissue growth. In parallel, the calcium signal originated in stem cells has propagated to the neighbour cells, possibly through membrane GAPs. Intermingled with stem cells, goblet cells receive the calcium signal which is also generated by activation of muscarinic receptors in their membrane. Increase in cytosolic calcium in goblet cells mediates a rapid cellular response where calcium binds to the calcium sensor KChiP3 and promotes the fusion of the mucus globules with the plasma membrane and the release of mucus. At the same time, the calcium signal has propagated up the crypt axis activating other cells. The increase in cytosolic calcium activates epithelial chloride transport which is brought inside the cell by NKCC1 and the Cl^- channel and released by the apical Cl^- channel and the cAMP-activated CFTR which also releases HCO_3^-. This activated epithelial chloride transport induces the release of fluid which follows the anion transport via osmosis. In goblet cells this mechanism also helps to hydrate the secreted mucus enabling its unfolding and expansion. In enteroendocrine cells, the characteristics of this signal have not been studied but it is possible that the same mechanism could be implicated in the release of hormones. The proposed mechanism of the regulation of the different physiological functions exerted in the colonic epithelium in response to the muscarinic-coupled calcium signal is displayed in **Figure 6.6**.

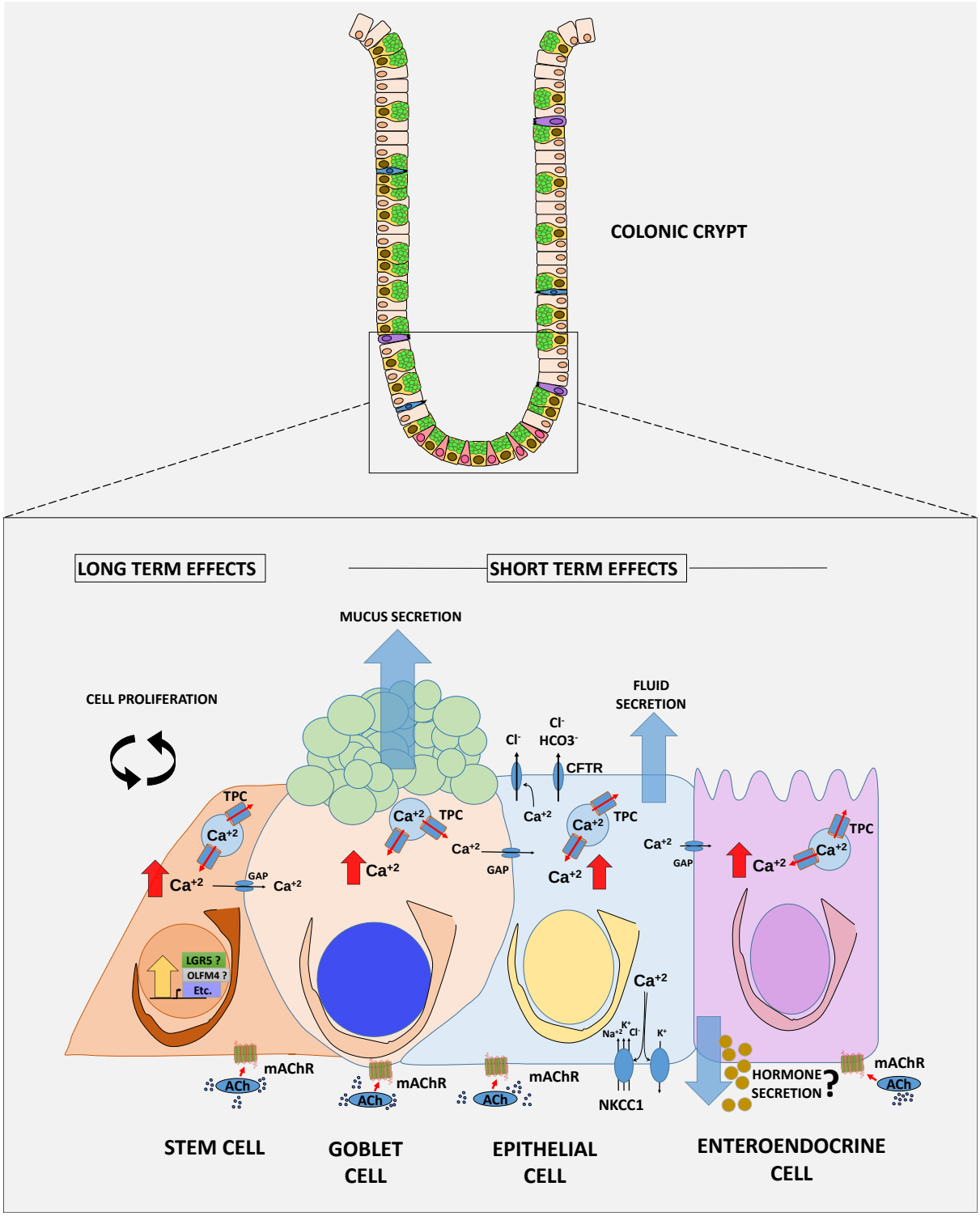

Figure 6.6. Physiological functions of the muscarinic-coupled calcium signalling pathway in the colon epithelium. Activation of the muscarinic signalling pathway induces an intracellular signal that results in the activation of TPCs and release of calcium to the cytoplasm. This signal is amplified by CICR and in stem cells promotes gene transcription of proliferative genes. In goblet cells this signal induces mucus secretion and together with other epithelial cells the activation of epithelial chloride

transport resulting in fluid secretion to the lumen. In enteroendocrine cells, this signal could potentially induce hormone release.

6.5 Integrated model for muscarinic-coupled calcium regulation of epithelial barrier

The colon epithelium is formed by a monolayer of cells that separates the luminal contents from the underlying mucosa. To be protected from the harsh luminal environment, the colonic epithelium requires the constant presence of a barrier which is generated by the secretion of mucins, antimicrobial peptides and the release of fluid to flush noxious substances. Importantly, the stem cells, which are key in maintaining the constant cellular turnover and tissue renewal are safely located in the base of the crypt where they are safeguarded from any potential threat. Tissue regeneration and mucus secretion are mechanisms by which colonic crypts respond to bacterial infection. The results of this thesis suggest the following scenario for the regulation of the epithelial barrier of the colon epithelium: Under homeostatic conditions, stem cells maintain a constant cell turnover to renew the epithelium and preserve the tissue integrity. Goblet cells present a moderate baseline secretion of mucus which is used to replace the mucus layer that is constantly being degraded by the microbiota. In the event of a tissue injury such as a bacterial infection, the specialised tuft cells can sense the presence of bacterial antigens and respond by releasing ACh. Tuft cells in the vicinity of the stem cell niche can secrete ACh to activate stem and goblet cells and possibly other cell types in a paracrine fashion. Alternatively, tufts cells might be able to activate cholinergic neurons via release of ACh, and in turn, these neurons can release ACh in close proximity to the stem cells to activate the generation of the defence mechanism. Stem cells first sense ACh by activation of muscarinic receptors. This induces a calcium signal which is mediated by calcium release from endolysosomes via TPCs. The amplification of the signal activates the gene expression of proliferation genes which results in the generation of more daughter cells which migrate and differentiate to regenerate the injured tissue. At the same time, guardian goblet cells residing in the stem cell niche are immediately activated by the same calcium signal which is transmitted from the stem cells and generated via muscarinic activation. This signal induces release of mucus into the lumen by compound exocytosis and promotes the quick refill of the mucus granules. In parallel, the calcium signal that has propagated through the crypt axis activates the release of fluid into the lumen which is used to flush the content out of the crypt. After expelling the pathogens, the mucus barrier is restored, and the colonic epithelium returns to constant homeostatic levels of proliferation and mucus secretion (**Figure 6.6**).

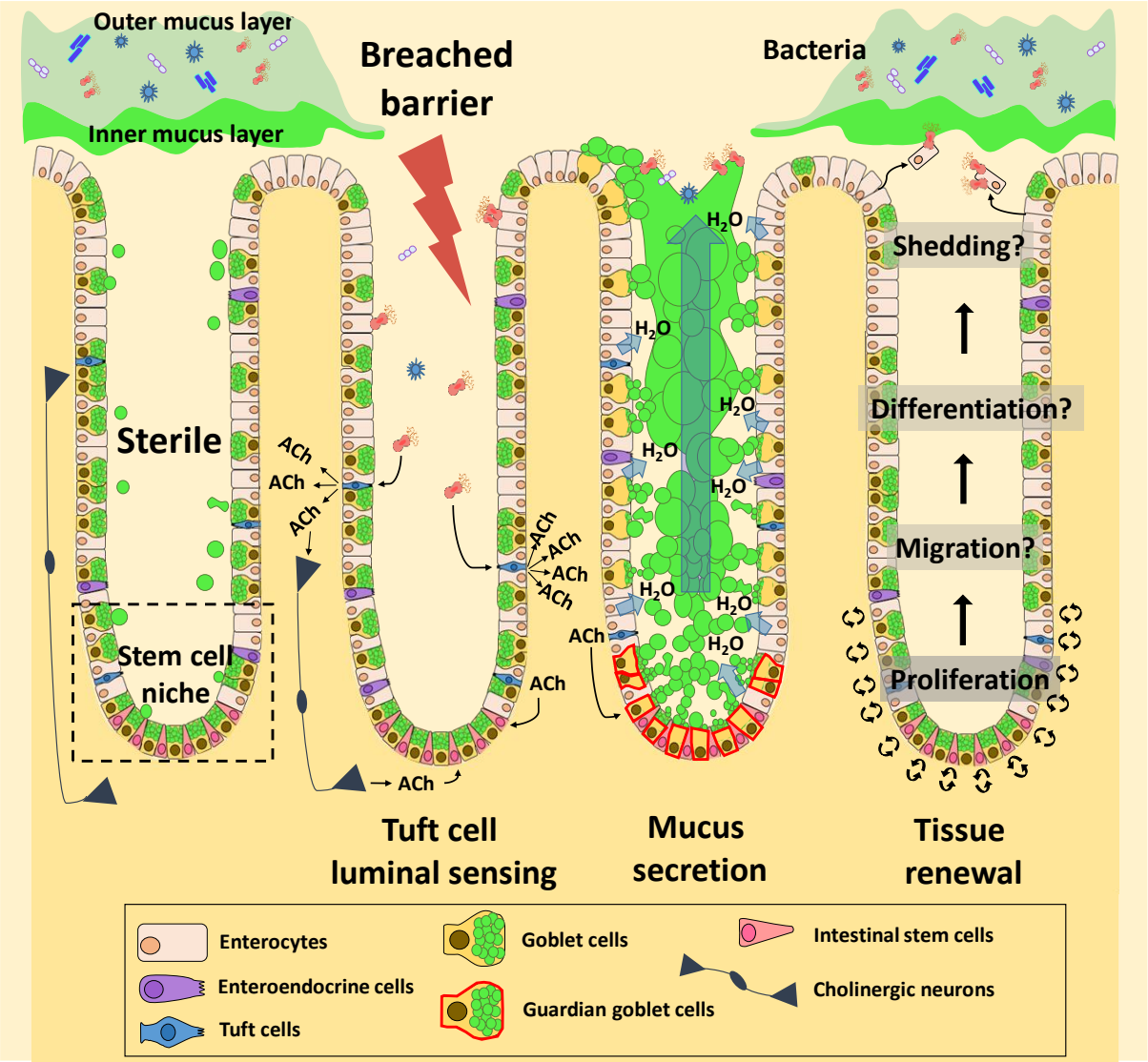

Figure 6.7. Proposed mechanism for the regulation of the epithelial barrier. Bacteria can penetrate the epithelial barrier inducing an infection. Tuft cells sense their presence and secrete ACh in response, to activate cholinergic neurons or directly the stem cell niche. Activation of the muscarinic-coupled calcium signal induces stem proliferation and tissue regeneration. In goblet cells, the same signal activates release of mucus into the lumen and in the rest of epithelial cells induces fluid secretion to flush the luminal content.

6.6 Implications for the study of diseases of the colonic epithelium.

The colonic epithelium is susceptible to the onset of diseases like IBD and cancer. Inflammatory bowel disease is characterised by the presence of intestinal inflammation and integrates Crohn's disease and ulcerative colitis. These diseases have an increasing incidence in society; however, they remain poorly understood. In both diseases the epithelial mucus barrier is altered and in ulcerative colitis this barrier is weakened facilitating the penetration of bacteria. In this disease, an abnormal

mucus production deteriorates the inner mucus layer resulting in bacterial infection and inflammation (Van Der Post et al., 2019).

Colorectal cancer (CRC) is characterised by an aberrant stem cell turnover due the alteration of gene expression of oncogenes and tumour suppression genes (Kuipers et al., 2015). Although there is a substantial heterogeneity in the specific mutations between tumours, CRC is often initiated with the alteration of the Wnt signalling pathway (Parsons et al., 2005). In the colon epithelium, Tuft cells promote intestinal epithelial regeneration during homeostasis. However, these cells are found highly expressed during the development of colorectal cancer and have been proposed as cancer initiating cells (Westphalen et al., 2014). In addition, aberrant secretion of ACh from tuft cells and cholinergic neurons in the epithelium of the GI tract has been suggested to induce tumorigenesis via MACh3R-dependent activation of the Wnt signalling pathway (Hayakawa et al., 2016).

Altered intracellular calcium signalling has been found in a number of cancers including colorectal cancer. Cancer cells present alterations in the expression and distribution of the different calcium channels which dysregulates the normal calcium fluxes across the cell. Recent studies suggest that a high expression of IP3Rs is associated with aggressive forms of colon cancer (Shibao et al., 2010). Overexpression of the SERCA pump was also found in colorectal cancer cells (Fan et al., 2014). In addition, dysregulation of TPC-dependent calcium signalling has been suggested to drive tumorigenesis in the endothelial tissue (Favia et al., 2016). Abnormal expression of TPC1 and 2 has been shown in cell cancer lines from bladder, blood and liver (Patel and Kilpatrick, 2018). Moreover, novel discoveries functionally demonstrated that NAADP stimulates mobilisation of calcium from TPCs in a model of human colorectal cancer (Faris et al., 2019). Furthermore, overexpression of the transcription factors NFATc3 and YAP has been confirmed to induce tumorigenesis in the gastrointestinal tract (Tripathi et al., 2014; Hayakawa et al., 2016).

This thesis demonstrates the role of muscarinergic-coupled calcium signals in the regulation of the epithelial barrier and tissue regeneration. In view of our results, we hypothesise that aberrant ACh release and a dysregulated expression of the calcium toolkit components can be responsible for the loss of tissue integrity observed in IBD and colorectal cancer. Defective intracellular calcium signalling can result in the incorrect secretion and formation of mucus, which is a phenotype observed during IBD. Increased secretion of ACh via cholinergic neurons and tuft cells and/or the aberrant expression of the elements of the calcium toolkit can results in the overexpression of transcription factors such as NFAT and YAP which ultimately result in the uncontrolled gene expression of stem cell markers which drives tumorigenesis (**Figure 6.8**).

The characterisation of this signalling pathway presents the opportunity to investigate the role of muscarinic-coupled intracellular calcium in IBD and cancer. Studies on this signalling pathway hold the potential for the finding of therapeutic targets. Recently, the Williams lab has developed an organoid culture system of tumour colonic epithelium (tumouroid). This model together with the use of the healthy matching sample can be used to study the characteristics of the calcium signals and to potentially find targets for the treatment of cancer.

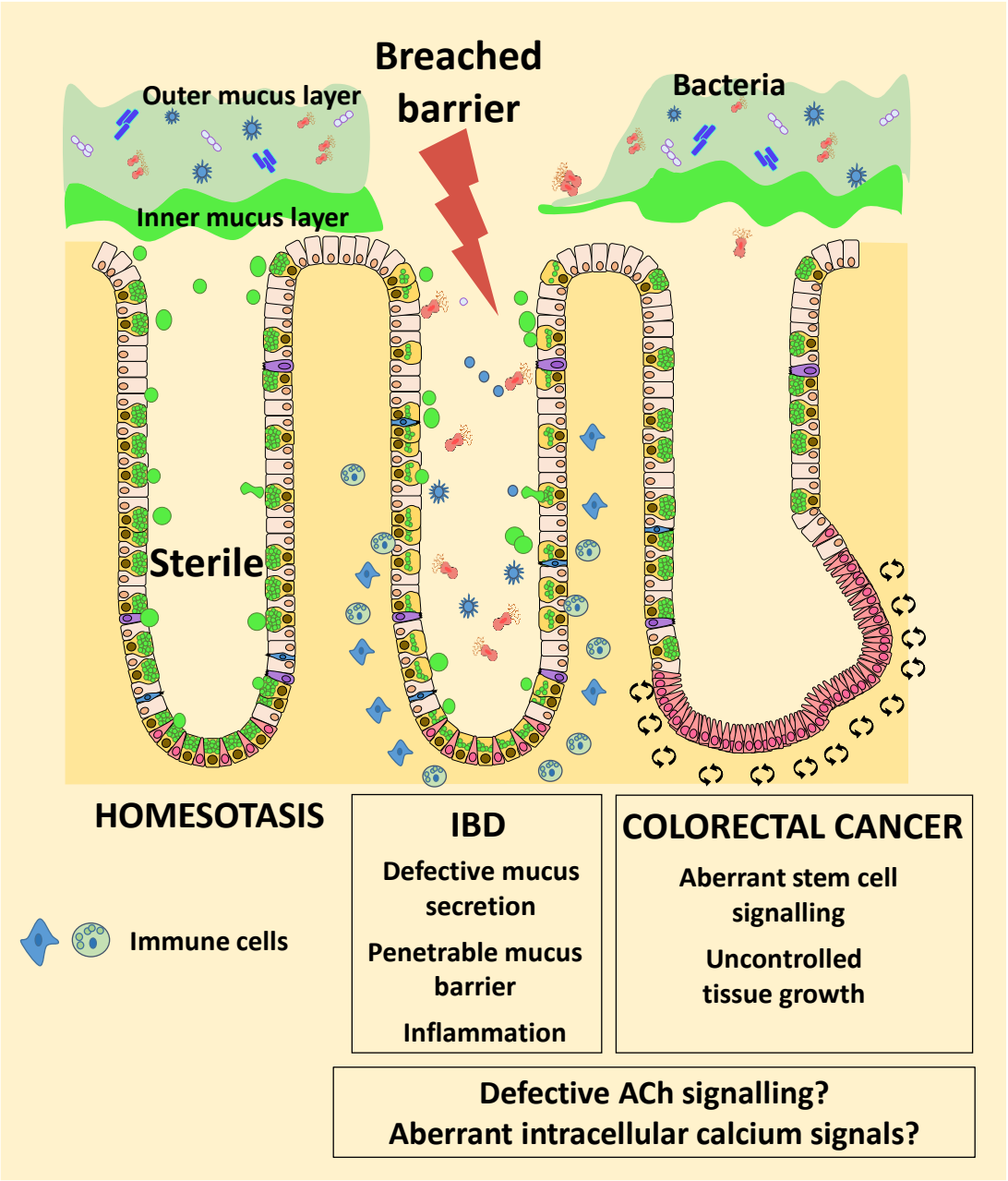

Figure 6.8. Potential role of ACh and intracellular calcium signalling in the onset of IBD and colorectal cancer. Aberrant calcium signals can result in the improper release and production of

mucus in goblet cells. In stem cells, the alteration of this signals can induce gene overexpression and uncontrolled tissue growth.

6.7 Concluding remarks

The work on thesis has helped to decipher the role of calcium signals in colon epithelium. It has been demonstrated that in response to ACh stimulation, a calcium signal is triggered which is mediated by the TPCs present in the acidic stores. The integration of this signal by calcium has been shown to modulate different cellular functions in the epithelial cells of the stem cell niche. In goblet cells these signals have been shown to induce mucus secretion and the release of fluid together with epithelial cells; two physiological functions required for the maintenance of the epithelial barrier. In stem cells, it has been demonstrated that stimulation of these calcium signals induces calcium-dependent transcription factor activation, which promotes stem cell proliferation and tissue regeneration. The development of a human organoid culture system that recapitulates the *in vivo* physiological conditions, provides an extraordinary opportunity to investigate human epithelial cell biology in health and disease. The novel characterisation of this intracellular calcium signalling and its regulation of the different physiological functions of the crypt epithelium, makes it a good candidate for the study of its status during intestinal diseases such as colorectal cancer and IBD, and the potential discovery of new therapeutic strategies.

Bibliography

Abdullah, L. H. *et al.* (1997) 'Protein kinase C and Ca2+ activation of mucin secretion in airway goblet cells', *American Journal of Physiology - Lung Cellular and Molecular Physiology*, 273(1 17-1).

Adebanjo, O. A. *et al.* (1999) 'A new function for CD38/ADP-ribosyl cyclase in nuclear Ca2+ homeostasis', *Nature Cell Biology*, 1(7), pp. 409–414. doi: 10.1038/15640.

Adler, K. B., Tuvim, M. J. and Dickey, B. F. (2013) 'Regulated mucin secretion from airway epithelial cells', *Frontiers in Endocrinology*, 4(SEP), pp. 1–9. doi: 10.3389/fendo.2013.00129.

Adli, M. (2018) 'The CRISPR tool kit for genome editing and beyond', *Nature Communications*. Springer US, 9(1). doi: 10.1038/s41467-018-04252-2.

Adolph, T. E. *et al.* (2013) 'Paneth cells as a site of origin for intestinal inflammation', *Nature*, 503(7475), pp. 272–276. doi: 10.1038/nature12599.

Agellon, L. B., Toth, M. J. and Thomson, A. B. R. (2002) 'Intracellular lipid binding proteins of the small intestine', *Molecular and Cellular Biochemistry*, 239(1–2), pp. 79–82. doi: 10.1023/A:1020520521025.

Albuquerque, E. X. *et al.* (2009) 'Mammalian Nicotinic Acetylcholine Receptors: From Structure to Function', *Physiology Review*, 89(1), pp. 73–120. doi: 10.1152/physrev.00015.2008.Mammalian.

Aliaga, J. C. *et al.* (2017) 'Requirement of the MAP kinase cascade for cell cycle progression and differentiation of human intestinal cells', *American Journal of Physiology-Gastrointestinal and Liver Physiology*, 277(3), pp. G631–G641. doi: 10.1152/ajpgi.1999.277.3.g631.

Almeqdadi, M. *et al.* (2019) 'Gut Organoids: Mini-Tissues in Culture to Study Intestinal Physiology and Disease', *American Journal of Physiology-Cell Physiology*, (46). doi: 10.1152/ajpcell.00300.2017.

Altmann, G. G. (1983) 'Morphological observations on mucus-secreting nongoblet cells in the deep crypts of the rat ascending colon', *American Journal of Anatomy*. John Wiley & Sons, Ltd, 167(1), pp. 95–117. doi: 10.1002/aja.1001670109.

Ambort, D. *et al.* (2012) 'Calcium and pH-dependent packing and release of the gel-forming MUC2 mucin', *Proceedings of the National Academy of Sciences*, 109(15), pp. 5645–5650. doi: 10.1073/pnas.1120269109.

Ambudkar, I. S. (2000) 'Regulation of calcium in salivary gland secretion', *Critical Reviews in Oral Biology and Medicine*, 11(1), pp. 4–25. doi: 10.1177/10454411000110010301.

Andrews, C., McLean, M. H. and Durum, S. K. (2018) 'Cytokine tuning of intestinal epithelial function', *Frontiers in Immunology*, 9(JUN). doi: 10.3389/fimmu.2018.01270.

Aoki, R. *et al.* (2016) 'Foxl1-Expressing Mesenchymal Cells Constitute the Intestinal Stem Cell Niche', *Cmgh*. Elsevier Inc, 2(2), pp. 175–188. doi: 10.1016/j.jcmgh.2015.12.004.

Arredouani, A. *et al.* (2015) 'NAADP and endolysosomal two-pore channels modulate membrane excitability and stimulus-secretion coupling in mouse pancreatic β cells', *Journal of Biological Chemistry*, 290(35), p. jbc.M115.671248. doi: 10.1074/jbc.M115.671248.

Artis, D. *et al.* (2004) 'RELM /FIZZ2 is a goblet cell-specific immune-effector molecule in the gastrointestinal tract', *Proceedings of the National Academy of Sciences*, 101(37), pp. 13596–13600. doi: 10.1073/pnas.0404034101.

Asfaha, S. *et al.* (2015) 'Krt19+/Lgr5- Cells Are Radioresistant Cancer-Initiating Stem Cells in the Colon and Intestine', *Cell Stem Cell*, 16(6), pp. 627–638. doi: 10.1016/j.stem.2015.04.013.

Ashby, M. C. *et al.* (2003) 'Long distance communication between muscarinic receptors and Ca2+ release channels revealed by carbachol uncaging in cell-attached patch pipette', *Journal of Biological Chemistry*, 278(23), pp. 20860–20864. doi: 10.1074/jbc.M302599200.

Atuma, C. *et al.* (2001) 'The adherent gastrointestinal mucus gel layer: thickness and physical state in vivo', *American Journal of Physiology-Gastrointestinal and Liver Physiology*, 280(5), pp. G922–G929. doi: 10.1152/ajpgi.2001.280.5.g922.

Azzolin, L. *et al.* (2014) 'YAP / TAZ Incorporation in the b -Catenin Destruction Complex Orchestrates the Wnt Response', *CELL*. Elsevier, 158(1), pp. 157–170. doi: 10.1016/j.cell.2014.06.013.

Azzouz, LL. Sharma, S. (2019) *Physiology, Large Intestine*, *StatPearls*. StatPearls. Available at: https://www.ncbi.nlm.nih.gov/books/NBK507857/.

Bader, S., Klein, J. and Diener, M. (2014) 'Choline acetyltransferase and organic cation transporters are responsible for synthesis and propionate-induced release of acetylcholine in colon epithelium', *European Journal of Pharmacology*. Elsevier, 733(1), pp. 23–33. doi: 10.1016/j.ejphar.2014.03.036.

Bagur, R. and Hajnoczky, G. (2017) 'Intracellular Ca2+ sensing: role in calcium homeostasis and

signaling', *Molecular Cell*, 66(6), pp. 780–788. doi: 10.1016/j.molcel.2017.05.028.

Bagur, R. and Hajnóczky, G. (2017) 'Intracellular Ca2+ Sensing: Its Role in Calcium Homeostasis and Signaling', *Molecular Cell*, 66(6), pp. 780–788. doi: 10.1016/j.molcel.2017.05.028.

Balseiro-Gomez, S. *et al.* (2015) 'Identification of a New Exo-Endocytic Mechanism Triggered by Corticotropin-Releasing Hormone in Mast Cells', *The Journal of Immunology*, 195(5), pp. 2046–2056. doi: 10.4049/jimmunol.1500253.

Banerjee, A., Coffey, R. J. and Lau, K. S. (2018) 'Interpreting heterogeneity in intestinal tuft cell structure and function', *J Clin Invest*, 128(5), pp. 1711–1719. doi: 10.1172/JCI120330.

Barber, R. D. *et al.* (2005) 'GAPDH as a housekeeping gene: Analysis of GAPDH mRNA expression in a panel of 72 human tissues', *Physiological Genomics*, 21, pp. 389–395. doi: 10.1152/physiolgenomics.00025.2005.

Barker, N. *et al.* (2007) 'Identification of stem cells in small intestine and colon by marker gene Lgr5', *Nature*, 449(7165), pp. 1003–1007. doi: 10.1038/nature06196.

Barker, N. (2014) 'Adult intestinal stem cells: critical drivers of epithelial homeostasis and regeneration.', *Nature reviews. Molecular cell biology*. Nature Publishing Group, 15(1), pp. 19–33. doi: 10.1038/nrm3721.

Barrett, K. E. and Keely, S. J. (2000) 'Chloride Secretion by the Intestinal Epithelium: Molecular Basis and Regulatory Aspects', *Annual Review of Physiology*, 62(1), pp. 535–572. doi: 10.1146/annurev.physiol.62.1.535.

Basak, O. *et al.* (2017) 'Induced Quiescence of Lgr5+ Stem Cells in Intestinal Organoids Enables Differentiation of Hormone-Producing Enteroendocrine Cells', *Cell Stem Cell*. Elsevier, 20(2), pp. 177-190.e4. doi: 10.1016/j.stem.2016.11.001.

Bedard, K. and Krause, K.-H. (2007) 'The NOX Family of ROS-Generating NADPH Oxidases: Physiology and Pathophysiology', *Physiological Reviews*, 87(1), pp. 245–313. doi: 10.1152/physrev.00044.2005.

Bekku, S. *et al.* (1998) 'Carbonic anhydrase I and II as a differentiation marker of human and rat colonic enterocytes', *Research in Experimental Medicine*, 198(4), pp. 175–185. doi: 10.1007/s004330050101.

Belley, A. and Chadee, K. (1999) 'Prostaglandin E2 stimulates rat and human colonic mucin

exocytosis via the EP4 receptor', *Gastroenterology*, 117(6), pp. 1352–1362. doi: 10.1016/S0016-5085(99)70285-4.

Bellono, N. W. *et al.* (2017) 'Enterochromaffin Cells Are Gut Chemosensors that Couple to Sensory Neural Pathways Article Enterochromaffin Cells Are Gut Chemosensors that Couple to Sensory Neural Pathways', *Cell*. Elsevier, 170(1), pp. 185-198.e16. doi: 10.1016/j.cell.2017.05.034.

Bennett, K. M. *et al.* (2016) 'Induction of Colonic M Cells during Intestinal Inflammation', *American Journal of Pathology*. American Society for Investigative Pathology, 186(5), pp. 1166–1179. doi: 10.1016/j.ajpath.2015.12.015.

Berkers, G. *et al.* (2019) 'Rectal Organoids Enable Personalized Treatment of Cystic Fibrosis', *Cell Reports*. ElsevierCompany., 26(7), pp. 1701-1708.e3. doi: 10.1016/j.celrep.2019.01.068.

Berridge, M. J. (2016) 'The Inositol Trisphosphate/Calcium Signaling Pathway in Health and Disease', *Physiological Reviews*, 96(4), pp. 1261–1296. doi: 10.1152/physrev.00006.2016.

Berridge, M. J., Bootman, M. D. and Roderick, H. L. (2003) 'Calcium signalling: dynamics, homeostasis and remodelling.', *Nature reviews. Molecular cell biology*, 4(7), pp. 517–29. doi: 10.1038/nrm1155.

Berridge, M. J., Lipp, P. and Bootman, M. D. (2000) 'The versatility and universality of calcium signalling.', *Nature reviews. Molecular cell biology*, 1(1), pp. 11–21. doi: 10.1038/35036035.

Beumer, J. *et al.* (2018) 'Enteroendocrine cells switch hormone expression along the crypt-to-villus BMP signalling gradient', *Nature Cell Biology*, 20(8), pp. 909–916. doi: 10.1038/s41556-018-0143-y.

Beumer, J. and Clevers, H. (2016) 'Regulation and plasticity of intestinal stem cells during homeostasis and regeneration', *Development*, 143(20), pp. 3639–3649. doi: 10.1242/dev.133132.

Beyaz, S. *et al.* (2016) 'High-fat diet enhances stemness and tumorigenicity of intestinal progenitors', *Nature*. Nature Publishing Group, 531(7592), pp. 53–58. doi: 10.1038/nature17173.

Bilgin, B. *et al.* (2016) 'Characterization of transcription factor response kinetics in parallel', *BMC Biotechnology*. BMC Biotechnology, 16(1), pp. 1–10. doi: 10.1186/s12896-016-0293-6.

Birchenough, G. M. H. *et al.* (2015) 'New developments in goblet cell mucus secretion and function', *Mucosal Immunology*, 8(4), pp. 712–719. doi: 10.1038/mi.2015.32.

Birchenough, G. M. H. *et al.* (2016) 'A sentinel goblet cell guards the colonic crypt by triggering

Nlrp6-dependent Muc2 secretion', *Science*, 352(6293), pp. 1535–1542. doi: 10.1126/science.aaf7419.

Bjerknes, M. and Cheng, H. (1999) 'Clonal analysis of mouse intestinal epithelial progenitors', *Gastroenterology*, 116(1), pp. 7–14. doi: 10.1016/S0016-5085(99)70222-2.

Bjerknes, M. and Cheng, H. (2001) 'Modulation of specific intestinal epithelial progenitors by enteric neurons.', *Proceedings of the National Academy of Sciences of the United States of America*, 98(22), pp. 12497–502. doi: 10.1073/pnas.211278098.

Boittin, F. X., Galione, A. and Evans, A. M. (2002) 'Nicotinic acid adenine dinucleotide phosphate mediates Ca2+ signals and contraction in arterial smooth muscle via a two-pool mechanism', *Circulation Research*, 91(12), pp. 1168–1175. doi: 10.1161/01.RES.0000047507.22487.85.

Bootman, M. D. *et al.* (2009) 'An update on nuclear calcium signalling', *Journal of Cell Science*, 122(14), pp. 2337–2350. doi: 10.1242/jcs.028100.

Bootman, M. D. and Bultynck, G. (2019) 'Fundamentals of Cellular Calcium Signaling: A Primer', *Cold Spring Harbor Perspectives in Biology*, (August), p. a038802. doi: 10.1101/cshperspect.a038802.

Boschero, A. C. *et al.* (1995) 'Oxotremorine-m potentiation of glucose-induced insulin release from rat islets involves M3 muscarinic receptors', *American Journal of Physiology - Endocrinology and Metabolism*, 268(2 31-2).

Boss, V., Talpade, D. J. and Murphy, T. J. (1996) 'Induction of NFAT-mediated transcription by Gq-coupled receptors in lymphoid and non-lymphoid cells', *Journal of Biological Chemistry*, 271(18), pp. 10429–10432. doi: 10.1074/jbc.271.18.10429.

Bou-Hanna, C. *et al.* (1994) 'Role of calcium in carbachol- and neurotensin-induced mucin exocytosis in a human colonic goblet cell line and cross-talk with the cyclic AMP pathway.', *The Biochemical journal*, 299 (Pt 2, pp. 579–585.

Brailoiu, E. *et al.* (2009) 'Essential requirement for two-pore channel 1 in NAADP-mediated calcium signaling', *Journal of Cell Biology*, 186(2), pp. 201–209. doi: 10.1083/jcb.200904073.

Brailoiu, G. C. *et al.* (2010) 'Acidic NAADP-sensitive calcium stores in the endothelium: Agonist-specific recruitment and role in regulating blood pressure', *Journal of Biological Chemistry*, 285(48), pp. 37133–37137. doi: 10.1074/jbc.C110.169763.

Brini, M. *et al.* (2014) 'Neuronal calcium signaling: Function and dysfunction', *Cellular and Molecular Life Sciences*, 71(15), pp. 2787–2814. doi: 10.1007/s00018-013-1550-7.

Brodskiy, P. A. and Zartman, J. J. (2018) 'Calcium as a signal integrator in developing epithelial tissues', *Physical Biology*, 15(5). doi: 10.1088/1478-3975/aabb18.

Brubaker, P. L. and Drucker, D. J. (2004) 'Minireview: Glucagon-like peptides regulate cell proliferation and apoptosis in the pancreas, gut, and central nervous system', *Endocrinology*, 145(6), pp. 2653–2659. doi: 10.1210/en.2004-0015.

Buchholz, M. and Ellenrieder, V. (2007) 'An emerging role for Ca2+/calcineurin/NFAT signaling in cancerogenesis', *Cell Cycle*, 6(1), pp. 16–19. doi: 10.4161/cc.6.1.3650.

Buczacki, S. J. a *et al.* (2013) 'Intestinal label-retaining cells are secretory precursors expressing Lgr5.', *Nature*, 495(7439), pp. 65–9. doi: 10.1038/nature11965.

Büller, N. V. J. A. *et al.* (2012) 'Hedgehog Signaling and Maintenance of Homeostasis in the Intestinal Epithelium', *Physiology*, 27(3), pp. 148–155. doi: 10.1152/physiol.00003.2012.

Calcraft, P. J. *et al.* (2009) 'NAADP mobilizes calcium from acidic organelles through two-pore channels.', *Nature*. Nature Publishing Group, 459(7246), pp. 596–600. doi: 10.1038/nature08030.

Cameron, H. L. and Perdue, M. H. (2007) 'Muscarinic acetylcholine receptor activation increases transcellular transport of macromolecules across mouse and human intestinal epithelium in vitro.', *Neurogastroenterol Motil*, 19(1), pp. 47–56. doi: 10.1111/j.1365-2982.2006.00845.x.

Campoy, F. J. *et al.* (2016) 'Cholinergic system and cell proliferation', *Chemico-Biological Interactions*, pp. 1–9. doi: 10.1016/j.cbi.2016.04.014.

Cane, M. C. *et al.* (2016) 'The two pore channel TPC2 is dispensable in pancreatic β-cells for normal Ca2+ dynamics and insulin secretion', *Cell Calcium*. Elsevier Ltd, 59(1), pp. 32–40. doi: 10.1016/j.ceca.2015.12.004.

Cantero-Recasens, G. *et al.* (2018) 'KChIP3 coupled to ca 2+ oscillations exerts a tonic brake on baseline mucin release in the colon', *eLife*, 7, pp. 1–20. doi: 10.7554/eLife.39729.

Capitani, M. and Sallese, M. (2009) 'The KDEL receptor: New functions for an old protein', *FEBS Letters*. Federation of European Biochemical Societies, 583(23), pp. 3863–3871. doi: 10.1016/j.febslet.2009.10.053.

Cárdenas, C. *et al.* (2010) 'Essential Regulation of Cell Bioenergetics by Constitutive InsP3 Receptor Ca2+ Transfer to Mitochondria', *Cell*, 142(2), pp. 270–283. doi: 10.1016/j.cell.2010.06.007.

Carreras-Sureda, A., Pihán, P. and Hetz, C. (2018) 'Calcium signaling at the endoplasmic reticulum: fine-tuning stress responses', *Cell Calcium*, 70(April 2017), pp. 24–31. doi: 10.1016/j.ceca.2017.08.004.

Catteral, W. A. (2011) 'Voltage-gated calcium channels', *Cold Spring Harbor Perspectives in Biology*, pp. 1–23. doi: 10.1101/cshperspect.a003947.

Chai, J. and Tarnaswski, A. S. (2002) 'Serum Response Factor: Discovery, Biochemistry, Biological Roles and Implications for Tissue Injury Healing', *Journa of Physiology and Pharmacology*, 53(2), pp. 147–157.

Chamero, P. *et al.* (2002) 'Dampening of cytosolic Ca2+ oscillations on propagation to nucleus', *Journal of Biological Chemistry*, 277(52), pp. 50226–50229. doi: 10.1074/jbc.C200522200.

Cheadle, G. a. *et al.* (2013) 'Enteric Glia Cells Attenuate Cytomix-Induced Intestinal Epithelial Barrier Breakdown', *PLoS ONE*, 8(7), pp. 1–11. doi: 10.1371/journal.pone.0069042.

Chen, E. Y. T. *et al.* (2011) 'Mucin secretion induced by titanium dioxide nanoparticles', *PLoS ONE*, 6(1), pp. 1–8. doi: 10.1371/journal.pone.0016198.

Chen, L. *et al.* (1998) 'Structure of the DNA-binding domains from NFAT, Fos and Jun bound specifically to DNA', *Nature*, 392(6671), pp. 42–48. doi: 10.1038/32100.

Cheng, H. and Leblond, C. P. (1974) 'Origin, differentiation and renewal of the four main epithelial cell types in the mouse small intestine I. Columnar cell', *American Journal of Anatomy*, 141(4), pp. 461–479. doi: 10.1002/aja.1001410403.

Cheng, K. *et al.* (2008) 'Acetylcholine release by human colon cancer cells mediates autocrine stimulation of cell proliferation', *Annual Journal of Physiology Gastrointest Liver Physiol*, 21201, pp. 591–597. doi: 10.1152/ajpgi.00055.2008.

Cheung, W. Y. (1979) 'Calmodulin Plays a Pivotal Role in Cellular Regulation', *Science*, 207, pp. 19–28.

Chieppa, M. *et al.* (2006) 'Dynamic imaging of dendritic cell extension into the small bowel lumen in response to epithelial cell TLR engagement', *The Journal of Experimental Medicine*, 203(13), pp. 2841–2852. doi: 10.1084/jem.20061884.

Chun-Mei Zhao, Yoku Hayakawa, Yosuke Kodama, Sureshkumar Muthupalani *et al.* (2014) 'Denervation suppresses gastric tumorigenesis', *Science Translational Medicine*, 6(250). doi: 10.1126/scitranslmed.3009569.

Churchill, G. C. *et al.* (2002) 'NAADP mobilizes Ca2+ from reserve granules, lysosome-related organelles, in sea urchin eggs', *Cell*, 111(5), pp. 703–708. doi: 10.1016/S0092-8674(02)01082-6.

Chuvpilo, S. *et al.* (2002) 'Autoregulation of NFATc1/A expression facilitates effector T cells to escape from rapid apoptosis', *Immunity*, 16(6), pp. 881–895. doi: 10.1016/S1074-7613(02)00329-1.

Clevers, H. (2013) 'The intestinal crypt, a prototype stem cell compartment', *Cell*. Elsevier Inc., 154(2), pp. 274–284. doi: 10.1016/j.cell.2013.07.004.

Clevers, H. C. and Bevins, C. L. (2013) 'Paneth Cells: Maestros of the Small Intestinal Crypts', *Annual Review of Physiology*, 75(1), pp. 289–311. doi: 10.1146/annurev-physiol-030212-183744.

Clevers, H., Loh, K. M. and Nusse, R. (2014) 'Stem cell signaling. An integral program for tissue renewal and regeneration: Wnt signaling and stem cell control.', *Science (New York, N.Y.)*, 346(6205), p. 1248012. doi: 10.1126/science.1248012.

Cobo, E. R. and Chadee, K. (2013) 'Antimicrobial human β-defensins in the colon and their role in infectious and non-infectious diseases', *Pathogens*, 2(1), pp. 177–192. doi: 10.3390/pathogens2010177.

Coe, H. and Michalak, M. (2009) 'Calcium binding chaperones of the endoplasmic reticulum', *General Physiology and Biophysics*, 28, pp. 96–103.

Collatz, M. B., Riidel, R. and Brinkmeier, H. (1997) 'Intracellular calcium chelator BAPTA protects cells against toxic calcium bverload but alsb alters Dhvsioloaical calcium responses', *Research Cell Cafcwn*, (6), pp. 453–459. Available at: https://pdf.sciencedirectassets.com/272490/1-s2.0-S0143416000X01662/1-s2.0-S0143416097900567/main.pdf?x-amz-security-token=AgoJb3JpZ2luX2VjEGAaCXVzLWVhc3QtMSJHMEUCIQClQ3x%2BcEaWyipA5lyb4m2f5BtsHDUEJKM3Ya1QHx4GOgIgBSz6JamP1NKDYO6VHDbq3%2FFhC8763Vy7lAJQoGBl.

Collins, Jason T. Badireddy, M. (2019) 'Anatomy, Abdomen and Pelvis, Small Intestine', in *Treasure Island (FL): StatPearls Publishing*. Available at: https://www.ncbi.nlm.nih.gov/books/NBK459366/.

Contreras, L. *et al.* (2010) 'Mitochondria: The calcium connection', *Biochimica et Biophysica Acta - Bioenergetics*. Elsevier B.V., 1797(6–7), pp. 607–618. doi: 10.1016/j.bbabio.2010.05.005.

Cooke, H. J. *et al.* (1991) 'Neural 5-hydroxytryptamine receptors regulate chloride secretion in guinea pig distal colon', *American Journal of Physiology - Gastrointestinal and Liver Physiology*, 261(5 24-5).

Cooke, H. J., Sidhu, M. and Wang, Y. Z. (1997) '5-HT activates neural reflexes regulating secretion in the guinea-pig colon.', *Neurogastroenterology and motility : the official journal of the European Gastrointestinal Motility Society*, 9(3), pp. 181–186.

Coyte, K. Z. and Rakoff-Nahoum, S. (2019) 'Understanding Competition and Cooperation within the Mammalian Gut Microbiome', *Current Biology*. Elsevier Ltd., 29(11), pp. R538–R544. doi: 10.1016/j.cub.2019.04.017.

Crabtree, G. R. (2001) 'Calcium, Calcineurin, and the Control of Transcription', *Journal of Biological Chemistry*, 276(4), pp. 2313–2316. doi: 10.1074/jbc.R000024200.

Dando, R. and Roper, S. D. (2012) 'Acetylcholine is released from taste cells, enhancing taste signalling', *Journal of Physiology*, 590(13), pp. 3009–3017. doi: 10.1113/jphysiol.2012.232009.

Date, S. and Sato, T. (2015) 'Mini-Gut Organoids: Reconstitution of Stem Cell Niche', *Annual Review of Cell and Developmental Biology*, 31(1), p. annurev-cellbio-100814-125218. doi: 10.1146/annurev-cellbio-100814-125218.

Davis, E. A., Zhou, W. and Dailey, M. J. (2018) 'Evidence for a direct effect of the autonomic nervous system on intestinal epithelial stem cell proliferation', *Physiological Reports*, 6(12), pp. 1–8. doi: 10.14814/phy2.13745.

Davis, H. *et al.* (2015) 'Aberrant epithelial GREM1 expression initiates colonic tumorigenesis from cells outside the stem cell niche', *Nature Medicine*. Nature Publishing Group, 21(1), pp. 62–70. doi: 10.1038/nm.3750.

Davis, L. C. *et al.* (2012) 'NAADP Activates two-pore channels on t cell cytolytic granules to stimulate exocytosis and killing', *Current Biology*. Elsevier Ltd, 22(24), pp. 2331–2337. doi: 10.1016/j.cub.2012.10.035.

Dawson, S. P., Keizer, J. and Pearson, J. E. (1999) 'Fire-diffuse-fire model of dynamics of intracellular calcium waves', *Proceedings of the National Academy of Sciences of the United States of America*, 96(11), pp. 6060–6063. doi: 10.1073/pnas.96.11.6060.

Deckmann, K. *et al.* (2014) 'Bitter triggers acetylcholine release from polymodal urethral

chemosensory cells and bladder reflexes', *Proceedings of the National Academy of Sciences*, 111(22), pp. 8287–8292. doi: 10.1073/pnas.1402436111.

Demitrack, E. S. and Samuelson, L. C. (2016) 'Notch regulation of gastrointestinal stem cells', *Journal of Physiology*, 594(17), pp. 4791–4803. doi: 10.1113/JP271667.

Deng, H., Gerencser, A. a. and Jasper, H. (2015) 'Signal integration by Ca2+ regulates intestinal stem-cell activity', *Nature*. Nature Publishing Group, pp. 1–26. doi: 10.1038/nature16170.

Devriese, S. *et al.* (2017) 'T84 monolayers are superior to Caco-2 as a model system of colonocytes', *Histochemistry and Cell Biology*. Springer Berlin Heidelberg, 148(1), pp. 85–93. doi: 10.1007/s00418-017-1539-7.

Dharmani, P. *et al.* (2009) 'Role of intestinal mucins in innate host defense mechanisms against pathogens', *Journal of Innate Immunity*, 1(2), pp. 123–135. doi: 10.1159/000163037.

Dickinson, K. E. J., Frizzell, R. a. and Sekar, M. C. (1992) 'Activation of T84 cell chloride channels by carbachol involves a phosphoinositide-coupled muscarinic M3 receptor', *European Journal of Pharmacology: Molecular Pharmacology*, 225(4), pp. 291–298. doi: 10.1016/0922-4106(92)90102-2.

Diwakarla, Shanti. Fothergill, Linda J. Fakhry, Josiane. Callaghan, Brid. Furnsess, J. B. (2017) 'Heterogeneity of enterochromaffin cells within the gastrointestinal tract', *Neurogastroenterol Motility*, 29(6). doi: 10.1093/oxfordjournals.bmb.a072118.

Dodd, A. N., Kudla, J. and Sanders, D. (2010) 'The Language of Calcium Signaling', *Annual Review of Plant Biology*, 61(1), pp. 593–620. doi: 10.1146/annurev-arplant-070109-104628.

Donaldson, G. P., Lee, S. M. and Mazmanian, S. K. (2017) 'HHS Public Access Gut biogeography of the bacterial microbiota', *Nature Reviews Microbiology*, 14(1), pp. 20–32. doi: 10.1038/nrmicro3552.Gut.

Duchalais, E. *et al.* (2018) 'Colorectal Cancer Cells Adhere to and Migrate Along the Neurons of the Enteric Nervous System', *Cmgh*. Elsevier Inc, 5(1), pp. 31–49. doi: 10.1016/j.jcmgh.2017.10.002.

Dupont, G. *et al.* (2011) 'Calcium Oscillations', *Cold Spring Harbor Perspectives in Biology*, 3, pp. 1–27. doi: 10.1101/cshperspect.a004226.

Eberhart, C. E. and Dubois, R. N. (1995) 'Eicosanoids in the gastrointestinal tract', *British Journal of Pharmacology*, 109, pp. 285–301. doi: 10.1111/bph.14178.

Edelblum, K. L. *et al.* (2006) 'Regulation of apoptosis during homeostasis and disease in the intestinal epithelium', *Inflammatory Bowel Diseases*, 12(5), pp. 413–424. doi: 10.1097/01.MIB.0000217334.30689.3e.

Efeyan, A. and Sabatini, D. M. (2010) 'MTOR and cancer: Many loops in one pathway', *Current Opinion in Cell Biology*, 22(2), pp. 169–176. doi: 10.1016/j.ceb.2009.10.007.

Eglen, R. M. (2006) 'Muscarinic receptor subtypes in neuronal and non-neuronal cholinergic function', *Autonomic and Autacoid Pharmacology*, 26(3), pp. 219–233. doi: 10.1111/j.1474-8673.2006.00368.x.

Erdmann, F. *et al.* (2010) 'The novel calcineurin inhibitor CN585 has potent immunosuppressive properties in stimulated human T cells', *Journal of Biological Chemistry*, 285(3), pp. 1888–1898. doi: 10.1074/jbc.M109.024844.

van Es, Johan. H. Sato, Toshiro. van de Wetering, Marc. Lyubimova, Anna. Gregorieff, Alex. Zeinstra, Laura. van den Born, Maaike. Korving, Jeroen. Martes, Anton. C.M. van dn Oudenaarden, Alexander. Clevers, H. (2013) 'Dll1 marks early secretory progenitors in gut crypts that can revert to stem cells upon tissue damage', *Nature cell biology*, 14(10), pp. 1099–1104. doi: 10.1038/ncb2581.Dll1.

Espinosa, A. *et al.* (2009) 'NADPH oxidase and hydrogen peroxide mediate insulin-induced calcium increase in skeletal muscle cells', *Journal of Biological Chemistry*, 284(4), pp. 2568–2575. doi: 10.1074/jbc.M804249200.

Evans, G. S. *et al.* (1992) 'The development of a method for the preparation of rat intestinal epithelial cell primary cultures.', *Journal of cell science*, 101 (Pt 1, pp. 219–31. Available at: http://www.ncbi.nlm.nih.gov/pubmed/1569126.

Fan, L. *et al.* (2014) 'Novel role of Sarco/endoplasmic reticulum calcium ATPase 2 in development of colorectal cancer and its regulation by F36, a curcumin analog', *Biomedicine and Pharmacotherapy*. Elsevier Masson SAS, 68(8), pp. 1141–1148. doi: 10.1016/j.biopha.2014.10.014.

Farin, H. F. *et al.* (2016) 'Visualization of a short-range Wnt gradient in the intestinal stem-cell niche.', *Nature*. Nature Publishing Group, 530(7590), pp. 340–3. doi: 10.1038/nature16937.

Farin, H. F., Van Es, J. H. and Clevers, H. (2012) 'Redundant sources of Wnt regulate intestinal stem cells and promote formation of paneth cells', *Gastroenterology*. Elsevier Inc., 143(6), pp. 1518-1529.e7. doi: 10.1053/j.gastro.2012.08.031.

Faris, P. *et al.* (2019) 'Nicotinic Acid Adenine Dinucleotide Phosphate (NAADP) Induces Intracellular Ca2+ Release through the Two-Pore Channel TPC1 in Metastatic Colorectal Cancer Cells', 11, pp. 1–19.

Favia, A. *et al.* (2014) 'VEGF-induced neoangiogenesis is mediated by NAADP and two-pore channel-2-dependent Ca2+ signaling.', *Proceedings of the National Academy of Sciences of the United States of America*, 111(44), pp. E4706-15. doi: 10.1073/pnas.1406029111.

Favia, A. *et al.* (2016) 'NAADP-Dependent Ca(2+) Signaling Controls Melanoma Progression, Metastatic Dissemination and Neoangiogenesis.', *Scientific reports*. Nature Publishing Group, 6(August 2015), p. 18925. doi: 10.1038/srep18925.

Fearon, E. R. and Volgelstein, B. (1990) 'A genetic model for colorectal cancer', *Cell*, 61(5), pp. 759–767. Available at: http://www.fundacion-barcelo.com.ar/oncologia-molecular/sesion 2/Bibliografia Sesion 2/j- Manuel Perucho-Genetica y epigenetica del Cancer/FearonOK - A genetic model for colorectal cancer.pdf.

Fevr, T. *et al.* (2007) 'Wnt/ -Catenin Is Essential for Intestinal Homeostasis and Maintenance of Intestinal Stem Cells', *Molecular and Cellular Biology*, 27(21), pp. 7551–7559. doi: 10.1128/mcb.01034-07.

Finnie, I. A. *et al.* (1995) 'Colonic mucin synthesis is increased by sodium butyrate', *Gut*, 36, pp. 93–99. Available at: https://www.ncbi.nlm.nih.gov/pmc/articles/PMC1382360/pdf/gut00519-0103.pdf.

van der Flier, L. G., Haegebarth, A., *et al.* (2009) 'OLFM4 Is a Robust Marker for Stem Cells in Human Intestine and Marks a Subset of Colorectal Cancer Cells', *Gastroenterology*. AGA Institute American Gastroenterological Association, 137(1), pp. 15–17. doi: 10.1053/j.gastro.2009.05.035.

van der Flier, L. G., van Gijn, M. E., *et al.* (2009) 'Transcription Factor Achaete Scute-Like 2 Controls Intestinal Stem Cell Fate', *Cell*. Elsevier Ltd, 136(5), pp. 903–912. doi: 10.1016/j.cell.2009.01.031.

Flint, H. J. *et al.* (2012) 'The role of the gut microbiota in nutrition and health', *Nature Reviews Gastroenterology & Hepatology*. Nature Publishing Group, 9(10), pp. 577–589. doi: 10.1038/nrgastro.2012.156.

Foskett, J. K. *et al.* (2007) ' Inositol Trisphosphate Receptor Ca 2+ Release Channels ', *Physiological Reviews*, 87(2), pp. 593–658. doi: 10.1152/physrev.00035.2006.

Foulke-Abel, J. *et al.* (2016) 'Human Enteroids as a Model of Upper Small Intestinal Ion Transport

Physiology and Pathophysiology', *Gastroenterology*. Elsevier, Inc, 150(3), pp. 638-649.e8. doi: 10.1053/j.gastro.2015.11.047.

France, M. M. and Turner, J. R. (2017) 'The mucosal barrier at a glance', *Journal of Cell Science*, 130(2), pp. 307–314. doi: 10.1242/jcs.193482.

Fre, S. *et al.* (2005) 'Notch signals control the fate of immature progenitor cells in the intestine', *Nature*, 435(7044), pp. 964–968. doi: 10.1038/nature03589.

Fridlyand, L. E., Tamarina, N. and Philipson, L. H. (2010) 'Bursting and calcium oscillations in pancreatic β-cells: Specific pacemakers for specific mechanisms', *American Journal of Physiology - Endocrinology and Metabolism*, 299(4). doi: 10.1152/ajpendo.00177.2010.

Frizzell, R. A. and Hanrahan, J. W. (2012) 'Physiology of epithelial chloride and fluid secretion', *Cold Spring Harbor Perspectives in Medicine*, 2(6), pp. 1–20. doi: 10.1101/cshperspect.a009563.

Fujii, M. *et al.* (2018) 'Human Intestinal Organoids Maintain Self-Renewal Capacity and Cellular Diversity in Niche-Inspired Culture Condition', *Cell Stem Cell*. Elsevier Inc., 23(6), pp. 787-793.e6. doi: 10.1016/j.stem.2018.11.016.

Fujii, M., Clevers, H. and Sato, T. (2019) 'Modeling Human Digestive Diseases With CRISPR-Cas9–Modified Organoids', *Gastroenterology*. Elsevier, Inc, 156(3), pp. 562–576. doi: 10.1053/j.gastro.2018.11.048.

Fujii, S. *et al.* (2016) 'PGE 2 is a direct and robust mediator of anion/fluid secretion by human intestinal epithelial cells', *Scientific Reports*, 6(February), pp. 1–15. doi: 10.1038/srep36795.

Fukuda, N. *et al.* (2008) 'Decreased olfactory mucus secretion and nasal abnormality in mice lacking type 2 and type 3 IP3 receptors', *European Journal of Neuroscience*, 27(10), pp. 2665–2675. doi: 10.1111/j.1460-9568.2008.06240.x.

Furness, J. B. (2012) 'The enteric nervous system and neurogastroenterology', *Nature Reviews Gastroenterology & Hepatology*. Nature Publishing Group, 9(5), pp. 286–294. doi: 10.1038/nrgastro.2012.32.

Furness, J. B. *et al.* (2013) 'The gut as a sensory organ', *Nature reviews. Gastroenterology & hepatology*. Nature Publishing Group, 10(12), pp. 729–740. doi: 10.1038/nrgastro.2013.180.

Galione, A. *et al.* (2010) 'NAADP as an intracellular messenger regulating lysosomal calcium-release

channels', *Biochemical Society Transactions*, 38(6), pp. 1424–1431. doi: 10.1042/BST0381424.

Galione, A. (2011) 'NAADP receptors', *Cold Spring Harbor perspectives in biology*, 38(3–4), pp. 273–280. doi: S0143-4160(05)00118-1 [pii] 10.1016/j.ceca.2005.06.031.

Galione, A., Lee, H. C. and Busa, W. B. (1991) 'Ca2+-induced Ca2+ release in sea urchin egg homogenates: Modulation by cyclic ADP-Ribose', *Science*, 253(5024), pp. 1143–1146. doi: 10.1126/science.1909457.

Garcher, C. (1998) 'CA 19-9 ELISA test: A new method for studying mucus changes in tears', *British Journal of Ophthalmology*, 82(1), pp. 88–90. doi: 10.1136/bjo.82.1.88.

Garcia-Cozar, F. J. *et al.* (1998) 'Two-site interaction of nuclear factor of activated T cells with activated calcineurin', *Journal of Biological Chemistry*, 273(37), pp. 23877–23883. doi: 10.1074/jbc.273.37.23877.

Garcia, M. A. S., Yang, N. and Quinton, P. M. (2009) 'Normal mouse intestinal mucus release requires cystic fibrosis transmembrane regulator-dependent bicarbonate secretion', *Journal of Clinical Investigation*, 119(9), pp. 2613–2622. doi: 10.1172/JCI38662.

Gassler, N. (2017) 'Paneth cells in intestinal physiology and pathophysiology', *World Journal of Gastrointestinal Pathophysiology*, 8(4), pp. 150–160. doi: 10.4291/wjgp.v8.i4.150.

Gaudier, E. *et al.* (2004) ' Butyrate specifically modulates MUC gene expression in intestinal epithelial goblet cells deprived of glucose ', *American Journal of Physiology-Gastrointestinal and Liver Physiology*, 287(6), pp. G1168–G1174. doi: 10.1152/ajpgi.00219.2004.

Gehart, H. and Clevers, H. (2019) 'Tales from the crypt: new insights into intestinal stem cells', *Nature Reviews Gastroenterology and Hepatology*. Springer US, 16(1), pp. 19–34. doi: 10.1038/s41575-018-0081-y.

Geibel, J. P. (2004) 'Secretion and Absorption By Colonic Crypts', *Annual Review of Physiology*, 67(1), pp. 471–490. doi: 10.1146/annurev.physiol.67.031103.153530.

Genazzani, A. A. *et al.* (1997) 'Pharmacological properties of the Ca2+-release mechanism sensitive to NAADP in the sea urchin egg', *British Journal of Pharmacology*, 121(7), pp. 1489–1495. doi: 10.1038/sj.bjp.0701295.

Gerbe, F. *et al.* (2011) 'Distinct ATOH1 and Neurog3 requirements define tuft cells as a new

secretory cell type in the intestinal epithelium', *Journal of Cell Biology*, 192(5), pp. 767–780. doi: 10.1083/jcb.201010127.

Gerbe, F. *et al.* (2016) 'Intestinal epithelial tuft cells initiate type 2 mucosal immunity to helminth parasites.', *Nature*. Nature Publishing Group, 529(7585), pp. 226–30. doi: 10.1038/nature16527.

Gerbe, F., Legraverend, C. and Jay, P. (2012) 'The intestinal epithelium tuft cells: Specification and function', *Cellular and Molecular Life Sciences*, 69(17), pp. 2907–2917. doi: 10.1007/s00018-012-0984-7.

Gerdes, J. *et al.* (1984) 'Cell cycle analysis of a cell proliferation-associated human nuclear antigen defined by the monoclonal antibody Why The JI ? Submit online . • Rapid Reviews ! 30 days * from submission to initial decision • No Triage ! Every submission reviewed by practic', *The Journal of Immunology*, 133(4), pp. 1710–1715.

Gerling, M. *et al.* (2016) 'Stromal Hedgehog signalling is downregulated in colon cancer and its restoration restrains tumour growth', *Nature Communications*, 7. doi: 10.1038/ncomms12321.

Gibson, Peter R. Van De Pol, Erika. Maxwell, Lesley E. Gabriel, Anastasia. Doe, W. F. (1989) 'Isolation of Colonic Crypts That Maintain Structural and Metabolic Viability In Vitro', *Gastroenterology*, 96(2), pp. 283–291.

Gifford, J. L., Walsh, M. P. and Vogel, H. J. (2007) ' Structures and metal-ion-binding properties of the Ca 2+ -binding helix–loop–helix EF-hand motifs ', *Biochemical Journal*, 405(2), pp. 199–221. doi: 10.1042/bj20070255.

Giorgi, C. *et al.* (2015) 'Mitochondria-Associated Membranes: Composition, Molecular Mechanisms, and Physiopathological Implications', *Antioxidants & Redox Signaling*. Mary Ann Liebert, Inc., publishers, 22(12), pp. 995–1019. doi: 10.1089/ars.2014.6223.

Giorgi, C., Marchi, S. and Pinton, P. (2018) 'The machineries, regulation and cellular functions of mitochondrial calcium', *Molecular and Cellular Biology*. Springer US, 19, pp. 713–720. doi: 10.1038/s41580-018-0052-8.

Godl, K. *et al.* (2002) 'The N terminus of the MUC2 mucin forms trimers that are held together within a trypsin-resistant core fragment', *Journal of Biological Chemistry*, 277(49), pp. 47248–47256. doi: 10.1074/jbc.M208483200.

Gómez-Suaga, P. *et al.* (2012) 'Leucine-rich repeat kinase 2 regulates autophagy through a calcium-

dependent pathway involving NAADP', *Human Molecular Genetics*, 21(3), pp. 511–525. doi: 10.1093/hmg/ddr481.

Goto, N. *et al.* (2019) 'Lineage tracing and targeting of IL17RB $^{+}$ tuft cell-like human colorectal cancer stem cells', *Proceedings of the National Academy of Sciences*, p. 201900251. doi: 10.1073/pnas.1900251116.

Graef, I. A. *et al.* (2001) 'Signals transduced by Ca 2+ /calcineurin and NFATc3/c4 pattern the developing vasculature', *Cell*, 105(7), pp. 863–875. doi: 10.1016/S0092-8674(01)00396-8.

Granados, M. P. *et al.* (2006) 'Dose-dependent effect of hydrogen peroxide on calcium mobilization in mouse pancreatic acinar cells', *Biochemistry and Cell Biology*, 84(1), pp. 39–48. doi: 10.1139/o05-150.

Grando, S. A. *et al.* (1993) 'Human keratinocytes synthesize, secrete, and degrade acetylcholine', *Journal of Investigative Dermatology*. Elsevier Masson SAS, 101(1), pp. 32–36. doi: 10.1111/1523-1747.ep12358588.

Greco, V. *et al.* (1967) 'Histochemistry of the colonic epithelial mucins in normal subjects and in patients with ulcerative colitis. A qualitative and histophotometric investigation.', *Gut*, 8(5), pp. 491–496. doi: 10.1136/gut.8.5.491.

Gregorieff, A. *et al.* (2015) 'Yap-dependent reprogramming of Lgr5 stem cells drives intestinal regeneration and cancer', *Nature*, 526. doi: 10.1038/nature15382.

Greicius, G. *et al.* (2018) ' PDGFRα + pericryptal stromal cells are the critical source of Wnts and RSPO3 for murine intestinal stem cells in vivo ', *Proceedings of the National Academy of Sciences*, 115(14), pp. E3173–E3181. doi: 10.1073/pnas.1713510115.

Gribble, F. M. and Reimann, F. (2019) 'Function and mechanisms of enteroendocrine cells and gut hormones in metabolism', *Nature Reviews Endocrinology*. Springer US, 15(4), pp. 226–237. doi: 10.1038/s41574-019-0168-8.

Grimm, C. *et al.* (2014) 'High susceptibility to fatty liver disease in two-pore channel 2-deficient mice', *Nature Communications*, 5. doi: 10.1038/ncomms5699.

Gross, E. R. *et al.* (2012) 'Neuronal serotonin regulates growth of the intestinal mucosa in mice', *Gastroenterology*. Elsevier Inc., 143(2), pp. 408–417. doi: 10.1053/j.gastro.2012.05.007.

Gunawardene, A. R., Corfe, B. M. and Staton, C. a. (2011) 'Classification and functions of enteroendocrine cells of the lower gastrointestinal tract', *International Journal of Experimental Pathology*, 92(4), pp. 219–231. doi: 10.1111/j.1365-2613.2011.00767.x.

Günther, C. *et al.* (2013) 'Apoptosis, necrosis and necroptosis: Cell death regulation in the intestinal epithelium', *Gut*, 62(7), pp. 1062–1071. doi: 10.1136/gutjnl-2011-301364.

Gustafsson, J. K. *et al.* (2012) 'Bicarbonate and functional CFTR channel are required for proper mucin secretion and link cystic fibrosis with its mucus phenotype', *The Journal of Experimental Medicine*, 209(7), pp. 1263–1272. doi: 10.1084/jem.20120562.

Gustafsson, J. K. *et al.* (2014) 'Carbachol-induced colonic mucus formation requires transport via NKCC1, K(+) channels and CFTR.', *Pflugers Archiv : European journal of physiology*, pp. 1403–1415. doi: 10.1007/s00424-014-1595-y.

Gut, P. *et al.* (2016) 'Chromogranin A - Unspecific neuroendocrine marker. Clinical utility and potential diagnostic pitfalls', *Archives of Medical Science*, 12(1), pp. 1–9. doi: 10.5114/aoms.2016.57577.

Guttman, J. A. and Finlay, B. B. (2009) 'Tight junctions as targets of infectious agents', *Biochimica et Biophysica Acta - Biomembranes*. Elsevier B.V., 1788(4), pp. 832–841. doi: 10.1016/j.bbamem.2008.10.028.

Haber, A. L. *et al.* (2017) 'A single-cell survey of the small intestinal epithelium', *Nature*. Nature Publishing Group, 551(7680), pp. 333–339. doi: 10.1038/nature24489.

Haberberger, R., Schultheiss, G. and Diener, M. (2006) 'Epithelial muscarinic M1 receptors contribute to carbachol-induced ion secretion in mouse colon', *European Journal of Pharmacology*, 530(3), pp. 229–233. doi: 10.1016/j.ejphar.2005.11.055.

Halm, D. R. and Halm, S. T. (2000) 'Secretagogue response of goblet cells and columnar cells in human colonic crypts.', *American journal of physiology. Cell physiology*, 278(1), pp. C212-33. doi: 10.1152/ajpcell.2000.278.1.C212.

Hamer, H. M. *et al.* (2008) 'Review article: The role of butyrate on colonic function', *Alimentary Pharmacology and Therapeutics*, 27(2), pp. 104–119. doi: 10.1111/j.1365-2036.2007.03562.x.

Hamilton, A. *et al.* (2018) 'Adrenaline stimulates glucagon secretion by Tpc2-Dependent ca2+ mobilization from acidic stores in pancreatic a-Cells', *Diabetes*, 67(6), pp. 1128–1139. doi:

10.2337/db17-1102.

Hardwick, J. C. H. *et al.* (2004) 'Bone Morphogenetic Protein 2 Is Expressed by, and Acts Upon, Mature Epithelial Cells in the Colon', *Gastroenterology*, 126(1 SUPPL. 1), pp. 111–121. doi: 10.1053/j.gastro.2003.10.067.

Hattrup, C. L. and Gendler, S. J. (2008) 'Structure and Function of the Cell Surface (Tethered) Mucins', *Annual Review of Physiology*, 70(1), pp. 431–457. doi: 10.1146/annurev.physiol.70.113006.100659.

Hayakawa, Y. *et al.* (2016) 'Nerve Growth Factor Promotes Gastric Tumorigenesis through Aberrant Cholinergic Signaling', *Cancer Cell*. Elsevier Inc., 31(1), pp. 21–34. doi: 10.1016/j.ccell.2016.11.005.

He, L. *et al.* (2018) 'Mechanical regulation of stem-cell differentiation by the stretch-activated Piezo channel', *Nature*. doi: 10.1038/nature25744.

Hebb, B. C. and Whittaker, V. P. (1958) 'Intracellular Distributions Of Acetylcholine And Choline Acetylase', *Journal of Physiology*, 142, pp. 187–196.

Heuberger, J. *et al.* (2014) 'Shp2/MAPK signaling controls goblet/paneth cell fate decisions in the intestine', *Proceedings of the National Academy of Sciences*, 111(9), pp. 3472–3477. doi: 10.1073/pnas.1309342111.

Hirota, C. L. and McKay, D. M. (2006) 'M3 muscarinic receptor-deficient mice retain bethanechol-mediated intestinal ion transport and are more sensitive to colitis.', *Canadian journal of physiology and pharmacology*, 84(11), pp. 1153–61. doi: 10.1139/y06-068.

Hogan, P. G. *et al.* (2003) 'Transcriptional regulation by calcium, calcineurin, and NFAT', *Genes and Development*, 17(18), pp. 2205–2232. doi: 10.1101/gad.1102703.GENES.

Hogan, S. P. *et al.* (2006) 'Resistin-like molecule β regulates innate colonic function: Barrier integrity and inflammation susceptibility', *Journal of Allergy and Clinical Immunology*, 118(1), pp. 257–268. doi: 10.1016/j.jaci.2006.04.039.

Homaidan, F. R. *et al.* (1997) 'Regulation of ion transport by histamine in mouse cecum', *European Journal of Pharmacology*, 331(2–3), pp. 199–204. doi: 10.1016/S0014-2999(97)00184-2.

Horiguchi, H. *et al.* (2017) 'ANGPTL2 expression in the intestinal stem cell niche controls epithelial regeneration and homeostasis.', *The EMBO journal*, 138(12), pp. 2700–2712. doi:

10.15252/embj.201695690.

Howe, J. R. *et al.* (1998) 'Mutations in the SMAD4/DPC4 gene in juvenile polyposis', *Science*, 280(5366), pp. 1086–1088. doi: 10.1126/science.280.5366.1086.

Howitt, Michael R. Lavoie, Sydney. Michaud, Monia. Blum, Arthur. M. Tran, Sara B. Weinstock, Joel V. Gallini, Carey A. Redding, K. Margolskee, Robert F. Osborne, Lisa C. Artis, David. Garrett, W. S. (2016) 'Tuft cells, taste-chemosensory cells, orchestrate parasite type 2 immunity in the gut', *Science*, 351(6279), pp. 1329–1333. doi: doi:10.1126/science.aaf1648.

Huang, J. *et al.* (2009) 'Activation of antibacterial autophagy by NADPH oxidases', *Proceedings of the National Academy of Sciences*, 106(15), pp. 6226–6231. doi: 10.1073/pnas.0811045106.

Iacob, S., Iacob, D. G. and Luminos, L. M. (2019) 'Intestinal microbiota as a host defense mechanism to infectious threats', *Frontiers in Microbiology*, 10(JAN), pp. 1–9. doi: 10.3389/fmicb.2018.03328.

Ikura, M. (1996) 'Calcium binding and conformational response in EF-hand proteins', *Trends in Biochemical Sciences*, 21(1), pp. 14–17. doi: 10.1016/S0968-0004(06)80021-6.

Inaba, T. *et al.* (2014) 'Mice lacking inositol 1,4,5-trisphosphate receptors exhibit dry eye', *PLoS ONE*, 9(6), pp. 1–10. doi: 10.1371/journal.pone.0099205.

Inomata, H., Haraguchi, T. and Sasai, Y. (2008) 'Robust stability of the embryonic axial pattern requires a secreted scaffold for chordin degradation', *Cell*, 134(5), pp. 854–865. doi: 10.1016/j.cell.2008.07.008.

Jadhav, Unmesh. Saxena, Madhurima. O'Neill, Nicholas. K. Saadatpour, Assieh. Yuan, Guo-Cheng. Herbert, Zachary. Murata, Kazutaka. Shivdasani, R. A. (2017) 'Dynamic reorganization of chromatin accessibility signatures during dedifferentiation of secretory precursors into Lgr5+ intestinal stem cells', *Cell Stem Cell*, 21(1), pp. 65–77. doi: 110.1016/j.bbi.2017.04.008.

Jain J *et al.* (1993) 'The T-cell transcription factor NFATp is a substrate for calcineurin and interacts wiht Fos and Jun.', *Nature*, 365(6444), pp. 352–355.

Janssen, K. P. *et al.* (2006) 'APC and Oncogenic KRAS Are Synergistic in Enhancing Wnt Signaling in Intestinal Tumor Formation and Progression', *Gastroenterology*, 131(4), pp. 1096–1109. doi: 10.1053/j.gastro.2006.08.011.

Jha, A. *et al.* (2014) 'Convergent regulation of the lysosomal two-pore channel-2byMg2+, NAADP,

PI(3,5)P2 and multiple protein kinases', *EMBO Journal*, 33(5), pp. 501–511.

Ji, Y. *et al.* (2000) 'Disruption of a single copy of the SERCA2 gene results in altered Ca 2+ homeostasis and cardiomyocyte function', *Journal of Biological Chemistry*, 275(48), pp. 38073–38080. doi: 10.1074/jbc.M004804200.

Jiang, H. *et al.* (2009) 'Cytokine/Jak/Stat Signaling Mediates Regeneration and Homeostasis in the Drosophila Midgut', *Cell*. Elsevier Ltd, 137(7), pp. 1343–1355. doi: 10.1016/j.cell.2009.05.014.

Johansson, Malin E.V. Hansson, G. C. (2011) 'Keeping Bacteria at a Distance', *Perspectives in Microbiology*, 334(0), pp. 1–2.

Johansson, M. E. V. and Hansson, G. C. (2016) 'Immunological aspects of intestinal mucus and mucins', *Nature Reviews Immunology*. Nature Publishing Group, 16(10), pp. 639–649. doi: 10.1038/nri.2016.88.

Johansson, M. E. V., Larsson, J. M. H. and Hansson, G. C. (2011) 'The two mucus layers of colon are organized by the MUC2 mucin, whereas the outer layer is a legislator of host-microbial interactions', *Proceedings of the National Academy of Sciences*, 108(Supplement_1), pp. 4659–4665. doi: 10.1073/pnas.1006451107.

Johansson, M. E. V., Sjövall, H. and Hansson, G. C. (2013) 'The gastrointestinal mucus system in health and disease', *Nature Reviews Gastroenterology and Hepatology*. Nature Publishing Group, 10(6), pp. 352–361. doi: 10.1038/nrgastro.2013.35.

Johansson, M. E. V *et al.* (2008) 'The inner of the two Muc2 mucin-dependent mucus layers in colon is devoid of bacteria.', *Pnas*, 105(39), pp. 15064–15069. doi: 10.1073/pnas.0803124105.

Johansson, M. E. V (2012) 'Fast renewal of the distal colonic mucus layers by the surface goblet cells as measured by in vivo labeling of mucin glycoproteins', *PLoS ONE*, 7(7). doi: 10.1371/journal.pone.0041009.

Johansson, M. E. V, Thomsson, K. A. and Hansson, G. C. (2009) 'Proteomic analyses of the two mucus layers of the colon barrier reveal that their main component, the Muc2 mucin, is strongly bound to the fcgbp protein', *Journal of Proteome Research*, 8(7), pp. 3549–3557. doi: 10.1021/pr9002504.

Johansson, Malin E V *et al.* (2011) 'Microbiology. Keeping bacteria at a distance.', *Science (New York, N.Y.)*, 334(6053), pp. 182–3. doi: 10.1126/science.1213909.

de Jonge, W. J. *et al.* (2005) 'Stimulation of the vagus nerve attenuates macrophage activation by activating the Jak2-STAT3 signaling pathway', *Nature Immunology*, 6(8), pp. 844–851. doi: 10.1038/ni1229.

Jung, P. *et al.* (2011) 'Isolation and in vitro expansion of human colonic stem cells', *Nat Med*. Nature Publishing Group, 17(10), pp. 1225–1227. doi: 10.1038/nm.2470.

Jung, P., Sommer, C., Barriga, Francisco M, *et al.* (2015) 'Isolation of Human Colon Stem Cells Using Surface Expression of PTK7', *Stem Cell Reports*. The Authors, 5(6), pp. 979–987. doi: 10.1016/j.stemcr.2015.10.003.

Jung, P., Sommer, C., Barriga, Francisco M., *et al.* (2015) 'Isolation of Human Colon Stem Cells Using Surface Expression of PTK7', *Stem Cell Reports*. The Authors, 5(6), pp. 979–987. doi: 10.1016/j.stemcr.2015.10.003.

Jurado, L. A., Chockalingam, P. S. and Jarrett, H. W. (2019) 'Apocalmodulin', 79(3), pp. 661–682.

Justet, C. *et al.* (2016) 'Fast calcium wave inhibits excessive apoptosis during epithelial wound healing', *Cell and Tissue Research*. Cell and Tissue Research, 365(2), pp. 343–356. doi: 10.1007/s00441-016-2388-8.

Kaelberer, M. M. *et al.* (2018) 'A gut-brain neural circuit for nutrient sensory transduction', *Science*, In Press. doi: 10.1126/science.aat5236.

Kang, J. W. *et al.* (2017) 'Synergistic mucus secretion by histamine and IL-4 through TMEM16A in airway epithelium', *American Journal of Physiology - Lung Cellular and Molecular Physiology*, 313(3), pp. L466–L476. doi: 10.1152/ajplung.00103.2017.

Katz, J. P. *et al.* (2002) 'The zinc-finger transcription factor Klf4 is required for terminal differentiation of goblet cells in the colon', *Developmente*, 129(11), pp. 2619–2628.

Kawashima, K. and Fujii, T. (2003) 'The lymphocytic cholinergic system and its biological function', *Life Sciences*, 72(18–19), pp. 2101–2109. doi: 10.1016/S0024-3205(03)00068-7.

Kay, S. K. *et al.* (2017) 'The role of the Hes1 crosstalk hub in Notch-Wnt interactions of the intestinal crypt', *PLoS Computational Biology*, 13(2), pp. 1–28. doi: 10.1371/journal.pcbi.1005400.

Keita, a.˚ V and Söderholm, J. D. (2010) 'The intestinal barrier and its regulation by neuroimmune factors', *Neurogastroenterology and Motility*, 22(7), pp. 718–733. doi: 10.1111/j.1365-

2982.2010.01498.x.

Kilbinger, H. *et al.* (1984) 'Comparison of affinities of muscarinic antagonists to pre- and postjunctional receptors in the guinea-pig ileum', *European Journal of Pharmacology*, 103(3–4), pp. 313–320. doi: 10.1016/0014-2999(84)90492-8.

Kim, Tae-Hee. Li, Fugen. Ferreiro-Neira, Isabel. Ho, Li-Lun. Luyten, Annouck. Nalapareddy, Kodandaramireddy. Long, Henry. Verzi, Michael. Shivdasani, R. A. (2014) 'Broadly permissive intestinal chromatin underlies lateral inhibition and cell plasticity', *Nature*, 506(7489), pp. 511–515. doi: 110.1016/j.bbi.2017.04.008.

Kim, T.-H., Escudero, S. and Shivdasani, R. A. (2012) 'Intact function of Lgr5 receptor-expressing intestinal stem cells in the absence of Paneth cells', *Proceedings of the National Academy of Sciences*, 109(10), pp. 3932–3937. doi: 10.1073/pnas.1113890109.

Kim, Y. S. and Ho, S. B. (2010) 'Intestinal goblet cells and mucins in health and disease: Recent insights and progress', *Current Gastroenterology Reports*, 12(5), pp. 319–330. doi: 10.1007/s11894-010-0131-2.

Kincaid, R. L. and Vaughan, M. (2006) 'Direct comparison of Ca2+ requirements for calmodulin interaction with and activation of protein phosphatase.', *Proceedings of the National Academy of Sciences*, 83(5), pp. 1193–1197. doi: 10.1073/pnas.83.5.1193.

Kindon, H. *et al.* (1995) 'Trefoil peptide protection of intestinal epithelial barrier function: Cooperative interaction with mucin glycoprotein', *Gastroenterology*, 109(2), pp. 516–523. doi: 10.1016/0016-5085(95)90340-2.

Kinnear, N. P. *et al.* (2004) 'Lysosome-sarcoplasmic reticulum junctions: A trigger zone for calcium signaling by nicotinic acid adenine dinucleotide phosphate and endothelin-1', *Journal of Biological Chemistry*, 279(52), pp. 54319–54326. doi: 10.1074/jbc.M406132200.

Kinzler, Kenneth W. Vogelstein, B. (1996) 'Lessons from Hereditary Colorectal Cancer', *Cell*, 87, pp. 159–170. doi: 10.1016/S0092-8674(00)81333-1.

Kjellev, S. (2009) 'The trefoil factor family - Small peptides with multiple functionalities', *Cellular and Molecular Life Sciences*, 66(8), pp. 1350–1369. doi: 10.1007/s00018-008-8646-5.

Knoop, K. A. and Newberry, R. D. (2018) 'Goblet cells: multifaceted players in immunity at mucosal surfaces', *Mucosal Immunology*. Springer US, 11(6), pp. 1551–1557. doi: 10.1038/s41385-018-0039-

y.

Knoop, K. a *et al.* (2014) 'Microbial sensing by goblet cells controls immune surveillance of luminal antigens in the colon.', *Mucosal immunology*. Nature Publishing Group, 8(1), pp. 198–210. doi: 10.1038/mi.2014.58.

Knott, G. J. and Doudna, J. A. (2018) 'CRISPR-Cas guides the future of genetic engineering', *Science*, 361(6405), pp. 866–869. doi: 10.1126/science.aat5011.

Kobayashi, K. *et al.* (2002) 'Human IgGFc Binding Protein (FcγBP) in Colonic Epithelial Cells Exhibits Mucin-like Structure', *Journal of Biological Chemistry*, 272(24), pp. 15232–15241. doi: 10.1074/jbc.272.24.15232.

Köenig, A. *et al.* (2010) 'NFAT-Induced Histone Acetylation Relay Switch Promotes c-Myc-Dependent Growth in Pancreatic Cancer Cells', *Gastroenterology*. Elsevier Inc., 138(3), pp. 1189-1199.e2. doi: 10.1053/j.gastro.2009.10.045.

Koninck, P. De and Schulman, H. (1998) 'Sensitivity of CaM Kinase II to the Frequency of Ca2 " Oscillations', *Science*, 279(5348), pp. 227–230.

Koo, B.-K. *et al.* (2011) 'Controlled gene expression in primary Lgr5 organoid cultures', *Nature Methods*. Nature Publishing Group, a division of Macmillan Publishers Limited. All Rights Reserved., 9, p. 81. Available at: https://doi.org/10.1038/nmeth.1802.

Korinek, V. *et al.* (1998) 'Depletion of epithelial stem-cell compartments in the small intestine of mice lacking Tcf-4', *Nature Genetics*, 19(4), pp. 379–383. doi: 10.1038/1270.

Kosinski, C. *et al.* (2007) 'Gene expression patterns of human colon tops and basal crypts and BMP antagonists as intestinal stem cell niche factors.', *Proceedings of the National Academy of Sciences of the United States of America*, 104(39), pp. 15418–15423. doi: 10.1073/pnas.0707210104.

Kosinski, C. *et al.* (2010) 'Indian hedgehog regulates intestinal stem cell fate through epithelial-mesenchymal interactions during development', *Gastroenterology*. Elsevier Inc., 139(3), pp. 893–903. doi: 10.1053/j.gastro.2010.06.014.

Kramer, W. *et al.* (2005) 'Aminopeptidase N (CD13) is a molecular target of the cholesterol absorption inhibitor Ezetimibe in the enterocyte brush border membrane', *Journal of Biological Chemistry*, 280(2), pp. 1306–1320. doi: 10.1074/jbc.M406309200.

Krasteva, G. *et al.* (2011) 'Cholinergic chemosensory cells in the trachea regulate breathing', *Proceedings of the National Academy of Sciences of the United States of America*, 108(23), pp. 9478–9483. doi: 10.1073/pnas.1019418108.

Krieger, T. and Simons, B. D. (2015) 'Dynamic stem cell heterogeneity', *Development*, 142(8), pp. 1396–1406. doi: 10.1242/dev.101063.

Krimi, R. B. *et al.* (2008) 'Resistin-like molecule β regulates intestinal mucous secretion and curtails TNBS-induced colitis in mice', *Inflammatory Bowel Diseases*, 14(7), pp. 931–941. doi: 10.1002/ibd.20420.

Kristen, E., Stefani, N. and Kelsey, N. (2014) 'Lymphocyte-derived ACh regulates local innate but not adaptive immunity', *PNAS*, 110(13), pp. 5269–5269. doi: 10.1073/pnas.1303818110.

Kuipers, E. J. *et al.* (2015) 'Colorectal cancer', *Nat Rev Dis Primers*, 1. doi: 10.3109/9781841847481.

Kulkarni, Devesha. H. McDonald, Keely. G. Knoop, Kathryn. A. Gustafsson, Jenny. K. Kozlowski, Konrad. M. Hunstad, David. A. Miller, Mark. Newberry, R. D. (2018) 'Goblet Cell Associated Antigen Passages are Inhibited During Salmonella typhimurium Infection to Prevent Pathogen Dissemination and Limit Responses to Dietary Antigens', *Mucosal Immunology*, 11(4), pp. 1103–1113. doi: 10.1002/cncr.31084.Talking.

Kuo, I. Y. and Ehrlich, B. E. (2015) 'Signaling in muscle contraction', *Cold Spring Harbor Perspectives in Biology*, 7(2), pp. 1–14. doi: 10.1101/cshperspect.a006023.

Kurzen, H. *et al.* (2004) 'Phenotypical and molecular profiling of the extraneuronal cholinergic system of the skin', *Journal of Investigative Dermatology*, 123(5), pp. 937–949. doi: 10.1111/j.0022-202X.2004.23425.x.

Labed, S. A. *et al.* (2018) 'Intestinal Epithelial Wnt Signaling Mediates Acetylcholine-Triggered Host Defense against Infection', *Immunity*. Elsevier, 48(5), pp. 963-978.e4. doi: 10.1016/j.immuni.2018.04.017.

Lamb, G. (2000) 'Excitation-contraction coupling in skeletal muscle: Comparisons with cardiac muscle', *Clinical and Experimental Pharmacology and Physiology.*, 27, pp. 1–9.

Lambert, D. *et al.* (2002) 'Molecular changes in the expression of human colonic nutrient transporters during the transition from normality to malignancy', *British Journal of Cancer*, 86(8), pp. 1262–1269. doi: 10.1038/sj.bjc.6600264.

Van Landeghem, L. *et al.* (2011) 'Enteric glia promote intestinal mucosal healing via activation of focal adhesion kinase and release of proEGF.', *American journal of physiology. Gastrointestinal and liver physiology*, 300(6), pp. G976–G987. doi: 10.1152/ajpgi.00427.2010.

Lanner, J. T. *et al.* (2010) 'Ryanodine Receptors: Structure, Expression, Molecular Details, and Function in Calcium Release', *Cold Spring Harbor Perspectives in Biology*, 2, pp. 1–21.

Laplante, M. and Sabatini, D. M. (2012) 'MTOR signaling in growth control and disease', *Cell*. Elsevier, 149(2), pp. 274–293. doi: 10.1016/j.cell.2012.03.017.

Lechleiter, J. *et al.* (1990) 'Distinct sequence elements control the specificity of G protein activation by muscarinic acetylcholine receptor subtypes.', *The EMBO Journal*, 9(13), pp. 4381–4390. doi: 10.1002/j.1460-2075.1990.tb07888.x.

Lei, W. *et al.* (2018) 'Activation of intestinal tuft cell-expressed Sucnr1 triggers type 2 immunity in the mouse small intestine', 115(21). doi: 10.1073/pnas.1720758115.

Lemieux, E. *et al.* (2011) 'Constitutive activation of the MEK/ERK pathway inhibits intestinal epithelial cell differentiation', *American Journal of Physiology-Gastrointestinal and Liver Physiology*, 301(4), pp. G719–G730. doi: 10.1152/ajpgi.00508.2010.

Leslie, J. L. *et al.* (2015) 'Persistence and toxin production by Clostridium difficile within human intestinal organoids result in disruption of epithelial paracellular barrier function', *Infection and Immunity*, 83(1), pp. 138–145. doi: 10.1128/IAI.02561-14.

Levine, B., Muzishima, N. and Virgin, H. W. (2011) 'Autophagy in immunity and inflammation', *Nature*, 469(7330), pp. 323–335. doi: 10.1038/nature09782.Autophagy.

Li, Ning. Nakauka-Ddamba, Angela. Tobias, John. Jensen, Shane. T. Lengner, C. J. (2016) 'Mouse Label-Retaining Cells Are Molecularly And Functionally Distinct From Reserve Intestinal Stem Cells', *Gastroenterology*, 151(1), pp. 298–310. doi: 10.1126/science.1249098.Sleep.

Li, P., Gu, M. and Xu, H. (2019) 'Lysosomal Ion Channels as Decoders of Cellular Signals', *Trends in Biochemical Sciences*. Elsevier Ltd, 44(2), pp. 110–124. doi: 10.1016/j.tibs.2018.10.006.

Lidell, M. E. *et al.* (2006) 'Entamoeba histolytica cysteine proteases cleave the MUC2 mucin in its C-terminal domain and dissolve the protective colonic mucus gel', *Proceedings of the National Academy of Sciences*, 103(24), pp. 9298–9303. doi: 10.1073/pnas.0600623103.

Lindemans, C. a. *et al.* (2015) 'Interleukin-22 promotes intestinal-stem-cell-mediated epithelial regeneration', *Nature*. Nature Publishing Group, 528(7583), pp. 560–564. doi: 10.1038/nature16460.

Lindqvist, S. *et al.* (2002) 'The colon-selective spasmolytic otilonium bromide inhibits muscarinic M 3 receptor-coupled calcium signals in isolated human colonic crypts', *British Journal of Pharmacology*, 137(7), pp. 1134–1142. doi: 10.1038/sj.bjp.0704942.

Lindqvist, S. M. *et al.* (1998) 'Acetylcholine-induced calcium signaling along the rat colonic crypt axis.', *Gastroenterology*, 115(5), pp. 1131–1143. doi: 10.1016/S0016-5085(98)70084-8.

De Lisle, R. C. and Borowitz, D. (2013) 'The cystic fibrosis intestine', *Cold Spring Harbor Perspectives in Medicine*, 3(9), pp. 1–17. doi: 10.1101/cshperspect.a009753.

Liu, W. *et al.* (2000) 'Mutations in AXIN2 cause colorectal cancer with defective mismatch repair', *Nature*, 26(october), pp. 146–147. doi: 10.1038/79859.

Liu, Z. *et al.* (2019) 'Induction of store-operated calcium entry (SOCE) suppresses glioblastoma growth by inhibiting the Hippo pathway transcriptional coactivators YAP/TAZ', *Oncogene*. Springer US, 38(1), pp. 120–139. doi: 10.1038/s41388-018-0425-7.

Lopez-Garcia, C. *et al.* (2010) 'Intestinal stem cell replacement follows a pattern of neutral drift', *Science*, 330(6005), pp. 822–825. doi: science.1196236 [pii]\n10.1126/science.1196236.

López-Sanjurjo, C. I. *et al.* (2013) 'Lysosomes shape Ins(1,4,5)P3-evoked Ca2+ signals by selectively sequestering Ca2+ released from the endoplasmic reticulum', *Journal of Cell Science*, 126(1), pp. 289–300. doi: 10.1242/jcs.116103.

Lundgren, O. *et al.* (2011) 'Intestinal epithelial stem/progenitor cells are controlled by mucosal afferent nerves.', *PloS one*, 6(2), p. e16295. doi: 10.1371/journal.pone.0016295.

Luo, C. *et al.* (2019) 'Mucinous colorectal adenocarcinoma: Clinical pathology and treatment options', *Cancer Communications*. BioMed Central, 39(1), pp. 1–13. doi: 10.1186/s40880-019-0361-0.

Luo, D. *et al.* (2008) 'Nuclear Ca2+ sparks and waves mediated by inositol 1,4,5-trisphosphate receptors in neonatal rat cardiomyocytes', *Cell Calcium*, 43(2), pp. 165–174. doi: 10.1016/j.ceca.2007.04.017.

Luo, F. *et al.* (2009) 'Mutated K-ras Asp12 promotes tumourigenesis in Apc Min mice more in the

large than the small intestines, with synergistic effects between K-ras and Wnt pathways', *International Journal of Experimental Pathology*, 90(5), pp. 558–574. doi: 10.1111/j.1365-2613.2009.00667.x.

Luo, X.-C. *et al.* (2019) ' Infection by the parasitic helminth Trichinella spiralis activates a Tas2r-mediated signaling pathway in intestinal tuft cells ', *Proceedings of the National Academy of Sciences*, 116(12), pp. 5564–5569. doi: 10.1073/pnas.1812901116.

Luzio, J. P., Pryor, P. R. and Bright, N. A. (2007) 'Lysosomes: Fusion and function', *Nature Reviews Molecular Cell Biology*, 8(8), pp. 622–632. doi: 10.1038/nrm2217.

Macgregor, A. *et al.* (2007) 'NAADP controls cross-talk between distinct Ca2+ stores in the heart', *Journal of Biological Chemistry*, 282(20), pp. 15302–15311. doi: 10.1074/jbc.M611167200.

Magnon, C., Freedland, S. J. and Frenette, P. S. (2013) 'Autonomic Nerve Development Contributes to Prostate Cancer Progression', *Science*, 314(2013). doi: 10.1126/science.1236361.

Mahoney, J. P. and Sunahara, R. K. (2016) 'Mechanistic insights into GPCR–G protein interactions', *Current Opinion in Structural Biology*. Elsevier Ltd, 41, pp. 247–254. doi: 10.1016/j.sbi.2016.11.005.

Mak, D. O. D. *et al.* (2013) 'Patch-clamp electrophysiology of intracellular Ca2+ channels', *Cold Spring Harbor Protocols*, 2013(9), pp. 787–797. doi: 10.1101/pdb.top066217.

Mak, D. O. D. and Foskett, J. K. (2015) 'Inositol 1,4,5-trisphosphate receptors in the endoplasmic reticulum: A single-channel point of view', *Cell Calcium*. Elsevier Ltd, 58(1), pp. 67–78. doi: 10.1016/j.ceca.2014.12.008.

Mak, I. W. Y., Evaniew, N. and Ghert, M. (2014) 'Lost in translation: Animal models and clinical trials in cancer treatment', *American Journal of Translational Research*, 6(2), pp. 114–118.

Malhas, A., Goulbourne, C. and Vaux, D. J. (2011) 'The nucleoplasmic reticulum: Form and function', *Trends in Cell Biology*. Elsevier Ltd, 21(6), pp. 362–373. doi: 10.1016/j.tcb.2011.03.008.

Mallilankaraman, K. *et al.* (2012) 'MICU1 is an essential gatekeeper for mcu-mediated mitochondrial Ca 2+ uptake that regulates cell survival', *Cell*, 151(3), pp. 630–644. doi: 10.1016/j.cell.2012.10.011.

Mammucari, C. *et al.* (2005) 'Integration of notch 1 and calcineurin/NFAT signaling pathways in keratinocyte growth and differentiation control', *Developmental Cell*, 8(5), pp. 665–676. doi: 10.1016/j.devcel.2005.02.016.

Manjarrez-Marmolejo, J. and Franco-Pérez, J. (2016) 'Gap Junction Blockers: An Overview of their Effects on Induced Seizures in Animal Models Joaquín', *Current Neuropharmacology*, 14, pp. 759–771. doi: 10.2174/1570159X14666160603115.

Mao, J. *et al.* (2010) 'Hedgehog signaling controls mesenchymal growth in the developing mammalian digestive tract', *Development*, 137(10), pp. 1721–1729. doi: 10.1242/dev.044586.

Marcobal, A. *et al.* (2013) 'A refined palate: Bacterial consumption of host glycans in the gut', *Glycobiology*, 23(9), pp. 1038–1046. doi: 10.1093/glycob/cwt040.

Marcon, M. A. *et al.* (1990) 'Inhibition of mucin secretion in a colonic adenocarcinoma cell line by DIDS and potassium channel blockers', *BBA - Molecular Cell Research*, 1052(1), pp. 17–23. doi: 10.1016/0167-4889(90)90051-E.

Marsh, V. *et al.* (2008) 'Epithelial Pten is dispensable for intestinal homeostasis but suppresses adenoma development and progression after Apc mutation', *Nature Genetics*, 40(12), pp. 1436–1444. doi: 10.1038/ng.256.

Martini, E. *et al.* (2017) 'Mend Your Fences: The Epithelial Barrier and its Relationship With Mucosal Immunity in Inflammatory Bowel Disease', *Cmgh*. Elsevier Inc, 4(1), pp. 33–46. doi: 10.1016/j.jcmgh.2017.03.007.

Maruyama, T. *et al.* (1997) '2APB, 2-Aminoethoxydophenyl Borate , a Membrane-Penetrable Modulator of Ins(1,4,5)P3-Induced Calcium Release', *Biochem, J*, 505, pp. 498–505.

Massagué, J. (2014) 'TGFb signaling in contest', *Nature Reviews Molecular Cell Biology*, 13(10), pp. 616–630. doi: 10.1038/nrm3434.TGF.

Massey-Harroche, D. (2000) 'Epithelial cell polarity as reflected in enterocytes', *Microscopy Research and Technique*, 49(4), pp. 353–362. doi: 10.1002/(SICI)1097-0029(20000515)49:4<353::AID-JEMT4>3.0.CO;2-8.

Matano, M. *et al.* (2015) 'Modeling colorectal cancer using CRISPR-Cas9-mediated engineering of human intestinal organoids', *Nature Medicine*. Nature Publishing Group, 21(3), pp. 256–262. doi: 10.1038/nm.3802.

Matsumoto, I. *et al.* (2011) 'Skn-1a/Pou2f3 specifies taste receptor cell lineage', *Nature Neuroscience*, 14(1), pp. 685–687.

Matsuo, A. *et al.* (2011) 'Nuclear choline acetyltransferase activates transcription of a high-affinity choline transporter', *Journal of Biological Chemistry*, 286(7), pp. 5836–5845. doi: 10.1074/jbc.M110.147611.

Matsuo, K. *et al.* (1997) 'Histochemistry of the surface mucous gel layer of the human colon', *Gut*, 40, pp. 782–789.

Matthiesen, S. *et al.* (2006) 'Muscarinic receptors mediate stimulation of human lung fibroblast proliferation', *American Journal of Respiratory Cell and Molecular Biology*, 35(6), pp. 621–627. doi: 10.1165/rcmb.2005-0343RC.

McCauley, H. a. and Guasch, G. (2015) 'Three cheers for the goblet cell: maintaining homeostasis in mucosal epithelia', *Trends in Molecular Medicine*, 21(8), pp. 1–12. doi: 10.1016/j.molmed.2015.06.003.

McCool, D. J., Forstner, J. F. and Forstner, G. G. (1994) 'Synthesis and secretion of mucin by the human colonic tumour cell line LS180', *Biochemical Journal*, 302(1), pp. 111–118. doi: 10.1042/bj3020111.

McCool, D. J., Forstner, J. F. and Forstner, G. G. (1995) 'Regulated and unregulated pathways for MUC2 mucin secretion in human colonic LS180 adenocarcinoma cells are distinct', *Biochemical Journal*, 312(1), pp. 125–133. doi: 10.1042/bj3120125.

McDole, J. R. *et al.* (2012) 'Goblet cells deliver luminal antigen to CD103 + dendritic cells in the small intestine', *Nature*. Nature Publishing Group, 483(7389), pp. 345–349. doi: 10.1038/nature10863.

McGuckin, M. A. and Hasnain, S. Z. (2017) 'Goblet cells as mucosal sentinels for immunity', *Mucosal Immunology*. Nature Publishing Group, 10(5), pp. 1118–1121. doi: 10.1038/mi.2016.132.

Medema, J. P. and Vermeulen, L. (2011) 'Microenvironmental regulation of stem cells in intestinal homeostasis and cancer.', *Nature*, 474(7351), pp. 318–26. doi: 10.1038/nature10212.

Medina, D. L. *et al.* (2015) 'Lysosomal calcium signalling regulates autophagy through calcineurin and TFEB', 17(3). doi: 10.1038/ncb3114.

Meissner, G. (1984) 'Adenine Nucleotide Stimulation of Ca2 + -induced Ca2 + Release in', *Journal of Biological Chemistry*, 259(4), pp. 2365–74.

Meissner, G. *et al.* (1997) 'Regulation of skeletal muscle Ca2+ release channel (ryanodine receptor)

by Ca2+ and monovalent cations and anions', *Journal of Biological Chemistry*, 272(3), pp. 1628–1638. doi: 10.1074/jbc.272.3.1628.

Meissner, G., Darling, E. and Eveleth, J. (1986) 'Kinetics of Rapid Ca2+ Release by Sarcoplasmic Reticulum. Effects of Ca2+, Mg2+, and Adenine Nucleotides', *Biochemistry*, 25(1), pp. 236–244. doi: 10.1021/bi00349a033.

Melo, F. de S. e *et al.* (2017) 'A distinct role for Lgr5+ stem cells in primary and metastatic colon cancer', *Nature*. Nature Publishing Group, 543(7647), pp. 676–680. doi: 10.1038/nature21713.

Meran, L., Baulies, A. and Li, V. S. W. (2017) 'Intestinal Stem Cell Niche: The Extracellular Matrix and Cellular Components', *Stem Cells International*, 2017. doi: 10.1155/2017/7970385.

Merritt, A. J. *et al.* (1994) 'The Role of p53 in Spontaneous and Radiation-induced Apoptosis in the Gastrointestinal Tract of Normal and p53-deficient Mice Advances in Brief The Role of p53 in Spontaneous and Radiation-induced Apoptosis in the Gastrointestinal Tract of Normal and p53-', *Aacr*, pp. 614–617. Available at: http://cancerres.aacrjournals.org/content/54/3/614.short.

Meyer-Hoffert, U. *et al.* (2008) 'Secreted enteric antimicrobial activity localises to the mucus surface layer', *Gut*, 57(6), pp. 764–771. doi: 10.1136/gut.2007.141481.

Meyer, T. *et al.* (1992) 'Calmodulin trapping by calcium-calmodulin-dependent protein kinase', *Science*, 256(5060), pp. 1199–1202. doi: 10.1126/science.256.5060.1199.

Middelhoff, M. *et al.* (2017) 'Dclk1-expressing tuft cells: critical modulators of the intestinal niche?', *American Journal of Physiology-Gastrointestinal and Liver Physiology*, 313(4), pp. G285–G299. doi: 10.1152/ajpgi.00073.2017.

Middendorp, S. *et al.* (2014) 'Adult Stem Cells in the Small Intestine Are Intrinsically Programmed with Their Location- Specific Function', *Stem Cells*, 32, pp. 1083–1091.

Mihaylova, M. M. *et al.* (2018) 'Fasting Activates Fatty Acid Oxidation to Enhance Intestinal Stem Cell Function during Homeostasis and Aging', *Cell Stem Cell*, pp. 769–778. doi: 10.1016/j.stem.2018.04.001.

Milano, J. *et al.* (2004) 'Modulation of Notch processing by γ-secretase inhibitors causes intestinal goblet cell metaplasia and induction of genes known to specify gut secretory lineage differentiation', *Toxicological Sciences*, 82(1), pp. 341–358. doi: 10.1093/toxsci/kfh254.

Mills, C. L., Dormer, R. L. and McPherson, M. A. (1991) 'Introduction of BAPTA into intact rat submandibular acini inhibits mucin secretion in response to cholinergic and β-adrenergic agonists', *FEBS Letters*, 289(2), pp. 141–144. doi: 10.1016/0014-5793(91)81054-C.

Miranti, C. K. *et al.* (1995) 'Calcium activates serum response factor-dependent transcription by a Ras- and Elk-1-independent mechanism that involves a Ca2+/calmodulin-dependent kinase.', *Molecular and Cellular Biology*, pp. 3672–3684. doi: 10.1128/mcb.15.7.3672.

Miron, N. and Cristea, V. (2012) 'Enterocytes: Active cells in tolerance to food and microbial antigens in the gut', *Clinical and Experimental Immunology*, 167(3), pp. 405–412. doi: 10.1111/j.1365-2249.2011.04523.x.

Mognol, GP. Carnerio, FRG. Robbs, BK. Faget, DV. Viola, J. (2016) 'Cell cycle and apoptosis regulation by NFAT transcription factors: new roles for an old player', *Cell Death and Disease*, 48(7), pp. 829–834. doi: 10.1038/cddis.2016.97.

von Moltke, J. *et al.* (2015) 'Tuft-cell-derived IL-25 regulates an intestinal ILC2–epithelial response circuit', *Nature*. Nature Publishing Group, 529(7585), pp. 221–225. doi: 10.1038/nature16161.

Moncada, D. M., Kammanadiminti, S. J. and Chadee, K. (2003) 'Mucin and Toll-like receptors in host defense against intestinal parasites', *Trends in Parasitology*, 19(7), pp. 305–311. doi: 10.1016/S1471-4922(03)00122-3.

Morgan, A. J. *et al.* (2011) 'Molecular mechanisms of endolysosomal Ca 2+ signalling in health and disease', *Biochemical Journal*, 439(3), pp. 349–374. doi: 10.1042/BJ20110949.

Morgan, A. J. (2016) 'Ca 2 + dialogue between acidic vesicles and ER', *Biochemical Society Transactions*, 44, pp. 546–553. doi: 10.1042//BST20150290.

Morgan, R. G., Mortensson, E. and Williams, A. C. (2018) 'Targeting LGR5 in Colorectal Cancer: Therapeutic gold or too plastic?', *British Journal of Cancer*. Springer US, 118(11), pp. 1410–1418. doi: 10.1038/s41416-018-0118-6.

Morin, P. J. *et al.* (1997) 'Activation of β-catenin-Tcf signaling in colon cancer by mutations in β-catenin or APC', *Science*, 275(5307), pp. 1787–1790. doi: 10.1126/science.275.5307.1787.

Moya, I. M. and Halder, G. (2019) 'Hippo–YAP/TAZ signalling in organ regeneration and regenerative medicine', *Nature Reviews Molecular Cell Biology*. Springer US, 20(4), pp. 211–226. doi: 10.1038/s41580-018-0086-y.

Mueller, F. *et al.* (2013) 'Quantifying transcription factor kinetics: At work or at play?', *Critical Reviews in Biochemistry and Molecular Biology*. Taylor & Francis, 48(5), pp. 492–514. doi: 10.3109/10409238.2013.833891.

Murata, J. *et al.* (2015) 'High-resolution mass spectrometry for detecting acetylcholine in arabidopsis', *Plant Signaling and Behavior*, 10(10). doi: 10.1080/15592324.2015.1074367.

Nachmansohn, D. and Machado, L. (1943) 'The Formation of Acetylcholine. A new enzyme: "Choline Acetylase"', *American Journal of Physiology*, pp. 397–403.

Nadjsombati, M. S. *et al.* (2018) 'Detection of Succinate by Intestinal Tuft Cells Triggers a Type 2 Innate Immune Circuit', *Immunity*. Elsevier Inc., 49(1), pp. 33-41.e7. doi: 10.1016/j.immuni.2018.06.016.

Nair, M. G. *et al.* (2008) ' Goblet Cell-Derived Resistin-Like Molecule β Augments CD4 + T Cell Production of IFN-γ and Infection-Induced Intestinal Inflammation ', *The Journal of Immunology*, 181(7), pp. 4709–4715. doi: 10.4049/jimmunol.181.7.4709.

Narciso, C. E. *et al.* (2017) 'Release of Applied Mechanical Loading Stimulates Intercellular Calcium Waves in Drosophila Wing Discs', *Biophysical Journal*. Biophysical Society, 113(2), pp. 491–501. doi: 10.1016/j.bpj.2017.05.051.

Nathanson, N. M. (2008) 'Synthesis, trafficking, and localization of muscarinic acetylcholine receptors.', *Pharmacology & therapeutics*, 119(1), pp. 33–43. doi: 10.1016/j.pharmthera.2008.04.006.

National Institue for Health and Care Excellence, N. in E. and W. (2012) *Crohn's disease: management*. Manchester.

National Institue for Health and Care Excellence, N. in E. and W. (2013) *Ulcerative colitis: management*. Manchester.

Naylor, E. *et al.* (2009) 'Identification of a chemical probe for NAADP by virtual screening', *Nature Chemical Biology*, 5(4), pp. 220–226. doi: 10.1038/nchembio.150.

Neal, J. W. and Clipstone, N. A. (2001) 'Glycogen Synthase Kinase-3 Inhibits the DNA Binding Activity of NFATc', *Journal of Biological Chemistry*, 276(5), pp. 3666–3673. doi: 10.1074/jbc.M004888200.

Neal, J. W. and Clipstone, N. A. (2003) 'A constitutively active NFATC1 mutant induces a transformed

phenotype in 3T3-L1 fibroblasts', *Journal of Biological Chemistry*, 278(19), pp. 17246–17254. doi: 10.1074/jbc.M300528200.

Neumüller, R. A. and Knoblich, J. A. (2009) 'Dividing cellular asymmetry: asymmetric cell division and its', *Genes & development*, 23(23), pp. 2675–2699. doi: 10.1101/gad.1850809.

Neunlist, M. *et al.* (2003) 'Human ENS regulates the intestinal epithelial barrier permeability and a tight junction-associated protein ZO-1 via VIPergic pathways', *American Journal of Physiology-Gastrointestinal and Liver Physiology*, 285(5), pp. G1028–G1036. doi: 10.1152/ajpgi.00066.2003.

Neunlist, M. *et al.* (2013) 'The digestive neuronal-glial-epithelial unit: a new actor in gut health and disease.', *Nature reviews. Gastroenterology & hepatology*. Nature Publishing Group, 10(2), pp. 90–100. doi: 10.1038/nrgastro.2012.221.

Neutra, M. and Leblond, C. P. (1966) 'Synthesis of the carbohydrate of mucus in the golgi complex as shown by electron microscope radioautography of goblet cells from rats injected with glucose-H3.', *The Journal of cell biology*, 30(1), pp. 119–136. doi: 10.1083/jcb.30.1.119.

Neutra, M. R., O'Malley, L. J. and Specian, R. D. (1982) 'Regulation of intestinal goblet cell secretion. II. A survey of potential secretagogues', *American Journal of Physiology-Gastrointestinal and Liver Physiology*, 242(4), pp. G380–G387. doi: 10.1152/ajpgi.1982.242.4.g380.

Nevo, S., Kadouri, N. and Abramson, J. (2019) 'Tuft cells: From the mucosa to the thymus', *Immunology Letters*, 210(January), pp. 1–9. doi: 10.1016/j.imlet.2019.02.003.

Nguyen, O. N. P. *et al.* (2017) 'Two-pore channel function is crucial for the migration of invasive cancer cells', *Cancer Research*, 77(6), pp. 1427–1438. doi: 10.1158/0008-5472.CAN-16-0852.

Notomi, T., Ezura, Y. and Noda, M. (2012) 'Identification of two-pore channel 2 as a novel regulator of osteoclastogenesis', *Journal of Biological Chemistry*, 287(42), pp. 35057–35064. doi: 10.1074/jbc.M111.328930.

Nozawa, K. *et al.* (2009) 'TRPA1 regulates gastrointestinal motility through serotonin release from enterochromaffin cells', *Proceedings of the National Academy of Sciences*, 106(9), pp. 3408–3413. doi: 10.1073/pnas.0805323106.

Nusse, R. and Clevers, H. (2017a) 'Wnt/β-Catenin Signaling, Disease, and Emerging Therapeutic Modalities', *Cell*. Elsevier Inc., 169(6), pp. 985–999. doi: 10.1016/j.cell.2017.05.016.

Nusse, R. and Clevers, H. (2017b) 'Wnt/β-Catenin Signaling, Disease, and Emerging Therapeutic Modalities', *Cell*. Elsevier Inc., 169(6), pp. 985–999. doi: 10.1016/j.cell.2017.05.016.

Nusse, Y. M. *et al.* (2018) 'Parasitic helminths induce fetal-like reversion in the intestinal stem cell niche', *Nature*. Springer US, 559(7712), pp. 109–113. doi: 10.1038/s41586-018-0257-1.

Nyström, E. E. L. *et al.* (2018) 'Calcium-activated Chloride Channel Regulator 1 (CLCA1) Controls Mucus Expansion in Colon by Proteolytic Activity', *EBioMedicine*. The Authors, 1, pp. 1–10. doi: 10.1016/j.ebiom.2018.05.031.

O'Malley, KE; Farrell, CB; O'Boyle, KM; Baird, A. (1995) 'Cholinergic activation of Cl-secretion in rat colonic epithelia', *European journal of pharmacology*, 275(1), pp. 83–89.

Oancea, E. and Meyer, T. (1998) 'Protein kinase C as a molecular machine for decoding calcium and diacylglycerol signals', *Cell*, 95(3), pp. 307–318. doi: 10.1016/S0092-8674(00)81763-8.

Ogobuiro, I. Tuma, F. (2019) *Physiology, Gastrointestinal*, *StatPearls*. Available at: https://www.ncbi.nlm.nih.gov/books/NBK537103/ (Accessed: 23 July 2019).

Ogunbayo, O. A. *et al.* (2011) 'Cyclic adenosine diphosphate ribose activates ryanodine receptors, whereas NAADP activates two-pore domain channels', *Journal of Biological Chemistry*, 286(11), pp. 9136–9140. doi: 10.1074/jbc.M110.202002.

Ogunbayo, O. A. *et al.* (2018) 'mTORC1 controls lysosomal Ca $^{2+}$ release through the two-pore channel TPC2', *Science Signaling*, 11(525), p. eaao5775. doi: 10.1126/scisignal.aao5775.

Okumura, R. and Takeda, K. (2018) 'Maintenance of intestinal homeostasis by mucosal barriers', *Inflammation and Regeneration*. Inflammation and Regeneration, 38(1), pp. 1–8. doi: 10.1186/s41232-018-0063-z.

Parikh, K. *et al.* (2019) 'Colonic epithelial cell diversity in health and inflammatory bowel disease', *Nature*. Springer US, p. 1. doi: 10.1038/s41586-019-0992-y.

Parker, I., Choi, J. and Yao, Y. (1996) 'Elementary events of InsP3-induced Ca2+ liberation in Xenopus oocytes: Hot spots, puffs and blips', *Cell Calcium*, 20(2), pp. 105–121. doi: 10.1016/S0143-4160(96)90100-1.

Parkesh, R. *et al.* (2008) 'Cell-permeant NAADP: A novel chemical tool enabling the study of Ca2+ signalling in intact cells', *Cell Calcium*, 43(6), pp. 531–538. doi: 10.1016/j.ceca.2007.08.006.

Parris, A. and Williams, M. (2015) 'A human colonic culture system to study regulation of stem cell-driven tissue renewal and physiological function', *Methods in Molecular Biology*, 1212, pp. 141–161.

Parsons, W. *et al.* (2005) 'Mutation in a signalling pathway', *Nature co*, 436.

Patel, K. K. *et al.* (2013) 'Autophagy proteins control goblet cell function by potentiating reactive oxygen species production', *The EMBO journal*. Nature Publishing Group, 32(24), pp. 3130–3144. doi: 10.1038/emboj.2013.233.

Patel, S. and Kilpatrick, B. S. (2018) 'Two-pore channels and disease', *Biochimica et Biophysica Acta - Molecular Cell Research*. Elsevier, 1865(11), pp. 1678–1686. doi: 10.1016/j.bbamcr.2018.05.004.

Pawel R, K. and Fayez K, G. (2016) 'Physiology of intestinal absorption', *Best Pract Res Clin Gastroenterol*, pp. 1–20. doi: 10.1016/j.bpg.2016.02.007.Physiology.

Pchitskaya, E., Popugaeva, E. and Bezprozvanny, I. (2018) 'Calcium signaling and molecular mechanisms underlying neurodegenerative diseases', *Cell Calcium*. Elsevier Ltd, 70, pp. 87–94. doi: 10.1016/j.ceca.2017.06.008.

Pereira, G. J. S. *et al.* (2011) 'Nicotinic Acid Adenine Dinucleotide Phosphate (NAADP) regulates autophagy in cultured astrocytes', *Journal of Biological Chemistry*, 286(32), pp. 27875–27881. doi: 10.1074/jbc.C110.216580.

Perez-Vilar, J. (2007) 'Mucin granule intraluminal organization', *American Journal of Respiratory Cell and Molecular Biology*, 36(2), pp. 183–190. doi: 10.1165/rcmb.2006-0291TR.

Perez-vilar, J. and Hill, R. L. (1999) 'The Structure and Assembly of Secreted Mucins', *The Journal of biological chemistry*, 274(45), pp. 31751–31754.

Petersen, O. H. and Tepikin, A. V. (2008) 'Polarized Calcium Signaling in Exocrine Gland Cells', *Annual Review of Physiology*, 70(1), pp. 273–299. doi: 10.1146/annurev.physiol.70.113006.100618.

Peterson, L. W. and Artis, D. (2014) 'Intestinal epithelial cells: regulators of barrier function and immune homeostasis.', *Nature reviews. Immunology*. Nature Publishing Group, 14(3), pp. 141–53. doi: 10.1038/nri3608.

Peuker, Kenneth. Muff, Stefanie. Wang, Jun. Kunzel, Sven. Bosse, Esther. Zeissig, Yvonne. Luzzi, Giuseppina. Basic, Marijana. Strigli, Anne. Ulbricht, Andrea. Kaser, Arthur. Arlt, Alexander. Chavakis, Triantafyllos. van den Brink, G.R. Schafmayer, Clemens, S. (2016) 'Epithelial calcineurin controls

microbiota-dependent intestinal tumor development', *Nat Med*, 22(5), pp. 506–515. doi: doi:10.1038/nm.4072.

Peuker, K. *et al.* (2016) 'Epithelial calcineurin controls microbiota-dependent intestinal tumor development', *Nature Medicine*, (April). doi: 10.1038/nm.4072.

Phillips, T. E. (1992) 'Both crypt and villus intestinal goblet cells secrete mucin in response to cholinergic stimulation', *American Journal of Physiology - Gastrointestinal and Liver Physiology*, 262(2 25-2).

Phillips, T. E., Phillips, T. H. and Neutra, M. R. (1984) 'Regulation of intestinal goblet cell secretion. III. Isolated intestinal epithelium', *American Journal of Physiology-Gastrointestinal and Liver Physiology*, 247(6), pp. G674–G681. doi: 10.1152/ajpgi.1984.247.6.g674.

Pickett, J. A. and Edwardson, J. M. (2006) 'Compound exocytosis: Mechanisms and functional significance', *Traffic*, 7(2), pp. 109–116. doi: 10.1111/j.1600-0854.2005.00372.x.

Pinto, D. *et al.* (2003) 'Canonical Wnt signals are essential for homeostasis of the intestinal epithelium', *Genes and Development*, 17(14), pp. 1709–1713. doi: 10.1101/gad.267103.

Pinton, P., Romagnoli, A. and Giorgi, R. R. and C. (2008) 'Ca2+ Signaling, Mitochondria and Cell Death', *Current Molecular Medicine*, pp. 119–130. doi: http://dx.doi.org/10.2174/156652408783769571.

Plaisancié, P. *et al.* (1998) 'Effects of neurotransmitters, gut hormones, and inflammatory mediators on mucus discharge in rat colon', *American Journal of Physiology-Gastrointestinal and Liver Physiology*, 275(5), pp. G1073–G1084. doi: 10.1152/ajpgi.1998.275.5.g1073.

Portal, C. *et al.* (2017) 'In vivo imaging of the Muc5b gel-forming mucin', *Scientific Reports*. Nature Publishing Group, 7, pp. 1–9. doi: 10.1038/srep44591.

Van Der Post, S. *et al.* (2019) 'Structural weakening of the colonic mucus barrier is an early event in ulcerative colitis pathogenesis', *Gut*, pp. 1–10. doi: 10.1136/gutjnl-2018-317571.

Potten, C. S. (1977) 'Extreme sensitivity of some intestinal crypt cells to X and γ irradiation', *Nature*, 269(5628), pp. 518–521. doi: 10.1038/269518a0.

Potten, C. S. *et al.* (1978) 'The segregation of DNA in epithelial stem cells', *Cell*, 15(3), pp. 899–906. doi: 10.1016/0092-8674(78)90274-X.

Potten, C. S. *et al.* (2003) 'Identification of a putative intestinal stem cell and early lineage marker; musashi-1', *Differentiation*. International Society of Differentiation, 71(1), pp. 28–41. doi: 10.1046/j.1432-0436.2003.700603.x.

Potten, C. S., Owen, G. and Booth, D. (2002) 'Intestinal stem cells protect their genome by selective segregation of template DNA strands.', *Journal of cell science*, 115(Pt 11), pp. 2381–8. Available at: http://www.ncbi.nlm.nih.gov/pubmed/12006622.

Rah, S., Lee, Y. and Kim, U. (2017) 'NAADP-mediated Ca 2 + signaling promotes autophagy and protects against LPS-induced liver injury', *FASEB Journal*, 31(7), pp. 3126–3137. doi: 10.1096/fj.201601290R.

Ramaschi, G. *et al.* (1996) 'Expression of cyclic ADP-ribose - Synthetizing CD38 molecule on human platelet membrane', *Blood*, 87(6), pp. 2308–2313.

Ramirez, V. T. *et al.* (2019) 'T-cell derived acetylcholine aids host defenses during enteric bacterial infection with Citrobacter rodentium', *PLoS pathogens*, 15(4), p. e1007719. doi: 10.1371/journal.ppat.1007719.

Rasmussen, C. D. and Means, A. R. (1989) 'Calmodulin is required for cell-cycle progression during G1 and mitosis.', *The EMBO Journal*, 8(1), pp. 73–82. doi: 10.1002/j.1460-2075.1989.tb03350.x.

Raufman, Jean-Pierre; Samini, Roxana; Shah, Nirish; Khurana, Sandeep; Shant, Jasleen; Drachenberg, Cinthia; Xie, Guofeng; Wess, J. C. K. (2008) 'Genetic Ablation of M3 Muscarinic Receptors Attenuates Murine Colon Epithelial Cell Proliferation and Neoplasia', *Cancer Research*, 68(10), pp. 3573–3578. doi: 10.1016/j.surg.2006.10.010.Use.

Renz, B. W. *et al.* (2018) 'Cholinergic signaling via muscarinic receptors directly and indirectly suppresses pancreatic tumorigenesis and cancer stemness', *Cancer Discovery*, 8(11), pp. 1458–1473. doi: 10.1158/2159-8290.CD-18-0046.

Resendes, M. C. *et al.* (1999) 'Nuclear localization of the 82-kDa form of human choline acetyltransferase', *Journal of Biological Chemistry*, 274(27), pp. 19417–19421. doi: 10.1074/jbc.274.27.19417.

Reynolds, A. *et al.* (2007) 'Dynamic and differential regulation of NKCC1 by calcium and cAMP in the native human colonic epithelium.', *The Journal of physiology*, 582, pp. 507–524. doi: 10.1113/jphysiol.2007.129718.

Reynolds, A. *et al.* (2013) 'Canonical Wnt signals combined with suppressed TGFβ/BMP pathways promote renewal of the native human colonic epithelium', *Gut*, 0, pp. 1–12. Available at: http://dx.doi.org/10.1136/.

Richmond, Camilla A. Shah, Manavasi S. Deary, Luke T. Trotier, Danny C. Thomas, Horatio. Ambruzs, Dana M. Jiang, Lijie. Whiles, Bristol B. Rickner, Hannah D. Montgomery, Robert K. Tovaglieri, Alessio. Carlone, Diana L. Breault, D. T. (2015) 'Dormant Intestinal Stem Cells are Regulated by PTEN and Nutritional Status', *Cell Reports*, 13(11), pp. 2403–2411. doi: 110.1016/j.bbi.2017.04.008.

Richmond, C. A. *et al.* (2018) 'JAK/STAT-1 Signaling Is Required for Reserve Intestinal Stem Cell Activation during Intestinal Regeneration Following Acute Inflammation', *Stem Cell Reports*. ElsevierCompany., 10(1), pp. 17–26. doi: 10.1016/j.stemcr.2017.11.015.

Ritsma, L. *et al.* (2014) 'Intestinal crypt homeostasis revealed at single-stem-cell level by in vivo live imaging', *Nature*. Nature Publishing Group, 507(7492), pp. 362–365. doi: 10.1038/nature12972.

Rock, J. *et al.* (2013) 'Notch-dependent differentiation of adult airway basal stem cells', *Cell Stem cell*, 8(6), pp. 639–648. doi: 10.1016/j.stem.2011.04.003.Notch-dependent.

Roderick, H. L., Lechleiter, J. D. and Camacho, P. (2000) 'Cytosolic phosphorylation of calnexin controls intracellular Ca2+ oscillations via an interaction with SERCA2b', *Journal of Cell Biology*, 149(6), pp. 1235–1247. doi: 10.1083/jcb.149.6.1235.

Rodríguez-Colman, M. J. *et al.* (2017) 'Interplay between metabolic identities in the intestinal crypt supports stem cell function', *Nature*. doi: 10.1038/nature21673.

Ronco, V. *et al.* (2015) 'A novel Ca2+-mediated cross-talk between endoplasmic reticulum and acidic organelles: Implications for NAADP-dependent Ca2+ signalling', *Cell Calcium*. Elsevier Ltd, 57(2), pp. 89–100. doi: 10.1016/j.ceca.2015.01.001.

Rossi, A. H. *et al.* (2007) 'Calcium signaling in human airway goblet cells following purinergic activation', *American Journal of Physiology - Lung Cellular and Molecular Physiology*, 292(1), pp. 92–98. doi: 10.1152/ajplung.00081.2006.

Rossi, A. H., Sears, P. R. and Davis, C. W. (2004) 'Ca2+ dependency of "Ca2+-independent" exocytosis in SPOC1 airway goblet cells', *Journal of Physiology*, 559(2), pp. 555–565. doi: 10.1113/jphysiol.2004.070433.

Rothenberg, M. E. *et al.* (2012) 'Identification of a cKit + colonic crypt base secretory cell that

supports Lgr5 + stem cells in mice', *Gastroenterology*. Elsevier Inc., 142(5), pp. 1195-1205.e6. doi: 10.1053/j.gastro.2012.02.006.

Ruas, M. *et al.* (2014) 'TPC1 Has Two Variant Isoforms, and Their Removal Has Different Effects on Endo-Lysosomal Functions Compared to Loss of TPC2', *Molecular and Cellular Biology*, 34(21), pp. 3981–3992. doi: 10.1128/mcb.00113-14.

Rusnak, F. and Mertz, P. (2000) 'Calcineurin: Form and function', *Physiological Reviews*, 80(4), pp. 1483–1521. doi: 10.1152/physrev.2000.80.4.1483.

Ryu, Y.-S. *et al.* (2010) 'Mitochondrial Ryanodine Receptors and Other Mitochondrial Ca2+ Permeable Channels', *FEBS Letters*, 584(10), pp. 1948–1955. doi: 10.1016/j.febslet.2010.01.032.Mitochondrial.

Sakurai, Y. *et al.* (2015) 'Two-pore channels control Ebola virus host cell entry and are drug targets for disease treatment', *Science*, 347(6225), pp. 995–998.

Sambuy, Y. *et al.* (2005) 'The Caco-2 cell line as a model of the intestinal barrier: Influence of cell and culture-related factors on Caco-2 cell functional characteristics', *Cell Biology and Toxicology*, 21(1), pp. 1–26. doi: 10.1007/s10565-005-0085-6.

Sancho, R., Cremona, C. A. and Behrens, A. (2015) 'Stem cell and progenitor fate in the mammalian intestine: Notch and lateral inhibition in homeostasis and disease', *EMBO reports*, 16(5), pp. 571–581. doi: 10.15252/embr.201540188.

Sangiorgi, Eugenio. Capecchi, M. R. (2008) 'Bmi1 is expressed in vivo in intestinal stem cells', *Nature Genetics*, 40(7), pp. 915–920. doi: 10.1038/ng.165.Bmi1.

Santos, A. J. M. *et al.* (2018) 'The Intestinal Stem Cell Niche: Homeostasis and Adaptations', *Trends in Cell Biology*. Elsevier Ltd, 28(12), pp. 1062–1078. doi: 10.1016/j.tcb.2018.08.001.

Sasaki, N. *et al.* (2016) 'Reg4+ deep crypt secretory cells function as epithelial niche for Lgr5+ stem cells in colon.', *Proceedings of the National Academy of Sciences of the United States of America*, 4, p. 201607327. doi: 10.1073/pnas.1607327113.

Sasaki, T. *et al.* (2002) 'Expression and distribution of laminin α1 and α2 chains in embryonic and adult mouse tissues: An immunochemical approach', *Experimental Cell Research*, 275(2), pp. 185–199. doi: 10.1006/excr.2002.5499.

Sasselli, V., Pachnis, V. and Burns, A. J. (2012) 'The enteric nervous system', *Developmental Biology*. Elsevier Inc., 366(1), pp. 64–73. doi: 10.1016/j.ydbio.2012.01.012.

Sato, T. *et al.* (2009) 'Single Lgr5 stem cells build crypt-villus structures in vitro without a mesenchymal niche.', *Nature*. Nature Publishing Group, 459(7244), pp. 262–5. doi: 10.1038/nature07935.

Sato, Toshiro *et al.* (2011) 'Long-term expansion of epithelial organoids from human colon, adenoma, adenocarcinoma, and Barrett's epithelium', *Gastroenterology*. Elsevier Inc., 141(5), pp. 1762–1772. doi: 10.1053/j.gastro.2011.07.050.

Sato, Toshiro. *et al.* (2011) 'Paneth cells constitute the niche for Lgr5 stem cells in intestinal crypts.', *Nature*. Nature Publishing Group, 469(7330), pp. 415–8. doi: 10.1038/nature09637.

Saucerman, J. J. and Bers, D. M. (2008) 'Calmodulin mediates differential sensitivity of CaMKII and calcineurin to local Ca2+ in cardiac myocytes', *Biophysical Journal*. Elsevier, 95(10), pp. 4597–4612. doi: 10.1529/biophysj.108.128728.

Saxena, K. *et al.* (2016) 'Human Intestinal Enteroids : a New Model To Study Human Rotavirus Infection, Host Restriction, and Pathophysiology', 90(1), pp. 43–56. doi: 10.1128/JVI.01930-15.Editor.

Schauber, J. *et al.* (2003) 'Expression of the cathelicidin LL-37 is modulated by short chain fatty acids in colonocytes: relevance of signalling pathways', *Gut*, 52, pp. 735–741.

Schepers, A. and Clevers, H. (2012) 'Wnt signaling, stem cells, and cancer of the gastrointestinal tract.', *Cold Spring Harbor perspectives in biology*, 4(4), pp. 1–14. doi: 10.1101/cshperspect.a007989.

Schewe, M. *et al.* (2016) 'Secreted Phospholipases A2 Are Intestinal Stem Cell Niche Factors with Distinct Roles in Homeostasis, Inflammation, and Cancer', *Cell Stem Cell*, 19(1), pp. 38–51. doi: 10.1016/j.stem.2016.05.023.

Schmitt, M. *et al.* (2018) 'Paneth Cells Respond to Inflammation and Contribute to Tissue Regeneration by Acquiring Stem-like Features through SCF/c-Kit Signaling', *Cell Reports*. ElsevierCompany., 24(9), pp. 2312-2328.e7. doi: 10.1016/j.celrep.2018.07.085.

Schneider, C. *et al.* (2018) 'A Metabolite-Triggered Tuft Cell-ILC2 Circuit Drives Small Intestinal Remodeling', *Cell*. Elsevier, 174(2), pp. 271-284.e14. doi: 10.1016/j.cell.2018.05.014.

Schneider, C., O'Leary, C. E. and Locksley, R. M. (2019) 'Regulation of immune responses by tuft cells', *Nature Reviews Immunology*, 3(1). doi: 10.1038/s41577-019-0176-x.

Schneider, H. *et al.* (2018) 'Study of mucin turnover in the small intestine by in vivo labeling', *Scientific Reports*. Springer US, 8(1), pp. 1–11. doi: 10.1038/s41598-018-24148-x.

Schölzel, S. *et al.* (2000) 'Carcinoembryonic antigen family members CEACAM6 and CEACAM7 are differentially expressed in normal tissues and oppositely deregulated in hyperplastic colorectal polyps and early adenomas', *American Journal of Pathology*, 156(2), pp. 595–605. doi: 10.1016/S0002-9440(10)64764-5.

Schuijers, J. *et al.* (2014) 'Robust cre-mediated recombination in small intestinal stem cells utilizing the Olfm4 locus', *Stem Cell Reports*. The Authors, 3(2), pp. 234–241. doi: 10.1016/j.stemcr.2014.05.018.

Schuijers, J. *et al.* (2015) 'Ascl2 acts as an R-spondin/wnt-responsive switch to control stemness in intestinal crypts', *Cell Stem Cell*. Elsevier Inc., 16(2), pp. 158–170. doi: 10.1016/j.stem.2014.12.006.

Schumacher, Y. *et al.* (2016) 'Dysregulated CRTC1 activity is a novel component of PGE2 signaling that contributes to colon cancer growth', *Oncogene*. Nature Publishing Group, 35(20), pp. 2602–2614. doi: 10.1038/onc.2015.283.

Schutte, A. *et al.* (2014) 'Microbial-induced meprin cleavage in MUC2 mucin and a functional CFTR channel are required to release anchored small intestinal mucus', *Proceedings of the National Academy of Sciences*, 111(34), pp. 12396–12401. doi: 10.1073/pnas.1407597111.

Schwank, G. *et al.* (2013) 'Functional repair of CFTR by CRISPR/Cas9 in intestinal stem cell organoids of cystic fibrosis patients', *Cell Stem Cell*. Elsevier Inc., 13(6), pp. 653–658. doi: 10.1016/j.stem.2013.11.002.

Schwartz, C. J. *et al.* (1974) 'Vasoactive intestinal peptide stimulation of adenylate cyclase and active electrolyte secretion in intestinal mucosa', *Journal of Clinical Investigation*, 54(3), pp. 536–544. doi: 10.1172/JCI107790.

Seidler, N. W. *et al.* (1989) 'Cyclopiazonic acid is a specific inhibitor of the Ca2+-ATPase of sarcoplasmic reticulum', *Journal of Biological Chemistry*, 264(30), pp. 17816–17823.

Serobyan, N. *et al.* (2007) 'The cholinergic system is involved in regulation of the development of the hematopoietic system', *Life Sciences*, 80, pp. 24–25. doi: 10.1016/j.lfs.2007.04.017.

Settembre, C. *et al.* (2013) 'Signals from the lysosome: A control centre for cellular clearance and energy metabolism', *Nature Reviews Molecular Cell Biology*. Nature Publishing Group, 14(5), pp. 283–296. doi: 10.1038/nrm3565.

Seung, H. Y. *et al.* (2007) 'Presence of secretogranin II and high-capacity, low-affinity Ca 2+ storage role in nucleoplasmic Ca2+ store vesicles', *Biochemistry*, 46(50), pp. 14663–14671. doi: 10.1021/bi701339m.

Shan, M. *et al.* (2013) 'Mucus enhances gut homeostasis and oral tolerance by delivering immunoregulatory signals', *Science*, 342(6157), pp. 447–453. doi: 10.1126/science.1237910.

Shaw, J.-P. *et al.* (1988) 'Identification of a putative regulator of early T cell activation genes. Science. 1988. 241: 202-205.', *Journal of immunology (Baltimore, Md. : 1950)*, 185(C), pp. 4972–4975. doi: 10.1126/science.3260404.

Shaywitz, A. J. and Greenberg, M. E. (1999) 'CREB: A Stimulus-Induced Transcription Factor Activated By A Diverse Array Of Extracellular Signals', *Annual Review of Biochemistry*, 68, pp. 821–861. doi: 10.1002/9783527678679.dg13514.

Shibao, K. *et al.* (2010) 'The type III inositol 1,4,5-trisphosphate receptor is associated with aggressiveness of colorectal carcinoma', *Cell Calcium*, 48(6), pp. 315–323.

Shoshkes-carmel, M. *et al.* (2018) 'Subepithelial telocytes are an important source of Wnts that supports intestinal crypts', *Nature*, 557, pp. 242–246. doi: 10.1038/s41586-018-0084-4.

Sicard, J.-F. *et al.* (2017) 'Interactions of Intestinal Bacteria with Components of the Intestinal Mucus', *Frontiers in Cellular and Infection Microbiology*, 7(September). doi: 10.3389/fcimb.2017.00387.

Siefjediers, A. *et al.* (2007) 'Characterization of inositol 1,4,5-trisphosphate (IP3) receptor subtypes at rat colonic epithelium', *Cell Calcium*, 41(4), pp. 303–315. doi: 10.1016/j.ceca.2006.07.009.

Simoes, B. M. *et al.* (2015) 'The role of steroid hormones in breast cancer stem cells', *Endocrine-Related Cancer*, 22(6), pp. T177–T186. doi: 10.1530/ERC-15-0350.

Skoczek, D. a *et al.* (2014) 'Luminal microbes promote monocyte-stem cell interactions across a healthy colonic epithelium.', *Journal of immunology (Baltimore, Md. : 1950)*, 193(1), pp. 439–51. doi: 10.4049/jimmunol.1301497.

van der Sluis, M. *et al.* (2008) 'Forkhead box transcription factors Foxa1 and Foxa2 are important regulators of Muc2 mucin expression in intestinal epithelial cells', *Biochemical and Biophysical Research Communications*, 369(4), pp. 1108–1113. doi: 10.1016/j.bbrc.2008.02.158.

Smirnova, M. G. *et al.* (2003) 'LPS up-regulates mucin and cytokine mRNA expression and stimulates mucin and cytokine secretion in goblet cells', *Cellular Immunology*, 221(1), pp. 42–49. doi: 10.1016/S0008-8749(03)00059-5.

Smyth, J. T. *et al.* (2010) 'Activation and regulation of store-operated calcium entry', *Journal of Cellular and Molecular Medicine*, 14(10), pp. 2337–2349. doi: 10.1111/j.1582-4934.2010.01168.x.

Snippert, H. J. *et al.* (2010) 'Intestinal crypt homeostasis results from neutral competition between symmetrically dividing Lgr5 stem cells', *Cell*. Elsevier Ltd, 143(1), pp. 134–144. doi: 10.1016/j.cell.2010.09.016.

Snoeck, V., Goddeeris, B. and Cox, E. (2005) 'The role of enterocytes in the intestinal barrier function and antigen uptake', *Microbes and Infection*, 7(7–8), pp. 997–1004. doi: 10.1016/j.micinf.2005.04.003.

Snyder, J. C. *et al.* (2013) 'Constitutive internalization of the Leucine-rich g protein-coupled receptor-5 (LGR5) to the trans-Golgi network', *Journal of Biological Chemistry*, 288(15), pp. 10286–10287. doi: 10.1074/jbc.M112.447540.

Soboloff, J. *et al.* (2012) 'STIM proteins: Dynamic calcium signal transducers', *Nature Reviews Molecular Cell Biology*. Nature Publishing Group, 13(9), pp. 549–565. doi: 10.1038/nrm3414.

Son, K. *et al.* (2018) 'A simple guideline to assess the characteristics of RNA-Seq Data', *BioMed Research International*, 2018. doi: 10.1155/2018/2906292.

Song, E. K. *et al.* (2012) 'NAADP Mediates Insulin-Stimulated Glucose Uptake and Insulin Sensitization by PPARγ in Adipocytes', *Cell Reports*. The Authors, 2(6), pp. 1607–1619. doi: 10.1016/j.celrep.2012.10.018.

de Sousa e Melo, F. and de Sauvage, F. J. (2019) 'Cellular Plasticity in Intestinal Homeostasis and Disease', *Cell Stem Cell*. Elsevier Inc., 24(1), pp. 54–64. doi: 10.1016/j.stem.2018.11.019.

Specian, R. D. and Neutra, M. R. (1980) 'Mechanism of rapid mucus secretion in goblet cells stimulated by acetylcholine', *Journal of Cell Biology*, 85(3), pp. 626–640. doi: 10.1083/jcb.85.3.626.

Specian, R. D. and Neutra, M. R. (1982) 'Regulation of intestinal goblet cell secretion. I. Role of parasympathetic stimulation', *American Journal of Physiology - Gastrointestinal and Liver Physiology*, 5(4), pp. 370–379.

Stange, Daniel E. Koo, Bon-Kyoung. Huch, Meritxell. Sibbel, Greg. Basak, Onur. yubimova, Anna. Kujala, Pekka. Barfeld, Sina. Koster, Jan. Geahlen, Jessica. H. Peters, Peter. J. van Es, Johan. H. van de Wetering, Marc. Mills, Jason. C. Clevers, H. (2013) 'Differentiated Troy+ chief cells act as "reserve" stem cells to generate all lineages of the stomach epithelium', *Cell*, 155(2), pp. 357–368. doi: 10.1371/journal.pone.0178059.

Sternini, C., Anselmi, L. and Rozengurt, E. (2008) 'Enteroendocrine cells: A site of "taste" in gastrointestinal chemosensing', *Current Opinion in Endocrinology, Diabetes and Obesity*, 15(1), pp. 73–78. doi: 10.1097/MED.0b013e3282f43a73.

Storm, E. E. *et al.* (2015) 'Targeting PTPRK-RSPO3 colon tumours promotes differentiation and loss of stem-cell function', *Nature*. Nature Publishing Group, 529(7584), pp. 97–100. doi: 10.1038/nature16466.

Streichert, L. C. and Sargent, P. B. (1992) 'The role of acetylcholinesterase in denervation supersensitivity in the frog cardiac ganglion.', *The Journal of Physiology*, 445(1), pp. 249–260. doi: 10.1113/jphysiol.1992.sp018922.

Stzepourginski, I. *et al.* (2017) ' CD34 + mesenchymal cells are a major component of the intestinal stem cells niche at homeostasis and after injury ', *Proceedings of the National Academy of Sciences*, 114(4), pp. E506–E513. doi: 10.1073/pnas.1620059114.

Sugimoto, K. *et al.* (2008) 'IL-22 ameliorates intestinal inflammation in a mouse model of ulcerative colitis', *The Journal of clinical investigation*, 118(2). doi: 10.1172/JCI33194DS1.

Suski, J. M. *et al.* (2014) 'Isolation of plasma membrane-associated membranes from rat liver', *Nature Protocols*. Nature Publishing Group, 9(2), pp. 312–322. doi: 10.1038/nprot.2014.016.

Swillens, S. *et al.* (1999) 'From calcium blips to calcium puffs: Theoretical analysis of the requirements for interchannel communication', *PNAS*, 96(24), pp. 1–6.

Takahashi, T. *et al.* (2014) 'Non-neuronal acetylcholine as an endogenous regulator of proliferation and differentiation of Lgr5-positive stem cells in mice.', *The FEBS journal*, 281(20), pp. 4672–90. doi: 10.1111/febs.12974.

Takahashi, T. (2018) 'Organoids for Drug Discovery and Personalized Medicine', *Annual Review of Pharmacology and Toxicology*, 59(1), pp. 447–462. doi: 10.1146/annurev-pharmtox-010818-021108.

Takahashi, T., Shiraishi, A. and Murata, J. (2018) 'The Coordinated Activities of nAChR and Wnt Signaling Regulate Intestinal Stem Cell Function in Mice', *International Journal of Molecular Sciences*, 19(3), p. 738. doi: 10.3390/ijms19030738.

Takaku, K. *et al.* (1999) 'Gastric and duodenal polyps in Smad4 (Dpc4) knockout mice', *Cancer Research*, 59(24), pp. 6113–6117.

Takeda, N. *et al.* (2011) 'Inter-conversion between intestinal stem cell populations in distinct niches', *Science*, 334(6061), pp. 1420–1424. doi: 10.1126/science.1213214.Inter-conversion.

Takeo, S. *et al.* (2002) 'The Wnt / calcium pathway activates NF-AT and promotes ventral cell fate in Xenopus embryos', *Nature*, 417(May), pp. 295–299.

Tapper, E. J., Powell, D. W. and Morris, S. M. (1978) 'Cholinergic-adrenergic interactions on intestinal ion transport', *American Journal of Physiology Endocrinology Metabolism and Gastrointestinal Physiology*, 4(4), pp. 402–409.

Tarasov, A. I., Griffiths, E. J. and Rutter, G. A. (2012) 'Regulation of ATP production by mitochondrial Ca2+', *Cell Calcium*. Elsevier Ltd, 52(1), pp. 28–35. doi: 10.1016/j.ceca.2012.03.003.

Tarlow, Branden, D. Pelz, Carl. Naugler, Willscott. E. Wakefield, Leslie. Wilson, Elizabeth. M. Finegold, Milton. J. Grompe, M. (2014) 'Bipotential adult liver progenitors are derived from chronically injured mature hepatocytes', *Cell Stem Cell*, 6(5), pp. 605–618. doi: 10.1371/journal.pone.0178059.

Taupin, D. and Podolsky, D. K. (2003) 'Trefoil factors: Initiators of mucosal healing', *Nature Reviews Molecular Cell Biology*, 4(9), pp. 721–732. doi: 10.1038/nrm1203.

Taylor, P. and Brown, J. (1999) 'Synthesis, Storage and Release of Acetylcholine', in Siegel, G., Agranoff, B., and Albers, R. (eds) *Basic Neurochemistry: Molecular, Cellular and Medical Aspects*. 6th editio. Philadelphia: Lippincott-Raven. Available at: https://www.ncbi.nlm.nih.gov/books/NBK28051/.

Tetteh, P. W. *et al.* (2016) 'Replacement of Lost Lgr5-Positive Stem Cells through Plasticity of Their Enterocyte-Lineage Daughters', *Cell Stem Cell*, 0(0). doi: 10.1016/j.stem.2016.01.001.

Thim, L. (1997) 'Trefoil peptides: from structure to function', *Cellular and Molecular Life Sciences*,

53(12), p. 888. doi: 10.1007/s000180050108.

Thorn, P. and Gaisano, H. (2012) 'Molecular control of compound Exocytosis: A key role for VAMP8.', *Communicative & integrative biology*, 5(1), pp. 61–613. doi: 10.4161/cib.18058.

Tian, H. *et al.* (2011) 'A reserve stem cell population in small intestine renders Lgr5-positive cells dispensable', *Nature*. Nature Publishing Group, 478(7368), pp. 255–259. doi: 10.1038/nature10408.

Tiwari, P. *et al.* (2013) 'Basic and modern concepts on cholinergic receptor: A review', *Asian Pacific Journal of Tropical Disease*, 3(5), pp. 413–420. doi: 10.1016/S2222-1808(13)60094-8.

Tomono, M. *et al.* (1998) 'Inhibitors of calcineurin block expression of cyclins A and E induced by fibroblast growth factor in Swiss 3T3 fibroblasts', *Archives of Biochemistry and Biophysics*, 353(2), pp. 374–378. doi: 10.1006/abbi.1998.0667.

Totaro, A., Panciera, T. and Piccolo, S. (2018) 'YAP/TAZ upstream signals and downstream responses', *Nature Cell Biology*. Springer US, 20(8), pp. 888–899. doi: 10.1038/s41556-018-0142-z.

Toyofuku, T. *et al.* (1998) 'Intercellular Calcium Signaling via Gap Junction in', *Journal of Biological Chemistry* , 273(3), pp. 1519–1528. doi: 10.1074/jbc.273.3.1519.

Tremaroli, V. and Bäckhed, F. (2012) 'Functional interactions between the gut microbiota and host metabolism', *Nature*, 489(7415), pp. 242–249. doi: 10.1038/nature11552.

Tripathi, M. K. *et al.* (2014) 'Nuclear factor of activated T-cell activity is associated with metastatic capacity in colon cancer', *Cancer Research*, 74(23), pp. 6947–6957. doi: 10.1158/0008-5472.CAN-14-1592.

Urso, K. *et al.* (2019) 'NFATc3 controls tumour growth by regulating proliferation and migration of human astroglioma cells', *Scientific Reports*, 9(1), pp. 1–14. doi: 10.1038/s41598-019-45731-w.

Vancamelbeke, M. and Vermeire, S. (2017) 'The intestinal barrier : a fundamental role in health and disease', *Expert Review of Gastroenterology & Hepatology*, 11(9), pp. 821–834. doi: 10.1080/17474124.2017.1343143.The.

Vandesompele, J. *et al.* (2002) 'Accurate normalization of real-time quantitative RT-PCR data by geometric averaging of multiple internal control genes', *Genome Biology*, 3(7), pp. 1–12. doi: https://doi.org/10.1186/gb-2002-3-7-research0034.

Vandussen, Kelli L. Samuelson, L. C. (2010) 'Mouse Atonal Homolog 1 Directs Intestinal Progenitors to Secretory Cell Rather than Absorptive Cell Fate', *Developmental Biology*, 346(2), pp. 215–223. doi: 10.1038/jid.2014.371.

Vanuytsel, T. *et al.* (2013) 'Major signaling pathways in intestinal stem cells', *Biochimica et Biophysica Acta - General Subjects*. Elsevier B.V., 1830(2), pp. 2410–2426. doi: 10.1016/j.bbagen.2012.08.006.

Velcich, A. *et al.* (2002) 'Colorectal Cancer in Mice Genetically Deficient in the Mucin Muc2', *Science*, 295. doi: 10.1126/science.1069094.

van Vliet, A. R., Verfaillie, T. and Agostinis, P. (2014) 'New functions of mitochondria associated membranes in cellular signaling', *Biochimica et Biophysica Acta - Molecular Cell Research*. Elsevier B.V., 1843(10), pp. 2253–2262. doi: 10.1016/j.bbamcr.2014.03.009.

Vu, D. *et al.* (2013) 'A structural basis for selective dimerization by NF-κB RelB', *Journal of Molecular Biology*, 425(11), pp. 1934–1945. doi: 10.1016/j.jmb.2013.02.020.

Wallon, C. *et al.* (2011) 'Eosinophils express muscarinic receptors and corticotropin-releasing factor to disrupt the mucosal barrier in ulcerative colitis', *Gastroenterology*. Elsevier Inc., 140(5), pp. 1597–1607. doi: 10.1053/j.gastro.2011.01.042.

Walseth, T. F. and Lee, H. C. (1993) 'Synthesis and characterization of antagonists of cyclic-ADP-ribose-induced Ca2+ release', *BBA - Molecular Cell Research*, 1178(3), pp. 235–242. doi: 10.1016/0167-4889(93)90199-Y.

Walsh, K. T. and Zemper, A. E. (2019) 'The Enteric Nervous System for Epithelial Researchers: Basic Anatomy, Techniques, and Interactions With the Epithelium', *Cellular and Molecular Gastroenterology and Hepatology*. The Authors, (July). doi: 10.1016/j.jcmgh.2019.05.003.

Wang, W. *et al.* (2015) 'Up-regulation of lysosomal TRPML1 channels is essential for lysosomal adaptation to nutrient starvation', *Proceedings of the National Academy of Sciences*, 112(11), pp. E1373–E1381. doi: 10.1073/pnas.1419669112.

Warhurst, G. *et al.* (1991) 'Stimulatory and inhibitory actions of carbachol on chloride secretory responses in human colonic cell line T84', *The American Journal of Physiology*, 261, pp. 220–228.

Wei, X. *et al.* (2017) 'Ascl2 activation by YAP1/KLF5 ensures the self-renewability of colon cancer progenitor cells', *Oncotarget*, 8(65), pp. 109301–109318. doi: 10.18632/oncotarget.22673.

Wessler, I. and Kirkpatrick, C. J. (2012) *Activation of Muscarinic Receptors by Non-neuronal Acetylcholine*. Muscarinic, *Handbook of experimental pharmacology*. Muscarinic. Edited by A. . F. et Al. Springer-Verlag. doi: 10.1007/978-3-642-23274-9_20.

Westphalen, C. B. *et al.* (2014) 'Long-lived intestinal tuft cells serve as colon cancer-initiating cells', *Journal of Clinical Investigation*, 124(3), pp. 1283–1295. doi: 10.1172/JCI73434.

van de Wetering, Marc. Sancho, Elena. Verweij, Cornelis. de Lau, Wim. Oving, Irma. Hurlstone, Adam. van der Horn, Karina. Batlle, Eduard. Coudreuse, Damien. Haramis, Anna-Pavlina. Tjon-Pon-Fong, Menno. Moerern, Petra. vand den Born, Maaike. Soete, Gwen, P, H. (2002) 'The Beta-Catenin/TCF-4 Complex Imposes a Crypt Progenitor Phenotype on Colorectal Cancer Cells Marc', *Cell*, 111, pp. 241–250. doi: 10.1016/S0092-8674(02)01014-0.

Whitehead, Robert. H. Brown, Anthony. Bhathal, P. S. (1987) 'A method for the isolation and culture of human colonic crypts in collagen gels', *In Vitro Cellular & Developmental Biology*, 23(6), pp. 436–442.

Willemsen, L. E. M. *et al.* (2003) 'Short chain fatty acids stimulate epithelial mucin 2 expression through differential effects on prostaglandin E1 and E2 production by intestinal myofibroblasts', *Gut*, 52(10), pp. 1442–1447. doi: 10.1136/gut.52.10.1442.

Williams, J. A. (2010) 'Regulation of acinar cell function in the pancreas', *Current Opinion in Gastroenterology*, 26(5), pp. 478–483. doi: 10.1097/MOG.0b013e32833d11c6.

Williams, J. M. *et al.* (2015) 'Epithelial Cell Shedding and Barrier Function: A Matter of Life and Death at the Small Intestinal Villus Tip', *Veterinary Pathology*, 52(3), pp. 445–455. doi: 10.1177/0300985814559404.

Winton, D. J., Blount, M. A. and Ponder, B. A. J. (1988) 'A clonal marker induced by mutation in mouse intestinal epithelium', *Nature*, 333(6172), pp. 463–466. doi: 10.1038/333463a0.

Withers, H. R., Brennand, J. T. and Elkind, M. M. (1970) 'The response of stem cells of intestinal mucosa to irradiation with 14 MeV neutrons', *The British Journal of Radiology*. The British Institute of Radiology, 43(515), pp. 796–801. doi: 10.1259/0007-1285-43-515-796.

Wlodarska, M. *et al.* (2014) 'NLRP6 inflammasome orchestrates the colonic host-microbial interface by regulating goblet cell mucus secretion', *Cell*. Elsevier Inc., 156(5), pp. 1045–1059. doi: 10.1016/j.cell.2014.01.026.

Wootten, D. *et al.* (2018) 'Mechanisms of signalling and biased agonism in G protein-coupled receptors', *Nature Reviews Molecular Cell Biology*. Springer US, 19(10), pp. 638–653. doi: 10.1038/s41580-018-0049-3.

Wrzosek, L. *et al.* (2013) 'Bacteroides thetaiotaomicron and Faecalibacterium prausnitzii influence the production of mucus glycans and the development of goblet cells in the colonic epithelium of a gnotobiotic model rodent', *BMC Biology*, 11. doi: 10.1186/1741-7007-11-61.

Wu, S. *et al.* (2018) 'Transcription factor YY1 promotes cell proliferation by directly activating the pentose phosphate pathway', *Cancer Research*, 78(16), pp. 4549–4562. doi: 10.1158/0008-5472.CAN-17-4047.

Wu, X. and Bers, D. M. (2007) 'Free and bound intracellular calmodulin measurements in cardiac myocytes', *Cell Calcium*, 41(4), pp. 353–364. doi: 10.1016/j.ceca.2006.07.011.

Wu, Y. *et al.* (2019) 'The role of autophagy in maintaining intestinal mucosal barrier', *Journal of Cellular Physiology*, (January), pp. 19406–19419. doi: 10.1002/jcp.28722.

Yajima, T. *et al.* (2011) 'Non-neuronal release of ACh plays a key role in secretory response to luminal propionate in rat colon', *Journal of Physiology*, 589(4), pp. 953–962. doi: 10.1113/jphysiol.2010.199976.

Yan, Kelley S. Gevaert, Olivier. Zheng, Grace. X.Y. Anchang, Benedict. Probert, Christopher. S. Larkin, Kathryn. A. Davies, Paige. S. Cheng, Zhuan-fen. Kaddis, John. S. Han, Arnold. Roelf, Kelly. Calderon, Ruben. I. Cynn, Esther. Hu, Xiaoyi. Mandleywala, C. J. (2017) 'Intestinal enteroendocrine lineage cells possess homeostatic and injury-inducible stem cell activity conducted experiments and analyzed data HHS Public Access', *Cell Stem Cell*, 21(1), pp. 78–90. doi: 10.1016/j.stem.2017.06.014.

Yan, K., Chia, L. and Li, X. (2012) 'The intestinal stem cell markers Bmi1 and Lgr5 identify two functionally distinct populations', *Pnas*, 109(2), pp. 466–471. doi: 10.1073/pnas.1118857109/-/DCSupplemental.www.pnas.org/cgi/doi/10.1073/pnas.1118857109.

Yan, K. S. and Kuo, C. J. (2015) 'Ascl2 reinforces intestinal stem cell identity', *Cell Stem Cell*. Elsevier Inc., 16(2), pp. 105–106. doi: 10.1016/j.stem.2015.01.014.

Yan Kelvin Yip, H. *et al.* (2018) 'Colon organoid formation and cryptogenesis are stimulated by growth factors secreted from myofibroblasts', *PLoS ONE*, 13(6). doi: 10.1371/journal.pone.0199412.

Yang, N., Garcia, M. A. S. and Quinton, P. M. (2013) 'Normal mucus formation requires cAMP-

dependent HCO3- secretion and Ca2+-mediated mucin exocytosis', *Journal of Physiology*, 591(18), pp. 4581–4593. doi: 10.1113/jphysiol.2013.257436.

Ye, Diana Z. Haestner, K. H. (2009) 'Foxa1 and Foxa2 Control the Differentiation of Goblet and Enteroendocrine L- and D-Cells in Mice', *Gastroenterology*, 137(6), pp. 2052-2–62. doi: 10.1038/jid.2014.371.

Yedgar, S. *et al.* (1992) 'Cyclic AMP-independent secretion of mucin by SW1116 human colon carcinoma cells. Differential control by Ca 2+ ionophore A23187 and arachidonic acid', *Biochemical Journal*, 283(2), pp. 421–426. doi: 10.1042/bj2830421.

Yilmaz, Ö. H. *et al.* (2012) 'mTORC1 in the Paneth cell niche couples intestinal stem-cell function to calorie intake.', *Nature*, 486(7404), pp. 490–5. doi: 10.1038/nature11163.

Yin, X. *et al.* (2016) 'Review Engineering Stem Cell Organoids', *Stem Cell*. Elsevier Inc., 18(1), pp. 25–38. doi: 10.1016/j.stem.2015.12.005.

Yousefi, M. *et al.* (2018) 'Calorie Restriction Governs Intestinal Epithelial Regeneration through Cell-Autonomous Regulation of mTORC1 in Reserve Stem Cells', *Stem Cell Reports*. ElsevierCompany., 10(3), pp. 703–711. doi: 10.1016/j.stemcr.2018.01.026.

Yu, D. H. *et al.* (2015) 'Postnatal epigenetic regulation of intestinal stem cells requires DNA methylation and is guided by the microbiome', *Genome Biology*, 16(1), pp. 1–16. doi: 10.1186/s13059-015-0763-5.

Yui, S. *et al.* (2012) 'Functional engraftment of colon epithelium expanded in vitro from a single adult $Lgr5^{+}$ stem cell.', *Nature medicine*. Nature Publishing Group, 18(4), pp. 618–23. doi: 10.1038/nm.2695.

Zhang, Y. *et al.* (2013) 'Mastermind-like transcriptional co-activator-mediated Notch signaling is indispensable for maintaining conjunctival epithelial identity', *Development*, 140(3), pp. 594–605. doi: 10.1242/dev.082842.

Zhao, C.-M. *et al.* (2014) 'Denervation suppresses gastric tumorigenesis', *Science Translational Medicine*, 6(250), pp. 250ra115-250ra115. doi: 10.1126/scitranslmed.3009569.

Zhao, F. *et al.* (2001) 'Dantrolene inhibition of ryanodine receptor Ca2+ release channels. Molecular mechanism and isoform selectivity', *Journal of Biological Chemistry*, 276(17), pp. 13810–13816. doi: 10.1074/jbc.M006104200.

Zheng, Leon. Kelly, Caleb J. Battista, Kayla D. Schaefer, Rachel. Lanis, Jordi M. Alexeev, Ericca E. Wang, Ruth X. Onyiah, Joseph C. Kominsky, Douglas J. Colgan, S. P. (2017) 'Microbial-derived Butyrate Promotes Epithelial Barrier Function Through IL-10 Receptor-dependent Repression of Claudin-2', *Journal of Immunology*, 199(8), pp. 2976–2984. doi: 110.1016/j.bbi.2017.04.008.

Zheng, H. *et al.* (2009) 'KLF4 gene expression is inhibited by the notch signaling pathway that controls goblet cell differentiation in mouse gastrointestinal tract', *American Journal of Physiology-Gastrointestinal and Liver Physiology*, 296(3), pp. G490–G498. doi: 10.1152/ajpgi.90393.2008.

Zietek, T. *et al.* (2015) 'Intestinal organoids for assessing nutrient transport, sensing and incretin secretion.', *Scientific reports*. Nature Publishing Group, 5, p. 16831. doi: 10.1038/srep16831.

Zong, X. *et al.* (2009) 'The two-pore channel TPCN2 mediates NAADP-dependent Ca2+-release from lysosomal stores', *Pflugers Archiv European Journal of Physiology*, 458(5), pp. 891–899. doi: 10.1007/s00424-009-0690-y.

Zumerle, S. *et al.* (2019) 'Intercellular Calcium Signaling Induced by ATP Potentiates Macrophage Phagocytosis', *Cell Reports*, 27(1), pp. 1-10.e4. doi: 10.1016/j.celrep.2019.03.011.

APENDIX A. RNAseq analysis of markers of cellular types and calcium signalling toolkit components

			Patient 1	Patient 2	Patient 3	Patient 4	Patient 5	Patient 6
STEM CELL MARKERS	LGR5	Mucosa	50	293.999	126	457.001	165	64
		Crypt	165	349	381.001	542.001	374.999	384
		Organoid	59	15	4	33	0	18
	OLFM4	Mucosa	2722	1483	5485	11831	4323	1899
		Crypt	6077	1653	9657	11422	9072	5800
		Organoid	22969	28054	37297	47941	309	102214
	ASCL2	Mucosa	208	471	232	1074	285	134
		Crypt	420	577	1385	835	417	435
		Organoid	143	53	170	173	10	95
	PTK7	Mucosa	205	537.001	355	426.999	585.001	285
		Crypt	384	728	646.998	475	687	722.002
		Organoid	96	116	231	106	200	96
GOBLET CELL MARKERS	MUC2	Mucosa	108681	170540	152400	122848	164343	89312.8
		Crypt	271472	289667	197532	174066	144038	65837.3
		Organoid	341150	217013	322913	347420	620698	167356
	WFDC2	Mucosa	4280.02	3836.97	2523.99	3900.99	4590.91	2034.01
		Crypt	5344.05	3272.95	6353.09	3119.05	4369.04	4012.01
		Organoid	9279.08	8862.91	13230.4	8157.39	15734.2	10664.2
	TFF1	Mucosa	1956	12856	4978	2931	3011	4689
		Crypt	1488	14790	5595	1893	1648	3196
		Organoid	23123	7790	52498	30030	7984	8806
	TFF2	Mucosa	24	172	86	73	78	51
		Crypt	34	185	109	51	64	47
		Organoid	2006.01	252	5489.85	3845.99	281	163
	TFF3	Mucosa	27824.7	36678.3	33190.6	47820.8	39219.6	24334.1
		Crypt	26068.5	32853.4	59631.4	37140.5	35304.3	33158.5
		Organoid	97747.4	67435.6	165520	114444	113458	65934.2
ENETEROCYTE MARKERS	CA1	Mucosa	189670	43149.6	38284.9	85080.6	80448.1	84010.3
		Crypt	129187	34623.8	25789	70881.9	86594.7	84799.7
		Organoid	17306.1	17345.5	11923	10607	53195.3	15274.8
	CA2	Mucosa	79888.2	89952.5	53358.3	56473	61751.6	64162.3
		Crypt	65497.2	76786.9	33191.2	48962.9	69586.6	72282.2
		Organoid	23846.2	25710.8	28516.1	27152.7	34042.5	26430.3
	FABP1	Mucosa	66323.7	120062	41081.4	84570.3	72123.3	73310.7
		Crypt	53849.6	93069.4	39178.8	72367.5	67107.2	64468
		Organoid	144935	121046	164768	182252	104857	153365
	FABP2	Mucosa	1329	4272	1814	3936	1309	3736
		Crypt	1002	1723	1646	3356	1056	3806
		Organoid	1447	3371	4346	4191	3867	4656
ENTEROENDOCRINE CELL MARKERS	CHGA	Mucosa	8310.29	10763	37271.4	8429.13	10591.1	9591.4
		Crypt	15050.1	19919.2	43579.7	8051.31	12338.1	16472.4
		Organoid	23884	35381.7	92258.3	21805.5	33418	34746.9
	GCG	Mucosa	5062.96	5353.9	4929.16	1356	2475.01	4352.05
		Crypt	4345.08	3738.06	7611.04	1000	2158.99	7260.13
		Organoid	669.997	1782.99	2381.98	802.001	1512.99	1465
TUFT CELL MARKERS	CHAT	Mucosa	5	34	18	10	15	3
		Crypt	2	4	1	8	9	4
		Organoid	0	0	0	0	1	0
	DCLK1	Mucosa	40	44	55	89	36	18
		Crypt	0	0	0	0	0	1
		Organoid	0	0	0	0	0	0
	PTGS1	Mucosa	199	765.001	341	312	618	487.001
		Crypt	36	157	88	75	289	86
		Organoid	12	6	12	2	22	16
	PTGS2	Mucosa	44	23	33	91	26	32
		Crypt	12	5	15	39	8	2
		Organoid	0	0	0	0	0	0
	POU2F3	Mucosa	16	148	28	23	99	30
		Crypt	16	49	34	27	82	49
		Organoid	59	25	44	38	22	24

Figure A.1. RNA expression of colonic epithelial cell types. The table illustrates the presence and quantity of the different colonic epithelial cell type markers obtained by RNA sequencing of isolated human colonic mucosa, crypts and organoids of 6 patients. Data is expressed in number of reads per kilobase million (RPKM).

			Patient 1	Patient 2	Patient 3	Patient 4	Patient 5	Patient 6
ITPR	ITPR1	Mucosa	71	102	216	134	126	226
		Isolated crypts	47	36	42	74	56	47
		Organoids	71	40	43	32	165	40
	ITPR2	Mucosa	1195	1003	1577	1664	1464	1179
		Isolated crypts	1931.99	1049	679	2131.01	1841.01	1772.99
		Organoids	1007	1137	1246	902	2578	908.999
	ITPR3	Mucosa	13315.5	12161.3	12451.7	11907.4	14307.5	10096.7
		Isolated crypts	19054.8	16305.2	7108.24	14622.6	17769.7	13401.1
		Organoids	22503.6	17038.9	24271.9	20967.3	19345.5	18177.7
RYR	RYR1	Mucosa	0	11	11	11	3	27
		Isolated crypts	4	7	2	4	0	3
		Organoids	1	0	0	4	0	2
	RYR2	Mucosa	3	4	5	4	3	6
		Isolated crypts	0	0	1	1	2	1
		Organoids	1	6	7	3	6	0
	RYR3	Mucosa	3	9	12	11	5	0
		Isolated crypts	0	0	0	0	0	0
		Organoids	0	2	0	0	0	0
TPC	TPC1	Mucosa	3250.99	3008	3240.98	4781.1	4270.99	3428
		Isolated crypts	5385.99	3870	2993	5643.98	4577.98	4297.06
		Organoids	4369.02	4311.05	5600.03	3803.02	4333.97	3263.98
	TPC2	Mucosa	578	646	453	688	682	590
		Isolated crypts	805	755	387	772	819	799.001
		Organoids	1179	895	912.999	1043	1297	959
ATP2	ATP2A1	Mucosa	1.431364	1.342423	1.477121	1.380211	1.531479	1.322219
		Isolated crypt	1.986772	1.748188	1.643453	1.612784	1.740363	1.681241
		Organoid	1.69897	1.556303	1.70757	1.380211	1.322219	1.681241
	ATP2A2	Mucosa	4.125722	4.357384	4.457526	4.273672	4.263866	4.165416
		Isolated crypt	4.220848	4.405962	4.175799	4.275935	4.334508	4.270709
		Organoid	4.368694	4.410556	4.479644	4.408801	4.390884	4.309707
	ATP2A3	Mucosa	4.299804	4.457628	4.288332	4.242745	4.396595	4.205332
		Isolated crypt	4.407843	4.560999	4.299228	4.263217	4.424231	4.367755
		Organoid	4.302565	4.208339	4.421849	4.081196	4.3987	4.176164
	ATP2B1	Mucosa	4316.01	6975	12550.3	5607.15	10777.9	6588.95
		Isolated crypt	3706.99	5485.05	5659.93	4482.96	10561.3	5971.92
		Organoid	3580	4464.07	4372.04	4852.96	4718.04	4234.92
	ATP2B2	Mucosa	3	0	2	1	1	0
		Isolated crypt	0	0	0	0	5	1
		Organoid	1	0	1	0	0	2
	ATP2B3	Mucosa	3	0	0	0	0	0
		Isolated crypt	0	0	1	0	0	0
		Organoid	1	0	2	1	0	0
	ATP2B4	Mucosa	952.999	603.001	409.999	913.002	1006	650.998
		Isolated crypt	1081	496	162	812.002	797	600.002
		Organoid	634.001	824.001	999.998	447.999	855.998	477.999
	ATP2C1	Mucosa	3217.99	4279.98	4800	4379.96	4624.96	3601.01
		Isolated crypts	3246.02	3457	3068	3743.04	4338	4438
		Organoids	4122.02	4843.99	5042	4818.01	5557.98	4526.97
	ATP2C2	Mucosa	5410.05	6494.87	5223.87	6288.07	6695.9	3872
		Isolated crypts	9213.94	8185.31	7657.05	8519.13	8126.15	8456.63
		Organoids	7451.88	5400.11	6076.82	5877.96	9226.65	6090.16

Figure A.2. RNA expression of main calcium signalling toolkit components. The table illustrates the presence and quantity of the markers for the main calcium toolkit components obtained by RNA sequencing of isolated human colonic mucosa, crypts and organoids of 6 patients. Data is expressed in number of reads per kilobase million (RPKM).

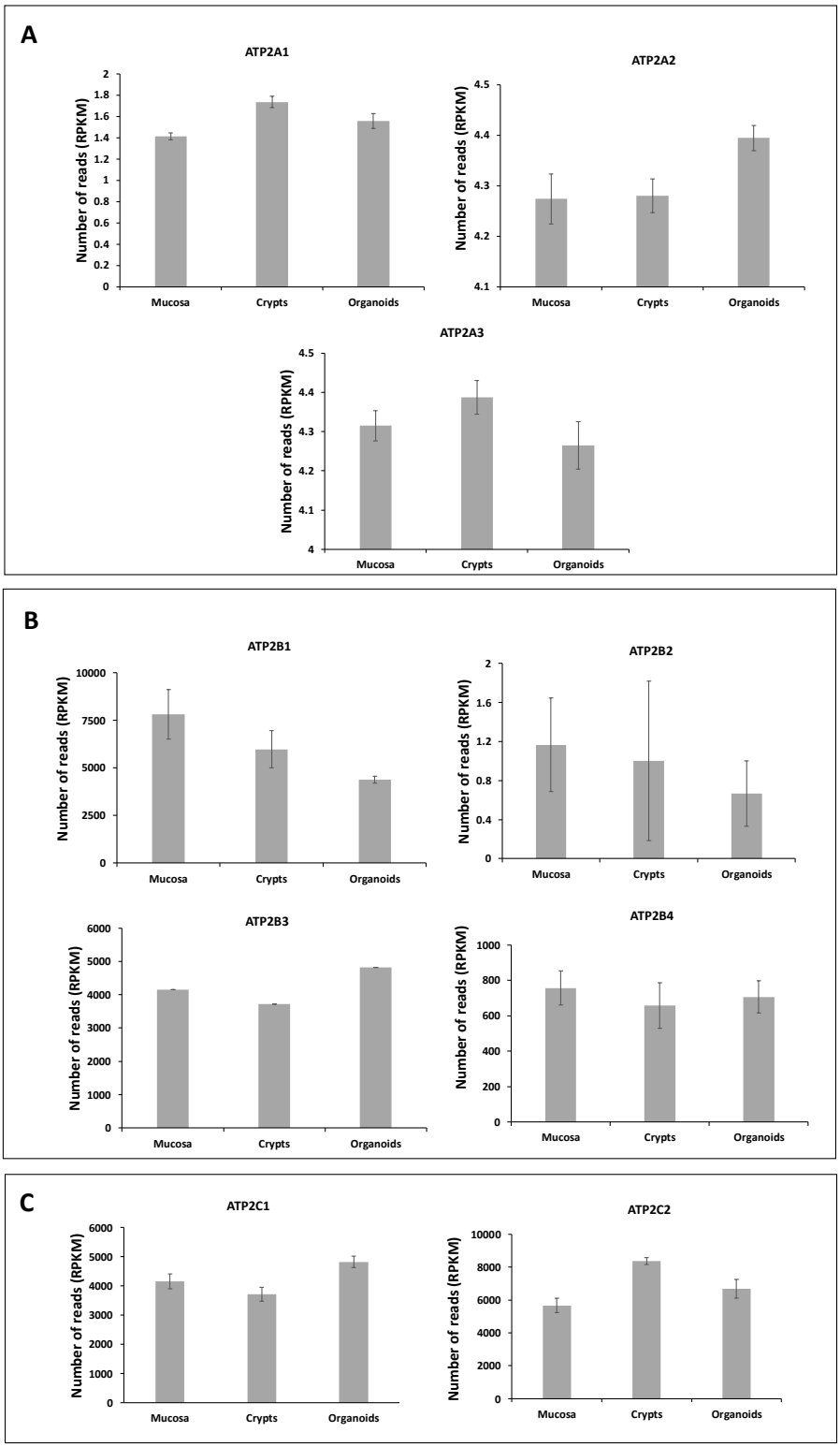

Figure A.3. Gene expression of cellular calcium ATPases. Bar charts represent the gene expression of the different isoforms of the SERCA pump (**A**), PMCA pump (**B**) and SPCA pump (**C**) on RNA samples obtained from isolated human colonic mucosa, crypts and organoids of 6 patients. Data is expressed as number of reads per kilobase million (RPKM).

APPENDIX B. Development of a MUC2 knock-in fluorescent reporter

The analysis of mucus secretion has advanced greatly over the last decades. The first approaches to study mucus secretion involved light and electron microscope radioautography of colon sections (Neutra and Leblond, 1966). The progress made in improving specificity of antibodies, fluorescent tags and the advances in confocal microscopy has helped to visualise with great accuracy the distribution and expression of proteins of interest including mucin-forming MUC2 in fixed samples. In addition, Johansson and colleagues made use of in vivo glycoprotein labelling to study mucus turnover. Using an azide-modified N-acetylgalactosamine, GalNAz, which is incorporated into glycans during protein biosynthesis, these researchers used fluorescent microscopy on fixed sections of the gut (Johansson, 2012; Schneider et al., 2018). The use of immunofluorescence labelling and confocal imaging has been instrumental in the development of this thesis, however, to get a better understanding of the spatio-temporal characteristics of mucus secretion, live imaging techniques are required. In order to do so, we aimed to develop a system to genetically engineer colonic crypt cells so they could permanently express a fluorescent reporter.

Genetic engineering of organoids has become a generalised tool in molecular biology that allows for a tailored modification of the cellular genome of a given cultured tissue, and a subsequent examination of the consequent phenotype. The CRISPR/Cas9 system has recently been demonstrated to be a precise instrument for gene editing as it introduces DNA double-strand breaks at specific genomic loci which permits a more efficient gene knock-out and knock-in, as well as enabling precise targeted gene regulation, epigenome editing, chromatin imaging, and chromatin topology manipulations (Adli, 2018; Fujii, Clevers and Sato, 2019). Because organoids allow for the potentially infinite expansion of tissues while retaining genetic and phenotypical stability, they are excellent models for genetic engineering. Indeed, recent work by Schwank and colleagues demonstrated the potential of this technique and made use of the CRISPR/Cas9 system to functionally repair the CFTR transporter in intestinal stem cell organoids of patients suffering from cystic fibrosis (Schwank et al., 2013).

In recent times, some research groups have demonstrated the possibility to edit the mouse genome to knock-in mucus fluorescent reporters. Portal et al. engineered a transgenic reporter mouse by homologous recombination, where the entire amino acid sequence of the mucus protein Muc5b was tagged with a monomeric enhanced GFP sequence. This tool allowed researchers to monitor the mucin live using confocal microscopy (Portal et al., 2017). Moreover, Birchenough and colleagues genetically engineered mice to express the mCherry-labelled human MUC2 protein. A BAC vector was constructed by homologous recombination of a BAC clone with a mCherry targeting cassette

inserted between the MUC2 CysD1 and CysD2 domains and delivered into RedMUC2^{98trTg} mice by pronuclear injection. The engineering of this fluorescent reporter allowed the researchers to visualise live mucus secretion and mucus layer growth in mouse explant crypt cultures using confocal microscopy (Birchenough et al., 2016).

In order to develop a MUC2 fluorescent reporter knock-in, we made use of the CRISPR/Cas9 technology for the advantages discussed previously. The CRISPR/Cas system consists of a series of components: the endonuclease Cas9, an enzyme that cleaves at specific target sites, a short mature CRISPR RNA (crRNA) which contains a 20 nucleotide sequence homologous to the target region of the MUC2 gene, and a trans-activating crRNA (tracrRNA) which helps creating a complex with the crRNA and the Cas9 enzyme to bind the target sequence. Once formed, the Cas9 complex can cleave the target sequence located 5' of the homologous target region, called protospacer adjacent motif (PAM), by double strand break of the DNA (**Figure B.1A**). A plasmid donor carrying the fluorescent reporter is co-transfected with the Cas9 complex via electroporation. This fluorescent reporter is flanked by two arms (5' and 3') that are homologous to the either side of the double strand break, and by a process termed homology-directed repair (HDR) the sequence of interest is inserted into the MUC2 gene. The fluorescent reporter used in our study was mKate2 (red) with excitation and emission of 588 nm and 633 nm respectively (**Figure B.1B**). In order to generate the mKate2 cassette, the flanking regions named 5' and 3' homology arms (HA) are generated by PCR amplification of the genomic organoid DNA using specific primers that contain adapters to the mKate2 reporter. The whole cassette containing the 5' and 3'HA, the mKate2 sequence and the plasmid backbone is ligated and transformed into *E. coli* competent cells. Next, the bacteria colonies are grown, and the plasmid DNA is isolated from antibiotic selective positive clones. The plasmid DNA is then Sanger-sequenced to confirm the presence of the right construct. The mKate2-containing plasmid along with Cas9 mRNA, the tracrRNA and the crRNA carrying the specific template recognition sequence are co-transfected by electroporation into colonic organoids. Next, the organoids are imaged under fluorescence microscopy to check for the functionality of the construct and its correct location. Successfully transfected organoids are then selected and clonally expanded until achieving a homogenous transfected population.

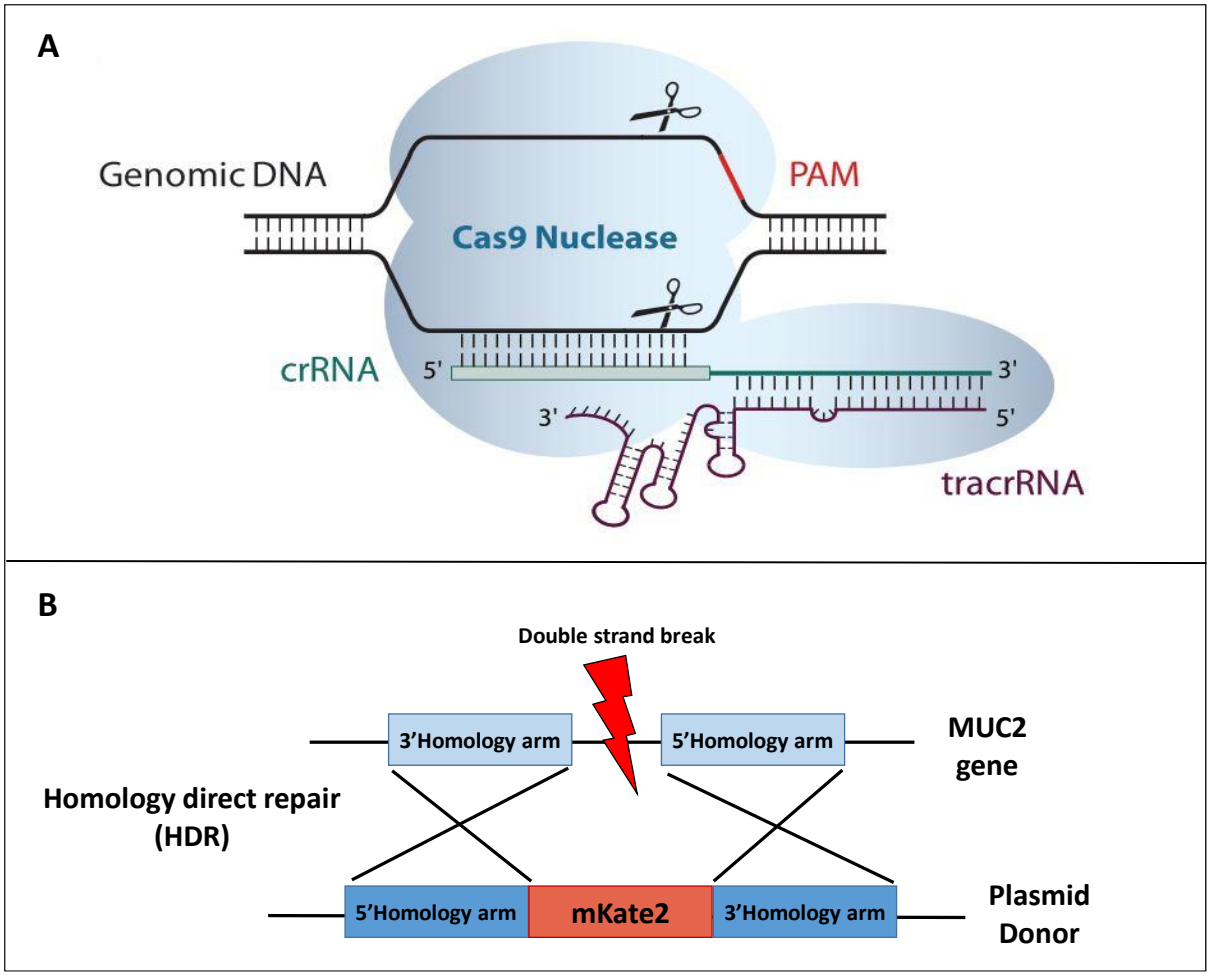

Figure B.1. CRISPR/Cas9-mediated insertion of fluorescent reporter. (**1**) The CRISPR/Cas9 complex is formed the crRNA that binds to the homologous region of the target sequence, the tracrRNA which stabilises the complex and the Cas9 enzyme that cleaves the target DNA upstream the PAM motif by double strand break (DBS). (**2**) The homology direct repair mechanism directs the insertion of the fluorescent reporter mKate2 into the DBS site. Diagram 1 adapted from Edit-R HDR Plasmid Donor technical manual, Dharmacon.

Firstly, a cleavage site was designed in the MUC2 gene for the Cas9 to induce the double strand break. This choice was based in the work of Birchenough and colleagues where they reportedly introduced an mCherry fluorescent reporter in between the CysteineD1 (CysD1) and CysteineD2 (CysD2) regions of human MUC2 gene, where it showed not to disrupt the protein function (Birchenough et al., 2016). Similarly, the MUC2 cleavage site was decided to be located at position 1398 in the PTS region after a threonine amino acid, which is situated immediately after the end of the CysD1 domain at position 1395. This decision was based on the work of Gold and colleagues who annotated the protein sequence of the N Terminus region of MUC2. With the purpose of studying the packaging of MUC2, these researchers engineered the N Terminus MUC2 region by inserting a

Myc tag domain and GFP domain immediately after the amino acid threonine at position1397. This construct allowed to visualise the status of the MUC2 N-terminal region under electron microscopy (Godl et al., 2002) (**Figure B.2**).

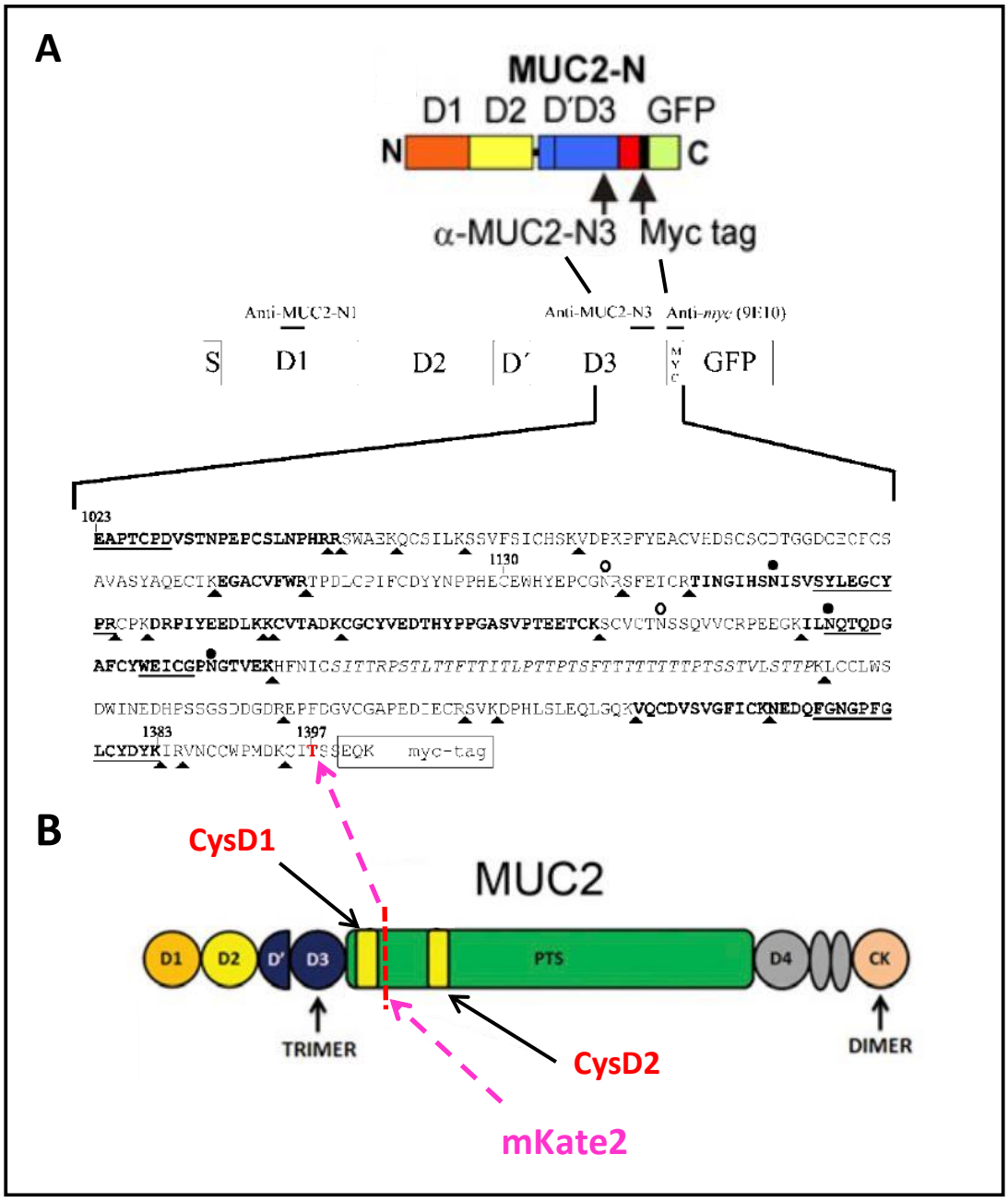

Figure B.2. Insertion of the mKate2 reporter in the MUC2 gene. (**1 top**) Schematic representation of the engineered MUC2 N Terminus containing a Myc tag and GFP fluorescent reporter in the C-terminal region. (**1 bottom**) Annotated amino acid sequence of the D3 and CysD1 domains of the MUC2 N Terminus construct. (**2**) Schematic representation of the full MUC2 monomer, highlighting

the desired Cas9-mediated cleavage site for the insertion of the mKate2 reporter. Figure 1 adapted from Gold et al., 2002. Figure 2 adapted from Nilsson et al., 2014.

Next, in order to create the mKate2 knock-in cassette, genomic DNA from colonic organoids was first isolated and purified to use as a template. To generate a homologous sequence to the template DNA that would allow recombination of mKate2, the 5' and 3'HA were amplified using PCR (**Figure B.3A**). PCR amplification of the 5'HA rendered a 634bp fragment (**Figure B.3B**). Amplification of the 3'HA was performed in two steps. Firstly, a PCR was carried out to amplify a region of 956bp containing the 3'HA (**Figure B.3C**) and secondly this PCR product was used to subsequently amplify the actual 3'HA region of 677bp (**Figure B.3D**) and the DNA was isolated and purified. In order to create the fully functional mKate2 cassette, the 5' and 3'HA were ligated together with the mKate2 fragment and the plasmid backbone and the resulting product transformed into competent *E. coli* cells (**Figure B.4A**). Bacterial colonies resistant to Carbenicillin (100 µg/mL) were screened for the presence of mKate2 cassette by performing colony PCR using primers to amplify the 5' fragment containing the 5'HA and part of the 5'mKate2 region and the 3' fragment containing the 3'HA and part of the 3'mKate2 region. 4 colonies presenting both the right 840bp 5' fragment (**Figure B.4B**) and the right 1092bp 3'fragment (**Figure B.4C**) were selected as potential candidates. Plasmid DNA of the selected candidates was sequenced using the Sanger methodology and the results blasted against the NCBI available MUC2 gene sequence. These results showed the presence of a correct 5' fragment in 3 out of 4 colonies, however, the 3' fragment had not been fully amplified in any of them which could result in a non-functional mKate2 cassette (data not shown).

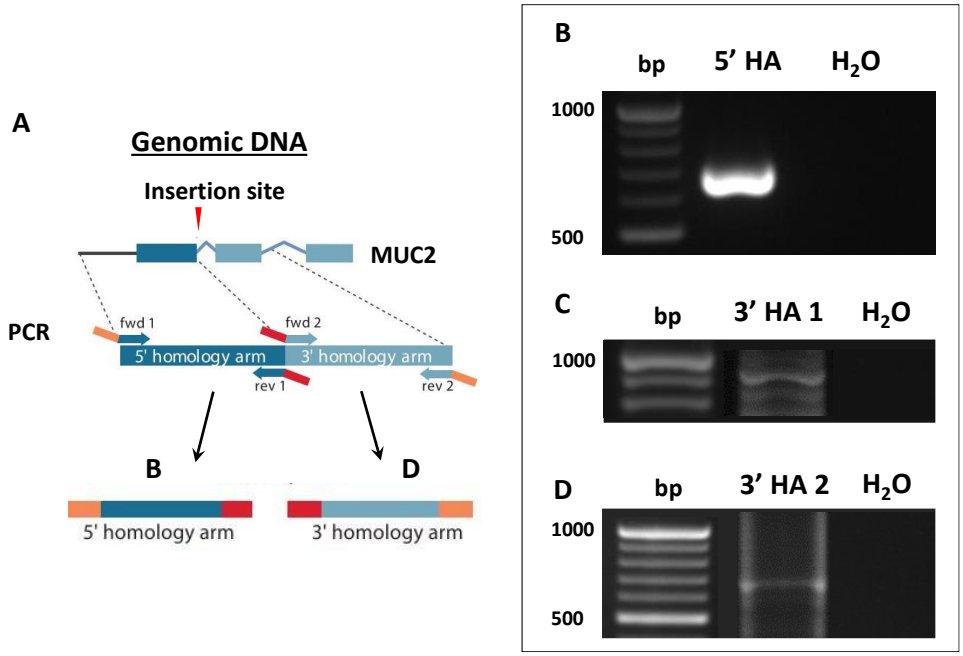

Figure B.3. Amplification of the 5' and 3' homology arms. (**A**) Schematic representing the generation of the 5' and 3'HA, homologous to the template DNA. (**B**) PCR gel showing the expression of the 5'HA. Band size, 634bp. (**C**) PCR gel showing the expression of a DNA region containing the 3'HA sequence. Band size, 956bp. (**D**) PCR gel showing the expression of the 3'HA amplified using a larger DNA region as template. Band size, 677bp. Schematic adapted from Edit-R HDR Plasmid Donor technical manual, Dharmacon.

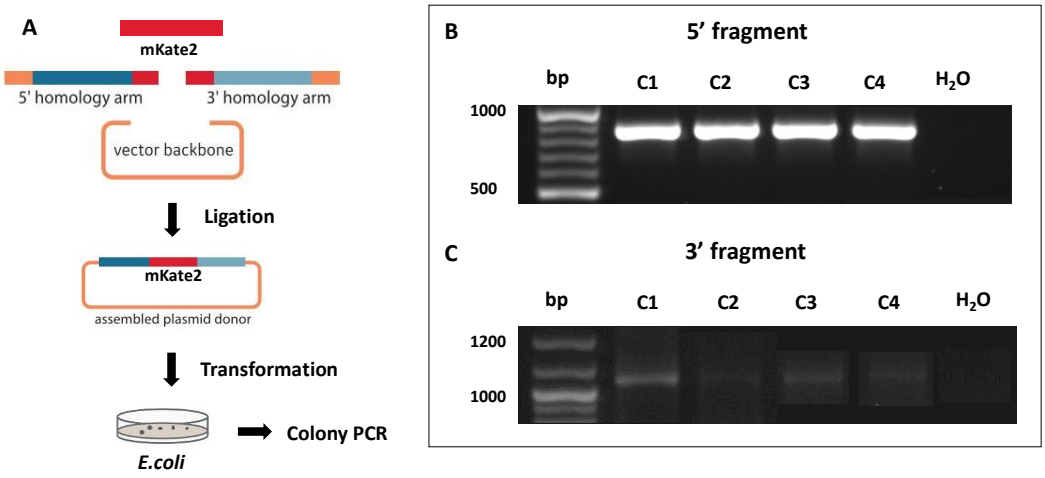

Figure B.4. Generation of a functional mKate2-conatining plasmid vector. (**A**) Schematic diagram illustrating the process of ligation of all the plasmid components and the transformation into *E.coli*. (**B**) PCR gel showing the expression of the 5' fragment in 4 bacterial colonies. Band size, 840bp. (**C**) PCR gel showing the expression of the 3' fragment in the same 4 bacterial colonies. Band size, 1092bp.